

Structural Reliability

Maurice Lemaire

in collaboration with
Alaa Chateauneuf and Jean-Claude Mitteau



ISTE

 **WILEY**

Structural Reliability

Maurice Lemaire

with the collaboration of
Alaa Chateauneuf and Jean-Claude Mitteau

Series Editor
Jacky Mazars



This page intentionally left blank

Structural Reliability

This page intentionally left blank

Structural Reliability

Maurice Lemaire

with the collaboration of
Alaa Chateauneuf and Jean-Claude Mitteau

Series Editor
Jacky Mazars



First published in France in 2005 by Hermes Science/Lavoisier entitled *Fiabilité des structures couplage mécano-fiabiliste statique* © LAVOISIER, 2005
First published in Great Britain and the United States in 2009 by ISTE Ltd and John Wiley & Sons, Inc.

Apart from any fair dealing for the purposes of research or private study, or criticism or review, as permitted under the Copyright, Designs and Patents Act 1988, this publication may only be reproduced, stored or transmitted, in any form or by any means, with the prior permission in writing of the publishers, or in the case of reprographic reproduction in accordance with the terms and licenses issued by the CLA. Enquiries concerning reproduction outside these terms should be sent to the publishers at the undermentioned address:

ISTE Ltd
27-37 St George's Road
London SW19 4EU
UK

www.iste.co.uk

© ISTE Ltd, 2009

John Wiley & Sons, Inc.
111 River Street
Hoboken, NJ 07030
USA

www.wiley.com

The rights of Maurice Lemaire to be identified as the author of this work have been asserted by him in accordance with the Copyright, Designs and Patents Act 1988.

Library of Congress Cataloging-in-Publication Data

Lemaire, Maurice.
[Fiabilité des structures. English]
Structural reliability / Maurice Lemaire.
p. cm.
Includes bibliographical references and index.
ISBN 978-1-84821-082-0
1. Structural engineering--Mathematics. 2. Reliability (Engineering) 3. Structural failures. I. Title.
TA640.L4613 2009
624.1--dc22

2008043201

British Library Cataloguing-in-Publication Data
A CIP record for this book is available from the British Library
ISBN: 978-1-84821-082-0

Printed and bound in Great Britain by CPI/Antony Rowe, Chippenham and Eastbourne.
Cover created from the author's photography of Anne and Patrick Poirier's artwork, *La Grande Colonne de Suchères*, 1984.



Cert no. SCS-COC-2993
www.fsc.org
© 1996 Forest Stewardship Council

Contents

Foreword	xv
Preface	xvii
Chapter 1. Introduction	1
1.1 An old history	1
1.2 A modern attitude	3
1.3 Reliability: a definition	6
1.4 Which risk is acceptable?	6
1.5 Today	10
1.6 A little glossary	12
1.7 The structure of this book	15
Chapter 2. Preliminary Approach to Reliability in Mechanics	19
2.1 General points	19
2.1.1 Reliability methods in mechanics	19
2.1.2 A new attitude: overcoming obstacles	20
2.2 Theoretical reliability in mechanics	21
2.2.1 Reliability approach in mechanics	21
2.2.2 Variables-component-system chain	21
2.2.3 Theoretical reliability	22
2.3 Stochastic modeling	23
2.3.1 Modeling based on available information	23
2.3.2 Construction of a stochastic model	24
2.3.3 Random variable or stochastic process	26
2.4 Mechanical modeling	28
2.4.1 Representation model of physics	28
2.4.2 Balance between resources and needs	29
2.5 Mechanical-reliability coupling	29
2.5.1 Reliability sensitivity analysis	30
2.5.2 Reliability analysis	31

2.5.3	Complexity of mechanical-reliability coupling	33
2.5.4	Actors in mechanical-reliability coupling	33
2.6	Fields of application	34
2.6.1	Reliability of offshore marine structures	35
2.6.2	Soil mechanics	35
2.6.3	Regulation	35
2.6.4	Stochastic dynamics	36
2.6.5	Integrity of structures	36
2.6.6	Stability	36
2.7	Conclusion	37
Chapter 3. Elementary $R - S$ Case		39
3.1	Presentation of the problem	39
3.1.1	Variables	39
3.1.2	Design model	40
3.1.3	Illustration	42
3.2	Definitions and assumptions	42
3.3	Random vector: a reminder	44
3.3.1	Random vector	44
3.3.2	Joint probability density	45
3.3.3	Moments and correlation	45
3.3.4	Independence and correlation	47
3.4	Expressions of the probability of failure	48
3.4.1	Probability of failure	48
3.4.2	Distributions of R and S and probability P_f	48
3.4.3	First expression of P_f	50
3.4.4	Second expression of P_f	51
3.4.5	Illustration	52
3.4.6	Generalization of the probability of failure	53
3.5	Calculation of the probability of failure	53
3.5.1	Calculation of P_f by direct integration	53
3.5.2	Calculation of P_f by numerical integration	54
3.5.3	Calculation of P_f by simulation	54
3.5.4	Calculation of P_f by sampling and integration	55
3.6	Rod under tension	57
3.6.1	Data	57
3.6.2	Probability of failure	58
3.6.3	Analytical integration	58
3.6.4	Simulation	60
3.7	Concept of reliability index	60
3.7.1	Rjanitzyne-Cornell index	61
3.7.2	Hasofer-Lind index	63
3.7.3	Naming point P^*	64

3.7.4	Application to the elementary Gaussian case	65
3.7.5	Rod under tension: Hasofer and Lind index	66
3.8	Equation $P_f = \Phi(-\beta)$	68
3.9	Exercises for illustration	68
3.9.1	Study of a frame	69
3.9.2	Resistance-stress problem	72
Chapter 4. Isoprobabilistic Transformation		77
4.1	Recapitulation of the problem and the notation	77
4.2	Case of independent variables	79
4.2.1	Gaussian variables	79
4.2.2	Independent variables	80
4.3	Rosenblatt transformation	82
4.3.1	Recapitulation	82
4.3.2	Formulation	83
4.3.3	Calculation of P_f	85
4.3.4	Example: double exponential	85
4.3.5	A warning about notation!	87
4.3.6	Gaussian variable couple	87
4.4	Approximation using a normal distribution	89
4.4.1	Principle	89
4.4.2	Uncorrelated variables	90
4.4.3	Correlated variables	91
4.5	Nataf transformation	92
4.5.1	Two random variables	92
4.5.2	Calculation of the correlation $\rho_{0,ij}$	93
4.5.3	Generalization to n variables	95
4.6	Example: correlated loads on a beam	98
4.6.1	Limit-state and design	98
4.6.2	Decorrelation of variables	99
4.6.3	Application of the Rosenblatt transformation	100
4.6.4	Application of the Nataf transformation	100
4.6.5	The uselessness of these calculations	101
4.6.6	Linear limit-state and Gaussian variables	101
4.7	Nataf transformation: example	101
4.8	Transformation by Hermite polynomials	102
4.8.1	Hermite polynomials	102
4.8.2	Isoprobabilistic transformation	104
4.8.3	Winterstein approximation [Win87, Win88]	106
4.8.4	Example: two uniform distributions	109
4.8.5	Conclusion on Hermite transformation	111
4.9	Conclusion	112

Chapter 5. Reliability Index	115
5.1 An optimization problem	115
5.1.1 Mechanical-reliability coupling	115
5.1.2 Formulation of the optimization problem	116
5.1.3 Optimality conditions	118
5.2 Optimization algorithms	119
5.2.1 Convergence [PW88]	119
5.2.2 Quality criteria	120
5.2.3 Principle of optimization algorithms	121
5.3 First order methods	124
5.3.1 Projected gradient method [HK85]	124
5.3.2 Penalty methods [HK85]	126
5.3.3 Augmented Lagrangian [PW88]	127
5.4 First order algorithms for the SDP	128
5.4.1 Hasofer-Lind-Rackwitz-Fiessler algorithm	128
5.4.2 Complements to first-order methods	131
5.5 Second order algorithms for the SDP	135
5.5.1 Newton method [PW88, HK85]	135
5.5.2 Sequential quadratic programming	136
5.5.3 Hybrid methods	137
5.6 Special problems	138
5.6.1 Limit-state with several minima	138
5.6.2 Search strategy for active constraints	139
5.7 Illustration using a simple example	140
5.7.1 HLRF algorithm	141
5.7.2 SQP, Abdo-Rackwitz and step control algorithms	143
5.8 Conclusion	144
Chapter 6. Products of Reliability Analysis	147
6.1 Sensitivity factors	147
6.1.1 Definitions	147
6.1.2 Mechanical sensitivity	148
6.2 Importance factors in reliability	149
6.2.1 Sensitivity of the reliability index	149
6.2.2 Sensitivity of β with respect to the distribution parameters $p_{i,\gamma}$	152
6.2.3 Sensitivity of β with respect to the performance function parameters	155
6.2.4 Sensitivity of the probability of failure [MKL86]	156
6.2.5 Elasticity of parameters	156
6.3 Omission factors	157
6.3.1 Linear limit-state	157
6.3.2 Non-linear limit-state	159

6.4	Representation of the results: an example	161
6.5	Conclusion	163
Chapter 7. Probability of Failure		165
7.1	Methodological framework	167
7.2	Approximation using a hyperplane: FORM	168
7.2.1	Principle of linear approximation	168
7.2.2	Expression of the probability of failure	169
7.2.3	Counter-example	172
7.2.4	Accuracy of the approximation	173
7.2.5	Reference example	174
7.3	Approximation using a second-order hypersurface	175
7.3.1	Curvature at the design point	176
7.3.2	Principle of approximations	177
7.3.3	Quadratic approximation	179
7.3.4	Elements of the approximation quadric	181
7.3.5	Parabolic approximation	183
7.3.6	Quadratic approximation	185
7.3.7	Reference example	185
7.3.8	Complement on quadratic approximations	186
7.3.9	Conclusion	189
7.4	'Asymptotic' SORM method	190
7.4.1	Breitung's formula	190
7.4.2	Reference example	194
7.4.3	Hohenbichler approximation	194
7.4.4	Tvedt approximation	194
7.4.5	Comments and conclusion	195
7.5	Exact SORM method in quadratic form	196
7.5.1	Characteristic function	196
7.5.2	Characteristic functions of quadratic forms	198
7.5.3	Results	199
7.5.4	Inversion of the characteristic function	200
7.5.5	Optimization of numerical calculation	200
7.5.6	Reference example	202
7.6	RGMR method	203
7.6.1	Motivation	203
7.6.2	Introduction to RGMR	204
7.6.3	Notion of solid angle	205
7.6.4	Integral of the solid angle	205
7.6.5	SORM integral	207
7.6.6	Calculation of the solid angle	208
7.6.7	Numerical aspects	211
7.6.8	Solid angle in the FORM approximation	212

7.6.9	Special two-dimensional case	215
7.6.10	Reference example	215
7.6.11	Conclusion	216
7.7	Numerical examples	218
7.7.1	Reference example: conclusions	218
7.7.2	Rod under tension	219
7.7.3	Plastic failure of a section	221
7.7.4	Approximations of the probability of failure	222
7.7.5	Example: double exponential	227
7.8	Conclusions	232
Chapter 8. Simulation Methods		233
8.1	Introduction	233
8.2	Uniform pseudo-random numbers	234
8.2.1	Composite congruential generator	234
8.2.2	Multiplicative generator	236
8.2.3	Congruential additive generator	237
8.2.4	Some generators as examples	237
8.2.5	How to test a generator	239
8.2.6	Conclusion	239
8.3	Generators of non-uniform distributions [Rub81, Dea90]	240
8.3.1	Inverse transformation method	240
8.3.2	Composition method [But56]	240
8.3.3	Rejection-acceptance method [VN51]	241
8.3.4	Gaussian distribution	242
8.3.5	Lognormal distribution	244
8.3.6	Weibull distribution with two parameters	244
8.3.7	Generation of a random vector	244
8.3.8	Conclusion	247
8.4	Simulation methods	247
8.4.1	Introduction	247
8.4.2	Crude Monte Carlo simulations	249
8.4.3	Directional simulations (DS) [Dea80, DBOH88, DMG90, Bje88]	253
8.5	Sampling methods using P^*	255
8.5.1	Importance sampling (IS) [Mel90]	255
8.5.2	Conditional sampling (CS) [BF87]	256
8.5.3	Latin hypercube (LH)	258
8.5.4	Adaptive sampling (AS) [Buc88]	259
8.5.5	Conditional importance sampling method	259
8.5.6	Stratified sampling method [Rub81]	260
8.6	Illustration of the methods	260
8.6.1	Crude Monte Carlo (MC)	260

8.6.2	Directional simulations (DS)	260
8.6.3	Conditional sampling with the knowledge of P^* (IS, CS, LH)	261
8.6.4	Outcome of the illustration	263
8.7	Conclusion	263
Chapter 9. Reliability of Systems		265
9.1	Combination of failure modes	265
9.1.1	Series combination	266
9.1.2	Parallel combination	266
9.1.3	Series combination of parallel systems	267
9.1.4	Parallel combination of series systems	268
9.1.5	Conditional parallel combination	268
9.1.6	Implementation and application	269
9.2	Bounds of the failure probability of a system	273
9.2.1	Hypothesis	273
9.2.2	A classic approximation	274
9.2.3	Correlation of events E_i and E_j	274
9.2.4	Uni-modal bounds	275
9.2.5	Bi-modal bounds	276
9.3	First-order approximation bounds	277
9.3.1	Hypothesis	277
9.3.2	Probability bounds of the intersection $P(E_i \cap E_j)$	277
9.3.3	Equivalent hyperplane	279
9.4	First-order system probability	281
9.4.1	Parallel system	282
9.4.2	Series system	282
9.4.3	Multinormal distribution function	282
9.5	Second-order system probability	286
9.6	System of two bars in parallel	289
9.6.1	Statement of the problem and data	290
9.6.2	Solution	291
9.6.3	First-order solution	293
9.6.4	Second-order solution	296
9.6.5	Conclusion of the illustration	296
9.7	Conclusion	297
Chapter 10. ‘Safety’ Coefficients		299
10.1	Bases of design	299
10.1.1	General information	299
10.1.2	Values associated with a variable	300
10.1.3	Design rule	303
10.1.4	Levels in the design approach	304

10.1.5 Illustration	305
10.2 Safety coefficients – elementary case	306
10.2.1 Probabilistic design	306
10.2.2 Global characteristic coefficient	309
10.2.3 Designing using partial coefficients	315
10.3 General definition of partial coefficients	319
10.3.1 Case of independent variables	319
10.3.2 Case of dependent variables	321
10.3.3 Comments	321
10.4 Calibration of partial coefficients	322
10.4.1 Calibration principle	322
10.4.2 A calibration method	324
10.4.3 Application example	326
10.5 Application examples	331
10.5.1 Linear fracture mechanics	331
10.5.2 Compound bending of a fragile material	336
10.6 Conclusion	339
Chapter 11. Mechanical-Reliability Coupling	341
11.1 Introduction	341
11.2 General information on the coupling with a FEM code	343
11.2.1 Control of the FEM code	343
11.2.2 Random variables	343
11.2.3 Mechanical-reliability variables	344
11.2.4 Dialog between FEM and reliability procedures	347
11.2.5 Implementation of the procedures	347
11.2.6 Numerical evaluation of gradients	349
11.3 Direct method	352
11.3.1 Description of the method	352
11.3.2 Overview	352
11.4 Response surface method	353
11.4.1 Introduction: polynomial response surface	353
11.4.2 Description of the method	355
11.4.3 Calculation of the coefficients of a QRS	359
11.4.4 Validation	360
11.4.5 Construction of a neural network	364
11.4.6 Summary	367
11.5 Two applications as examples	368
11.5.1 Sphere under pressure	369
11.5.2 Two correlated uniform distributions	371
11.5.3 Conclusion	376
11.6 Optimization method	377
11.6.1 Description of the method	377

11.6.2	Overview	380
11.6.3	Application	380
11.7	Example: isostatic truss	380
11.7.1	Data	380
11.7.2	Mechanical analysis	382
11.7.3	Reliability analysis	382
11.8	Conclusion	387
Chapter 12. Stochastic Finite Elements		391
12.1	Introduction	391
12.1.1	Definition and purpose	391
12.1.2	Random variables and random fields	392
12.1.3	Chapter plan	393
12.2	Spatial discretization of a random field	394
12.2.1	Random field [Cau88, CL67]	394
12.2.2	Stochastic mesh	398
12.2.3	A few discretization methods	399
12.2.4	Conclusion	400
12.3	Series expansion of a random field	401
12.3.1	Cholesky decomposition	401
12.3.2	Karhunen-Loëve expansion [GS91]	402
12.3.3	Polynomial chaos	402
12.3.4	Conclusion	404
12.4	Finite element method and gradient calculation	405
12.4.1	Assumptions and notations	405
12.4.2	FEM linear equations	405
12.4.3	Gradient calculation with constant mesh	406
12.4.4	Calculation of derivatives with a variable mesh	407
12.5	Perturbation method	410
12.5.1	Taylor expansion	410
12.5.2	Mean and covariance	411
12.5.3	Example: deflection of a beam	412
12.5.4	Neumann expansion	417
12.6	Polynomial chaos expansion	418
12.6.1	Random variable expansion	418
12.6.2	Application to the finite element method	420
12.6.3	Perspectives	424
12.6.4	Conclusion	425
12.7	Continuous random field methods	425
12.7.1	Weighted integral method	425
12.7.2	Spectral method	427
12.7.3	Conclusion	432
12.8	An illustration	432

12.8.1 Statement of the problem	432
12.8.2 Case 1: 4 random variables	433
12.8.3 Case 2: stiffness EA is a random field	435
12.9 Conclusion	437
12.9.1 Combination of the coupling and stochastic finite elements	438
12.9.2 Conclusion	439
Chapter 13. A Few Applications	441
13.1 Design of a wind bracing	441
13.2 Modeling of a mandrel	442
13.3 Failure of a cracked plate	443
13.4 Cooling of a cracked plate	444
13.5 Boiler casing subjected to a thermal field	445
13.6 Pressurized tank	446
13.7 Stability of a cylindrical shell	447
13.8 Reliability sensitivity for a cooling tower	448
13.9 Lifespan of an exhaust manifold	450
Chapter 14. Conclusion	453
14.1 Reliability methods in mechanics	453
14.2 Application of the methods	455
14.2.1 Design and maintenance	455
14.2.2 Software tools	458
14.3 Perspectives	459
14.3.1 Stochastic finite elements	460
14.3.2 The time factor	460
14.3.3 Data acquisition and processing	461
14.3.4 Mechanical-reliability optimization	461
14.4 Reliability analysis and sensitivity analysis	463
Bibliography	465
Annotations	481
A.1 Vectors and matrices	481
A.2 Operators	481
A.3 Random values	482
A.3.1 Scalar values and random variable couples	482
A.3.2 Statistical values	482
A.3.3 Vectorial values	483
A.3.4 Mechanical values	484
Index	485

Foreword

My colleague Maurice Lemaire has invited me to write a few words as a foreword to this treatise on structural reliability. The importance of the subject is obvious to everybody. Undertaking a scientific study of it requires a superior mastery of two disciplines, namely mechanics and probabilities. Maurice Lemaire was inspired by a remark made by the authors of the report that the President of the Republic Giscard d'Estaing had requested in 1980 from the Académie des Sciences, titled '*Les sciences mécaniques et l'avenir industriel de la France*' ('Mechanical sciences and the industrial future of France'). The report in fact observed that it was quite rare to find in French laboratories a team in which skills in these two disciplines mixed. This observation caught Lemaire's attention and motivated him to orient his research and that of his students in order to remedy the situation. This book testifies to the undeniable success of the decision made by Maurice Lemaire. I thank him for this opportunity to convey my heartfelt congratulations, and express my satisfaction in seeing that young researchers have found in this report an inspiration that has proved to be so fruitful.

The preface and the introduction present the content of this book as is customary, and also indicate its place in the history of mechanics. The reader can also discover how the book has been developed by its author, who has made good use of his lectures enriched by his personal reflections, tested his developments with his students and discussed his progress with colleagues abroad in international meetings and thus earned a well-merited reputation. That is why I believe that this book is a treatise, which I think will be a reference in this discipline for a long time to come.

Paul Germain
Honorary Permanent Secretary
Académie des Sciences

This page intentionally left blank

Preface

On 25 September 1975, I defended, before the Claude Bernard University and the National Institute of Applied Sciences of Lyon, a doctoral thesis in which I discussed how the new possibilities offered by computers in the numerical resolution of mechanical models opened up wide-ranging perspectives for developing behavior models of reinforced concrete and constructing their numerical implementation. At the end of this research work, one conclusion was obvious: a numerical solution consists of concatenating millions of operations performed with about 14 digits, whereas the knowledge of data is an uncertainty limited to two or three significant digits only.

It was this observation that inspired my approach on my arrival at the University of Clermont in September 1976. The spirit of Blaise Pascal still lingers here and perhaps made me aware of probabilities. But it was in 1980 that a founding text confirmed me in my approach. The President of the Republic had asked the Académie des Sciences for a report that was published under the title '*Les sciences mécaniques et l'avenir industriel de la France*'. It said:¹

It is evident that the stochastic point of view must play an increasingly greater role in mechanics and not only in academic research, but more importantly in industrial applications. While taking into account that developers are already introducing probability calculation into their reliability studies, and without forgetting research such as that undertaken for the definition of offshore oil platforms and the prediction of their resistance to sea and wind, we can no doubt say that it is quite rare in France (except for turbulence specialists) to find in laboratories a team in which skills in mechanics and in probability mix fully in equal parts.

All the calculations and all the predictions on safety coefficients must be definitively replaced by reasonable estimations of probabilities of failure. The French situation is a cause for concern and it seems advisable to promote the formation of cutting-edge

¹ La Documentation Française, September 1980, p. 198.

teams in the mechanical laboratories of the CNRS, engineering schools or universities.

Boosted by this direct confirmation of my conclusion, I strove from that day on to develop scientific research, and to set up a teaching program, on the theme of the marriage between models in mechanics and those in probability and statistics. A contribution to research gave me access to international debate, particularly through the International Conference on Applications of Statistics and Probability. It nurtured my teaching, firstly through a Master's course in Materials, Structures, and Reliability at the Blaise Pascal University.

In 1991, I was part of the creation of the Institut Français de Mécanique Avancée (IFMA). I then had the opportunity to promote the teaching of mechanical reliability as part of the curriculum for engineering students. It was the first time that such a course was offered, and I would like to thank Claude G. Bonthoux, founder and first director of IFMA, for placing his trust in me, and his successor Didier Marquis for his continued support.

More than 10 years after the publication of the report of the Académie des Sciences, during the inauguration of IFMA on 7 January 1994, I was able to demonstrate to the President of the Republic and to the Permanent Secretary of the Académie des Sciences the modest result of the reflection that the former had kindled and the latter fueled.

This book therefore embodies the experience acquired in a field in which we had to construct pedagogy and prove the relevance of such a degree course in an engineering school. As knowledge developed, numerical tools made lightning progress. If, even today, mechanical-reliability models consume considerable calculation resources, we have adequate means to actually address industrial problems. The development of methods and the increase in calculation power will make these models the routine tools of the designer in 10 or 15 years. If we are not convinced, we only need to ask ourselves whether the engineers of the 1970s could have imagined the non-linear calculations that are now possible thanks to finite elements.

Apart from IFMA and l'Ecole Doctorale Sciences pour l'Ingénieur de Clermont, this course, through my intervention or those of our team, also spread to other establishments, where it has been introduced in the last few years (Pôle Universitaire Léonard de Vinci, Institut National Polytechnique de Grenoble, Ecole des Mines Paris, Ecole Centrale Paris, etc.), and as a part of continuing education (Institut pour la Promotion des Sciences de l'Ingénieur, Ecole Polytechnique, etc.). It was also the basis for intervention in companies, going as far as to convince Jean-Marc Bourinet to join us.

The permanent dialog with engineering students proved to be a powerful driving force in the creation of this course, as it is true that everyone understands fully only what he is capable of teaching.

That is why I have great pleasure in thanking first of all the inner circle of engineering students of the Materials and Structures discipline at IFMA who, through the course and the projects, forced me to the limits of my resources to obtain satisfactory answers to their queries.

A second circle was made up of doctoral students who trusted me enough to venture onto the new path that I was showing them. They contributed extensively to the elaboration of this expertise. In order of appearance, my sincere thanks to Michel, Jean-Pierre, Ghassan (Claude), Alaa, Oscar, Nicolas, Clair, Pierre, Maurice, Céline, Nicolas, Ghias, Zakoua, Sébastien, Marc, Anthony, Lukas, François... That is why this book refers to their research.

My colleagues have also made precious contributions through the scientific and friendly discussions that we have had for so many years. Bernard Jacob, from the Laboratoire Central des Ponts et Chaussées, has been a particularly efficient accomplice in convincing ICASP to hold its congress in France. Jean Goyet, the delegate to the Bureau Veritas research department, allowed me to make use of his rich experience in his critique of my writing regarding ‘safety’ coefficients.

Jean-Claude Mitteau and Alaa Chateauneuf (Mohamed) joined the Laboratoire de Recherches et Applications en Mécanique Avancée (Institut Français de Mécanique Avancée and Blaise Pascal University), which has today become the Laboratoire de Mécanique et Ingénieries (LaMI), and were kind enough to associate themselves with my research. As colleagues, they have made particularly significant contributions, and have shared their experience and their observations. They are naturally part of this book.

For the last few years, we have forged a collaboration with Electricité de France, firstly under the impetus of Patrick Hornet, joined thereafter by Bruno Sudret. This collaboration was formalized by a partnership agreement signed on 16 June 2000 and extended since. The meeting of industrial, pedagogical and scientific preoccupations has also been a powerful motor in the development of mechanical-reliability methods.

These methods are now reaching sufficient maturity to form a tool of industrial performance. Maurice Pendola was so convinced of this that he created PHIMECA Engineering S.A. to develop this knowhow.

I take this opportunity to express my sincere gratitude to all, students, teachers, researchers and industrialists, for all that they have contributed.

This book deals with mechanical reliability, and of course it can be judged by the reliability of its writing, and as the French proverb says, a man is punished by the very things through which he sins! Is this book reliable? It is perhaps reliable with a sufficiently weak probability of failure. The electronic file contains 17 MB. A reasonable target failure of 10^{-5} would result in 170 typing errors. The reality is much lower, we hope!

Nurtured by contact with mechanical engineering students, this book is based on standard knowledge in the fields of mechanics (continuous media, structures) and numerical modeling (finite elements). It requires at least some knowledge of probability and statistics (random variables, distributions). These basic concepts are not repeated in the book as they can be found in classic textbooks. The ambition of the book is to allow an engineering student or an engineer to discover the advantages of reliability methods, to understand the approach and the tools: that is why, in addition to theoretical developments, simple examples describe how results are obtained. This is also the reason why the book not only describes the methods that are the most widely used today, but also presents methods that have made their contribution to the current doctrine, as it is true that, just as in politics, we can understand current affairs only in the light of history. Then everyone can move on to applications, first academic and then industrial, with the help of general or dedicated tools, and also access the international literature on the subject.

Preface to the English edition

The translation of this book, published in French over four years ago, was a daunting task, undertaken at the suggestion of and with the help of the publisher. It was possible thanks to the faultless collaboration of David Turner, a linguist capable of accepting the compromises which are inevitable in a scientific text. I would particularly like to thank him for his open-mindedness and for the care with which he accomplished this task.

A translation is not the same as writing a book directly in the target language. It conserves a style and a presentation which, showing a certain ‘French touch’, reveal its origin. Its context is a set of references which underline the contribution of French studies to the field, although they are of course not exclusive. The author begs the readers to excuse him for this, certain that they will easily find the necessary standard works in their own environment, especially in mechanics, probability and statistics.

Some useful changes have been made to the original French text, and some points have been explained in more detail. The book has largely contributed to the initiation of numerous students and engineers working in France. I hope that tomorrow it will play the same role for those who are about to discover it.

Maurice Lemaire
Maurice.Lemaire@ifma.fr

Chapter 1

Introduction

1.1 An old history

It would be fascinating to take some time to go back in history in order to understand how man gradually conquered enough ‘certainties’ to accept rationally the risk of his uncertainties. We will find that great personalities have reflected on this question and contributed to the gradual acquisition of more comprehensive heuristic and axiomatic information, which has made it possible to design more and more ambitious structures and systems.

It is certainly Hammurabi’s code that first established rules governing the acceptance of risk in construction.¹ Around 1755 B.C., this Babylonian sovereign put together a set of prescriptions, dictated by the gods, constituting the first legal code ever known. It remained in force in Mesopotamia for a thousand years. The code related to the construction of houses, and the mason’s responsibility was strongly binding.² Let us judge for ourselves:

Article 229: If a mason has constructed a house for someone but has not strengthened his construction, and if the house that he has constructed collapses and kills the house owner, that mason shall be put to death.

Article 230: If it is the child of the house owner that has been killed, one of the mason’s children shall be put to death.

It is interesting to note that the insistence on safety was then based on the transfer onto the builder of a risk that related to his own security: linking the notion of risk to the outcome of the feared event remains quite a contemporary mindset.

In fact, risk is defined by the existence of a feared event that has a probability (or a possibility) of occurrence, and by the gravity of the consequences of this event.

¹ *Les Grands Procès*, under the guidance of N. Laneyrie-Dagen, Larousse, Paris, 1995.

² *Le Code d’Hammourabi*, A. Finet, Editions du Cerf, Paris, 1983.

2 Structural Reliability

The following equation is often given:

$$\text{Risk} = \text{Probability} \times \text{Gravity.}$$

In order to diminish the probability of an event feared by the user, the penalty should be increased for the person who takes the responsibility for the construction. This is a direct application of the Farmer graph illustrated in Figure 1.1, according to which the mason will try to reduce the probability of the occurrence of a feared event if its consequences are disastrous for him.³

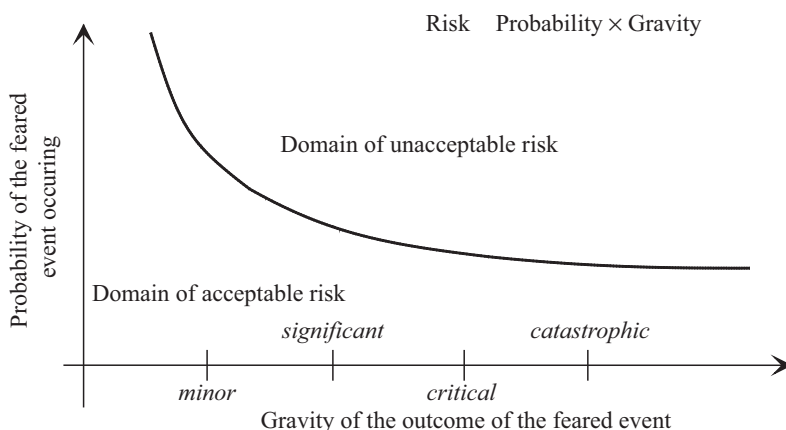


Figure 1.1 Farmer graph (1967): probability-gravity.

Hammurabi imposed responsibility for results and left the choice of the means of achieving them open. He anticipated what the European Union would much later call *directives*. Today this practice seems barbaric, whereas it essentially aimed at limiting the effects of an endless vendetta between the concerned parties due to the application of the law of ‘an eye for an eye’.

Humanity’s scientific quest therefore consisted of accumulating experience and constructing projected models that give today, not for one man but collectively to engineers, the possibility of taking on the risks of civil and mechanical constructions on behalf of society with real success, in a context in which great catastrophes are a reminder that humility is always necessary.

³ Concepts et méthodes probabilistes de base de la sécurité, A. Desroches, Editions Lavoisier, Paris, 1995.

1.2 A modern attitude

If the knowledge of geometry and static mechanics advanced rapidly in ancient times, the mastery of the uncertain in the construction of cathedrals in the Middle Ages proceeded by trial and error and led to well-known failures.⁴ Leonardo da Vinci (1452–1519) was one of the first to look for a relationship between load effect and resistance in the case of beams. A little later, Galileo was particularly interested in the optimization of the resistance of a cantilever beam, thereby initiating the first modeling.⁵

We know the great developments in modeling the behavior of materials and constructions that followed. This conquest could lead us to believe that one day the knowledge of laws, models and solutions will attain such perfection that engineers will be able to trust them completely. However, in parallel and sometimes simultaneously, scientists explained that we should live with chance.

Should we return to a philosophical debate by wondering whether chance exists, or whether what we call chance is only the fruit of our ignorance and our inability to take into account all the initial conditions of a process? Using the language of fluid mechanics, the Lagrange approach to chance is impossible because it requires monitoring a trajectory, whereas the Euler approach is content to observe the variability at the time and the place where the observer is placed. This debate is certainly futile for us today, and it is no doubt more pragmatic to think that between the present mastery of knowledge and physical reality, there will always be a gap that cannot be modeled with certainty. Moreover, we all know very well that very small disturbances of an initial state can lead to huge potential differences in the consequences, as seen in the phenomena of instability, for example in meteorology or in structural mechanics.

On the other hand, perfectly determined outcomes can be predicted by methods based on the modeling of uncertainty. This is the case for geostatistics, for example, where the content of an ore is considered a unique outcome of a random process.

In view of this inability to master all the data – which he possesses in theory, however, as they are in front of him and he has only to know how to read them – man gambles, and most often he wins.

Blaise Pascal (1623–1662) invites us to reflect on this theme:

when we work for tomorrow, and do so on an uncertainty, we act reasonably; for we ought to work for an uncertainty according to the doctrine of chance which has been demonstrated.

⁴ Trials on the construction of very high vaults ended at Beauvais with a partial collapse in 1284.

⁵ *Discorsi e Dimostrazioni Matematiche, intorno à due nuove scienze, attenenti alla Mecanica & i Movimenti Locali*, Galiléo Galiléi Lincéo, Leida 1638.

4 Structural Reliability

The first part of this proposition is simple. We work for tomorrow using studies that contribute to strengthening scientific progress, to increasing our knowledge of phenomena and to creating models in order to anticipate; we work for the uncertain because all the data will never be at our disposal for sure. Pascal tells us that we do it with reason, and he justifies it by the hope of success. It is therefore important to know what success brings us, and what makes us fear failure. Replying to Chevalier de Méré, Pascal demonstrated how to share – in other words, to give everyone his due – in a game which is subject to risk-taking and hopes of success. The doctrine of chance therefore enables each person to justify his commitment depending on his hopes.

This *pensée* by Pascal regarding a commercial stake can also be applied relevantly to a technical context. In his quest for knowledge, in his desire to want to achieve the most daring of constructions or machines, man takes risks, hoping for progress, for the benefit of humankind. Thus, Pascal made a contribution to decision-making in uncertainty, by showing that chance, whatever its origin, has a geometry: Pascal thereby laid the foundations for the calculation of probabilities.

If everyone accepts the uncertainty of data, the uncertainty of models has only recently been admitted.

One of the most powerful drivers in the advancement of science was the observation of the solar system, as much by what it induced in terms of the capacity for precise measurements as in the capacity for modeling. Until the end of the 19th century, the majority of astronomer–mathematicians were searching for mathematical laws to describe the movement of the planets, particularly in terms of the well-known problem of three bodies in gravitational interaction (sun, earth, moon). According to them, it would have been enough to add to the main components of movement successive corrections brought about by weak perturbations, in order to obtain exact predictions of the ephemerids. The works of Henri Poincaré, on the occasion of the award given in 1889 by the King of Sweden and Norway, Oscar II, led to a conclusion accepted with difficulty: *unpredictability* had its place in deterministic systems.⁶ Poincaré wrote in 1903, in his book *Science et méthode*:

A very small cause, which escapes us, produces a considerable effect that we cannot avoid seeing, and then we say that this effect is due to chance. If we knew the laws of nature exactly and the situation of this very universe at its initial instant, we would be able to predict exactly the situation of the same universe at a later time. However, even though the laws of nature would no longer have any secrets for us, we could know the initial situation only *approximately*. If this allows us to anticipate the latter situation with the *same*

⁶ *Le Chaos dans le système solaire*, Ivars Peterson, Pour la Science, Paris, 1995.

approximation, it is all that we need; we say that the phenomenon was anticipated, that it is governed by laws. But it is not always so; sometimes small differences in the initial conditions generate large ones in the final phenomena: a small error in the former will cause an enormous error in the latter. Prediction becomes impossible and we have a random phenomenon.

This does not challenge the principles of Newtonian mechanics in any way. For this, we had to wait for the theory of relativity, once again in relation to astronomy: an elucidation of Mercury's trajectory, then quantum mechanics uniting a certain macroscopic determinism with the necessary taking into account of the random of uncertainty in the infinitely small.

Furthermore, the 20th century has also removed certain illusions following Kurt Gödel's incompleteness theorem (1931), which introduced the *undecidability* of certain propositions. The theorem results in the impossibility of solving certain well-formulated problems algorithmically.

Unpredictability and *undecidability* therefore invite us to assume considerable humility in our hope of analyzing risks – humility that the engineer should have permanently in his mind each time he is confronted with a decision about reliable and economic design.

In risk analysis, reliable design belongs to the engineer, and the gravity of the consequences belongs to the economist and citizen. Serious accidents and lower tolerance toward damages on the part of society, though often paradoxical, have recently given rise to a political deliberation leading to the evolution of an essentially deterministic French approach via the integration of probabilistic concepts into risk analysis. The French law of 30 July 2003 makes the following provision:

the measures envisaged in plans for the prevention of technological risks ... are implemented progressively depending particularly on the probability, the gravity and the kinetics of potential accidents as well as the relationship between the cost of the measures envisaged and the expected benefit in terms of safety.⁷

However, O. Gudmestad reminds us that constraints owing to budgets or unrealistic schedules are never taken into account in risk analysis, and suggests the restoration of the role of court jester in a project team, for he is the only person capable of telling the truth!⁸

⁷ Law of 30 July 2003 regarding the prevention of technological and natural risks and repair of damages.

⁸ ASRaNet Conference, Barcelona, 5 July 2004, 'Implementation of human factors analysis in QRA & SRA'.

1.3 Reliability: a definition

We still need to be sure that mastery of the uncertain is sufficient for risks to be well evaluated and remain acceptable; otherwise, it would be like playing the sorcerer's apprentice. This is the objective of theories of *reliability*.

A technical definition of this word is given in the text retained by AFNOR:

the ability of a system to accomplish a required function in given conditions, during a given period ... the term is also used as an attribute describing a probability of success or a percentage of success.⁹

This text demonstrates the importance of a closely associated qualitative definition (ability) and quantitative definition (probability).

It should be noted that such a definition immediately settles a possible debate by associating the analysis of the uncertain with probabilistic modeling. It favors an approach using random variables and stochastic processes, which is not the only choice: the methods and tools of fuzzy logic, convex sets and robustness may also play their role.

Reliability may be considered as an element of a larger whole, constituting the 'ities' RAMS: which can be understood as *reliability* (the subject of this book), as *availability* (the ability of a device or a commodity to accomplish a required purpose at a given moment), as *Maintainability* (the ability of a device or a commodity to be maintained or re-established with the intention of accomplishing a required purpose), and finally as *safety* (concerning risks of physical, material and environmental damage related to the system or commodity considered).

1.4 Which risk is acceptable?

As we have just seen, the theory of reliability uses the estimation of probability as a measure. Whether this probability is acceptable or not is a very complex question, and it is clear that a decision involves taking into consideration the quality of the available information, the estimated level of the risk, the consequences of a failure, such as material and human damage, and the duration of exposure to the risk, given that certain risks are imposed on everyone by living conditions and that others are freely accepted. One reasoned argument, two research studies and a few expert opinions will enable us to define the values of the probabilities that we will be searching for.

The reasoning is by Laplace. If an event has been observed n times consecutively, the probability that it will take place $n + 1$ times is $n/(n + 1)$, and the probability that it will not take place $n + 1$ times is therefore $1/(n + 1)$.

⁹ AFNOR, NF X50-120, 1988.

Activity	Rate
Plague epidemic in London in 1665	15,000
Training for rock climbing on a rockface	4,000
Firefighter in London during the air raids in 1940	1,000
Travel by helicopter	500
Travel by motorbike or moped	300
Travel by bicycle	60
An average police officer in North Ireland	70
Using tobacco	40
Walking along the road	20
Travel by plane	15
Travel by car	15
Travel by train	5
Accident during construction	1
Travel by bus	1
Accidents at home	1
Acceptable limit when facing an unexpected exceptional event	1
Effects of natural radon	0.1
Terrorist attack in a street in London	0.1
Collapse of a building	0.002

Source: from J. P. Menzies.

Table 1.1 Risk rate by activity, per hour for 10^8 people exposed.

According to the estimated duration of the universe (around 15 billion years), the probability that the sun will not rise tomorrow is of the order 10^{-12} . It is pointless to be interested in such weak probabilities.¹⁰

The first study is that of J. P. Menzies, who carried out an *objective* evaluation of death risks in the United Kingdom by type of activity.¹¹ Table 1.1 represents some values of the fatal accident rate per hour of activity for 10^8 persons exposed. It is possible to draw two conclusions from it. The first is the extremely low risk due to the collapse of buildings in comparison with many other risks of daily life, although the duration of exposure is very long. The second is the definition of an acceptable limit when facing an unexpected exceptional event, that is, the level of risk accepted more or less consciously by everyone, which is $\tau = 10^{-8}/h$.

¹⁰ Quoted by A. Leroy and J. P. Signoret, *Le Risque technologique*, PUF, Paris, 1992.

¹¹ Quoted by J. A. Calgaro, *Fiabilité des matériaux et des structures*, Hermès, Paris, 1998.

8 Structural Reliability

Activity	Rate τ ($10^8/\text{h}$)	Exposure n_e (h/yr)	Rate τ_a ($10^4/\text{yr}$)	Ratio
Mountain climbing (international)	2,700	100	27	
Trawl fishing (deep sea, 1958–1972)	59	2,900	17	
Flying (crew)	120	1,000	12	$\ll 1$
Coal mining	21	1,600	3.3	
Automobile travel	56	400	2.2	20
Construction	7.7	2,200	1.7	450
Flying (passengers)	120	100	1.2	$\ll 1$
Home accidents	2.1	5,500	1.1	
Factory work	2	2,000	0.4	
Building fires	0.15	5,500	0.08	5
Structural failure	0.002	5,500	0.001	6

Source: H. O. Madsen *et al.*, *Methods of Structural Safety* (Prentice Hall, 1986).

Table 1.2 Risk rate by activity.

Menzies' study can be compared with Table 1.2, given by H. O. Madsen *et al.*, who also concluded that there is a very low risk due to structural failure, with the same value.¹² This table also introduces hours of exposure per year n_e , the annual rate τ_a and the ratio between the number of injured and the number of dead.

These figures represent different levels of risk well, but do not directly introduce a subjective appreciation of risks. For the population, risk is subjectively different if it is freely accepted or if it is imposed (nobody has to fly a plane or to climb a mountain) and if it allows – or not – a high chance of survival (is the plane any safer than the car?).

The level of risk acceptable to the population is not a totally objective value. It depends on social relations: the level of nuclear risk apparently tolerated in Germany, France and even in Russia is not the same. It also depends on constraints, because no-one can escape the risk associated with consuming food without the certainty of dying of hunger.

Structural reliability seems a trivial issue in this context, but that would be to forget that certain catastrophes are linked not only to an installation, but also to its environment. This is the case, for example, with industrial risks inducing pollution that it is not possible to contain, such as oil slicks and radioactive

¹² *Methods of Structural Safety*, H. O. Madsen, S. Krenk, N. C. Lind, Prentice Hall, New York, 1986 (source: CIRIA, 1977).

Average number of people placed in danger	Economic consequences		
	Not serious	Serious	Very serious
Small (<0.1)	10^{-3}	10^{-4}	10^{-5}
Average	10^{-4}	10^{-5}	10^{-6}
Large (> 10)	10^{-5}	10^{-6}	10^{-7}

Table 1.3 Order of magnitude of target probabilities in construction.

pollution. It would also be forgetting the localization of strong natural risks such as earthquakes and floods.

A probability of structural failure causing a risk of 10^{-7} deaths per year therefore appears a sufficiently strong value to prompt particular attention from designers. However, it is not the only criterion, and the level of reliability also depends on an economic optimization. A lower level is perfectly acceptable if the consequent risks remain well within strict geographical and temporal limits. Table 1.3, often quoted in documents on civil construction, suggests target values according to various situations in construction, yet without clearly specifying the reference period.¹³ The table shows the order of magnitude of target probabilities in construction. Hence, very small quantities in relation to one have to be estimated – something that poses specific problems in terms of data and calculations.

Figure 1.2 adopts the principle of the Farmer graph by demarcating zones for which the design is acceptable, and others for which the design is unacceptable.¹⁴ Obviously, designers seek to place themselves in the most favorable economic situation, that is, the closest possible to the danger zone. The figure shows that installations in the North Sea were designed for a much higher risk than those in the rest of the world; the representative point of the Piper Alpha platform, destined for tragedy, is indeed in the zone of unacceptable design.

Figure 1.3 summarizes probabilities of failure estimated by experts in different industrial areas involving all the greatest risks, but with very different lifetimes.¹⁵

Any decision-making supposes the acceptance of a more or less well-assessed risk. Reliability methods help by contributing to better identification of the component of the risk associated with the occurrence of a feared event.

¹³ Suggested by the Norwegian NKB regulations in 1978.

¹⁴ Suggested by J. P. Signoret, Total company, in his speech during the ‘Risks and Reliability of Industrial Systems’ course at the SPI Doctoral School of Clermont-Ferrand, 11 June 2001.

¹⁵ Source: EDF.

10 Structural Reliability

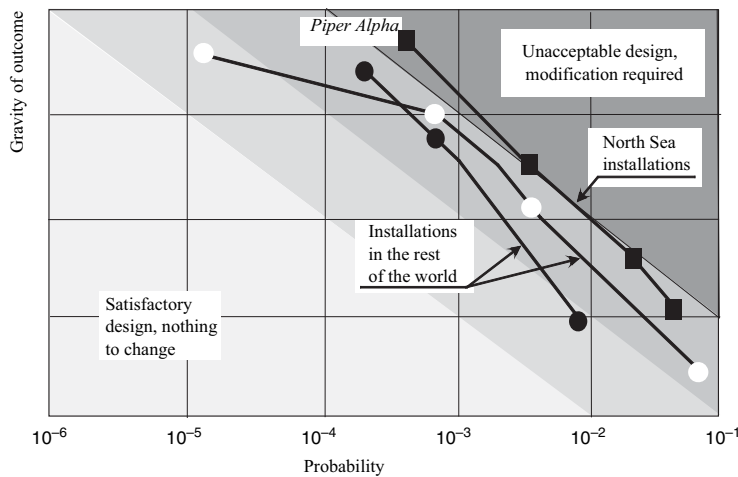


Figure 1.2 Diagram of gravity of outcome versus probability: positioning of various petroleum research installations (from J. P. Signoret).

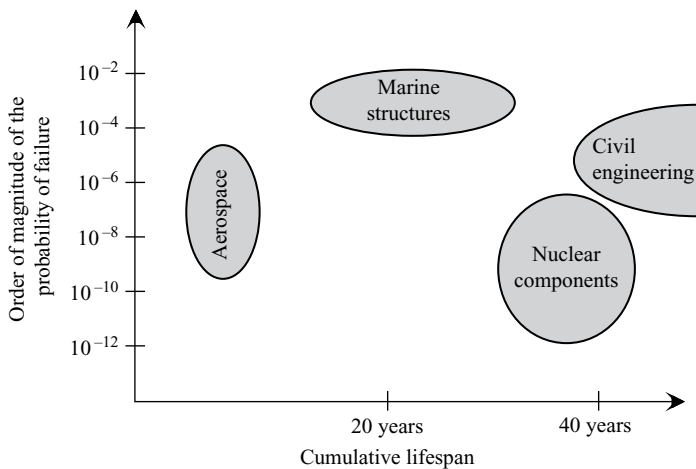


Figure 1.3 Level of probabilities estimated in different industrial branches.

1.5 Today

Enriched by a mechanical and probabilistic culture, progressively accepting the uncertain, the 20th century first of all gave rise to pioneers who attempted progressively to rationalize the concepts of reliability in structural mechanics.

In Germany, M. Mayer was certainly one of the first to suggest, in 1926, the use of average values and variances of variables in design.¹⁶ However, it was in 1947 that A. M. Freudenthal initiated, in an article, the present scientific debate:

place the concept of safety of structures in the realm of physical reality, where there is no absolute and where knowledge is not perfect.¹⁷

At practically the same time, A. R. Rjanitzyn introduced, in the context of metallic construction, a *characteristic of safety* γ .¹⁸ This is equal to the inverse of the coefficient of variation of a performance function, and it became the first definition of a reliability index. The Soviet school was distinguished by V. V. Bolotin in particular.¹⁹ In Europe, we should mention the research studies of J. Ferry-Borges and M. Castanheta at the Laboratório Nacional de Engenharia Civil in Lisbon, whose summary was outlined in 1971.²⁰

In France, we can note, for example, the anticipatory study of R. Lévi published in the *Annales des Ponts et Chaussées*²¹ in 1949 and in the *Revue Générale des Chemins de Fer*²² in 1951.

For over half a century now, ongoing scientific advancement has enabled researchers and engineers to construct design methods that take into account predictable limits and uncertainties. It is of course those fields where these advances were the greatest which have mobilized efforts – for civil engineering first of all, and geotechnics in particular, for natural loads and then for mechanical structures and constructions. Thus the application of probabilities and statistics to engineering problems is becoming more and more necessary for design and maintenance.

Any probabilistic approach involves the explicit acknowledgment of a risk that appears not to exist in a deterministic approach because it is not identified. Thus, it is naturally subject to rejection, and the application must overcome cultural and also educational inertia.

Risk analysis first of all results from expert and axiomatic knowledge. As illustrated in Figure 1.4, these two forms of knowledge grow exponentially with the development of humanity and, in every age, man depends on one or the

¹⁶ Die Sicherheit der Bauwerke, M. Mayer, Springer Verlag, Berlin, 1926.

¹⁷ ‘The Safety of Structures’, A. M. Freudenthal, *ASCE transactions* 112, 1947.

¹⁸ Stroevenmorizdat, 1949. French translation, *Calcul à la rupture et plasticité des constructions*, Eyrrolles, Paris, 1959.

¹⁹ *Statistical Methods in Structural Mechanics*, translated from Russian, Holden Day, San Francisco, 1969.

²⁰ *Structural Safety*, 1971.

²¹ ‘Calculs probabilistes de la sécurité des constructions’, R. Lévi, *Annales des Ponts et Chaussées* 26, July–August 1949.

²² ‘Conceptions modernes relatives à la sécurité des constructions’, M. Prot and R. Lévi, *Revue Générale des Chemins de Fer*, June 1951.

12 Structural Reliability

other. However, the modern age also constructs theories and tools of reliability. By contributing to probability theory they bring, according to A. M. Hasofer, ‘an additional precision’.²³

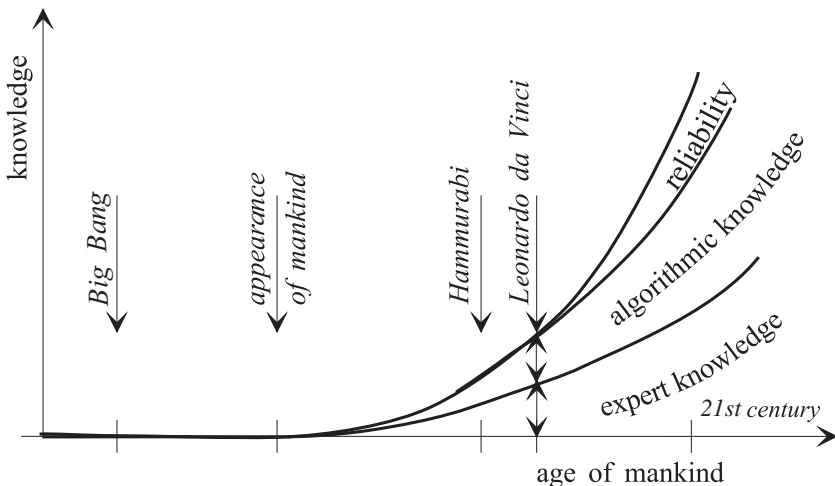


Figure 1.4 *The evolution of knowledge in history.*

If probabilistic approaches to the RAMS of systems, particularly electronic systems, and the management of breakdowns have been developing for several years now, it is only very recently that they have penetrated civil and mechanical engineering for risk analysis linked to dimensional choice. They also constitute a link between modeling in mechanics and the codes and rules of design, and represent an essential element in the transfer of knowledge between research and regulation.

The combination of mechanical modeling to simulate (in the physical sense) mechanical behavior and reliability modeling constitutes a **mechanical-reliability coupling** indispensable for an approach to design that includes risk analysis in an economic context.

1.6 A little glossary

All disciplines use a vocabulary whose current meaning should be clarified. Some words will be repeated frequently and hence deserve to be explained,

²³ Quotation taken from a lecture delivered at the University of Clermont in the framework of doctoral training ‘Matériaux, Structures, Fiabilité’, 29 January 1992.

either from classic definitions found in books on mechanics or probability theory or based on a more general meaning.²⁴

In mechanics

Action (load) – a force, or field of forces, translating the effect of the environment on a medium or a system that consequently undergoes transformations. Example: gravity.

Load effect (internal strength) – the result of an action on any medium, on a structure. Example: stress. The term is often wrongly used in the place of ‘action’. The effect of the loading induces internal stresses in a structure. Due to the essential role of stresses, a typical variable is noted by the letter S , but S includes all load effect variables such as displacements, strains, etc. More generally, S is a demand variable.

Resistance – the capacity of materials to resist actions, which is also called ‘strength of materials’. The chosen letter is R . More generally, R is a resource variable. A typical problem is the elementary case $R-S$ which compares the balance between the resource and the demand, the resistance and the stress.

Structure – an orderly assembly of materials conforming to a geometry. A structure has relations and, placed in a field of action, it undergoes load effects. Example: a beam. The entire set of actions constitutes the **loading** of a structure.

Structural component – a geometric and material element belonging to a structure. Example: a rod in a framework.

On reliability approaches

Hazard – from Arabic *az-zahr*, a game of dice; the word is variously linked, to good luck in its Arabic origin, to the uncertain in French and to danger in English.

Chance – attributed to any phenomenon of which the root cause is unknown. This ignorance leads to the impossibility of determined prediction. Is chance a confession of our ignorance or does it have an existence of its own? ‘Chance is a vehicle used by God when He wants to travel incognito’ is a quotation sometimes attributed to A. Einstein, but it seems to go back to the first centuries of our era.

Random – from the old French verb ‘randir’. A ‘randy’ foal is a young horse that is gamboling in any direction, without having a precise goal. Example: a random number is any number selected in a set, such as 1 or 2 or 3 or 4 or 5 or 6, when playing dice.

Stochastic – from Greek *στοχαστής*, soothsayer. The word characterizes phenomena related to chance. ‘Random’ and ‘stochastic’ are equivalents, and the use of one or the other is more from habit than a semantic

²⁴ See, for example, *Le Trésor, dictionnaire des sciences*, under the direction of Michel Serres and Nayla Farouki, Flammarion, Paris, 1997.

14 Structural Reliability

difference. Example: ‘random processes’ and ‘stochastic processes’ are often used interchangeably.

Test – a protocol aimed at obtaining a particular result among several possible results: the set of possible results from a test constitutes the universe Ω (or event space). A result is a selection $\omega_i \in \Omega$. Example: throwing a die (not loaded) with six sides and obtaining one of the following results {1, 2, 3, 4, 5, 6}.

Outcome – the result of a test, it is therefore a selection $\omega_i \in \Omega$. Example: rolling a 6 when throwing a die. The word ‘outcome’ interprets a physical and concrete concept.

Event – a part of Ω that can be defined by a logical proposition (statement) corresponding or not to an outcome. The event is realized if the logical proposition is true. The word ‘event’ expresses a mathematical and abstract concept. An event may not correspond to any physical outcome. Example: rolling 2 and 3 in a single throw of the die.

Protocol – all the formal conditions of an experiment.

Random experiment – a test in which the repetition of the same protocol leads to different results.

Probability – frequency definition: associated with the frequency of an event, that is, with the number of favorable situations out of the total number of situations. Axiomatic definition of probability P as a mathematical measure (A. N. Kolmogorov, 1933).

Uncertain – characterizes all the possible outcomes in a given situation. Example: the weather is uncertain; it could rain in the afternoon.

Unexpected – characterizes an event that has not been predicted. Example: the destruction of the Tacoma Narrows bridge was due to an unexpected phenomenon, the coupling of vibrations of bending and of torsion.²⁵

Imprecise – characterizes a result evaluated in a very summary manner; also applicable to reasoning. Example: the imprecision of a measurement.

Error – the result of a test is an error when the protocol has not been respected.

Imprecise leads to error – when there is an imprecision it induces a difference between the result potentially anticipated and the result obtained. The difference is therefore called an error. Example: measurement error.

Reliability component – a complete description of a protocol including a structural component and its mode of mechanical operation with respect to a test. Example: a rod in elastic traction tested in relation to its yield limits.

²⁵ The Tacoma Narrows bridge was situated in the State of Washington in the United States. It collapsed in 1940 under very moderate wind conditions.

Safety and security – The meaning of the words ‘safety’ and ‘security’ tends to vary, depending on the communities which use them. In the reliability context, this book is addressed to engineers for whom safety is related to the performance of a mechanical system, and security is related to the risk which dysfunction could occasion for people and for the environment.

Let us note that the word ‘simulation’ takes on a different meaning depending on whether it is used in a physical or a mathematical context. If it relates to representing a physical phenomenon by a mathematical model, it is the word ‘modeling’ that is accepted. The ‘resolution’ of a model is therefore the process that moves from modeling to numerical operation. In this context, the word ‘simulation’ is reserved for the repetition of the solution with random data.

1.7 The structure of this book

This book is located within the framework of mechanical-reliability coupling, that is, the coupling between mechanical and probability methods, with the objective of a reliable design of structures. It has been written in such a way as to introduce the concepts in as simple a manner as possible and it remains limited to an approach independent of time; we will, however, note that a number of phenomena repeated in time may be modeled using the statistics of extremes. It is dependent on probabilistic methods using reliability indexes. This book provides study material aimed at defining an essential tool for students and engineers confronted with the use of probabilistic methods in mechanics. The structure is as follows.

1. **Introduction:** this chapter.
2. **Preliminary Approach to Reliability in Mechanics:** first of all, this chapter is about situating the hypotheses within the framework of the book, and then opening up certain fields of application.
3. **Elementary $R - S$ Case:** this chapter introduces the basic concepts (failure scenario, random design variables) in the elementary case of two variables, resistance R and internal strength or stress S . It presents elementary methods of resolution – direct or by simulation – and introduces the notion of the reliability index.
4. **Isoprobabilistic Transformation:** the calculation of the index uses a transformation between physical and standardized random variables. This chapter studies three transformation principles (Rosenblatt, Nataf and Hermite).
5. **Reliability Index:** this concerns the problem of non-linear optimization for which the general methods (of gradient, by quadratic programming) are adapted to the particular form of research on the reliability index.

16 Structural Reliability

6. **Products of Reliability Analysis:** apart from the index and the probability of failure, reliability analysis also produces important factors associated with sensitivity.
7. **Probability of Failure:** this chapter deals with approximations of the calculation of probability of failure, P_f , from the reliability index.
8. **Simulation Methods:** they offer the possibility of researching the probability of failure, either directly or in combination with reliability index methods.
9. **Reliability of Systems:** in cases where failure may result from several components, this chapter studies their combination.
10. **'Safety' Coefficients:** from the knowledge of failure parameters, this chapter shows how to define partial coefficients, and introduces methods for reliable design.
11. **Mechanical-Reliability Coupling:** the finite elements method is the essential tool for modeling in mechanics. This chapter shows how to couple mechanical and reliability models.
12. **Stochastic Finite Elements:** the introduction of randomness into the variational models of the finite elements method or at the discretized level leads to new families of finite elements, called stochastic finite elements.
13. **A Few Applications:** demonstration of the potential of reliability methods.
14. **Conclusion:** certain remarks in conclusion, and to pursue the subject further.

Being study material, this book is complemented first of all by comprehension exercises, and also by the presentation of results obtained for certain engineering problems.

This is intended to be a methodological preliminary. For implementation, it should be embedded within various types of knowledge:

- knowledge of statistical methods and random modeling using random variables,
- knowledge of specific scientific fields (integrity of structures, fatigue, cracking and rupture, stability and instability of shells, and so on) which call for reliability approaches,
- knowledge of technical fields (civil engineering, mechanical construction, naval construction, aeronautics, inspection, maintenance, repair, and so on) which introduce random analysis in their design rules.

All these scientific and technical questions are the subject of numerous publications that the reader can refer to later.

Remarks: *it is quite obvious that the calculation of probabilities of failure is concerned with orders of magnitude, and that the engineer cannot assert a large number of significant digits in a result, taking into account what he knows about the data. We will depart from this rule because, on the methodological level, the comparison of methods and axioms should be carried out with the greatest possible precision.*

This page intentionally left blank

Chapter 2

Preliminary Approach to Reliability in Mechanics

Before discussing reliability in mechanics, we must specify the context in which the proposed approach is relevant. In fact, reliability covers both widely used methods, like the use of statistical techniques for production control, and new methods concerning failure modes and contributing to risk evaluation. These new methods rely on an approach which is still novel and whose underlying philosophy must be defined.

It is therefore the purpose of this chapter to describe the context and the objective with the aid of general concepts, in the hope of arousing in the reader an interest for a reliability approach to design.

2.1 General points

2.1.1 Reliability methods in mechanics

We are interested in methods that are developed primarily in relation to the modeling of materials and structures. They allow mechanics to take advantage of many advances made in scientific disciplines, like the theory of probability, and experiments in other technological fields. They are characterized by a close relationship with mechanical behavior models. In the words of Hasofer (author, with Lind, of the first invariant definition of the reliability index [HL74]), they '*offer an additional precision*' to the designer.

The designer plans structures and machines whose development and operating conditions, throughout the expected lifespan, are not perfectly known: design takes place in an imprecise and uncertain universe, which can be, at least in certain cases, modeled by a random hazard. This is not the only modeling approach possible, and some have suggested the use of fuzzy sets; this is not always possible: gross error, or even blunder, is not probabilizable!

By accepting a probability-based approach, reliability methods in mechanics help calculate reliability estimates: the *notional* or conditional probability, reliability index and sensitivity of the failure to a stochastic data description.

Three fields of application are particularly targeted:

- Exceptional or highly innovative structures for which the experience accumulated in the last few centuries is inadequate. It is no coincidence if the first to take advantage of reliability methods were engineers in charge of building offshore platforms.
- Structures and constructions which are quite ordinary, but whose design relies on codes or regulations whose current evolution offers the possibility of a calibration of *partial coefficients* using reliability methods.
- The monitoring of structures during their lifespan, which often brings to light a degraded state – following, for example, fatigue leading to a crack – for which the inspection-maintenance-repair strategy can be optimized through reliability.

2.1.2 A new attitude: overcoming obstacles

An article [ASC83] as early as 1983 highlighted the advantage of reliability methods which:

- offer a realistic processing of uncertainties and a method for evaluating safety factors that are too often arbitrary,
- offer decision-making support for a more economic and better-balanced design,
- analyze failure modes and measure the reliability provided by the application of regulations,
- allow an optimal distribution of materials among the various components of a structure,
- can benefit from the experience acquired in design by updating based on feedback from experience,
- support maintenance and repair decision-making with the twofold purpose of safety and economy,
- expand the knowledge of uncertainties in the response of structures.

These methods were presented so attractively that everyone must have wondered about the reason for their indifferent development at the time. The article also underlined the obstacles to their implementation, which are:

- *inertial*, because they demand a new attitude, a calling into question of our thinking and working patterns,
- *cultural*, because probabilities (mainly) and statistics (to a lesser extent) are more a part of the knowledge of the mathematician, who can doubt, rather than that of the engineer, who must have certainties,

- *philosophical*, because they explicitly underscore the acceptance of a risk which is only implicit, behind the reassuring notion of the ‘*safety*’ coefficient, because they demand judgment and decision,
- obstacles arising from a *lack of conviction* on account of the novelty of the developments and the infancy of tools that were still immature and without informed users.

Since 1983, significant progress has been made both in the construction of efficient methods and tools and in the calculating power available.

2.2 Theoretical reliability in mechanics

2.2.1 Reliability approach in mechanics

A reliability approach in mechanics is often used in the framework of quality controls. These help observe the dispersion of a particular quantity, reject outcomes outside tolerance limits and monitor their variability. Statistics is the primary tool used for this, and modeling based on random variables relies on experience feedback. The reliability approach to risk in design, applied to rare events, does not allow (quite fortunately) feedback on the part or product in question. It is therefore not a prediction validated by statistical control.

It is based firstly on a statistical knowledge of the elementary variables (or basic design variables) entering into mechanical modeling: knowledge of material properties, geometry, boundary conditions and actions.

The combination of elementary variables composes a deterministic complex mechanical model, and is used in certain areas: each localized model forms a *component*:

a component is composed of a geometric element (physical component) and its mechanical behavior.

The latter cannot, in general, be studied using the statistics of failure, that is, of non-satisfaction of expected performance; it does not present a binary operation (in service or out of service); it functions most often in downgraded modes.

Failure generally brings into play a simple combination of complex components rather than a complex combination of simple components. This last case is more frequently encountered when dealing with system reliability.

2.2.2 Variables-component-system chain

The variables-component-system chain is represented in Figure 2.1. As regards elementary variables, we must have a minimal *statistical* knowledge of all the parameters entering into the modeling. From this, we can deduce a *probabilistic*

knowledge of the component and, lastly, of the assembly of components. This gives rise to three fields of investigation, each with its specific tools:

- *Stochastic modeling* of elementary design variables of the mechanical model, undertaken most often by the analysis of statistical data: adjustment of probability density functions and estimation of their parameters (mean value, standard deviation), evaluation of coefficients of correlation between variables.
- Probabilistic study of the *failure of components*, based on simulation, integration or approximation methods.
- Probabilistic study of the *failure of systems* (system reliability), with the aid of either simulation methods or approximation methods (multinormal integration).

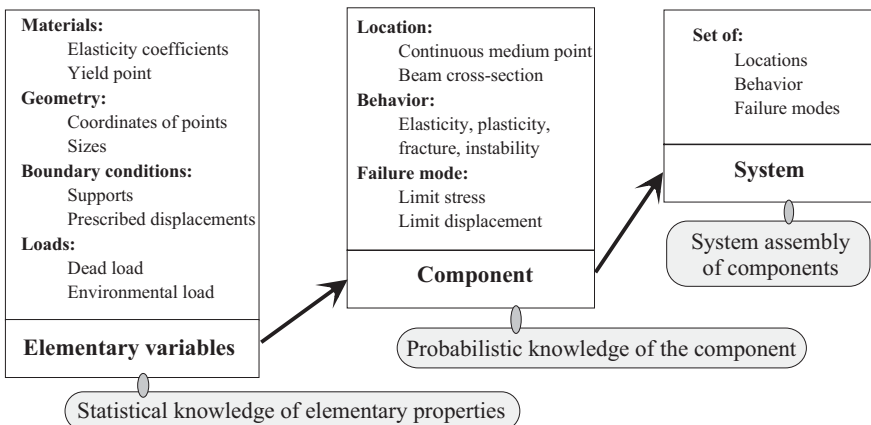


Figure 2.1 Elementary variables-component-system chain.

2.2.3 Theoretical reliability

The analysis of a potential failure supposes (Figure 2.2):

- *In design:* examining all the failure modes possible, i.e. all the relations between the elementary variables, components and systems. This preliminary analysis is a vital step, since the simple identification of a potential failure implies the implementation of measures for minimizing the risks, and this without any particular reliability calculation. There is no use in devoting considerable effort to a well-identified situation if a critical situation has been overlooked.

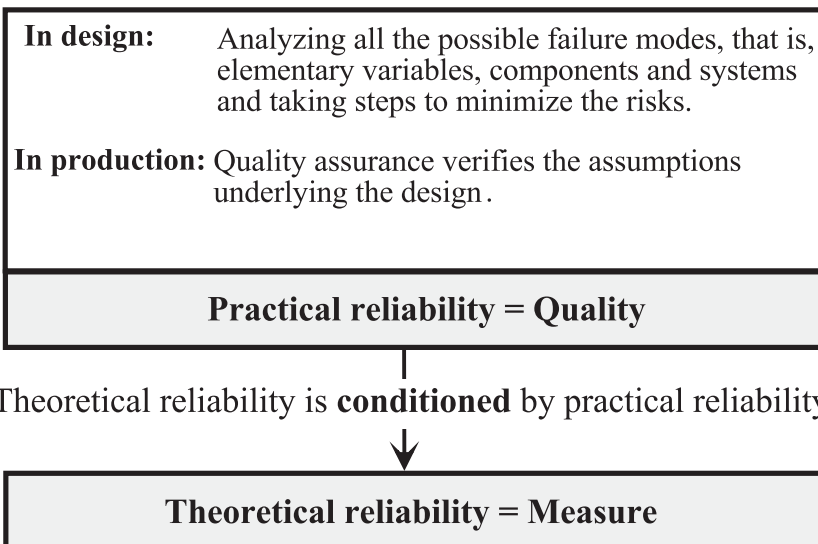


Figure 2.2 Practical reliability and theoretical reliability.

- *In production:* implementing a quality assurance system that verifies the adherence to assumptions made during design for the modeling of variables and that preempts gross errors.

Such an attitude is often called practical reliability, synonymous in fact with quality. Quality plays a vital role both in design and in production. Thus, designing welds in fatigue in accordance with Eurocode 3 supposes that they are performed according to well-established procedures.

Theoretical reliability can then be calculated: its aim is to arrive at a measure of reliability, a probability that can only be a conditional probability, based on an ideal representation of data and models.

Theoretical reliability is conditioned by practical reliability.

2.3 Stochastic modeling

2.3.1 Modeling based on available information

The modeling of elementary variables implies that we have information, however inadequate (Figure 2.3) it may be.

We must sometimes be content with a *summary estimation* made from a judgment based on limited experience:

The variable V is of the order v_s .

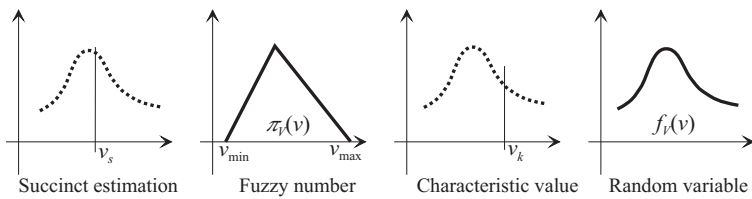


Figure 2.3 Representation of variables.

An expert's evaluation replaces an uncertain variable by a *fuzzy number*. In a given interval, a degree of possibility is associated with each value of the variable:

The variable V ranges between v_{\min} and v_{\max} .

The possibility $\pi_V(v)$ is associated with V .

An engineer typically uses *characteristic values* obtained generally by increasing or decreasing a value considered average, depending on the direction necessary to approach safety:

The variable V is represented by the characteristic value v_k .

Lastly, a statistician sees whether the variable can be represented by a known *distribution*:

The variable V is a random variable with the density $f_V(v)$.

To mark the random nature of a variable, it is denoted by $V(\omega)$, and an outcome is then $v = V(\omega = \omega_0)$, where $\omega \in \Omega$, is the event space.

The reliability approach must be compatible with the available information. It always makes a contribution, since a probabilistic calculation contains a deterministic calculation. It is sufficient to make the standard deviation tend toward zero to return to a mean-based determinist calculation, but why should we calculate based on means? This is not what is done normally.

The study, on a case-by-case basis, of the random nature of each variable must be completed by a study of the relations between the variables, translated into an initial approximation (to the second order) by *correlation*.

2.3.2 Construction of a stochastic model

Constructing a stochastic model of variables means establishing a representation of their variability by the best-suited probability density. Two approaches are possible.

Naturalist's approach

The naturalist's approach relies on the observation of a sample from which estimates of the mean, the variance and other statistical moments are assessed. Statistical methods offer an ad hoc estimation or an estimation by interval. We must keep in mind that these estimates are themselves random variables. Then, the best adjustment of a probability density must be found and the objective of statistical tests such as the χ^2 test or the Kolmogorov-Smirnov test is to give a solution for 'goodness-of-fit' of the assumption (for a practical example, see [Col95]). It is also possible to search for the best density in parametrized families whose performances have been studied in [Pen00].

Physicist's approach

The physicist's approach seeks to understand the variability of material behavior on a macroscopic scale based on the state of this material on a lower meso- or microscopic scale. The very nature of the origin of variability physics results in proposing a compatible form of density. Thus, Weibull [Wei51] introduced his famous probability density function in order to explain the mechanism of failure of a material containing internal defects of random dimensions.

Problems in stochastic modeling

This question is not dealt with here, since it requires in-depth development beyond the scope of this book. The designer who intends to perform a reliability calculation must be conscious that the results he will produce depend on the quality of the data and that these data are always insufficient. Three problems are underlined below.

Size of test samples: a common practice consists of validating a design using a test and then constructing by adding a margin and by ensuring that the test conditions are reproduced. It is paradoxical to think that the greater the number of tests, the greater the chance of stumbling upon an unsatisfactory test and the more the design will suffer! A probabilistic approach resolves this paradox by showing how better accuracy of the information benefits the designer [PHLM00].

Infinite domain – Gauss distribution: if Gauss distribution is the most famous of the probability representations of variability, it is certainly thanks more to its wonderful mathematical properties (additivity, central limit theorem) than to the virtues of physics, because how can we accept an infinite domain? It is nevertheless true that if some truncations are made, it is certainly very well

adapted, since it represents central tendencies satisfactorily, as underscored by J. Gleick [Gle89], see Figure 2.4. From this point of view, a bounded density is preferable, but the bounds become random variables.

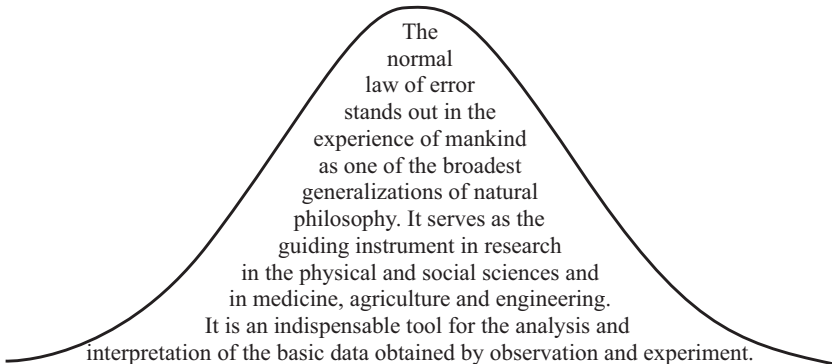


Figure 2.4 Gauss density, as viewed by J. Gleick.

Distribution tails: reliability calculation for rare events concerns distribution tails for which information is evidently rare. The approach using extreme value statistics provides a preliminary response and a physical examination. Moreover, it is possible to compare different assumptions to search for an envelope.

Conclusion

This book does not deal with the stochastic modeling of data, the importance of which has been highlighted in this section. The reliability engineer must work with the statistician.

2.3.3 Random variable or stochastic process

$V(\omega)$ is a function $\omega \in \Omega$ defined on the random set Ω : it is a random variable. Fixing ω is tantamount to extracting an outcome from this variable $v = V(\omega = \omega_0)$.

Let us now consider a function $V(x, t, \omega)$ on the space, the time and the random set. An outcome $v(x, t, \omega_0)$ is a trajectory of this function for a fixed element of the random set.

The term *stochastic process* (or random process) denotes such a function. It can be indexed only by time (example: the acceleration of an earthquake at a point) or in space (example: the spatial distribution of an elasticity modulus). In this latter case, we can also speak of a random field.

Without entering into the theory of the processes, we can note that it is possible to perform a discretization. A vector $\{V\}$ whose components are correlated (matrix $[\rho]$) is then substituted for the process:

$$V(x, t, \omega) \longrightarrow \{V(t, \omega)\} = \left\{ \begin{array}{l} v_1(x = x_1, t, \omega) \\ v_2(x = x_2, t, \omega) \\ \vdots \\ v_n(x = x_n, t, \omega) \end{array} \right\}$$

$$[\rho] = \begin{bmatrix} 1 & \rho_{12} & \cdots & \rho_{1n} \\ \rho_{21} & 1 & \cdots & \rho_{2n} \\ \vdots & \vdots & \ddots & \vdots \\ \rho_{n1} & \rho_{n2} & \cdots & 1 \end{bmatrix}$$

Such a discretization quickly results in large vectors that current methods and software have difficulty in handling. This is discussed in detail, for spatial processes, in Chapter 12 in the framework of stochastic finite elements.

Depending on time, most actions rely on modeling by stochastic processes indexed by time. However, in many cases, it is possible to use an extreme value distribution to express the maximum (and respectively the minimum) of an action for a given period. If we consider a random variable V , modeling for instance, the maximum wind speed in a year:

$$F_V(v) = \text{Prob}(V \leq v)$$

is the probability that the annual maximal speed does not exceed v . In the N successive years, owing to the slow evolution of the climate, it is possible to consider that annual probabilities are independent, with the same distribution functions. If Y_N is the random variable modeling the maximum speed for N years, then:

$$\text{Prob}(V_1 \leq v) \text{ Prob}(V_2 \leq v) \cdots \text{Prob}(V_N \leq v) = (F_V(v))^N = F_{Y_N}(v)$$

The asymptotic behavior of $F_{Y_N}(v)$ when $N \rightarrow \infty$ has been studied for various related functions. It leads to three types of extreme value distributions: Gumbel, Fréchet and Weibull distributions [Gum58, MKL86]. It is thus possible to represent a repeated function of time by a random variable. The modeling of data by random variables or processes is an essential step in a reliability analysis.

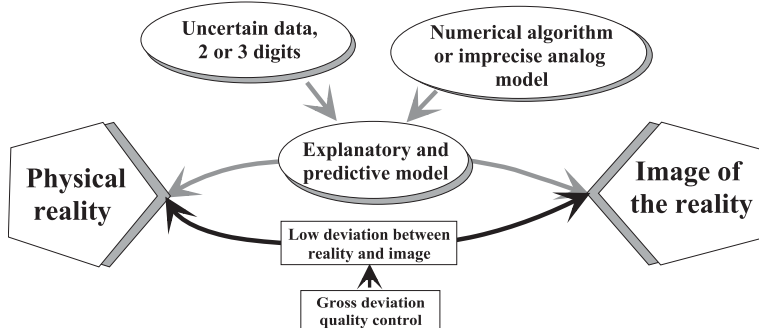


Figure 2.5 Approximated representation of physical reality.

2.4 Mechanical modeling

2.4.1 Representation model of physics

The purpose of modeling is to construct explanatory and predictive models of physical phenomena, theoretical models and numerical solutions (Figure 2.5). There will always be a difference between a behavior model of a structure and the physical reality. No material, no structure is required to obey the laws promulgated by human beings. Modeling deviation is normal and acceptable, and procedures for the validation of models are used to control it. It is not totally random and contains a systematic bias. On the other hand, gross errors must be prevented by a process of quality assurance guaranteeing an application and a use that conform to the requirements laid down. Two questions must be posed:

- Does the model represent the physics of the phenomenon well?

Mathematical modeling must explain and represent the physics; numerical modeling must control the accuracy of the results. The deviation between the physics and its image must be low, with quality control avoiding a gross deviation. It is therefore necessary to have a validated mechanical modeling approach, validation of the model and the numerical solution (density of the finite element mesh, convergence tests, etc.), and, even better, have a measure of the bias of the model and of a deviation random variable.

- Do the uncertainties in data influence the variables of the model?

The data introduced into a calculation model are known with only a few significant digits (not more than 2 or 3 very often). They are uncertain, and the designer must forgo the certainty of his habits and reflect on the significance of the values that he chooses when he initiates a calculation code.

2.4.2 Balance between resources and needs

Mechanical models are used to evaluate the *needs*, which are the expected internal strengths or stresses, and the required *resources*, which are the availability of materials and their resistance (Figure 2.6). Theoretical reliability analysis is based on a *failure scenario* combining the evaluation of internal strengths and that of their resistances, which are a function of elementary variables. The scenario reflects the balance between the resource and the need and is expressed by a *performance function*.

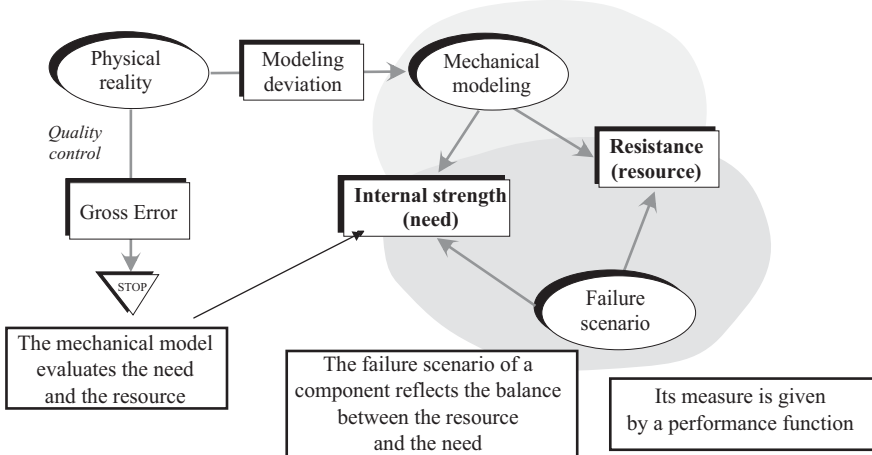


Figure 2.6 Failure scenario in mechanics.

Two complementary objectives must be achieved: estimating the parameters (mean, standard deviation, etc.) and adjusting if possible a distribution of internal strength or resistance variables; and estimating the probabilities of occurrence of failure scenarios, these theoretical probabilities being conditioned by a practical reliability of an acceptable level, avoiding any gross error.

It is the purpose of reliability sensitivity analysis, and reliability analysis, respectively, to meet these two objectives by applying a coupling between mechanical and stochastic models.

2.5 Mechanical-reliability coupling

A model that associates a mechanical calculation procedure and a reliability-based calculation procedure is a mechanical-reliability model.

2.5.1 Reliability sensitivity analysis

The mechanical model ensures the transition between input data (basic elementary variables) and output variables (Figure 2.7). The problem is then to calculate the statistical parameters of the output variables with respect to the statistical parameters of the input data. Such an analysis is called a reliability sensitivity analysis, characterizing the sensitivity of the response to the variability of the input. Firstly, a deterministic sensitivity analysis consists of a calculation of the gradient around a point, whereas a reliability sensitivity analysis searches for the relation between the respective variation coefficients of an output variable and an input variable.

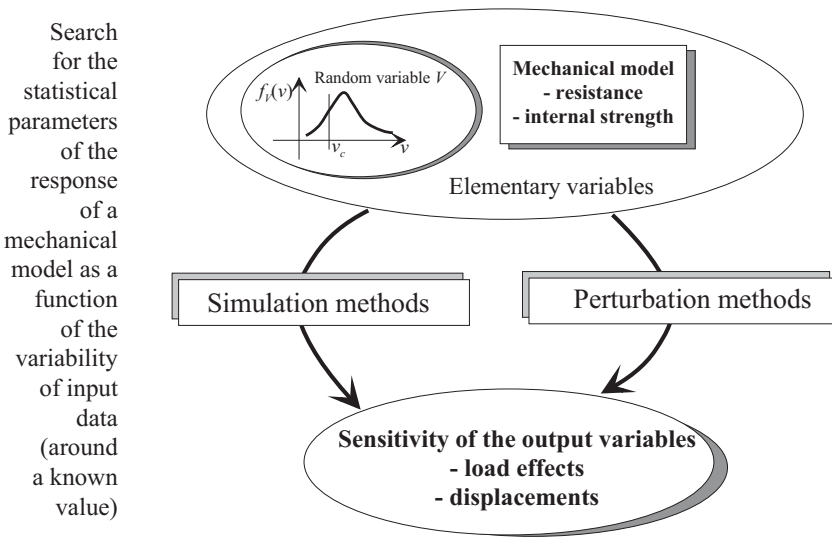


Figure 2.7 Reliability sensitivity analysis.

Two main methods are used: the *Monte Carlo method* (Chapter 8), which proceeds by simulation, and the *perturbation method* (Chapter 12), which requires calculation of the derivatives of the performance function with respect to the random data. The Monte Carlo method constructs a sample from which we can deduce the statistical moments without *a priori* any limitation of order. The perturbation method is generally limited to the first two moments. The solution is relatively simple when the (external) random element only affects the actions and when the model is linear; it becomes more delicate in the case of internal random variables for the state parameters of the mechanical system and non-linear behavior.

A sensitivity analysis is in general performed around the mean operating point and not around a particularly interesting point, *the most probable failure point*, which is introduced in Chapter 3. It determines whether the variability of a datum is damped or, on the contrary, amplified by the mechanical model, with the risks of instability that this gives entails.

In a dynamic context, *stochastic dynamic* methods are now well adapted to the study of the response process of a determined system excited by an input process, at least if it is Gaussian and stationary.

In simulation, the sensitivity analysis relies on the capacity to construct synthetic statistical data samples (quality of the random number generator, stochastic process generator) and on the capacity to identify samples of output variables or processes.

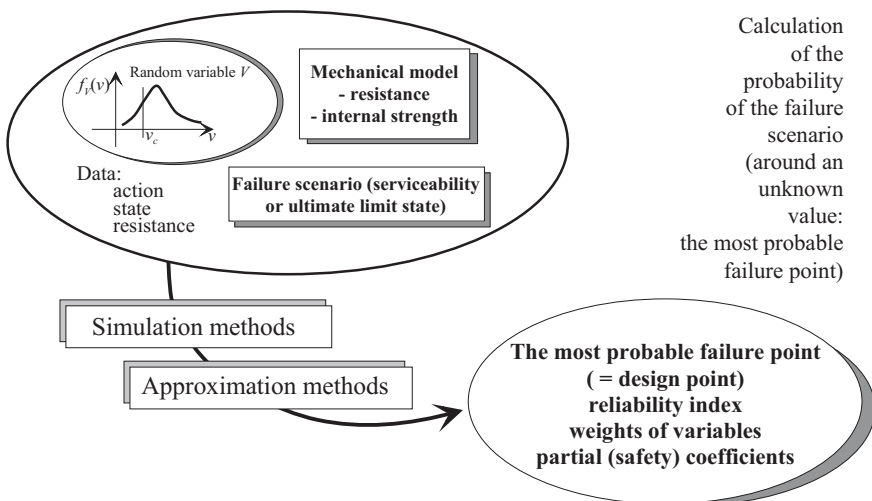


Figure 2.8 Reliability analysis.

2.5.2 Reliability analysis

Reliability analysis requires, in addition, a failure scenario (Figure 2.8). It separates the situations that the designer decides to consider acceptable from those that he decides to consider unacceptable. In the words of our colleague Vidal-Cohen [MML94]: *reliability consists of the probabilities plus the decision*. The decision can be totally determined and separates two domains in a binary manner; it can be *fuzzy* by associating an increasing degree of satisfaction progressively from failure situations with safe operating situations.

The scenario is represented by one (or more) performance function(s) delimiting the two domains, namely, the safety domain, when the performance function takes positive values, and the failure domain, when it takes negative or zero values. Failure states correspond to situations considered unacceptable, regardless of whether they are really unacceptable, in the case of damage, or whether they are less significant malfunctions, nevertheless conventionally defined as also being unacceptable situations. The concepts of the ultimate limit-state and serviceability limit-state illustrate these two types of situation.

The limit-state function is therefore the zero performance function; it is expressed as a function of basic variables. These include data relative to actions, state parameters, but also resistances.

It is often possible to construct two independent calculation models, one resulting in the evaluation of internal strengths, and the other in the evaluation of resistances. In this case, the difference between internal strength and resistance is a margin, which is a random variable. In a static context, the objective of the reliability analysis is then to evaluate the probability that the margin has a positive value.

This concept complements that of the '*safety*' coefficient, to which we must be careful to give a meaning by indicating whether it is a mean coefficient, a characteristic coefficient or a partial coefficient (Chapter 10).

Based on the data (action, state, resistance) and a reliability model, the objective is to calculate a reliability index and to approximate a probability. In addition to this, the products of reliability analysis include the most probable failure point (or design point), the sensitivity factors to failure and an evaluation of partial (safety) coefficients.

We can say that the calculation procedure of the reliability model *excites* the internal strength and resistance models by a judicious choice of data to produce the required results. The Monte Carlo simulation methods or reliability index approximation methods are some excitation strategies.

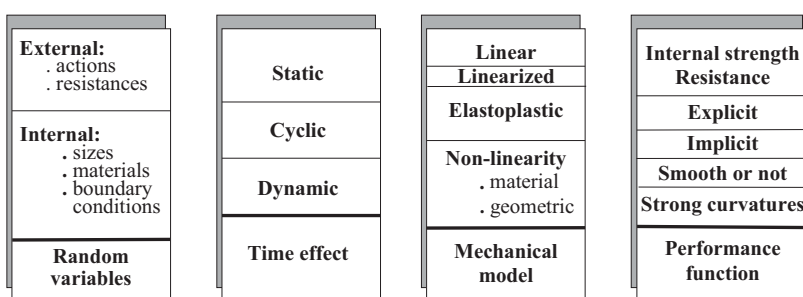


Figure 2.9 Complexity of mechanical-reliability coupling.

2.5.3 Complexity of mechanical-reliability coupling

Four criteria, depending on the modalities they take, help define the complexity of the coupling of a mechanical model and a reliability model (Figure 2.9); they relate to:

- **the nature of the random variables:**
 - external (actions and resistances),
 - internal (states),
 - independence or not of the variables.
- **the effect of time:**
 - static context,
 - cyclical or dynamic,
 - aging (mechanical, physical and chemical degradation).
- **the mechanical model:**
 - linear elastic calculation,
 - elastoplastic calculation by linear or linearized sequences,
 - elastoplastic calculation by limit-state theorems,
 - elastoplastic calculation by explicit or implicit linear formulation,
 - geometric and material non-linear calculation,
 - linear dynamic calculation,
 - non-linear dynamic calculation.
- **the form of the performance function:**
 - with separation of internal strength and resistance variables,
 - explicit and linear form of random variables,
 - smooth or not,
 - with strong curvatures,
 - with singular points,
 - explicit, implicit.

Simple problems including external variables and a linear, static, explicit resistance-internal strength function are easy to solve, whereas those resulting in implicit functions in non-linear models will require substantial calculation resources. It is the extent of the risk that will decide the accuracy of the modeling and the resources to be employed.

2.5.4 Actors in mechanical-reliability coupling

Figure 2.10 recalls the partners in a mechanical-reliability approach. There is no orchestra conductor *a priori* – this depends on the nature of the problem posed – but exchanges and a very high interaction are necessary between the

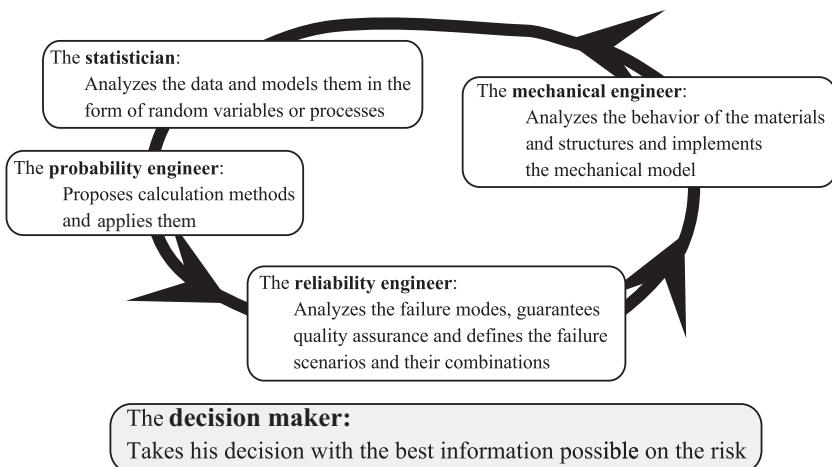


Figure 2.10 *Actors in mechanical-reliability coupling.*

various specialties that collectively provide the decision maker with additional information:

- The *statistician* analyzes the data, conditions them and models them as a function of a predictable use. He identifies the random variables and the processes. He must have a dialog with the mechanical engineer or the material specialist who can provide him information on the physical origin of the variabilities.
- The *probability engineer* proposes the methods and the tools for the calculation of probabilities. He uses them.
- The *reliability engineer* analyzes the failure modes, guarantees quality assurance and defines the failure scenarios and their combinations.
- The *mechanical engineer* analyzes the behavior of the materials and the structures, and guarantees the proper use of the mechanical models used.

2.6 Fields of application

Our purpose here is not to describe in detail the applications coupling a mechanical calculation and a reliability-based calculation, but to give a few indications of some industrial problems discussed in the mechanical-reliability context.

The proceedings of the three French JN'FIAB conferences (Cachan [MML94], Marne-la-Vallée [MBB98] and Bordeaux [BMB01]) illustrate the wide range of scientific research in France. It will also be interesting to

consult the proceedings of the two main conferences in this field, including the latest events: *International Conference on Applications of Statistics and Probability* (ICASP'7 – Paris [LFM95], ICASP'8 – Sydney [MS99], San Francisco (2003), Tokyo (2007)) and *International Conference for Structural Safety and Reliability* (ICOSSAR'7, Kyoto [SS97], Los Angeles [SS01], Rome (2005)). A book has been devoted to industrial applications [ESR98], and Chapter 13 also presents some of them.

2.6.1 Reliability of offshore marine structures

As early as 1983, the *Committee on Reliability of Offshore Structures of the Committee on Structural Safety and Reliability of the Structural Division* (ASCE) published an important article justifying and analyzing the potential of reliability-based methods [ASC83]. In view of the environmental uncertainties and the difficulties in predicting the behavior of offshore marine structures, oil engineering has made considerable efforts to evaluate the risk of the failure of platforms. Reliability indexes are arguments taken into account for the re-evaluation of the reliability of damaged or modified structures, as well as for the planning of maintenance operations. The mechanical models include the phenomena of plastification, cracking, instability and fatigue.

2.6.2 Soil mechanics

Structures relying on soil mechanics are a favored field of application of reliability methods owing to the great uncertainties in the knowledge of materials in place and their spatial variability. Following Matheron [Mat65], researchers have developed methods for analyzing and identifying random fields (exploration of soils, correlation, geostatistic methods) and methods for processing continuous or discretized random fields.

2.6.3 Regulation

Regulation is the collection of rules for ensuring the reliability of constructions. These rules result from heuristic knowledge (derived from experience) and from algorithmic knowledge (derived from models); they allow a design at an acceptable cost with sufficient reliability, though still seldom quantified.

By coupling an accurate mechanical model and a reliability model, it is possible to calibrate the existing codes and formulate proposals for the evolution of partial ‘*safety*’ coefficients. This does not mean asking the designer to perform a probabilistic calculation, but enabling him to develop a deterministic design based on underlying probabilistic principles. The *International Organization for Standardization* published as early as 1986 a

document dealing with the bases of the reliability of constructions [ISO86]¹ and the first Eurocodes document [AFN96]² recalls the theory of reliability as a tool for the elaboration of future European codes.

2.6.4 Stochastic dynamics

When random actions are time-dependent and induce dynamic responses, we are in the domain of stochastic dynamics [KS83, Soi94]. The first problem is to determine the parameters of the process and to identify the acceptable assumptions: Gaussian process or not, stationarity, ergodicity. We must then determine the properties of the response processes representing an output variable of a structure. The simplest model is made up of the oscillator with one degree of freedom excited by a random input.

These two problems have produced a number of results, at least under the assumption of a linear response.

Stochastic dynamics finds a field of application every time a natural action varies rapidly in time: earthquakes, winds, waves.

2.6.5 Integrity of structures

This term encompasses the various phenomena that combine to bring about a loss of structural integrity and thus a failure, in general by rupture: damage, fatigue and fracture. The initiation of a crack and the propagation of the crack depend on random defects and uncertain parameters. Furthermore, the evaluation of the decrease in the safety margin owing to a crack state is an important element in the decision to engage, or not, maintenance operations.

Among the fields concerned, we can cite damage by fatigue of civil engineering works, and the safety of pressure vessels and aircraft [Ver94]. For all structures subjected to a time-dependent degradation, optimization of maintenance by reliability is a challenge for the future.

2.6.6 Stability

The geometric stability of thin shells or slender structures is highly dependent on defects likely to initiate significant displacements. Limit loads, unlike critical loads, can be considerably reduced, depending on the faults taken into account. Any outcome presents imperfections in geometry or in the material. The scope of application includes constructions using sheets or hardened composite slabs (metallic bridges, naval constructions and aeronautics).

¹ The ISO standard 2394 has been revised since.

² Currently EC1, probably EC0 shortly.

2.7 Conclusion

The objective of this chapter was above all to present the main concepts in reliability and to arouse interest and curiosity. First, it sought to recall and convince us that:

- risk is always present in human activity,
- there are failure modes that we must identify carefully,
- quality assurance is the first condition of reliability,
- it is not always possible to take refuge behind rules for innovating,
- '*too strong has never failed*' can prove to be expensive and even inefficient,
- an innovative design must be a reliable design.

Then, it showed that mechanical-reliability methods based on certain statistical knowledge and the calculation of probabilities could provide additional precision, which proves, even now, useful in several disciplines and technical fields. After taking this first step, we can now present to the reader the bases of reliability methods in mechanical design.

This page intentionally left blank

Chapter 3

Elementary $R - S$ Case

Before presenting more general methods, this chapter introduces and illustrates the basic principles of reliability applied to problems in the mechanics of materials or structures: failure scenario, safety and failure domains, limit-state, probability of failure and index. For the sake of clarity, several simplifying assumptions are introduced progressively, and the number of variables is finally limited to two:

- a *resistance* random variable, R , an outcome of which is r ,
- an *internal strength* or *stress* random variable, S , an outcome of which is s .

3.1 Presentation of the problem

Based on a general presentation, we will show which assumptions can be used to arrive at a simple resistance-stress problem.

3.1.1 Variables

Mechanical materials or structures are considered as systems comprising an input, a state and an output. The organizational scheme of the variables is given in Figure 3.1.

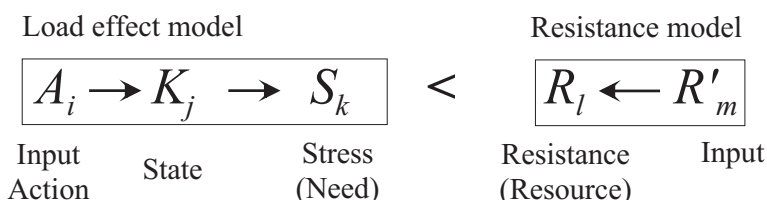


Figure 3.1 Link diagram of variables for a load model and a resistance model.

Let us note:

- $A_i(t)$, $i = 1, \dots, p$ – *input data* of the mechanical system, as a function of time t , relative to the loading, to the applied loads to the system and to the prescribed displacements,
- $R'_m(t)$, $m = 1, \dots, s'$ – *input variables* of the available resource; in a mechanical context, these are the parameters of material resistance, the geometric characteristics of cross-sections and the admissible displacements,
- $K_j(t)$, $j = 1, \dots, q$ – *state data* of the mechanical system (except those that can be included in the output variables), separated into two categories: $K_{j_f}^f$ (j_f data imposed by the specifications) and $K_{j_p}^p$ (j_p data at the disposal of the designer); this separation is useful in a design or optimization context. They contain the geometric characteristics, the characteristics of the materials and the boundary conditions.

A first calculation model is used to simulate (in the physical and not statistical sense) an outcome of the needs (stresses) which constitute $k = 1, \dots, r$ output variables of the model, denoted by $S_k(t)$. If $F(\dots)$ is a mathematical operator representative of the mechanical model, then there is an equation of the type:

$$F(t, A_i, K_{j_f}^f, K_{j_p}^p, S_k) = 0 \quad (3.1)$$

This model can be very complex, for example, when it results from advanced modeling with a finite element resolution. Likewise, a second mechanical model is used to construct the outcomes of the resources that constitute $l = 1, \dots, s$ variables $R_l(t)$. Generally, this model is simple, and the equation between R' and R is often identity, and it is not explained here. We must however note that the separation between the variables S and R , as it appears in Figure 3.1, is not always possible, as certain variables can be found both in the load model and the resistance model. This is the case in fatigue when the successive loads degrade the resistance.

3.1.2 Design model

The success of a design is seen in the verification of an inequality function of time t , of type:

$$G(S_k(t), R_l(t)) > 0 \quad \forall t \in [0, T] \quad (3.2)$$

and in a simple case of separation of variables, for each significant couple k, l :

$$S_k(t) < R_l(t) \quad \forall t \in [0, T]$$

where $[0, T]$ is the required lifespan or reference period for which the design is studied. The designer then tries to determine the best design, that is, the one that optimizes a target criterion (often, the generalized cost) for a given level of reliability. He proposes and justifies the values to be given to the variables $K_{j_p}^p$.

$G(\dots)$ is the performance function associated with an operating rule; it expresses the *failure scenario* introduced in section 2.4.2. The equation $G(\dots) = 0$ constitutes the *limit-state*.

The variables A_i , R'_m and K_j are the basic variables, whereas S_k and R_l are the output variables.

In the calculation of structures, the identification of the variables is simple. We have, for example, in the context of the finite element method:

- the input is the vector of external forces $\{F\}$,
- the state is characterized by the stiffness matrix $\{K\}$,
- the output is given by the displacement vector $\{q\}$ and the solution of the equation $\{F\} = \{K\}\{q\}$ in a linear assumption. The other elements of S_k , forces, stresses, strains, etc., are calculated from $\{q\}$.

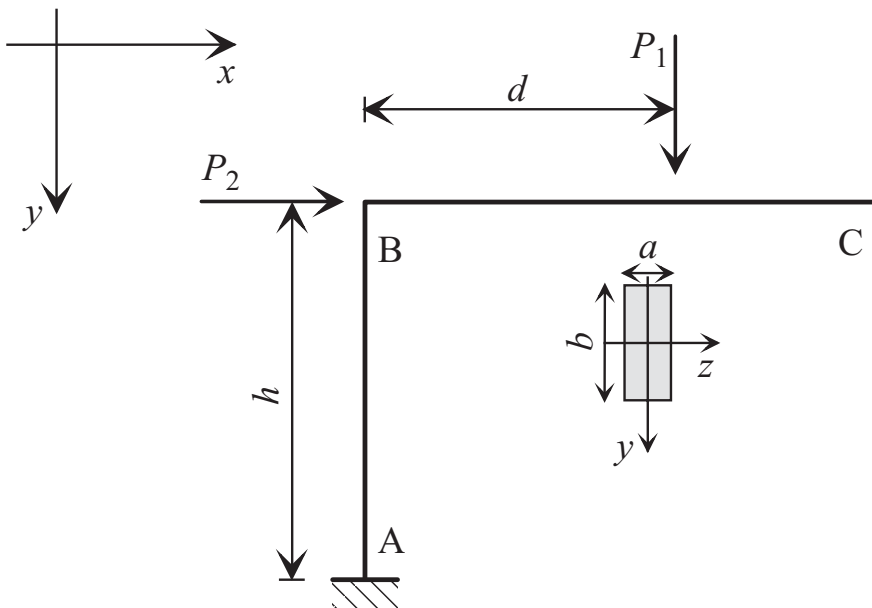


Figure 3.2 Definition of the variables for a frame.

3.1.3 Illustration

Figure 3.2 represents a frame clamped in A for which the following variables are identified:

- $A_i = \langle P_1, P_2 \rangle$, applied loads,
- $K_j = \langle h, d \rangle$, geometric state variables, to be completed by the elasticity modulus, the cross-section areas and the inertias, if the calculation of displacements is required,
- $S_k = \langle P_1d, P_1d + P_2h \rangle$ the maximum values of the bending moment, respectively in beams BC and AB,
- $R_l = \langle M_{BC}, M_{AB} \rangle$, the absolute values of the resisting moment, respectively in beams BC and AB,
- $R'_m = \langle f_y, a, b \rangle$ under the assumption of a resisting moment equal to the elastic moment in a rectangular cross-section of sides a and b : the resisting moment is then $M_{\text{resisting}} = ab^2 f_y / 6$.

3.2 Definitions and assumptions

- *Basic random space*: the basic random variables are the input variables A_i and R'_m as well as the state variables contained in K_j ; these are directly accessible physical values such as the geometric dimensions of a construction and the mechanical and physical-chemical characteristics of the constituent materials and the applied loads. They form the basic random space.
- *Output random space*: the output random variables are the values S_k as a function of the basic random variables, which express the state of the structure. They are calculated using the mathematical and numerical model of Equation (3.1). They are also the resource variables R_l derived from R'_m . They are related to a reliability condition representing the failure scenario (3.2). They form the output random space.

The simplest formulation consists of considering the resistance R and the stress S as time-independent output variables. It is then possible to describe the state of the structure using a single global random variable, the margin $Z = R - S$, which forms the *elementary case* of resistance-stress.

- *Safety domain and failure domain*: let $X_n = (A_{i=1,\dots,p}, K_{j=1,\dots,q}, R'_{m=1,\dots,s})$; $n = 1, \dots, p+q+s'$ or $X_n = (S_{k=1,\dots,r}, R_{l=1,\dots,s})$; $n = 1, \dots, r+s$, the random vector composed of the random variables in question. Equations (3.1) and (3.2) define a function $G_\kappa(\dots)$ for each possible operating scenario κ .

The functions $G_\kappa(X_n); \kappa = 1, \dots, \mu$ describe the state of the structure.

- $G_\kappa(X_n) > 0$ defines the safety domain D_s , the domain inside the limit-state, the domain of success events.
- $G_\kappa(X_n) \leq 0$ defines the failure domain D_f , the domain outside the limit-state, the domain of failure events.
- $G_\kappa(X_n) = 0$ conventionally defines the limit-state surface, the boundary (if D_f exists) between the two domains D_s (inside) and D_f (outside): this is the limit-state function. The choice of including the limit-state $G_\kappa(X_n) = 0$ in the failure domain is arbitrary. If the variables are continuous, the measure of the probability of failure in the limit-state is zero; if the variables are discrete, this choice is unfavorable from the safety perspective.

Let us take the example of the frame (Figure 3.2). Two limit-states are identified:

$$\text{Failure of beam BC: } G_1 = \frac{ab^2 f_y}{6} - |P_1 d| = 0$$

$$\text{Failure of beam AB: } G_2 = \frac{ab^2 f_y}{6} - |P_1 d + P_2 h| = 0$$

The failure domain D_f corresponds to the outcome of either condition $G_1 \leq 0$ or $G_2 \leq 0$. It is the union of the two failure domains, represented by the hatched part of Figure 3.3. The representation of the concentric elliptical curves will be justified later. Note that this figure must be completed by symmetry in order to take into account absolute values present in the expressions of the limit-states.

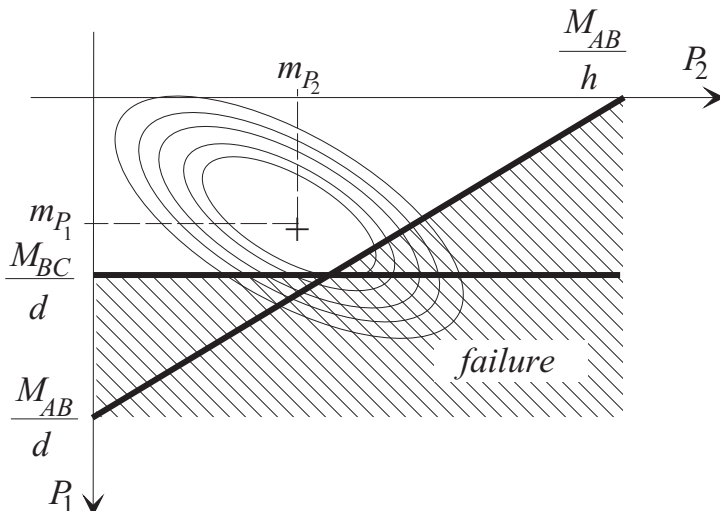


Figure 3.3 Representation of the failure domain of the frame.

The safety domain corresponds to the acceptable outcomes of the mechanical system. These are realizable physically. The failure domain corresponds to unacceptable outcomes. It is possible that they do not correspond to realistic situations. For example, in the case of rupture under tension of an isolated bar, there are no physical outcomes of failure at points other than those belonging to the limit-state. In fact, if T is the tensile force and R is the resistance, it is possible to perform a test (or a calculation) for $T \leq R$, but it is not possible to do so if $T > R$.

The concept of the scenario underlines a decision which must be made to separate the acceptable from the unacceptable. It depends on the modeling level necessary and the risks involved. The acceptable can include only elastic outcomes, for example, or accept elastoplastic behavior. Behavioral continuity in the safety domain and in the limit-state at least reflects the fact that the operation is considered as being in a downgraded mode.

Lastly, this presentation is based on a binary criterion of acceptance or rejection, but it is also possible to propose a fuzzy criterion in a given zone, with a degree of satisfaction from 0 to 1.

In this chapter, we will only consider the particular case of two random variables, resistance R and stress S : this is the *elementary resistance-stress*. We thus have:

Output variables: S and R

Vectors of random variables: $\langle X \rangle = \langle R, S \rangle$

Limit-state function: $G(\{X\}) = R - S = 0$

Safety domain: $G(\{X\}) = R - S > 0$

Failure domain: $G(\{X\}) = R - S \leq 0$

However, a study of this simple case requires a few reminders of the theory of probabilities, which are given in the next section.

3.3 Random vector: a reminder

In this section we remind the reader (see, e.g. [Rad91]) of a few results for the distribution of a random vector, which will subsequently characterize the distribution of R, S .

3.3.1 Random vector

A n -dimensional random vector $\{X\}$ is a vector, each component of which X_i is a random variable.

3.3.2 Joint probability density

The joint probability density of the vector $\{X\}$ is denoted by $f_{\{X\}}(\{x\})$. It verifies the following property:

$$\int_{\mathbb{R}^n} f_{\{X\}}(\{x\}) dx_1 \cdots dx_n = 1$$

The marginal distribution of a component (note: x_k and X_k are respectively an outcome and a random variable indexed with k and not a vector!) is obtained by integrating over all the variables except for x_k :

$$f_{X_k}(x_k) = \int_{\mathbb{R}^{n-1}} f_{\{X\}}(\{x\}) \prod_{i \neq k} dx_i$$

When two components are statistically independent, their joint density distribution is the product of the densities of each:

$$f_{X_i, X_j}(x_i, x_j) = f_{X_i}(x_i) f_{X_j}(x_j)$$

An illustration is given by the Gaussian distribution of a vector whose joint probability density is the product of the exponential functions if the correlation is zero; for example, for two centered and standardized variables $\mathcal{N}(0, 1)$:

$$f_{U_i, U_j}(u_i, u_j) = \frac{1}{2\pi} e^{-\frac{1}{2}(u_i^2 + u_j^2)} = \frac{1}{\sqrt{2\pi}} e^{-\frac{u_i^2}{2}} \frac{1}{\sqrt{2\pi}} e^{-\frac{u_j^2}{2}}$$

$$f_{U_i, U_j}(u_i, u_j) = f_{U_i}(u_i) f_{U_j}(u_j)$$

where the notation U_i , corresponding to u_i , is used for a Gaussian variable $\mathcal{N}(0, 1)$ in this entire book, with the exception of Chapter 12, if the variables i are independent.

3.3.3 Moments and correlation

Each component X_i is associated with a mean m_{X_i} (first-order moment) and a standard deviation σ_{X_i} (the square – the variance – is the second-order centered moment) whose expressions are:

$$\mathbb{E}[X_i] = m_{X_i} = \int_{-\infty}^{\infty} x_i f_{X_i}(x_i) dx_i$$

$$\mathbb{E}[(X_i - \mathbb{E}[X_i])^2] = \sigma_{X_i}^2 = \int_{-\infty}^{\infty} (x_i - m_{X_i})^2 f_{X_i}(x_i) dx_i$$

or

$$\sigma_{X_i}^2 = \int_{-\infty}^{\infty} x_i^2 f_{X_i}(x_i) dx_i - m_{X_i}^2$$

Mechanical engineers will recall that these are the definitions of the center of gravity and inertia.

In the case of a random vector, for each couple of random variables a new quantity is introduced, the second-order mixed moment:

$$\mathbb{E}[X_i X_j] = \int_{-\infty}^{\infty} \int_{-\infty}^{\infty} x_i x_j f_{X_i, X_j}(x_i, x_j) dx_i dx_j$$

The correlation coefficient of the variables X_i and X_j is defined by:

$$\rho_{X_i X_j} = \frac{\mathbb{E}[X_i X_j] - \mathbb{E}[X_i] \mathbb{E}[X_j]}{\sigma_{X_i} \sigma_{X_j}} = \frac{\text{cov}[X_i, X_j]}{\sqrt{\text{var}[X_i] \text{var}[X_j]}}$$

where the numerator of the above expression is the second order centered mixed moment; this is called the covariance.

All the terms $\text{cov}[X_i, X_j]$ (centered moments $\mathbb{E}[(X_i - \mathbb{E}[X_i])(X_j - \mathbb{E}[X_j])]$) form a square matrix called the covariance matrix:

$$[C_X] = \begin{bmatrix} \text{var}[X_1] & \text{cov}[X_1, X_2] & \dots & \text{cov}[X_1, X_n] \\ \text{cov}[X_2, X_1] & \text{var}[X_2] & \dots & \text{cov}[X_2, X_n] \\ \vdots & \vdots & \ddots & \vdots \\ \text{cov}[X_n, X_1] & \text{cov}[X_n, X_2] & \dots & \text{var}[X_n] \end{bmatrix}$$

The correlation matrix is the matrix of coefficients $\rho_{X_i X_j}$. For example, the general expression of the multinormal distribution of a Gaussian vector is:

$$f_{\{X\}}(\{x\}) = \frac{1}{(2\pi)^{n/2}} \frac{1}{\sqrt{\det[C_X]}} e^{-(1/2)\{\{x-m_X\}\}^t [C_X]^{-1} \{\{x-m_X\}\}} \quad (3.3)$$

The quadratic form appearing as an exponential can be diagonalized, and there is a change of coordinate system defined by the eigenvectors of $[C_X]$ for which the components of the random vector are decorrelated. A change of variables then gives centered standardized components $\mathcal{N}(0, 1)$. $[C_X]$ is a symmetric positive-defined matrix, and a change of coordinates is always possible.

In two dimensions, the standardized, centered and correlated Gaussian density is given by:

$$\phi_2(\hat{u}_1, \hat{u}_2, \rho) = \frac{1}{2\pi\sqrt{1-\rho^2}} \exp\left(-\frac{1}{2(1-\rho^2)}(\hat{u}_1^2 + \hat{u}_2^2 - 2\rho\hat{u}_1\hat{u}_2)\right) \quad (3.4)$$

where

$$[C_U] = \begin{bmatrix} 1 & \rho \\ \rho & 1 \end{bmatrix}$$

The isodensities $\phi_2(\hat{u}_1, \hat{u}_2, \rho) = \text{constant}$ are ellipses and circles when $\rho = 0$. This representation is frequently used (Figure 3.4). The notation \hat{U}_i , with corresponding \hat{u}_i , is used for a Gaussian variable $\mathcal{N}(0, 1)$ in this entire book, in the case of correlation.

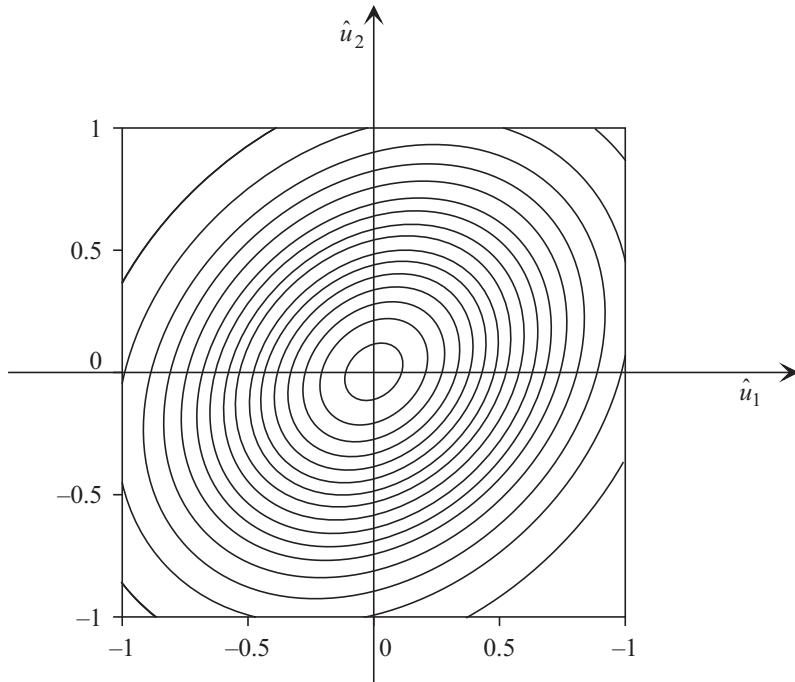


Figure 3.4 Representation of the isodensities of the standardized, centered Gaussian distribution, for a correlation $\rho = 0.25$.

In practical cases, the information available is generally poor. Statistics provides knowledge of the means and the standard deviations of the random variables, but has more difficulty with the distribution of each random variable, and even more difficulty with joint distribution.

3.3.4 Independence and correlation

Decorrelation: two random variables are decorrelated if there is factorization of the mathematical expectations:

$$\mathrm{E}[XY] = \mathrm{E}[X]\mathrm{E}[Y]$$

Independence: independence requires in addition the factorization of the probability densities:

$$f_{X,Y}(x,y) = f_X(x)f_Y(y)$$

Hence the following results:

1. independence leads to decorrelation,
2. decorrelation does not lead to independence,
3. but, in the case of two Gaussian variables, a zero correlation leads to factorization, hence independence!

3.4 Expressions of the probability of failure

3.4.1 Probability of failure

The operating scenario is the availability of a resistance greater than the stress, such that:

$$G(r,s) = r - s > 0$$

and the non-operating or failure scenario is:

$$G(r,s) = r - s \leq 0$$

The *measure of the failure* is then the probability associated with the event $\{R - S \leq 0\}$, that is:

$$\text{Probability of failure} = P_f = \text{Prob}(\{R - S \leq 0\})$$

Reliability is then defined as the complement of the probability of failure:

$$\text{Reliability} = 1 - P_f$$

3.4.2 Distributions of R and S and probability P_f

R and S are two random variables characterized by a *joint probability density* denoted by $f_{R,S}(r,s)$.

The probability of failure P_f , associated with the margin Z , is the *probabilistic weight* of the part of the space composed by the domain $\mathcal{D}_f : z = r - s \leq 0$:

$$P_f = \text{Prob}(R - S \leq 0) = \int_{r-s \leq 0} f_{R,S}(r,s) \, dr \, ds \quad (3.5)$$

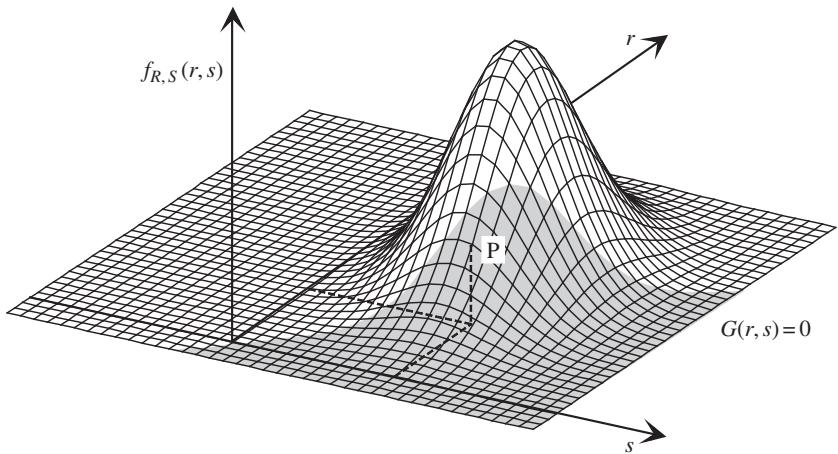


Figure 3.5 Three-dimensional representation of P_f for a Gaussian distribution of two correlated variables R and S .

The illustration of Equation (3.5) is given in Figure 3.5 where the joint probability density of variables R and S is Gaussian, as the variables are correlated. The probabilistic weight, P_f , is the volume located under the gray-shaded part. In fact, in the case of two variables, $f_{R,S}(r,s)$ is a surface and P_f is a volume, much smaller than 1 if the structure is well designed. It is also shown in Figure 3.6 where the ellipses are probability isodensity ‘level curves’. The correlation is expressed by the rotation of the main axes of the ellipses with respect to the coordinate axes of the random variables. These level curves are shown in Figure 3.3 where they show the correlation of actions P_1 and P_2 .

If the two variables are statistically *independent*, then the joint probability density is the product of the densities of each variable:

$$f_{R,S}(r,s) = f_R(r)f_S(s) \quad (\text{independent variables})$$

In this case, we denote the probability densities and the distribution functions of R and S by:

$$\text{for } R: f_R(r) \text{ and } F_R(r) \quad \text{and} \quad \text{for } S: f_S(s) \text{ and } F_S(s)$$

Two expressions proposed for P_f are now established with the assumption of independence.

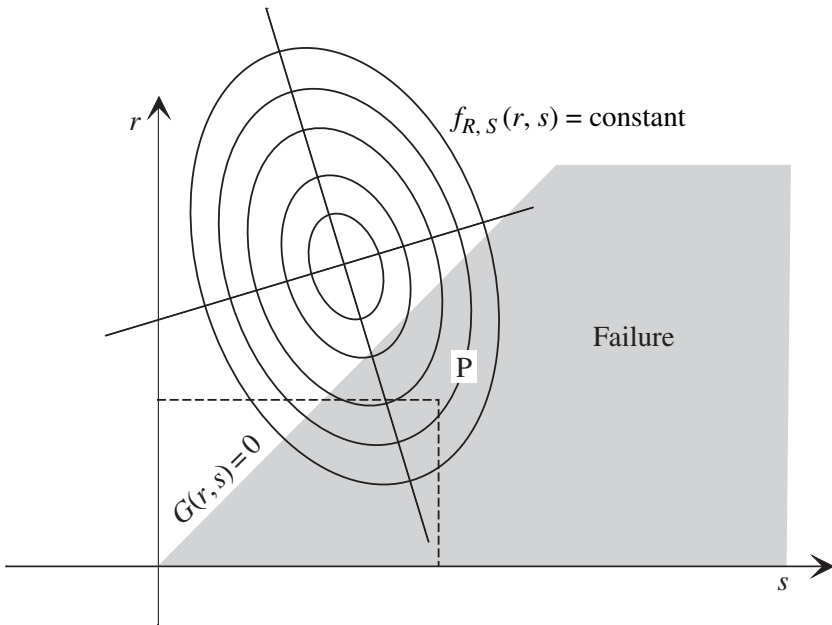


Figure 3.6 Representation of P_f by probability isodensity curves.

3.4.3 First expression of P_f

Let A be the event $\{\text{stress } S \in [x, x+dx]\}$ and B the event $\{\text{resistance } R < x\}$. The probability of failure for stresses ranging between x and $x+dx$ (Figure 3.7) is the probability of the event $\{A \cap B\}$:

$$\text{Prob}\{A\} = f_S(x) dx \quad \text{and} \quad \text{Prob}\{B\} = \int_{-\infty}^{\infty} f_R(\xi) d\xi = F_R(x)$$

As the events are independent:

$$dP_f = \text{Prob}\{A \cap B\} = \text{Prob}\{A\} \text{Prob}\{B\} = f_S(x) dx F_R(x)$$

For all possible stresses:

$$P_f = \int_{-\infty}^{\infty} f_S(x) F_R(x) dx \quad (R, S \text{ independent}) \quad (3.6)$$

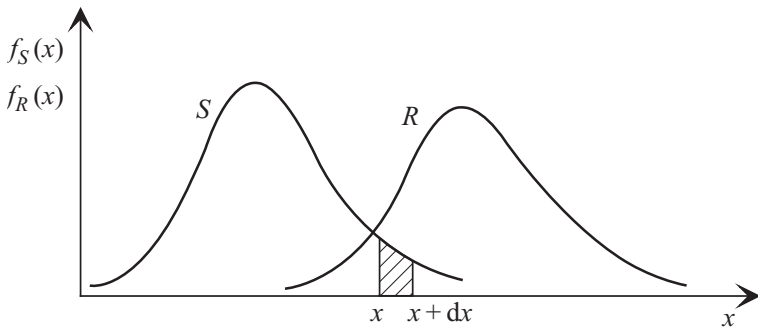


Figure 3.7 Densities of R and S : first form of P_f .

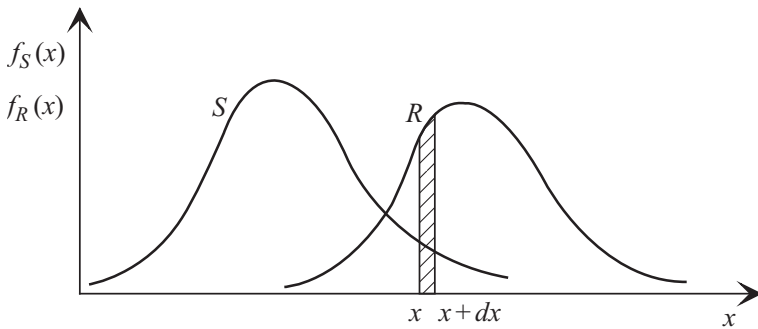


Figure 3.8 Densities of R and S : second form of P_f .

3.4.4 Second expression of P_f

Another expression of P_f is obtained from the events (Figure 3.8):

$$A = \{\text{resistance } R \in [x, x + dx]\} \implies \text{Prob}\{A\} = f_R(x) dx$$

$$B = \{\text{stress } S < x\} \implies \text{Prob}\{B\} = \int_{-\infty}^{\infty} f_S(\xi) d\xi = F_S(x)$$

Failure is the intersection of events $\{A\}$ and $\{\bar{B}\}$, complementary to $\{B\}$:

$$P_f = \int_{-\infty}^{\infty} (1 - F_S(x)) f_R(x) dx \quad (R, S \text{ independent}) \quad (3.7)$$

The calculation of the reliability $P_s = 1 - P_f$ is deduced from this equation:

$$P_s = 1 - \left(\int_{-\infty}^{\infty} f_R(x) dx - \int_{-\infty}^{\infty} F_S(x) f_R(x) dx \right) = \int_{-\infty}^{\infty} F_S(x) f_R(x) dx$$

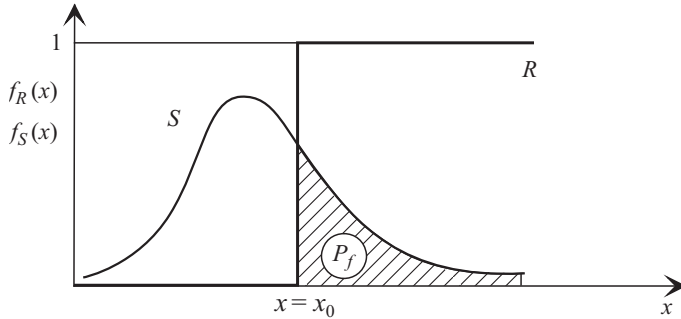


Figure 3.9 Random stress and determined resistance.

3.4.5 Illustration

Determined resistance

A few particular cases provide a graphical illustration. For example, when the resistance is deterministic, the hatched area of Figure 3.9 is the probability of failure; in fact:

$$F_R(x) = \begin{cases} 0 & \text{if } x \leq x_0 \\ 1 & \text{if } x > x_0 \end{cases} \implies P_f = \int_{x_0}^{\infty} f_S(x) dx$$

In the case of two variables, the probability of failure is represented by a volume as illustrated in Figures 3.5 and 3.6. The probability density $f_{R,S}(r,s)$ is a surface, and the probability of failure, P_f , is a volume, the volume limited by the plane $f_{R,S}(r,s) = 0$, the surface and the plane $r = s$.

Correlated binormal distribution

Let us consider two random variables R and S whose means and standard deviations are respectively m_R , m_S , σ_R and σ_S . The correlation coefficient is ρ_{RS} . We obtain:

$$f_{R,S}(r,s) = \frac{1}{2\pi\sigma_R\sigma_S\sqrt{1-\rho_{RS}^2}} \exp \left[-\frac{1}{2(1-\rho_{RS}^2)} \left[\frac{(r-m_R)^2}{\sigma_R^2} - \frac{2\rho_{RS}(r-m_R)(s-m_S)}{\sigma_R\sigma_S} + \frac{(s-m_S)^2}{\sigma_S^2} \right] \right]$$

There is no independence, and expressions (3.6) and (3.7) are not applicable. An integration is possible, and this is given in Chapter 9. A convenient representation is to plot the probability isodensity curves in the r,s plane.

Here these are ellipses, centered on the mean point and whose main axes are parallel to the coordinate axes only in the case of the independence of the variables ($\rho_{RS} = 0$). Figure 3.6 is a representation of the normal distribution for two correlated variables.

3.4.6 Generalization of the probability of failure

The equations established in the case of two random variables can be generalized to that of a random vector $\{X\}$. $f_{\{X\}}(\{x\})$ is the probability density of vector $\{X\}$ and $G(\{X\})$ is the limit-state function. The probability of failure is then:

$$P_f = \int_{G(\{X\}) \leq 0} f_{\{X\}}(\{x\}) dx_1 \cdots dx_n \quad (3.8)$$

The expression obtained is the general form of the probability of failure; the integral is spread to the entire failure domain. If this formulation is simple, it is theoretical and its use supposes that the joint probability density of vector $\{X\}$ is known and that direct integration is possible, two requirements that are seldom satisfied.

3.5 Calculation of the probability of failure

The elementary forms of the expression of the probability of failure help to evaluate it in particular cases.

3.5.1 Calculation of P_f by direct integration

This calculation can be performed only in particular favorable cases where the density functions have simple forms. The following example considers a resistance and a stress represented by uniform density functions.

Example: two independent uniform distributions

Resistance R is uniform in the interval $[a, b]$, and stress S is uniform in the interval $[c, d]$, with $c < a < d < b$ (Figure 3.10). We thus deduce the expression of the distribution function of R :

$$F_R(x) = \begin{cases} 0 & \text{if } x \leq a \\ (x-a)/(b-a) & \text{if } x \in]a, b] \\ 1 & \text{if } x > b \end{cases}$$

and that of the density function of S :

$$f_S(x) = \begin{cases} 0 & \text{if } x \leq c \\ 1/(d-c) & \text{if } x \in]c, d] \\ 0 & \text{if } x > d \end{cases}$$

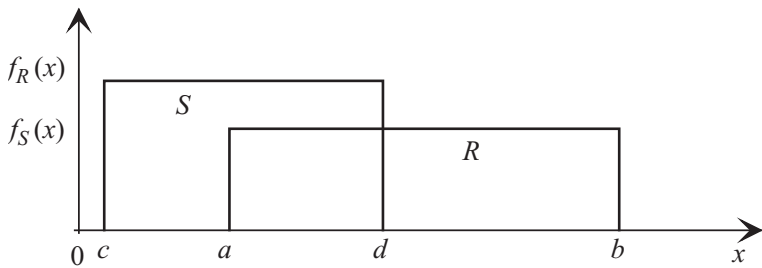


Figure 3.10 Two uniform distributions, resistance R and stress S .

The intersection of the two definition domains of the density functions is $[a, d]$ and $f_S(x) = 1/(d - c)$ for $x \in [a, d]$; Equation (3.6) reads:

$$P_f = \int_a^d \frac{1}{d - c} \frac{x - a}{b - a} dx = \frac{(d - a)^2}{2(d - c)(b - a)}$$

Example: two independent Gaussian distributions

A direct integration is given in the example of the rod under tension in Section 3.6.3.

3.5.2 Calculation of P_f by numerical integration

The integration can *a priori* be performed numerically; however, the values, in principle very small, of the probability of failure result in significant errors as P_f is of the order of magnitude of the integration error. Furthermore, the integration domain is not always bounded. Formal or numerical calculation software is a very useful aid for this integration.

3.5.3 Calculation of P_f by simulation

Mathematical procedures are used to simulate an outcome of a random variable of a given distribution. The Monte Carlo method, for example, consists of simulating outcomes of the limit-state and counting the number of failure events obtained. If n is the number of simulations, we admit that the frequency of failure events tends toward the probability of failure when $n \rightarrow \infty$:

$$P_f = \lim_{n \rightarrow \infty} \frac{\text{Number of events where } G \leq 0}{\text{Total number of simulated events}}$$

Such a procedure presents the advantage of simplicity, provided we know how to simulate a variable of a given distribution, but has a very slow convergence

	m_X	σ_X	$\tilde{m}_{X_{1,000}}$	$\tilde{\sigma}_{X_{1,000}}$	$\tilde{m}_{X_{10,000}}$	$\tilde{\sigma}_{X_{10,000}}$
R	4.500	1.443	4.462	1.456	4.503	1.441
S	2.000	1.155	2.073	1.167	1.993	1.152
\tilde{P}_f	$\{0.093 - 0.133\}$				$\{0.096 - 0.108\}$	

Table 3.1 Results of the simulation of the probability of failure for the example of two uniform distributions.

(in \sqrt{n}), all the more so as the number of simulations must be far higher than the inverse of the probability of failure. The convergence is given by the Shooman formula [Sho68]:

$$\% S = 200 \sqrt{\frac{1 - \tilde{P}_f}{n \tilde{P}_f}} \quad (3.9)$$

where \tilde{P}_f is the estimated frequency and n is the number of simulations. This percentage corresponds to a probability of 95% that the exact value of P_f belongs to the interval $\tilde{P}_f (1 \pm \% S)$: this is the 95% confidence interval. The simulation methods are presented in Chapter 8.

Example: two independent uniform distributions

A uniform sample generator is widely available under names such as RND, RANDOM, ... and it is therefore very simple to run a simulation in the case of two uniform distributions. It is illustrated for the following data: $a = 2, b = 7, c = 0$ and $d = 4$, which results in $P_f = 0.100$. The calculation is performed using MATHCAD software [Sof01]. Table 3.1 gives the results for 1,000 and 10,000 simulations. We recall that if X is a uniform random variable $\in [a, b]$, then $m_X = (b+a)/2$ and $\sigma_X = (b-a)/\sqrt{12}$. The results are given as they are found, and another simulation will give different results. The means and standard deviations demanded and obtained ($\tilde{\cdot}$) are slightly different, but the result is satisfactory; the probability bounds indicated correspond to a 5% confidence level. The necessity for a large number of simulations is seen clearly; 10,000 simulations are used here for a very high probability of 0.100.

3.5.4 Calculation of P_f by sampling and integration

This method uses a simulation for integrating expression (3.7). We first construct a sample of N elements of variable R and a sample of M elements of variable S .

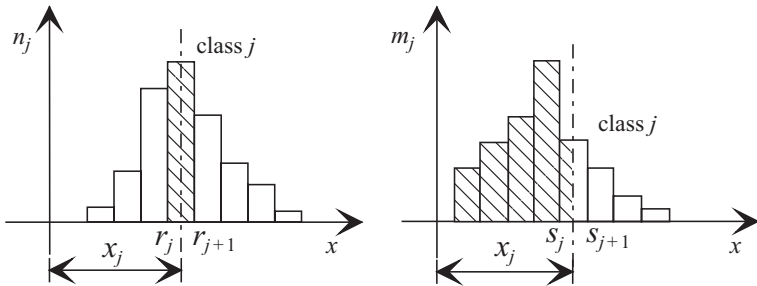


Figure 3.11 Histograms of R and S .

N and M are not necessarily equal. These two samples are distributed in identical classes:

- The sample of R is decomposed into n classes $j, [r_j, r_{j+1}[$ whose sizes are n_j (Figure 3.11).
- The sample of S is decomposed into $m = n$ classes $j, [s_j = r_j, s_{j+1} = r_{j+1}[$ whose sizes are m_j .

Equation (3.7) is then written:

$$f_R(x)\Delta x_j = \frac{n_j}{N}$$

$$P_f = \sum_{j=1}^n \frac{n_j}{N} (1 - F_S(x_j)) \quad \text{with } x_j = \frac{r_j + r_{j+1}}{2} = \frac{s_j + s_{j+1}}{2} \quad (3.10)$$

and we have to calculate $F_S(x_j)$:

$$F_S(x_j) = \sum_{i=1}^j \frac{m_i}{M} - \frac{1}{2} \frac{m_j}{M} = \frac{1}{2M} \left(\sum_{i=1}^j 2m_i - m_j \right) \quad (3.11)$$

By introducing (3.11) into (3.10), we obtain, after the calculation:

$$P_f = 1 - \frac{1}{2NM} \left[\sum_{j=1}^n \left(n_j \left(2 \sum_{i=1}^j m_i - m_j \right) \right) \right].$$

Analytical evaluation methods and methods using numerical simulation of P_f have a very limited application. Since the 1970s, a method of approximation of P_f by *reliability indexes* has been progressively developed. Before presenting it, let us first illustrate our statement with an example.

3.6 Rod under tension

The purpose of this example (Figure 3.12) is to illustrate the concepts presented above in a simple case, with assumptions that allow an explicit calculation of the solutions and which do not correspond to assumptions confirmed by experience, as the choice of distributions representing the random variables is not the best possible. This example is used repeatedly as a leitmotiv according to the developments of the theories presented.

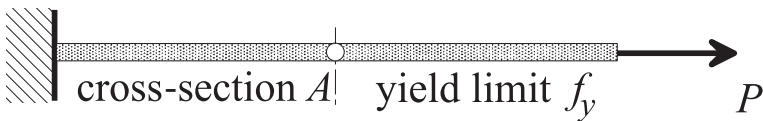


Figure 3.12 Rod under tension.

3.6.1 Data

We have chosen to study the reliability of the design of a rod subjected to an axial force by the application of a tension or compression action P . The cross-section area is A and the yield limit is f_y . We have:

- action data: the load P ,
- state data: the cross-section A ,
- stress: $\sigma = P/A$,
- resistance: f_y ,
- design rule: $P/A < f_y$.

The vector of the basic variables is $\{X\} = \{P, A, f_y\}^t$ and the limit-state is $G(\{X\}) = f_y A - P$. The quantity $f_y A$ is the resistance denoted by R , and P is equal to the internal strength denoted by S .

In order to obtain a simple representation and to retain linearity, only two variables are assumed to be random: P and f_y . The numerical data are as follows:

- P , with a mean of 70 MN and a standard deviation of 15 MN, represents the maximum value of an action variable over a certain duration,
- f_y , with a mean of 272.72 MPa and a standard deviation of 16.36 MPa, is assumed to be homogeneous in a defined population. The mean decreased by two standard deviations gives an elastic limit value of 240 MPa corresponding to construction steel.

These variables are *Gaussian* and *uncorrelated*. The value of A is fixed at 0.42 m^2 ; the choice of this design and the numerical data is justified in the study

of ‘safety’ coefficients in Chapter 10. They correspond to the usual values for the design of such a mechanical system. The reader may be surprised at the numerical values chosen. Their origin, now old, draws from the first studies initiated by Elf-Aquitaine, and these values are extracted from very simplified models of equivalent elements in offshore structures.

3.6.2 Probability of failure

With the defined data, probability of failure is expressed as follows (Equation (3.5)):

$$P_f = \int_{f_y A - P \leq 0} f_{f_y A, P}(f_y A, P) A \, df_y \, dP$$

with

$$\begin{aligned} f_{f_y A, P}(f_y A, P) \\ = \frac{1}{2\pi\sigma_{f_y A}\sigma_P} \exp\left(-\frac{1}{2}\left(\frac{(f_y A - m_{f_y A})^2}{\sigma_{f_y A}^2} + \frac{(P - m_P)^2}{\sigma_P^2}\right)\right) \end{aligned} \quad (3.12)$$

The probability isodensities are ellipses whose main axes are parallel to the coordinate axes, as the variables are uncorrelated. The simple forms of probability and limit-state allow an integration, giving the value $P_f = 0.0035$ for the design chosen. A complete analytical integration is not possible, and we must resort to tabulated or approximated values for the distribution function of the centered reduced normal distribution $\Phi(x)$.

3.6.3 Analytical integration

Analytical integration is possible using the usual techniques. They form the basis of the concept of the reliability index, which is thus introduced. For the analytical integration of (3.12), it is necessary to:

1. standardize the space,
2. perform a rotation of the axes (Figure 3.13).

Let us carry out the following changes in variables to obtain centered standardized variables:

$$\begin{aligned} r = f_y A & \quad s = P & \quad u = \frac{r - m_R}{\sigma_R} & \quad v = \frac{s - m_S}{\sigma_S} \\ dr = \sigma_R \, du & \quad ds = \sigma_S \, dv \end{aligned}$$

The joint density of (U, V) is then written:

$$f_{U,V}(u, v) = \frac{1}{2\pi} \exp\left(-\frac{1}{2}(u^2 + v^2)\right)$$

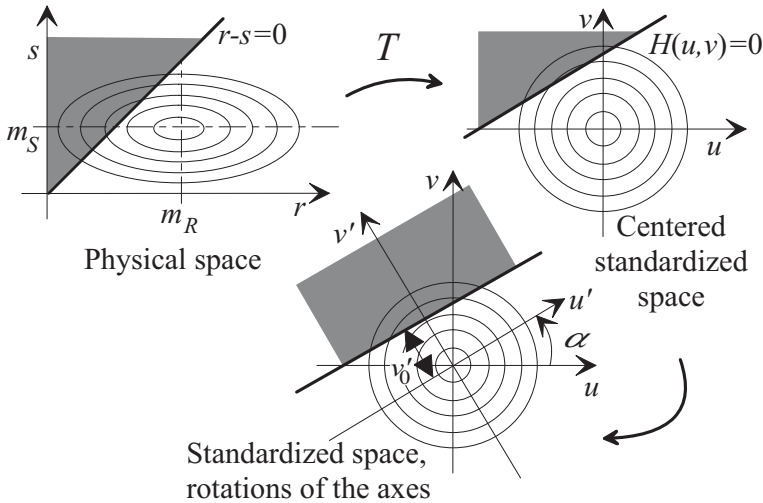


Figure 3.13 Steps in the integration of P_f : transformation from physical space to standardized space and rotation of the axes.

Note that joint density is obtained by carrying out the transformation of variables in (3.12) and by introducing the standardization condition: $\int_{-\infty}^{+\infty} \int_{-\infty}^{+\infty} f_{U,V}(u,v) du dv = 1$. The probability of failure is given by:

$$P_f = \frac{1}{2\pi} \int_{\sigma_R u - \sigma_S v + m_R - m_S \leq 0} \exp\left(-\frac{1}{2}(u^2 + v^2)\right) du dv$$

as the failure condition $r-s < 0$ becomes $\sigma_R u - \sigma_S v + m_R - m_S \leq 0$ (limit-state straight line).

This integral can be calculated by performing a rotation of the axes by an angle $\alpha = (\vec{u}, \vec{u}')$:

$$\begin{bmatrix} u \\ v \end{bmatrix} = \begin{bmatrix} \cos \alpha & -\sin \alpha \\ \sin \alpha & \cos \alpha \end{bmatrix} \begin{bmatrix} u' \\ v' \end{bmatrix}$$

and the limit-state straight line becomes:

$$H(u', v') = (\sigma_R \cos \alpha - \sigma_S \sin \alpha)u' - (\sigma_R \sin \alpha + \sigma_S \cos \alpha)v' + m_R - m_S = 0$$

The coefficient of u' is canceled for $\tan \alpha = \sigma_R / \sigma_S$ and:

$$v' = \frac{m_R - m_S}{\sigma_R \sin \alpha + \sigma_S \cos \alpha} = v'_0 \quad \text{for } \alpha = \tan^{-1}\left(\frac{\sigma_R}{\sigma_S}\right)$$

$$H(u', v') = -v' + v'_0 \leq 0 \quad \text{that is } v' \geq v'_0.$$

The determinant of the Jacobian of the rotation is equal to 1, and $du' dv' = du dv$. The expression of P_f becomes:

$$P_f = \frac{1}{2\pi} \int_{v'=v'_0}^{\infty} \left(\int_{-\infty}^{\infty} e^{-u'^2/2} du' \right) e^{-v'^2/2} dv'$$

The integral between brackets is equal to $\sqrt{2\pi}$ and finally:

$$P_f = \frac{1}{\sqrt{2\pi}} \int_{v'=v'_0}^{\infty} e^{-v'^2/2} dv' = \frac{1}{\sqrt{2\pi}} \int_{-\infty}^{-v'_0} e^{-v'^2/2} dv' = \Phi(-v'_0)$$

With the numerical data:

$$v'_0 = 2.700 \quad \text{and} \quad P_f = 0.00347$$

This result, which is more accurate than necessary, is given for the purpose of comparison with other evaluations. The distance v'_0 is the *reliability index*. This concept is generalized in the next section.

3.6.4 Simulation

Table 3.2 illustrates a simulation application for this example, using MATHCAD. The slowness of the convergence and the large number of simulations show the limitation of the method.

Number of simulations	10^2	10^3	10^4	10^5	10^6
\tilde{P}_f (estimated)	0	0.00400	0.00350	0.00360	0.00351
95% confidence	∞	$\pm 99.8\%$	$\pm 33.75\%$	$\pm 10.52\%$	$\pm 3.44\%$
$(\hat{P}_f - P_f)/P_f$		15%	1%	4%	1%

Table 3.2 Rod under tension: results obtained by simulation.

3.7 Concept of reliability index

It seems that the first proposed reliability index can be attributed to Rjanitzyn [Rzh49, Rja59], in the 1950s, in the Soviet Union. However, it was Cornell [BC70] who popularized this idea. Thereafter, several proposals were made, but the most complete form is credited to Hasofer and Lind [HL74], who gave it a precise definition. We will discuss only the Rjanitzyn and Cornell index and the Hasofer and Lind index.

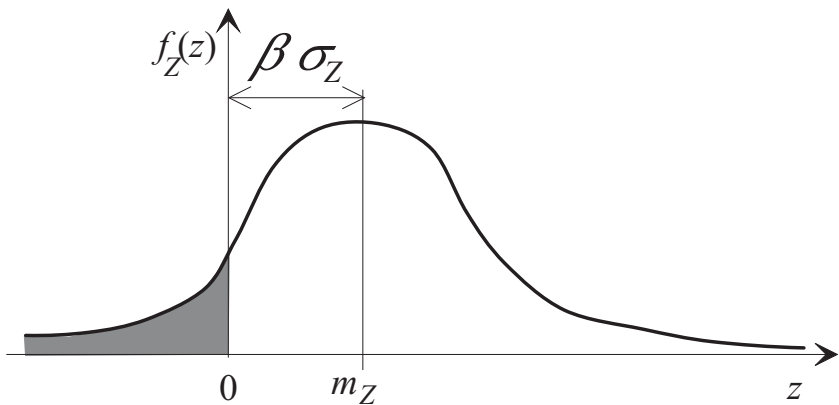


Figure 3.14 Representation of the Cornell index.

3.7.1 Rjanitzyne-Cornell index

The definition proposed is very simple: the index β_c is obtained from the mean, m_Z , and the standard deviation, σ_Z , of the margin variable $Z = R - S$:

$$\beta_c = \frac{m_Z}{\sigma_Z} \quad (3.13)$$

The index β_c thus appears as the inverse of the coefficient of variation of the random variable Z . The graphical representation (Figure 3.14) shows that this index indicates the number of standard deviations between the mean point, m_z , and the limit-state ($z = 0$). β_c is a number without physical dimension. It reflects the frequent practice in engineering of moving by a few standard deviations from the mean in order to be in the safety domain, and the usual values of a reliability index are a few units.

$R - S$ case

If $Z = R - S$:

$$m_Z = m_R - m_S \quad \text{and} \quad \sigma_Z = \sqrt{\sigma_R^2 + \sigma_S^2} \implies \beta_c = \frac{m_R - m_S}{\sqrt{\sigma_R^2 + \sigma_S^2}} \quad (3.14)$$

If the variables are correlated, the result is valid, noting that:

$$\sigma_Z^2 = \sigma_R^2 + \sigma_S^2 - 2 \operatorname{cov}[R, S]$$

R and S are Gaussian variables

Under this assumption, Z is also a Gaussian variable. Figure 3.14 shows that the probability of failure is given by:

$$P_f = \int_{-\infty}^0 f_Z(z) dz = \frac{1}{\sigma_Z \sqrt{2\pi}} \int_{-\infty}^0 \exp\left(-\frac{1}{2}\left(\frac{z - m_Z}{\sigma_Z}\right)^2\right) dz$$

and, by assuming $u = (z - m_Z)/\sigma_Z$,

$$P_f = \frac{1}{\sqrt{2\pi}} \int_{-\infty}^{-\beta_c} \exp\left(-\frac{u^2}{2}\right) du = \Phi(-\beta_c)$$

where $\Phi(\dots)$ is the distribution function of the reduced centered normal distribution. The transformation $z \rightarrow u$ introduces the variable u , a Gaussian with zero mean and unit standard deviation. Such a variable $\mathcal{N}(0, 1)$ plays a vital role in the following sections.

Critique of the β_c index

The situation – Gaussian variables and linear limit-state – is the only one for which the method of the Rjanitzyn and Cornell index is rigorous. In fact, a different representation of the margin Z , for the same limit-state, results in a different value of β_c . For example, if the margin is now defined by $Z = R/S - 1$, the calculation of the mean and the standard deviation of Z is no longer possible analytically and Z is not a Gaussian random variable. If R and S are Gaussian, Z is a Cauchy variable, which does not even have any moments. If $Z = R - S$ and if R and S are not Gaussian, expression (3.14) gives a β_c index, but the equation with P_f now depends on the distribution of Z .

Here we come up against two difficulties:

- the first is due to the non-invariance of the reliability index β_c in various representations of the same limit-state function. The Hasofer and Lind index solves this problem,
- the second is due to the move from the index to the probability of failure. This will be remedied by the first order and second order approximations (Chapter 7).

The β_c index can be considered as an approximation of the exact and invariant reliability index by a first order development, but we must perform this development around a particular point, the most probable failure point, which will be discussed further below.

The β_c index is correct in the case of Gaussian variables and a linear limit-state in the physical space. This condition is sufficient, but not necessary.

3.7.2 Hasofer-Lind index

Isoprobabilistic transformation

To compensate for the non-invariance of β_c , Hasofer and Lind [HL74] proposed not considering a physical variable space, but performing a transformation of variables, as in the example in Section 3.6, to a new space of statistically independent Gaussian variables, with zero mean and unit standard deviations:

$$X_i \longrightarrow U_i \text{ Gaussian vector } \mathcal{N}(0, 1), m_{U_i} = 0, \sigma_{U_i} = 1, \rho_{ij} = 0, \forall i, \forall j$$

The transformation from physical space to standardized space (or normalized space) is immediate in the case of independent Gaussian variables:

$$u = \frac{x - m_X}{\sigma_X} \quad (\text{reduced variables, here Gaussian})$$

and it retains the linearity of the limit-state.

For independent variables of any distribution, the principle of the transformation consists of writing the equality of the distribution functions:

$$\Phi(u) = F_X(x) \implies x \longrightarrow u = \Phi^{-1}(F_X(x)) \quad (3.15)$$

The resulting transformation of Equation (3.15) is called an *isoprobabilistic transformation*; it is denoted by T hereafter. It is applied here to a variable, and it supposes that $F_X(x)$ is continuous and strictly increasing. For the case where the variables are not independent, a general form of the transformation has been given by Rosenblatt [Ros52]. This point, as well as other transformations, is discussed in Chapter 4.

Definition of the exact and invariant reliability index

In the standard Gaussian space of variables u_i , the reliability index β is defined as the distance between the origin O and the point P^* closest to the origin in the limit-state surface. P^* is the *most probable failure point* (this misused name is discussed in Section 3.7.3). The example of the rod under tension (Figure 3.13) illustrates this definition; the distance v'_0 is the Hasofer-Lind reliability index $\beta_{HL} = \beta$:

$$\beta_{HL} = \beta = \text{distance } O, G(\{x_i(u_j)\}) = 0 = \min_{G(\{x_i(u_j)\}) \leq 0} \sqrt{\{u\}^t \{u\}} \quad (3.16)$$

A distance is essentially positive: by convention, index β is considered positive if the origin point belongs to the safety domain; if not, it is negative.

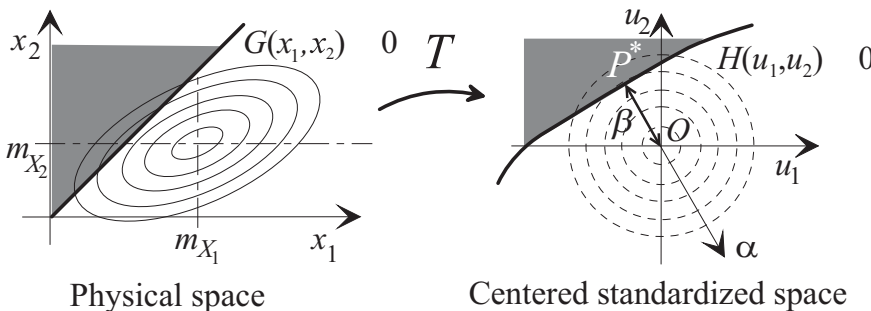


Figure 3.15 Representation of the Hasofer-Lind index.

Assuming the transformation of variables into standardized space, this procedure allows an invariant determination of an index β_{HL} which can be simple to carry out when the physical variables are Gaussian (or lognormal, see Section 3.7.5) and the limit-state linear, or require the use of numerical calculation to use the necessary algorithms.

Apart from the index, important information is given by the direction cosines α_i (Figure 3.15) of the straight line P^*O oriented from P^* toward O ; in fact:

$$u_i^* = -\beta \alpha_i$$

The value α_i represents the influence of the random variable U_i in the limit-state and an approximation of the influence of the physical variable X_i which is associated with it. Note that if:

$$u_i^* = -\beta \alpha_i \quad \text{then } \alpha_i u_i^* = -\beta \alpha_i \alpha_i = -\beta$$

Discussion of the transformation from physical space to standardized space can be found in Chapter 4. We should note that it is not unique.

3.7.3 Naming point P^*

Owing to the symmetry of revolution of the multinormal Gaussian density and its decrement from the origin, point P^* is the point in the limit-state corresponding to the maximum density of probability in the standardized space. It was therefore called, first by Freudenthal (1956), *the most probable failure point*. This name reflects the role of this point in reliability analysis in the sense of the Hasofer-Lind index. Considered from the point of view of partial coefficients, its name is *design point*, which is absolutely satisfactory. We will discuss it in this role in Chapter 10. The book by Ditlevsen and Madsen [DM96]

employs the term ‘most central limit-state point’ or ‘most central failure point’, thus abandoning the original name. These hesitations arise from a certain difficulty: what, in fact, is the relation between this point and the one obtained by the maximum likelihood theory?

In physical variable space, the real operating point of the structure, with coordinates x_i , is distributed according to a probability distribution $F_{X_i}(x_i)$. According to the maximum likelihood theory, the most probable failure point, which is not necessarily unique, is the one in which the density of probability allows a maximum value in the failure domain, which has meaning only if the distribution $F_{X_i}(x_i)$ allows a density $f_{X_i}(x_i)$ at any point in the failure domain, including on the edges of the domain.

Let us now move to standardized space. Density is a standardized multinormal Gaussian distribution $\phi_n(u_i)$, and its maximum is in P^* in view of the symmetry of revolution and its decrement as a function of β , the distance to the origin.

Density in physical space is obtained in one way or another by the product $\phi_n(u_i)$ and the Jacobian of transformation $u_i \rightarrow x_i$. There is no reason for the physical density function to allow a maximum also in the corresponding point, and nothing enables us to affirm that the image of P^* in physical space is the maximum likelihood point. This is however true for linear transformations, since the Jacobian is constant.

It seems possible to use the maximum likelihood theory, but it does not generally lead us exactly to point P^* as it is defined. These remarks justify our hesitations concerning the vocabulary used, and in this book, it is the term ‘the most probable failure point’ which is first used, despite its shortcomings, and therefore the term ‘design point’ is used in relation to partial coefficients and design.

3.7.4 Application to the elementary Gaussian case

The vector of the random variables is chosen equal to $X_i = \langle R, S \rangle$, with components assumed to be Gaussian and statistically independent. The transformation is then:

$$u_R = \frac{r - m_R}{\sigma_R} \quad \text{and} \quad u_S = \frac{s - m_S}{\sigma_S}$$

The limit-state surface in physical variable space is $r - s = 0$; its expression becomes:

$$u_R \sigma_R - u_S \sigma_S + m_R - m_S = 0$$

This is a straight line Δ of \mathbb{R}^2 , and the Hasofer-Lind index is the distance from the origin to the straight line:

$$\beta = \text{distance } (0, \Delta) = \frac{m_R - m_S}{\sqrt{\sigma_R^2 + \sigma_S^2}}$$

This expression is identical to that of β_c , taking into account the assumptions, and the probability of failure is obtained exactly:

$$P_f = \Phi(-\beta_c) = \Phi(-\beta)$$

The coordinates of P^* in standardized space are u_R^* and u_S^* and in physical space:

$$\begin{aligned} r^* &= u_R^* \sigma_R + m_R = m_R - \beta \alpha_R \sigma_R = m_R(1 - \beta \alpha_R c_R) \\ s^* &= u_S^* \sigma_S + m_S = m_S - \beta \alpha_S \sigma_S = m_S(1 - \beta \alpha_S c_S) \end{aligned}$$

3.7.5 Rod under tension: Hasofer and Lind index

Case of Gaussian variables

To obtain index β , we must transform the variables into standardized space. It is enough to take:

$$u_1 = \frac{r - m_R}{\sigma_R} \quad u_2 = \frac{s - m_S}{\sigma_S}$$

The limit-state becomes:

$$\begin{aligned} \sigma_R u_1 - \sigma_S u_2 + m_R - m_S &= 0 \\ 6.87u_1 - 15u_2 + 44.54 &= 0 \end{aligned}$$

This is the equation of a straight line whose distance to the origin is index β :

$$\beta = \frac{m_R - m_S}{\sqrt{\sigma_R^2 + \sigma_S^2}} = 2.700$$

The probability of failure is $\Phi(-\beta) = 0.00347$; the calculation here is exact under the assumptions chosen.

Note that the Rjanitzyne-Cornell index, β_c , is here confused with the Hasofer-Lind index.

The most probable failure point is P^* , whose coordinates are:

$$u_{1P^*} = -\beta \cos \alpha \quad u_{2P^*} = -\beta \sin \alpha$$

and the physical point is:

$$f_{yP^*} = 254.39 \text{ MPa} \quad P_{P^*} = 106.9 \text{ MN}$$

α is the angle of the direction u_1 with the normal to the limit-state directed toward the reliability domain.

Figure 3.16 gives the representation of the limit-state in standardized variables (dotted line).

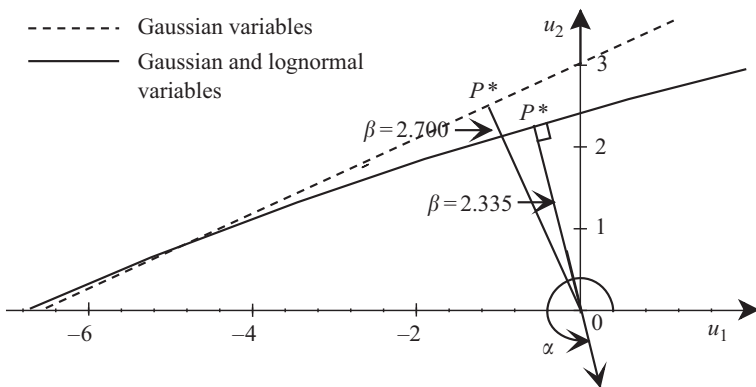


Figure 3.16 Rod under tension: limit-states.

R Gaussian and S lognormal

In this case, too, analytical calculations are possible. If S is lognormal, $Y = \ln S$ is Gaussian, with value:

$$m_{\ln S} = m_Y = \lambda_S = \ln \left(\frac{m_S}{\sqrt{1 + \left(\frac{\sigma_S}{m_S} \right)^2}} \right)$$

and standard deviation:

$$\sigma_{\ln S} = \sigma_Y = \xi_S = \sqrt{\ln \left(1 + \left(\frac{\sigma_S}{m_S} \right)^2 \right)}$$

The variable transformation is then:

$$u_2 = \frac{\ln s - \lambda_S}{\xi_S}$$

thus, the equation of the limit-state with the numerical values chosen is:

$$6.87 u_1 + 114.54 - \exp(0.212 u_2 + 4.226) = 0$$

This limit-state is plotted (continuous line) in Figure 3.16, and the distance to the origin is $\beta = 2.335$, obtained by an iterative numerical calculation. The probability given by $P_f = \Phi(-\beta) = 0.00978$ is then only an approximation, as the limit-state is not linear in standardized space. The physical coordinates of the most probable failure point are, respectively:

$$f_y^* = 261.92 \text{ MPa} \quad \text{and} \quad P^* = 110.01 \text{ MN}$$

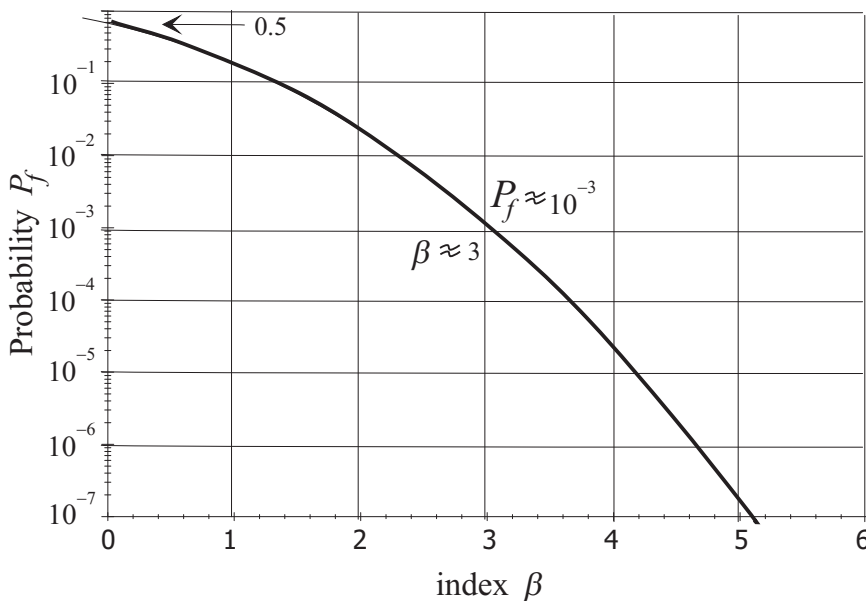


Figure 3.17 $P_f = \Phi(-\beta)$.

3.8 Equation $P_f = \Phi(-\beta)$

This equation gives the correspondence between the probability and the index. It is exact if the limit-state is linear in the reduced variable space. Its illustration is given in Figure 3.17. The two significant points $P_f \approx 10^{-3}$ for $\beta = 3$ and $P_f = 0.5$ for $\beta = 0$ must be retained.

The equation between P_f and β is a change of scale.

The value of the index is a few units, whereas in the case of probability, it is the exponent n of $P_f = 10^{-n}$ which is the interesting number. The scale of β is an approximately logarithmic scale of reliability, which best corresponds to a subjective appreciation of the order of magnitude of acceptable risks.

3.9 Exercises for illustration

The two exercises below illustrate direct applications of calculation of the indexes.

3.9.1 Study of a frame

Description of the problem

The calculation of the strength of the materials¹ of the frame shown in Figure 3.18 yields the following value for the bending moment at B :

$$M_B = -0.496 p a^2$$

where p is the random distributed load and a is a deterministic unit of length taken equal to 1. The resisting moment is M_R , a random variable. We consider that there is failure when:

$$|M_B| \geq M_R$$

The data are as follows:

var. X	var. U	m_X	σ_X	Distribution (case 1)	Distribution (case 2)	Distribution (case 3)
p	U_1	1,000	200	normal	lognormal	lognormal
M_R	U_2	800	40	normal	normal	lognormal

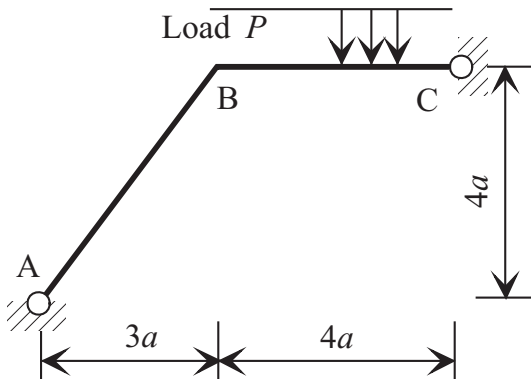


Figure 3.18 A simple frame.

¹ The result corresponds to a constant cross-section of the two beams and particular cross-section area characteristics; the energy effects of the bending moment, the axial force and the shear force are taken into account.

Questions

1. Show that the failure corresponds to two limit-states, each of which specify the composition, one being without significance.
2. Calculate the Cornell index.
3. Give the expression of the limit-state in standardized variables when the two variables are normal (case 1); deduce the Hasofer-Lind index and the direction cosines α_i .
4. Give the expression of the limit-state in standardized variables when p is lognormal and M_R is normal (case 2).
5. Calculate the Hasofer-Lind index for lognormal distributions (case 3).

Solution

1. *Two limit-states.* The failure condition $|M_B| \geq M_R$ introduces an absolute value. We consider M_R as a positive datum. Failure is therefore the union of events $M_B \geq M_R$ and $-M_B \geq M_R$. The mean of p being positive, the case $M_B \geq M_R$ corresponds to negative outcomes of p , very improbable if the variable is Gaussian and impossible if it is lognormal. The probability associated with this event is therefore negligible. We can also consider that M_R has negative outcomes, which is also without significance. This point underlines the fact that it is possible that the stochastic modeling of the variables is not physically realizable. This is often the case when densities with unbounded support are chosen.

2. *Cornell index.* It is given by:

$$\beta_c = \frac{800 - 0.496 \times 1,000}{\sqrt{40^2 + (0.496 \times 200)^2}} = 2.84$$

3. *Hasofer-Lind index, normal variables.* The variables are normal and the limit-state is linear, and the Hasofer-Lind index is equal to the Cornell index. Let us transform the variables:

$$u_1 = \frac{p - m_p}{\sigma_p} \quad u_2 = \frac{M_R - m_{M_R}}{\sigma_{M_R}}$$

We obtain:

$$40 u_2 - 0.496 \times 200 u_1 + 800 - 0.496 \times 1,000 = 0$$

and by standardizing:

$$0.374 u_2 - 0.927 u_1 + 2.84 = 0$$

hence:

$$\beta = 2.84 \quad \alpha_1 = -0.927 \quad \alpha_2 = 0.374$$

The limit-state is linear and the probability of failure is:

$$P_f = \Phi(-\beta) = 2.24 \cdot 10^{-3}$$

4. *Hasofer-Lind index, lognormal p and normal M_R .* The parameters of the normal distribution associated with the lognormal distribution of p are:

$$c_p = \frac{\sigma_p}{m_p} \quad \lambda_p = \ln \frac{m_p}{\sqrt{1 + c_p^2}} = 6.888 \quad \xi_p = \sqrt{\ln(1 + c_p^2)} = 0.198$$

hence:

$$40 u_2 + 800 - \exp(0.198 u_1 + 6.888 + \ln 0.496) = 0$$

The calculation gives the following results:

$$\beta = 2.43 \quad \alpha_1 = -0.968 \quad \alpha_2 = 0.252$$

The limit-state is not linear and the probability of failure is approximated only by:

$$P_f \approx \Phi(-\beta) = 7.47 \times 10^{-3}$$

5. *Hasofer-Lind index, lognormal variables.* Let us transform the limit-state:

$$\ln M_R - \ln 0.496 - \ln p = 0$$

$$\lambda_{M_R} = \ln \frac{m_{M_R}}{\sqrt{1 + c_{M_R}^2}} = 6.683 \quad \xi_{M_R} = \sqrt{\ln(1 + c_{M_R}^2)} = 0.050$$

hence:

$$0.050 u_2 + 6.683 - 0.198 u_1 - 6.888 - \ln 0.496 = 0$$

that is, by standardizing:

$$0.245 u_2 - 0.970 u_1 + 2.43 = 0 \implies \beta = 2.43$$

Note that the limit-state is linear in the reduced variable space and therefore:

$$P_f = \Phi(-\beta) = 7.54 \times 10^{-3}$$

3.9.2 Resistance-stress problem

Statement of the problem and the questions

Discrete problem. We consider a failure defined by the limit-state $G(R, S) = R - S$, where the failure events are given by the performance function $G(R, S) = R - S \leq 0$. Note that $R - S = 0$ belongs to the failure domain.

R is the resistance whose simulated outcomes are obtained by throwing two unloaded dice with six sides numbered from 1 to 6 (an outcome r is the sum of the values indicated on the two top sides).

S is the stress whose simulated outcomes are obtained by throwing only one unloaded die, with six sides numbered from 1 to 6 (an outcome s is the value indicated on the top side). The two variables are independent:

1. Calculate the mean and the standard deviation of the random variables R and S .
2. Calculate the exact probability of failure $P_f = \text{Prob}(R - S \leq 0)$.
3. Calculate the Cornell index and the approximation of P_f .

Continuous problem. We will now consider the same problem with continuous random variables R and S . R is a Gaussian variable with mean 7 and standard deviation 2.415. S is a uniform variable between 0.5 and 6.5:

1. Calculate the mean and standard deviation of S .
2. Calculate the Cornell index; deduce an approximate value for P_f .
3. Calculate the exact probability of failure.
4. Give the expression of the limit-state in the centered standardized space by choosing $R \rightarrow U_1$, $S \rightarrow U_2$.
5. Calculate the Hasofer-Lind index β , and deduce an approximate value of P_f .

Solution of the problem

Discrete problem

- Means and standard deviations. The equations used are:

$$m = \frac{1}{N} \sum_{i=1}^N x_i = E[X] \quad \sigma^2 = E[X^2] - (E[X])^2$$

Hence:

$$m_S = 3.5 \quad \sigma_S = 1.708 \quad m_R = 7 \quad \sigma_R = 2.415$$

- Note: the standard deviation σ_R can be deduced from σ_S . In fact, R is the sum of two random variables with the same means (3.5) and the same standard deviation values: (1.708), therefore $\text{var}[R = S + S] = 2 \text{ var}[S] = 2\sigma_S^2$ and then $\sigma_R = \sqrt{2}\sigma_S$.
- Exact probability of failure: this is obtained by considering the following events, which are independent:

$$(S = 1 \cap R \leq 1) \cup (S = 2 \cap R \leq 2) \cup \dots \cup (S = 6 \cap R \leq 6)$$

The probability of $S = i$ ($i = 1, 2, \dots, 6$) is $1/6$, the probabilities $R \leq i$ are respectively $0, 1/36, 3/36, 6/36, 10/36$ and $15/36$ and the probability of failure is then $P_f = 0.162$.

By considering the failure limit-state $R - S < 0$, the probability of failure is $P_f = 0.093$.

- Cornell index and approximation of P_f . By definition:

$$\beta_c = \frac{m_{R-S}}{\sigma_{R-S}} = \frac{m_R - m_S}{\sqrt{\sigma_R^2 + \sigma_S^2}} = 1.183 \quad \Phi(-\beta_c) = 0.118$$

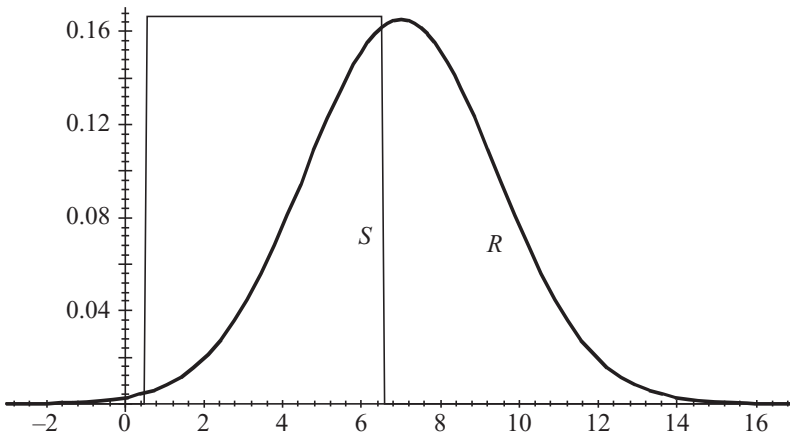


Figure 3.19 Probability densities of S and R .

Continuous problem. The problem is discussed for two variables: resistance R Gaussian $\mathcal{N}(m_R, \sigma_R^2)$ and stress S uniform in $a, b : \mathcal{U}(a, b)$.

- Mean and standard deviation of S :

$$m_S = \frac{b+a}{2} = 3.5 \quad \sigma_S = \frac{b-a}{\sqrt{12}} = \sqrt{3}$$

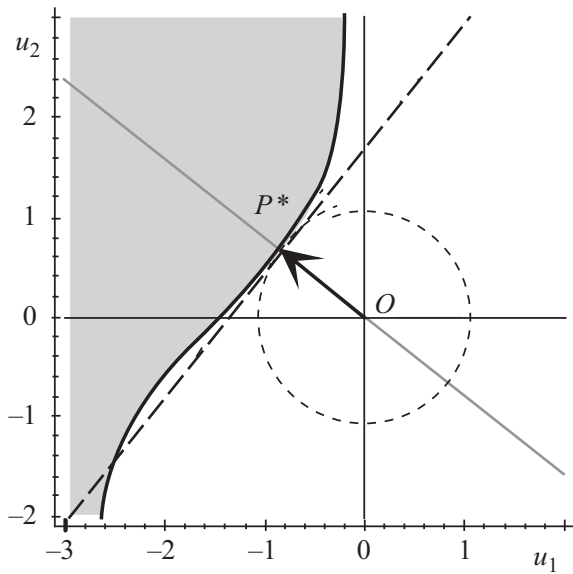


Figure 3.20 Limit-state in standardized variables.

- Cornell index and approximation of P_f :

$$\beta_c = \frac{m_{R-S}}{\sigma_{R-S}} = \frac{m_R - m_S}{\sqrt{\sigma_R^2 + \sigma_S^2}} = 1.178 \quad \Phi(-\beta_c) = 0.119$$

- Exact probability of failure: this is obtained by the equation:

$$P_f = \int_{-\infty}^{\infty} (1 - F_S(x)) f_R(x) dx$$

where $f_R(x)$ is the Gaussian density and $F_S(x)$ is the distribution function of the stress, given by:

$$F_S(x) = \begin{cases} 0 & \text{if } x \leq a \\ (x - a)/(b - a) & \text{if } a < x \leq b \\ 1 & \text{if } x > b \end{cases}$$

Let us assume:

$$u = \frac{x - m_R}{\sigma_R} \quad u_a = \frac{a - m_R}{\sigma_R} \quad u_b = \frac{b - m_R}{\sigma_R}$$

and the integral P_f becomes:

$$\begin{aligned} & \int_{-\infty}^{u_a} (1 - 0)\phi(u) \, du + \int_{u_a}^{u_b} \left(1 - \frac{\sigma_R u + m_R - a}{b - a}\right) \phi(u) \, du \\ & + \int_{u_b}^{\infty} (1 - 1)\phi(u) \, du \\ P_f = \Phi(u_a) + \frac{b - m_R}{b - a}(\Phi(u_b) - \Phi(u_a)) + \frac{\sigma_R}{b - a}(\phi(u_b) - \phi(u_a)) \end{aligned}$$

whose value is $P_f = 0.122$ (which corresponds to $\beta = 1.165$) for the numerical values proposed.

- Limit-state in the standardized space. The expression of $F_S(x)$ was given in the previous section, $F_S^{-1}(x) = (b - a)x + a$ for $a \leq x \leq b$. The transformation of S is then:

$$s = (b - a)\Phi(u_2) + a \quad (3.17)$$

and $r = \sigma_R u_1 + m_R$, hence:

$$H(u_1, u_2) = \sigma_R u_1 + m_R - (b - a)\Phi(u_2) - a = 0$$

Numerical resolution, for the values proposed, gives:

$$\begin{aligned} \beta &= 1.068 \quad u_1^* = -0.836 \quad u_2^* = 0.665 \quad \alpha_1^* = 0.783 \quad \alpha_2^* = -0.622 \\ P_f &\approx \Phi(-\beta) = 0.143 \end{aligned}$$

which illustrates the limited quality of the first-order approximation (17%) in this case, where the curvature of the limit-state is still relatively moderate. This error is no more than 8% for the reliability index, whose logarithmic scale best corresponds to the scale of appreciation of a risk of failure.

Graphical representation. Figure 3.19 represents the probability densities of the stress and resistance variables:

$$f_S(x) = \begin{cases} 0 & \text{if } x \leq 0.5 \\ 1/6 & \text{if } 0.5 < x \leq 6.5 \\ 0 & \text{if } 6.5 < x \end{cases} \quad f_R(x) = \frac{1}{2.415\sqrt{2\pi}} \exp\left(-\frac{1}{2}\left(\frac{x-7}{2.415}\right)^2\right)$$

The limit-state is shown in Figure 3.20 in standardized space. The radius of the circle is β . Variable u_1 is defined from $-\infty$ to $+\infty$, and variable u_2 is defined only for $s \in [a, b]$. The limits are also given by Equation (3.17), that is, $u_2 \in [-\infty, \infty]$.

This page intentionally left blank

Chapter 4

Isoprobabilistic Transformation

The calculation of the reliability index β , according to the definition by Hasofer and Lind [HL74], comprises two essential steps, mentioned in Chapter 3:

- the transformation from physical variable space to standardized, centered and independent variables, which will be discussed in this chapter,
- the calculation of the distance between the origin and the boundary of the limit-state in standardized space, which will be discussed in Chapter 5.

We will describe below a few possible transformations from physical variable space to standardized variable space, depending on the information available on the distributions of random vectors. It must be noted that in the case of independent variables, there is a standard transformation T and that the problem is largely simplified.

4.1 Recapitulation of the problem and the notation

The formulation, which is now classic, of the reliability index β according to Hasofer and Lind's definition assumes a transformation from physical variable space X_i into a space of standardized Gaussian variables U_i .

Suppose that the reliability of a component is defined by the knowledge of a limit-state function $G(X_i) = 0$ of the design variables X_i chosen as random variables. Among the design variables, some are considered to be random; others are considered as deterministic and are called limit-state function parameters. They do not appear explicitly in the notation.

The knowledge of an explicit form of the limit-state function is not necessary; it is enough to have a means to calculate an outcome $G(x_i)$ of G for an outcome x_i of X_i . However, solely implicit knowledge of $G(X_i)$ complicates

the resolution considerably. By convention, we choose:

$$\text{safety domain: } G(X_i) > 0 \quad \text{and failure domain: } G(X_i) \leq 0$$

Lastly, the definition of a limit-state function separating the physical variable domain into two sub-domains, the safety domain and the failure domain, may seem too brutal to be satisfactory. It could be appropriate to consider a more or less large satisfaction zone around the limit-state and the acceptance of a safety state; otherwise a failure state would fall less under binary logic than fuzzy logic, which will not be covered here. However, a positive outcome which is very close to the limit-state, if it is acceptable, is nevertheless penalized by a short distance to the limit-state. If there are a large number of positive outcomes close to the limit-state, this will result in low partial coefficients that do not guarantee the necessary operational safety (Chapter 10).

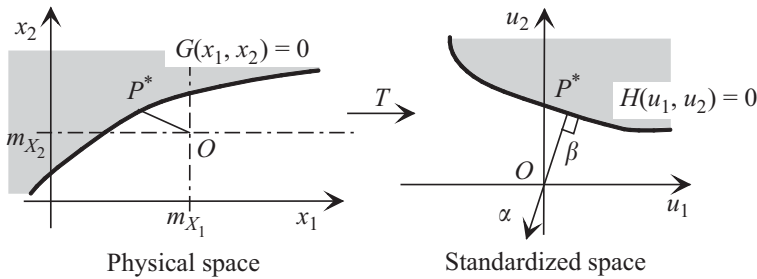


Figure 4.1 Transformation of physical space into standardized space; definition of geometric index.

Hasofer and Lind have shown that the measure of the reliability index must be performed in a standardized Gaussian space. For this, we must define a transformation T , represented in Figure 4.1 as:

$$u_i = T_i(x_j) \quad \text{and} \quad H(u_i) = G(T_j^{-1}(u_i)) \quad (4.1)$$

The reliability index is then the shortest distance between the origin of the space of variables u_i and the domain $H(u_i) \leq 0$, which is expressed in the form of a minimization problem:

$$\beta = \min \left(\sqrt{\{u\}^t \{u\}} \right) \quad \text{under the constraint } H(u_i) \leq 0 \quad (4.2)$$

The methods used to solve this problem are given in Chapter 5. We must then evaluate the probability of failure, which will be discussed in Chapter 7.

Let us first study transformation T by starting with simple cases.

4.2 Case of independent variables

There is independence if the joint density is the product of marginal densities. In this case, it is possible to construct transformation T variable by variable:

$$u_i = T_i(x_i)$$

4.2.1 Gaussian variables

Transformation T

As a first illustration case, consider the case of independent Gaussian variables. The transformation from physical space to standardized space is then immediate:

$$x_i \xrightarrow{T} u_i = \frac{x_i - m_{X_i}}{\sigma_{X_i}}$$

This is a linear transformation which associates a Gaussian distribution for x_i with a Gaussian distribution (with zero mean and unit variance $\mathcal{N}(0, 1)$) for u_i .

Example

Consider the fundamental example of the form (resistance $R = X_1$) – (stress $S = X_2$):

$$G(R, S) = R - S$$

whose expression in standardized space is:

$$H(u_1, u_2) = \sigma_{X_1}u_1 - \sigma_{X_2}u_2 + m_{X_1} - m_{X_2}$$

or:

$$H(u_1, u_2) = \sigma_R u_1 - \sigma_S u_2 + m_R - m_S$$

This is the equation of a straight line Δ whose distance to the origin O is given by the classic equation:

$$d(O, \Delta) = \frac{m_R - m_S}{\sqrt{\sigma_R^2 + \sigma_S^2}} = \beta$$

which corresponds to the result obtained in Chapter 3.

4.2.2 Independent variables

Transformation T

If the variables X_i are *a priori* of any distributions $F_{X_i}(x_i)$, it is possible to express transformation T by writing the equality of probabilities for variables x_i and u_i and hence the *isoprobabilistic transformation*:

$$x_i \xrightarrow{T} u_i \quad \text{defined by: } \Phi(u_i) = F_{X_i}(x_i)$$

and therefore:

$$x_i \xrightarrow{T} u_i = \Phi^{-1}(F_{X_i}(x_i))$$

Reciprocally, if F_{X_i} is invertible for any value of x_i , the inverse transformation is defined as:

$$u_i \xrightarrow{T^{-1}} x_i = F_{X_i}^{-1}(\Phi(u_i))$$

For all distributions, transformations T and T^{-1} can be constructed only numerically, point by point. There are, however, cases where an analytical form can be found.

The equation $\Phi(u_i) = F_{X_i}(x_i)$ for $u_i = 0$ shows that the origin point of standardized space is the image of the *median physical point* and not mean physical point; in fact, $F_{X_i}(x_i \mid u_i = 0) = 1/2$.

Note on the derivation

From:

$$\Phi(u_i) = F_{X_i}(x_i)$$

we have:

$$\begin{aligned} \frac{d\Phi(u_i)}{du_i} du_i &= \frac{dF_{X_i}(x_i)}{dx_i} dx_i \\ \phi(u_i) du_i &= f_{X_i}(x_i) dx_i \end{aligned} \tag{4.3}$$

$$\frac{du_i}{dx_i} = \frac{f_{X_i}(x_i)}{\phi(u_i)} = \frac{f_{X_i}(x_i)}{\phi(\Phi^{-1}(F_{X_i}(x_i)))}$$

Case of lognormal distribution

X_i is a lognormal random variable, with mean m_{X_i} and standard deviation σ_{X_i} ; then $\ln(X_i)$ follows a Gaussian distribution with mean λ_{X_i} and standard deviation ξ_{X_i} , with:

$$\lambda_{X_i} = \ln \left(\frac{m_{X_i}}{\sqrt{1 + c_{X_i}^2}} \right) \quad \text{and} \quad \xi_{X_i} = \sqrt{\ln(1 + c_{X_i}^2)} \quad \text{with } c_{X_i} = \frac{\sigma_{X_i}}{m_{X_i}}$$

and transformation T is then:

$$x_i \xrightarrow{T} u_i = \frac{\ln(x_i) - \lambda_{X_i}}{\xi_{X_i}}$$

Consider as an example another form of the resistance – stress limit-state with $R, S > 0$:

$$G(R, S) = \frac{R}{S} - 1 = 0$$

which can also be written as:

$$\ln R - \ln S = \ln 1 = 0$$

in which R and S are lognormal random variables; hence:

$$\xi_R u_1 - \xi_S u_2 + \lambda_R - \lambda_S = 0$$

where ξ_R and ξ_S respectively represent the standard deviations of the random variables $\ln R$ and $\ln S$, and λ_R and λ_S their means, which gives the index β :

$$\beta = \frac{\lambda_R - \lambda_S}{\sqrt{\xi_R^2 + \xi_S^2}}$$

Another example: E1-max Gumbel distribution

X_i is a random variable with mean m_{X_i} and standard deviation σ_{X_i} , and X_i follows an E1-max Gumbel distribution with parameters a and b ; then:

$$u_i = \Phi^{-1} \left(\exp \left(- \exp \left(- \frac{x_i - b}{a} \right) \right) \right)$$

with $m_{X_i} = f a + b$ where $f = 0.5772156649\dots$ Euler-Mascheroni constant:

$$\sigma_{X_i} = \pi \frac{a}{\sqrt{6}}$$

and:

$$a = \frac{\sqrt{6}}{\pi} \sigma_{X_i} \quad \text{and} \quad b = m_{X_i} - f \frac{\sqrt{6}}{\pi} \sigma_{X_i}$$

The inverse transformation is given by:

$$x_i = b - a \ln \left(- \ln (\Phi(u_i)) \right)$$

As we do not have an explicit form of function Φ , and even less of Φ^{-1} , such expressions must be evaluated numerically. That is why we must proceed in this manner for the various possible distribution functions.

4.3 Rosenblatt transformation

This section deals with dependent variables.

4.3.1 Recapitulation

For a recapitulation of probability concepts, it is useful to consult the book by Radix [Rad91], which presents them by taking into account the problems which are faced more by an engineer than a mathematician.

We denote by $F_{X_1, X_2, \dots, X_n}(x_1, x_2, \dots, x_n)$ the joint distribution function of random variable vector X_i and $f_{X_1, X_2, \dots, X_n}(x_1, x_2, \dots, x_n)$ the joint density function of this vector. The marginal density of sub-vector X_k , $1 \leq k \leq j$, extracted from X_i , $i = 1, n$, is given by:

$$\begin{aligned} & f_{X_1, X_2, \dots, X_j}(x_1, x_2, \dots, x_j) \\ &= \int_{-\infty}^{\infty} \cdots \int_{-\infty}^{\infty} f_{X_1, X_2, \dots, X_n}(x_1, \dots, x_j, t_{j+1}, \dots, t_n) dt_{j+1} \cdots dt_n \end{aligned} \quad (4.4)$$

Similarly, the *conditional density* of vector X_1, \dots, X_j , for fixed X_{j+1}, \dots, X_n , is given by:

$$\begin{aligned} & f_{X_1, X_2, \dots, X_j}(x_1, x_2, \dots, x_j | x_{j+1}, \dots, x_n) \\ &= \frac{f_{X_1, X_2, \dots, X_n}(x_1, x_2, \dots, x_j, x_{j+1}, \dots, x_n)}{f_{X_{j+1}, \dots, X_n}(x_{j+1}, \dots, x_n)} \end{aligned} \quad (4.5)$$

which is a form of the classical equation:

$$\text{Prob}(A | B) = \frac{\text{Prob}(A \cap B)}{\text{Prob}(B)}$$

The *conditional distribution* function is obtained by integrating with respect to non-fixed variables:

$$\begin{aligned} & F_{X_1, X_2, \dots, X_j}(x_1, x_2, \dots, x_j | x_{j+1}, \dots, x_n) \\ &= \frac{\int_{-\infty}^{x_1} \cdots \int_{-\infty}^{x_j} f_{X_1, X_2, \dots, X_n}(t_1, t_2, \dots, t_j, x_{j+1}, \dots, x_n) dt_1 \cdots dt_j}{f_{X_{j+1}, \dots, X_n}(x_{j+1}, \dots, x_n)} \end{aligned}$$

Based on the joint probability density, $f_{X_1, X_2, \dots, X_n}(x_1, x_2, \dots, x_n)$, that we can write for fixed x_1, \dots, x_{n-1} (Equation (4.5)):

$$f_{X_1, X_2, \dots, X_n}(x_1, x_2, \dots, x_n) = f_{X_n}(x_n | x_1, \dots, x_{n-1}) f_{X_1, \dots, X_{n-1}}(x_1, \dots, x_{n-1})$$

and by recurrence:

$$\begin{aligned}
 f_{X_1, X_2, \dots, X_{n-1}}(x_1, x_2, \dots, x_{n-1}) \\
 = f_{X_{n-1}}(x_{n-1} | x_1, \dots, x_{n-2}) f_{X_1, \dots, X_{n-2}}(x_1, \dots, x_{n-2}) \\
 \vdots \\
 f_{X_1, X_2}(x_1, x_2) = f_{X_2}(x_2 | x_1) f_{X_1}(x_1) \\
 f_{X_1}(x_1) = f_{X_1}(x_1)
 \end{aligned}$$

We finally obtain a general form:

$$f_{X_i}(x_i | x_1, \dots, x_{i-1}) = \frac{f_{X_1, X_2, \dots, X_i}(x_1, x_2, \dots, x_i)}{f_{X_1, \dots, X_{i-1}}(x_1, \dots, x_{i-1})} \quad (4.6)$$

which gives the distribution function:

$$F_{X_i}(x_i | x_1, \dots, x_{i-1}) = \frac{\int_{-\infty}^{x_i} f_{X_1, X_2, \dots, X_i}(x_1, x_2, \dots, x_{i-1}, t_i) dt_i}{f_{X_1, \dots, X_{i-1}}(x_1, \dots, x_{i-1})} \quad (4.7)$$

$F_{X_i}(x_i | x_1, \dots, x_{i-1})$ can also be obtained by the integration of the conditional density:

$$F_{X_i}(x_i | x_1, \dots, x_{i-1}) = \int_{-\infty}^{x_i} f_{X_i}(t_i | x_1, \dots, x_{i-1}) dt_i$$

4.3.2 Formulation

When the random variables X_i are independent, the previous results (Section 4.2.2) are used to associate u_i with x_i , *variable by variable*. This is not the case when the variables X_i are dependent. Rosenblatt's [Ros52] transformation provides a solution when the joint distribution function $F_{X_1, X_2, \dots, X_n}(x_1, x_2, \dots, x_n)$ is known, but this is particularly difficult to obtain. This transformation is not unique, as it assumes the choice of an order of variables. Madsen *et al.* [MKL86] believe that the differences are small, except in pathological cases. The choice gives different reliability indexes, but with the same probability of failure, provided we know how to evaluate it accurately. The transformation is written as:

$$x_i \xrightarrow{T} u_i = T_i(x_j)$$

with:

$$\begin{aligned}
 u_1 &= \Phi^{-1}(F_{X_1}(x_1)) \\
 u_2 &= \Phi^{-1}(F_{X_2}(x_2 | x_1)) \\
 &\vdots \\
 u_i &= \Phi^{-1}(F_{X_i}(x_i | x_1, x_2, \dots, x_{i-1})) \\
 &\vdots \\
 u_n &= \Phi^{-1}(F_{X_n}(x_n | x_1, x_2, \dots, x_{n-1}))
 \end{aligned} \tag{4.8}$$

In these expressions, $F_{X_i}(x_i | x_1, x_2, \dots, x_{i-1})$ is the distribution function of X_i conditioned by $X_1 = x_1, X_2 = x_2, \dots, X_{i-1} = x_{i-1}$ (Equation (4.7)).

The inverse transformation is obtained in the same manner:

$$\begin{aligned}
 x_1 &= F_{X_1}^{-1}(\Phi(u_1)) \\
 &\vdots \\
 x_n &= F_{X_n}^{-1}(\Phi(u_n) | x_1, \dots, x_{n-1})
 \end{aligned}$$

These equations include those for independent variables; they must be evaluated numerically in most cases. They require a very full knowledge, as the joint probability density must be estimated while only the marginal distribution and the correlation are accessible in most cases. It should be noted that this is sufficient for vectors of Gaussian or lognormal variables.

Section 4.3.4 gives an example of a non-Gaussian pair for which the calculation is performed analytically.

Jacobian transformation

We note $[\partial u_i / \partial x_l]$ the Jacobian matrix of the Rosenblatt transformation. u_i depends only on variables x_1 to x_i , $\partial u_i / \partial x_l = 0$ if $l > i$; the matrix is lower triangular and its determinant is the product of the diagonal elements. Each diagonal element is given by Equation (4.3):

$$\frac{du_i}{dx_i} = \frac{f_{X_i}(x_i | x_1, \dots, x_{i-1})}{\phi(u_i)} = \frac{f_{X_i}(x_i | x_1, \dots, x_{i-1})}{\phi(\Phi^{-1}(F_{X_i}(x_i | x_1, \dots, x_{i-1})))} \tag{4.9}$$

Point P^*

By definition, coordinates u_k^* are given by:

$$u_k^* = \max_{\mathcal{D}_{f\text{-standardized}}} \phi_n(u_k) = \max_{\mathcal{D}_{f\text{-standardized}}} \phi(u_1) \cdots \phi(u_n)$$

which gives, when passing into physical space:

$$\begin{aligned} x_k^* &= \max_{\mathcal{D}_{f-\text{physical}}} f_{X_1}(x_1) \cdots f_{X_n}(x_n | x_1, \dots, x_{n-1}) \frac{dx_1}{du_1} \cdots \frac{dx_n}{du_n} \\ x_k^* &= \max_{\mathcal{D}_{f-\text{physical}}} f_{X_1, \dots, X_n}(x_1, \dots, x_n) \det [\partial x_m / \partial u_l] \end{aligned}$$

which shows that point P^* is not at the maximum of the probability density in physical space, owing to the presence of the Jacobian.

4.3.3 Calculation of P_f

The probability of failure is given by the equation:

$$P_f = \int_{\mathcal{D}_{f-\text{physical}}} f_{X_1, \dots, X_n}(x_1, \dots, x_n) dx_1 \cdots dx_n$$

in which the change of variable $u_i = T_i(x_1, \dots, x_n)$ is performed.

The Rosenblatt transformation decomposes the joint density into a product of conditional densities:

$$P_f = \int_{\mathcal{D}_{f-\text{physical}}} f_{X_1}(x_1) f_{X_2}(x_2 | x_1) \cdots f_{X_n}(x_n | x_1, \dots, x_{n-1}) dx_1 \cdots dx_n$$

and then transforms the variables:

$$\Phi(u_i) = F_{X_i}(x_i | x_1, \dots, x_{i-1}), \quad i = 1, \dots, n$$

By differentiating, according to Equation (4.9), we have:

$$\phi(u_i) du_i = f_{X_i}(x_i | x_1, \dots, x_{i-1}) dx_i, \quad i = 1, \dots, n$$

and therefore:

$$\begin{aligned} P_f &= \int_{\mathcal{D}_{f-\text{standardized}}} \phi(u_1) \cdots \phi(u_n) du_1 \cdots du_n \\ &= \int_{\mathcal{D}_{f-\text{standardized}}} \phi_n(u_k) du_1 \cdots du_n \end{aligned}$$

4.3.4 Example: double exponential

A classic illustration [Dol83] is presented in various forms [AT84, MKL86, DM96]. Consider two random variables X_1 and X_2 whose joint distribution function is given by an exponential distribution:

$$\begin{aligned} F_{X_1, X_2}(x_1, x_2) &= 1 - e^{-x_1} - e^{-x_2} + e^{-(x_1+x_2+\theta x_1 x_2)} \\ \text{with } x_1 &\geq 0 \quad \text{and} \quad x_2 \geq 0, \quad \theta = \text{constant} \end{aligned}$$

The joint probability density is then obtained by deriving twice, with respect to x_1 and then to x_2 :

$$f_{X_1, X_2}(x_1, x_2) = (1 - \theta(1 - x_1 - x_2) + \theta^2 x_1 x_2) e^{-(x_1 + x_2 + \theta x_1 x_2)}$$

and the marginal densities are respectively:

$$f_{X_1}(x_1) = e^{-x_1} \quad \text{and} \quad f_{X_2}(x_2) = e^{-x_2}$$

Demonstration – The marginal density:

$$f_{X_1}(x_1) = \int_0^\infty f_{X_1, X_2}(x_1, x_2) dx_2$$

is obtained by integration by parts. That is:

$$f_{X_1}(x_1) = \int_0^\infty (1 - \theta + \theta x_1 + x_2(\theta + \theta^2 x_1)) e^{(-x_1 + x_2(-1 - \theta x_1))} dx_2$$

Assuming:

$$\begin{aligned} A &= \theta + \theta^2 x_1 \\ B &= 1 - \theta + \theta x_1 \\ C &= -1 - \theta x_1 \\ D &= -x_1 \end{aligned}$$

we have:

$$\begin{aligned} f_{X_1}(x_1) &= \int_0^\infty (A x_2 + B) e^{C x_2 + D} dx_2 \quad \theta \geq 0 \quad C < 0 \\ &= \left[(A x_2 + B) \frac{e^{C x_2 + D}}{C} \right]_0^\infty - \int_0^\infty \frac{e^{C x_2 + D}}{C} A dx_2 \\ &= \left[\left[\frac{A x_2 + B}{C} - \frac{A}{C^2} \right] e^{C x_2 + D} \right]_0^\infty \end{aligned}$$

By replacing and simplifying, we have:

$$f_{X_1}(x_1) = e^{-x_1}$$

The distribution function is then:

$$F_{X_1}(x_1) = 1 - e^{-x_1}$$

and:

$$F_{X_2}(x_2 | x_1) = \frac{\int_0^{x_2} f_{X_1, X_2}(x_1, t_2) dt_2}{f_{X_1}(x_1)} = \frac{e^{-x_1} - (1 + \theta x_2)e^{-(x_1+x_2+\theta x_1 x_2)}}{e^{-x_1}}$$

$$F_{X_2}(x_2 | x_1) = 1 - (1 + \theta x_2)e^{-(x_2+\theta x_1 x_2)}$$

and finally, the transformation is written as:

$$u_1 = \Phi^{-1}(1 - e^{-x_1}) \quad \text{and} \quad u_2 = \Phi^{-1}(1 - (1 + \theta x_2)e^{-(x_2+\theta x_1 x_2)})$$

A second solution is obtained by permuting the indexes. The consequences of the choice of order are examined in detail in Section 7.7.5.

If θ is equal to 0, the two variables are uncorrelated; the value $\theta \neq 0$ expresses a correlation. If $\theta = 1$, the correlation coefficient is $\rho = -0.40$ [AT84].

4.3.5 A warning about notation!

The notation U is reserved for standardized (unit variance), centered (zero mean) and independent Gaussian variables $\mathcal{N}(0, 1)$. Intermediate steps introduce other variables. The transformation:

$$\hat{U} = \frac{X - m_X}{\sigma_X}$$

introduces variables that are standardized and centered but dependent and with *a priori* non-Gaussian distributions if X is non-Gaussian.

4.3.6 Gaussian variable couple

Let X_1 and X_2 be a Gaussian variable couple with means $m_{X_1} = m_1$ and $m_{X_2} = m_2$ and standard deviations $\sigma_{X_1} = \sigma_1$ and $\sigma_{X_2} = \sigma_2$. The correlation coefficient is $\rho_{X_1 X_2} = \rho$, $|\rho| < 1$, and the joint probability density is then:

$$f_{X_1, X_2}(x_1, x_2) \\ = k \exp \left(- \frac{\left(\frac{x_1 - m_1}{\sigma_1} \right)^2 - 2\rho \left(\frac{x_1 - m_1}{\sigma_1} \frac{x_2 - m_2}{\sigma_2} \right) + \left(\frac{x_2 - m_2}{\sigma_2} \right)^2}{2(1 - \rho^2)} \right)$$

with:

$$k = \frac{1}{2\pi \sigma_1 \sigma_2 \sqrt{1 - \rho^2}}$$

Let us transform the variables:

$$\hat{u}_1 = \frac{x_1 - m_1}{\sigma_1} \quad \text{and} \quad \hat{u}_2 = \frac{x_2 - m_2}{\sigma_2}$$

whose Jacobian is:

$$\begin{bmatrix} \frac{1}{\sigma_1} & 0 \\ 0 & \frac{1}{\sigma_2} \end{bmatrix}$$

hence:

$$f_{\hat{U}_1, \hat{U}_2}(\hat{u}_1, \hat{u}_2) = \frac{1}{2\pi\sqrt{1-\rho^2}} \exp\left(-\frac{1}{2(1-\rho^2)}(\hat{u}_1^2 - 2\rho\hat{u}_1\hat{u}_2 + \hat{u}_2^2)\right)$$

Let us first calculate $f_{\hat{U}_1}(\hat{u}_1)$ [Rad91]:

$$f_{\hat{U}_1}(\hat{u}_1) = \int_{-\infty}^{\infty} f_{\hat{U}_1, \hat{U}_2}(\hat{u}_1, t_2) dt_2 = \frac{1}{\sqrt{2\pi}} e^{-\frac{1}{2}\hat{u}_1^2} = \phi(\hat{u}_1)$$

and similarly:

$$f_{\hat{U}_2}(\hat{u}_2) = \int_{-\infty}^{\infty} f_{\hat{U}_1, \hat{U}_2}(t_1, \hat{u}_2) dt_1 = \frac{1}{\sqrt{2\pi}} e^{-\frac{1}{2}\hat{u}_2^2} = \phi(\hat{u}_2)$$

We then obtain:

$$F_{\hat{U}_1}(\hat{u}_1) = \int_{-\infty}^{\hat{u}_1} \phi(t_2) dt_2 = \Phi(\hat{u}_1)$$

and for $f_{\hat{U}_2}(\hat{u}_2 | \hat{u}_1)$, Equation (4.6):

$$f_{\hat{U}_2}(\hat{u}_2 | \hat{u}_1) = \frac{\frac{1}{2\pi\sqrt{1-\rho^2}} \exp\left(-\frac{1}{2(1-\rho^2)}(\hat{u}_1^2 - 2\rho\hat{u}_1\hat{u}_2 + \hat{u}_2^2)\right)}{\frac{1}{\sqrt{2\pi}} e^{-\frac{1}{2}\hat{u}_1^2}}$$

$$f_{\hat{U}_2}(\hat{u}_2 | \hat{u}_1) = \frac{1}{\sqrt{2\pi}\sqrt{1-\rho^2}} \exp\left(-\frac{1}{2}\left(\frac{\hat{u}_2 - \rho\hat{u}_1}{\sqrt{1-\rho^2}}\right)^2\right)$$

where $(\hat{u}_2 - \rho\hat{u}_1)/\sqrt{1-\rho^2}$ has zero mean and unit standard deviation; hence:

$$F_{\hat{U}_2}(\hat{u}_2 | \hat{u}_1) = \int_{-\infty}^{\hat{u}_2} f_{\hat{U}_2}(t_2 | \hat{u}_1) dt_2 = \Phi\left(\frac{\hat{u}_2 - \rho\hat{u}_1}{\sqrt{1-\rho^2}}\right)$$

and the Rosenblatt transformation is written as:

$$u_1 = \hat{u}_1 = \frac{x_1 - m_1}{\sigma_1} \quad \text{and} \quad u_2 = \frac{\hat{u}_2 - \rho\hat{u}_1}{\sqrt{1-\rho^2}} = \frac{1}{\sqrt{1-\rho^2}}\left(\frac{x_2 - m_2}{\sigma_2} - \rho\frac{x_1 - m_1}{\sigma_1}\right)$$

Note that the Rosenblatt transformation matrix is the lower matrix of the Cholesky decomposition of the correlation matrix in the form:

$$\begin{aligned} [\rho] = [L][L]^t &\implies \begin{bmatrix} 1 & \rho \\ \rho & 1 \end{bmatrix} = \begin{bmatrix} 1 & 0 \\ \rho & \sqrt{1-\rho^2} \end{bmatrix} \begin{bmatrix} 1 & \rho \\ 0 & \sqrt{1-\rho^2} \end{bmatrix} \\ (\hat{u}_1) &= \begin{bmatrix} 1 & 0 \\ \rho & \sqrt{1-\rho^2} \end{bmatrix} (u_1) \\ (u_1) &= [L]^{-1} (\hat{u}_1) \quad [L]^{-1} = \begin{bmatrix} 1 & 0 \\ -\rho & \frac{1}{\sqrt{1-\rho^2}} \\ \sqrt{1-\rho^2} & \frac{1}{\sqrt{1-\rho^2}} \end{bmatrix} \end{aligned}$$

This equation can be generalized: if \hat{U} is a vector of centered, standardized and correlated Gaussian variables, then:

$$\text{if } [\rho] = [L][L]^t \quad \{U\} = [L]^{-1}\{\hat{U}\} \quad (4.10)$$

is a vector of centered, standard and uncorrelated Gaussian variables.

Note: it is easy to verify that the following four expressions of $[L]$:

$$\begin{array}{ccc} \begin{bmatrix} 1 & 0 \\ \rho & \sqrt{1-\rho^2} \end{bmatrix} & \begin{bmatrix} 1 & 0 \\ \rho & -\sqrt{1-\rho^2} \end{bmatrix} & \begin{bmatrix} -1 & 0 \\ -\rho & \sqrt{1-\rho^2} \end{bmatrix} \\ & \begin{bmatrix} -1 & 0 \\ -\rho & -\sqrt{1-\rho^2} \end{bmatrix} & \end{array}$$

are also solutions of $[\rho] = [L][L]^t$. They give four transformations having the same reliability index but not the same direction cosines. As indicated above, the only one we must choose is the first; that is, the positive square root of the Cholesky decomposition.

4.4 Approximation using a normal distribution

4.4.1 Principle

The Rosenblatt transformation gives a solution to the decomposition and standardization of a random variable vector when the joint probability density is known. However, most of the time we have only a very small amount of information, which is made up of:

- the marginal distribution of each random variable $F_{X_i}(x_i)$, and therefore
 - the mean m_{X_i} of X_i ,
 - the standard deviation σ_{X_i} of X_i ,
- the correlation coefficients $\rho_{X_i X_j}$ of variables X_i, X_j .

Approximation using a normal distribution is based on the search, *point by point*, for the mean $m_{X_i}^N$ and the standard deviation $\sigma_{X_i}^N$ of the normal distribution for which the functions Φ and $F_{X_i}(x_i)$ have the same values at the point under consideration.

In such methods, the marginal density of each component of vector X can be unrestricted and can involve statistical moments at an order as high as possible. On the other hand, the statistical equation between the components is limited to the first mixed moment, the moment of order 2 (covariance or correlation). The high-order equations are unknown, since the information that would help to take them into account is generally unknown.

4.4.2 Uncorrelated variables

The equivalent normal distribution is obtained by writing the equality between the values of the distribution functions at the point in question:

$$\text{equality of distribution functions: } \Phi\left(\frac{x_i - m_{X_i}^N}{\sigma_{X_i}^N}\right) = F_{X_i}(x_i)$$

and, by deriving with respect to x_i :

$$\frac{1}{\sigma_{X_i}^N} \phi\left(\frac{x_i - m_{X_i}^N}{\sigma_{X_i}^N}\right) = f_{X_i}(x_i)$$

From these two equations, we deduce the unknowns $m_{X_i}^N$ and $\sigma_{X_i}^N$:

$$\sigma_{X_i}^N = \frac{\phi(\Phi^{-1}(F_{X_i}(x_i)))}{f_{X_i}(x_i)} \quad m_{X_i}^N = x_i - \sigma_{X_i}^N \Phi^{-1}(F_{X_i}(x_i)) \quad (4.11)$$

Example: lognormal distribution

By using the equations of lognormal distribution, we obtain:

$$F_{X_i}(x_i) = \Phi\left(\frac{\ln x_i - \lambda_{X_i}}{\xi_{X_i}}\right) \implies \sigma_{X_i}^N = x_i \xi_{X_i} \quad \text{and} \quad m_{X_i}^N = x_i(1 - \ln x_i + \lambda_{X_i})$$

4.4.3 Correlated variables

Let X_i and X_j be two correlated variables characterized by their covariance. Let us express this covariance as:

$$\text{cov} [X_i, X_j] = \mathbb{E} [X_i X_j] - \mathbb{E} [X_i] \mathbb{E} [X_j]$$

Let us perform the transformation necessary to center and standardize the variables:

$$\hat{U}_i = \frac{X_i - m_{X_i}^N}{\sigma_{X_i}^N} \quad (4.12)$$

where the notation \hat{u}_i indicates that the variable is standardized and centered, but underlines that vector \hat{u}_k is not uncorrelated and furthermore that it is not Gaussian. Hence:

$$\begin{aligned} \text{cov}[X_i, X_j] &= \mathbb{E} \left[\left(\sigma_{X_i}^N \hat{U}_i + m_{X_i}^N \right) \left(\sigma_{X_j}^N \hat{U}_j + m_{X_j}^N \right) \right] - m_{X_i}^N m_{X_j}^N \\ \text{cov}[X_i, X_j] &= \sigma_{X_i}^N \sigma_{X_j}^N \mathbb{E} [\hat{U}_i \hat{U}_j] + m_{X_i}^N \mathbb{E} [\hat{U}_j] + m_{X_j}^N \mathbb{E} [\hat{U}_i] \\ &\quad + m_{X_i}^N m_{X_j}^N - m_{X_i}^N m_{X_j}^N \end{aligned}$$

Variables \hat{U}_i and \hat{U}_j have zero means and the expression can be written as:

$$\text{cov} [X_i, X_j] = \sigma_{X_i}^N \sigma_{X_j}^N \mathbb{E} [\hat{U}_i \hat{U}_j] = \sigma_{X_i}^N \sigma_{X_j}^N \rho_{ij}$$

where ρ_{ij} is the correlation coefficient of variables X_i and X_j . This equation is in fact the definition of the correlation.

The application of the transformation by equivalent Gaussian variables leads to \hat{U}_i variables with zero mean, unit standard deviation and correlation coefficients $\text{cor}[X_i, X_j]$. In general, it is this matrix that forms the data on variable dependence. For a n -dimensional random vector X_i , there is therefore an n -dimensional correlation matrix notated $[C_{\hat{U}}]$ whose element is $\text{cor}[X_i, X_j]$. A new transformation is then necessary to switch into the eigencoordinates of $[C_{\hat{U}}]$.

This matrix is symmetric and positive defined. It possesses n eigenvalues λ_i arranged in the diagonal matrix $[\lambda]$. A set of eigenvectors R_i defines the transformation of coordinates $[R]$

$$[R] = [\{R_i\}, i = 1, n] \quad \text{such that} \quad [R]^t [C_{\hat{U}}] [R] = [\lambda].$$

A set of *uncorrelated* variables \tilde{U}_i , but with *non-unit standard deviations*, is obtained by shifting into the main axes:

$$\{\tilde{U}\} = [R]^t \{\hat{U}\}$$

This last transformation does not retain standardization, as the covariance matrix of \tilde{U}_i is written as:

$$\begin{aligned} [C_{\tilde{U}}] &= E[\{\tilde{U}\}\{\tilde{U}\}^t] = E[[R]^t \{\hat{U}\}\{\hat{U}\}^t [R]] \\ &= [R]^t E[\{\hat{U}\}\{\hat{U}\}^t] [R] = [R]^t [C_{\hat{U}}] [R] \end{aligned} \quad (4.13)$$

$$[C_{\tilde{U}}] = [\lambda] = [\sigma_{\tilde{U}}]^t [\sigma_{\tilde{U}}] \quad (4.14)$$

where $[\sigma_{\tilde{U}}]$ is the diagonal matrix of standard deviations of \tilde{U}_i . Finally:

$$\begin{aligned} \{U\} &= T(\{X\}) = [\sigma_{\tilde{U}}]^{-1} \{\tilde{U}\} = [\sigma_{\tilde{U}}]^{-1} [R]^t \{\hat{U}\} \\ &= [\sigma_{\tilde{U}}]^{-1} [R]^t [\sigma_X^N]^{-1} (\{X\} - \{m_X^N\}) \end{aligned}$$

and:

$$\{X\} = T^{-1}(\{U\}) = [\sigma_X^N] [R] [\sigma_{\tilde{U}}] \{U\} + \{m_X^N\} \quad (4.15)$$

which forms the necessary transformation T .

4.5 Nataf transformation

As with approximation using a normal distribution (see Section 4.4.1), the Nataf transformation [Nat62] requires only to know the means m_{X_i} , the standard deviations σ_{X_i} , the correlation matrix $\rho_{X_i X_j} = \rho_{ij}$ and the marginal distributions of X_i . Der Kiureghian and Liu [DKL86] have suggested, in this case, the use of such a transformation.

4.5.1 Two random variables

First consider two correlated random variables X_1 and X_2 . The marginal functions $F_{X_i}(x_i)$ are known, \hat{U}_1 and \hat{U}_2 are standard and normal, but correlated, variables, obtained by the transformation:

$$\hat{u}_i = \Phi^{-1}(F_{X_i}(x_i)) \quad i = 1, 2. \quad (4.16)$$

According to Nataf, we can associate a joint density function with variables X_1 and X_2 , knowing that variables \hat{U}_1 and \hat{U}_2 have a normal joint distribution, by the following equation:

$$f_{X_1, X_2}(x_1, x_2) = \phi_2(\hat{u}_1, \hat{u}_2, \rho_{0,12}) \frac{f_{X_1}(x_1) f_{X_2}(x_2)}{\phi(\hat{u}_1) \phi(\hat{u}_2)} \quad (4.17)$$

where $f_{X_i}(x_i) = dF_{X_i}(x_i)/dx_i$ and $\phi_2(\hat{u}_1, \hat{u}_2, \rho_{0,12})$ is the 2-dimensional normal density, with zero means, unit standard deviations and correlation $\rho_{0,12}$:

$$\phi_2(\hat{u}_1, \hat{u}_2, \rho_{0,12}) = \frac{1}{2\pi\sqrt{1-\rho_{0,12}^2}} \exp \left[-\frac{\hat{u}_1^2 - 2\rho_{0,12}\hat{u}_1\hat{u}_2 + \hat{u}_2^2}{2(1-\rho_{0,12}^2)} \right]$$

The equation between $\rho_{0,12}$ and ρ_{12} is obtained from the definition of the correlation. We can express $\rho_{0,12}$ as a function of the marginal densities of X_i . First consider the left-hand side of Equation (4.17):

$$\int_{-\infty}^{\infty} \int_{-\infty}^{\infty} \frac{x_1 - m_{X_1}}{\sigma_{X_1}} \frac{x_2 - m_{X_2}}{\sigma_{X_2}} f_{X_1, X_2}(x_1, x_2) dx_1 dx_2 = \rho_{12}$$

Then let us apply the same operation to the right-hand side:

$$\rho_{12} = \int_{-\infty}^{\infty} \int_{-\infty}^{\infty} \frac{x_1 - m_{X_1}}{\sigma_{X_1}} \frac{x_2 - m_{X_2}}{\sigma_{X_2}} \phi_2(\hat{u}_1, \hat{u}_2, \rho_{0,12}) \frac{f_{X_1}(x_1) f_{X_2}(x_2)}{\phi(\hat{u}_1) \phi(\hat{u}_2)} dx_1 dx_2$$

and, by introducing the equation between $d\hat{u}_i$ and dx_i (Equation (4.16)), $dx_i = \phi(\hat{u}_i)/f_{X_i}(x_i) d\hat{u}_i$, we have:

$$\rho_{12} = \int_{-\infty}^{\infty} \int_{-\infty}^{\infty} \frac{x_1(\hat{u}_1) - m_{X_1}}{\sigma_{X_1}} \frac{x_2(\hat{u}_2) - m_{X_2}}{\sigma_{X_2}} \phi_2(\hat{u}_1, \hat{u}_2, \rho_{0,12}) d\hat{u}_1 d\hat{u}_2 \quad (4.18)$$

This equation thus determines the correlation coefficient $\rho_{0,12}$ to be used. According to the authors, the model presented is applicable if:

1. the search for \hat{u}_i is carried out one at a time; this is possible if all the marginal distribution functions are known and are strictly increasing,
2. the values of $\rho_{0,12}$ range between -1 and 1 , which is not always verified insofar as $\rho_{0,12}$ is a dummy correlation.

The difference between $\rho_{0,12}$ and ρ_{12} is small for most of the distribution functions, and in most practical conditions the second condition is satisfied.

4.5.2 Calculation of the correlation $\rho_{0,ij}$

The use of Equation (4.18) is delicate and the authors [DKL86] have introduced a semi-empirical equation between the correlation coefficients to make the calculation easier:

$$f = \frac{\rho_{0,ij}}{\rho_{ij}}$$

In the above equation, for 2 r.v. X_i and X_j of correlation ρ_{ij} , f has the following properties:

- f in general depends on ρ_{ij} and on the parameters of the two marginal distributions,

- $f \geq 1$ for arbitrary values of ρ_{ij} and marginal distributions of any type,
 - f is independent of ρ_{ij} if one of the variables is normal,
 - f is invariant for linear transformations of X_i and X_j ,
 - further, based on the last property, for distribution functions with two parameters, f is independent of the distribution of parameters X_i if the distribution is reducible to the standard form by a linear transformation.
- If not, f is a function of the coefficient of variation:

$$c_{X_i} = \sigma_{X_i}/m_{X_i}$$

Distributions that are reducible to the standard form by a linear transformation are called Group I distributions (Uniform, Exponential, Rayleigh, E1-max and E1-min). Group II distributions, studied by Der Kiureghian *et al.*, cannot be brought down to the standard form by a linear transformation (lognormal, Gamma, extreme type II, extreme type III (Weibull)).

Der Kiureghian *et al.* show how to apply this transformation, and give the tables to evaluate f according to the distributions and their parameters, such that it is not necessary to evaluate the exact expression. Five categories are proposed:

1. f is constant if X_i is normal and X_j follows a distribution of Group I,
2. $f = f(c_{X_j})$ if X_i is normal and X_j follows a distribution of Group II,
3. $f = f(\rho_{ij})$ if X_i and X_j follow distributions of Group I,
4. $f = f(\rho_{ij}, c_{X_j})$ if X_i follows a distribution of Group I and X_j follows a distribution of Group II,
5. $f = f(\rho_{ij}, c_{X_i}, c_{X_j})$ if X_i and X_j follow distributions of Group II.

The formulae for calculating f have been developed based on polynomial expressions obtained from the exact results given by Equation (4.18). The values of variation coefficients used to calculate the values of f for categories (2), (4) and (5) range between 0.1 and 0.5. Outside this domain, errors can be greater.

Tables 4.1, 4.2, 4.3, 4.4 and 4.5 give the values of f and of the maximum error according to the categories described.

Distribution	f	Error (%)
Uniform	1.023	0.0
Exponential	1.107	0.0
Rayleigh	1.014	0.0
E1-max	1.031	0.0
E1-min	1.031	0.0

Table 4.1 Category (1): $f = \text{constant}$, X_i normal and X_j distribution of Group I.

Distribution	f	Error (%)
Lognormal	$c_{X_j} / \sqrt{\ln(1 + c_{X_j}^2)}$	Exact
Gamma	$1.001 - 0.007 c_{X_j} + 0.118 c_{X_j}^2$	0.0
E2-max	$1.030 + 0.238 c_{X_j} + 0.364 c_{X_j}^2$	0.1
E3	$1.031 - 0.195 c_{X_j} + 0.328 c_{X_j}^2$	0.1

Table 4.2 Category (2): $f = f(c_{X_j})$, X_i normal and X_j distribution of Group II.

Distribution	Uniform	Exponential	E1-max
Uniform	$1.047 - 0.047 \rho^2$ (0.0%)		
Exponential	$1.133 + 0.029 \rho^2$ (0.0%)	$1.229 - 0.367 \rho$ $+0.153 \rho^2$ (1.5%)	
E1-max	$1.055 + 0.015 \rho^2$ (0.0%)	$1.142 - 0.154 \rho$ $+0.031 \rho^2$ (0.2%)	$1.064 - 0.069 \rho$ $+0.005 \rho^2$ (0.0%)

Table 4.3 Category (3): $f = f(\rho_{ij} = \rho)$, X_i and X_j distributions of Group I.

One of the advantages of this transformation is that the reliability index is invariant, depending on the order chosen to perform the transformation.

4.5.3 Generalization to n variables

The generalization to n variables is simple. We must define the unit centered normal variables $\hat{U} = (\hat{U}_1, \dots, \hat{U}_n)$, which are correlated two by two.

The joint density model is then:

$$f_{\{X\}}(\{x\}) = \phi_n(\{\hat{u}\}, [\rho_0]) \frac{f_{X_1}(x_1) \cdots f_{X_n}(x_n)}{\phi(\hat{u}_1) \cdots \phi(\hat{u}_n)}$$

where $\phi_n(\{\hat{u}\}, [\rho_0])$ is the n -dimensional (multinormal) joint probability function and $[\rho_0]$ is the matrix of correlation coefficients. The elements of $[\rho_0]$ are obtained from the equation for two variables (Equation (4.18)) or from the tables given by Der Kiureghian, depending on the marginal distributions and the correlation coefficient.

Distribution	Uniform
Lognormal	$1.019 + 0.014c_{X_j}$ + $0.010\rho^2 + 0.249c_{X_j}^2$ (0.7%)
Gamma	$1.023 - 0.007c_{X_j}$ + $0.002\rho^2 + 0.127c_{X_j}^2$ (0.1%)
E3	$1.061 - 0.237c_{X_j}$ - $0.005\rho^2 + 0.379c_{X_j}^2$ (0.5%)
Exponential	
Lognormal	$1.098 + 0.003\rho + 0.019c_{X_j}$ + $0.025\rho^2 + 0.303c_{X_j}^2 - 0.437\rho c_{X_j}$ (1.6%)
Gamma	$1.104 + 0.003\rho - 0.008c_{X_j}$ + $0.014\rho^2 + 0.173c_{X_j}^2 - 0.296\rho c_{X_j}$ (0.9%)
E3	$1.147 + 0.145\rho - 0.271c_{X_j}$ + $0.010\rho^2 + 0.459c_{X_j}^2 - 0.467\rho c_{X_j}$ (0.4%)
E1-max	
Lognormal	$1.029 + 0.001\rho + 0.014c_{X_j}$ + $0.004\rho^2 + 0.233c_{X_j}^2 - 0.197\rho c_{X_j}$ (0.3%)
Gamma	$1.031 + 0.001\rho - 0.007c_{X_j}$ + $0.003\rho^2 + 0.131c_{X_j}^2 - 0.132\rho c_{X_j}$ (0.3%)
E3	$1.064 + 0.065\rho - 0.210c_{X_j}$ + $0.003\rho^2 + 0.356c_{X_j}^2 - 0.211\rho c_{X_j}$ (0.2%)

Table 4.4 Category (4): $f = f(\rho_{ij}, c_{X_j})$, X_i Group I and X_j Group II.

Distribution	Lognormal
Lognormal	$\frac{\ln(1 + \rho c_{X_i} c_{X_j})}{\rho \sqrt{\ln(1 + c_{X_i}^2) \ln(1 + c_{X_j}^2)}}$ (exact)
Gamma	$1.001 + 0.033\rho + 0.004c_{X_i} - 0.016c_{X_j}$ $+ 0.002\rho^2 + 0.223c_{X_i}^2 + 0.130c_{X_j}^2$ $- 0.104\rho c_{X_i} + 0.029c_{X_i}c_{X_j} - 0.119\rho c_{X_j}$ (4.0%)
E3	$1.031 + 0.052\rho + 0.011c_{X_i} - 0.210c_{X_j}$ $+ 0.002\rho^2 + 0.220c_{X_i}^2 + 0.350c_{X_j}^2$ $+ 0.005\rho c_{X_i} + 0.009c_{X_i}c_{X_j} - 0.174\rho c_{X_j}$ (2.4%)
	Gamma
Gamma	$1.002 + 0.022\rho - 0.012(c_{X_i} + c_{X_j})$ $+ 0.001\rho^2 + 0.125(c_{X_i}^2 + c_{X_j}^2)$ $- 0.077\rho(c_{X_i} + c_{X_j}) + 0.014c_{X_i}c_{X_j}$ (4.0%)
E3	$1.032 + 0.034\rho - 0.007c_{X_i} - 0.202c_{X_j}$ $+ 0.121c_{X_i}^2 + 0.339c_{X_j}^2$ $- 0.006\rho c_{X_i} + 0.003c_{X_i}c_{X_j} - 0.111\rho c_{X_j}$ (4.0%)
	E3
E3	$1.063 - 0.004\rho - 0.200(c_{X_i} + c_{X_j})$ $- 0.001\rho^2 + 0.337(c_{X_i}^2 + c_{X_j}^2)$ $+ 0.007\rho(c_{X_i} + c_{X_j}) - 0.007c_{X_i}c_{X_j}$ (2.6%)

Table 4.5 Category (5): $f = f(\rho_{ij}, c_{X_i}, c_{X_j})$, X_i and X_j distribution of Group II.

The model is valid if every marginal distribution is (a) continuous and strictly increasing and (b) if matrix $[\rho_0]$ is positive defined.

Condition (b) requires that $|\rho_{0,ij}|$ is strictly less than 1 for any $i \neq j$. It is satisfied for most practical cases.

The transformation into independent variables is then written as:

$$u_i = T_i(x_j) = \sum_j \Gamma_{0,ij} \hat{u}_j = \sum_j \Gamma_{0,ij} \Phi^{-1}(F_{X_j}(x_j)) \quad (4.19)$$

where $[\Gamma_0] = [L]^{-1}$ (Equation (4.10)) is the inverse of the lower triangular matrix of the Cholesky decomposition of $[\rho_0]$. For non-normal variables, the transformation is non-linear.

4.6 Example: correlated loads on a beam

This example illustrates the results obtained in this chapter for the decorrelation of variables. Consider a simply supported beam, Figure 4.2, subjected to two concentrated loads P and Q placed respectively at $l/3$ and $2l/3$. These loads are the only random data. They are Gaussian, with means m_P and m_Q and standard deviations σ_P and σ_Q . They are correlated and the correlation coefficient is ρ . The other deterministic data are the length l and the plastic bending moment resistance M_P .

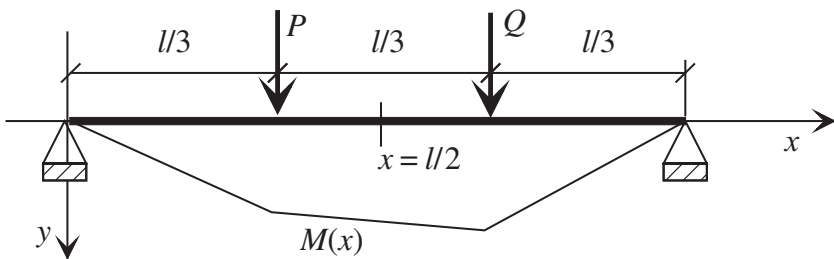


Figure 4.2 Beam on two supports subjected to two random loads.

4.6.1 Limit-state and design

The resistance R is the moment M_P and the bending moment is the internal stress S . Limiting ourselves to the section located at $l/2$, even though it is not the most critical in all cases, the limit-state is:

$$M_P - \frac{(P + Q)l}{6}$$

Design is performed for the chosen characteristic values P_k and Q_k , equal to the mean increased by two standard deviations, which gives the value of the plastic moment M_P :

$$M_P = \frac{(m_P + 2\sigma_P + m_Q + 2\sigma_Q)l}{6}$$

Suppose $P = X_1$ and $Q = X_2$; hence:

$$G(X_1, X_2) = M_P - \begin{bmatrix} \frac{l}{6} & \frac{l}{6} \end{bmatrix} \begin{pmatrix} X_1 \\ X_2 \end{pmatrix} = 0$$

Let us introduce the standardized centered variables \hat{U}_1 and \hat{U}_2 (of correlation ρ):

$$\hat{H}(\hat{U}_1, \hat{U}_2) = M_P - \frac{l}{6}(m_P + m_Q) - \begin{bmatrix} \frac{l\sigma_P}{6} & \frac{l\sigma_Q}{6} \end{bmatrix} \begin{pmatrix} \hat{U}_1 \\ \hat{U}_2 \end{pmatrix} = 0$$

4.6.2 Decorrelation of variables

The equations in Section 4.4.3 are illustrated here. The correlation matrix $\begin{bmatrix} 1 & \rho \\ \rho & 1 \end{bmatrix}$ has eigenvalues $\lambda_1 = 1 - \rho$ and $\lambda_2 = 1 + \rho$ and the change of coordinate matrix is $[R] = \frac{1}{\sqrt{2}} \begin{bmatrix} 1 & 1 \\ -1 & 1 \end{bmatrix}$, and hence the expression of the limit-state with respect to variables \tilde{U}_i :

$$\tilde{H}(\tilde{U}_1, \tilde{U}_2) = M_P - \frac{l}{6}(m_P + m_Q) - \begin{bmatrix} \frac{l\sigma_P}{6} & \frac{l\sigma_Q}{6} \end{bmatrix} \frac{1}{\sqrt{2}} \begin{bmatrix} 1 & 1 \\ -1 & 1 \end{bmatrix} \begin{pmatrix} \tilde{U}_1 \\ \tilde{U}_2 \end{pmatrix} = 0$$

This is a linear limit-state of variables \tilde{U}_i and the calculation of β is immediate, not forgetting that variables \tilde{U}_i no longer have a standard deviation equal to 1, in fact (Equation (4.14)):

$$[C_{\tilde{U}}] = [\lambda] = [\sigma_{\tilde{U}}]^t [\sigma_{\tilde{U}}] = \begin{bmatrix} \lambda_1 & 0 \\ 0 & \lambda_2 \end{bmatrix} = \begin{bmatrix} 1 - \rho & 0 \\ 0 & 1 + \rho \end{bmatrix}$$

hence the equation for standardizing $\{\tilde{U}\}$ ($\text{var}[\tilde{U}_1] = (1 - \rho)$ and $\text{var}[\tilde{U}_2] = (1 + \rho)$):

$$\begin{pmatrix} \tilde{U}_1 \\ \tilde{U}_2 \end{pmatrix} = \begin{bmatrix} \sqrt{1 - \rho} & 0 \\ 0 & \sqrt{1 + \rho} \end{bmatrix} \begin{pmatrix} U_1 \\ U_2 \end{pmatrix}$$

Suppose:

$$c = M_P - \frac{l}{6}(m_P + m_Q) \quad \text{and} \quad [a_1 \quad a_2] = - \begin{bmatrix} \frac{l\sigma_P}{6} & \frac{l\sigma_Q}{6} \end{bmatrix} \frac{1}{\sqrt{2}} \begin{bmatrix} 1 & 1 \\ -1 & 1 \end{bmatrix}$$

$$H(U_1, U_2) = c + [a_1 \quad a_2] \begin{bmatrix} \sqrt{1 - \rho} & 0 \\ 0 & \sqrt{1 + \rho} \end{bmatrix} \begin{pmatrix} U_1 \\ U_2 \end{pmatrix} = 0$$

hence:

$$\beta = \frac{c}{\sqrt{a_1^2(1-\rho) + a_2^2(1+\rho)}} \quad (4.20)$$

4.6.3 Application of the Rosenblatt transformation

Based on the equations given in the case of a Gaussian variable couple applied directly to the correlated variables \hat{U}_1 and \hat{U}_2 , we obtain the equation below:

$$\begin{pmatrix} \hat{U}_1 \\ \hat{U}_2 \end{pmatrix} = \begin{bmatrix} 1 & 0 \\ \rho & \sqrt{1-\rho^2} \end{bmatrix} \begin{pmatrix} U_1 \\ U_2 \end{pmatrix}$$

hence:

$$H(U_1, U_2) = M_P - \frac{l}{6}(m_P + m_Q) - \begin{bmatrix} l\sigma_P & l\sigma_Q \\ 6 & 6 \end{bmatrix} \begin{bmatrix} 1 & 0 \\ \rho & \sqrt{1-\rho^2} \end{bmatrix} \begin{pmatrix} U_1 \\ U_2 \end{pmatrix} = 0$$

This is again a linear limit-state of variables U_i and the calculation of β is immediate; variables U_i are now unit variables. Assuming:

$$c = M_P - \frac{l}{6}(m_P + m_Q) \quad \text{and} \quad [a_1 \quad a_2] = - \begin{bmatrix} l\sigma_P & l\sigma_Q \\ 6 & 6 \end{bmatrix} \begin{bmatrix} 1 & 0 \\ \rho & \sqrt{1-\rho^2} \end{bmatrix}$$

we have:

$$\beta = \frac{c}{\sqrt{a_1^2 + a_2^2}} \quad (4.21)$$

After expansion, the two expressions (4.20) and (4.21) are identical and are expressed as:

$$\beta = \frac{M_P - (l/6)(m_P + m_Q)}{(l/6)\sqrt{\sigma_P^2 + 2\rho\sigma_P\sigma_Q + \sigma_Q^2}}$$

but these are not coincidental lines in the plane (U_1, U_2) .

4.6.4 Application of the Nataf transformation

The variables are Gaussian and the application is trivial. Note that:

$$[\rho_0] = [\rho] = \begin{bmatrix} 1 & \rho \\ \rho & 1 \end{bmatrix} = \begin{bmatrix} 1 & 0 \\ \rho & \sqrt{1-\rho^2} \end{bmatrix} \begin{bmatrix} 1 & \rho \\ 0 & \sqrt{1-\rho^2} \end{bmatrix} = [L][L]^t$$

where we find the Rosenblatt transformation matrix.

4.6.5 The uselessness of these calculations

If the calculations given in this example are not useless (hopefully!) for illustrating the proposed methods, they are however useless for obtaining a result that gives β . Indeed, note that the limit-state is linear for Gaussian variables P and Q , that the sum of two Gaussian random variables is Gaussian and that the transformations are linear. The reliability index is then the quotient of mean over standard deviation (Cornell index):

$$\beta = \frac{m_G}{\sigma_G} = \frac{M_P - (l/6)(m_P + m_Q)}{(l/6)\sqrt{\sigma_P^2 + 2\rho\sigma_P\sigma_Q + \sigma_Q^2}}$$

where the square of the denominator is nothing but the variance of the sum of the correlated random variables P and Q according to the equation:

$$\text{var}[P + Q] = \text{var}[P] + \text{var}[Q] + 2 \text{cov}[P, Q]$$

4.6.6 Linear limit-state and Gaussian variables

The above example can be generalized to any limit-state of Gaussian variables, and the calculation of index β is immediate. Let:

$$G(\{x\}) = a_0 + \{A\}^t \{x\}$$

The Cornell index is then correct and is written as:

$$\beta = \beta_c = \frac{m_G}{\sigma_G} = \frac{a_0 + \{A\}^t \{m_X\}}{\sqrt{\{A\}^t [\text{cov}_X] \{A\}}} \quad (4.22)$$

Moreover, in this case, the probability of failure is given exactly by $P_f = \Phi(-\beta)$. The demonstration of Equation (4.22) comes from the definitions:

$$\begin{aligned} m_G &= a_0 + \{A\}^t \{m_X\} \\ G(\{x\})^2 &= a_0^2 + 2a_0 \{A\}^t \{x\} + \{A\}^t \{x\} \{x\}^t \{A\} \\ \sigma_G^2 &= E[G(\{x\})^2] - m_G^2 \\ &= a_0^2 + 2a_0 \{A\}^t \{m_X\} + \{A\}^t E[\{x\} \{x\}^t] \{A\} \\ &\quad - a_0^2 - 2a_0 \{A\}^t \{m_X\} - \{A\}^t \{m_X\} \{m_X\}^t \{A\} \\ \sigma_G^2 &= \{A\}^t (E[\{x\} \{x\}^t] - \{m_X\} \{m_X\}^t) \{A\} = \{A\}^t [\text{cov}_X] \{A\} \end{aligned}$$

4.7 Nataf transformation: example

This example shows the application of the Nataf transformation for two correlated uniform distributions. The data are those chosen in Chapter 3.

Resistance R is uniform over $[2, 7]$ and the load S is uniform over $[0, 4]$. According to the results in Table 4.3, the correlation of the normal distribution is given by:

$$\rho_0 = \rho(1.047 - 0.047\rho^2) \quad (4.23)$$

The correlated, centered, standardized variables are:

$$r = 2 + 5\Phi(\hat{u}_1) \Rightarrow \hat{u}_1 = \Phi^{-1}\left(\frac{r-2}{5}\right) \quad s = 4\Phi(\hat{u}_2) \Rightarrow \hat{u}_2 = \Phi^{-1}\left(\frac{s}{4}\right)$$

and the independent variables:

$$\begin{bmatrix} u_1 \\ u_2 \end{bmatrix} = \begin{bmatrix} 1 & 0 \\ -\rho_0 & 1 \\ \sqrt{1-\rho_0^2} & \sqrt{1-\rho_0^2} \end{bmatrix} \begin{bmatrix} \hat{u}_1 \\ \hat{u}_2 \end{bmatrix}$$

r and s varying between 2 and 4, the intersection of their variation domains, u_1 and u_2 are calculated and the minimum of $\sqrt{u_1^2 + u_2^2}$ is obtained and hence β . Table 4.6 gives a few results illustrated in Figure 4.3.

ρ	-0.5	0	0.5
β	0.876	1.077	1.546
$\Phi(-\beta)$	0.190	0.141	0.061
P_f	0.166	0.100	0.032

Table 4.6 Correlation of uniform r.v.

4.8 Transformation by Hermite polynomials

This transformation is used to take into account the information known about the distributions of random variables beyond the second-order moment, particularly on third- or fourth-order moments, while including the correlation of the variables.

4.8.1 Hermite polynomials

This introduction to Hermite polynomials is taken from [DM96].

Definition

Let us first consider the function ϕ , Gauss density $\mathcal{N}(0, 1)$ and the equation:

$$\frac{\phi(t-x)}{\phi(x)} = \exp\left[-\frac{1}{2}t(t-2x)\right]$$

For zero correlation, calculation of the probability of failure is a simple problem of calculation of the area of a triangle. In case of non-zero correlation, results have been obtained by simulation and by RGMR algorithm (see Chapter 7). The strong curvatures of limited-states shown in the figure explain the deviations observed between FORM approximation and P_f .

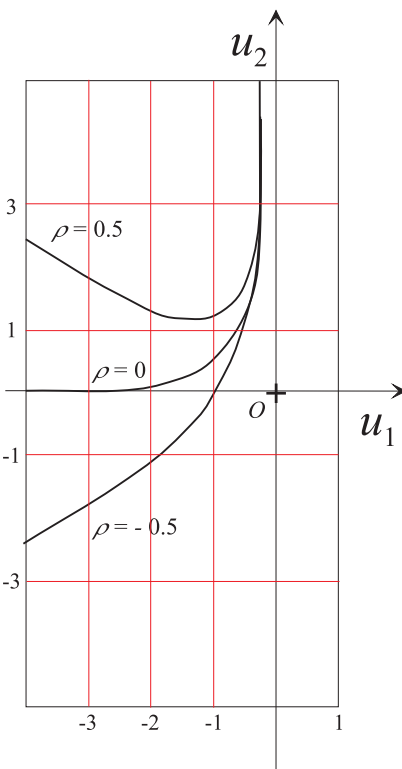


Figure 4.3 Representation of the limit-state functions for correlated uniform variables.

which is written in view of the expansion $\exp(-(1/2)u) = \sum_0^{\infty} (-1)^n (u^n / (2^n n!))$:

$$\begin{aligned}
 \frac{\phi(t-x)}{\phi(x)} &= \sum_{n=0}^{\infty} (-1)^n \frac{t^n (t-2x)^n}{2^n n!} \\
 &= \sum_{n=0}^{\infty} \frac{(-1)^n}{2^n n!} \sum_{i=0}^n \binom{n}{i} (-2x)^{n-i} t^{n+i} \quad (\text{binomial expansion}) \\
 &= \sum_{n=0}^{\infty} \frac{(-1)^n}{2^n n!} \sum_{i=0}^n \frac{n!}{i! (n-i)!} (-2x)^{n-i} t^{n+i} \\
 &= \sum_{k=0}^{\infty} \frac{t^k}{k!} \sum_{i=0}^{[k/2]} \frac{(-1)^i k!}{i! (k-2i)!} \frac{x^{k-2i}}{2^i} = \sum_{k=0}^{\infty} \frac{t^k}{k!} H_k(x)
 \end{aligned}$$

where $[k/2] = k/2$ if k is even and $[k/2] = (k - 1)/2$ if k is odd. The last equation defines the polynomial of order k :

$$H_k(x) = \sum_{i=0}^{[k/2]} \frac{(-1)^i k!}{i! (k-2i)!} \frac{x^{k-2i}}{2^i}$$

The first Hermite polynomials $H_i(x)$ are:

$$\begin{aligned} H_0(x) &= 1 \\ H_1(x) &= x \\ H_2(x) &= x^2 - 1 \\ H_3(x) &= x^3 - 3x \\ H_4(x) &= x^4 - 6x^2 + 3 \end{aligned}$$

Properties

The polynomials have the following properties:

$$\begin{aligned} H_k(x)\phi(x) &= \left. \frac{d^k}{dt^k} \phi(t-x) \right|_{t=0} = (-1)^k \frac{d^k}{dx^k} \phi(x) \\ \frac{d}{dx} H_k(x) &= kH_{k-1}(x) \end{aligned}$$

The polynomials are ϕ -orthogonal and verify that:

$$\int_{-\infty}^{\infty} \phi(x) H_m(x) H_n(x) dx = n! \delta_{mn}$$

4.8.2 Isoprobabilistic transformation

Definition of the transformation

Consider two standardized, centered Gaussian random variables \hat{U}_i and \hat{U}_j , with covariance $\rho_{ij} = \text{cov}[\hat{U}_i, \hat{U}_j]$. The first two statistical properties are verified below:

$$\begin{aligned} E[H_0(\hat{U})] &= 1 & E[H_k(\hat{U})] &= 0 \quad \text{for } k = 1, 2, 3, \dots \\ \text{cov}[H_m(\hat{U}_i), H_n(\hat{U}_j)] &= \begin{cases} 0 & \text{for } n \neq m \\ n! \rho_{ij}^n & \text{for } m = n > 0 \end{cases} \end{aligned} \tag{4.24}$$

The transformation:

$$X_i = \sum_{k=0}^N a_{ik} H_k(\hat{U}_i) \quad (4.25)$$

where coefficients a_{ik} are constant, is then proposed. The linearity of transformation (4.25) gives:

$$\begin{aligned} E[X_i] &= \sum_{k=0}^N a_{ik} E[H_k(\hat{U}_i)] = a_{i0} \\ \text{cov}[X_i, X_j] &= \sum_{k=1}^N a_{ik} a_{jk} k! \rho_{ij}^k \end{aligned}$$

because the product of the two sums only retains the terms with the same order k according to orthogonality condition (4.24), and the 0 order term is constant.

Application to order $N = 3$

Third- and fourth-order moments of a distribution. The third- and fourth-order moments of a distribution introduced here respectively characterize skewness and kurtosis. Let us first consider the third-order moment: $E[X^3]$. It is interesting to calculate the centered moment and to standardize it, thus bringing to light a coefficient without dimension, α_3 :

$$\frac{E[(X - E[X])^3]}{\text{var}[X]^{3/2}} = \alpha_3$$

This coefficient is called the skewness coefficient or first Fisher coefficient. It expresses the skewness of the distribution and has the value 0 for a symmetric distribution, particularly for a Gauss distribution.

We likewise define the second Fisher coefficient, representing the kurtosis of the distribution:

$$\frac{E[X - E[X]^4]}{\text{var}[X]^2} = \alpha_4$$

For a Gauss distribution, its value is 3.

Case of a variable X close to a Gaussian variable. \hat{U} being a standardized, centered, Gaussian variable, its successive moments are:

$$E[\hat{U}] = 0 \quad E[\hat{U}^2] = 1 \quad E[\hat{U}^3] = 0 \quad E[\hat{U}^4] = 3 \dots$$

$$E[\hat{U}^n] = \begin{cases} 0 & \text{for odd } n \\ 1 \times 3 \times \dots \times (n-1) & \text{for even } n \end{cases}$$

The moments of the variable X can be calculated as:

$$\begin{aligned} \mathbb{E}[X^n] &= \mathbb{E}\left[\left(\sum_{k=0}^3 a_k H_k(\hat{U})\right)^n\right] \\ &= \mathbb{E}\left[(a_0 + a_1 \hat{U} + a_2 (\hat{U}^2 - 1) + a_3 (\hat{U}^3 - 3\hat{U}))^n\right] \end{aligned}$$

Let us choose the centered and standardized X , which does not diminish the generality. For $n = 1$, $\mathbb{E}[X] = \mathbb{E}[a_0] = a_0 = 0$; for $n = 2$, $\mathbb{E}[X^2] = a_1^2 + 2a_2^2 + 6a_3^2$; hence $a_1^2 + 2a_2^2 + 6a_3^2 = 1$, whose solution is $a_2 = \pm\sqrt{(1 - a_1^2 - 6a_3^2)/2}$ provided that $a_1^2 + 6a_3^2 \leq 1$.

The third- and fourth-order moments are respectively denoted by α_3 and α_4 . They are expressed as a function of a_1 and a_3 by:

$$\begin{aligned} \alpha_3 &= \pm\sqrt{2(1 - a_1^2 - 6a_3^2)}(2 + a_1^2 + 18a_1a_3 + 42a_3^2) \\ \alpha_4 &= 15 + 288a_1a_3 + 936a_3^2 - 12a_1^4 - 264a_1^3a_3 \\ &\quad - 864a_1^2a_3^2 - 432a_1a_3^3 - 2808a_3^4 \end{aligned}$$

If the distribution of X is hardly different from a normal distribution, $|\alpha_3| \ll 1$ and $|\alpha_4 - 3| \ll 1$, we obtain:

$$\begin{aligned} |a_3| &\ll 1, \quad a_1 = 1 - \varepsilon \quad \text{with} \quad \varepsilon \ll 1 \\ a_2 &\simeq \pm\sqrt{\varepsilon} \\ \alpha_3 &\simeq 2\sqrt{\varepsilon}(3 - 2\varepsilon + 18a_3) \\ \alpha_4 &\simeq 3 + 48\varepsilon + 24a_3 \end{aligned} \tag{4.26}$$

and finally, by taking into account $a_3 \rightarrow 0$ and $\varepsilon \rightarrow 0$:

$$X \simeq \left(1 - \frac{\alpha_3^2}{36}\right)\hat{U} + \frac{\alpha_3}{6}(\hat{U}^2 - 1) + \left(\frac{\alpha_4 - 3}{24} - \frac{\alpha_3^2}{18}\right)(\hat{U}^3 - 3\hat{U}) \tag{4.27}$$

Such a equation helps introduce into the probabilistic transformation the information resulting from the third- and fourth-order moments of the random variable, in this case slightly different from a Gaussian variable. In a more general case, it is a starting point for an exact resolution.

If X is Gaussian, we verify that $X = \hat{U}$ for $\alpha_3 = 0$ and $\alpha_4 = 3$.

4.8.3 Winterstein approximation [Win87, Win88]

Let us consider a random vector X_i whose variable distributions are undetermined. The information available is made up only of:

- the first four statistical moments of each variable X_i ,
- the correlation $\text{cor}[X_i, X_j] = \rho_{ij}$.

The steps are then as follows:

1. We first carry out a transformation to obtain centered, standardized (non-Gaussian) variables:

$$Y_i = (X_i - \text{E} [X_i]) / \sqrt{\text{var} [X_i]}$$

with correlation $\text{cor}[Y_i, Y_j] = \rho_{ij}$.

2. For each variable Y_i , we calculate coefficients a_{ik} by solving (index i omitted):

$$\begin{aligned} \alpha_3 &= \pm \sqrt{2(1 - a_1^2 - 6a_3^2)}(2 + a_1^2 + 18a_1a_3 + 42a_3^2) \\ \alpha_4 &= 15 + 288a_1a_3 + 936a_3^2 - 12a_1^4 - 264a_1^3a_3 \\ &\quad - 864a_1^2a_3^2 - 432a_1a_3^3 - 2808a_3^4 \\ a_2 &= \pm \sqrt{(1 - a_1^2 - 6a_3^2)/2} \quad \text{with } a_1^2 + 6a_3^2 \leq 1 \end{aligned} \tag{4.28}$$

3. Each variable Y_i is then replaced by:

$$Y_i = \sum_{k=0}^3 a_{ik} H_k(\hat{U}_i)$$

4. The equivalent correlation (as for the Nataf transformation) $\rho_{0,ij}$ of variables \hat{U}_i and \hat{U}_j is obtained by solving:

$$\begin{aligned} \text{cor} [Y_i, Y_j] &= \sum_{k=1}^3 a_{ik} a_{jk} k! \rho_{0,ij}^k \\ \implies 6a_{i3}a_{j3}\rho_{0,ij}^3 + 2a_{i2}a_{j2}\rho_{0,ij}^2 + a_{i1}a_{j1}\rho_{0,ij} - \rho_{ij} &= 0 \end{aligned} \tag{4.29}$$

5. Variables \hat{U}_i are correlated Gaussian variables, and decorrelation is performed using the standard procedure (Equation (4.10)):

$$U_i = L_{ij}^{-1} \hat{U}_j$$

If the distribution is symmetric, $\alpha_3 = 0$; hence $a_1^2 = 1 - 6a_3^2$ and a_3 is given by the equation:

$$\alpha_4 = 3 + 216a_3^2 + 1944a_3^4 + 24a_3(1 + 48a_3^2)\sqrt{1 - 6a_3^2} \tag{4.30}$$

It must be noted that the other equation for canceling α_3 : $2 + a_1^2 + 18a_1a_3 + 42a_3^2 = 0$ does not yield possible solutions.

A reminder about notation

- X_i is a random vector, each of whose variables has a distribution of any type, known by its first four moments; second-order dependence is represented by the correlation $\text{cor}[X_i, X_j]$.
- Y_i is a vector of centered, standardized variables and unknown distributions; second-order dependence is represented by the correlation $\text{cor}[Y_i, Y_j] = \text{cor}[X_i, X_j]$.
- \hat{U}_i is a vector of correlated, Gaussian, centered and standardized random variables.

Example – Gamma distribution

Let us consider a family of Gamma distributions of parameter k (mean k and standard deviation \sqrt{k}). Density is given by:

$$f_X(x, k) = \frac{1}{\Gamma(k)} x^{k-1} e^{-x} \quad k > 0 \quad x \geq 0$$

and the Fisher coefficients are:

$$\alpha_3 = \frac{2}{\sqrt{k}} \quad \alpha_4 = 3 + \frac{6}{k}$$

The calculation of coefficients a_i for various values of k is performed in Ditlevsen and Madsen [DM96]. The results are recalculated here for $k = 4$ (Table 4.7).

a_i	Exact (4.28)	Approximate (4.26)	Approximate (4.27)
a_1	0.9729	0.9755	0.9722
a_2	0.1632	0.1566	0.1667
a_3	0.0066	0.0135	0.0069

Table 4.7 Coefficients of the Gamma distribution for $k = 4$.

Strangely, the result for a_3 appears less satisfactory in column (2), whereas in principle it should be a better approximation. Columns (2) and (3) assume that $a_3 \rightarrow 0$.

In order to verify the approximation, it is now possible to calculate the density of the random variable $X = g(U)$. The principle [Rad91] consists of writing the conservation of probability mass when we go from du to dx . If $g(u)$ is monotonic and derivable, then $u = g^{-1}(x)$ yields a single solution and:

$$f_X(x) = \frac{\phi(u)}{|g'(u)|} \Big|_{u=g^{-1}(x)}$$

If the equation $x = g(u)$ gives several real roots u_i , then:

$$f_X(x) = \sum_i \frac{\phi(u_i)}{|g'(u_i)|} \quad (4.31)$$

The comparative plot of origin and approximate densities does not help to distinguish them, and therefore Figure 4.4 shows the relative deviation between the approximation and the density for $x \in [\varepsilon, m_X + 5\sigma_X]$. For numerical reasons, the approximation below the threshold ε could not be obtained. Beyond this, the approximation is very satisfactory up to five standard deviations.

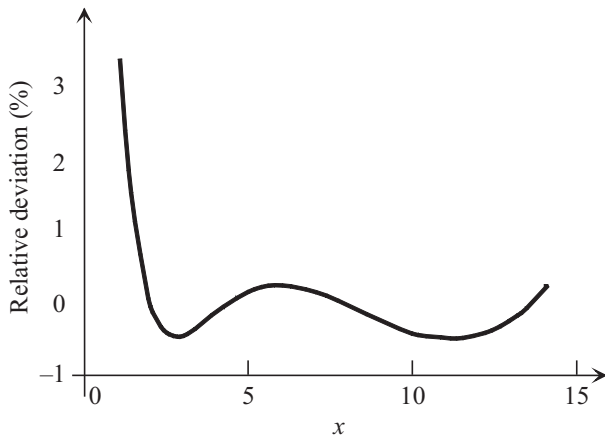


Figure 4.4 Relative deviation between density approximation and Gamma density for $k = 4$.

4.8.4 Example: two uniform distributions

This example is chosen since uniform distribution is particularly remote from Gauss distribution and it has a discontinuity. It is therefore a tough test that cannot be solved exactly.

Representation of a uniform distribution

Let us first consider a random variable Y with uniform distribution, with zero mean and unit standard deviation, that is, distributed on the segment $[-\sqrt{3}, +\sqrt{3}]$. The calculation of the various parameters gives:

$$\mathbb{E}[Y] = 0 \quad \mathbb{E}[Y^2] = 1 \quad \alpha_3 = 0 \quad \alpha_4 = 1.800$$

The resolution of Equation (4.30) does not give any real solution. The minimum value possible for α_4 is 1.849 for which $a_1 = 0.9484$, $a_2 = 0$ and $a_3 = -0.1294$. The Hermite approximation is then:

$$Y = 0.9484 U - 0.1294 (U^3 - 3U)$$

Figure 4.5 gives a comparison between the uniform density and the approximate density $f_X(x)$. It presents an infinite value for the roots of $g'(u) = 0$ (Equation (4.31)). The roots of $g'(u)$ should be $\pm\sqrt{3} = \pm 1.732$; however, the accepted approximation for α_4 of 1.849 instead of 1.800 results in a shrinkage of the density between the roots ± 1.655 . The density satisfies $\int_{-\infty}^{\infty} f_X(x) dx = 1$ and the other statistical moments because of Equation (4.30).

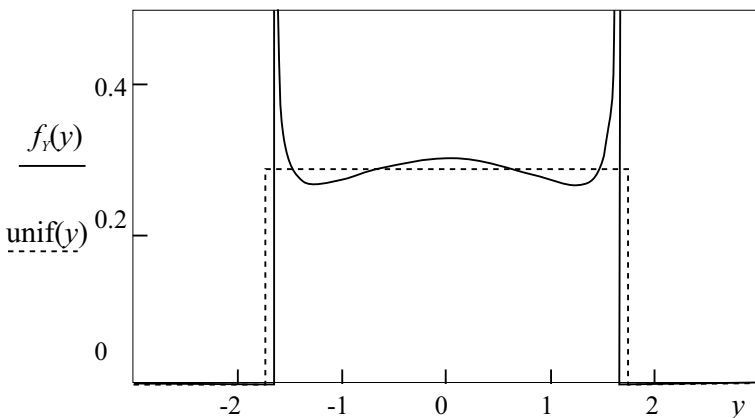


Figure 4.5 Representation of uniform density by Hermite polynomials.

Basic example

Let us now consider the example $R - S$ with two uniform distributions (Section 4.7):

$$Y_1 = \frac{R - m_R}{\sigma_R} \quad Y_2 = \frac{S - m_S}{\sigma_S}$$

and the limit-state function is written as:

$$\sigma_R Y_1 - \sigma_S Y_2 + m_R - m_S = 0$$

where functions Y_i are replaced by the Hermite expansion:

$$\sigma_R (a_1 U_1 + a_3 (U_1^3 - 3U_1)) - \sigma_S (a_1 U_2 + a_3 (U_2^3 - 3U_2)) + m_R - m_S = 0$$

The numerical application ($m_R = 4.5$; $\sigma_R = 1.4434$; $m_S = 2$; $\sigma_S = 1.1547$; $a_1 = 0.9484$ and $a_3 = -0.1294$) gives $\beta_{\text{FORM}} = 1.074$ for $\rho = 0$ to be compared with the result $\beta = 1.077$ in Table 4.6.

The Hermite transformation also provides a means of calculating the equivalent correlation. Table 4.8 compares the correlations obtained by the approximate equation of Nataf transformation (4.23) and that of Hermite transformation (4.29).

Correlation $\pm\rho$	Nataf $\pm\rho_0$	Hermite $\pm\rho_0$
0	0	0
0.25	0.2610	0.2756
0.50	0.5176	0.5384
0.75	0.7654	0.7806
1	1	1

Table 4.8 Correlation according to Nataf and Hermite.

4.8.5 Conclusion on Hermite transformation

The expansion procedure using Hermite polynomials is not advantageous compared to the exact transformation for a variable if the marginal distribution of X_i is known. We can nevertheless observe interesting perspectives:

- To obtain the coefficients of the decomposition of any random variable in the form:

$$X = \sum_{k=0}^{\infty} a_k H_k(U) \quad (4.32)$$

let us multiply (4.32) by $H_l(U)$ and express the expectation [PPS02]:

$$\mathbb{E}[X H_l(U)] = a_k \sum_{k=0}^{\infty} \mathbb{E}[H_k(U) H_l(U)] = a_k \mathbb{E}[H_k^2(U)] = a_k k!$$

because of orthogonality (4.24). Let us now introduce the isoprobabilistic transformation:

$$F_X(x) = \Phi(u) \longrightarrow x = F_X^{-1}(\Phi(u))$$

and finally:

$$\begin{aligned} \mathbb{E}[X H_k(U)] &= \int_{\mathbb{R}} F_X^{-1}(\Phi(u)) H_k(u) \phi(u) du \\ a_k &= \frac{1}{k!} \int_{\mathbb{R}} F_X^{-1}(\Phi(u)) H_k(u) \phi(u) du \end{aligned}$$

which provides an effective means of calculating the coefficients at any order. There is an analytical solution for normal and lognormal variables; in other cases, we must use quadrature methods.

- It makes it possible to get closer to the processing of the available information by directly using statistics on experimental samples whose moments are estimated. These moments can also result from a quadrature to evaluate the distribution of $G(X_k)$:

$$\begin{aligned} \mathbb{E}[G(X_k)] &= \int_{\mathbb{R}^n} G(x_k) f_{X_k}(x_k) dx_1 \cdots dx_n \\ &= \mathbb{E}\left[\left(G(X_k) - \frac{1}{\text{if } i>1} \mathbb{E}[G(X_k)]\right)^i\right] \\ &= \int_{\mathbb{R}^n} (G(x_k) - \mathbb{E}[G(X_k)])^i f_{X_k}(x_k) dx_1 \cdots dx_n \end{aligned}$$

When the objective sought is also to obtain a representation of the density, other methods must be explored:

1. approximation by a Pearson distribution [Bal99],
2. approximation based on an exponential of a polynomial [Er98, Pen00].

A recent article [LG03] calls into question this approach, advocated by Zhao and Ono [ZO00, ZO01], by showing its limits arising from the modeling of distribution tails, which is not necessarily a drawback when the approach is based on the sensitivity analysis around the average.

- It proposes an expansion base common to several random variables thus opening up interesting perspectives for stochastic finite elements – Chapter 12 – which are based largely on multidimensional Hermite polynomials.

4.9 Conclusion

If the Rosenblatt transformation offers a general solution to construct the transformation from physical variable space into centered and decorrelated standardized variable space, it presents two drawbacks:

- We must know the joint density of the random variables, which is ‘rich’ knowledge but rarely available.
- The transformation is not unique and the reliability index depends on it in a limited manner.

The use of approximation by normal distribution or Nataf transformation requires poorer information, limited to the marginal distributions of the

Available information	Transformation	Notes
Joint distribution of the vector X_i	Rosenblatt	Non-unique transformation.
Marginal distributions of X_i and correlation $\text{cor}[X_i, X_j]$	Normal distribution	Information sufficient for normal and lognormal X_i , correlation taken into account directly.
Marginal distributions of X_i and correlation $\text{cor}[X_i, X_j]$	Nataf	Information sufficient for normal and lognormal X_i , equivalent correlation to be calculated.
Marginal moments of X_i and correlation $\text{cor}[X_i, X_j]$	Hermite	The interest would lie in an expansion base common to diverse variables.

Table 4.9 Overview of the various transformations.

components of the random vector and to the mixed second-order moment which yields the correlation. If the influence of order moments greater than the second order is sought, the Hermite transformation can be used without requiring the choice of a probability distribution.

Table 4.9 summarizes the various possibilities. These are classified from the richest information to the poorest information. Between the Rosenblatt transformation and the approximations, what is lost is the knowledge of all the mixed moments other than the second-order moment. It is difficult to believe that this information can significantly influence the calculation of the index or the probability.

The approximation of the reliability index from the marginal densities and the correlation now constitutes an efficient solution consistent with the available information. This results in an approximation of the value of β whose quality can be estimated in the passage from β to P_f , the latter value being the objective to be achieved. This point will be discussed in Chapter 7.

Before this, we must specify the search algorithm for β .

This page intentionally left blank

Chapter 5

Reliability Index

Calculation of the reliability index requires a search for the most probable failure point, P^* , as was defined in Chapter 3. This point is also considered from the design point of view as a reference point for designing, which will be discussed in Chapter 10. Its determination belongs to a non-linear optimization method, which must be adapted to the distinctive nature of the problem. This chapter deals with the methods which make the search for P^* , and thus the reliability index β and the direction cosines $\{\alpha\}$, possible. It first summarizes the formulation of the optimization problem, and then presents an introduction to the method of resolution. It later explains in detail the principal algorithms adapted to the search for the design point and gives illustrations for these.

5.1 An optimization problem

5.1.1 Mechanical-reliability coupling

The most effective methods at present for reliability calculation are based on the Search for Design Point P^* (SDP). Knowledge of the latter is at the root of approximations of the probability of failure in the context of first-/second-order reliability methods – FORM/SORM – which will be presented in Chapter 7.

These methods constitute a coupling between the mechanical model and the reliability model, in which the responsibility for driving the search direction is given to the reliability model, whereas the mechanical model deals with the evaluation of the limit-state function. The rate of convergence is the responsibility of the reliability model, whereas the calculation cost of each stage is that of the mechanical model.

Figure 5.1 illustrates the two transformations, isoprobabilistic and mechanical, and the two representations of P^* , in physical space and in standardized space. It is *a priori* possible to work in one or the other; however, the notion of distance is defined simply in standardized space, which is therefore preferred, even if the designer has better knowledge of physical space. Moving back and forth between these two spaces is constantly necessary.

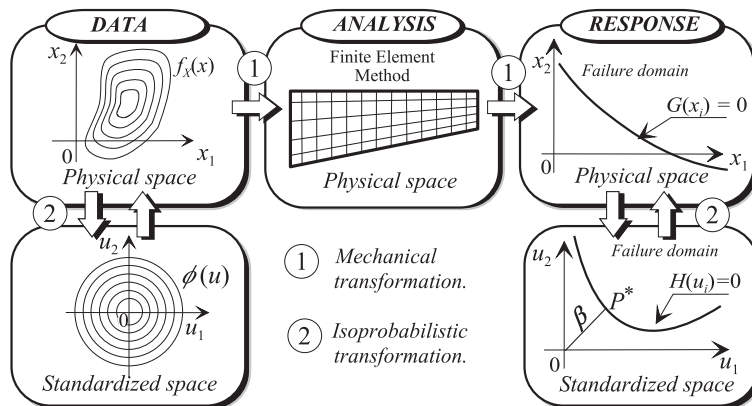


Figure 5.1 Isoprobabilistic and mechanical transformations in the search for the most probable failure point (or design point).

5.1.2 Formulation of the optimization problem

In standardized space, the design point is the closest point of the failure domain to the origin. The definition of the reliability index β is interpreted geometrically as the length of vector OP^* (Figure 5.1).

Calculation of the reliability index is thus reduced to the resolution, in standardized space, of the following optimization problem (Equation (4.2) of Chapter 4):

$$\beta = \min d(u_k) = \min \left(\sqrt{\sum_i u_i^2} \right) \quad \text{under the constraint } H(u_k) \leq 0 \quad (5.1)$$

Resolution poses the classic optimization problems:

- How should convergence to the global minimum be ensured?
- Can we have derivatives of the first order, or even of the second order with the constraint $H(u_k) \leq 0$?
- What is the necessary cost of calculation to obtain a solution?

There is no definitive answer, and if the solution can be very simple when the limit-state function is explicit and shows good properties, it can also mobilize considerable numerical resources, for example, when it depends implicitly on results from a non-linear calculation using finite elements (Chapter 11). Moreover, the approximation of the probability of failure requires knowledge

not only of the absolute minimum but also of the series of secondary minima located at admittedly higher, but comparable, distances.

The SDP is therefore the resolution of an optimization problem with constraints of inequality. An important class of optimization algorithms is based on the use of gradients to determine the direction of descent. These algorithms are rendered efficient by being adapted to the specificity of the reliability problem.

Reliability of components (single limit-state)

In the analysis of reliability components, we have a single failure scenario and consequently a single limit-state. The objective function d is a positive or zero scalar; the optimal point without constraint is of course the origin of the reference (trivial solution!). We are therefore certain that the optimum is on the limit-state (i.e. at the boundary between the failure domain and the safety domain) unless the origin is a failure point which corresponds to an unacceptable design showing a very high probability of failure. This implies that constraint $H(u_k) \leq 0$ is always active: $H(u_k^*) = 0$ in P^* . It is therefore more interesting to use methods which are efficient with constraints of equality, and problem (5.1) becomes:

$$\begin{aligned} &\text{finding } u_k^* \\ &\text{to minimize } d^2(u_k) = \sum_i u_i^2 \\ &\text{under the constraint } H(u_k) = 0 \end{aligned} \tag{5.2}$$

by noting that minimizing $d^2(u_k)$ is better adapted than simply $d(u_k)$, because the calculation of the derivatives is simpler.

Reliability of systems (several limit-states)

In the case of the analysis of a system composed of logical combinations of reliability components (Chapter 9), there is no general rule for the active and inactive constraints. The optimization procedure should be more general and should be able to identify the set of local minima. The problem of looking for the global minimum is written as:

$$\begin{aligned} &\text{finding } u_k^* \\ &\text{to minimize } d^2(u_k) = \sum_i u_i^2 \\ &\text{under the constraints } H_l(u_k) \leq 0 \end{aligned}$$

where $H_l(u_k)$ is the function of the limit-state number l . The problem with inequalities is solved by searching for the combination of active constraints,

for which optimization under equality is applied. The algorithms are identical to components (5.2), but add a strategy of activation and deactivation of constraints.

5.1.3 Optimality conditions

Necessary condition for components

Let us consider the problem of minimization (5.2). The Lagrangian L associated with this problem is:

$$L(u_k, \lambda) = d^2(u_k) + \lambda H(u_k) \quad (5.3)$$

in which λ is the Lagrange multiplier. It is non-zero $\lambda \neq 0$ (and even $\lambda > 0$) if the constraint $H(u_k)$ is active. The equivalent problem to solve is:

$$\begin{aligned} &\text{finding } (u_k^*, \lambda^*) \\ &\text{to make stationary } L(u_k, \lambda) \end{aligned}$$

If there is a solution, the optimality conditions (or Kuhn-Tucker conditions) are:

$$\begin{aligned} \frac{\partial L(u_k, \lambda)}{\partial u_i} &= 0 \\ \frac{\partial L(u_k, \lambda)}{\partial \lambda} &= 0 \end{aligned}$$

By taking into account $\partial d^2(u_k)/\partial u_i = 2u_i$, the previous expression becomes:

$$\begin{aligned} 2u_i + \lambda \frac{\partial H(u_k)}{\partial u_i} &= 0 \\ H(u_k) &= 0 \end{aligned} \quad (5.4)$$

The solution should be a saddle-point: a minimum according to u_k and a maximum according to λ . The Hessian of the Lagrangian is semi-positive defined.

Necessary condition for systems

The Lagrangian of the system takes the form:

$$L(u_k, \lambda_l) = d^2(u_k) + \sum_l \lambda_l H_l(u_k)$$

in which λ_l is the Lagrange multiplier associated with the limit-state $H_l(u_k)$, with $\lambda_l = 0$ if $H_l(u_k) < 0$ and $\lambda_l > 0$ if $H_l(u_k) = 0$. The optimality conditions (or Karush-Kuhn-Tucker conditions [Kar39]) are now:

$$\begin{aligned}\frac{\partial L(u_k, \lambda_l)}{\partial u_i} &= 0 \\ \frac{\partial L(u_k, \lambda_l)}{\partial \lambda_j} &= 0 \quad \text{for active constraints} \\ \lambda_j &= 0 \quad \text{for inactive constraints}\end{aligned}$$

which implies:

$$\begin{aligned}2u_i + \sum_l \lambda_l \frac{\partial H_l(u_k)}{\partial u_i} &= 0 \\ \lambda_j H_j(u_k) &= 0\end{aligned}$$

5.2 Optimization algorithms

An optimization algorithm is characterized by the criteria of convergence and quality.

5.2.1 Convergence [PW88]

The convergence of the method is measured by the number of iterations necessary to reach the optimal point with a given level of accuracy.

Global and local convergence

Global convergence expresses the capacity of the algorithm to find the optimal point from any initial point, not necessarily in the vicinity of the optimum. Convergence is therefore not affected by the choice of the starting point.

Local convergence expresses the capacity of the algorithm to move rapidly to the optimum from a point in its vicinity.

Convergence rate

An algorithm is said to be convergent if:

$$\lim_{k \rightarrow \infty} \frac{\epsilon^{(k+1)}}{\epsilon^{(k)}} = 0$$

where $\epsilon^{(k)}$ is the error in the variables at iteration (k) : $\epsilon^{(k)} = \|\{u\}^{(k)} - \{u\}^{(k-1)}\|$.

By introducing the real error given by $\bar{\epsilon}^{(k)} = \|\{u\}^{(k)} - \{u^*\}\|$, the convergence rate is a measure of the reduction in the error between two successive iterations, and it is expressed by a measure γ as follows:

$$\text{linear convergence } \bar{\epsilon}^{(k+1)} \leq \gamma \bar{\epsilon}^{(k)} \quad \text{with } 0 < \gamma < 1$$

$$\text{overlinear convergence } \bar{\epsilon}^{(k+1)} \leq \gamma_k \bar{\epsilon}^{(k)} \quad \text{with } \lim_{k \rightarrow \infty} \gamma_k = 0$$

$$\text{quadratic convergence } \bar{\epsilon}^{(k+1)} \leq \gamma \bar{\epsilon}^{(k)2} \quad \text{with } \gamma \in \mathbb{R}$$

Approaching the optimum is of course faster for methods whose convergence is quadratic, but the cost of calculation becomes exorbitant for a high number of variables. It should be noted that, in their raw state, methods with a quadratic rate (such as the Newton method) are not necessarily convergent, whereas the robust methods (such as gradient methods) are not efficient, with linear convergence rates. It is therefore necessary to introduce modifications with a view to reaching the *best* compromise between efficiency and robustness, concepts which are clarified in the following section. In practice, the choice of a method is in itself an optimization problem under the limitations of data processing resources and according to the information available about the problem.

5.2.2 Quality criteria

In an optimization algorithm, three criteria are to be taken into account:

- *Efficiency*, which is identified by the number of calls to the limit-state function (i.e. to the mechanical model), necessary to reach convergence to a threshold of predefined numerical accuracy.
- *Robustness*, which is defined by the capacity of the algorithm to find the *good design* point, whatever the configuration of the problem and, in particular, whatever the initial point. It is very difficult to identify a method as being ‘the best’, because the criteria ‘efficiency’ and ‘robustness’ do not have the same requirements in terms of cost of calculation.
- the *capacity* of the method to process problems of large size (high number of random variables) or with complex limit-states, for the given data processing resources.

In the SDP, some methods require only results from the performance function (methods of order 0), others are based on the calculation of the gradient (methods of order 1) or even the Hessian (methods of order 2). By using a method of high order, we reduce the number of iterations, but increase the cost of calculation in each of these iterations. The choice of the method to be followed depends on the nature of the problem posed and the possibilities offered by the mechanical model (calculation time, direct calculation – or not – of gradients, of curvatures, etc.).

5.2.3 Principle of optimization algorithms

The principle of optimization algorithms consists, starting from an initial point, of determining the best direction of descent and in covering a certain path depending on this direction. The choice of the direction results from information on the function, its first or even second derivatives. The distance to be covered is solved by the optimization of a merit function. An iteration (k) is written in a form of the type:

$$\{u\}^{(k+1)} = \{u\}^{(k)} + \alpha^{(k)} \{S\}^{(k)} \quad (5.5)$$

where $\alpha^{(k)} > 0$ is the length of the optimal step and $\{S\}^{(k)}$ is the direction of descent. It can be completed by a projection.

Calculation of the search direction

The literature offers us numerous algorithms to solve a problem of minimization under constraints, among which we have distinguished four main categories:

1. Zero order methods:

- dichotomy,
- non-linear simplex.

2. First order methods:

- gradient method,
- projected gradient method,
- penalty method,
- augmented Lagrangian method.

3. Second order methods:

- Newton method,
- sequential quadratic programming method.

4. Hybrid methods:

- Davidson-Fletcher-Powell (DFP) method,
- Broyden-Fletcher-Goldfarb-Shanno (BFGS) method.

The advantage of the zero order methods would be that they do not require the calculation of gradients. However, their convergence is slow and would demand, in the case of reliability problems, a very large number of calculations of the performance function.

Such methods are not adapted to reliability problems, except for a non-derivative limit-state.

This section discussed some elements concerning the calculation of the optimal step, and the following sections concern the adaptation of general methods to reliability problems.

Calculation of the optimal step length

Design point search methods are based on the definition of the direction of descent which minimizes the objective function.

We thus know the shortest path to approach the design point, but we do not know the distance we must travel along it. It is quite possible for the algorithm to approach the optimum and then converge by chance or else, in most cases, diverge. This behavior is observed more when the calculation point is in the vicinity of the design point, because the gradient of the Lagrangian approaches zero. Figure 5.2 shows an example where point 1 can *jump* in the following iteration to point 2 above the minimum without detecting it.

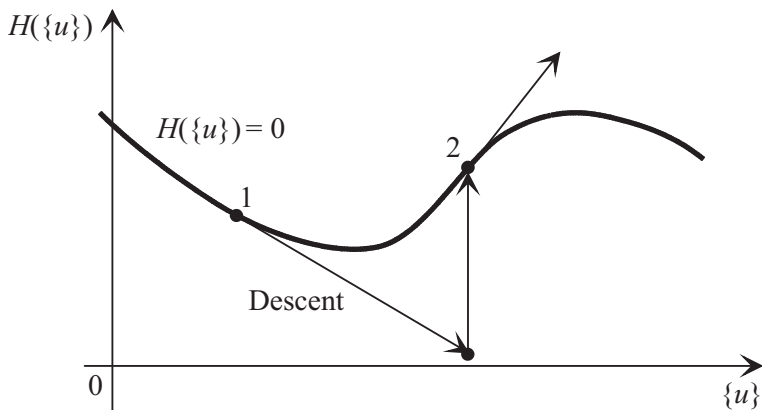


Figure 5.2 Illustration of possible divergence due to the length of the vector of descent.

To obtain the best behavior, the distance α in Equation (5.5) should be checked carefully, a good choice leading to an acceleration of convergence. The calculation of α results from a line minimization procedure (*line search – LS*) of an objective function with a single parameter, the merit function Ψ : to find $\alpha^{(k)}$ which minimizes the function $\Psi(\{u\}^{(k)} + \alpha^{(k)} \{S\}^{(k)})$, where $\{u\}^{(k)}$ is the current point and $\{S\}^{(k)}$ is the direction of descent.

Solving this problem adds an additional cost to the algorithm, but allows us to reduce the total number of iterations. The outcome is generally very positive. We describe three approaches to solve this problem: quadratic interpolation, cubic interpolation and the Newton method.

Quadratic interpolation [HK85]: it is wise to construct a quadratic interpolation for which we can determine simply the minimum. A small number of iterations enables us to find the optimal step.

Let us assume:

$$p(\alpha) = a\alpha^2 + b\alpha + c \approx \Psi(\{u\} + \alpha\{S\}) \quad (5.6)$$

By supposing that $\{S\}$ is the minimizing direction Ψ (i.e. $\alpha > 0$), the calculation procedure is summed up by the following stages:

1. calculate the merit function at the starting point: $p_0 = \Psi(\{u\})$,
2. choose a length of step ξ and calculate $p_1 = \Psi(\{u\} + \xi\{S\})$ and $p_2 = \Psi(\{u\} + 2\xi\{S\})$,
3. determine the polynomial coefficients as:

$$a = \frac{p_0 - 2p_1 + p_2}{2\xi^2} \quad b = \frac{-3p_0 + 4p_1 - p_2}{2\xi} \quad c = p_0$$

4. calculate the value α_m for which $p(\alpha)$ is extreme:

$$\alpha_m = -\frac{b}{2a} = \xi \frac{-3p_0 + 4p_1 - p_2}{-2p_0 + 4p_1 - 2p_2}$$

5. verify that α_m minimizes the merit function (i.e. $a > 0$); if this is not verified, or else if α_m exceeds the maximum authorized value, take this latter as the increment value,
6. obtain a new point as $\{u\} + \alpha_m\{S\}$,
7. repeat 2–6 until α_m stabilizes.

Cubic interpolation [PW88]: in this method, a cubic interpolation is adopted by using the gradients at the extremities of the calculation interval:

$$p(\alpha) = a\alpha^3 + b\alpha^2 + c\alpha + d$$

The procedure is thus as follows:

1. evaluate $p_0 = \Psi(\{u\})$ and $p'_0 = \langle S \rangle \{\nabla_u \Psi(\{u\})\}$ and verify that $p'_0 < 0$,
2. choose a length of step ξ (use, for example, a quadratic interpolation),
3. calculate $p_1 = \Psi(\{u\} + \xi\{S\})$ and $p'_1 = \langle S \rangle \{\nabla_u \Psi(\{u\} + \xi\{S\})\}$,
4. if $p'_1 < 0$ and $p_1 < p_0$, replace ξ by 2ξ and go to 3,
5. calculate:

$$a = \frac{p_0 + p'_1 + 2e}{3\xi^2} \quad b = -\frac{p'_0 + e}{\xi} \quad c = p'_0 \quad d = p_0$$

with: $e = \frac{3}{\xi}(p_0 - p_1) + p'_0 + p'_1$

6. calculate the value of α_m as:

$$\alpha_m = \xi \frac{p'_0 + e + \sqrt{e^2 - p'_0 p'_1}}{p'_0 + p'_1 + 2e}$$

7. use the interval $(0, \alpha_m)$ if $p'(\alpha_m) \geq 0$; otherwise, use the interval (α_m, ξ) and go to 4,
8. obtain a new point as $\{u\} + \alpha_m \{S\}$,
9. repeat 2–8 until α_m is stabilized,
10. if α_m maximizes the merit function, continue by taking the maximum authorized step.

Newton method [PW88]: at the extreme point, we have $\partial\Psi(\{u\})/\partial\alpha = 0$. With the expansion of this derivative to the first order, we obtain:

$$\left. \frac{\partial\Psi(\{u\})}{\partial\alpha} \right|_{(k+1)} = \left. \frac{\partial\Psi(\{u\})}{\partial\alpha} \right|_{(k)} + \left. \frac{\partial^2\Psi(\{u\})}{\partial\alpha^2} \right|_{(k)} (\alpha^{(k+1)} - \alpha^{(k)}) = 0$$

(k) being the number of the iteration. The iterative equation for solution is therefore:

$$\alpha^{(k+1)} = \alpha^{(k)} - \left. \frac{\partial\Psi(\{u\})/\partial\alpha}{\partial^2\Psi(\{u\})/\partial\alpha^2} \right|_{(k)}$$

in which we must verify $\partial^2\Psi(\{u\})/\partial\alpha^2 > 0$ to reach the minimum.

5.3 First order methods

5.3.1 Projected gradient method [HK85]

The principle of the projected gradient method is to search for the optimum while moving in the space tangent to the active constraints. These latter constitute an active sub-space in which we solve the problem of minimization. The procedure is divided into two phases (Figure 5.3):

- *Descent phase:* this is a question of defining the direction of descent which minimizes the objective function in tangent space. This phase allows us to displace the calculation point in the direction of the most effective minimization (the highest slope is in the direction opposite to that of the gradient). The trajectory being rectilinear, the resulting calculation point does not remain on the departure constraints, unless these are linear.
- *Projection phase:* to prevent the active constraints from being violated, a correction of the movement is necessary. This is carried out by projecting the new point onto the active sub-space. The direction of projection is determined by the normal to this sub-space.

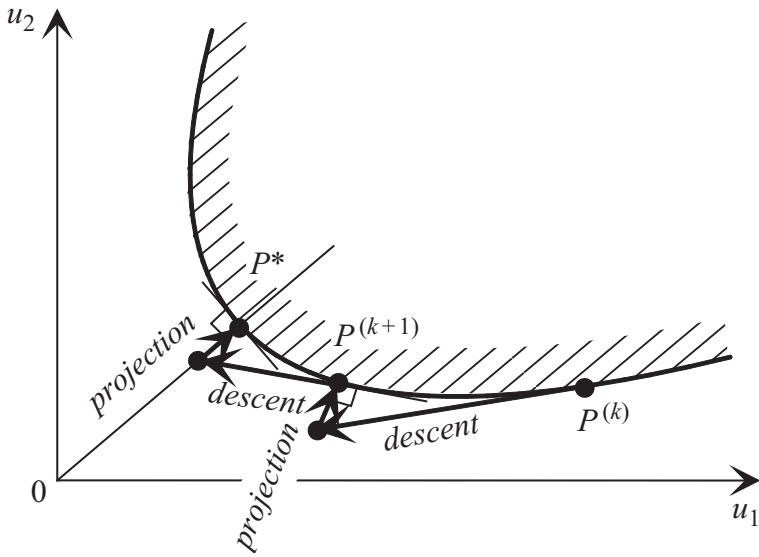


Figure 5.3 Iterative method with projected gradient.

Let us consider the problem:

$$\begin{aligned} & \text{to minimize } d^2(u_k) \\ & \text{under the constraint } \langle \nabla_u H \rangle \{u\} + c = 0 \end{aligned}$$

where the constraint is linearized to point $P^{(k)}$ and to carry out an iteration of the form (5.5):

$$\{u\}^{(k+1)} = \{u\}^{(k)} + \alpha^{(k)} \{S\}^{(k)}$$

As we wish to find the minimum in the active sub-space, it is necessary that $\{u\}^{(k)}$ and $\{u\}^{(k+1)}$ satisfy the equation of the constraint (i.e. $H(u_k) = 0$).

This is possible only if:

$$\langle \nabla_u H \rangle \{S\} = 0$$

The Lagrangian associated with the problem is:

$$L(u_k, \lambda) = d^2(u_k) + \lambda(\langle \nabla_u H \rangle \{u\} + c)$$

and the first Kuhn-Tucker condition is written as:

$$\{\nabla_u d^2\} + \lambda \{\nabla_u H\} = \{0\}$$

As the constraint is not linear, this equation is not respected in the course of the iterations. We define the residue as:

$$\{R\} = \{\nabla_u d^2\} + \lambda \{\nabla_u H\}$$

The objective is now to minimize this residue (to remain nearest to the active constraint); the least squares method gives:

$$\|\langle R \rangle\{R\}\|^2 = \lambda^2 \langle \nabla_u H \rangle \{\nabla_u H\} + 2\lambda \langle \nabla_u H \rangle \{\nabla_u d^2\} + \langle \nabla_u d^2 \rangle \{\nabla_u d^2\}$$

which is minimal for $\partial \|\langle R \rangle\{R\}\|^2 / \partial \lambda = 0$, and it becomes:

$$\langle \nabla_u H \rangle \{\nabla_u H\} \lambda + \langle \nabla_u H \rangle \{\nabla_u d^2\} = 0$$

from which the Lagrange multiplier:

$$\lambda = -[\langle \nabla_u H \rangle \{\nabla_u H\}]^{-1} \langle \nabla_u H \rangle \{\nabla_u d^2\}$$

$\{R\} = 0$ implies:

$$\begin{aligned} \{\nabla_u d^2\} - \{\nabla_u H\} [\langle \nabla_u H \rangle \{\nabla_u H\}]^{-1} \langle \nabla_u H \rangle \{\nabla_u d^2\} &= 0 \\ ([I] - \{\nabla_u H\} [\langle \nabla_u H \rangle \{\nabla_u H\}]^{-1} \langle \nabla_u H \rangle) \{\nabla_u d^2\} &= 0 = [P] \{\nabla_u d^2\} \end{aligned}$$

where $[P]$ is the matrix of the projection on the sub-space tangent to the active constraint. The direction of descent is therefore:

$$\{S\} = [P] \{\nabla_u d^2\} \quad \text{with } [P] = [I] - \{\nabla_u H\} [\langle \nabla_u H \rangle \{\nabla_u H\}]^{-1} \langle \nabla_u H \rangle$$

5.3.2 Penalty methods [HK85]

The principle of penalty methods follows from observations of everyday life and from the code of Hammurabi: laws are all the more respected when the punishment is severe! A penalty is thus introduced when the constraints are violated. As in politics, new laws have more chance of being respected if the penalties are applied in a progressive manner (a very brutal application of a strong penalty could lead to revolution!). In optimization, this has an explanation: a high penalty makes the function curvature very strong, and the problem becomes ill-conditioned, leading to the divergence of the search algorithm.

The optimization problem is written in the form:

$$\text{Minimize } \Pi(\{u\}, r) = d^2(\{u\}) + \Psi(r, H(\{u\}))$$

where r is the penalty parameter and Ψ is a penalization function (or merit function). The *external penalty* method consists of applying the penalization

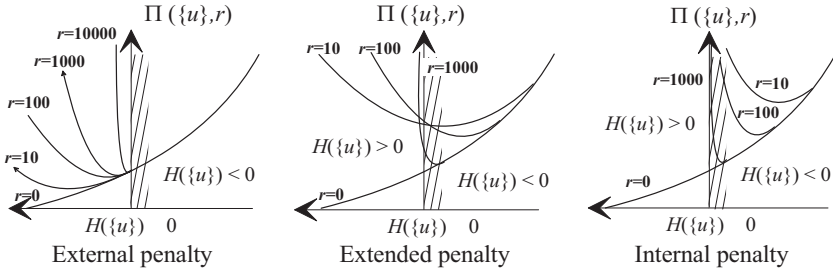


Figure 5.4 Representation of three possible forms of penalization.

function if the constraint is violated, whereas the *internal penalty* does not allow us to exceed the constraint; we also find an approach called the *extended internal penalty* where we tolerate violation of the constraint by applying the penalty in the admissible domain. These forms of penalization are shown in Figure 5.4.

Several forms of the penalization function are proposed in the literature, from which we show here an example of each category:

- External penalization: $\Pi(\{u\}, r) = d^2(\{u\}) + r(H(\{u\}))^2$.
- Extended penalization: $\Pi(\{u\}, r) = d^2(\{u\}) + rf(H(\{u\}))$.
- Internal penalization: $\Pi(\{u\}, r) = d^2(\{u\}) + r(1/H(\{u\}))$.

$$\text{with } f(H(\{u\})) = \begin{cases} 1/H(\{u\}) & \text{for } H(\{u\}) \geq H_0 \\ (1/H_0)[2 - H(\{u\})/H_0] & \text{for } H(\{u\}) \leq H_0 \end{cases}$$

Generally, the penalization function makes the system resolve in an ill-conditioned manner. Consequently, the first-order methods converge very slowly. It is also proved that the penalty methods are still slower for constraints of equality. As with reliability, the probability of failure is very sensitive to the index value β ; it is therefore necessary to be able to determine the design point in a very accurate manner. This is only possible when the penalty tends to infinity, which induces still more numerical problems. Liu and Der Kiureghian [LDK90] conclude that this family of methods is not adapted to the reliability problem because of the lack of efficiency and robustness.

5.3.3 Augmented Lagrangian [PW88]

The problem of poor conditioning of the penalty method can be avoided by adding the merit function, not to the objective function, but to the Lagrangian of the system. This is the augmented Lagrangian method.

The augmented Lagrangian can be defined as:

$$\text{minimize } \Pi(\{u\}, \lambda, r) = d^2(\{u\}) + \lambda H(\{u\}) + \frac{1}{2} r(H(\{u\}))^2$$

The performance of this method is better than that of the rough penalty method. However, it is difficult to implement because its efficiency depends on the choice of the initial values of λ and r .

5.4 First order algorithms for the SDP

In this section, the principles of reliability algorithms are applied, taking into account some special cases.

5.4.1 Hasofer-Lind-Rackwitz-Fiessler algorithm

Construction of the algorithm

The Hasofer-Lind-Rackwitz-Fiessler (HLRF) algorithm [Rac76, RF79] is a good adaptation of a first order optimization algorithm to special problems in the search for the most probable failure point according to the definition of Hasofer and Lind. It is shown to be effective in many situations even if its convergence is not assured in all cases. The works of Schittkowski on quadratic programming [Sch86], from 1981 to 1986, have led to some improvements made by Rackwitz [AR90] in a globally convergent algorithm which is described in Section 5.5.3. In this section, we present the principle of the Rackwitz-Fiessler algorithm illustrated in Figure 5.5.

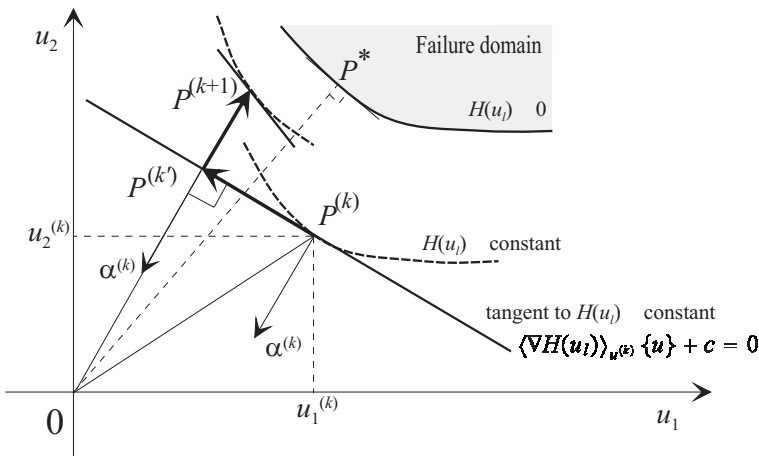


Figure 5.5 Illustration of the iteration of HLRF algorithm.

To determine the design point, we start at a point $P(k)$ with coordinates $\{u\}^{(k)}$, the point of origin of the iteration (k). This point does not necessarily

belong to the constraint and $H(u_l)$ can be different from zero. The Taylor expansion around this point reads:

$$H(u_l) = H\left(u_l^{(k)}\right) + \langle \nabla H(u_l) \rangle_{u^{(k)}} \left(\{u\} - \{u\}^{(k)}\right) + O^2$$

which gives the equation of the hyperplane tangent to $H(u_l)$ in $\{u\}^{(k)}$:

$$\langle \nabla H(u_l) \rangle_{u^{(k)}} \{u\} + c = 0$$

If the point $P^{(k+1)}$ satisfies the constraint, we can write:

$$H\left(u_l^{(k+1)}\right) = H\left(u_l^{(k)}\right) + \langle \nabla H(u_l) \rangle_{u^{(k)}} \left(\{u\}^{(k+1)} - \{u\}^{(k)}\right) = 0 \quad (5.7)$$

Let us divide this equation by the norm of the gradient $\|\nabla H(u_l)\|_{u^{(k)}}$ and let us introduce the vector of the direction cosines $\{\alpha\}$:

$$\{\alpha\} = \frac{\{\nabla H(u_l)\}}{\|\nabla H(u_l)\|} \quad (5.8)$$

We obtain the limit-state (5.7) in the form:

$$\frac{H\left(u_l^{(k)}\right)}{\|\nabla H(u_l)\|_{u^{(k)}}} + \langle \alpha \rangle^{(k)} \left(\{u\}^{(k+1)} - \{u\}^{(k)}\right) = 0$$

or:

$$\frac{H\left(u_l^{(k)}\right)}{\|\nabla H(u_l)\|_{u^{(k)}}} + \left(\langle u \rangle^{(k+1)} - \langle u \rangle^{(k)}\right) \{\alpha\}^{(k)} = 0$$

This leads to:

$$\langle u \rangle^{(k+1)} \{\alpha\}^{(k)} = \langle u \rangle^{(k)} \{\alpha\}^{(k)} - \frac{H\left(u_l^{(k)}\right)}{\|\nabla H(u_l)\|_{u^{(k)}}} \quad (5.9)$$

At the limit when $k \rightarrow \infty$, $d(u_l)^{(k)} = \beta$ and $\{u\} = -\beta \{\alpha\}$ if the algorithm is convergent. At the iteration (k) , let us set:

$$\{u\}^{(k+1)} = -\beta^{(k)} \{\alpha\}^{(k)} \implies \beta^{(k)} = -\langle u \rangle^{(k+1)} \{\alpha\}^{(k)} \quad (5.10)$$

which leads to the iterative equation giving the reliability index:

$$\beta^{(k)} = -\left(\langle u \rangle^{(k)} \{\alpha\}^{(k)}\right) + \frac{H\left(u_l^{(k)}\right)}{\|\nabla H(u_l)\|_{u^{(k)}}} \quad (5.11)$$

If the initial point $\{u\}^{(k)}$ belongs to the limit-state, Equation (5.11) is simplified because $H(u_l^{(k)}) = 0$. This formulation constitutes the initial HLRF algorithm.

Physical interpretation

With reference to coordinates $\{u\}$, the iteration of the HLRF algorithm is written by introducing (5.11) into (5.10):

$$\{u\}^{(k+1)} = \left(\langle u \rangle^{(k)} \{\alpha\}^{(k)} \right) \{\alpha\}^{(k)} - \frac{H(u_l^{(k)})}{\|\nabla H(u_l)\|_{u^{(k)}}} \{\alpha\}^{(k)} \quad (5.12)$$

It contains two terms:

- the first projects $P^{(k)}$ in $P^{(k')}$ (Figure 5.5) in the normal direction $\alpha^{(k)}$ passing through the origin: part $(\langle u \rangle^{(k)} \{\alpha\}^{(k)}) \{\alpha\}^{(k)}$ of expression (5.12),
- the second $P^{(k')} \rightarrow P^{(k+1)}$ is a correction according to the gradient: part $-H(u_l^{(k)})/\|\nabla H(u_l)\|_{u^{(k)}} \{\alpha\}^{(k)}$ of expression (5.12); it can be completed by carrying out a projection of $\{u\}^{(k+1)}$ on $H(u_l) = 0$ according to the projected gradient method described in Section 5.4.2.

Summary of the algorithm

The algorithm is summarized by the following steps:

1. choose a starting point $\{u\}^{(0)}$, generally the origin of the space in the absence of specific information ($k = 0$),
2. evaluate the limit-state function $H(u_l^{(k)})$,
3. calculate the limit-state gradient $\{\nabla H(u_l)\}^{(k)}$ and its norm $\|\nabla H(u_l)\|^{(k)}$, by deducing $\{\alpha\}^{(k)}$ using (5.8),
4. calculate $\beta^{(k)}$ using Equation (5.11),
5. calculate $\{u\}^{(k+1)}$ using Equation (5.10),
6. if $\|\{u\}^{(k+1)} - \{u\}^{(k)}\| \leq \varepsilon$ stop the calculation; otherwise set $k = k + 1$ and go to step 2.

After convergence, we can verify that $\{u\}^{(k+1)} = \{u\}^{(k)}$ and $H(u_l^{(k)}) = 0$. The algorithm is stopped according to a criterion calculated either from a norm of vector $\{u\}$, for example, $\|\{u\}^{(k+1)} - \{u\}^{(k)}\| < \varepsilon$ or, better still, from a tolerance on all the components of the vector $\{u\}$.

Case of a linear limit-state

In the case of a linear limit-state, gradient $\{\alpha\}$ is constant and convergence is reached in a single iteration. If $\{u\}$ is any point, the limit-state is written as:

$$\frac{H(u_l)}{\|\nabla H(u_l)\|} = \langle \alpha \rangle (\{u^*\} - \{u\}) = 0 \quad (5.13)$$

and the coordinates of P^* are according to 5.9:

$$\{u^*\} = -\beta\{\alpha\} = \left(\langle u \rangle \{\alpha\} - \frac{H(u_l)}{\|\nabla H(u_l)\|} \right) \{\alpha\}$$

The distance of this hyperplane from the origin is:

$$\beta = -\langle \alpha \rangle \{u\} \Big|_{H(u_l)=0}$$

Isoprobabilistic transformation

If the performance function is known only in the physical domain, the derivatives in standardized space are calculated from the Jacobian of the isoprobabilistic transformation (Chapter 4):

$$\left\{ \frac{\partial H}{\partial \{u\}} \right\} = [J]^{-1} \left\{ \frac{\partial G}{\partial \{x\}} \right\} \quad \text{with } [J] = \left[\frac{\partial \{T(\{x\})\}}{\partial \{x\}} \right]$$

5.4.2 Complements to first-order methods

iHLRF algorithm

An improved version of HLRF was proposed by Zhang and Der Kiureghian [ZDK95] by integrating a search for the optimal step. The authors demonstrate the unconditional convergence of the algorithm. The HLRF iteration (5.12) is first rewritten in the form (5.5):

$$\begin{aligned} \{u\}^{(k+1)} &= \{u\}^{(k)} + \alpha^{(k)} \{S\}^{(k)} \\ \{u\}^{(k+1)} &= \{u\}^{(k)} + \alpha^{(k)} \left(\frac{\langle u \rangle^{(k)} \{\alpha\}^{(k)} - H(u_l^{(k)})}{\|\nabla H(u_l)\|_{u^{(k)}}} \{\alpha\}^{(k)} - \{u\}^{(k)} \right) \end{aligned}$$

making the direction of descent $\{S\}$ and the step $\alpha^{(k)}$ appear. The HLRF algorithm corresponds to a choice of $\alpha^{(k)} = 1$. An optimal choice of $\alpha^{(k)}$ is obtained by minimizing a merit function of the form:

$$\alpha^{(k)} = \min_{\alpha} \left(\Psi \left(\{u\}^{(k)} + \alpha \{S\}^{(k)} \right) \right)$$

which can be obtained from linear research methods discussed in Section 5.2.3. However, the difficulty of resolution leads us to accept not the optimal solution $\alpha^{(k)}$, but a sufficiently approximate solution. The Armijo rule [Lue86] is applied ($a, b > 0$):

$$\alpha^{(k)} = \max_l \left(b^l \mid \Psi \left(\{u\}^{(k)} + b^l \{S\}^{(k)} \right) - \Psi \left(\{u\}^{(k)} \right) \leq a b^l \left\| \nabla \Psi \left(\{u\}^{(k)} \right) \right\|^2 \right)$$

The merit function Ψ proposed by Zhang and Der Kiureghian [ZDK95] is:

$$\Psi(\{u\}) = \frac{1}{2} \|\{u\}\|^2 + c |H(\{u\})|$$

in which the choice of a constant $c > \|\{u\}\| / \|\nabla H(\{u\})\|$ assures us of conditions sufficient for unconditional convergence.

Gradient method with projection

The HLRF iteration includes a correction term which constitutes only the first step of a projection on constraint $H(u_l) = 0$. A complete projection is possible according to the outline described here.

Principle: the initial algorithm can be improved by introducing the projection on the limit-state at each iteration, which requires the resolution of an equation in β whose nature depends on that of the limit-state. We thus establish:

1. knowing a point $\{u\}^{(k)}, \{\alpha\}^{(k)}$, we express $\{u\}^{(k)}$ as a function of $\beta^{(k)}$:

$$\{u\}^{(k)} = -\beta^{(k)}\{\alpha\}^{(k)} \quad (5.14)$$

2. this quantity is introduced in the expression of $H(u_l) = 0$, which gives an equation in $\beta^{(k)}$,
3. this equation is solved by a Newton-type procedure, Figure 5.6.

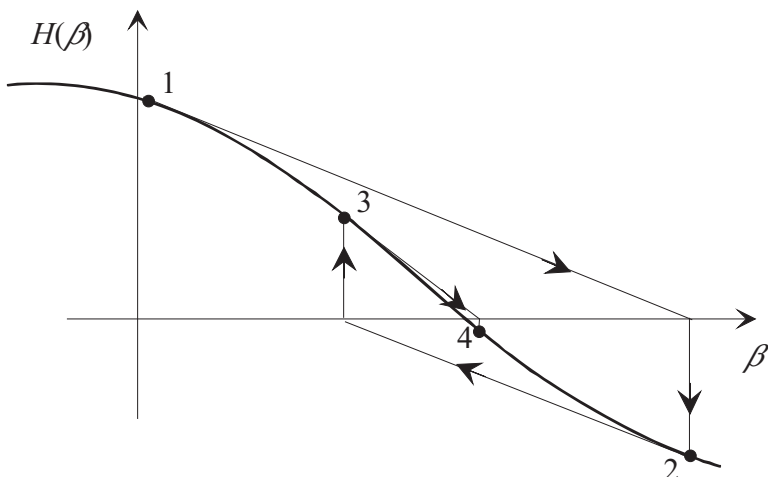


Figure 5.6 Iterative resolution of the equation $H(\beta) = 0$.

According to this formulation, the algorithm leads to a double system of iterations. The first on the successive points $\{u\}^{(k)}$ and the second for the resolution of the equation in $\beta^{(k)}$. This method is very efficient if the solution of the equation in β can be obtained easily.

Illustration: we look for the reliability index relative to the limit-state:

$$H(\{u\}) = 12.5 u_1 u_2 + 250 u_1 + 100 u_2 - 200 u_3 + 1,000 = 0$$

stemming from the example which is explained in detail in section 7.7.3. Table 5.1 gives the first iterations, first without projection (sp) and then with projection (ap).

Iteration (k)	Calculation point $\langle u \rangle^{(k)}$	Limit-state $H(u_l^{(k)})$	Index $\beta^{(k)}$
(0) $^{sp/ap}$	$\langle 0 \ 0 \ 0 \rangle$	1,000	2.981
(1) sp	$\langle -2.222 - 0.889 \ 1.778 \rangle$	24.691	3.050
(2) sp	$\langle -2.278 - 0.689 \ 1,907 \rangle$	-0.139	3.049
(3) sp	$\langle -2.289 - 0.678 \ 1.897 \rangle$	-0.001	3.049
(1) ap	$\langle -2.278 - 0.689 \ 1,907 \rangle$	0	3.049
(2) ap	$\langle -2.290 - 0.677 \ 1.896 \rangle$	0	3.049

Table 5.1 Illustration of the convergence according to the first-order algorithms.

Conclusion: the algorithm is presented here expressed directly from the knowledge of function $H(u_l)$ and not that of $G(x_l)$. Its operation is illustrated in Figure 5.7 for the case of two variables.

At any point $P^{(k)}$, we calculate the value of the performance function and the corresponding normal vector $\{\alpha\}^{(k)}$. Then we carry out the projection of point $P^{(k)}$ in the direction parallel to $\{\alpha\}^{(k)}$, passing through the origin of the space (which amounts to the projection of the origin on the plane tangent to $H(\{u\})$ in $P^{(k)}$). The point obtained, $P^{(k')}$, is later corrected by a step depending on the gradient (Equation (5.12)), or otherwise by a projection on $H(\{u\}) = 0$ (equation in β). The new starting point is then $P^{(k+1)}$. The repetition of these operations makes it possible generally to converge toward a design point P^* (as long as the limit-state is not circular).

This algorithm leads to satisfactory results for performance functions of weak curvatures; however, we have observed divergence for some cases with high curvature, $\kappa_i, |\beta \kappa_i| > 1$, in which the algorithm oscillates indefinitely around

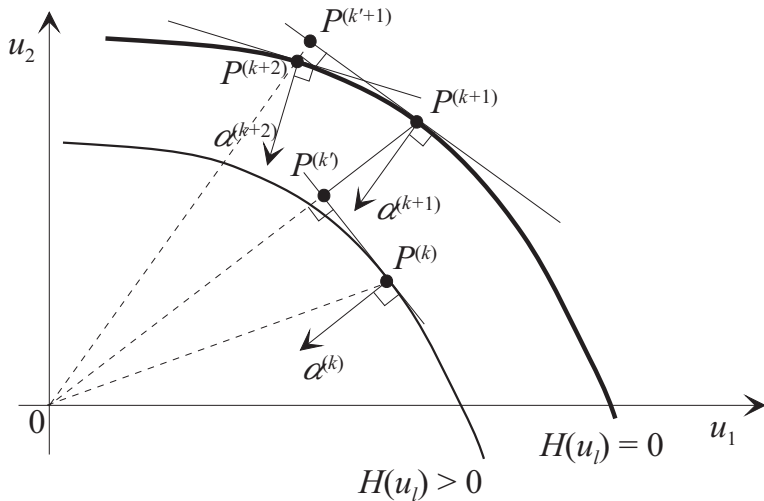


Figure 5.7 Search algorithm for P^* , with projection on the limit-state.

the most probable failure point (illustrated in Section 5.7.1). In addition, the algorithm can converge toward a relative minimum.

From physical space, the implementation can be rendered difficult for all the possible forms of transformation T , and the uniqueness of the solution for the equation in $\beta^{(k)}$ is not guaranteed. It is relatively simple by using the approximation with respect to a normal PDF (Chapter 4) and can be implemented according to the procedure described hereafter.

Application of the approximation of T according to a normal PDF

Let us first recall the notations introduced in Section 4.4.1. The variables $\{x\}$ are first standardized:

$$\hat{u} = \frac{x - m_X^N}{\sigma_X^N} \quad \{\hat{u}\} = [\sigma_X^N]^{-1}(\{x\} - \{m_X^N\})$$

in which variables $\{\hat{u}\}$ are correlated (matrix $[C_{\tilde{U}}]$, such that $[R]^t [C_{\tilde{U}}] [R] = [\lambda] = [\sigma_{\tilde{U}}]^t [\sigma_{\tilde{U}}]$) and m_X^N and σ_X^N are, respectively, the mean and the standard deviation of the equivalent normal PDF. Transformation T^{-1} is then written with iteration (k) , Equation (4.15):

$$\{u\} \xrightarrow{T^{-1}} \{x\}^{(k)} = \{m_X^N\}^{(k)} + [\sigma_X^N]^{(k)} [R]^{(k)} [\sigma_{\tilde{U}}]^{(k)} \{u\}^{(k)}$$

The gradient $\{\nabla H(\{u\})\}$ is decomposed (see the following remark):

$$\{\nabla H(u_l)\} = \left\{ \frac{\partial H}{\partial \{u\}} \right\} = \left[\frac{\partial H}{\partial \{\hat{u}\}} \frac{\partial \{\hat{u}\}}{\partial \{\tilde{u}\}} \frac{\partial \{\tilde{u}\}}{\partial \{u\}} \right]^t = [\sigma_{\tilde{U}}][R]^t \{\nabla H(\hat{u}_l)\} \quad (5.15)$$

and the direction cosines $\{\alpha\}$ are given by:

$$\begin{aligned} \{\alpha\} &= \frac{\{\nabla H(u_l)\}}{\sqrt{\langle \nabla H(u_l) \rangle \{\nabla H(u_l)\}}} \\ &= \frac{[\sigma_{\tilde{U}}][R]^t \{\nabla H(\hat{u}_l)\}}{\sqrt{\langle \nabla H(\hat{u}_l) \rangle [R][\sigma_{\tilde{U}}]^t [\sigma_{\tilde{U}}][R]^t \{\nabla H(\hat{u}_l)\}}} \end{aligned}$$

or otherwise by introducing the correlation of standardized variables $\{\hat{U}\}$, identical to the correlation of physical variables $\{X\}$:

$$\{\alpha\} = \frac{[\sigma_{\tilde{U}}][R]^t \{\nabla H(\hat{u}_l)\}}{\sqrt{\langle \nabla H(\hat{u}_l) \rangle [C_{\hat{U}}] \{\nabla H(\hat{u}_l\}}}}$$

Remark: Equation (5.15) must be written in vectorial and matrix form by transposing the product of successive derivations. To take this into account, it is sufficient to express an equation of this type in indicial notation. So, for example, $G = G(u_i(x_j))$ with $u_i = t_{ij} x_j$. It becomes:

$$\frac{\partial G}{\partial x_i} = \frac{\partial G}{\partial u_j} \frac{\partial u_j}{\partial x_i} = \frac{\partial u_j}{\partial x_i} \frac{\partial G}{\partial u_j} = t_{ji} G_{,j}$$

and in matrix form:

$$\{u\} = [T]\{x\} \quad \{\nabla G(x_l)\} = \left\{ \frac{\partial G}{\partial \{x\}} \right\} = \left(\frac{\partial G}{\partial \{u\}} \frac{\partial \{u\}}{\partial \{x\}} \right)^t = [T]^t \{\nabla G(u_l)\}$$

5.5 Second order algorithms for the SDP

5.5.1 Newton method [PW88, HK85]

In the Newton method, the objective function is expanded to the second order around point $\{u\}^{(k)}$, whereas the constraints are in the first order only. Let us put $\{\Delta u\} = \{u\} - \{u\}^{(k)}$; the problem of minimization is written as:

$$\begin{aligned} \text{minimize} \quad & \langle \nabla d^2 \rangle \{\Delta u\} + \frac{1}{2} \langle \Delta u \rangle [\nabla^2 d^2] \{\Delta u\} \\ \text{under} \quad & \langle \nabla H \rangle \{\Delta u\} + c = 0 \end{aligned}$$

where ∇ is the gradient and ∇^2 is the Hessian. For this system, the Lagrangian takes the form:

$$L(\{\Delta u\}, \lambda) = \langle \nabla d^2 \rangle \{\Delta u\} + \frac{1}{2} \langle \Delta u \rangle [\nabla^2 d^2] \{\Delta u\} + \lambda (\langle \nabla H \rangle \{\Delta u\} + c)$$

whose optimality conditions lead to the following system:

$$\begin{bmatrix} [\nabla^2 d^2] & \{\nabla H\} \\ \langle \nabla H \rangle & 0 \end{bmatrix} \begin{bmatrix} \{\Delta u\} \\ \lambda \end{bmatrix} = \begin{bmatrix} -\{\nabla d^2\} \\ -c \end{bmatrix}$$

Let us recall that $\{\nabla d^2\}$ is equal to $2\{u\}$ and that $[\nabla^2 d^2] = 2[I]$ ($[I]$ being the unit matrix), the previous system is reduced to:

$$\begin{bmatrix} 2[I] & \{\nabla H\} \\ \langle \nabla H \rangle & 0 \end{bmatrix} \begin{bmatrix} \{\Delta u\} \\ \lambda \end{bmatrix} = \begin{bmatrix} -2\{u\} \\ -c \end{bmatrix} \quad (5.16)$$

However, we remind the reader that this algorithm is not necessarily convergent!

5.5.2 Sequential quadratic programming

Such an algorithm [PW88] uses information of the second order on the limit-state function; in addition to the gradients, the sequential quadratic programming (SQP) method uses the curvatures to improve convergence. The solution is therefore accurate for quadratic functions.

Let us first consider the problem of optimization to be solved:

$$\begin{aligned} & \text{minimize} && \|\{u\}\|^2 \\ & \text{subject to} && H(u_l) = 0 \end{aligned}$$

which is equivalent to the minimization of the Lagrangian:

$$L(\{u\}, \lambda) = \|\{u\}\|^2 + \lambda H(u_l)$$

The optimality conditions are:

$$\begin{aligned} \nabla_u L(\{u\}, \lambda) &= 0 \\ H(u_l) &= 0 \end{aligned}$$

Let us develop $\nabla_u L$ and H into Taylor expansions to the first order around point $\{u\}^{(k)}$ to obtain:

$$\begin{aligned} \nabla_u L(\{u\}, \lambda) &= 2\{u\}^{(k)} + \lambda \{\nabla_u H(u_l)\}^{(k)} + [\nabla_u^2 L(\{u\}, \lambda)]^{(k)} \{\Delta u\} \\ H(u_l) &= H(u_l)^{(k)} + \langle \nabla_u H(u_l) \rangle^{(k)} \{\Delta u\} \end{aligned}$$

and hence the system of equations is:

$$\begin{bmatrix} [\nabla_u^2 L(\{u\}, \lambda)]^{(k)} & \{\nabla_u H(u_l)\}^{(k)} \\ \langle \nabla_u H(u_l) \rangle^{(k)} & 0 \end{bmatrix} \begin{bmatrix} \{\Delta u\} \\ \lambda \end{bmatrix} = \begin{bmatrix} -2\{u\}^{(k)} \\ -H(u_l)^{(k)} \end{bmatrix}$$

The resolution of this iterative system allows us to determine the direction of descent $\{\Delta u\}$. The SQP algorithm is efficient and robust. Its only defect is the need to evaluate the second derivatives (i.e. Hessian), which represents a non-negligible cost of calculation, especially in the presence of a large number of random variables. Several authors have proposed approximations to reduce the calculation cost, but these can weaken the algorithm.

5.5.3 Hybrid methods

We have seen that the first order methods are relatively slow, whereas quadratic convergence methods entail a high calculation cost. The principal cost of the latter lies in the evaluation of the Hessian. It was proposed to make this calculation more economical, through hybrid methods.

In these methods, we avoid calculating the Hessian by using approximation formulae which converge toward the exact Hessian in the course of the iterations. Two formulations are very well known:

- Davidon-Fletcher-Powell (DFP) [Dav59],
- Broyden-Fletcher-Goldfarb-Shanno (BFGS) [FP63, Bro70, Fle70, Gol70, Sha70, Sha78].

The BFGS method has proved its robustness and its stability very well. It can therefore be integrated into a procedure of quadratic calculation in the place of the Hessian.

Abdo-Rackwitz algorithm [AR90]

To avoid calculating the Hessian, Abdo and Rackwitz have proposed suppressing the contribution of the second derivatives of the limit-state; this algorithm is implemented in COMREL®. The Hessian of the Lagrangian is reduced to:

$$[\nabla^2 L(\{u\}, \lambda)] \approx [\nabla^2(\|\{u\}\|^2)] = 2[I]$$

in which $[I]$ is the identity matrix. The system to be solved is therefore:

$$\begin{bmatrix} 2[I] & \{\nabla H(u_l)\}^{(k)} \\ \langle \nabla H(u_l) \rangle^{(k)} & 0 \end{bmatrix} \begin{bmatrix} \{\Delta u\} \\ \lambda \end{bmatrix} = \begin{bmatrix} -2\{u\}^{(k)} \\ -H(u_l)^{(k)} \end{bmatrix}$$

This formula is quite simply Newton formula (5.16). The solution is given by:

$$\begin{aligned} \lambda &= \frac{2(H(u_l)^{(k)} - \langle \nabla H(u_l) \rangle^{(k)} \{u\}^{(k)})}{\|\nabla H(u_l)^{(k)}\|^2} \\ \{u\}^{(k+1)} &= -\frac{\lambda}{2} \{\nabla H(u_l)\}^{(k)} \end{aligned}$$

The advantage of this method lies in the saving of time, thanks to the elimination of the Hessian calculation. According to the authors, the method is very efficient for a large number of random variables (more than 50 variables). Coupled with an optimization of the step length, it converges a little more slowly than the SQP method.

5.6 Special problems

5.6.1 Limit-state with several minima

When a limit-state shows several local minima, there are no robust and efficient methods guaranteeing identification of the set of these minima. In this case, there is no certainty of convergence and, if it exists, it can detect the presence of a local minimum. Figure 5.8 illustrates the case of two local minima and the perturbation technique used. The algorithm leads to one or the other, according to the initial starting point, in general the median point.

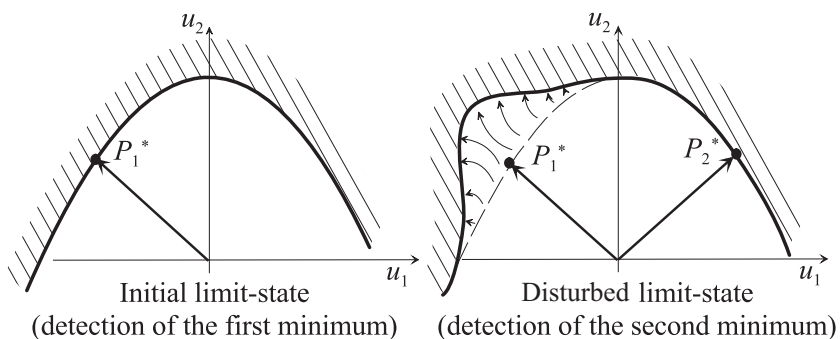


Figure 5.8 Case of local minima.

To detect subsequent relative minima, the following procedure can be used [DKD98]:

1. find a first minimum of the problem,
2. apply a transformation of the limit-state by a disturbance, moving the point found away from the origin; in other words, by dilating the limit-state in the vicinity of the identified minimum,
3. find the following minimum by the solution of the new optimization problem for the disturbed limit-state,
4. repeat 2 and 3 until all the minima are identified or until the number of fixed minima is reached.

5.6.2 Search strategy for active constraints

In the case of the reliability of systems, which will be discussed in Chapter 9, there are several limit-states which are not necessarily active at the global minimum of the problem. To identify the active sub-space, it is necessary to define a strategy for the activation and deactivation of the constraints.

The projected gradient method can be effective in finding the minimum of the problem. An algorithm to search for the active set is proposed [PW88]:

1. begin from an admissible initial point and a starting sub-space,
2. verify the Karush-Kuhn-Tucker conditions; if the point is not optimal, either continue with the same sub-space, or go to 7,
3. calculate a direction of descent $\{S\}$,
4. evaluate the step length α according to $\{S\}$ which minimizes $d(\{u\} + \alpha\{S\})$; if α violates a constraint, continue; otherwise, go to 6,
5. add the violated constraint to the active sub-space and reduce the step length to the maximum possible within the admissible domain,
6. make $\{u\}^{(k+1)} = \{u\}^{(k)} + \alpha^{(k)} \{S\}^{(k)}$,
7. modify the work sub-space (if necessary) by eliminating a constraint, update the different quantities and go to 2.

This procedure is illustrated in Figure 5.9 for the case of the intersection of three constraints. At point P^* , the two constraints H_2 and H_3 are activated.

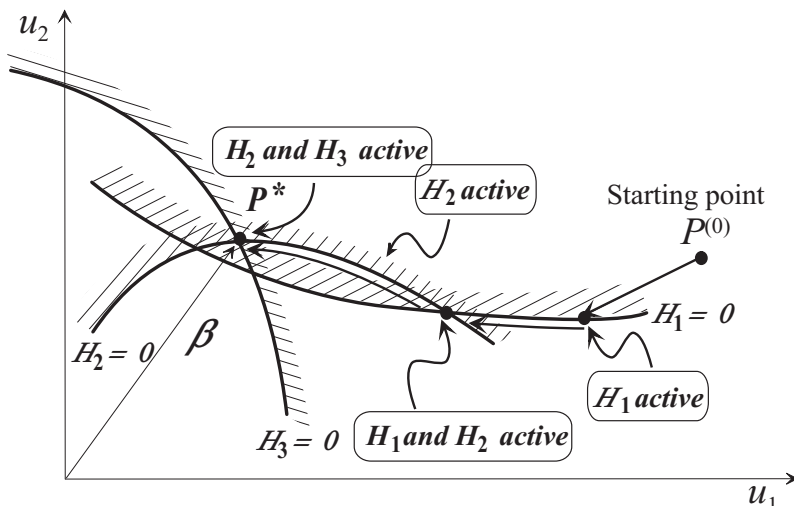


Figure 5.9 Search for P^* in the case of several limit-states.

To search for the set of minima of the problem, the designer should use his experience to test the validity of potential scenarios in any combination of the limit-states. Three compatibility situations can be presented:

- *Impossibility*: this is the case in which the failure scenarios cannot exist in a simultaneous manner, and the associated events are exclusive. Thus, no solution is possible. This combination should definitely be discarded from the analysis.
- *Inadmissibility*: this is the case in which certain scenarios can exist together, but their intersection violates other limit-states. For example, we can have a crack in a beam and damage to the material, but in a configuration in which we have already exceeded the acceptable displacement limit. The solution for this configuration exists, but it is not admissible. This combination is also excluded.
- *Admissibility*: this is the case in which the combination of scenarios exists and is admissible. In this case, we resolve the optimization problem with *constraints of equality* for each of the admissible combinations, which allows us to obtain the global minimum and the set of minima of the problem. The interesting part of this approach is that resolution with constraints of equality is more efficient than that with constraints of inequality.

5.7 Illustration using a simple example

In order to illustrate the implementation of the search for P^* , we will discuss the results of calculations in a simple case, but presenting some numerical difficulties. It is a resistance – stress problem calculated for three correlations ($\rho = -0.5; 0; 0.5$ examples discussed in Section 4.7). In fact, the curvature of the limit-state increases with the correlation, leading to a non-convergence of some algorithms for $\rho = 0.5$. The reference result is obtained using the RGMR method (Chapter 7):

ρ	-0.5	0.0	0.5
β	0.876	1.077	1.546
κ	0.208	0.528	1.154
$\kappa\beta$	0.182	0.569	1.784

The curvature is given for P^* as well as the product $\kappa\beta$, which must be lower than 1.

The limit-state is simply written as:

$$G(R, S) = R - S$$

Application of the formulae of Der Kiureghian and Liu gives the equivalent correlation:

$$\rho_0 = \rho(1.047 - 0.047\rho^2)$$

The standardized correlated variables are:

$$\hat{u}_1 = \Phi^{-1} \left(\frac{r-2}{5} \right) \quad \hat{u}_2 = \Phi^{-1} \left(\frac{s}{4} \right)$$

and the standardized decorrelated variables are given by:

$$\begin{bmatrix} u_1 \\ u_2 \end{bmatrix} = [\Gamma_0] \begin{bmatrix} \hat{u}_1 \\ \hat{u}_2 \end{bmatrix}$$

with:

$$[\Gamma_0] = \begin{bmatrix} 1 & 0 \\ \frac{-\rho_0}{\sqrt{1-\rho_0^2}} & \frac{1}{\sqrt{1-\rho_0^2}} \end{bmatrix}$$

5.7.1 HLRF algorithm

In this section, we show a few detailed iterations of the search for the most probable failure point. The starting point for the calculations is taken as being $r^{(0)} = 4$ and $s^{(0)} = 2$; the limit-state function is therefore 2 ($G^{(0)} = r^{(0)} - s^{(0)}$).

Iteration 0 – case $\rho = 0$

In standardized space, the gradients are:

$$\frac{\partial H}{\partial u_R} = 1.932 \quad \text{and} \quad \frac{\partial H}{\partial u_S} = -1.596$$

which gives:

$$\begin{aligned} \{\alpha\}^{(0)} &= \frac{\{\nabla H(u_l)\}^{(0)}}{\|\nabla H(u_l)\|^{(0)}} = \begin{bmatrix} 0.771 \\ -0.637 \end{bmatrix} \\ \beta^{(0)} &= -\frac{\langle \nabla H(u_l) \rangle^{(0)} \{\alpha\}^{(0)} - H^{(0)}}{\|\nabla H(u_l)\|^{(0)}} = 0.994 \\ \{u\}^{(1)} &= -\beta^{(0)} \{\alpha\}^{(0)} = \begin{bmatrix} -0.766 \\ 0.633 \end{bmatrix} \\ \{x\}^{(1)} &= \{T^{-1}(\{u\}^{(0)})\} = \begin{bmatrix} 3.109 \\ 2.946 \end{bmatrix} \end{aligned}$$

Iteration 1 – case $\rho = 0$

It becomes:

$$\frac{\partial H}{\partial u_R} = 1.488 \quad \text{and} \quad \frac{\partial H}{\partial u_S} = -1.306$$

and:

$$\begin{aligned}\{\alpha\}^{(1)} &= \frac{\{\nabla H(u_l)\}^{(1)}}{\|\nabla H(u_l)\|^{(1)}} = \begin{bmatrix} 0.751 \\ -0.660 \end{bmatrix} \\ \beta^{(1)} &= -\frac{\langle \nabla H(u_l) \rangle^{(1)} \{u\}^{(1)} - H^{(1)}}{\|\nabla H(u_l)\|^{(1)}} = 1.075 \\ \{u\}^{(2)} &= -\beta^{(1)} \{\alpha\}^{(1)} = \begin{bmatrix} -0.808 \\ 0.710 \end{bmatrix} \\ \{x\}^{(2)} &= \{T^{-1}(\{u\}^{(1)})\} = \begin{bmatrix} 3.048 \\ 3.044 \end{bmatrix}\end{aligned}$$

A correct result is obtained with two iterations only. It is confirmed by subsequent iterations.

Convergence and results, case $\rho = 0.5$

Figure 5.10 shows the convergence obtained – or not – by the HLRF algorithm for three cases of correlation. The case $\rho = 0.5$ is non-convergent because of its strong curvature. The evolution of the main variables is summarized in Table 5.2. We note that the algorithm seems to converge until the second iteration, and then it diverges by showing some oscillations around a position removed from the expected solution.

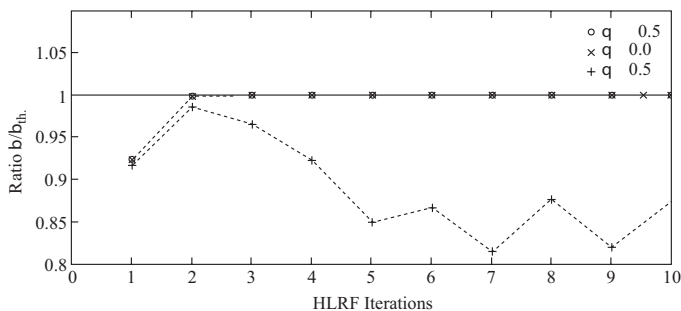


Figure 5.10 Convergence of the HLRF algorithm for different correlation values.

Iteration	r	s	u_R	u_S	$G/G^{(0)}$	β
0	4	2	-0.253	0.153	1	0
1	2.931	2.738	-0.892	1.101	0.097	1.417
2	3.244	3.172	-0.679	1.366	0.036	1.525
3	2.719	2.540	-1.064	1.047	0.089	1.493
4	3.762	3.346	-0.379	1.375	0.208	1.426
5	2.665	2.035	-1.113	0.699	0.315	1.314
6	4.026	3.369	-0.240	1.319	0.328	1.340
7	2.686	1.952	-1.093	0.626	0.367	1.260
8	3.978	3.365	-0.265	1.329	0.306	1.355
9	2.682	1.964	-1.097	0.637	0.359	1.268

Table 5.2 Iterations according to the HLRF algorithm, $\rho = 0.5$.

5.7.2 SQP, Abdo-Rackwitz and step control algorithms

Application of the SQP algorithm leads to a very rapid convergence, illustrated in Figure 5.11, without even introducing a step control. The Abdo-Rackwitz algorithm diverges like HLRF, but a step control, performed here by quadratic interpolation, allows us to conserve a slow convergence at the price of a judicious choice of the merit function and the parameter ξ and of a limitation of the maximum step length.

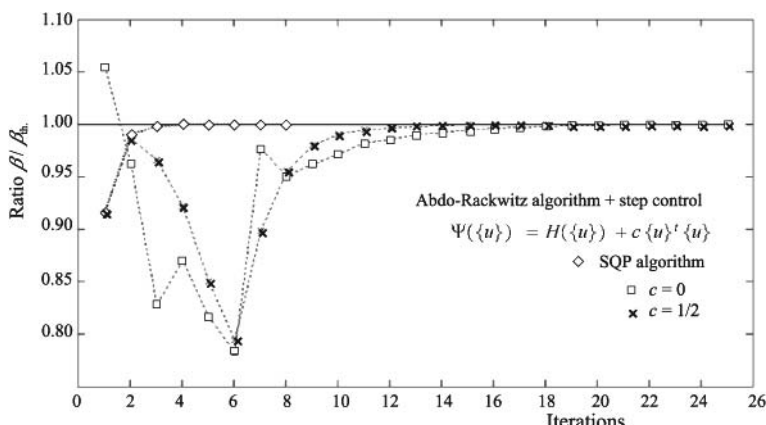


Figure 5.11 Convergence of the SQP algorithm and the Abdo-Rackwitz algorithm with step length check.

5.8 Conclusion

It is very difficult to identify a solution method as being the ‘best’. For each problem, certain methods are better adapted than others. Taken as a whole, methods based on the calculation of the gradients are of very high performance in the search for the design point. As the gradient calculation is generally carried out through finite differences, the cost of calculation becomes very high with a large number of variables. Some efficient methods of calculation of the gradients with the aid of sensitivity operators are proposed [ML98].

Liu and Der Kiureghian [LDK90] compare the performance of some of the principal methods and arrive at the following conclusions:

- the projected gradient and penalty methods are very robust, but expensive,
- the Rackwitz-Fiessler method, utilizing the characteristics of the problem very well, is economical, but its convergence is not guaranteed,
- a step control is necessary to ensure unconditional convergence,
- the SQP method appears to be robust.

Optimization algorithms are certainly going to progress in the coming years. They are increasingly being included in the codes for finite element calculations, for mechanical optimization, and they can also be used to calculate an index β , in applications coupled (or not) with mechanical modeling. This point will be examined in Chapter 11.

In the present situation, the solution of the optimization problem in the search for the most probable failure point requires great attention from the designer. A guarantee of obtaining a good solution cannot be given merely by some algorithmic criteria. All the expertise of the designer and his knowledge of the problem should be used to validate the convergence, confirm the global character of the minimum obtained and verify whether some secondary minima are present. In fact, as we will see in Chapter 7, the presence of several minima at some comparable distances from the origin can influence the probability of failure.

Table 5.3 summarizes the different methods and emphasizes their advantages and disadvantages.

Method	Derivatives	Convergence	Comments
Penalty	Dependent on the technique	Dependent on the technique	+ Robust; capable of managing several limit-states; possibility of avoiding gradient calculation.
			- Arbitrary choice of penalties; numerical slowness.

Table 5.3 Summary of the different methods of optimization of the search for the design point.

Augmented Lagrangian	Dependent on the technique	Dependent on the technique	+ Very robust; good compromise between Lagrangian and penalty methods.
			- Arbitrary choice of penalties; average numerical performance.
Projected gradient	Gradient	Linear	+ Very robust; easy coupling with a strategy of activation of constraints.
			- Not adapted to problems with high curvature of the limit-state.
HLRF	Gradient	Linear	+ Simple to implement; adapted to the reliability problem; cost of calculation very much reduced.
			- No convergence in the case of strong curvature; failure on spherical limit-state.
iHLRF	Gradient	Linear	+ Adapted to the reliability problem; very robust.
			- Cost of calculation in the search for the optimal step.
Newton-Abdo-Rackwitz	Gradient	Super linear	+ Good efficiency; low cost of calculation; adapted to large number of variables.
			- Bad approximation of the Hessian.
BFGS	Gradient	Super linear	+ Very good efficiency; robustness close to SQP; adapted to large number of variables.
			- Approximate Hessian, particularly during first iterations.
SQP	Gradient and Hessian	Quadratic	+ Very high efficiency; very robust, particularly when a search for the optimal step is adopted.
			- Calculation of the Hessian.

Table 5.3 *Continued.*

This page intentionally left blank

Chapter 6

Products of Reliability Analysis

By *products* of reliability analysis, we mean the different results stemming from the calculations. In addition to the reliability index β and the direction cosines α_i already introduced, there are the *sensitivity and elasticity factors*, often grouped under the name *importance factors*. This chapter also introduces the omission factors characterizing the effect of a variable whose random character is omitted.

6.1 Sensitivity factors

6.1.1 Definitions

To know the importance of a variable, it is necessary to identify the influence of its variation on the state of a mechanical system. The aim of such a study is to select the most significant variables, which enables us to control them better according to their role with respect to mechanical behavior or to reliability. On the reliability level, the most significant variables should be subjected to some severe quality controls; on the other hand, those which play a small role can be less controlled and supposed to be deterministic to simplify the mechanical-reliability analysis.

The importance of a variable is considered with respect to two objectives:

- its influence on the performance function: this is the study of *mechanical sensitivities* because it is related to the function of mechanical transformation that influences the behavior of a system. It is to be noted that this study is purely deterministic,
- its influence on the reliability index: this is the study of *reliability sensitivities* because it is related to the variation in reliability of the structure. It also deals with the influence of distribution parameters on the performance function.

In the rest of this section, we review the standard concepts of mechanical sensitivity.

6.1.2 Mechanical sensitivity

We are interested here in the variation of the performance function when a variable changes. The mechanical sensitivity s_i is then the derivative of the performance function $G(\{x\})$ with respect to the variables x_i :

$$s_i = \frac{\partial G(\{x\})}{\partial x_i} = \nabla_i G(\{x\})$$

The gradient appears as the measure of sensitivities with respect to the design variables.

If we look for the importance of a compound variable, sensitivity is given by the classic rule of derivation:

$$s_i = \frac{\partial G(\{x(\{y\})\})}{\partial y_i} = \sum_j \frac{\partial G(\{x(\{y\})\})}{\partial x_j} \frac{\partial x_j(\{y\})}{\partial y_i}$$

In general, the analysis of mechanical sensitivities is carried out with particular representative values $\{x_r\}$ of different variables such as the mean or any other value used by the engineer. Let us note that the value of the derivative is not objective, because it depends on the numerical magnitudes considered, which can deceive the designer during the comparison of different variables. In order to be able to carry out more significant comparisons, it is more interesting to *standardize* the results in the form:

$$\bar{s}_i = \frac{\partial G(\{x\})}{\partial x_i} \frac{x_i}{G(\{x\})} \Big|_{\{x\}=\{x_r\}}$$

This a-dimensional quantity is called *mechanical elasticity*. It is not possible to standardize at the most probable failure point where $G(\{x^*\}) = 0$.

The result of the study of mechanical sensitivities is very useful in the choice of the random variables which need to be taken into account. It allows us to distinguish stress variables from resistance variables by the sign of the sensitivity. These indications are exploited to choose more favorable initial values in the reliability calculation algorithm and in the calculation of gradients.

Moreover, the analysis of mechanical sensitivities enables us to identify the variables whose influence is amplified or weakened during the mechanical transformation. Thus, we can limit the mechanical-reliability analysis to the variables which have the most influence on the performance function.

Only those variables which allow us to economize calculation resources are considered random. However, in the reliability context, this conclusion is not always true for several reasons:

- The performance function is generally non-linear. Sensitivities to the representative values can be very different from those at the most probable failure point. Deviation is greater when non-linearity is stronger.
- The variables can have a small mechanical influence, but present a large probabilistic dispersion. In spite of the small effect on the performance function, the variability of the data can be an essential factor in the failure.
- The types of distribution, as well as the correlations of the random variables, can modify the importance of the random variables for the same standard deviation, according to the flattening of the density function.

Nevertheless, the calculation of mechanical sensitivities offers, in most practical cases, reasonable indications of the importance of the different variables of the system.

6.2 Importance factors in reliability

The study of the importance of random variables and of their distribution parameters enables us to have a clear and precise idea of mechanical-reliability behavior. We therefore look for the effects of variations on the failure of the system measured by β at the most probable point of failure. There are several measures of importance:

- the sensitivity of the reliability index to design variables,
- the sensitivity of β to the distribution parameters of the probability density function,
- the sensitivity of β to the performance function parameters,
- the sensitivity of the probability of failure,

to which it is also possible to associate the corresponding elasticities.

6.2.1 Sensitivity of the reliability index

Sensitivity of β to standardized random variables

Let us consider the FORM limit-state written in the standardized form:

$$H(\{u\}) = \{\alpha\}^t \{u\} + \beta = 0 \quad (6.1)$$

in which the direction cosines are given by:

$$\alpha_i = \frac{\nabla_i H(\{u\})}{\sqrt{\langle \nabla H(\{u\}) \rangle \langle \nabla H(\{u\}) \rangle}} \Big|_{\{u^*\}} = \frac{\nabla_i H(\{u\})}{\|\{\nabla H(\{u\})\}\|} \Big|_{\{u^*\}}$$

From (6.1), it becomes:

$$\beta = -\{\alpha\}^t \{u\} \implies \frac{\partial \beta}{\partial \{u\}} \Big|_{\{u^*\}} = -\{\alpha\} \text{ or } \frac{\partial \beta}{\partial u_i} \Big|_{\{u^*\}} = -\alpha_i \quad (6.2)$$

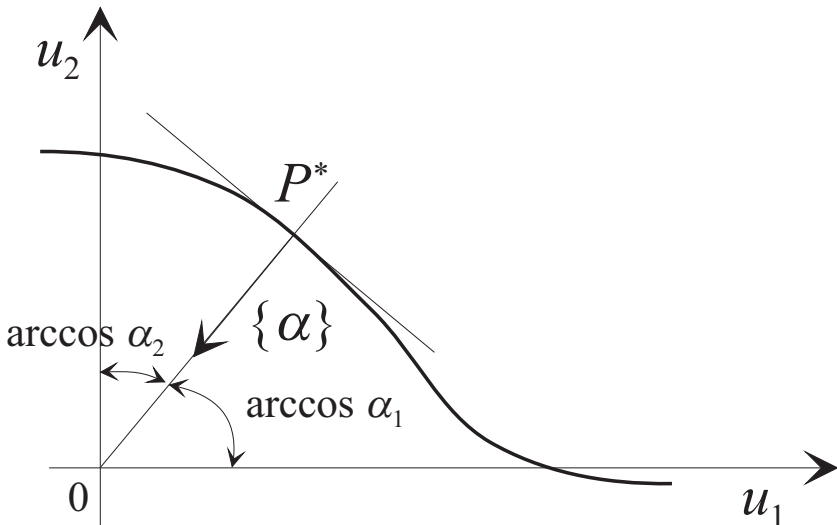


Figure 6.1 Direction cosines at the design point.

in which $\{u^*\}$ is the vector of the design point coordinates in standardized space (Figure 6.1). The direction cosines represent the sensitivities of the reliability index in standardized space *vis-à-vis* each of the standardized random variables.

Sensitivity of β to physical random variables

The sensitivity of β to physical random variables is obtained by the rule of derivation. By introducing the isoprobabilistic transformation $u_j = T_j(\{x\})$, it becomes:

$$\frac{\partial \beta}{\partial x_i} = \sum_j \frac{\partial \beta}{\partial u_j} \frac{\partial u_j}{\partial x_i} = - \sum_j \alpha_j \frac{\partial T_j(\{x\})}{\partial x_i} \Big|_{\{x^*\}} = -[J]^t \{\alpha\}$$

By choosing the negative definition and standardizing it, we obtain a factor of physical importance:

$$\{\gamma_{\text{phys}}\} = \frac{[J]^t \{\alpha\}}{\|[J]^t \{\alpha\}\|} \quad (6.3)$$

This equation shows that sensitivities in physical space integrate the Jacobian $[J]$ of the isoprobabilistic transformation. The role of distributions and correlations can amplify the influence of certain variables.

Case of dependent physical variables

Equation (6.2) is satisfactory for independent variables; it is not so in the case of dependence, and therefore the importance factor must be corrected. The limit-state (6.1) can also be written as:

$$H(\{u\}) = \{\alpha\}^t \{u\} + \beta = \{\alpha\}^t (\{u\} - \{u^*\}) = 0$$

in which we can introduce the isoprobabilistic transformation linearized at the failure point:

$$\{u\} \approx \{u^*\} + [J](\{x\} - \{x^*\}) \quad \text{with } [J] = \frac{\partial T_i(\{x\})}{\partial x_j} \Big|_{\{x^*\}} \quad (6.4)$$

$$\text{or } \{u\} = \{u^*\} + [J](\hat{x} - \{x^*\})$$

in which equality is obtained for a value $\{\hat{x}\}$ close to $\{x\}$. The linear equation between $\{u\}$ and $\{\hat{x}\}$ implies the Gaussian character of $\{\hat{x}\}$:

$$\{\hat{x}\} = [J]^{-1}(\{u\} - \{u^*\}) + \{x^*\}$$

whose moments are:

$$\begin{aligned} E[\{\hat{x}\}] &= -[J]^{-1}\{u^*\} + \{x^*\} = \{m_{\hat{X}}\} \\ E[(\{\hat{x}\} - \{m_{\hat{X}}\})^2] &= [J]^{-1} [J]^{-1 t} = [\text{cov}_{\hat{X}}] \end{aligned}$$

Point \hat{P} of coordinates $\{\hat{x}\}$ is the standard equivalent of P^* . Let us introduce (6.4) into (6.1):

$$\hat{H}(\{u\}) = \{\alpha\}^t [J](\hat{x} - \{x^*\})$$

from which we can calculate the mean and the variance:

$$\begin{aligned} m_{\hat{H}} &= -\{\alpha\}^t [J] [J]^{-1} \{u^*\} = \beta \\ \sigma_{\hat{H}}^2 &= \{\alpha\}^t [J] [\text{cov}_{\hat{X}}] [J]^t \{\alpha\} = 1 \end{aligned}$$

It remains for us to identify the weight of each variable in the total variance. For this, we introduce the diagonal matrix of standard deviations of $\{\hat{X}\}$, marked $[\sigma_{\hat{X}}]$. The covariance matrix $[\text{cov}_{\hat{X}}]$ is then split up:

$$[\text{cov}_{\hat{X}}] = [\sigma_{\hat{X}}] [\sigma_{\hat{X}}] + [\text{cov}_{\hat{X}}] - [\sigma_{\hat{X}}] [\sigma_{\hat{X}}]$$

which gives, in the expression of $\sigma_{\hat{H}}^2$:

$$\begin{aligned} \sigma_{\hat{H}}^2 &= \{\alpha\}^t [J] ([\sigma_{\hat{X}}] [\sigma_{\hat{X}}] + [\text{cov}_{\hat{X}}] - [\sigma_{\hat{X}}] [\sigma_{\hat{X}}]) [J] \{\alpha\} = 1 \\ &= \{\alpha\}^t [J] [\sigma_{\hat{X}}] [\sigma_{\hat{X}}] [J]^t \{\alpha\} \\ &\quad + \{\alpha\}^t [J] ([\text{cov}_{\hat{X}}] - [\sigma_{\hat{X}}] [\sigma_{\hat{X}}]) [J]^t \{\alpha\} \end{aligned}$$

The first term of the decomposition can be considered as the importance of variables $\{\hat{x}\}$ in the total variance. The importance vector $\{\gamma\}$ is the first term, after normalization:

$$\{\gamma\} = \frac{[\sigma_{\hat{X}}] [J]^t \{\alpha\}}{\|[\sigma_{\hat{X}}] [J]^t \{\alpha\}\|}$$

Case of independent physical variables: the isoprobabilistic transformation is reduced to:

$$\hat{x}_i = \sigma_{\hat{X}_i} u_i + m_{\hat{X}_i} \implies [J]^{-1} = [\sigma_{\hat{X}}]$$

and:

$$\{\gamma\} = \{\alpha\} \quad \text{independent variables}$$

When the physical variables are independent, the vector of direction cosines represents the importance factors of the reliability index very well. When they are dependent, the notion of standard equivalent allows us to construct the vector of the importance factors.

Illustration: case of two uniform variables

Let us look again at the example dealt with in Section 4.7. The results obtained are given in Table 6.1. A positive value (or negative) indicates a variable of resistance type (or stress type).

ρ	-0.5		0		0.5	
$\langle \alpha \rangle$	0.896	-0.444	0.755	-0.655	0.551	-0.835
$\langle \gamma \rangle$	0.770	-0.638	0.755	-0.655	0.735	-0.679

Table 6.1 Importance factors of the two random variables in the elementary case with uniform distributions.

6.2.2 Sensitivity of β with respect to the distribution parameters p_{i_γ}

The calculation of the sensitivities of β with respect to parameters $\{p\}$ intervening in the probability density functions (means, standard deviations, etc.) enables us to identify the measures which must be taken to control (or not) the quality.

The parameter considered here is the γ th parameter of variable X_i , and it is denoted as p_{i_γ} . By extension, this notation also includes parameters which

are not linked to a single random variable, for example, a correlation ρ_{ij} . The effect of its variation on the reliability is defined by:

$$\alpha_{i_\gamma} = \left. \frac{\partial \beta}{\partial p_{i_\gamma}} \right|_{\{u^*\}}$$

calculated in $\{u^*\}$.

Let us express β as a function of variables u_j :

$$\alpha_{i_\gamma} = \sum_j \left. \frac{\partial \beta}{\partial u_j} \frac{\partial u_j}{\partial p_{i_\gamma}} \right|_{\{u^*\}}$$

and let us point out that $\partial \beta / \partial u_j = -\alpha_j = u_j^* / \beta_j$; the expression of α_{i_γ} becomes:

$$\begin{aligned} \alpha_{i_\gamma} &= \sum_j \left. \frac{u_j^*}{\beta} \frac{\partial u_j}{\partial p_{i_\gamma}} \right|_{\{u^*\}} = - \sum_j \alpha_j \frac{\partial T_j(\{x^*\}, \{p\})}{\partial p_{i_\gamma}} \\ &= \sum_j \frac{u_j^*}{\beta} \frac{\partial T_j(\{x^*\}, \{p\})}{\partial p_{i_\gamma}} \end{aligned} \quad (6.5)$$

which shows the isoprobabilistic transformation T that depends on the parameter p_{i_γ} . T is a value function in (u_1, \dots) of variables p_{i_γ}, x_1, \dots Two special cases allow us to continue the calculation.

Case of independent variables: the quantities $\partial u_j / \partial p_{i_\gamma}$ are zero for $i \neq j$ and transformation T is inferred simply from:

$$\Phi(u_i) = F_{X_i}(x_i, p_{i_\gamma}) \longrightarrow u_i = T_i(x_i, p_{i_\gamma})$$

By differentiation with respect to p_{i_γ} , it becomes:

$$\begin{aligned} \frac{\partial \Phi(u_i)}{\partial u_i} \frac{\partial u_i}{\partial p_{i_\gamma}} &= \frac{\partial F_{X_i}(x_i, p_{i_\gamma})}{\partial p_{i_\gamma}} = \phi(u_i) \frac{\partial u_i}{\partial p_{i_\gamma}} \\ \frac{\partial u_i}{\partial p_{i_\gamma}} &= \frac{1}{\phi(u_i)} \frac{\partial F_{X_i}(x_i, p_{i_\gamma})}{\partial p_{i_\gamma}} \\ \alpha_{i_\gamma} &= \left. \frac{\partial \beta}{\partial p_{i_\gamma}} \right|_{\{u^*\}} = \left. \frac{\partial \beta}{\partial u_i} \frac{\partial u_i}{\partial p_{i_\gamma}} \right|_{\{u^*\}} = -\alpha_i \frac{1}{\phi(u_i^*)} \frac{\partial F_{X_i}(x_i^*, p_{i_\gamma})}{\partial p_{i_\gamma}} \end{aligned} \quad (6.6)$$

where x_i^* is defined by $\Phi(u_i^*) = F_{X_i}(x_i^*, p_{i_\gamma})$.

Case of correlated variables: according to Nataf transformation (4.19):

$$u_j = \sum_k \Gamma_{0,jk} \Phi^{-1}(F_{X_k}(\{x\}, \{p\})) = \sum_k \Gamma_{0,jk} \hat{u}_k$$

and the sensitivities are calculated as follows.

$$\alpha_{i_\gamma} = \frac{\partial \beta}{\partial p_{i_\gamma}} \Big|_{\{u^*\}} = \sum_j \frac{\partial \beta}{\partial u_j} \frac{\partial u_j}{\partial p_{i_\gamma}} \Big|_{\{u^*\}} = - \sum_j \alpha_j \frac{\partial}{\partial p_{i_\gamma}} \left(\sum_k \Gamma_{0,jk} \hat{u}_k \right) \Big|_{\{u^*\}}$$

and if $\Gamma_{0,jk}$ does not contain the parameter p_{i_γ} :

$$\alpha_{i_\gamma} = - \sum_j \alpha_j \sum_k \Gamma_{0,jk} \frac{\partial \hat{u}_k}{\partial p_{i_\gamma}} \Big|_{\{u^*\}}$$

and if $\partial \hat{u}_k / \partial p_{i_\gamma} = 0$ for $k \neq i$:

$$\alpha_{i_\gamma} = - \sum_j \alpha_j \Gamma_{0,ji} \frac{\partial \hat{u}_i}{\partial p_{i_\gamma}} = - \sum_j \alpha_j \Gamma_{0,ji} \frac{1}{\phi(\hat{u}_i^*)} \frac{\partial F_{X_i}(x_i^*, p_{i_\gamma})}{\partial p_{i_\gamma}}$$

In general, it is necessary to use the calculation of the Jacobian matrix of the isoprobabilistic transformation at the design point, by including the derivation with respect to the parameter of the probability density function.

Illustration – Gaussian density: let us consider the example of a standardized density $\mathcal{N}(m, \sigma^2)$; the transformation is:

$$u_i = T_i(\{x\}) = \frac{x_i - m}{\sigma} \quad \text{and} \quad x_i = m + \sigma u_i$$

Sensitivity with respect to the mean is given as (Equation (6.5)):

$$\alpha_m = - \frac{1}{\sigma} \frac{u_i^*}{\beta} \quad (\text{independent Gaussian variable})$$

and with respect to the standard deviation:

$$\alpha_\sigma = - \frac{(x_i^* - m)}{\sigma^2} \frac{u_i^*}{\beta} = - \frac{u_i^{*2}}{\sigma \beta} \quad (\text{independent Gaussian variable})$$

This expression shows well that the sensitivity of the standard deviation is always negative (β is assumed to be positive); the increase in the standard deviation diminishes the reliability of the system systematically, whether the variable is of stress or of resistance.

The result is also obtained from the general Equation (6.6) by noting that $F_X = \Phi((x - m)/\sigma)$ for the mean:

$$\alpha_m = \frac{u_i^*}{\beta} \frac{1}{\phi(u_i^*)} \frac{\partial F_X}{\partial m} = \frac{u_i^*}{\beta} \frac{1}{\phi(u_i^*)} \frac{\partial \Phi}{\partial u_i} \frac{\partial u_i}{\partial m} = -\frac{1}{\sigma} \frac{u_i^*}{\beta}$$

and for the standard deviation:

$$\alpha_\sigma = \frac{u_i^*}{\beta} \frac{1}{\phi(u_i^*)} \frac{\partial F_X}{\partial \sigma} = \frac{u_i^*}{\beta} \frac{1}{\phi(u_i^*)} \frac{\partial \Phi}{\partial u_i} \frac{\partial u_i}{\partial \sigma} = -\frac{u_i^{*2}}{\sigma \beta}$$

6.2.3 Sensitivity of β with respect to the performance function parameters

In the previous case, we considered the parameters of the distribution functions. These parameters intervene only in the isoprobabilistic transformation.

Let us now examine the case of parameters intervening in the limit-state function $G(\{X\})$ (i.e. the mechanical transformation). We are interested in the evolution of the design point during the variation of parameter p_i . As the design point should remain on the limit-state, the total derivative with respect to the parameter is always zero:

$$\frac{dG(\{x\}, \{p\})}{dp_i} \equiv \frac{dH(\{u\}, \{p\})}{dp_i} = \frac{\partial H(\{u\}, \{p\})}{\partial p_i} + \sum_j \frac{\partial H(\{u\}, \{p\})}{\partial u_j} \frac{\partial u_j}{\partial p_i} = 0$$

Let us divide this expression by the norm of the gradient vector to obtain:

$$\frac{1}{\|\nabla H(\{u\}, \{p\})\|} \frac{\partial H(\{u\}, \{p\})}{\partial p_i} + \sum_j \alpha_j \frac{\partial u_j}{\partial p_i} = 0 \quad (6.7)$$

Now, the reliability index is defined by:

$$\beta = - \sum_j \alpha_j u_j|_{u_j=u_j^*}$$

and it becomes:

$$\begin{aligned} \frac{\partial \beta}{\partial p_i} &= - \sum_j u_j \frac{\partial \alpha_j}{\partial p_i} - \sum_j \alpha_j \frac{\partial u_j}{\partial p_i} \\ &= \sum_j \alpha_j \beta \frac{\partial \alpha_j}{\partial p_i} - \sum_j \alpha_j \frac{\partial u_j}{\partial p_i} \end{aligned}$$

Vectors α_j and $\partial \alpha_j / \partial p_i$ are orthogonal at the design point because:

$$\sum_j \alpha_j \alpha_j = 1 \implies \frac{\partial (\sum_j \alpha_j \alpha_j)}{\partial p_i} = 2 \sum_j \alpha_j \frac{\partial \alpha_j}{\partial p_i} = 0$$

and we obtain from this:

$$\frac{\partial \beta}{\partial p_i} = - \sum_j \alpha_j \frac{\partial u_j}{\partial p_i}$$

Let us introduce this expression into the formula of the total derivative of the limit-state (6.7) to obtain:

$$\frac{\partial \beta}{\partial p_i} = \frac{1}{\|\{\nabla H(\{u\}, \{p\})\}\|} \frac{\partial H(\{u\}, \{p\})}{\partial p_i}$$

6.2.4 Sensitivity of the probability of failure [MKL86]

If we admit a first-order approximation of the probability of failure, we know that:

$$P_f \approx \Phi(-\beta) = 1 - \Phi(\beta)$$

The variation of P_f with respect to any parameter p_i can be obtained as:

$$\frac{\partial P_f}{\partial p_i} = \frac{\partial P_f}{\partial \beta} \frac{\partial \beta}{\partial p_i} = -\phi(\beta) \left. \frac{\partial \beta}{\partial p_i} \right|_{\{u^*\}}$$

where ϕ is the standardized Gaussian density function. For a distribution parameter:

$$\frac{\partial P_f}{\partial p_{i_\gamma}} = -\phi(\beta) \left. \frac{\partial \beta}{\partial p_{i_\gamma}} \right|_{\{u^*\}} = -\phi(\beta) \alpha_{i_\gamma}$$

6.2.5 Elasticity of parameters

As in the calculation of mechanical sensitivities, the values of reliability sensitivities cannot be exploited for the comparison of variables and parameters. To remedy this problem, we must normalize the sensitivities to obtain *elasticities* defined by:

$$e_{p_i} = \frac{p_i}{\beta} \left. \frac{\partial \beta}{\partial p_i} \right|_{\{u^*\}}$$

In the example of the Gauss distribution, elasticity with respect to the mean is:

$$e_m = -\frac{u_i^* m}{\sigma \beta} = \frac{\alpha_i m}{\beta \sigma}$$

in which α_i is the direction cosine of variable u_i . With respect to the standard deviation:

$$e_\sigma = -\frac{\sigma u_i^*}{\sigma \beta^2} = -\alpha_i^2$$

As $\sum_i \alpha_i^2 = 1$, it is usual to represent the influence of the variability of the design variables in the form of a pie diagram of unit surface (Figure 6.5).

6.3 Omission factors

Omission factors [DM96] express the relative error of the reliability index when a random variable is replaced by a deterministic value:

$$\zeta(U_i = u_i) = \frac{\beta_{\{U\}|U_i=u_i}}{\beta}$$

in which ζ is the omission factor, β is the Hasofer-Lind index and $\beta_{\{U\}|U_i=u_i}$ is the conditional index calculated for the deterministic variable U_i equal to u_i .

6.3.1 Linear limit-state

In standardized space, a linear limit-state is written in the form:

$$H(\{U\}) = \beta + \sum_i \alpha_i U_i = 0$$

If we set the value of $U_k = u_k$, the limit-state becomes:

$$H(\{U\}|U_k = u_k) = \beta + \alpha_k u_k + \sum_{i \neq k} \alpha_i U_i = 0$$

The conditional reliability index is therefore:

$$\beta_{\{U\}|U_k=u_k} = \frac{\beta + \alpha_k u_k}{\sqrt{\sum_{i \neq k} \alpha_i^2}} = \frac{\beta + \alpha_k u_k}{\sqrt{1 - \alpha_k^2}}$$

and the corresponding omission factor:

$$\zeta(U_k = u_k) = \frac{\beta_{\{U\}|U_k=u_k}}{\beta} = \frac{1 + \alpha_k u_k / \beta}{\sqrt{1 - \alpha_k^2}}$$

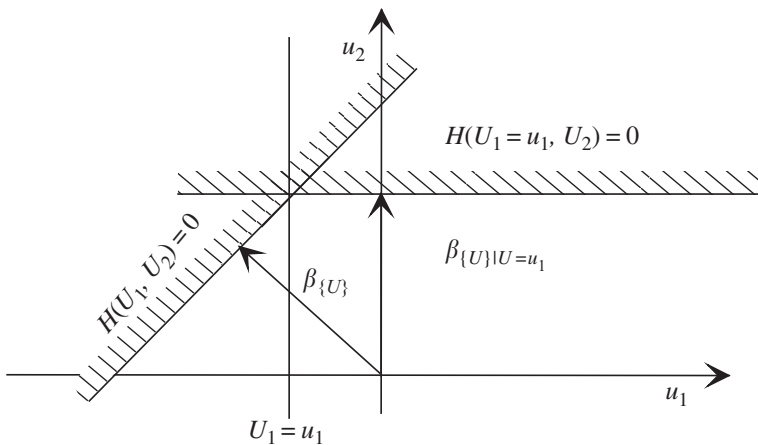


Figure 6.2 Limit-state in standardized space and conditional limit-state.

Illustration: let us consider the example of a limit-state formed from two independent normal variables (Figure 6.2):

$$G(X_1, X_2) = X_1 - X_2$$

in which X_1 is a normal variable of average 5 and of standard deviation 0.8 and X_2 is a normal variable of average 2 and of standard deviation 0.6; the corresponding normalized variables are:

$$U_1 = \frac{X_1 - 5}{0.8} \quad \text{and} \quad U_2 = \frac{X_2 - 2}{0.6}$$

It becomes:

$$H(U_1, U_2) = 3 + 0.8U_1 - 0.6U_2$$

We have:

$$\beta = 3 \quad \{\alpha^*\} = \begin{bmatrix} 0.8 \\ -0.6 \end{bmatrix} \quad \{u^*\} = \begin{bmatrix} -2.4 \\ +1.8 \end{bmatrix}$$

By imposing the value of the first variable, the limit-state becomes:

$$H(U_1 = u_1, U_2) = 3 + 0.8u_1 - 0.6U_2$$

whose corresponding reliability index is:

$$\beta_{\{U\}|U_1=u_1} = (3 + 0.8u_1)/0.6$$

$$\zeta(U_1 = u_1) = \frac{1 + 0.8u_1/3}{0.6}$$

The omission factor for $x_1 = 5$ (mean, $u_1 = 0$) becomes:

$$\zeta(U_1 = 0) = \frac{1}{0.6} = 1.67$$

that is, $\beta_{\{U\}|U_1=u_1} = 1.67\beta = 5$. However, it can be more judicious to replace a random variable by a characteristic value rather than by the mean. X_1 is a value of resistance type, and we choose the mean reduced by two standard deviations $u_1 = -2$, $\zeta(U_1 = -2) = 0.78$. The reliability index conditioned by a hypothesis of certainty of a weak resistance falls from 3 to 2.33.

6.3.2 Non-linear limit-state

If the limit-state is non-linear, the exact solution requires two mechanical-reliability calculations: the first by considering all the random variables and the second by considering one of these as a deterministic variable, and this is true for all the variables for which we wish to calculate the omission factors. This method can lead to a large number of calculations, and therefore some approximations are required.

A first approximation can be carried out by replacing the limit-state by the plane tangent to the design point. However, in the case of strong curvatures or of a large deviation between the imposed values and those of the design point, the tangent plane method can give erroneous results.

The calculation of the conditional reliability index $\beta_{\{U\}|U_k=u_k}$ corresponds to the classic index β for all the variables, but by fixing $U_k = u_k$. From the probabilistic point of view, this can be interpreted as a very narrow truncation of the distribution of U_k around point u_k , and the interval of truncation is $[u_k - \varepsilon, u_k + \varepsilon]$, $\varepsilon > 0$ being a small number. In the case where we fix the variable to its mean, we are simply attributing a zero standard deviation to the variable considered $\sigma_{X_k} \rightarrow 0$. From the geometric point of view, we search for reliability for a new limit-state $H^{(k)}(\{U\} | U_k = u_k)$ defined by the intersection of the initial limit-state $H(\{U\})$ with the plane $U_k = u_k$ (Figure 6.3).

To solve this problem, we propose a quadratic approximation of the limit-state surface. This procedure is similar to that developed to approximate the limit-state from a finite element model, explained in detail in Chapter 11. The approach is as follows:

1. Using any procedure, we calculate the reliability index of the system for the initial limit-state $H(\{U\}) = 0$.
2. We construct a quadratic approximation of the limit-state function from the evaluations carried out during the search for the design point (step 1); we can improve the approximation by calculating some points close to the

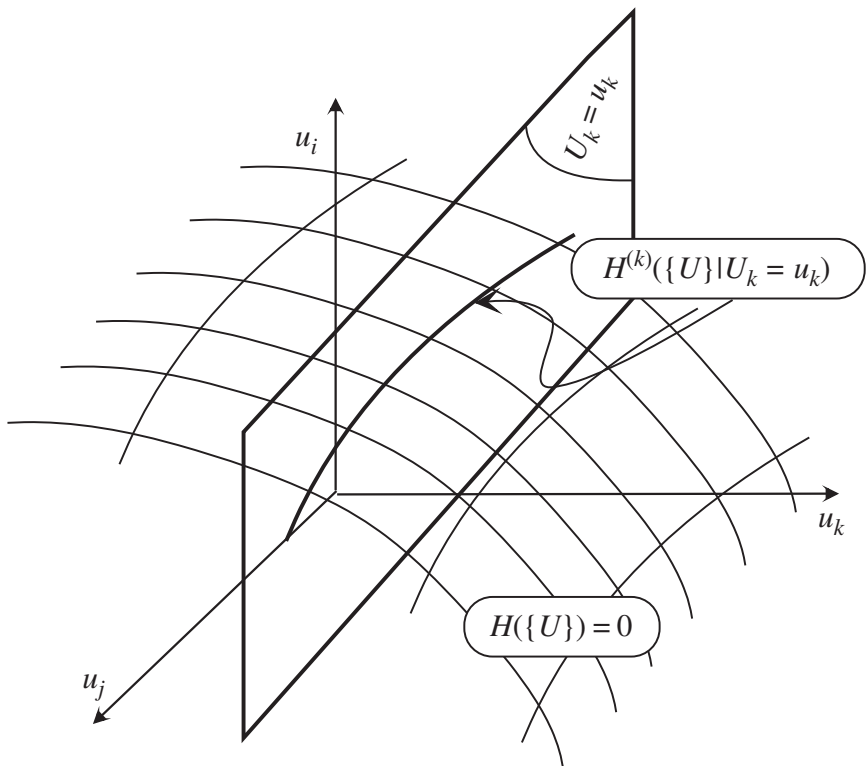


Figure 6.3 Intersection with the plane $U_k = u_k$.

plane $U_k = u_k$; regression gives an expression in the form:

$$H(\{U\}) \approx Q(\{U\}) = a_0 + \sum_i a_i U_i + \sum_i \sum_j b_{ij} U_i U_j$$

3. For each variable, we look for the intersection of the approximate limit-state with the plane of the variable $U_k = u_k$. The limit-state becomes:

$$\begin{aligned} Q^{(k)}(\{U\}|U_k = u_k) &= a_0 + a_k u_k + b_{kk} u_k^2 + 2u_k \sum_{i \neq k} b_{ki} U_i \\ &\quad + \sum_{i \neq k} a_i U_i + \sum_{i \neq k} \sum_{j \neq k} b_{ij} U_i U_j \end{aligned}$$

4. For this limit-state, we calculate the reliability index $\beta_{\{U\}|U_k = u_k}$ (in the plane $U_k = u_k$).

5. The omission factor for variable U_k is evaluated according to the definition:

$$\zeta(U_k = u_k) = \frac{\beta_{\{U\} | U_k = u_k}}{\beta}$$

6. We repeat steps 3–5 for each variable to be considered.

Let us note that this procedure does not require additional calculations of the limit-state function. The quadratic approximation $Q(\{U\})$ is evaluated once and for all.

6.4 Representation of the results: an example

In order to illustrate the concepts introduced, we consider a frame (Figure 6.4) made up of tubular sections. Here, the elastoplastic limit-state is given by the equation:

$$\cos\left(\frac{\pi}{2} \frac{N}{N_p}\right) \pm \frac{M}{M_p} = 0$$

in which N and M are respectively the axial force and the bending moment acting in the section considered, and N_p, M_p are the admissible plastic axial force and bending moment. A strength of materials calculation determines the influence coefficients P_i of the horizontal action due to swell H and of the dead load q in the form:

$$M = P_1 H + P_2 q \quad N = P_3 H + P_4 q$$

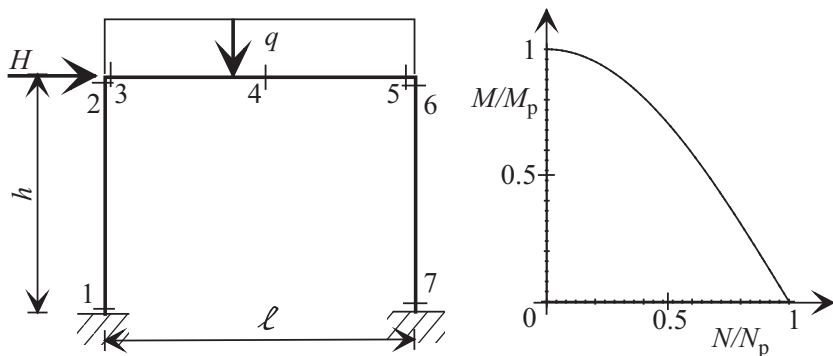


Figure 6.4 Tubular frame: elastoplastic limit-state.

and this is done for each section $S_i, i = 1, \dots, 7$ studied. The plastic limit efforts are functions of the yield limit f_y :

$$M_p = P_5 f_y \quad N_p = P_6 f_y$$

All the parameters P_i are considered deterministic, whereas H, q and f_y are random variables. The limit-state is then written in the form:

$$G(H, q, f_y, P_i) = \cos\left(\frac{\pi}{2} \frac{P_3 H + P_4 q}{P_6 f_y}\right) \pm \frac{P_1 H + P_2 q}{P_5 f_y} = 0$$

Typical results obtained are shown in Figure 6.5.

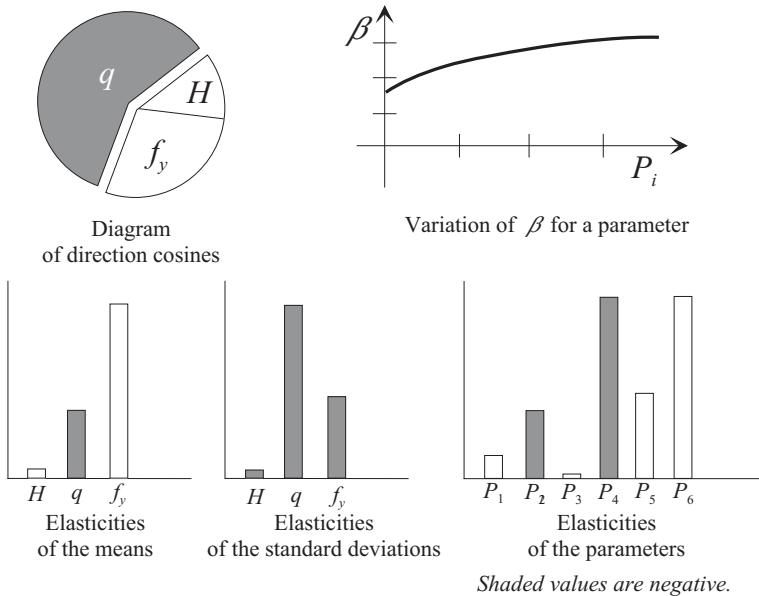


Figure 6.5 Reliability analysis results (cross-section 2).

These results are those associated with cross-section 2. The squares of the direction cosines are shown in a pie chart. The negative values are shaded. The influence of a parameter P_i on the reliability index β can be studied. The elasticity of the means shows that the horizontal component H has a slightly favorable effect: it is therefore necessary to underestimate it in a safety analysis. This comes from the fact that the bending moment in cross-section 2 due to action H is of the opposite sign to that of the moment due to q . This remark disappears if the sign of H is liable to change. Nevertheless, it reminds us that systematically increasing actions does not necessarily bring about safety.

Quite obviously, an increase in f_y is favorable. The elasticity of the standard deviations is always negative; this is a general result, since an increase in variability never tends toward safety. Finally, the elasticities of the parameters identify those parameters whose values must be controlled as well as possible. They depend here only on geometric variables and they are not independent.

6.5 Conclusion

Although the probability of failure is always conditioned by the mechanical scenario and the stochastic modeling of data, importance factors are particularly significant elements for the designer. Sensitivity to means is a determining factor for the design to retain; sensitivity to the standard deviations underlines the role of quality control.

By analogy, the reliability index is a measure on a badly graduated thermometer on which, in addition, it is difficult to know the level of comfort desired, whereas the importance factors indicate whether the temperature increases or decreases, which is a strong element in knowing how to improve the design.

This page intentionally left blank

Chapter 7

Probability of Failure

The most universally adopted method for quantifying reliability depends on the calculation of probabilities. Normalization recognizes the direct link between the notion of reliability and its measure by a probability. Probabilities constitute a common language among speakers: decision makers, engineers, scientists, financiers, etc. They can be applied to a very large number of problems of different origins.

The detailed discussions in the previous chapters emphasized the general objective of probability calculation. They later described quantifications based on the notions of indexes, as well as the corresponding calculation methods, but ultimately we refer to probability when we wish to refine reliability analyses and compare the results obtained with those arising from other sources.

This chapter aims at presenting a number of methods for calculating the probability of failure. We will see that different levels of approximation are possible, depending on the characterization of the limit-state, when relying on the notions seen in the previous chapters, which continue to play an important role in the methods proposed.

The evaluation of a probability by simulation is approached in Chapter 8. The plan for the current chapter is as follows:

1. methodological framework,
2. approximation using a hyperplane: first-order reliability method (FORM),
3. approximation using a hypersurface,
4. ‘asymptotic’ second-order reliability method (SORM),
5. method using the characteristic function,
6. Riemannian geometric method for reliability (RGMR),
7. numerical examples,
8. conclusions.

A reference example – the case of hyperbolas: to enable the reader to familiarize himself with these different methods, an example has been selected [Ric80] because it can be dealt with in an elementary way. It is approached using a series of methods.

The limit-state function is defined by:

$$G(x_1, x_2) = \varepsilon(2x_1 x_2 - y)$$

where y and ε are parameters of the problem, whose values are given in Table 7.1.

Case	y	ε
0	0.005	1
1	100	-1

Table 7.1 Reference example – definition of the data.

We therefore examine the values of x_1 and x_2 for which the quadratic form $2x_1 x_2$ has values lower than 0.005 or higher than 100.

The probabilistic model is the following: X_1 and X_2 are Gaussian random variables of averages 3 and 5 and standard deviations 1 and 2, respectively. The two variables have a correlation equal to 0.5.

A physical interpretation of this model is, for example, constituted by a system of two water processing plants in series whose outputs are modeled by random variables (Figure 7.1). We are interested in the output of the complete system.

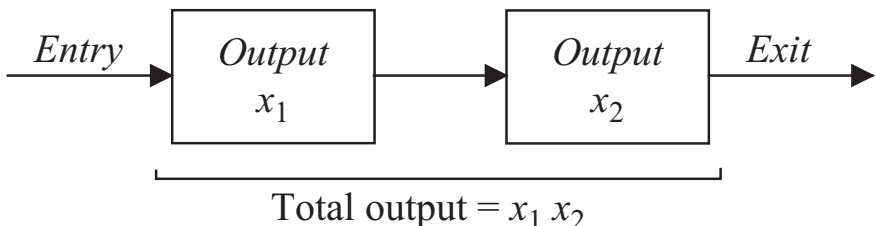


Figure 7.1 Illustration of the reference example.

7.1 Methodological framework

We suppose that there exists a sufficiently regular¹ transformation $T: \mathcal{X} \rightarrow \mathcal{U}$ which allows us to transform the physical variable space \mathcal{X} into a standardized variable space \mathcal{U} . By definition, T respects the measure of probability. We have called such a transformation an *isoprobabilistic transformation*. As a transformation, it is reversible.

The dimension of space \mathcal{X} , normally equal to that of \mathcal{U} , corresponds to the number of independent random variables of the problem. It is written n in the continuation of this chapter.²

When the physical variable space is formed of Gaussian random variables, T is a simple affinity.

The search for an isoprobabilistic transformation in the general case was explained in detail in Chapter 4. With the usually satisfactory hypotheses for the distribution functions, there exists at least one way of defining T .

The compound function $H = G \circ T^{-1}$ defines, by the inequation $H(\mathbf{u}) \leq 0$, $\mathbf{u} \in \mathcal{U}$, the failure domain \mathcal{D}_f in the standardized variable space. The boundary of \mathcal{D}_f is written $\partial\mathcal{D}_f$ in the following text.

By the construction of T , we have:

$$P_f = \text{Prob}(\tilde{\mathcal{D}}_f) = \int_{\mathcal{D}_f} \phi_n(\mathbf{u}) \, d\text{vol}(\mathbf{u})$$

where P_f is the probability of failure; $\text{Prob}(\tilde{\mathcal{D}}_f)$ is the probability associated with the domain $\tilde{\mathcal{D}}_f = T^{-1}(\mathcal{D}_f)$ in space \mathcal{X} ; ϕ_n is the multidimensional Gaussian centered density of probability, of variance 1 for all the coordinates, without correlation:

$$\phi_n(\mathbf{u}) = (2\pi)^{-n/2} e^{(-\|\mathbf{u}\|^2/2)}$$

where $\|\cdot\|$ designates the Euclidean norm in space \mathcal{U} and $d\text{vol}(\mathbf{u}) = du_1 du_2 \cdots du_n$ represents the element of the multidimensional volume. Some mathematical hypotheses are implicit in all the calculations carried out, as recalled in the note. The boundary of \mathcal{D}_f must be a sufficiently differentiable hypersurface, at least at the design point. Point P^* , of coordinates \mathbf{u}^* , is the point on \mathcal{D}_f which is closest to the origin. It should in general be unique.

¹ We will not come back each time to the question of mathematical hypotheses indispensable for the validity of constructions. The regularity of domains is a condition rarely clarified *a priori*. The non-convergence of design point search algorithms is often due to such irregularities. When this case is extended, a specific study emerges normally at the end of the problem. The case in which the gradient of the performance function would cancel out or would become very weak at the design point must also be remembered.

² In order to simplify the notation, a vector of \mathcal{U} is written \mathbf{u} in this chapter in place of the notation $\{u\}$, retained in other instances.

In practice, these hypotheses are almost always verified, except perhaps in certain complex cases for which several limit-states can be in competition. If \mathcal{D}_f is not differentiable at the design point, problems generally arise during the search for this point; the corresponding reliability index is then inaccessible using classical methods. A representation by a series and (or) parallel system is then often an interesting solution, if it is possible to show that each component of the system presents good properties. This approach is presented in Chapter 9.

Notation and definitions: we use the geometric description of the failure domain presented in Chapters 4 and 5. We call the design point the nearest point in the failure domain to the origin, in standardized variable space. This notion has no sense when the nominal conditions, corresponding to the point where the probability density is maximum, are already located in the failure domain (β is then implicitly negative).

In the course of this chapter, an approximation of the function H , in the equation for the limit-state in standardized space, is written as \tilde{H} . This approximation is of the first order for FORM methods, where the limit-state is replaced by its hyperplane tangential to the design point. The approximation is of the second order for the SORM method, the limit-state being, in this case, replaced by a hyperquadratic osculating at the design point.

The reference example: the two variables being Gaussian, $\hat{u}_1 = x_1 - 3$ and $\hat{u}_2 = (x_2 - 5)/2$ are normal-centered but correlated.

Decorrelation uses the matrix $[L]$ of Cholesky's decomposition of the correlation matrix (see Section 4.3.6):

$$[\rho] = \begin{bmatrix} 1 & \rho \\ \rho & 1 \end{bmatrix} = [L][L]^t$$

where ρ is the correlation coefficient.

The change of variables is defined by $u_1 = \hat{u}_1$ and $\sqrt{3}u_2 = -\hat{u}_1 + 2\hat{u}_2$. The two failure domains are shown in Figure 7.2. The number of extrema is four for case 0, of which three are minima, and two for case 1.

7.2 Approximation using a hyperplane: FORM

This method is applied in standardized space \mathcal{U} .

7.2.1 Principle of linear approximation

Resolution of the problem:

$$\beta = \min \left(\sqrt{\sum_i u_i^2} \right) \quad \text{under the constraint } H(\mathbf{u}) \leq 0$$

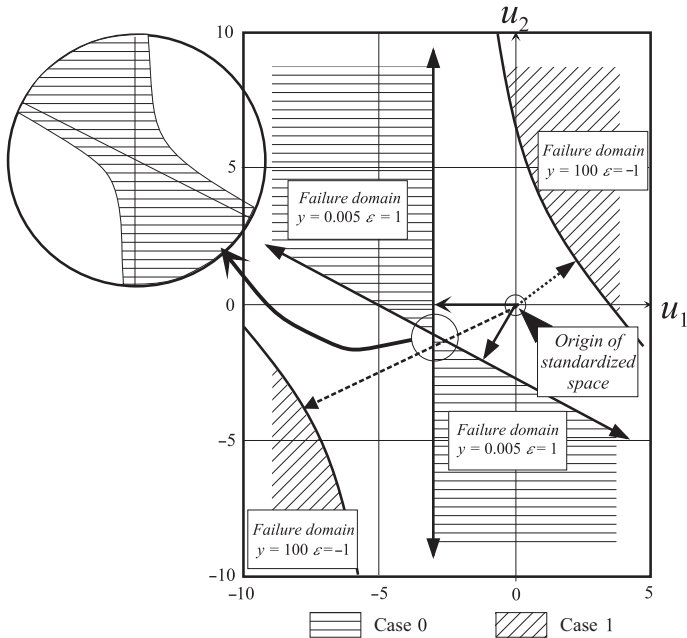


Figure 7.2 Reference example: representation of two failure domains.

leads to the determination of β (or of a β if there is no uniqueness) and of the direction cosines of vector P^*O written as α in Figure 7.3 – we remind the reader that these are the direction cosines of the gradient of H at point P^* ; the gradient must not be null.

A simple remark is at the origin of the development of the FORM methods (this is equally true for SORM): *at the point of domain D_f which is closest to the origin, that is to say, at the design point, the probability density is maximum in D_f ; in the presence of a limited number of random variables, this density decreases rapidly when the distance from the origin increases.*

This results from the analytical form of the probability density of the normal Gaussian density. However, this property becomes less and less verified when the number of random variables of the problem increases. This point is discussed in Section 7.6.8.

7.2.2 Expression of the probability of failure

The FORM approximation consists of associating with the value of β the probability $\Phi(-\beta)$. This hypothesis consists of replacing the surface of the real limit-state $H(\mathbf{u}) = 0$ by a hyperplane at the design point (Figure 7.3). The

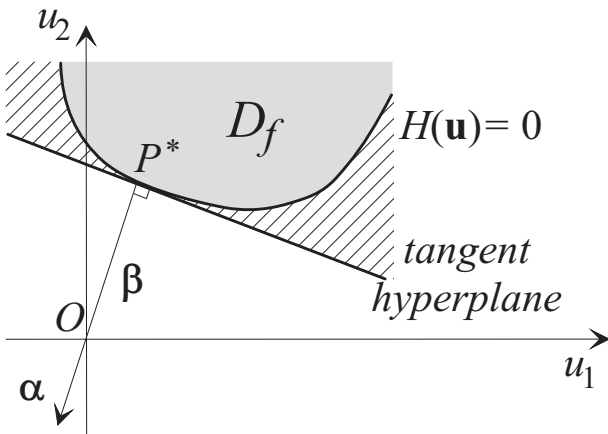


Figure 7.3 Principle of the FORM approximation: construction of the hyperplane tangent at P^* .

equation of such a hyperplane (Π) is given by:

$$(\Pi): \quad \tilde{H}(\mathbf{u}) = \sum_i \alpha_i u_i + \beta = 0$$

By constructing point P^* (of coordinates \mathbf{u}^*) as the point located at the minimum distance from the origin, this hyperplane is orthogonal to the vector P^*O of direction cosines α_i . $\partial\mathcal{D}_f$ being defined by the implicit equation $H(\mathbf{u}) = 0$, we are certain that a tangent plane exists at point P^* representing the minimum distance if:

1. H admits a gradient written as ∇H at the point of coordinates \mathbf{u}^* ,
2. $\nabla H(\mathbf{u})|_{\mathbf{u}^*} \neq 0$.

Proposition 1. Let (Π) be a hyperplane in standardized variable space \mathcal{U} , located at a distance β from the origin. Let \mathcal{D}_f be the halfspace delimited by (Π) not containing the origin. Then the probability of domain \mathcal{D}_f is given by the equation:

$$\text{Prob}(\mathcal{D}_f) = \Phi(-\beta)$$

in which Φ is the Gaussian one-dimensional centered distribution probability function $\mathcal{N}(0, 1)$.

Proof. The rotations of space \mathcal{U} will make the probability density ϕ_n invariant. Let us note n as the dimension of the space \mathcal{U} (number of random variables).

By a rotation in this space, we can bring (II) to be perpendicular to the n th direction.

In these conditions, the probability is written as:

$$\text{Prob}(\mathcal{D}_f) = \int_{u_n \geq \beta} (2\pi)^{-n/2} e^{-\|\mathbf{u}\|^2/2} du_1 \cdots du_n \quad (7.1)$$

Taking into account the equation:

$$\|\mathbf{u}\|^2 = \sum_{i=1}^{n-1} u_i^2 + u_n^2$$

the function to be integrated in (7.1) becomes:

$$(2\pi)^{-n/2} \exp\left(-\frac{\sum_{i=1}^{n-1} u_i^2}{2}\right) e^{-(u_n^2/2)}$$

We can apply Fubini's theorem to the integral (7.1):

$$\begin{aligned} \text{Prob}(\mathcal{D}_f) &= \int_{u_n \geq \beta} \frac{1}{\sqrt{2\pi}} e^{-u_n^2/2} \\ &\times \left[\int_{-\infty}^{\infty} \cdots \int_{-\infty}^{\infty} (2\pi)^{-(n-1)/2} \exp\left(-\frac{\sum_{i=1}^{n-1} u_i^2}{2}\right) du_1 \cdots du_{n-1} \right] du_n \end{aligned}$$

The integral between square brackets is equal to 1, and thus we obtain the result, taking into account the definition of Φ :

$$\Phi(-\beta) = \frac{1}{\sqrt{2\pi}} \int_{-\infty}^{-\beta} e^{-u^2/2} du = 1 - \Phi(\beta) \quad \square$$

Another approach: let us calculate the probability, that is to say $\text{Prob}(\sum_i \alpha_i U_i + \beta \leq 0)$, the probability of outcomes located in the failure domain \mathcal{D}_f :

$$\text{Prob}(\mathcal{D}_f) = \text{Prob}\left(\sum_i \alpha_i U_i + \beta \leq 0\right) = \text{Prob}\left(\sum_i \alpha_i U_i \leq -\beta\right)$$

In this expression, $Z = \sum_i \alpha_i U_i$ is a linear combination of the standardized variables U_i , and α_i is a vector of direction cosines; it results from this that Z is a standardized Gaussian random variable and:

$$\text{Prob}(\mathcal{D}_f) = \text{Prob}\left(\sum_i \alpha_i U_i \leq -\beta\right) = \text{Prob}(Z \leq -\beta) = \Phi(-\beta)$$

Calculation of Φ : no expression for Φ exists from classic functions. It is given in tables or approximate expressions and by a large number of modern calculators. An approximation is obtained using the following equation [AS72] (giving an error lower than $\pm 7.5 \times 10^{-8}$):

$$\Phi(x) = 1 - \frac{1}{\sqrt{2\pi}} e^{-(x^2/2)} (u(b_1 + u(b_2 + u(b_3 + u(b_4 + b_5 u)))))$$

$$b_1 = 0.319381530 \quad b_2 = -0.356563782 \quad b_3 = 1.781477937$$

$$b_4 = -1.821255978 \quad b_5 = 1.330274429$$

$$\text{with } u = \frac{1}{1 + 0.2316419x}$$

This formula is valid if $x > 0$. For negative values, it is sufficient to take the absolute value and the complement to 1 from the result $\Phi(-x) = 1 - \Phi(x)$.

We thus have a very rapid means of obtaining an approximate idea of the probability of failure P_f as soon as we have determined the Hasofer-Lind index.

FORM method: as a first approximation, when we replace the surface of the limit-state by its hyperplane tangent at the design point P^* , the probability of failure is given by:

$$P_f \approx \Phi(-\beta) = 1 - \Phi(\beta)$$

Once β is calculated, this approximation is obtained at no cost. However, it is necessary to accept the result only after evaluation. The following example constitutes one of the most severe cases challenging it.

7.2.3 Counter-example

In certain cases, the approximation thus found for P_f can be very imprecise. A frequently presented example is as follows: the limit-state function H (hyperparaboloid of revolution, Figure 7.4) is given by:

$$H(\mathbf{u}) = 3 + u_1 - \frac{1}{6} \sum_{i=2}^{n=10} u_i^2$$

A very simple geometric study shows that $\beta = 3$, leading to a FORM probability of 1.35×10^{-3} . The exact value obtained by a numerical calculation is 0.111. We see that in this case the error is very great.

However, it would be wrong to conclude that the FORM method is not interesting. In fact, the example is very special. The hyperparaboloid is chosen in such a manner that the parabola is just outside the circle of radius β . It

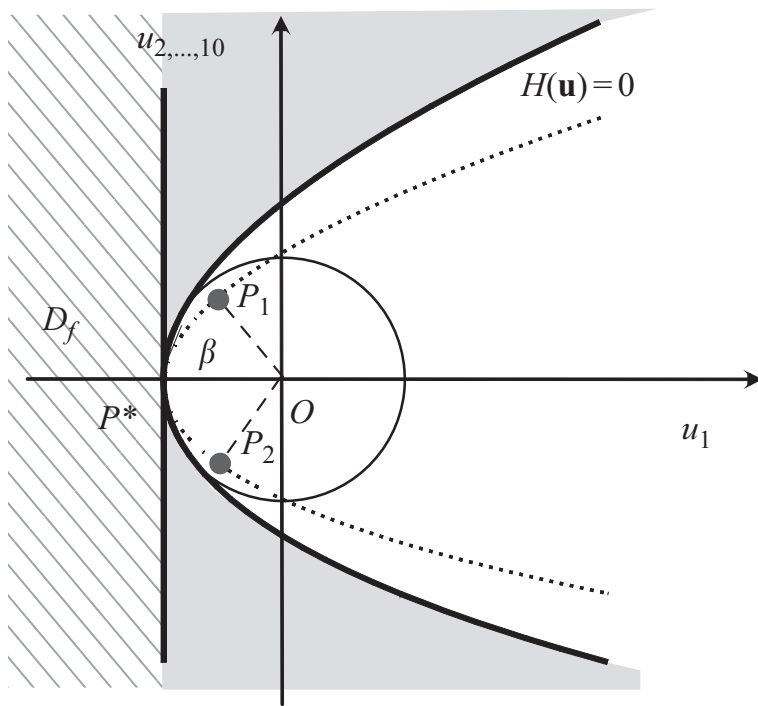


Figure 7.4 FORM counter-example – hyperparaboloid of revolution.

has a second order contact with the circle and hence an even curvature radius. By increasing the curvature slightly, some design points appear which are not located on the axis of symmetry. For two variables, these are P_1 and P_2 in Figure 7.4 and the probability calculation can then be conducted by the FORM approximation on condition that these points are introduced in a series system from hyperplane tangents to the points P_i . For $n \geq 3$, there is an infinity of points P_i .

We can ascertain that, in simple problems, FORM provides a good order of magnitude of the probability P_f . It is simply necessary to validate the obtained result carefully.

7.2.4 Accuracy of the approximation

It is clear that the accuracy of the FORM approximation depends on the form of the limit-state at the most probable failure point. The solution is exact only if the limit-state is linear in the reduced variable space. This is produced (a sufficient but not necessary condition) if we have simultaneously:

- a linear limit-state in the physical variable space \mathbf{x} ,
- Gaussian variables \mathbf{X} ; the transformation $\mathbf{x} \rightarrow \mathbf{u}$ is therefore linear.

Let us note that special cases can also lead to linear limit-states, for example if $G(\mathbf{x})$ is a combination of the product quotient of lognormal random variables.

By positioning ourselves in standardized space \mathcal{U} , we can deduce from the curvature the following approximations:

- concavity of $H(\mathbf{u})$: the concavity is turned toward the origin; the probability of failure is higher than the FORM approximation and a bound formula has been given by Hasofer (probability of the space external to the sphere of radius β):

$$1 - \chi_n^2(\beta^2) \geq P_f \geq \Phi(-\beta) \quad \text{concave surface}$$

where $\chi_n^2(\cdot)$ indicates the distribution of χ^2 at n degrees of freedom (n is the number of random variables). This is the case of Figure 7.4 which leads to the bounds $0.468 \geq P_f \geq 0.00135$,

- in the convex case, the bound formula is trivial, but too broad:

$$\Phi(-\beta) \geq P_f \geq 0 \quad \text{convex surface}$$

These bounds require that all the curvatures be of the same sign and they remain very imprecise.

Case	y	ε	β	$P_{f,\text{FORM}}$	β'
0	0.005	1	2.499	6.222×10^{-3}	2.999
1	100	-1	2.604	4.602×10^{-3}	8.950

Table 7.2 Reference example – results of the FORM approximation.

7.2.5 Reference example

Figure 7.2 shows that there are several design points. In case 0, Table 7.8 gives the points obtained. In case 1, the convexity is turned toward the origin and there is 1 point located on each of the connected components.

The nearest design point provides, in each of the cases, the FORM approximation. The results are given in Table 7.2, in which the second index β' is reported as well.

We can see that in case 0, the ‘contribution’ FORM of the second relative minimum is $\Phi(-2.999) \approx 1.35 \times 10^{-3}$ and is not therefore negligible, whereas it is so in case 1.

7.3 Approximation using a second-order hypersurface

Several authors endeavor to give the best approximation of the probability of failure from a more complete knowledge of the geometry of the limit-state function in the vicinity of the design point. The limit-state function is then approximated by a second degree hypersurface, complete or incomplete. A restriction by hypercones has also been proposed [M  90], but we will not take that up here.

This section examines geometric approximations of the second order. The following sections present the SORM results, in terms of the probability, possibly resulting from a better knowledge of the limit-state at the design point.

The notation used in existing publications has been retained as much as possible. Later, a first rotation placing point P^* on the last coordinate axis of unit vector e_n is systematically carried out (Figure 7.5). Under these conditions, point P^* takes the coordinates:

$$P^* = (0, \dots, 0, \beta)$$

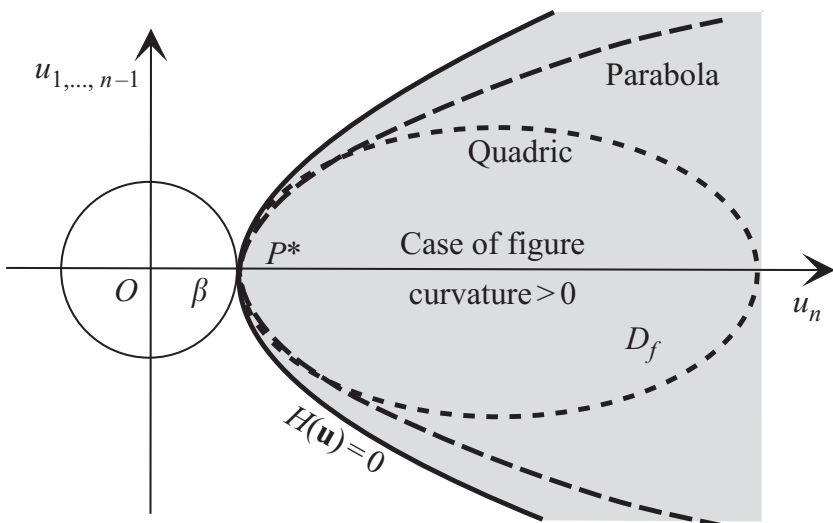


Figure 7.5 SORM approximations.

7.3.1 Curvature at the design point

We see clearly in Figure 7.4 that the defect of the FORM calculation is principally caused by the curvature of the limit-state hypersurface at point P^* , of coordinates \mathbf{u}^* , the shaded portion representing the weight of the probability ‘forgotten’ by FORM.

Let us consider the problem as it is posed after having made the vector OP^* coincide with the last coordinate axis aligned on the unit vector e_n . Let us take the limit-state defined by the implicit equation $H(\mathbf{u}) = 0$. Let $\bar{\mathbf{u}} = (u_1, \dots, u_{n-1})$. We discuss directly from the function of origin H and not from any approximation.

Because the gradient of H is not canceled out at point P^* and is collinear with OP^* , the theorem of implicit functions enables us to assert that, in the vicinity of 0 for $\bar{\mathbf{u}}$, we can find a real function ψ of $n - 1$ variables such that the equation:

$$H \left(u_1, u_2, \dots, u_{n-1}, \underbrace{\beta + \psi(u_1, u_2, \dots, u_{n-1})}_{u_n} \right) = 0 \quad (7.2)$$

is verified in every case. This defines the hypersurface $H(\mathbf{u}) = 0$ by the equation:

$$u_n = \beta + \psi(\bar{\mathbf{u}}) = \beta + \psi(u_1, \dots, u_{n-1})$$

Let us calculate the derivatives of ψ , using the following notation: i, j are indexes varying from 1 to $n - 1$; $\partial_i, \partial_{ij}$ indicate the partial derivatives:

$$\partial_i = \frac{\partial}{\partial u_i} \quad \partial_{ij} = \frac{\partial^2}{\partial u_i \partial u_j}$$

and $\partial_n H$ indicates the partial derivative of H with respect to the last coordinates.

The first derivatives of ψ are deduced from identity (7.2):

$$\partial_i H + \partial_n H \partial_i \psi = 0$$

which shows that at the origin, these first derivatives are zero, which is evident from the situation of point P^* . The second derivatives at the origin are given, after removal of zero terms, by:

$$\partial_{ij} H + \partial_n H \partial_{ij} \psi = 0$$

Taking into account the choice of reference, $\partial_{ij} \psi$ represents the tensor of curvature of the hypersurface $H(\mathbf{u}) = 0$ at P^* and the curvature in a direction $\bar{\mathbf{u}}_0$ is:

$$\sum_i \sum_j \partial_{ij} \psi \bar{u}_{0i} \bar{u}_{0j}$$

We therefore have the following result: we suppose that two hypersurfaces Σ_1 and Σ_2 , defined respectively by the implicit equations $H_1(\mathbf{u}) = 0$ and $H_2(\mathbf{u}) = 0$, verify the following hypothesis:

1. Σ_1 and Σ_2 have point P^* in common,
2. at P^* , these two hypersurfaces are tangent,
3. at P^* , H_1 and H_2 have the same gradient, of length 1, aligned on P^*O ,
4. P^* is located on the axis of unit vector e_n (last coordinate axis).

Then Σ_1 and Σ_2 have the same principal curvatures at point P^* only if the quadratic forms of coefficients $\partial_{ij}H_1$ and $\partial_{ij}H_2$ admit the same eigensystems (eigenvalues and eigenvectors) with respect to the Euclidean metric system.

This is true, particularly if we have $\partial_{ij}H_1 = \partial_{ij}H_2$. This result enables the simplest characterization of the curvatures of a hypersurface:

with the hypotheses made, the principal curvatures are given by the eigenvalues of the quadratic form of coefficients, $\partial_{ij}\psi$, $i, j = 1, \dots, n - 1$, relative to the Euclidean metric.

The simplicity of this formulation results from the system of special coordinates representing the hypersurfaces.

The general calculation of curvatures can always be performed using this method, applicable after having carried out the orthogonal transformation bringing P^* onto the last axis carried by vector e_n , then having standardized the function H , that is to say $\partial H_n = -1$.

The knowledge of the curvatures leads to an asymptotic approximation of the probability of failure, presented in Section 7.4.

7.3.2 Principle of approximations

The asymptotic method based on the sole knowledge of the curvatures which will be developed in Section 7.4 suffers from the shortcomings of all the methods of this type: we have no direct means of obtaining information on the quality of the approximation. It is therefore natural to have attempted to render the calculations more exact. The principle followed is to construct a domain approaching the failure domain so as to respect a certain number of significant elements in the vicinity of the design point. We can think that the most important part of the probability density is concentrated in this zone, at least when the number of random parameters is not too large. The significant elements usually chosen are the position of the design point, the tangent plane at this point and the curvatures. The domain is defined by a simple analytical expression. In practice, we use a quadratic form whose equation is now established.

The actual calculation of the integral of probability on the quadratic domains is presented in Sections 7.5 and 7.6. Let us accept that it is possible to calculate in an accurate manner the integral of probability on the domains defined by the quadratic equations.

The approach to the curvature here is different from that of the asymptotic case because we should define more precisely what the approximation is: this is obtained by considering quadratic domains \mathcal{D}_Q , defined by the inequalities $Q(\mathbf{u}) \leq 0$, where Q is any quadratic form. The approximation is defined by the property for \mathcal{D}_Q to be tangent and osculatory at the failure domain at a design point P^* , *oscularity at the considered point P^* means that the two hypersurfaces bordering the domains admit the same principal curvatures and the same principal directions for these curvatures.*

These criteria can be implemented directly from the elements of Section 7.3.1. If H is the performance function and P^* the design point, we consider a quadratic form Q such that:

1. $Q(\mathbf{u}^*) = 0$,
2. $\nabla H(\mathbf{u}^*)$ and $\nabla Q(\mathbf{u}^*)$ are collinear: the hypersurfaces defined by the implicit equation $Q(\mathbf{u}) = 0$ and $H(\mathbf{u}) = 0$ then have the same tangent planes as P^* ,
3. these hypersurfaces have the same curvatures in P^* .

We can use the method from Section 7.3.1 to characterize the last condition. We start by placing the design point P^* on the last axis by a rotation, then we standardize the function H . This calculation is carried out in the following subsections.

Two elements should be taken into account for the practical efficiency of this new method: on the one hand, there are many possible geometric approximations of the failure domain, leading to values for the probability of failure which can be very diverse. The effective choice therefore results from elements coming from the mechanical part of the problem. On the other hand, all the points of the approximation domain are not necessarily physically admissible. It is advisable in this case to interpret the mathematical results obtained.

The real mathematical reason for this difficulty is the following: whatever the quantity of information that we possess on a hypersurface at one of its points, we can in no way prejudge its form at other points, particularly as regards its behavior at infinity.

In spite of all these difficulties, these methods are very often used because they provide results which cannot be obtained otherwise. Except in some cases of very irregular behavior, such as limit-states concurrent at the design point leading to some angular points, the calculations are very powerful.

This method has some links with the quadratic response surface method (Chapter 11). In fact, we construct in both cases a quadratic surface forced to represent the failure domain as closely as possible. We can moreover note that the use of response surfaces also requires the intervention of the engineer's judgment.

7.3.3 Quadratic approximation

In the FORM method, the equation $H(\mathbf{u}) = 0$ is replaced by the equation $\tilde{H}(\mathbf{u}) = (\mathbf{u} - \mathbf{u}^*) \cdot \mathbf{u}^* = 0$, where $\mathbf{v} \cdot \mathbf{u}$ indicates the scalar product of vectors \mathbf{u} and \mathbf{v} of \mathcal{U} .

To take the curvatures into account, we now use a quadratic approximation of H . Usually there are two ways of constructing such an approximation (Figure 7.5):

- either we consider the paraboloid tangent at point P^* at its apex at $\partial\mathcal{D}_f$, the hypersurface limit, admitting at this point the same principal curvatures as $\partial\mathcal{D}_f$ and e_n for the principal direction at infinity,
- or we consider a quadric tangent at point P^* at its apex at $\partial\mathcal{D}_f$, the hypersurface limit, admitting at this point the same principal curvatures as $\partial\mathcal{D}_f$ and admitting equally e_n for the principal direction. We will see that this second problem is incompletely determined.

It is also possible to consider quadratic forms for which the axis carrying u_n is not the principal axis. In this case, the calculation of curvatures is more complex. The reference example is moreover a case of this type.

A second orthogonal transformation (rotation) is then carried out to diagonalize the two quadratic forms. This operation is always possible. It is not the same as a parabolic approximation or a quadratic approximation.

Paraboloid case

This first method is the most generally used. If we force the vector PO^* to be found on the last coordinate axis (Figure 7.5), the paraboloid equation $\tilde{H}(u) = 0$ is given by an expression of the type $u_n = \beta + Q(u_1, \dots, u_{n-1})$, where Q is a homogeneous quadratic form.

After diagonalization and leaving the invariant vector carried by axis e_n (new coordinates $y_i, i = 1, \dots, n-1, y_n = u_n$), the inequation approaching the failure condition in a new normal coordinate space becomes:

$$m_P(\mathbf{y}) = -y_n + \sum_{i=1}^{n-1} \lambda_i y_i^2 \leq -\beta \quad (7.3)$$

where the coefficients λ_i are the eigenvalues of the form Q (the calculation is presented in Section 7.3.5).

In the case of Equation (7.3), the principal curvatures κ_i are deduced in a simple manner from the expression.

We have in fact:

$$\kappa_i = 2\lambda_i \quad i = 1, \dots, n-1 \quad (7.4)$$

which is a result of the geometry of conics.

Quadratic case

In this case, the limit-state is approximated by an expression $Q(u_1, \dots, u_n) = 0$ where Q is a general quadratic form, not necessarily homogeneous (but admitting e_n for the principal direction).

An orthogonal operation (rotation) around the axis enables us to diagonalize the second degree terms. Representing the coordinates more generally, Tvedt [Tve90] writes the condition $Q(\mathbf{y}) \leq 0$ in the form:

$$m_Q(\mathbf{y}) = \nu + \sum_{i=1}^n (\lambda_i y_i^2 + \gamma_i y_i) \leq -\beta \quad (7.5)$$

an expression where ν , λ_i and γ_i are constants which are deduced from the Taylor expansion of H in the vicinity of P^* (see Section 7.3.6). The index β is thus shown. Q is standardized, $\|\nabla Q(\mathbf{y})|_{\mathbf{y}^*}\| = 1$.

This second method is slightly simpler than in the case of the paraboloid: the equation of the quadric is directly deduced from the Hessian (second derivative matrix) of function $H(\mathbf{u})$, once the latter has been standardized for a unit gradient at the design point.

Another formulation is used by Rice [Ric80]:

$$m_{Q'}(\mathbf{y}) = \sum_{i=1}^n \mu_i (y_i - \omega_i)^2 \leq 0 \quad (7.6)$$

The coefficient-passing formulae are:

$$\lambda_i = C \mu_i \quad \gamma_i = -2C \mu_i \omega_i \quad \nu + \beta = C \sum_{i=1}^n \mu_i \omega_i^2 \quad (7.7)$$

C being a normalization constant.

We can note that formulation (7.5) is more general than (7.6). An equation must link ν , λ_i and γ_i for the calculation of μ_i and ω_i : if all the μ_i are different from 0, we must replace the condition of compatibility:

$$\nu + \beta = \sum_{i=1}^n \frac{\gamma_i^2}{\lambda_i}$$

We can also note that in the case where direction OP^* would not be the principal direction of the quadric, the diagonalization displaces point P^* which, for that reason, is no longer located on the axis of vector e_n .

In the case of the general quadratic formula, the calculation of the principal curvatures is more complex than in the parabolic case. The principal curvatures which intervene in the asymptotic formula are deduced from coefficients ν , λ_i and γ_i .

It is important to verify the sign of the curvatures carefully. In the definition which is presented in this document, the curvatures are positive when the concavity of the limit-state is on the opposite side of the origin (see Figure 7.5). This convention is not always chosen by other authors.

In practice, we determine coefficients λ_i using the method given in the following section (if we have an analytical formulation of the limit-state, either at the start or after having constructed a response surface – see Chapter 11). Let us note that values λ_i or μ_i are defined with the exception of a multiplicative factor. Equation (7.4) is verified only if a gradient of the form Q has been standardized at the design point.

In general, for pure numerical data, it is always possible to carry out a numerical differentiation (to the second order). The calculation algorithm is then a transcription of the method in Section 7.3.4.

The interest of the above-mentioned formulae becomes evident for the methods using the characteristic function. The calculation of the Fourier transform of expressions (7.3), (7.5) and (7.6) is in fact simple.

7.3.4 Elements of the approximation quadric

Let us take up again the formulae presented in the previous sections, after rotation of the reference axes in standardized space. We are going to study a special case of approximation.

We distinguish the cases of Equations (7.3) (parabolic) and (7.5) (quadratic). The case of (7.6) is deduced from (7.5) by an algebraic calculation. The presentation follows the method discussed in [Tve90].

We start from the function $H(\mathbf{u})$ obtained after isoprobabilistic transformation. The problem is purely geometric. It consists of looking for the quadrics (hypersurfaces defined by the set of roots of a non-homogeneous quadratic form) which admit:

1. the design point P^* as the minimum distance to the origin,
2. the same second derivatives at this point as the function defining the limit-state hypersurface.

In all cases, we begin by calculating the Taylor expansion of H at point \mathbf{u}^* .

This gives, with the exception of the second order, the function:

$$H_0(\mathbf{u}) = \nabla H(\mathbf{u})|_{\mathbf{u}^*} (\mathbf{u} - \mathbf{u}^*) + \frac{1}{2} (\mathbf{u} - \mathbf{u}^*) \nabla^2 H(\mathbf{u})|_{\mathbf{u}^*} (\mathbf{u} - \mathbf{u}^*)$$

$\nabla^2 H$ indicating, in this expression, the second derivatives matrix of H , usually called the *Hessian* of H . There is no constant term since point P^* is located on the limit-state.

For reasons of homogeneity, we standardize the gradient. The new function \tilde{H} , proportional to H_0 , defines the same limit-state; it is given by the matrix formulae:

$$\begin{aligned}\tilde{H}(\mathbf{u}) &= \alpha (\mathbf{u} - \mathbf{u}^*) + (\mathbf{u} - \mathbf{u}^*) [B] (\mathbf{u} - \mathbf{u}^*) \\ \alpha &= \left. \frac{\nabla H(\mathbf{u})}{\|\nabla H(\mathbf{u})\|} \right|_{\mathbf{u}^*} \\ [B] &= \left. \frac{\nabla^2 H(\mathbf{u})}{2\|\nabla H(\mathbf{u})\|} \right|_{\mathbf{u}^*} \quad ([B] \text{ is symmetric})\end{aligned}$$

This calculation can be carried out only if the *gradient* $\nabla H(\mathbf{u})$ is not zero. If this was not the case, all the calculations which follow would be indeterminate; it would be necessary then to use an approximation to the third order, leading to more complex calculations.

A quadric approximation of $\partial\mathcal{D}_f$ is defined by the equation $\tilde{H}(\mathbf{u}) = 0$. We will see below that quite a family of quadrics exists, having the same principal curvatures in P^* . Among them, there exists a special one, parabolic to axis e_n . However, all are osculatory in P^* to that defined by $\tilde{H}(\mathbf{u}) = 0$.

A more practical formulation is calculated below, in order to obtain the functions m_P and m_Q of the previous section. We carry out at first an orthogonal change of coordinates (Grahm-Schmidt procedure). Noting $\mathbf{v} = [R]\mathbf{u}$, constructed in order to obtain the coordinates $\mathbf{v}^* = [R]\mathbf{u}^*$ of point $(0, \dots, 0, \beta)$, we have in these conditions, with $\beta = -\alpha \cdot \mathbf{u}^*$:

$$\mathbf{v} = [R]\mathbf{u} = \begin{bmatrix} [R_{n-1}] \\ -\alpha^t \end{bmatrix} \quad \mathbf{u} = \begin{bmatrix} [R_{n-1}]\mathbf{u} \\ -\alpha^t \mathbf{u} \end{bmatrix} = \left\{ \begin{array}{l} [R_{n-1}]\mathbf{u} \\ v_n \end{array} \right\}$$

where $[R_{n-1}]$ represents the first $n-1$ lines of $[R]$. We can see that the vector α is that of the direction cosines of P^*O in the initial space. In this new coordinate system, the function \tilde{H} is written as:

$$\tilde{H}(\mathbf{v}) = (-v_n + \beta) + \left\{ \begin{array}{l} \bar{\mathbf{v}} \\ v_n - \beta \end{array} \right\}^t [R][B][R]^t \left\{ \begin{array}{l} \bar{\mathbf{v}} \\ v_n - \beta \end{array} \right\} \quad (7.8)$$

by writing the vector $\bar{\mathbf{v}}$ with $(n - 1)$ components (v_1, \dots, v_{n-1}) . It is useful to break the matrix $[R][B][R]^t = [A]$ down into blocks adapted to the decomposition of the vector:

$$[A] = \begin{bmatrix} [A_{n-1}] & \mathbf{C} \\ \mathbf{C}^t & a_{nn} \end{bmatrix} \quad (7.9)$$

where \mathbf{C} is an $(n - 1)$ -column vector, $[A]$ is symmetric and $[A_{n-1}]$ is also symmetric. With these notations, the function \tilde{H} is now written as:

$$\tilde{H}(\mathbf{v}) = -v_n + \beta + \bar{\mathbf{v}}[A_{n-1}]\bar{\mathbf{v}} + 2(v_n - \beta)\mathbf{C}^t\bar{\mathbf{v}} + a_{nn}(v_n - \beta)^2 \quad (7.10)$$

It is from expressions (7.8) and (7.10), which are quite general, that the parabolic and quadratic approximations are determined. Extending the case, a matrix operation enables us to pass from coordinates \mathbf{v} to coordinates \mathbf{y} appearing in Equations (7.3), (7.5) and (7.6).

7.3.5 Parabolic approximation

Proposition 2. *The hypersurface defined by the equation:*

$$\beta - v_n + \bar{\mathbf{v}}[A_{n-1}]\bar{\mathbf{v}} = 0 \quad (7.11)$$

is a paraboloid of axis OP^ which admits a contact of order 2 at point P^* with the hypersurface defined by:*

$$H(\mathbf{v}) \equiv H[R(\mathbf{u})] = 0 \quad (7.12)$$

where β is the Hasofer-Lind index and $[A_{n-1}]$ is the first minor of order $n - 1$ of the standardized Hessian written in the form (7.9).

Proof. That (7.11) defines a paraboloid of axis OP^* is evident by going back to (7.3) (any symmetric matrix is diagonalizable).

Equation (7.12) is still written as $H(v_1, v_2, \dots, v_n) = 0$. With the arguments already developed, we determine a real function ψ of $n - 1$ variables such that:

$$H[v_1, v_2, \dots, v_{n-1}, \beta + \psi(v_1, v_2, \dots, v_{n-1})] = 0 \quad (7.13)$$

is verified in every case. This defines the hypersurface $H(\mathbf{v}) = 0$ by the equation:

$$v_n = \beta + \psi(\bar{\mathbf{v}}) = \beta + \psi(v_1, \dots, v_{n-1})$$

Let us first carry out a limited expansion of standardized H . Let us put $\mathbf{w} = \mathbf{v} - \mathbf{v}^*$. This function being quadratic, we have:

$$\tilde{H}(\mathbf{w} + \mathbf{v}^*) = a + \sum_{i=1}^n b_i w_i + \sum_{i=1}^n \sum_{j=1}^n c_{ij} w_i w_j \quad (7.14)$$

As P^* is located on the hypersurface, we have $a = 0$.

In the same manner, let us carry out an expansion of ψ , limited to the second order; by noting that for $i = 1, \dots, n-1$, we have $w_i = v_i$; we obtain:

$$\psi(v_1, \dots, v_{n-1}) = A + \sum_{i=1}^{n-1} B_i v_i + \sum_{i=1}^{n-1} \sum_{j=1}^{n-1} C_{ij} v_i v_j + \dots$$

As a result of definition (7.13) of ψ , we also have $A = 0$. Let us transfer this expression in (7.14). By considering only the terms of the first and second orders, we obtain:

$$\begin{aligned} & \sum_{i=1}^{n-1} b_i v_i + b_n \left(\sum_{i=1}^{n-1} B_i v_i + \sum_{i=1}^{n-1} \sum_{j=1}^{n-1} C_{ij} v_i v_j \right) + \sum_{i=1}^{n-1} \sum_{j=1}^{n-1} c_{ij} v_i v_j \\ & + 2 \sum_{i=1}^{n-1} c_{in} v_i \left(\sum_{j=1}^{n-1} B_j v_j \right) + c_{nn} \left(\sum_{i=1}^{n-1} B_i v_i \right)^2 + \dots = 0 \end{aligned}$$

an equality verified in every case.

Separating then the terms of the same order, we obtain by identification the following equations:

$$\begin{aligned} b_i + b_n B_i &= 0 \quad \text{for } i = 1, \dots, n-1 \\ b_n C_{ij} + c_{ij} + 2c_{in} B_j + c_{nn} B_i B_j &= 0 \quad \text{for } i, j = 1, \dots, n-1 \end{aligned}$$

These equations are simplified if we consider the specially chosen coordinate system: we have $b_i = 0$, $i = 1, \dots, n-1$ and $b_n = -1$.

The previous equations then become:

$$\begin{aligned} B_i &= 0 \quad \text{for } i = 1, \dots, n-1 \\ C_{ij} &= c_{ij} \quad \text{for } i, j = 1, \dots, n-1 \end{aligned}$$

We have therefore shown that the hypersurface $H(\mathbf{v}) = 0$ accepted a second-order contact with the hypersurface defined by the equation of the type given by formula (7.11) which is now written as:

$$v_n = \beta + \sum_{i=1}^{n-1} \sum_{j=1}^{n-1} c_{ij} v_i v_j$$

After diagonalization of c_{ij} it is a matter of Equation (7.3). \square

7.3.6 Quadratic approximation

The calculation is much simpler. It is sufficient in fact to diagonalize the symmetric matrix $[A]$.

Let $[P]$ be an orthogonal matrix of change of coordinates diagonalizing $[A]$ and let $[\Lambda]$ be the diagonal matrix of eigenvalues λ_i . Let us stipulate $\mathbf{y} = [P]^t \mathbf{v}$.

Expression (7.8) becomes:

$$\tilde{H}(\mathbf{y}) = \beta - \mathbf{P}_n \cdot \mathbf{y} + \mathbf{y} [\Lambda] \mathbf{y} - 2\beta \mathbf{P}_n [\Lambda] \mathbf{y} + a_{nn} \beta^2$$

where P_n is the vector of the n th line of $[P]$. Let us note that in general, point P^* is no longer necessary on axis e_n . $[\Lambda]$ is the diagonal matrix of eigenvalues λ_i . If we define the n -vector γ by:

$$\gamma = -([I] + 2\beta [\Lambda]) \mathbf{P}_n$$

and the real ν by:

$$\nu = a_{nn} \beta^2$$

function \tilde{H} goes into the form (7.5) already given:

$$\tilde{H}(\mathbf{y}) = \beta + \nu + \sum_{i=1}^n (\lambda_i y_i^2 + \gamma_i y_i) = m_Q(\mathbf{y}) + \beta$$

Note: *in theory, we arrive at exactly the same result by diagonalizing matrix $[B]$ directly. However, in practice, point P^* is not necessarily known with great accuracy, which can have an influence on the curvatures.*

It can therefore be interesting, numerically, to begin with transformation $[R]$. We find at times that the gradient vector is not exactly oriented on the last axis, which does not introduce an appreciable error as long as the deviation is low.

Let us also note that in general, point P^* is no longer on axis e_n . This is what happens with the hyperbolas in the reference example. The condition such that point $(0, \dots, 0, \beta)$ is P^* in (7.5) is:

$$\nu + \lambda_n \beta^2 + (\gamma_n + 1)\beta = 0 \quad \gamma_i = 0 \quad i = 1, \dots, n-1 \quad (7.15)$$

7.3.7 Reference example

Diagonalization leads us to position the coordinate axes according to the principal directions (see Figure 7.2). The performance function must also be standardized. Only case 0 is dealt with.

The elements of the calculation are:

$$\alpha = \begin{Bmatrix} 0.500 \\ 0.866 \end{Bmatrix} \quad [B] = \begin{bmatrix} 0.286 & 0.247 \\ 0.247 & 0 \end{bmatrix}$$

The matrix of rotation is:

$$[R] = \begin{bmatrix} -0.866 & 0.500 \\ -\alpha_1 & -\alpha_2 \end{bmatrix} = \begin{bmatrix} -0.866 & 0.500 \\ -0.500 & -0.866 \end{bmatrix}$$

The results are:

$$A_{1,1} = \lambda_1 = -1.753 \times 10^{-4} \quad C_1 = 0.247 \quad a_{22} = 0.286$$

We find the curvature $\kappa = 2\lambda_1 = -3.505 \times 10^{-4}$.

The quadratic form is written, after rotation, according to (7.10):

$$\tilde{H}(\mathbf{v}) = -v_2 + \beta + A_{1,1}v_1^2 + 2C_1(v_2 - \beta)v_1 + a_{22}(v_2 - \beta)^2$$

The passage into the eigensystem of the quadratic form is performed by the transformation:

$$[P] = \begin{pmatrix} 0.866 & 0.500 \\ -0.500 & 0.866 \end{pmatrix} \quad [\Lambda] = \begin{pmatrix} -0.143 & 0 \\ 0 & 0.429 \end{pmatrix}$$

which gives, with the exception of a factor C arising from the normalization of H , the quadratic form:

$$m_{Q'}(\mathbf{y}) = C \left[\left(y_1 - \frac{1}{2} \right)^2 - 3 \left(y_2 - \sqrt{\frac{121}{12}} \right)^2 \right]$$

The center of symmetry of the hyperbolae has the coordinates $(1/2, \sqrt{121/12})$. Point P^* has then the approximate coordinates $(-1.249; 2.165)$. It is no longer located on axis e_2 .

7.3.8 Complement on quadratic approximations

Non-uniqueness of a quadratic approximation

Let us now attempt to construct directly a hyperquadric approximating the hypersurface defined by $H(\mathbf{u}) = 0$. After rotation and normalization, the performance function is written as $H(\mathbf{v}) = 0$.

Let us write the conditions so that this quadric has a second order contact with the hypersurface at point P^* and respects the other usual conditions. The most general equation of the quadric is:

$$a + \sum_{i=1}^n b_i v_i + \sum_{i=1}^n \sum_{j=1}^n c_{ij} v_i v_j = 0$$

We assume at first that this equation is normalized, which signifies that the gradient at point P^* is of norm 1, directed toward the origin and passing through it, and merged with the last coordinate axis.

For point P^* of coordinates $(0, \dots, 0, \beta)$ to be on this quadric, we must have:

$$a + b_n \beta + c_{nn} \beta^2 = 0 \quad (7.16)$$

For the gradient on this point to be aligned with vector OP^* , in the direction e_n and of unit length, we must have:

$$b_i + 2 \sum_{j=1}^n c_{ij} v_j = b_i + 2c_{in} \beta = 0 \quad i = 1, \dots, n-1 \quad (7.17)$$

$$b_n + 2 \sum_{j=1}^n c_{nj} v_j = b_n + 2c_{nn} \beta = -1 \quad (7.18)$$

By combining (7.16) and (7.18), we obtain:

$$a = \beta + c_{nn} \beta^2$$

Finally, the condition of the second order is given by the previous calculation and results of the Hessian. The second order coefficients of the limited expansion around P^* have for value the coefficients c_{ij} of the quadratic form. These coefficients are given by the coefficients of matrix $[A_{n-1}]$ up to the order $n-1$. The coefficients of the last column are arbitrary. Let us name them K_i , $i = 1, \dots, n$.

We have therefore the following result:

Proposition 3. All the hyperquadrics given by the equations:

$$\begin{aligned} & \beta + K_n \beta^2 - 2 \sum_{i=1}^{n-1} K_i \beta v_i - (1 + 2K_n \beta) v_n \\ & + \sum_{i=1}^{n-1} \sum_{j=1}^{n-1} A_{ij} v_i v_j + 2 \sum_{i=1}^{n-1} K_i v_i v_n + K_n v_n^2 = 0 \end{aligned}$$

are osculatory with the hypersurface defined by $H(\mathbf{v}) = 0$ at the design point P^* .

In this formula, the quantities K_i are unspecified; β and A_{ij} ($i, j = 1, \dots, n-1$), the coefficients of $[A_{n-1}]$, are defined previously: after normalization and rotation $[R]$, the matrix $[A_{n-1}]$ is the sub-matrix of rank $n-1$ of the Hessian obtained by canceling the last column and the last line.

Among the matrices thus obtained, there is the matrix of the second derivatives of H , and the parabolic approximation appears, but it is not the only one.

Coefficients of the parabolic form

The coefficients λ_i of formula (7.3) are the eigenvalues of the matrix A_{n-1} obtained by deleting the last line and the last column of matrix $[A]$ of formula (7.9):

$$[A_{n-1}] = [R_{n-1}] \frac{[\nabla^2 H(\mathbf{u})]_{\mathbf{u}^*}}{2\|\nabla H(\mathbf{u})\|_{\mathbf{u}^*}} [R_{n-1}]^t$$

Numbers λ_i are real and can be of any sign. At point \mathbf{u}^* , the first derivatives are zero and numbers λ_i are linked to the principal curvatures κ_i by the equation $\kappa_i = 2\lambda_i$. In the case of quadratic approximation, the new quantities λ_i are not directly linked to the quantities of the same name in the parabolic approximation.

Construction of matrix $[R]$: the construction of matrix $[R]$ follows a Gram-Schmidt procedure. We construct a rotation matrix bringing the vector $(0, \dots, 0, \beta)$ onto the unit vector $OP^*/|OP^*|$. For this we use a function allowing the calculation of a base of the kernel of a linear operator L , that is to say the vectorial sub-space of null image by L . We start from the operator which projects the whole space onto $OP^*/|OP^*|$ and we extract a vector of the kernel which constitutes, after normalization, a unit vector orthogonal to the previous one. The process is repeated as many times as necessary.

Three dimensions: in three dimensions, it is sufficient to choose an unspecified vector V orthogonal to OP^* . We then construct the vectorial product $V \wedge OP^*$ which we standardize to obtain the third vector of the base.

Calculation of curvatures

We have seen that the calculation was immediate in the case of the parabolic approximation given in the form (7.3):

$$\kappa_i = 2\lambda_i$$

In the case of the quadratic approximation, this result is still true, provided that the axis OP^* is the principal axis for the quadric (condition (7.15)) – which is frequently the case – and that the approximation is standardized (unit gradient at the design point).

In the general case of formula (7.5) or (7.6), the calculation of the curvature calls for a complete calculation of the fundamental forms of the hyperspace. The simplest way is to refer again to the start of the chapter. It is necessary for this to find the design point, which is obtained by one of the solutions to the problem

of the constrained extreme:

$$\begin{aligned} \sum_{i=1}^n v_i^2 & \text{ minimum} \\ \nu + \sum_{i=1}^n (\lambda_i v_i^2 + \gamma_i v_i) & = -\beta \end{aligned}$$

by considering, for example, the case of (7.5). The solution (see (5.4)) is given by looking for the sets made up of a Lagrange multiplier Λ and a point (v_1, \dots, v_n) , solutions of:

$$\begin{aligned} 2v_i + \Lambda(2\lambda_i v_i + \gamma_i) & = 0 \\ \nu + \sum_{i=1}^n (\lambda_i v_i^2 + \gamma_i v_i) & = -\beta \end{aligned}$$

We obtain a finite number of solutions $\Lambda_1, \dots, \Lambda_N$, among which the absolute minimum or minima should be found. Once point P^* is thus determined, we look for the rotation leading to this point on a coordinate axis, and we then continue with the method already described.

In practice, the calculation of curvatures is performed before the second rotation, by looking again for the eigenvalues of the sub-matrix $[A_{n-1}]$, see Equation (7.9).

Two-dimensional case: in the case of the reference example, the curvature value is obtained directly by putting the limit-state in the form of a function graph (see the treatment of the reference example in Section 7.4.2). Elementary geometry gives, for the curvature of the graph:

$$\kappa = f''(1 + f'^2)^{-3/2}$$

in a system of Euclidean coordinates and:

$$\kappa = (\rho^2 + 2\rho'^2 - \rho\rho'')(\rho^2 + \rho'^2)^{-3/2}$$

in polar coordinates. In the two cases, the sign requires adjustment depending on the conventions already mentioned (positive curvature if the concavity is on the opposite side of the origin).

7.3.9 Conclusion

This section has clarified the geometric approximation of the limit-state at the design point. The knowledge can be that of the *curvature tensor*, of a *parabolic approximation* or of a complete *quadratic approximation*. This information is now used to improve the approximation of the probability of failure.

7.4 ‘Asymptotic’ SORM method

The knowledge of the curvature of the limit-state at point P^* leads to an asymptotic correction of the FORM approximation, and it constitutes a SORM approximation.

7.4.1 Breitung’s formula

The influence of curvature on the probability of failure is intuitively easy to foresee. Figure 7.5 shows that a positive curvature (convexity turned toward the origin) has a tendency to *diminish the probability of failure* with respect to the FORM approximation. In a quantitative manner, the influence is calculated asymptotically using the Breitung formula [Bre84]. What does the word asymptotic signify here? It signifies that if we bring about an affinity of the space (dilation) by increasingly large coefficients, we can calculate the limit of the coefficient of correction to be applied to the probability given by the FORM formula to obtain an approximation taking the curvatures into account.

Theorem 1. K. Breitung: let a hypersurface of limit-state be defined by the equation $H(\mathbf{u}) = 0$.

If H , twice continuously differentiable, verifies:

1. $\inf_{H(\mathbf{u}) \leq 0} |\mathbf{u}| = \beta > 0$,
2. there exists a number at the most finite (upperscript $\alpha = 1, \dots, \eta$) of points $\mathbf{u}^{(\alpha)}$ such that $\|\mathbf{u}^{(\alpha)}\| = \beta$,
3. in these points, the gradient of H is not zero,
4. in these points the principal curvatures of the hypersurface $H(\mathbf{u}) = 0$ verify:

$$\kappa_j^{(\alpha)} \beta > -1, \quad j = 1, \dots, n-1$$

with α varying on the set of minimal points,

we then have an approximation, for $\beta \rightarrow \infty$, of the probability of failure (Breitung formula) as:

$$P_f \approx \Phi(-\beta) \left(\sum_{\alpha=1}^{\eta} \left(\prod_{j=1}^{n-1} \left(1 + \beta \kappa_j^{(\alpha)} \right)^{-1/2} \right) \right) \quad (7.19)$$

In practice, the equation is generally used with a unique point:

$$P_f \approx \Phi(-\beta) \left(\prod_{j=1}^{n-1} \frac{1}{\sqrt{1 + \beta \kappa_j}} \right) \quad (7.20)$$

For the proof, we refer to the original article, some elements of which are used again below.

Proof. The starting point is the equation giving expression (7.3) of the limit-state in a parabolic form:

$$m_P(\mathbf{y}) = -y_n + \sum_{j=1}^{n-1} \lambda_j y_j^2 \quad H(\mathbf{u}) \equiv m_P(\mathbf{y}) + \beta = 0$$

The limit-state is expressed, around point P^* , in the form of a hyperparaboloid whose coordinate y_n is oriented according to OP^* . Moreover, coordinates y_j are chosen in the principal reference of curvature. It results from this that coefficients λ_j are linked with the curvatures κ_j by $2\lambda_j = \kappa_j$.

The probability of failure is expressed as:

$$P_f = \text{Prob}[m_P(\mathbf{y}) \leq -\beta] = \text{Prob}\left[-y_n + \sum_{j=1}^{n-1} \lambda_j y_j^2 \leq -\beta\right]$$

To calculate P_f , we use the notion of a characteristic function (see Section 7.5.1). The characteristic function of a continuous random variable Y of density $f_Y(y)$ is given, for ω and $y \in \mathbb{R}$, by:

$$\mathcal{G}_Y(\omega) = E[e^{i\omega y}] = \int_{-\infty}^{+\infty} e^{i\omega y} f_Y(y) dy$$

as long as this integral is convergent, verified with the conditions:

$$\int_{-\infty}^{+\infty} f_Y(y) dy = 1 \quad \text{and} \quad |e^{i\omega y}| = 1 \quad i = \sqrt{-1}$$

Let us define the random variable M_P by $M_P = -y_n + \sum_{j=1}^{n-1} \lambda_j y_j^2$. Variables y_j being $\mathcal{N}(0, 1)$, the characteristic function is written as:

$$\mathcal{G}_{M_P}(\omega) = \frac{1}{(2\pi)^{n/2}} \int_{-\infty}^{+\infty} \cdots \int_{-\infty}^{+\infty} \exp\left(i\omega(-y_n + \sum_{j=1}^{n-1} \lambda_j y_j^2) - \frac{1}{2} \sum_{j=1}^n y_j^2\right) dy_1 \cdots dy_n$$

As variables y_j are independent, the previous expression is reduced to:

$$\begin{aligned} \mathcal{G}_{M_P}(\omega) &= \frac{1}{(2\pi)^{n/2}} \int_{-\infty}^{+\infty} \exp\left(-i\omega y_n - \frac{1}{2} y_n^2\right) dy_n \\ &\times \int_{-\infty}^{+\infty} \cdots \int_{-\infty}^{+\infty} \exp\left(-\frac{1}{2} \sum_{j=1}^{n-1} (1 - 2i\omega \lambda_j) y_j^2\right) dy_1 \cdots dy_{n-1} \end{aligned}$$

By comparing the last integration with the multinormal density function, we note that the coefficients $(1 - 2i\omega\lambda_j)$ play the role of the inverse of the variance; it becomes:

$$\mathcal{G}_{M_P}(\omega) = \frac{e^{-\omega^2/2}}{\sqrt{2\pi}} \int_{-\infty}^{+\infty} e^{-1/2(i\omega+y_n)^2} dy_n \prod_{j=1}^{n-1} \frac{1}{\sqrt{1 - 2i\omega\lambda_j}}$$

The calculation of this integral gives $\sqrt{2\pi}$; thus, the characteristic function of M_P takes the form:

$$\mathcal{G}_{M_P}(\omega) = e^{-\omega^2/2} \prod_{j=1}^{n-1} \frac{1}{\sqrt{1 - 2i\omega\lambda_j}}$$

The probability density of variable M_P is obtained by the Fourier inverse transformation:

$$\begin{aligned} f_{M_P}(\xi) &= \frac{1}{2\pi} \int_{-\infty}^{+\infty} e^{-i\omega\xi} \mathcal{G}_{M_P}(\omega) d\omega \\ &= \frac{1}{2\pi} \int_{-\infty}^{+\infty} e^{-i\omega\xi - \omega^2/2} \prod_{j=1}^{n-1} \frac{1}{\sqrt{1 - 2i\omega\lambda_j}} d\omega \end{aligned}$$

or otherwise:

$$\begin{aligned} f_{M_P}(\xi) &= \frac{e^{-\xi^2/2}}{2\pi} \int_{-\infty}^{+\infty} \exp \left[\frac{(i\omega - \xi)^2}{2} - \frac{1}{2} \sum_{j=1}^{n-1} \ln(1 - 2i\omega\lambda_j) \right] d\omega \\ &= \frac{e^{-(\xi^2/2)}}{2\pi} I(\xi) \end{aligned}$$

As long as the poles $\omega = 0$ and $\omega = 1/2\lambda_j$ are not exceeded, the integral $I(\xi)$ is independent of the trajectory of integration; it is appropriate to take a trajectory parallel to the imaginary axis tracing the outline of pole $\omega = 0$. The probability of failure is given by the distribution function of M_P :

$$P_f = \text{Prob}[M_P \leq -\beta] = \frac{1}{2\pi} \int_{-\infty}^{-\beta} e^{-(\xi^2/2)} I(\xi) d\xi \quad (7.21)$$

As the term $e^{-\xi^2/2}$ shows a rapid decrease, especially when $\xi \rightarrow \pm\infty$, the essential weight of this integration is located in the vicinity of $-\beta$. The term $I(\xi)$ can be evaluated in $\xi \rightarrow -\beta$, without seriously affecting the result. Given the exponential expansion of the integrand and with the hypotheses $\beta \rightarrow \infty$ and $\lambda_j > -1/(2\beta)$, K. Breitung obtains the following result:

$$\lim_{\beta \rightarrow \infty} \left| \frac{I(-\beta)}{\sqrt{2\pi} \prod_{j=1}^{n-1} \frac{1}{\sqrt{1+2\beta\lambda_j}}} \right| = 1$$

□

Let us introduce this result into the expression of the probability of failure (Equation (7.21)); we obtain:

$$P_f = \frac{1}{\sqrt{2\pi}} \int_{-\infty}^{-\beta} e^{-\xi^2/2} d\xi \prod_{j=1}^{n-1} \frac{1}{\sqrt{1 + 2\beta \lambda_j}}$$

which gives the Breitung formula already cited (Equation (7.20)) in the form:

$$P_f \simeq \Phi(-\beta) \prod_{j=1}^{n-1} \frac{1}{\sqrt{1 + \beta \kappa_j}}$$

where $\kappa_j = 2\lambda_j$.

Note: Let us remember once again that the principal curvatures are defined in this result as being positive if the convexity is turned toward the origin. The use of (7.19) implies the positivity of the term $1 + \beta \kappa_j^{(\alpha)}$. If the curvature is negative, this cannot be the case. However, Figure 7.6 shows that if the curvature is smaller than $-1/\beta$, point P^* , the apex of the approximation parabola, is no longer the closest point to the origin.

In this case, it is necessary to consider the nearest symmetric points to obtain a good approximation. With a positive sign for κ_j (convexity turned toward the origin), we verify easily that $P_f < \Phi(-\beta)$.

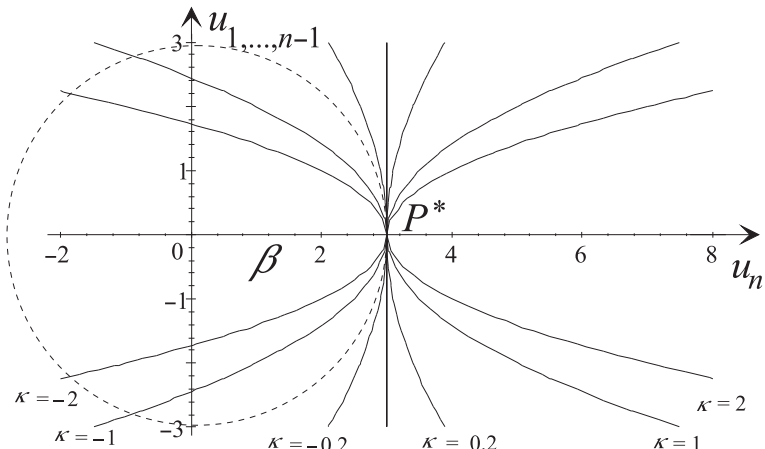


Figure 7.6 Parabolic approximations – representation according to different curvatures for $\beta = 3$.

7.4.2 Reference example

In the case of two variables, the calculation of the curvature pertains to elementary analytical geometry: if a curve is given by the equation $y = f(x)$, the curvature at a point of the abscissa x_0 is then:

$$\kappa = f''(x_0)[1 + f'^2(x_0)]^{-3/2}$$

In case 0, the curvature, calculated in Section 7.3.7, is practically zero and the SORM value coincides with the FORM value. For case 1, the quadratic form is written as:

$$u_1^2 + \sqrt{3}u_1u_2 + 8u_1 + 3\sqrt{3}u_2 - 35 = 0$$

which can be solved as the function $u_2 = f(u_1)$ with:

$$f(u) = \frac{35 - u^2 - 8u}{\sqrt{3}(u + 3)}$$

The precise results are given in Table 7.3.

Case	β	$\Phi(-\beta)$	κ	$P_{f\text{-Breitung}}$	$P_{f\text{-Tvedt}}$
0	2.499	6.222×10^{-3}	-3.505×10^{-4}	6.225×10^{-3}	6.225×10^{-3}
1	2.604	4.602×10^{-3}	5.752×10^{-2}	4.292×10^{-3}	4.255×10^{-3}

Table 7.3 Reference example – results of SORM-Breitung and SORM-Tvedt approximations for the first point.

The corrective factor in case 0 is 1.0004 and it is therefore practically equal to 1. In case 1, it is preferable to take the correction into account.

7.4.3 Hohenbichler approximation

An improvement has been brought to the asymptotic Breitung formula by Hohenbichler [HGKR87]. It is written as:

$$P_f \simeq \Phi(-\beta) \prod_{j=1}^{n-1} \frac{1}{\sqrt{1 + \frac{\phi(\beta)}{\Phi(-\beta)} \kappa_j}}$$

7.4.4 Tvedt approximation

The asymptotic method was developed in two directions: in order to take into account the multiple limit-states on the one hand (this point is dealt with in Chapter 9, Section 9.5) and by introducing the higher order terms into the Breitung formula.

Tvedt [Tve83] calculated the successive terms of an asymptotic formula. The calculation is given for a single design point, whose Hasofer-Lind index is β .

The first three terms of the asymptotic expansion of the probability of failure:

$$P_f = A_1 + A_2 + A_3 + \dots \quad (7.22)$$

are defined by the following equations:

- A_1 is the first term, calculated by Breitung, Equation (7.20),
- A_2 , using the same data and the density, ϕ , of the standardized Gaussian distribution, is:

$$A_2 = [\beta \Phi(-\beta) - \phi(\beta)] \left\{ \prod_{j=1}^{n-1} (1 + \beta \kappa_j)^{-1/2} - \prod_{j=1}^{n-1} [1 + (\beta + 1) \kappa_j]^{-1/2} \right\} \quad (7.23)$$

- A_3 also uses the same quantities:

$$A_3 = (\beta + 1)[\beta \Phi(-\beta) - \phi(\beta)]C \quad (7.24)$$

with:

$$C = \prod_{j=1}^{n-1} (1 + \beta \kappa_j)^{-1/2} - \operatorname{Re} \left\{ \prod_{j=1}^{n-1} [1 + (\beta + i) \kappa_j]^{-1/2} \right\}$$

The sign conventions used in this book for the principal curvatures, κ_j , are respected in these formulae. Re indicates the real part of a complex number and $i = \sqrt{-1}$. The last column of Table 7.3 gives the results for the reference example.

We can note that such an asymptotic expansion is not unique. An expansion with three different terms has also been proposed by other authors, for example, [KN94]. The authors of the latter article carried out a detailed comparison of different cases on a certain number of types of examples. For these different cases, the probability of failure can be calculated exactly in an analytical or numerical manner.

7.4.5 Comments and conclusion

It is important to emphasize the difficulties of implementation of the asymptotic SORM method:

1. We must not forget that asymptotic Equation (7.20) improves when the value of the index increases. In practice, it is necessary to consider indexes verifying at least $\beta \geq 3$, which is not verified in the reference example.

2. Knowledge of the second order elements of the performance function at the design point enables the use of an asymptotic method. However, the validity of the results depends closely on the number of random variables and on the distance to the critical value -1 of the term $\beta \kappa$ (concavity turned toward the origin); see the example of Section 7.2.3 which cannot be dealt with by the asymptotic method ($\beta \kappa_i = -1$).
3. A geometric approximation of the limit-state surface, defined in the vicinity of a design point, is no longer necessarily valid as soon as we move away from this point. This can lead to values without any real significance, when the failure domain differs in too radical a manner from a regular form.
4. The calculation, often numerical, of the Hessian should be carried out with care.

It is therefore essential to experiment with the asymptotic SORM-type methods and to ensure correct implementation during applications. They have the considerable advantage of often allowing a precise evaluation of the probability of failure for a limited calculation cost, especially in the context of coupling with the finite element method (FEM). The constraint of this efficiency is that they cannot be used without judgment.

7.5 Exact SORM method in quadratic form

Let us now turn to the exact calculation of the probability of failure for a quadratic limit-state. The original article is that of Rice [Ric80]. The idea is the following: in a space \mathcal{U} with n variables provided with a Gaussian distribution of probabilities, let us consider the values of a quadratic form Q . The values $Q(\mathbf{u})$ of this quadratic form for $\mathbf{u} \in \mathcal{U}$ are outcomes of a random variable from which it is possible to calculate the distribution using the characteristic function.

By obtaining the inverse of the characteristic function, we can then calculate the probability density function (PDF) and the cumulated distribution of the values of $Q(u)$, in particular, the quantity $\text{Prob}(Q(\mathbf{u}) \leq 0)$ which is the probability of failure sought. The method has been extended by Tvedt [Tve90, Tve88].

7.5.1 Characteristic function

Definition

Two expressions of the characteristic function of a continuous random variable Y of density $f_Y(y)$ are proposed, depending on whether we consider the pure imaginary axis or the whole complex plane. We use the imaginary $i = \sqrt{-1}$. In

the first case [Rad91], the variable is $p \in \mathbb{R}$; in the second case, it is $z \in \mathbb{C}$:

$$\begin{aligned} \mathcal{G}_Y(p) &= E[e^{ipY}] = \int_{-\infty}^{+\infty} e^{ipY} f_Y(y) dy \quad p \in \mathbb{R} \\ G_Y(z) &= E[e^{zy}] = \int_{-\infty}^{+\infty} e^{zy} f_Y(y) dy \quad z \in \mathbb{C} \end{aligned}$$

It is this second definition that is retained.

If \mathbf{Y} is a random vector of PDF $f_{\mathbf{Y}}(\mathbf{y})$, the characteristic function is then:

$$G_{\mathbf{Y}}(\mathbf{z}) = E[e^{\mathbf{z}^t \mathbf{y}}]$$

A few results

Table 7.4 gives some useful results for the calculation of characteristic functions of the forms (7.3), (7.5) and (7.6). The last three lines call for a complex square root. It is therefore necessary to pay attention to questions of determination. Point $\frac{1}{2}$ is a remarkably isolated point. The square root is real when z is real and lower than $\frac{1}{2}$. We have a choice between the two signs and this choice is generally +. The characteristic function cannot be defined totally, and it is necessary to define a continuous determination along the integration path.

$Y: \mathcal{N}(0, 1)$ a, b : constants	$Q(Y)$	$G_{Q(Y)}(z) \quad z \in \mathbb{C}$
Gaussian variable	Y	$e^{z^2/2}$
Linear application	$aY + b$	$e^{zb} G_Y(az)$
Sum of independent random variables	$\sum_{i=1}^n Y_i$	$\prod_{j=1}^n G_{Y_j}(z)$
Random variable square	Y^2	$\pm(1 - 2z)^{-1/2}$
Sum of squares of random variables χ_n^2	$\chi_n^2 = \sum_{j=1}^n Y_j^2$	$\pm(1 - 2z)^{-n/2}$
'Translated' square	$(Y - a)^2$	$\pm \frac{\exp(a^2/2(1/(1 - 2z) - 1))}{\sqrt{1 - 2z}}$

Table 7.4 A few characteristic functions.

If $G_Y(z)$ is the characteristic function of the PDF, then the values of the distribution function are deduced from $\frac{1}{z}G_Y(z)$.

If the PDF is absolutely integrable and at least twice continuously differentiable, we can obtain the inverse of the Fourier transformation and:

$$f_Y(y) = \frac{1}{2\pi} \int_{t=-\infty}^{t=\infty} e^{-ity} \mathcal{G}_Y(t) dt$$

Following the properties and the theoretical context, this inversion formula can take different forms; in particular, the inverse transform can be put in the following form:

$$f_Y(y) = \frac{1}{2\pi i} \int_{\Delta} e^{-zy} G_Y(z) dz$$

where Δ is the imaginary axis of the complex plane, running in the direction of increasing ordinate values ($-i\infty, i\infty$).

7.5.2 Characteristic functions of quadratic forms

The equations in Table 7.4 enable the calculation of the characteristic functions G_{M_P} (Equation (7.3)), G_{M_Q} (Equation (7.5)) and $G_{M_{Q'}}$ (Equation (7.6)) of random variables Y_i , $\mathcal{N}(0, 1)$. The sign + is chosen systematically. We note that all the functions obtained have isolated singular points in finite number in $1/\lambda_j$ (respectively $1/\mu_j$).

Parabolic case (Equation (7.3))

$$\begin{aligned} m_P(\mathbf{y}) &= -y_n + \sum_{j=1}^{n-1} \lambda_j y_j^2 \\ Y_n \longrightarrow G_{Y_n}(z) &= \int_{-\infty}^{+\infty} e^{zy_n} \frac{1}{\sqrt{2\pi}} e^{-\frac{y_n^2}{2}} dy_n = e^{\frac{z^2}{2}} \\ Y_j^2 \longrightarrow G_{Y_j^2}(z) &= (1 - 2z)^{-\frac{1}{2}} \\ \lambda_j Y_j^2 \longrightarrow G_{\lambda_j Y_j^2}(z) &= (1 - 2\lambda_j z)^{-\frac{1}{2}} \\ G_{M_P}(z) &= e^{\frac{z^2}{2}} \prod_{j=1}^{n-1} (1 - 2\lambda_j z)^{-\frac{1}{2}} \end{aligned}$$

Quadratic case (Equation (7.5))

$$m_Q(\mathbf{y}) = \nu + \sum_{j=1}^n (\lambda_j y_j^2 + \gamma_j y_j)$$

The constant ν has the characteristic function $e^{z\nu}$. The term under the sum should be adapted as:

$$\begin{aligned} \lambda_j y_j^2 + \gamma_j y_j &= \lambda_j \left(y_j + \frac{\gamma_j}{2\lambda_j} \right)^2 - \frac{\gamma_j^2}{4\lambda_j} \\ \rightarrow G_{\lambda_j y_j^2 + \gamma_j y_j}(z) &= (1 - 2\lambda_j z)^{-\frac{1}{2}} e^{\frac{\gamma_j^2}{8\lambda_j^2} \left(\frac{1}{1-2\lambda_j z} - 1 \right)} e^{-\frac{z\gamma_j^2}{4\lambda_j}} \\ \rightarrow G_{\lambda_j y_j^2 + \gamma_j y_j}(z) &= (1 - 2\lambda_j z)^{-\frac{1}{2}} e^{\frac{\gamma_j^2 z^2}{2(1-2\lambda_j z)}} \\ G_{M_Q}(z) &= e^{\nu z} \prod_{j=1}^n (1 - 2\lambda_j z)^{-\frac{1}{2}} e^{\frac{\gamma_j^2 z^2}{2(1-2\lambda_j z)}} \end{aligned}$$

Quadratic case (Equation (7.6))

$$\begin{aligned} m_{Q'}(\mathbf{y}) &= \sum_{j=1}^n \mu_j (y_j - \omega_j)^2 \\ (Y_j - \omega_j)^2 &\longrightarrow G_{(Y_j - \omega_j)^2}(z) = (1 - 2z)^{-\frac{1}{2}} e^{\frac{\omega_j^2}{2} \left(\frac{1}{1-2z} - 1 \right)} \\ G_{M_{Q'}}(z) &= \prod_{j=1}^n (1 - 2\mu_j z)^{-\frac{1}{2}} e^{\frac{\omega_j^2}{2} \left(\frac{1}{1-2\mu_j z} - 1 \right)} \end{aligned}$$

7.5.3 Results

The previous results can be put in the form of a theorem.

Theorem 2. *Let Y be a random variable of n -dimensional normal PDF (Gaussian, centered, variance 1, without correlation).*

We define the random variables in one dimension M_P , M_Q and $M_{Q'}$ given by the values of the quadratic forms:

$$\begin{aligned} m_P(\mathbf{y}) &= -y_n + \sum_{j=1}^{n-1} \lambda_j y_j^2 \\ m_Q(\mathbf{y}) &= \nu + \sum_{j=1}^n (\lambda_j y_j^2 + \gamma_j y_j) \\ m_{Q'}(\mathbf{y}) &= \sum_{j=1}^n \mu_j (y_j - \omega_j)^2 \end{aligned}$$

Then the characteristic functions – expressed using the complex variable $z \in \mathbb{C}$ – of the random variables M_P , M_Q and $M_{Q'}$, marked respectively G_{MP} , G_{MQ} and $G_{MQ'}$, are given by the expressions:

$$G_{MP}(z) = e^{\frac{z^2}{2}} \prod_{j=1}^{n-1} (1 - 2\lambda_j z)^{-1/2} \quad (7.25)$$

$$G_{MQ}(z) = e^{\nu z} \prod_{j=1}^n (1 - 2\lambda_j z)^{-1/2} e^{\frac{1}{2}\gamma_j^2 z^2 / (1 - 2\lambda_j z)} \quad (7.26)$$

$$G_{MQ'}(z) = \prod_{j=1}^n (1 - 2\mu_j z)^{-1/2} e^{\frac{\omega_j^2}{2} [(1 - 2\mu_j z)^{-1} - 1]} \quad (7.27)$$

The first formula corresponds to the parabolic approximation of the failure domain; the second corresponds to the quadratic approximation in the formulation given by [Tve90]; the third corresponds to the formulation of [Ric80]. A useful reference is the work of Johnson and Klotz [JK70].

7.5.4 Inversion of the characteristic function

The following result gives the value of the PDF and of the CDF of a random variable of the given characteristic function.

Theorem 3. Let M be a real random variable of the characteristic function $G = e^\varphi$, G being equal to one of the given functions of the previous theorem; φ is to be determined such that $\varphi = \ln G$. The determination of φ is chosen such that its argument is zero if G is real.

Then the PDF $f_M(m)$ and the CDF $F_M(m)$ of M are given by the integrals:

$$f_M(m) = \frac{1}{i2\pi} \int_{-i\infty}^{i\infty} e^{-z m + \varphi(z)} dz \quad (7.28)$$

$$F_M(m) = \int_m^\infty f_M(t) dt = \frac{1}{i2\pi} \int_{-i\infty}^{i\infty} \frac{1}{z} e^{-z m + \varphi(z)} dz \quad (7.29)$$

This theorem results from Fourier's inversion formula. It is to be noted that $P_f(m) = 1 - F_M(m)$.

7.5.5 Optimization of numerical calculation

Equations (7.28) and (7.29) are calculated by a direct numerical integration using the trapezium method. However, a difficulty is that these integrals generally have a very slow convergence: they cannot be absolutely convergent.

To improve the situation, we modify the integration path by optimizing the new path for the fastest possible convergence (point-saddle method).

The fact that modification of the path might be possible results from the fact that the function φ is holomorph, except possibly in a finite number of isolated singular points.

Unfortunately, these singular points are not always poles. We can, however, thanks to Jordan's lemma, displace the integration path, as is usual in Cauchy's theory.

The technique used is that of the demonstration of Paley-Wiener theorems; see, for example [Rud75].

In the simplest version, we replace integrals (7.28) and (7.29) by carrying out a translation of the imaginary integration axis from a real u_0 : we replace the integration path $z(t) = it$ by the path $z(t) = u_0 + it$.

The singularities are located on the real axis and have for abscissas $1/2\lambda_j$ in the case of formulae (7.25) and (7.26), and $1/2\mu_j$ in the other cases. If u_0 is negative, it is occasionally necessary to use the residue formula to add the contribution of the singularity $m = 0$ to the value of $f_M(m)$ or $F_M(m)$.

Let us note that the function φ is symmetric with respect to the real axis: $\varphi(\bar{u}) = \overline{\varphi(u)}$. $f_M(m)$ having a real value is given by the expression:

$$\begin{aligned} f_M(m) &= \frac{1}{i2\pi} \left(\int_{u_0-i\infty}^{u_0} e^{-z m + \varphi(z)} dz + \int_{u_0}^{u_0+i\infty} e^{-z m + \varphi(z)} dz \right) \\ &= \frac{1}{i2\pi} \int_{u_0}^{u_0+i\infty} e^{-z m + \varphi(z)} dz - e^{-\bar{z}m + \varphi(\bar{z})} d\bar{z} \\ &= \frac{1}{i\pi} \int_{u_0}^{u_0+i\infty} \frac{1}{2} (e^{-z m + \varphi(z)} + e^{-\bar{z}m + \varphi(\bar{z})}) dz \\ &= \operatorname{Re} \left[\frac{1}{i\pi} \int_{u_0}^{u_0+i\infty} (e^{-z m + \varphi(z)}) dz \right] \end{aligned}$$

A similar calculation can be made for $F_M(m)$. Thus, we obtain the formulae:

$$f_M(m) = \operatorname{Re} \left[\frac{1}{i\pi} \int_{u_0}^{u_0+i\infty} e^{-z m + \varphi(z)} dz \right] \quad (7.30)$$

$$F_M(m) = \operatorname{Re} \left[\frac{1}{i\pi} \int_{u_0}^{u_0+i\infty} \frac{1}{z} e^{-z m + \varphi(z)} dz \right] \quad u_0 > 0 \quad (7.31)$$

If we write the integrand of (7.30) with a real variable t , we must study an alternate integral:

$$\int_0^\infty e^{-m u_0 - i t m + \varphi(u_0 + i t)} dt \quad (7.32)$$

The decrease in this integral is given by the term $e^{-m u_0 + \varphi(u_0)}$. The fastest decrease is obtained for the minimum of this quantity (7.32) and u_0 must verify the equation:

$$u_0 \text{ saddle point, solution of } m = \frac{d\varphi(u)}{du}$$

The search for solutions to this equation enables us to consider the best possible integration. We can note that obtaining an approximate value is sufficient but that the discussion concerning a true minimum must be carried out.

Other paths are conceivable [Ric80]. It is the case of the reference example in which the integration path is inclined on the real axis.

Note: *the various documents published on these methods call for different sign conventions depending on the authors.*

Note: *since the publication of the works of S.O. Rice, different software packages for formal calculations have appeared. Inversion of the Fourier transformation is generally included. The results which have been obtained are excellent. All the operations to be carried out are easy to implement, especially the search for the minima of the function $e^{-m u + \varphi(u)}$.*

7.5.6 Reference example

This method is used by Rice for the calculation [Ric80].

The characteristic function G of the values of the quadratic form $Q(x_1, x_2) = \varepsilon(2x_1 x_2 - y)$ is:

$$G(z) = \frac{\exp\left(\frac{1}{2}\left[\frac{121}{12}\frac{6z}{1-6z} - \frac{1}{4}\frac{2z}{1+2z}\right]\right)}{\sqrt{(1-6z)(1+2z)}}$$

with the exception of the term in y .

We choose a determination of the complex logarithm $\varphi = \ln(G)$. The integration is carried out along the path:

$$z = u_0 + \frac{1+i\sqrt{3}}{y} v$$

where $y > 0$ is the value limited by the quadratic form ($y = 0.005$ or $y = 100$) and v is a real variable.

Before using the trapezium formula, a second change of variable is carried out:

$$t \mapsto v = e^{t-e^{-t}}$$

Integral (7.31) is then calculated using the trapezium method with N points and an interval h . [Ric80] gives the numerical results of Table 7.5.

Case	u_0	h	N	P_f	$\beta_1 = -\phi^{-1}(P_f)$
0	-0.32	0.05	133	7.15228×10^{-3}	2.4500
1	0.07	0.15	45	4.25734×10^{-3}	2.6314

Table 7.5 Reference example – Rice’s original results.

The results given are extremely precise, with a low calculation cost, but requiring intensive theoretical preparation. We can, however, examine the validity of the figures: it is necessary to make an error calculation for the trapezium method.

7.6 RGMR method

This section presents a method of ‘exact’ calculation of the probability of failure, in the sense that the only approximations carried out are of numerical type, in contrast to the FORM and SORM methods which start with a geometric approximation of the hypersurface of the limit-state whose impact on the probability is difficult to evaluate. It is called RGMR (Riemannian Geometric Method for Reliability). It comes from the works of J.C. Mitteau.

7.6.1 Motivation

Beyond the problems posed by statistical identification, for example as regards conjoint PDF of random variables, it is necessary to be able to certify the quality of the numerical chain:

$$(\mathcal{X}, G, F_{\mathbf{X}}(\mathbf{x})) \longrightarrow P_f$$

which goes from the mechanical-reliability model to the corresponding probability of failure.

In this formulation, the mechanical model is given by the performance function $G : \mathcal{X} \rightarrow \mathbb{R}$ and the probabilistic model by the conjoint CDF

F_X . The latter is always present, when it results from a complete statistical identification, allowing the use of a Rosenblatt transformation, or when the identification is partial, resulting then from methods such as the Nataf transformation or Hermite polynomials (see Chapter 4).

Certification of the calculations necessitates evaluation of numerical errors. This evaluation is not possible by the FORM and SORM methods, which have an asymptotic significance.

The use of simulation methods (Chapter 8) enables calculation of a confidence interval using the Shooman formula, but this evaluation results from the application of asymptotic theorems of statistics. It is not therefore a calculation of error in the strict sense.

Finally, knowledge of the error generated by a given method is indispensable for economic reasons. If we want to define economical calculation methods for reliability evaluation, it is necessary to be able to obtain, in each case, the best compromise between accuracy and volume, and thus the cost of calculation.

7.6.2 Introduction to RGMR

The calculation of the error committed in a numerical method results from a detailed analysis of a mathematically exact algorithm.

This is the case for the RGMR method, which is a numerical evaluation of integrals of low value, based on the use of quadrature points in the known directions of standardized space. These directions are distributed in a not necessarily uniform but controlled manner. The knowledge of the geometry of the quadrature points makes an error analysis possible.

In order to simplify the formulation, the method uses Riemannian geometry, allowing the calculation of hypersurfaces in spaces of any dimension. Direct numerical evaluation, often considered inaccessible by many authors, becomes optimal, in the sense that the number of calculations is minimal for a required calculation accuracy.

The method is based on a numerical evaluation of the integral of a function $\varphi(\delta)$ whose variable is a direction (non-oriented) in space \mathcal{U} of normal variables (centered, independent). By going in oriented directions in space, it also enables us to integrate functions defined on a hypersphere.

The method is especially adapted to the calculation of reliability integrals in standardized space, since the probability density admits a spherical symmetry.

The stages of the method are as follows:

1. To define the algorithm to calculate G , the performance function. As in the simulation methods, the algorithm need not lead to differentiable values.
2. To construct the chosen isoprobabilistic transformation.

3. To write the limit-state function in \mathcal{U} by combining the two previous operations. Two options are possible, depending on whether the distance of the limit-state with respect to the origin in a given direction is known or not:

- in the first case, we can integrate the directions directly in space to obtain the probability of failure,
- if we do not know this distance, we make the choice of a certain number of values of the distance, and we calculate later the probability of failure by an one-dimensional integration.

7.6.3 Notion of solid angle

For each radius $\rho > 0$, we define the solid angle $\theta(\rho)$ as the number of directions which admit a failure point at the distance ρ . The solid angle is mathematically identical to the $(n - 1)$ -volume of the intersection of the hypersphere of radius ρ with the failure domain, in standardized space.

For practical reasons, we consider the ratio with $(n - 1)$ -total volume of the hypersphere of radius ρ . This is a relative solid angle. Its expression is:

$$\theta(\rho) = \frac{\text{vol}(\Sigma_{n-1,\rho} \cap \mathcal{D}_f)}{\text{vol}(\Sigma_{n-1,\rho})} \Big|_{(n-1)\text{-volume}} \quad (7.33)$$

where $\Sigma_{n-1,\rho}$ indicates the hypersphere (and not the hyperball) of the n -dimensional space, centered at the origin, of radius ρ .

We can trace the solid angle as a function of ρ , which provides interesting information on the structure of the failure domain in the vicinity of the design point. The example in Section 7.6.8 gives the elements to trace Figure 7.7. Figure 7.8 represents the special case in dimension $n = 2$. It then becomes:

$$\theta(\rho) = \frac{\text{vol}(\Sigma_{2-1,\rho} \cap \mathcal{D}_f)}{\text{vol}(\Sigma_{2-1,\rho})} \Big|_{(2-1)\text{-volume}} = \frac{\text{vol}(\Sigma_{1,\rho} \cap \mathcal{D}_f)}{2\pi\rho}$$

7.6.4 Integral of the solid angle

Performed in standardized space, the calculation of the probability of failure is that of a multiple integral.

We note that the probability density depends only on the distance from the point in space to the origin. This enables us to decompose the following probability integral:

$$\frac{1}{(2\pi)^{n/2}} \int_{\mathcal{D}_f} e^{-\rho^2/2} du_1 \cdots du_n = \frac{1}{(2\pi)^{n/2}} \int_{\beta}^{\infty} \left[\int_{\mathcal{D}_{f,\rho}} d\sigma_{\rho} \right] e^{-\rho^2/2} d\rho$$

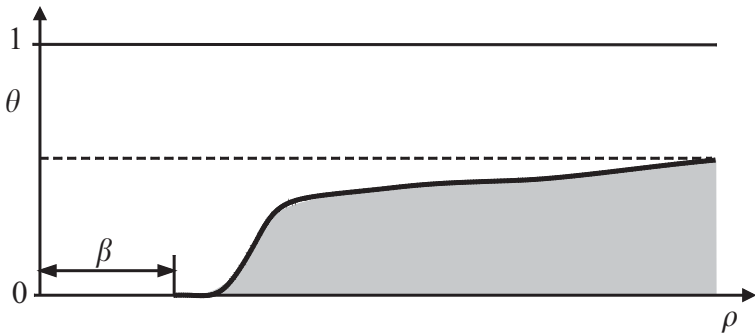


Figure 7.7 Typical form of the solid angle function $\theta(\rho)$.

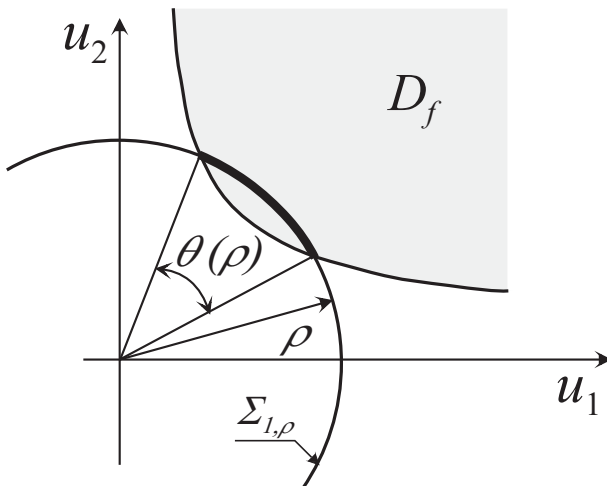


Figure 7.8 Illustration of the solid angle in a two-dimensional space.

in which $\mathcal{D}_{f,\rho} = \Sigma_{n-1,\rho} \cap \mathcal{D}_f$ is the intersection of the failure domain with the hypersphere of radius ρ , and $d\sigma_\rho$ is the differential element of the surface on this hypersphere.

The term in square brackets is written as:

$$\int_{\mathcal{D}_{f,\rho}} d\sigma_\rho = \theta(\rho) \text{vol}(\Sigma_{n-1,\rho}) = \theta(\rho) \rho^{n-1} \text{vol}(\Sigma_{n-1,1})$$

and finally:

$$P_f = \frac{\text{vol}(\Sigma_{n-1,1})}{(2\pi)^{n/2}} \int_{\beta}^{\infty} \theta(\rho) e^{-\rho^2/2} \rho^{n-1} d\rho \quad (7.34)$$

where the solid angle function $\theta(\rho)$ is given by (7.33). The numerical evaluation of the solid angle function therefore provides the probability of failure by a numerical quadrature. No hypothesis is formulated on the form of the limit-state; it is sufficient to know how to calculate the solid angle (Section 7.6.6).

7.6.5 SORM integral

Another decomposition of the probability integral is possible; it would be interesting if there exists an algorithmic means of calculating the intersection of each direction with the failure domain, and this is particularly simple when the failure domain is given by a quadratic inequation.

Let δ be a straight line in space. Let us indicate by I_δ (Figure 7.9) the intersection:

$$I_\delta = \delta \cap \mathcal{D}_f$$

We can note that in the case of the SORM integral, I_δ is made up of zero, one or two intervals whose limits are given by trinomial solutions.

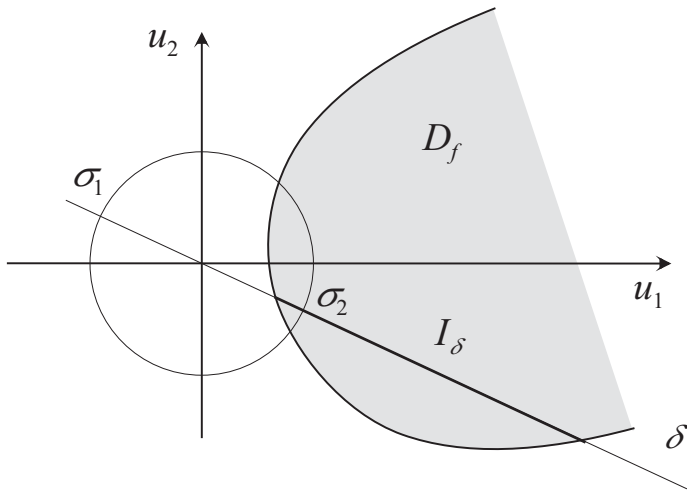


Figure 7.9 Representation of SORM integration; the same straight line δ is defined by points σ_1 and σ_2 .

The expression of the probability of failure:

$$P_f = \frac{1}{(2\pi)^{n/2}} \int_{\mathcal{D}_f} e^{-\rho^2/2} du_1 \cdots du_n$$

is written as previously in the coordinate system (σ, ρ) , and the integration is carried out this time by starting along the directions and then according to the complete set of directions. As I_δ is defined as the intersection of the straight line δ with the failure domain, the set of directions is identified with the hemisphere, in a manner that will not take the integral into account twice. Let us note $\Sigma_{n-1,1}^+$ the hemisphere and note that $du_1 \cdots du_n = \rho^{n-1} d\rho d\sigma_1$; it becomes:

$$P_f = \frac{1}{(2\pi)^{n/2}} \int_{\Sigma_{n-1,1}^+} \left[\int_{I_\delta} \rho^{n-1} e^{-\rho^2/2} d\rho \right] d\sigma_1 = \frac{1}{(2\pi)^{n/2}} \int_{\Sigma_{n-1,1}^+} f(\delta) d\sigma_1$$

In this case, which corresponds more particularly to that of the SORM integrals, the result is then obtained by an integration, along the space of the directions, of the function:

$$f(\delta) = \int_{I_\delta} \rho^{n-1} e^{-\rho^2/2} d\rho \quad (7.35)$$

By putting $u = \rho^2/2$ and by noting a , the value of ρ at the intersection, supposedly unique here, it becomes:

$$f(\delta) = \int_0^a \rho^{n-2} e^{-\rho^2/2} \rho d\rho = 2^{(n-2)/2} \int_0^{a^2/2} u^{(n-2)/2} e^{-u} du$$

whose values are deduced from the incomplete function Γ :

$$\Gamma(t, x) = \int_0^x u^{t-1} e^{-u} du \quad \text{with } x = \frac{a^2}{2} \text{ and } t = \frac{n}{2}$$

This function gives the Rayleigh's PDF of order $n, n \geq 1$ [BF87]; we find its algorithm of calculation in the usual mathematics libraries of scientific programming languages. This method is to be compared with directional simulations, described in Section 8.4.3, but the calculation is not performed here for random directions.

7.6.6 Calculation of the solid angle

Principle of calculation

In the two cases presented above, the calculation of the probability of failure is based on that of integrals of functions defined on the unit hypersphere of the n -dimensional space of the standardized variables:

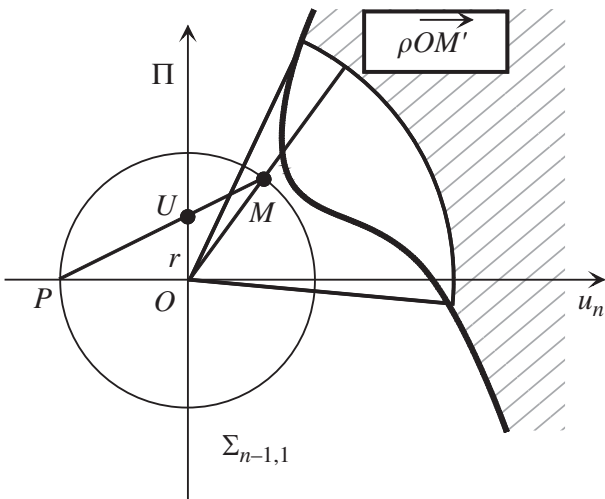


Figure 7.10 Representation of stereographic projection.

1. The calculation of the solid angle is obtained by integrating the constant function 1 on the set of points defined by the inequality:

$$H(\rho \overrightarrow{OM}) \leq 0$$

\overrightarrow{OM} indicating a unit vector of the space.

2. The calculation of the SORM integrals is obtained by integrating the function f defined in Section 7.3.5 on the direction space which is identified with a half hypersphere.

RGMR method calculations are carried out by a change of specially adapted variables, the stereographic transformation. This gives simple analytical formulae:

- Let us consider a point of the unit hypersphere, called the pole P . It is used as the point of projection (Figure 7.10). The choice of this point is not critical, but the further its direction is from the design point, the better the results obtained are.
- Let us note Π the hyperplane passing through the origin, orthogonal to direction OP . Any point U of Π is projected on the unit hypersphere in M , the intersection other than P of the straight line PU with the hypersphere.
- Let us choose any system of orthonormal coordinates u_i , $i = 1, \dots, n - 1$, in Π completed by the last axis u_n according to the straight line oriented along \overrightarrow{PO} .

This projection covers the hypersphere in a one-to-one manner, with the exception of P , and is written in an analytical manner by the formulae:

$$\overrightarrow{OM} = \left(\frac{2u_1}{1+r^2}, \dots, \frac{2u_{n-1}}{1+r^2}, \frac{1-r^2}{1+r^2} \right) \quad \|\overrightarrow{OM}\| = 1$$

with $r = \sqrt{u_1^2 + \dots + u_{n-1}^2}$.

The determinant of the Jacobian of the transformation $U \rightarrow M$ is:

$$|J| = \left(\frac{2}{1+r^2} \right)^{n-1}$$

The integrals along the sphere are therefore:

- for the solid angle (Equation (7.33)):

$$\theta(\rho) = \frac{1}{\text{vol}(\Sigma_{n-1,1})} \left[\int_{\mathbf{u} \in \mathcal{D}_U^+(\rho)} |J| du_1 \cdots du_{n-1} + \int_{\mathbf{u} \in \mathcal{D}_U^-(\rho)} |J| du_1 \cdots du_{n-1} \right] \quad (7.36)$$

with:

$$\begin{aligned} \mathcal{D}_U^+(\rho) &= \{U \in \Pi \mid H(\rho \overrightarrow{OM}(U)) \leq 0\} \\ \mathcal{D}_U^-(\rho) &= \{U \in \Pi \mid H(-\rho \overrightarrow{OM}(U)) \leq 0\} \end{aligned}$$

- for the SORM integral:

$$P_f = \int_{B_{n-1,1}} f(\overrightarrow{OM}) |J| du_1 \cdots du_{n-1}$$

where f is given by (7.35) and $B_{n-1,1}$ is the unit sphere (full sphere) of Π . These integrals are easy to calculate numerically: they are quadratures in a $(n-1)$ -dimensional space.

Illustration in three dimensions

An illustration has been given by [And02], which is presented in Figure 7.11. Expression (7.36) becomes:

$$\begin{aligned} \theta(\rho) &= \frac{1}{\text{vol}(\Sigma_{2,1})} \left[\int_{\mathbf{u} \in \mathcal{D}_U^+(\rho)} \left(\frac{2}{1+r^2} \right)^2 du_1 du_2 \right. \\ &\quad \left. + \int_{\mathbf{u} \in \mathcal{D}_U^-(\rho)} \left(\frac{2}{1+r^2} \right)^2 du_1 du_2 \right] \end{aligned}$$

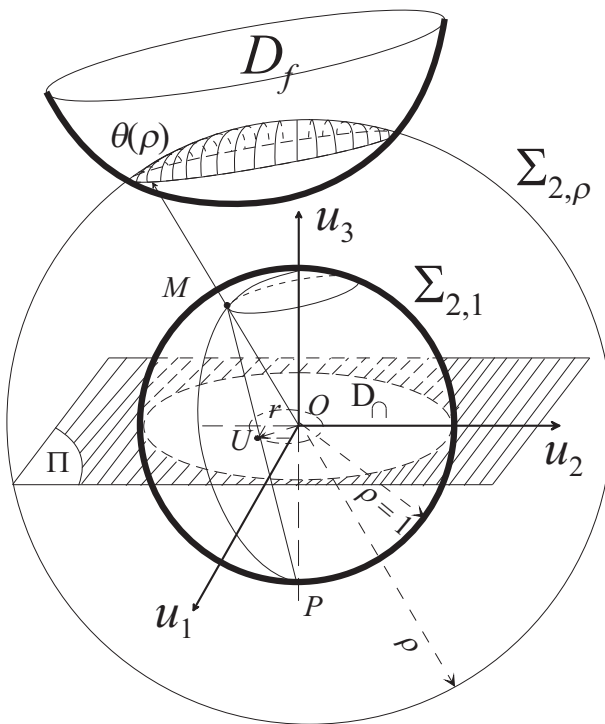


Figure 7.11 Illustration of the calculation of the solid angle in three dimensions.

where:

- \mathbf{u} is the coordinate vector of U , any point of the plane Π , belonging to the intersection $D_\cap = \{U \in \Pi \mid r(U) \leq 1\}$,
- $r = \sqrt{u_1^2 + u_2^2} = \|\overrightarrow{OU}\|$,
- $\mathcal{D}_U^+(\rho)$ is the set of points $U \in \Pi$ such as $H(\rho \overrightarrow{OM}(U)) \leq 0$, which is true in the case of the figure,
- $\mathcal{D}_U^-(\rho)$ is the set of points $U \in \Pi$ such that $H(-\rho \overrightarrow{OM}(U)) \leq 0$,
- $\text{vol}(\Sigma_{2,1})$ is the volume of the two-dimensional sphere, that is to say 4π .

7.6.7 Numerical aspects

Quadrature points

The calculation of the integrals on the sphere is therefore reduced to a classical calculation of a multidimensional integral. The simplest way is to consider a

regular network of points with a step h in all the directions of a reference chosen in Π . The use of a distribution of points adapted to the performance function H , concentrating the quadrature points in the sectors of interest and eliminating zones without interest, enable us to limit the calculations to the values of variables having a physical significance.

Calculation of the integration error

The use of explicit numerical formulae for the different quadratures enables a calculation error analysis of the type which is used generally in numerical analysis [Mit99].

Boundary effects

Attention must be paid to the boundary effects when they arise from points of the failure domain sufficiently close to the limit in a direction forming part of plane Π (Figure 7.10). The volume element, at this point, must be truncated by the condition $r \leq 1$. This condition is not simple to write down. We run the risk of integrating the same points twice.

Several methods exist to get round this difficulty:

- We can write an approximation of the volume of the truncated cells. This type of method is the prevailing one in numerical analysis. This is what has been used in the examples dealt with in this work.
- The point of projection P can be placed in such a manner as to avoid this situation.
- Finally, we can consider integrating along the orientation directions instead of integrating as has been done above. The disadvantage comes from introducing points of plane Π which can be far from the origin, but we are sure not to count the same points twice.

7.6.8 Solid angle in the FORM approximation

Problem: calculate the solid angle function of a halfspace located at a distance β from the origin, as a function of the number n of random variables. Study more particularly the behavior of the solid angle function in the vicinity of $\rho = \beta$.

The solid angle is a cone for which it is easy to calculate the angle at the apex, α_0 . For a given radius ρ , the apex angle is such that $\cos \alpha_0 = \beta/\rho$. The ratio between the volume cut off by the cone of the angle at the apex α_0 on the n -dimensional sphere and the total volume of this sphere remains to be calculated.

In Equation (7.33), the set $\Sigma_{n-1,\rho} \cap \mathcal{D}_f$ is made up of points such that $\alpha \leq \alpha_0$ (Figure 7.12). These points form a spherical cap. To calculate its

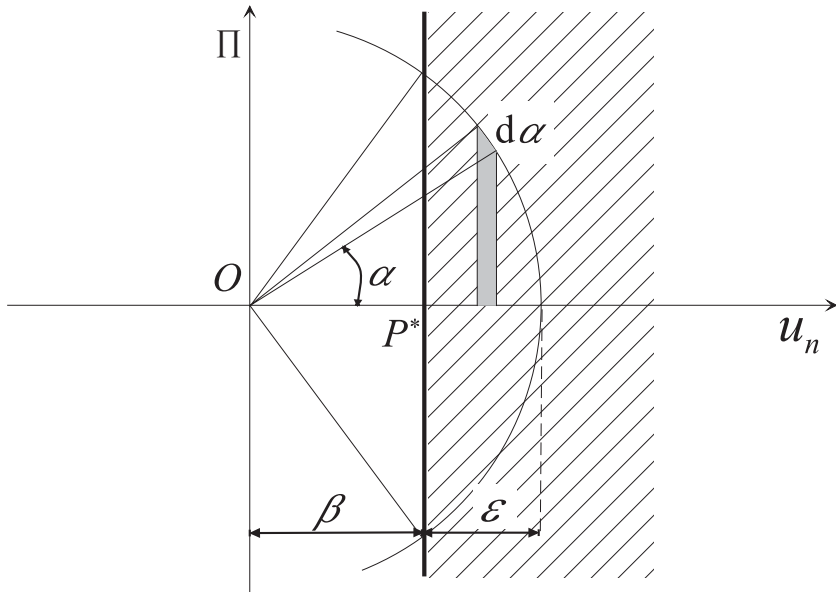


Figure 7.12 Calculation of the FORM solid angle.

volume, let us consider for each value α , the sphere $\Sigma_{n-2,\rho \sin \alpha}$ defined by the values $\alpha = \text{constant}$. Let us integrate in α :

$$\text{vol}(\Sigma_{n-1,\rho} \cap \mathcal{D}_f) = \text{vol}(\Sigma_{n-2,1}) \rho^{n-1} \int_0^{\alpha_0} (\sin \alpha)^{n-2} d\alpha$$

which gives the solid angle:

$$\begin{aligned} \theta(\rho) &= \frac{\text{vol}(\Sigma_{n-2,1}) \rho^{n-1}}{\text{vol}(\Sigma_{n-1,\rho})} \int_0^{\alpha_0} (\sin \alpha)^{n-2} d\alpha \\ &= \frac{\text{vol}(\Sigma_{n-2,1})}{\text{vol}(\Sigma_{n-1,1})} \int_0^{\alpha_0} (\sin \alpha)^{n-2} d\alpha \end{aligned} \quad (7.37)$$

and the constant $\text{vol}(\Sigma_{n-2,1})/\text{vol}(\Sigma_{n-1,1})$ is obtained from the same integral with $\alpha_0 = \pi$. In three dimensions, it becomes:

$$\theta(\rho) = \frac{\text{vol}(\Sigma_{3-2,1})}{\text{vol}(\Sigma_{3-1,1})} \int_0^{\alpha_0} (\sin \alpha)^{3-2} d\alpha = \frac{2\pi}{4\pi} \int_0^{\alpha_0} \sin \alpha d\alpha = \frac{1}{2}(1 - \cos \alpha_0)$$

More generally, (7.37) is an incomplete Wallis integral and can be calculated numerically from the incomplete Eulerian function $\Gamma(x, u) = \int_0^u t^{x-1} e^{-t} dt$.

What is of interest to us here is the behavior in the vicinity of the design point $\rho = \beta$. Let us develop for this Equation (7.37) in the vicinity of this point. Let us define $\varepsilon = \rho - \beta$. We have $\sin \alpha \approx \alpha$. The integration gives $\theta(\rho) \approx K \alpha_0^n$.

Furthermore, we have:

$$\cos \alpha_0 = \frac{\beta}{\beta + \varepsilon} \approx 1 - \frac{\alpha_0^2}{2}$$

leading to $\alpha_0 \approx \sqrt{2\varepsilon / \beta}$.

Finally, the behavior of the solid angle function is of the order of $\varepsilon^{(n-1)/2}$, with the exception of a multiplication constant dependent on β . This remark shows behavior varying greatly with the number n of random variables. When this number increases, the points which contribute significantly to the probability of failure move progressively away from the origin. This emphasizes the more and more approximate character of the FORM and SORM methods when the number of random variables is high.

The multinormal density is written as $\phi_n(\rho) = (2\pi)^{-n/2} \exp(-\rho^2/2)$. Figure 7.13 shows the derivative $d\phi_n(\rho)/d\rho$ for different values of n . It illustrates the fact that the decrease is much less rapid when the number n of variables is high.

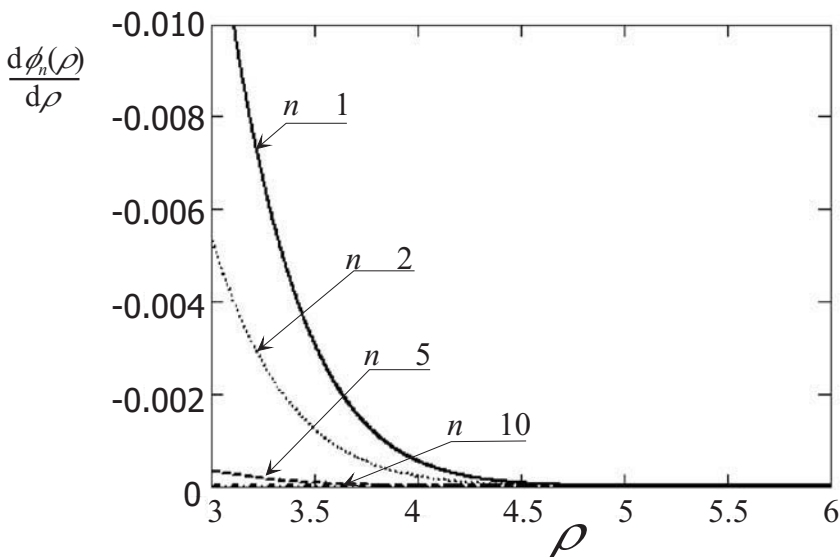


Figure 7.13 Decrease of the multinormal function for a radius $\rho > 3$.

7.6.9 Special two-dimensional case

An interesting special case of the calculation of reliability is that where only two random variables are present. Over and above the pedagogic interest illustrated in Section 7.7.4, this case arises when the probabilistic model has been sufficiently simplified by identifying the variables having the most significant importance factors. The RGMR method is then identical with the calculation of a curvilinear integral.

In polar coordinates:

$$P_f = \frac{1}{2\pi} \int_{\mathcal{D}_f} e^{-(u_1^2 + u_2^2)/2} du_1 du_2 = \frac{1}{2\pi} \int_{\mathcal{D}_f} \rho e^{-\rho^2/2} d\rho d\theta$$

which is written by decomposing the failure domain according to the radius and the angle:

$$\begin{aligned} P_f &= \frac{1}{2\pi} \int_{\theta_1}^{\theta_2} \left\{ \int_{\rho_1(\theta)}^{\rho_2(\theta)} \rho e^{-\rho^2/2} d\rho \right\} d\theta \\ &= \frac{1}{2\pi} \int_{\theta_1}^{\theta_2} \left[e^{-\rho_1^2(\theta)/2} - e^{-\rho_2^2(\theta)/2} \right] d\theta \end{aligned}$$

The two integrals correspond to an integration of θ_1 to θ_2 , one of θ_1 toward θ_2 and the other of θ_2 toward θ_1 , hence:

$$P_f = \frac{1}{2\pi} \int_{\theta_1}^{\theta_2} e^{-\rho_1^2(\theta)/2} d\theta + \int_{\theta_2}^{\theta_1} e^{-\rho_2^2(\theta)/2} d\theta = \frac{1}{2\pi} \int_{\Gamma} e^{-\rho^2(\theta)/2} d\theta$$

where Γ is the contour of the failure domain defined by its angular limits.

7.6.10 Reference example

A spreadsheet enables us to program the curvilinear integral: the variation of angle θ is divided into 200 points. For a given direction θ , we calculate the roots of the trinomial $\cos\theta(\cos\theta + \sqrt{3}\sin\theta)\rho^2 + (8\cos\theta + 3\sqrt{3}\sin\theta)\rho + 15 = y/2$, y taking the values 0.005 or 100. These values $\rho(\theta)$ define a parametric representation of the limit-state. It is advisable to study the different possible cases, according to the values of angle θ .

Let us take case 1, $y = 100$. According to Figure 7.2, θ varies usefully between -0.58 and 1.65 radians, values for which the straight line of the angle θ is practically tangent to the hyperbola. The domain is separated into two parts for which it is sufficient to add the integrals. The constant term is -35 . The calculation shows that the value on one of the branches is negligible because ρ is altogether higher than the second β , itself reduced by 8.9. For case 0, $y = 0.005$, we integrate on the totality of the circle, from 0 to 2π .

The trapezium method is applied for the numerical calculation of the integral. The values obtained are given in Table 7.6, in which β_{rgmr} is $-\Phi^{-1}(P_{f,\text{rgmr}})$.

Case	y	ε	$P_{f,\text{RGMR}}$	β_{RGMR}
0	0.005	1	7.15×10^{-3}	2.450
1	100	-1	4.257×10^{-3}	2.631

Table 7.6 Reference example – results from RGMR integration.

An error calculation for the trapezium method is carried out by using the error formula of the trapezium integral:

$$\frac{(b-a)^3}{12 n^3} \sum_{j=1}^n M_j$$

where $[a, b]$, $a < b$ is the integration interval, n is the number of intervals of the method and M_j is a superior bound, in each interval, of the absolute value of the second derivative.

Evaluation of the second derivative of $\rho(\theta)$ for the first branch of the hyperbola leads to the graph in Figure 7.14 which enables us to increase the derivative.

The results obtained show that the error in case 0 is of the order of 10^{-4} , which gives a probability value of $(7.2 \pm 0.1)10^{-3}$. The situation is more favorable in case 1, since the error is of the order of 2×10^{-6} . It is not therefore illusory to give four significant figures, $(4.257 \pm 0.002)10^{-3}$.

7.6.11 Conclusion

A critical study of the approximation methods of the multinormal integrals in reliability shows that the results obtained are often difficult to interpret.

In particular, it is practically impossible to date to determine the magnitude of the approximations made using different methods, which might be FORM or SORM methods or random sampling methods.

The RGMR method enables us to deal with these questions. We have seen that its principle consists of taking up a position in the direction space passing through the origin in standardized variable space and studying the intersection of a direction with the failure domain [MBL95].

The direction space is provided with a mathematical structure which enables us to refer to the distance of two directions and to integrate according to the set of directions. This structure is based on the use of Riemannian geometry, which is very well formalized today.

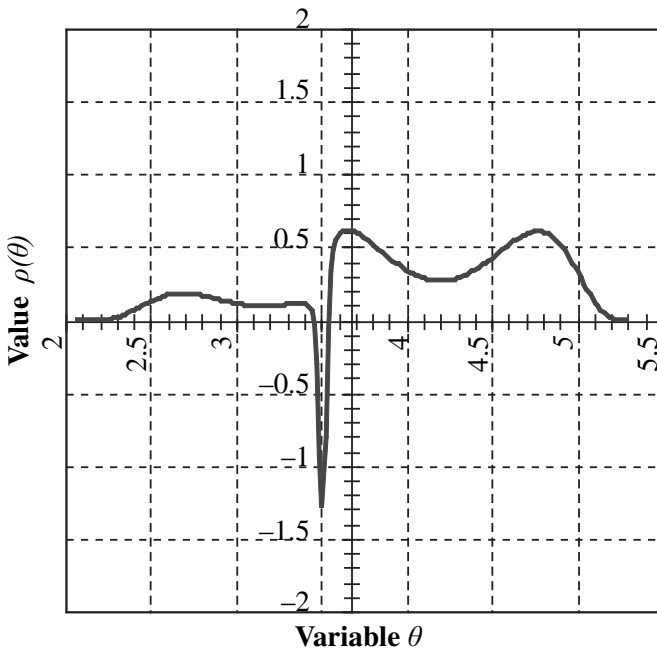


Figure 7.14 Second derivative of $\rho^{(\theta)}$.

From this formalism, we can carry out the following operations:

1. Look for the nearest point in all possible directions. This is the search for the Hasofer-Lind index. We can thus obtain the absolute minimum of the distance and not a relative minimum:

$$\beta = \min_U(\rho) \mid U \in \mathcal{D}_U(\rho) = \{U \in \Pi \mid H(\rho \overrightarrow{OM}(U)) \leq 0\}$$

and all the secondary extremes are identified.

2. Refine the calculation of β , for a precise investigation of the design point, by a method without gradient.
3. Determine the failure interval in a given direction. The integral in the given direction is obtained by an analytical formula, reducing the integration dimension by one unit. We then benefit, with full spherical symmetry, from the distribution in normal variable space.
4. Determine the solid angle for a given radius ρ , that is to say, the ratio between the total volume of direction space and that of directions for which at least one of the points at distance ρ is in the failure domain.

The probability results then from the integral of this solid angle from the $\chi^2 = \sqrt{\sum u_i^2}$ density.

Not using directly the differentiation properties of the limit-state enables an investigation of the design point when function G is directly defined by the computer algorithms. This is the case, for example, of complex systems of failure scenarios. Few problems of convergence appear in the investigation of the reliability index, and the different forms of isoprobabilistic transformations can be integrated directly in the source code.

However, all these advantages have a cost. The calculation time depends essentially on the number of variables and the accuracy required. This method is obviously more unwieldy to implement than the FORM/SORM methods, but it gives many more results. The use of an error calculation enables us to optimize the cost for the accuracy required of the calculation [Mit96].

7.7 Numerical examples

7.7.1 Reference example: conclusions

On the approximation of the probability of failure

Table 7.7 summarizes the results obtained. We can note the proximity of the results of the last two lines, obtained with approximately equivalent calculation costs and a definitely simpler preparation for RGMR. The characteristic function gives a crude result, obtained without error calculation. The FORM/SORM results are obtained with only the first design point.

	$10^3 P_f$		$\beta_1 = -\Phi^{-1}(P_f)$	
Method	$y = 0.005$	$y = 100$	$y = 0.005$	$y = 100$
FORM (7.2)	6.222	4.602	2.499	2.604
SORM (7.3)	6.225	4.292	2.495	2.628
Charact. funct. (7.5)	7.15228	4.25734	2.450	2.631
RGMR (2D.) (7.6)	7.2 ± 0.1	4.257 ± 0.002	2.450	2.631

Table 7.7 Reference example – review of results from the first design point.

On the multiplicity of calculation points

In case 0, $y = 0.005$, the SORM approximation, limited to one point, is not excellent. This is due to the existence of four extremes giving indexes sufficiently close, of which three are placed on the first branch of the hyperbola (Table 7.8). However, point 3 is a maximum.

Point	$1 = P^*$	2	3	4
u_1^*	-1.250	-2.999	-2.974	-3.027
u_2^*	-2.164	-0.000	-1.115	-1.192
β	2.499	2.999	3.176	3.253
P_{f_FORM}	6.222×10^{-3}	1.355×10^{-3}		0.570×10^{-3}
κ	-3.5×10^{-4}	-1.9×10^{-3}	-6.9	7.1
P_{f_SORM}	6.225×10^{-3}	1.359×10^{-3}		0.116×10^{-3}

Table 7.8 Reference example: combination of local minima in case 0, $y = 0.005$.

The reliability system gives the means of taking into account these three significant points. For a first approximation, it is sufficient to apply Equation (9.7) of Chapter 9 with a positive correlation (the asymptotes make an angle greater than $\pi/2$), for points 1 and 2, and then to withdraw the influence of point 4 to take into account the fact that the failure domain is located only between the hyperbolas. The result obtained is:

$$6.11 \times 10^{-3} \leq P_f \leq 7.46 \times 10^{-3}$$

which restricts the expected value satisfactorily. More precise methods of composition are given in Chapter 9.

7.7.2 Rod under tension

This example illustrates the different approaches for the data proposed in Figure 3.12; the resistance is assumed to be Gaussian and the stress is lognormal. The equation of the limit-state is then:

$$6.87u_1 + 114.54 - \exp(0.212 u_2 + 4.226) = 0$$

The result obtained is $\beta = 2.335$, $u_1^* = -0.660$, $u_2^* = 2.240$, $P_{f_FORM} = \Phi(-\beta) = 0.00978$.

Breitung formula

The curvature is calculated directly by rewriting the limit-state as:

$$u_1 = \frac{1}{6.87} [\exp(0.212 u_2 + 4.226) - 114.54]$$

by the equation $|\kappa| = |u''_1|/(1 + u'_1)^{3/2}$, with $\kappa = -0.0162$, a negative value because the concavity contains the origin, whence:

$$P_{f,\text{Breitung}} \approx \frac{\Phi(-\beta)}{\sqrt{1 + \beta\kappa}} = 0.00997$$

RGMR integration

Numerical integration gives:

$$P_{f,\text{RGMR}} = 0.01009$$

Monte Carlo simulation

The result is obtained using a technique of conditional simulations presented in Chapter 8:

$$P_{f,\text{simulation}} = 0.01024$$

The number of simulations is much higher than is necessary, as shown by the convergence curve given in Figure 7.15.

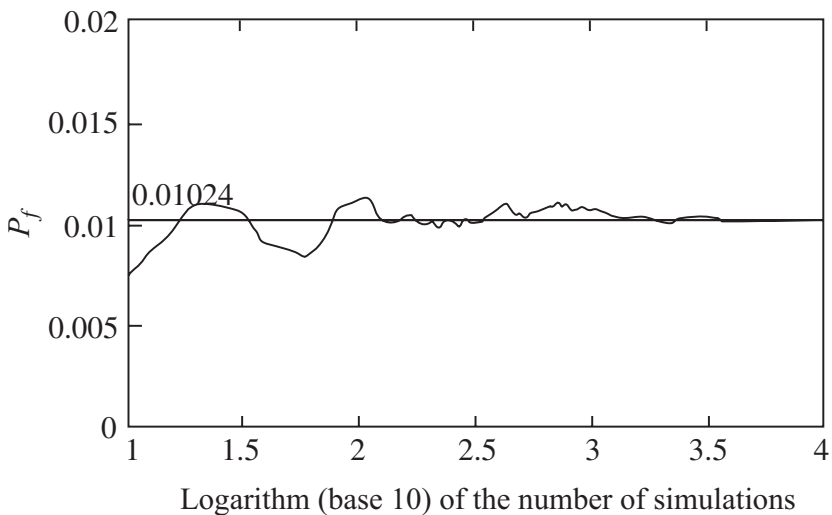


Figure 7.15 Solution by conditional simulations.

7.7.3 Plastic failure of a section

Problem

The plastic resistance of a cross-section of a bending beam is given by the equation:

$$M_P = z f_y$$

where M_P is the plastic moment, z is the plastic bending modulus and f_y is the yield limit. The stress is the bending moment M and the elastoplastic failure is then given by:

$$G(\mathbf{x}) = f_y z - M = x_1 x_2 - x_3$$

The three variables $f_y = X_1$, $z = X_2$, $M = X_3$ are Gaussian variables (for simplicity of calculation) whose data are in Table 7.9.

	v.a.	$\mathcal{N}(0, 1)$	Mean	Standard deviation
f_y	X_1	U_1	40	5
z	X_2	U_2	50	2.5
M	X_3	U_3	1,000	200

Table 7.9 Data of random variables.

Questions

1. By carrying out a linearization of the limit-state function around the mean (by a first-order expansion of $G(\mathbf{x})$), calculate the Cornell reliability index and the direction cosines α .
2. Give the expression of the limit-state function $H(\mathbf{u})$ as a function of normal variables \mathbf{u} , centered, reduced, associated with \mathbf{x} and of the numerical coefficients and calculate the Hasofer-Lind index β .
3. Give a first approximation of the probability of failure P_f .
4. Give the approximation of P_f using Breitung's formula.

Linearization

The linearization of the limit-state function around the mean is written as:

$$G(\mathbf{x}) = G(\mathbf{m}_X) + \begin{pmatrix} m_{X_2} & m_{X_1} & -1 \end{pmatrix} \begin{pmatrix} x_1 - m_{X_1} \\ x_2 - m_{X_2} \\ x_3 - m_{X_3} \end{pmatrix}$$

After replacing by numerical values, it becomes:

$$m_G = 1,000 \quad \sigma_G = 335.41 \implies \beta_C = 2.981$$

Limit-state in centered reduced variables

The variables are Gaussian and the change of variable is given by:

$$u_i = \frac{x_i - m_{X_i}}{\sigma_{X_i}}$$

and:

$$H(\{u\}) = 12.5 u_1 u_2 + 250 u_1 + 100 u_2 - 200 u_3 + 1,000 = 0$$

This limit-state is the one that we dealt with in Section 5.4.2: $\beta = 3.049$ and $\langle \alpha \rangle = \langle 0.751 \ 0.222 \ -0.622 \rangle$.

FORM approximation of P_f

It is given by:

$$P_{f_FORM} \approx \Phi(-\beta) = 0.001148$$

Breitung's formula

We obtain:

$$\kappa_1 = -0.032 \quad \kappa_2 = 0.019 \quad P_{f_Breitung} = 0.001174$$

The FORM/SORM coefficient of correction is $c = 1.023$. This correction is weak, and the FORM approximation takes advantage of the fact that the two curvatures are of opposite signs. For comparison, RGMR gives $P_{f_RGMR} = 0.001187$.

7.7.4 Approximations of the probability of failure

FORM and SORM approximations

We consider the following limit-state function, defined in Gaussian variable space, standardized and centered:

$$H(\mathbf{u}) = u_1^2 - 2\sqrt{3} u_1 u_2 + 3u_2^2 - 2\sqrt{3} u_1 - 2u_2 + 12 = 0$$

The point of coordinates $(0, 0)$ belongs to the safety domain:

1. Represent graphically this function.
2. Deduce, by geometric reasoning, the coordinates of the most probable failure point P^* .
3. Calculate the gradient $\nabla H(\mathbf{u})$ in P^* , by deducing the direction cosines α in P^* and the index β .
4. Give the FORM approximation of $P_{f,\text{FORM}}$ and, if possible, of the bounds of the correct value.
5. Express $H(\mathbf{u})$ in reduced form by dividing by the norm of the vector $\nabla H(\mathbf{u})$ calculated in P^* .
6. Calculate the curvature at point P^* by deducing the SORM approximation of $P_{f,\text{SORM}}$ according to Breitung. Give the corresponding value of β .

Representation: the representation of the limit-state is given in Figure 7.16. It is a parabola whose axis makes an angle of 30° with Ou_1 .

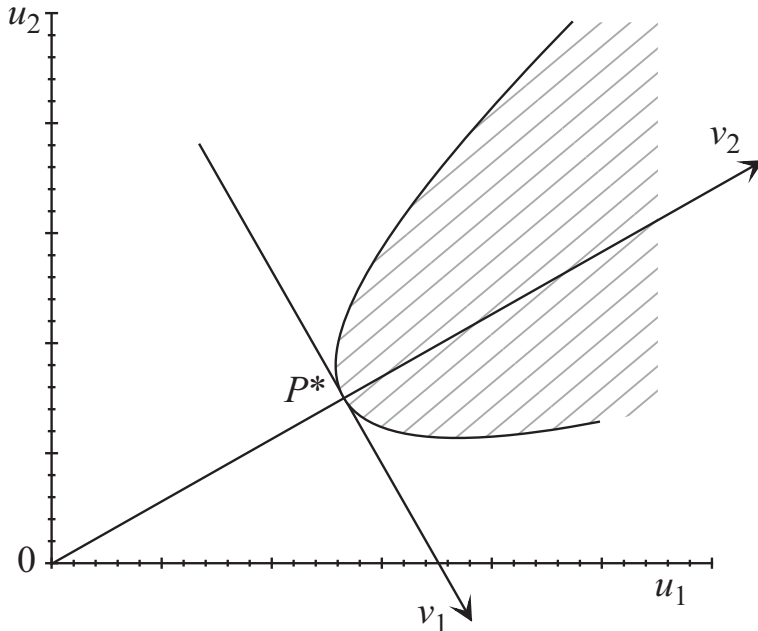


Figure 7.16 Representation of the limit-state in standardized space.

The most probable failure point: geometrically, $\beta = 3$ and $u_1^* = 3\sqrt{3}/2$, $u_2^* = 3/2$. Such a graph is obtained from the calculation of a few points.

Calculation of β

$$\{\nabla H(\mathbf{u})\} = \begin{bmatrix} 2u_1 - 2\sqrt{3}u_2 - 2\sqrt{3} \\ -2\sqrt{3}u_1 + 6u_2 - 2 \end{bmatrix} \implies \{\nabla H^*(\mathbf{u})\} = \begin{bmatrix} -2\sqrt{3} \\ -2 \end{bmatrix}$$

from which $\|\nabla H^*(\mathbf{u})\| = 4$ and:

$$\beta = 3 \quad \langle \alpha \rangle = \left\langle -\frac{\sqrt{3}}{2}, -\frac{1}{2} \right\rangle$$

FORM approximation: this is given by:

$$P_{f,\text{FORM}} \approx \Phi(-\beta) = 0.001350$$

and taking into account the convexity toward the origin, $P_{f,\text{FORM}} > P_f > 0$.

Reduced form of $H(\mathbf{u})$

$$H(\mathbf{u}) = u_1^2 - 2\sqrt{3}u_1u_2 + 3u_2^2 - 2\sqrt{3}u_1 - 2u_2 + 12 = 0$$

Calculation of the curvature and the second order approximation.

First method – reduction of the quadratic form: $H(\mathbf{u})$ contains a quadratic form $u_1^2 - 2\sqrt{3}u_1u_2 + 3u_2^2$ of matrix:

$$[Q] = \begin{bmatrix} 1 & -\sqrt{3} \\ -\sqrt{3} & 3 \end{bmatrix}$$

whose eigenvalues λ_i and eigenvectors ϕ_i are:

$$\lambda_1 = 0 \quad \phi_1 = \begin{bmatrix} \sqrt{3}/2 \\ 1/2 \end{bmatrix} \quad \lambda_2 = 4 \quad \phi_2 = \begin{bmatrix} 1/2 \\ -\sqrt{3}/2 \end{bmatrix}$$

A possible rotation of axis is then:

$$[R] = \begin{bmatrix} \frac{1}{2} & \frac{\sqrt{3}}{2} \\ \frac{-\sqrt{3}}{2} & \frac{1}{2} \end{bmatrix} \quad \mathbf{u} = [R]\mathbf{v}$$

and:

$$H(v_1, v_2) = 4v_1^2 - 4v_2 + 12 = 0 \implies v_2 = v_1^2 + 3$$

Under this form, it immediately becomes $\kappa = 2$ (radius = 0.5).

Second method – application of the general approach:

$$\begin{aligned} [B] &= \frac{\nabla^2 H(\mathbf{u})}{2\|\nabla H(\mathbf{u})\|} \Big|_{\mathbf{u}^*} = \frac{1}{4} \begin{bmatrix} 1 & -\sqrt{3} \\ -\sqrt{3} & 3 \end{bmatrix} \\ [R] &= - \begin{bmatrix} r_{11} & r_{12} \\ -\alpha_1 & -\alpha_2 \end{bmatrix} = \begin{bmatrix} r_{11} & r_{12} \\ \frac{\sqrt{3}}{2} & \frac{1}{2} \end{bmatrix} \end{aligned}$$

where r_{11} and r_{12} are such that:

$$\begin{aligned} \frac{\sqrt{3}}{2} r_{11} + \frac{1}{2} r_{12} &= 0 \quad (\text{orthogonality of the vectors}) \\ r_{11}^2 + r_{12}^2 &= 1 \quad (\text{normalized vector}) \end{aligned}$$

which gives:

$$[R] = \begin{bmatrix} 1/2 & -\sqrt{3}/2 \\ \sqrt{3}/2 & 1/2 \end{bmatrix} \quad [A] = [R][B][R]^t = \begin{bmatrix} 1 & 0 \\ 0 & 0 \end{bmatrix}$$

The curvature is then $\kappa = 2\lambda = 2$.

SORM equation

$$P_{f_{-\text{SORM}}} = \Phi(-\beta) \frac{1}{\sqrt{1 + \kappa\beta}} = 0.000510 \quad \beta = 3.285$$

Tvedt's equation gives $P_{f_{-\text{TVEDT}}} = 0.000477$, and $\beta = 3.304$.

Accurate calculation of P_f

In polar coordinates (method from Section 7.6.9):

$$P_f = \frac{1}{2\pi} \int_{\Gamma} e^{-\rho^2(\theta)/2} d\theta$$

where Γ is the contour of the failure domain. Returning to Cartesian coordinates:

$$\rho^2(\theta) = u_1^2(\theta) + u_2^2(\theta) \quad (= v_1^2(\theta) + v_2^2(\theta))$$

$$\tan \theta = \frac{u_2}{u_1} \quad \left(= \frac{v_2}{v_1} \right)$$

$$(1 + \tan^2 \theta) d\theta = \frac{u_1 du_2 - u_2 du_1}{u_1^2} = \frac{u_1^2 + u_2^2}{u_1^2} d\theta$$

$$d\theta = \frac{u_1 du_2 - u_2 du_1}{u_1^2 + u_2^2}$$

$$P_f = \frac{1}{2\pi} \int_{\Gamma} e^{-(u_1^2 + u_2^2)/2} \frac{u_1 du_2 - u_2 du_1}{u_1^2 + u_2^2}$$

The latter equation enables integration if the equation between u_1 and u_2 is known along Γ . Care must be taken to travel along the contour in the positive direction.

The application is run, for the example, for coordinates v_1, v_2 .

$$v_2 = v_1^2 + 3$$

$$P_f = -\frac{1}{2\pi} \int_{-\infty}^{\infty} e^{-(v_1^4 + 7v_1^2 + 9)/2} \frac{v_1^2 - 3}{v_1^4 + 7v_1^2 + 9} dv_1$$

where the sign ‘–’ occurs, so that the path from $-\infty$ to ∞ according to v_1 leads to θ turning in the negative direction.

This integral is calculated numerically in MATHCAD:

$$P_f = 0.000481 \quad \text{or} \quad \beta = 3.302$$

RGMR result: the application of RGMR gives $\beta = 3.301$ and $P_f = 0.000482$.

The convergence is illustrated in Figure 7.17. This represents the results obtained according to different values of the calculation path h (Section 7.6.7). We note that they converge according to the number of calls n to the limit-state function.

Statement

Table 7.10 summarizes the results and shows their good concordance, with the exception of FORM.

	FORM	Breitung	TVEDT	MATHCAD	RGMR
β	3.000	3.285	3.304	3.302	3.301
$10^4 P_f$	13.500	5.10	4.77	4.81	4.82

Table 7.10 Approximations of the probability of failure.

Integration using the trapezium method with 1,500 points gives the bounds:

$$0.0004796 \leq P_f \leq 0.0004806$$

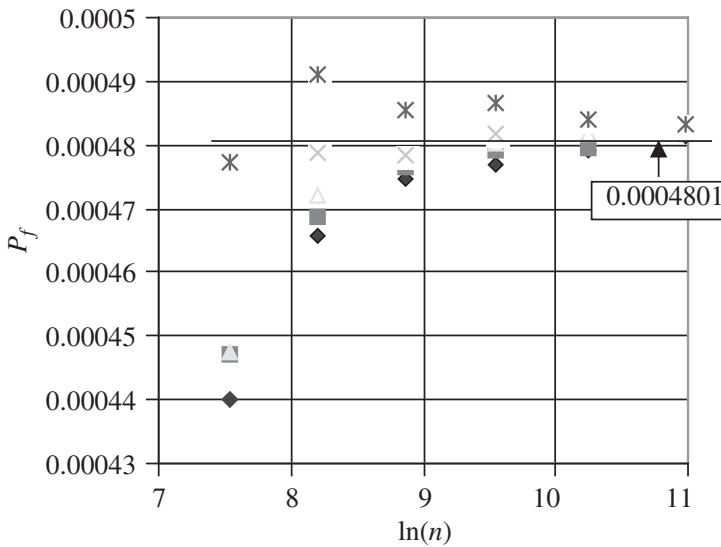


Figure 7.17 Convergence toward the probability of failure by RGMR for two variables.

Integration is limited to $\rho(\theta) < 5.8$, which leads to a truncation error lower than 0.5×10^{-7} .

Quite obviously, such calculation accuracy is only of methodological interest.

7.7.5 Example: double exponential

This classic example, seen in the literature [Dol83], is interesting for several reasons. It enables us to show first how two transformations can be constructed according to the order of the variables. Each leading to the existence of a second minimum, close in distance to the first, it then illustrates the importance of these secondary minima for the calculation of the probability of failure.

Statement of the problem

The example considers a performance function defined by:

$$G(X_1, X_2) = 18 - 3X_1 - 2X_2$$

where X_1 and X_2 are two correlated random variables whose joint distribution function is given by:

$$F_{X_1, X_2}(x_1, x_2) = 1 - \exp(-x_1) - \exp(-x_2) + \exp[-(x_1 + x_2 + x_1 x_2)]$$

with $x_1 > 0$ and $x_2 > 0$. The corresponding density function is therefore:

$$f_{X_1, X_2}(x_1, x_2) = (x_1 + x_2 + x_1 x_2) \exp[-(x_1 + x_2 + x_1 x_2)]$$

Two Rosenblatt transformations can be constructed depending on the choice of the order of variables x_1 and x_2 . The analytical calculation was dealt with in Section 4.3.4. This leads to:

- first Rosenblatt transformation:

$$u_1 = \Phi^{-1}[1 - \exp(-x_1)]$$

$$u_2 = \Phi^{-1}[1 - (1 + x_2) \exp(-(x_2 + x_1 x_2))]$$

- second Rosenblatt transformation:

$$u_1 = \Phi^{-1}[1 - \exp(-x_2)]$$

$$u_2 = \Phi^{-1}[1 - (1 + x_1) \exp(-(x_1 + x_1 x_2))]$$

The graphic representation is given in Figure 7.18. It creates a situation in which two minima, close in distance, are obtained (respectively $P_{(1)}^*$, $P_{(1)}^{(2)}$ and $P_{(2)}^*$, $P_{(2)}^{(1)}$), for each of the transformations. Moreover, the positions of the two minima are permuted, that is, the most probable point of failure is highly dependent on the choice of the order of the transformation. The calculation of the probability of failure should then be performed by taking into account the existence of these two minima.

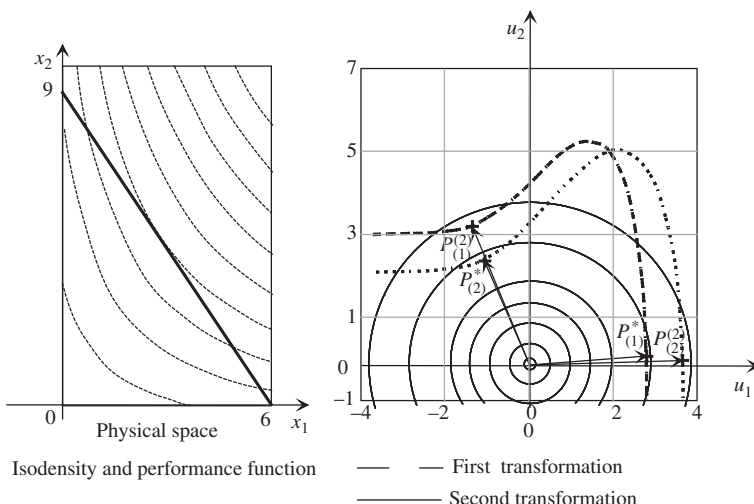


Figure 7.18 Representation of the limit-state.

First order results [MKL86]

In *standardized coordinates*: the calculation of the probability of failure by numerical integration gives $P_f = 2.940 \times 10^{-3}$, $\beta = 2.631$. t_1 and t_2 , respectively, are relative to the two transformations and the results are summarized in Table 7.11.

	β	$\Phi(-\beta)$	$\beta^{(2)}$	\mathbf{u}_1^*	\mathbf{u}_2^*	$\mathbf{u}_1^{(2)}$	$\mathbf{u}_2^{(2)}$
t_1	2.784	2.68×10^{-3}	3.501	2.783	0.087	-1.296	3.253
t_2	2.649	4.04×10^{-3}	3.633	-1.124	2.400	3.630	0.142

Table 7.11 MKL results.

In *physical coordinates*: it is simple to verify that the point of maximum joint probability density has coordinates $x_1^{*p} = 6$; $x_2^{*p} = 0$. A second minimum is obtained for $x_1^{(2)p} = 0$; $x_2^{(2)p} = 9$. These points are not the images of points P^* and $P^{(2)}$ coming from the two transformations as shown in Table 7.12, but are close to them.

	\mathbf{u}_1^*	\mathbf{u}_2^*	$\mathbf{u}_1^{(2)}$	$\mathbf{u}_2^{(2)}$	\mathbf{x}_1^*	\mathbf{x}_2^*	$\mathbf{x}_1^{(2)}$	$\mathbf{x}_2^{(2)}$
t_1	2.783	0.087	-1.296	3.253	5.917	0.128	0.103	8.848
t_2	-1.124	2.400	3.630	0.142	5.910	0.140	0.091	8.862

Table 7.12 Coordinates of points P^* in physical space.

It is interesting to note that the two transformations return to the same physical points, with the exception of a slight difference that it is possible to attribute to the accuracy of the calculation of the standardized coordinates of the extremes.

Calculation of P_f : a better approximation of P_f is obtained by combining the two hyperplanes defined at points P^* and $P^{(2)}$. We will find the presentation of the combination method in Chapter 9. The correlation is calculated by:

$$\rho = \frac{\mathbf{u}^{*^t} \mathbf{u}^{(2)}}{\|\mathbf{u}^*\| \|\mathbf{u}^{(2)}\|} = -0.337 \text{ (for } t_1) \text{ and } \rho = -0.388 \text{ (for } t_2)$$

and:

$$\text{for } t_1: P_f \approx 1 - \Phi_2(\beta, \beta^{(2)}; \rho) = 2.92 \times 10^{-3} \text{ and } \beta \approx 2.755$$

$$\text{for } t_2: P_f \approx 1 - \Phi_2(\beta, \beta^{(2)}; \rho) = 4.18 \times 10^{-3} \text{ and } \beta \approx 2.638$$

The combination of two linearized limit-states in the t_1 case is remarkably satisfactory, whereas the t_2 case leads to a less accurate solution. The reason for the less advantageous performance of t_2 can be found in the fact that the curvature is very much higher in $P_{(2)}^*$ than in $P_{(1)}^*$. This hypothesis is verified by introducing a SORM correction.

Second order results

SORM asymptotic method: the calculation is given here for the t_1 case. x_1 is chosen as a parameter and we express the limit-state by the function $x_2 = g(x_1) = 9 - 3x_1/2$. u_1 and u_2 are then functions of x_1 only. The curvature is given by:

$$\kappa = \frac{u'_1 u''_2 - u''_1 u'_2}{(u'^2_1 + u'^2_2)^{3/2}}$$

Let $F_1(v) = 1 - e^{-v}$ and $F_2(v) = 1 - (10 - 3v/2)e^{(1+v)(9-3v/2)}$. We have $u_1(v) = \Phi^{-1}(F_1(v))$ and $u_2(v) = \Phi^{-1}(F_2(v))$. By deriving the expression $\Phi \circ \Phi^{-1} = \text{Id}$, we obtain the second order derivatives of the inverse of Φ :

$$u'_1 = \sqrt{2\pi} e^{u_1^2/2} F'_1 \quad u''_1 = 2\pi u_1 e^{u_1^2} F'^2_1 + \sqrt{2\pi} e^{u_1^2/2} F''_1$$

and the corresponding quantities for u_2 , identical with the exception of the name of the indexes.

For the t_1 transformation, the greatest curvature is in $P_{(1)}^{(2)}$. Numerical calculation provides at this point $v = 0.1026$ and the values given in Table 7.13.

u_1	u_2	β	u'_1	u''_1	u'_2	u''_2	κ
-1.296	3.253	3.501	5.235	-40.74	2.089	-1.996	0.417

Table 7.13 Calculation of the curvatures in the example of the double exponential for point $P_{(1)}^{(2)}$.

The application of Breitung's formula leads to a corrector coefficient of $(1 + \beta \kappa)^{-1/2} = 0.637$. The absolute minimum, obtained with $v = 5.915$ and $\beta = 2.784$, has a weak curvature.

RGMR method: the use of the curvilinear integral method leads to $P_f = 2.940 \times 10^{-3}$ by integrating on 200 points. The curve is parametrized by x_1 in the case of the first Rosenblatt transformation and by x_2 in the other case. x_2 is then obtained by the limit-state equation $2x_2 = 18 - 3x_1$ and then u_1 and u_2 by the Rosenblatt transformation. The only difficulty is that this representation leads to very important variations in the argument of the quadrature points according to the position on the curve. It is therefore recommended to use a trapezium method with a variable step.

Of course, integration leads to the same value in the two cases of transformation, u_1 then u_2 , or u_2 then u_1 . The numerical results give the value 2.940×10^{-3} in both cases.

Comments

Table 7.14 summarizes the results.

	β	$\Phi(-\beta)$	κ	$P_{f,B}$	$P_{f,2\beta,\text{FORM}}$	$P_{f,2\beta,\text{SORM}}$
The probabilities are to be multiplied by 10^{-3}						
t_1	2.784	2.68	-0.025	2.78	2.92	2.93
t_2	2.649	4.04	0.400	2.81	4.18	2.96
	$\beta^{(2)}$	$\Phi(-\beta^{(2)})$	$\kappa^{(2)}$	$10^3 P_{f,B}^{(2)}$	$P_{f,\text{exact}} = 2.940 \times 10^{-3}$	
t_1	3.501	0.23	0.416	0.15	$P_{f,\text{exact}} = P_{f,\text{RGMR}}$	
t_2	3.633	0.14	-0.031	0.15		

Table 7.14 Results of the double exponential.

The result of column β is the smallest distance according to the definition of Hasofer-Lind. Column $\beta^{(2)}$ gives the distance from the second minimum. The following comments can be observed:

- the solution $P_f = 2.940 \times 10^{-3}$ is considered as the exact solution, obtained by numerical integration and RGMR,
- κ and $\kappa^{(2)}$ give respectively the curvatures relative to the first and then to the second minimum,
- the application of Breitung's formula $P_{f,B}$, by considering only a single β , slightly corrects the FORM result in the t_1 case but is significant for the t_2 case; to be noted is the opposite conclusion for points $P^{(2)}$,
- the FORM combination (column $P_{f,2\beta,\text{FORM}}$) is very favorable for the t_1 case but leads to a poor result for t_2 (in fact, in this case, the curvature is high for the dominant point),
- the SORM combination (column $P_{f,2\beta,\text{SORM}}$) shows the correction brought about by the effect of curvature, and the two transformations lead to entirely satisfactory results.

Ditlevsen and Madsen had already taken up this example. The table given in p. 131 of [DM96] confirms the results, with the exception of the second curvature for transformation t_1 which is given as being equal to 0.2973 (instead of 0.4163). The difference in the results in terms of probabilities is very weak. A discussion with the author confirms the result obtained here (0.4163).

7.8 Conclusions

The choice of reliability analysis tools depends strongly on the problem posed. There does not exist any universal method allowing us to cope with the multiplicity of situations of practical reality. Methodological decisions result therefore from the experience acquired in the profession.

We can, however, formulate a few recommendations.

The FORM approximation presents in practice a great advantage: it requires a generally low calculation effort to obtain a good approximation in most cases.

To go even further, we use SORM approximations, which as we have seen are multiple. They are based on a knowledge of the geometry of the failure domain around P^* , and the quality of the solution depends on that of the approximation: parabolic or quadratic. The difficulties of implementation of the SORM methods and their accuracy are being investigated continuously. The reader will be able to consult references [Mit95, Mit99, ZO99a, ZO99b] in particular. It is to be noted that SORM can sometimes give less accurate results than FORM; its use must therefore be controlled in a certain number of significant cases.

For this, we frequently propose the use of the simulation methods developed in Chapter 8. Besides their intrinsic interest, they can also be used to confirm – or not – a FORM or SORM result. The information obtained by FORM or SORM enables us to limit the number of simulations considerably.

Finally, RGMR enables a calculation of the probability in all cases, accompanied by an error calculation. In terms of cost, the method is of the same type as the directional simulations. It presents, on the other hand, with respect to the latter, the advantage of being able to be optimized for a given accuracy requirement. However, it should be noted that this last method requires a considerable effort to express the propagation of errors in the calculation process.

Chapter 8

Simulation Methods

8.1 Introduction

To *simulate* signifies to represent a phenomenon by an equivalent model; *numerical simulations* are representations by numerical models. *Monte Carlo simulations*¹ imply representation by random samples.

Generally, Monte Carlo simulations represent the most expensive methods, but these are certainly the safest for the evaluation of the probability of failure, subject to the quality of the pseudo-random number generator. [Rub81] gives an ample description. Simulations enable us to obtain reference results and to control other approximation methods. The result is simply an estimation of the probability of failure accompanied by an evaluation of variance estimate. It should be noted that simulations, unless in the case of a specific adaptation, provide only limited information regarding the failure point and the importance factors of the random variables.

The principle of simulation methods is to carry out a random sampling in the variable space, which could be physical or standardized. For each of the samples, the limit-state function is evaluated to conclude whether the configuration drawn is in the safety domain or the failure domain. A calculation of failures enables us to estimate the probability sought. Therefore, the steps of the procedure are as follows:

1. generate outcomes of random variables according to their joint probability density, or at least according to their marginal distributions and their correlations,
2. calculate the value of the limit-state function,

¹ The designation Monte Carlo simulations comes from a confidential project of the American army, during the Second World War, dealing with random problems; the code for the project was Monte Carlo, in reference to the games of chance played in its casinos. A Monte Carlo algorithm is a probabilistic approximation algorithm, in contrast to the Atlantic City and Las Vegas algorithms which give, although not always, exact solutions.

3. depending on the case:
 - if there is no failure, go to 1,
 - if there is a failure, increment the counter of the failing cases,
4. repeat 1 to 3 until a sufficient number of samples is obtained,
5. estimate the probability as a function of the number of failing cases with respect to the total number of tests carried out.

This chapter first presents a few concepts of pseudo-random number generators and then of the construction of samples according to a given distribution. This point is particularly important and the validation of the quality of the generator is essential, in particular for a multidimensional analysis.

Application of the direct Monte Carlo method is not economical and, moreover, is often impossible because its efficiency depends on the frequency of points in the failure domain. Appropriate conditioning, taking into account the information available from FORM or SORM approximations, leads to much more efficient conditional simulation methods, which are presented later and illustrated with examples.

8.2 Uniform pseudo-random numbers

Generation of pseudo-random numbers is at the root of all simulation methods. It is indispensable for the creation of random variable outcomes obeying a given distribution. As generation by any distribution passes initially through the generation of outcomes of variables in a uniform distribution on the interval $[0, 1[$, we present the latter first.

Generation algorithms are based on *deterministic* recursive functions. The set of numbers created is therefore repeatable if we inject the same starting conditions, the same seed. It is for this reason that we call them '*pseudo-random numbers*'.

While the process of generation is totally deterministic, it is possible to demonstrate that the generated numbers obey a uniform distribution and are relatively independent. This can be verified by testing hypotheses, as in the χ^2 test [Sap90, Col95].

8.2.1 Composite congruential generator

The most widely-used method for generating a series x_i is based on the calculation of the remainder of a division by an integer m ; the most common expression is written in the form:

$$x_{i+1} = (a x_i + c) \pmod{m} \quad i = 1, \dots, n \quad (8.1)$$

in which the multiplier a , the increment c and the denominator m are *non-negative integers*; mod is the operator of integer division: $A \text{ (mod } B)$ = the remainder from the integer division of A by B . The previous notation is equivalent to:

$$x_{i+1} = a x_i + c - m k_i \quad \text{with } k_i = \text{integer} \left(\frac{ax_i + c}{m} \right)$$

in which the operator $\text{integer}(\cdot)$ indicates the integer part of the division. Let us note that the number obtained, x_i , belongs to the interval $[0, m[$. In order to have a number u_i belonging to the interval $[0, 1[$, it is sufficient to divide by m :

$$u_i = \frac{x_i}{m}$$

It is clear that such a procedure is periodic. Each period is lower than or equal to m and contains a maximum of m distinct numbers. The procedure carries out a unlimited number of loops by passing over the same values within rounded off errors in each cycle.

In order to ensure a significant number of non-repeated values, it is necessary to choose the largest possible m . Let us take p to be the period (i.e. the dimension of the non-repeated sequence). We say that the generator possesses a *complete period* when $p = m$. This is realized if and only if:

- (1) c and m are prime numbers,
- (2) $a \equiv 1 \pmod{g}$ for any g , prime factor of m ,
- (3) $a \equiv 1 \pmod{4}$ if m is a multiple of 4.

The first condition implies that the highest common factor of c and m is one. The second condition implies that $a = g \text{ integer}(a/g) + 1$, with prime factor g of m . The third condition implies that $a = 4 \text{ integer}(a/4) + 1$ if $(m/4)$ is an integer.

Greenberger [Gre61] has shown that the correlation between X_i and X_{i+1} is bounded by:

$$\frac{1}{a} - \left(\frac{6c}{am} \right) \left(1 - \frac{c}{m} \right) \pm \frac{a}{m}$$

and that the upper bound is reached when $a = \sqrt{m}$, whatever the value of c .

Choice of algorithm parameters

From the data processing point of view, it has been demonstrated that the calculation of the remainder of division is fastest when the denominator is equal to the length of the word defined according to the calculator type. Two main types are largely used.

Binary calculator (base 2): for a binary calculator, the choice of $m = 2^\beta$ (where β is the word length) guarantees a complete period. Condition (1) implies that c is odd. Condition (3) implies $a \equiv 1 \pmod{4}$, which is satisfied if $a = 2^r + 1$ with $r \geq 2$.

From experience, if the compiler is capable of dealing with integers of this size, a good choice is obtained by:

$$m = 2^{35} \quad a = 1 + 2^7 \quad c = 1$$

Decimal calculator (base 10): in this case, efficiency is obtained with the choice $m = 10^\beta$ (where β is the word length). To have a complete period, it is necessary that c be neither divisible by $g = 2$ nor by $g = 5$, and with condition (3) that $a \equiv 1 \pmod{20}$ or $a = 10^r + 1$; $r > 1$.

Satisfactory results are obtained using:

$$a = 101 \quad r \geq 4 \quad c = 1$$

8.2.2 Multiplicative generator

This category is obtained by putting $c = 0$ in Equation (8.1) of the composite generator:

$$x_{i+1} = a x_i \pmod{m}$$

In this case, the complete period cannot be attained, but a maximum period is to be sought. This is achieved if x_0 is not a prime factor of m and if a respects certain conditions.

Binary calculator (base 2): we let $m = 2^\beta$ with a view to obtaining maximum calculation efficiency. The size of the period is lower than or equal to $m/4$. The period is maximum if $a = 8r \pm 3$, where r is any positive integer.

We choose x_0 as an odd number close to $2^{\beta/2}$. A good combination is given as follows ($\beta = 35$):

$$m = 2^{35} \quad a = 3 + 2^{17}$$

Decimal calculator (base 10): as in the previous case, we choose $m = 10^\beta$. The maximum period is obtained using $a = 200r \pm p$, where r is any positive integer and p is any number of the set $\{3, 11, 13, 19, 21, 27, 29, 37, 53, 59, 61, 67, 69, 77, 83, 91\}$.

We choose x_0 as an odd number not divisible by 5 which is close to $10^{\beta/2}$. A good combination is given as follows ($\beta = 10$):

$$m = 10^{10} \quad a = 10^5 \pm 3$$

8.2.3 Congruential additive generator

This generator takes the form:

$$x_{i+1} = x_i + x_{i-k} \pmod{m} \quad k = 1, 2, \dots, i-1$$

When $k = 1$, we obtain the Fibonacci sequence, which can also be obtained using the multiplicative generator with $a = (1 + \sqrt{5})/2$. The statistical properties of this generator are not satisfactory, but they improve as the value of k increases.

General comments on generators

- The initial number x_0 (the seed) can be chosen arbitrarily. We can take the last number of the previous call or otherwise a function of the current date and time.
- The number m must be large; the speed of the calculation of the remainder is optimal if m is equal to the word length. The calculation of the remainder must be performed exactly, without any rounding error.
- If m is a power of 2 (binary calculator), choose a such that $a \pmod{8} = 5$. If m is a power of 10 (decimal calculator), choose a such that $a \pmod{200} = 21$.
- The number a must be greater than \sqrt{m} (and preferably $a > m/100$) and less than $m - \sqrt{m}$ (take a number at random such that $a = 3141592621$).
- The constant c must be odd if m is a power of 2, and odd and indivisible by 5 if m is a power of 10.

The least significant digits of x_i are not really random, and it is therefore necessary to reason with respect to the most significant digits. This is why it is preferable to use the variable $u_i = x_i/m$.

If we want a uniform distribution defined on the interval $[0, k[$, it is sufficient to multiply u_i by k .

8.2.4 Some generators as examples

IBM System/360 generator

The IBM System/360 used a multiplicative generator. For this type of device, the word length is equal to 32 bits, whose first bit is reserved for the sign; the denominator m is therefore taken as equal to 2^{31} . The maximum size of the period is equal to $m/4 = 2^{29}$. The size of the period depends on the initial value, too. When m is a prime factor, the maximum size of the period is $m - 1$; the greatest prime factor lower than or equal to 2^{31} is given by $2^{31} - 1$. The value of the multiplier a is chosen as equal to 7^5 to satisfy statistical performances.

The generator is summarized by:

$$x_0 > 0 \quad x_{i+1} = 7^5 x_i (\text{mod } 2^{31} - 1) \quad u_i = \frac{x_i}{(2^{31} - 1)}$$

This generator, which has been very frequently used in several other systems developed by IBM, has proved to be of poor quality [PTVF92].

HP25 generator

This generator is defined as:

$$u_{i+1} = \text{fractional part of } (\pi + u_i)^5 \quad \text{with } u_0 \in [0, 1[$$

Let us note that this procedure directly gives numbers ranging between 0 and 1.

This equation, tested by the authors, has given satisfaction in numerous applications. It has proved to lead to poor quality results when it was at the root of the Weibull distribution simulation (with two parameters). The mean and the standard deviation of the samples generated for a resistance variable R and for a stress variable S appeared correct, whereas the simulation of the margin $R - S$ did not give a satisfactory result. Hence, there seems to exist an equation between the two samples, whereas different methods were tested: simulate r_i then s_i then $r_{i+1} \dots$ or otherwise all the r_i then all the s_i .

In such a simple problem, numerical integration is possible (performed using MATHCAD). It has enabled us to verify the correct operation of the generator on all the couples tested, except Weibull. This experiment is mentioned to alert the reader to the need for the greatest prudence in the use of generators.

NR generator

This generator is proposed by [PTVF92], whose authors primarily discuss the construction of random numbers.

The solution retained is version RAN2, Chapter 7, p. 272. Its implementation does not demonstrate the dysfunctioning observed with the HP generator and hence it remains a good solution, until proven otherwise!

The basic idea is to select a sequence of values randomly instead of selecting each value successively.

MT generator

Matsumoto and Nishimura have more recently proposed [MN98] a generator, *Mersenne Twister*, of period $2^{19937} - 1$. Its period is remarkably high and it is reputed to be very fast.

8.2.5 How to test a generator

The quality of a generator is defined by a good representation of uniform distribution, statistical independence, repeatability and speed of generation. A compromise is therefore sought with these requirements. For this, we can use the following methods:

- statistical χ^2 and Kolmogorov-Smirnov criteria to test the sample generated with respect to a uniform distribution hypothesis,
- succession test to verify the independence between the successive outcomes of a sample,
- tendency test to compare a set of values obtained with a previous or following set; it is thus possible to detect tendencies to rise or fall during successive generations,
- cavity test to look for the absence of generation of a value contained in a given interval,
- finally, it is always desirable to compare the unbiased estimates of the statistical moments (mean, variance, moments of order 3 and 4, etc.) of the samples generated with their theoretical values.

Generally, the validation of a generator implies the acceptance of a statistical hypothesis applied to a sample. References [Rub81, Gib71, Gor67, Knu81] will be consulted for this purpose.

Control of uniformity [Rad91]: let a series of n values be x_i belonging to an interval $[a, b]$. The interval is divided into k partitions whose respective populations are n_i . We then calculate the quantity:

$$\chi^2 = \sum_{i=1}^k \frac{(n_i - E[n_i])^2}{n/k}$$

in which $E[n_i]$ is the theoretical expectation of partition i . The value of χ^2 is compared with a maximum permitted value for a probability threshold.

8.2.6 Conclusion

If the generation of uniform random numbers on the interval $[0, 1[$ seems a simple question since we find RAN, RANDOM, RND or similar functions on any calculator, it is necessary to be prudent with regard to their use. Simple tests of comparison with analytical results and a statistical study of the obtained samples constitute indispensable precautions before any use in a reliability analysis.

8.3 Generators of non-uniform distributions [Rub81, Dea90]

In the following, U , of outcome u , indicates a random variable obeying a *uniform* distribution. To generate any distribution numbers, we have at our disposal three general methods and specific methods with certain distributions such as Gaussian distributions.

8.3.1 Inverse transformation method

It is easy to demonstrate that for U , a random variable uniformly distributed on the interval $[0, 1]$, the variable X , defined by:

$$X = F_X^{-1}(U)$$

possesses a distribution function $F_X(x)$. In fact, since F_X is strictly increasing:

$$\text{Prob}(X \leq x) = \text{Prob}[F_X^{-1}(U) \leq x] = \text{Prob}[U \leq F_X(x)] = F_X(x)$$

it is sufficient to give a number u_i and to deduce the corresponding variable x_i as $x_i = F_X^{-1}(u_i)$ (Figure 8.1).

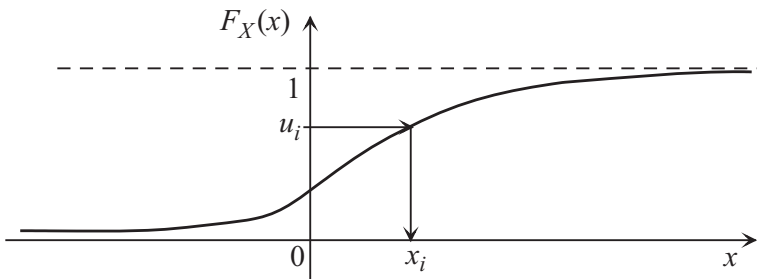


Figure 8.1 Construction of a random variable by inversion of probability distribution.

Even if the analytical form of $F_X^{-1}(x)$ exists explicitly, the inverse transformation method is not always the most efficient. The method becomes very slow when it is a matter of inverting $F_X(x)$ by an iterative procedure (as, for example, in the case of normal variables).

8.3.2 Composition method [But56]

In this method, the probability density to be generated is expressed by a combination of a certain number of judiciously chosen distributions. Let us

say $g_X(x | u)$ is a probability density, where u defines a unique function $g_X(x)$. If an outcome of U is drawn from a uniform distribution function $F_U(u)$ on $[a, b[$ and if X is drawn from $g_X(x)$ for a given value of u , the density of X is:

$$f_X(x) = \int g_X(x | u) dF_U(u)$$

This technique allows us to generate complex distributions from more simple distributions which can be generated by the inverse transformation method. Another advantage is that decomposition can be performed in a manner such that strong probabilities are associated with density functions that are easy to evaluate, and weak probabilities are associated with density functions whose evaluation is expensive.

Example: we consider density $f_X(x)$ on support $[0, b]$ with $0 \leq a \leq b$:

$$f_X(x) = \begin{cases} 0 & \text{if } (x < 0) \cup (x \geq b) \\ 2x/(ab) & \text{if } 0 \leq x < a \\ -2(x-b)/b/(b-a) & \text{if } a \leq x < b \end{cases}$$

It is partitioned into two segments of respective weights $c_1 = a/b$ and $c_2 = 1 - c_1$ to which the following functions are associated:

$$\begin{aligned} g_1(x) &= \frac{1}{c_1} \frac{2x}{ab} && \text{conditioned by } U \leq c_1 \\ g_2(x) &= -\frac{1}{c_2} \frac{2(x-b)}{b(b-a)} && \text{conditioned by } U > c_1 \end{aligned}$$

Different equivalent conditionings are possible.

8.3.3 Rejection-acceptance method [VN51]

This method is based on drawing a random number from an appropriate distribution and later testing this number with a view to determining whether it is rejected or accepted.

Let $f_X(x)$ be the density to be generated. We choose an auxiliary density $h(x)$ and a constant C such that $\forall x, f_X(x) \leq Ch(x)$. This procedure is then followed (Figure 8.2).

We generate two random variables: U from a uniform distribution $[0, 1[$ and V from $h(v)$; we then test the condition $u_i \leq g(v_i) = f_X(v_i)/Ch(v_i)$:

- if $u_i \leq g(v_i)$ we accept v_i as a number generated from $f_X(x)$,
- if $u_i > g(v_i)$ we reject the couple (u_i, v_i) and we start the sampling again.

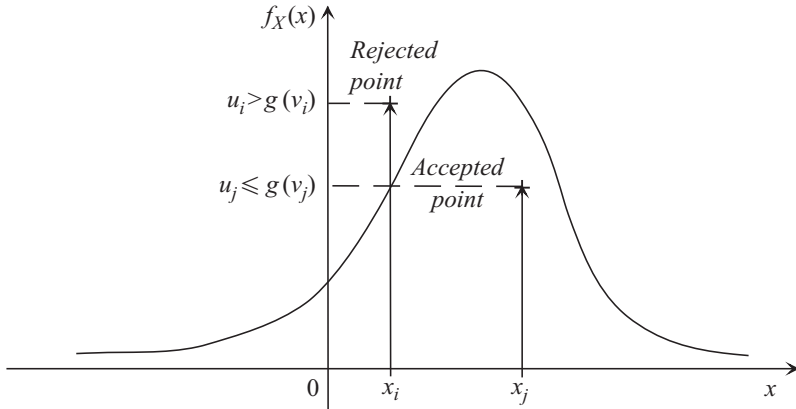


Figure 8.2 Construction of a random variable by the rejection-acceptance method.

Efficiency of the method: this is defined as the ratio between the number of accepted points and the number of sampled points, and is equal to $\int f_X(x) dx / C \int h(x) dx = 1/C$ because $f_X(x)$ and $h(x)$ are densities. It is not useful to calculate the exact value of C because an over-estimate is sufficient. Density $h(x)$ must be chosen in a manner to facilitate the sampling of V by the inverse transformation method.

Convergence of the method: let p be the probability of having an accepted sample. The probability of n successive rejected samples is $(1 - p)^n$ which tends toward 0 when $n \rightarrow \infty$. Convergence exists, but it can be slow.

Improvement: an improvement consists of introducing, when it is possible, a function $g(x)$, such that $f_X(x) = C h(x)g(x)$, to improve efficiency.

Example: to simulate a density $\mathcal{N}(0, 1)$, choose $h(x) = \exp(-x)$ and $C = \sqrt{e/2\pi}$ by utilizing symmetry to generate the negative outcomes. The function $g(x) = \exp(-(x - 1)^2/2)$ is then convenient.

8.3.4 Gaussian distribution

A Gaussian distribution can be advantageously constructed using specific methods, because the inverse transformation method is then very expensive due to the inversion which must be carried out by an iterative procedure. However, the use of an approximation of Φ^{-1} could be preferred if the distribution tails are significant, which is the case in reliability.

The density of a Gaussian distribution $\mathcal{N}(m, \sigma^2)$ is defined as:

$$f_Z(z) = \frac{1}{\sigma\sqrt{2\pi}} \exp\left[-\frac{(z-m)^2}{2\sigma^2}\right] \quad -\infty < z < \infty$$

Box and Müller [BM58] have shown that if two variables U_1 and U_2 are uniform, independent and defined on $[0, 1[$, variables:

$$X_1 = \sqrt{-2 \ln U_1} \sin(2\pi U_2)$$

$$X_2 = \sqrt{-2 \ln U_1} \cos(2\pi U_2)$$

are two reduced and independent, centered, normal variables.

Demonstration: let us write the previous expression in the form:

$$X_1 = \sqrt{2V} \sin(2\pi U) \quad X_2 = \sqrt{2V} \cos(2\pi U)$$

where $V = -\ln U_1$ and $U = U_2$. Thus, we have:

$$X_1^2 + X_2^2 = 2V \quad \text{and} \quad \frac{X_1}{X_2} = \tan(2\pi U)$$

The Jacobian of the transformation is:

$$|J| = \begin{vmatrix} \partial u / \partial x_1 & \partial u / \partial x_2 \\ \partial v / \partial x_1 & \partial v / \partial x_2 \end{vmatrix} = \begin{vmatrix} x_2 / (4\pi v) & -x_1 / (4\pi v) \\ x_1 & x_2 \end{vmatrix} = \frac{1}{4\pi v} (x_1^2 + x_2^2) = \frac{1}{2\pi}$$

Remembering that exponential density is the transformation of uniform density by the equation $V = -\ln U_1$, it becomes:

$$f_{X_1, X_2}(x_1, x_2) = f_{U,V}(u, v) |J| = \frac{1}{2\pi} \exp\left(-\frac{x_1^2 + x_2^2}{2}\right)$$

which represents the joint density function of two independent variables.

To obtain a normal non-standardized variable Z , it is sufficient to introduce:

$$Z = m_Z + \sigma_Z X \quad \text{with } X \text{ of distribution } \mathcal{N}(0, 1)$$

Inverse Φ^{-1} : Φ^{-1} can be estimated with the following approximation:

$$c_0 = 2.515517 \quad c_1 = 0.802853 \quad c_2 = 0.010328$$

$$d_1 = 1.432788 \quad d_2 = 0.189269 \quad d_3 = 0.001308$$

$$\Phi^{-1}(x) = -\sqrt{-\ln(x^2)} + \frac{c_0 + c_1 \sqrt{-\ln(x^2)} - c_2 \ln(x^2)}{1 + d_1 \sqrt{-\ln(x^2)} - d_2 \ln(x^2) + d_3 (\sqrt{-\ln(x^2)})^3}$$

which is valid only if $0 < x \leq 0.5$; otherwise take $-\Phi^{-1}(1-x)$. Error is less than 10^{-5} .

8.3.5 Lognormal distribution

The density function takes the form:

$$f_X(x) = \frac{1}{x \xi_X \sqrt{2\pi}} \exp \left[-\frac{(\ln x - \lambda_X)^2}{2\xi_X^2} \right] \quad \text{for } x > 0$$

To generate variables X having a lognormal distribution of parameters $\lambda_X = m_{\ln X}$, $\xi_X = \sigma_{\ln X}$, it is sufficient to generate a normal distribution $\mathcal{N}(\lambda_X, \xi_X^2)$ of a variable Y and then to carry out:

$$X = e^Y$$

It is necessary to note that for large values of y_i the capacity of the computer can easily be exceeded during the calculation of $x_i = e^{y_i}$.

8.3.6 Weibull distribution with two parameters

This is expressed as a function of the parameters:

- α : scale factor, $\alpha > 0$,
- β : form factor, $\beta > 0$,
- γ : position factor, taken here as equal to 0.

The density function is given by:

$$f_X(x) = \frac{\beta}{\alpha} \left(\frac{x}{\alpha} \right)^{\beta-1} \exp \left(- \left(\frac{x}{\alpha} \right)^\beta \right) \quad x \geq 0$$

and the distribution function by:

$$F_X(x) = 1 - \exp \left(- \left(\frac{x}{\alpha} \right)^\beta \right) \quad x \geq 0$$

The direct transformation is:

$$u = F_X(x) = 1 - e^{-(x/\alpha)^\beta}$$

and hence the inverse transformation is expressed as:

$$x = F_X^{-1}(u) = \alpha[-\ln u]^{1/\beta}$$

because if U is uniform on $[0, 1]$ then $(1 - U)$ is, too.

8.3.7 Generation of a random vector

Normal distribution without correlation

The simplest method, and the most used by far, of generating a series of n -dimensional random vectors consists of taking successive samples of size n in

a succession of samples t_1, t_2, \dots . In practice, designating by \mathbf{t} the vector of components (t_1, t_2, \dots, t_n) , we have the correspondence:

$$\begin{aligned}\mathbf{t}_1 &= (t_1, t_2, \dots, t_n) \\ \mathbf{t}_2 &= (t_{n+1}, t_{n+2}, \dots, t_{2n}) \\ &\vdots \quad \vdots \quad \vdots \\ \mathbf{t}_i &= (t_{(i-1)n+1}, t_{(i-1)n+2}, \dots, t_{in}) \\ &\vdots \quad \vdots \quad \vdots\end{aligned}$$

Such a method necessarily supposes that:

1. all the components follow the same probability distribution,
2. there is independence between the components.

It is essentially used with distributions which are uniform on the segment $[0, 1]$. We end up thus in a uniform filling of the paving block $[0, 1]^n$ of dimension n .

The use of the transformation from Section 8.3.4, or the inverse function Φ^{-1} of the one-dimensional normal distribution, enables us to construct, from these outcomes, a sample of the standardized distribution in n -dimensional space.

Non-normal and correlated distributions

In practice, we start from the standardized distribution constructed above; the simplest method is then to use an isoprobabilistic transformation. If $[\rho]$ is the correlation matrix and $\{U\}$ a vector of independent Gaussian variables, the vector of correlated variables $\{\hat{U}\}$ is given by the equation (see Section 4.10, Chapter 4):

$$\{\hat{U}\} = [L]\{U\} \quad \text{with } [\rho] = [L][L]^t$$

The only delicate case occurs when the inversion of the isoprobabilistic transformation is computer time-consuming. This is the case, for example, when it is necessary to systematically look for a root using a Gaussian method. This fortunately occurs rather rarely and can be solved by the use of techniques based on an incomplete implementation of the joint probability of the vector (Nataf transformation).

There is also the possibility of using several generators started simultaneously. The method should then be adapted case-by-case, according to the joint probability distribution of the vector being simulated.

Vectorial properties of generators

Although it is relatively easy to obtain series of satisfactory random numbers, the passage to a dimension greater than 1 poses serious problems of generator quality.

There are very few references presenting these questions, still a subject of research. This section is based on two works. The first is a rather old, but still valid, report, presenting the question from a practical point of view [DC75]. The second is a colloquium report presenting more theoretical aspects [Nie94].

The new phenomenon which appears in the domain of vectorial random generation is that of striation: in certain cases and for certain values of the dimension, the points are distributed preferentially on linear sub-spaces of dimension $p < n$ of n -dimensional space. We understand that, in the case where the limit-state surface is positioned in an unfortunate manner with respect to a sub-space, the calculated probability of failure could be strongly affected.

Only numerical experiments, which can be voluminous, allow us to qualify the good generators. We know for example that all the points of the congruential additive generator (Fibonacci series) $x_{i+1} = x_i + x_{i-1}$ in three-dimensional space are distributed in two planes at most. This is an extreme case. The calculation of a probability by simulation is, in such a case, very hazardous. This phenomenon is, moreover, easily verified graphically in two dimensions.

We have shown that the IBM RANDU routine generator was also strongly striated.

The following procedure constructs a generator which has passed different tests with success. It combines two generators:

- Let two integers i_1 and i_2 be generated randomly. We apply a procedure called EXOR: i_1 and i_2 , being written in binary notation, are compared bit by bit. The resulting number, $i_3 = i_1 \hat{+} i_2$, has 1 in this position if the bits of the initial numbers are different, and 0 otherwise. This is an exclusive OR bit-by-bit logical operation.
- The generator recommended by [DC75] following H. Marqvardsen in 1973 is an EXOR generator in which the first number is provided by a congruential generator $i_1(n+1) = (2^7 + 1)i_1(n) + 907\,633\,385 \bmod 2^{32}$. The second is a Fibonacci series $i_2(n+1) = i_2(n) + i_2(n-1) \bmod 2^{32} - 99$. It is necessary to specify the choice of starting values.

Directional generator

In 1980, an article by Deák [Dea80] provided a new idea in the search for random vectorial generation.

The principle is to use the random series to construct a transformation of n -dimensional space. These ideas are the basis of directional simulation [DHOH88].

Generation of a uniform vector on a unit sphere

To generate vectors of uniform distribution on a sphere surface of unit radius in n dimensions, we can simulate a unitary vector in a hypercube $-1 \leq x_i \leq +1$

with $i = 1, 2, \dots, n$, and then we reject the sample if the points (x_1, x_2, \dots, x_n) are outside the sphere. The algorithm takes the following form:

1. generate u_1, \dots, u_n uniform independent variables $[0, 1[$,
2. center the variables $y_i = 1 - 2u_i$; the radius is hence $R^2 = \sum_{i=1}^n y_i^2$,
3. if $R^2 < 1$, accept the point and keep the result $x_i = y_i/R$,
4. go to 1.

8.3.8 Conclusion

The tools of pseudo-random number generation are not lacking, which tends to prove that there is no unanimously accepted solution. Any user should take the trouble to carefully validate the procedure he uses through tests and calculate estimates of known samples. Every use must be finely analyzed and all the data concerning the generator used, particularly the initial values, should be mentioned in a calculation report using the Monte Carlo method.

8.4 Simulation methods

This section shows the application of the Monte Carlo simulation, independently of results obtained by FORM/SORM reliability analyses.

8.4.1 Introduction

Calculation of an integral

Monte Carlo simulations constitute an integration method which, with respect to numerical integration, represents an ‘economical’ means of choosing only some points by chance in the integration domain instead of systematically scanning in all directions. The value of the integration is thus deduced from the mathematical expectations of the sampling.

Let us consider the integral of a function $g(x)$ on the domain $[a, b]$:

$$I = \int_a^b g(x) dx$$

This integral is represented by the surface under curve $g(x)$ in Figure 8.3.

Let us suppose that we have at our disposal a framework of $g(x)$ in the integration domain: $0 \leq g(x) < c$ for $a \leq x < b$. Two independent uniform variables (X, Y) are generated with $x \in [a, b[$ and $y \in [0, c[$, and their joint distribution is:

$$f_{X,Y}(x, y) = \begin{cases} 1/(c(b-a)) & \text{if } X, Y \in [a, b[, [0, c[} \\ 0 & \text{if } X, Y \notin [a, b[, [0, c[} \end{cases}$$

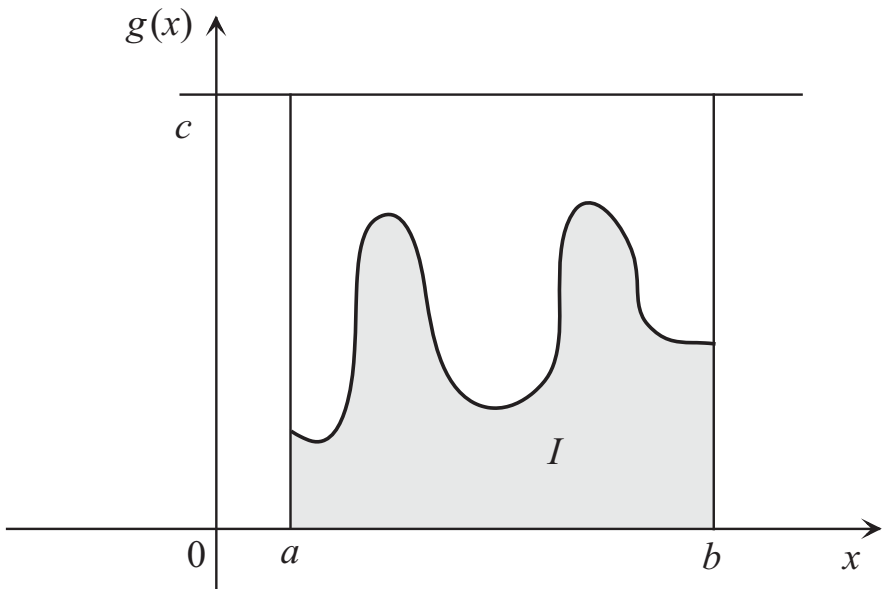


Figure 8.3 Calculation of an integral by simulation.

The ratio of the surface under $g(x)$ with respect to the domain is therefore:

$$p = \frac{\int_a^b g(x) dx}{(c - 0)(b - a)} = \frac{I}{c(b - a)}$$

After having carried out N random samples of the couple (X, Y) , the above ratio can be estimated as:

$$\tilde{p} = \frac{N_{y \leq g(x)}}{N}$$

where $N_{y \leq g}$ is the number of samples for which $g(x_i) \leq y_i$. The estimation of this integral is therefore:

$$I \simeq c(b - a) \frac{N_{y \leq g}}{N}$$

and the expectation of the integral is:

$$\mathbb{E}[I] = \int_{y \leq g(x)} f_{X,Y}(x, y) dx dy$$

Let us note that in this procedure the useful samples are only those for which $y \leq g(x)$. The other samples involve a cost to evaluate $g(x)$ without contributing to the calculation of $E[I]$. The efficiency of the method therefore depends on the ratio $N_{y \leq g}/N$.

Implementation in reliability problems

In practice, a failure counter is activated if the outcome of the limit-state belongs to the failure domain. An estimation of the probability (frequency) is therefore given as a function of the failures observed. Some variance reduction techniques enable us to choose sampling which improves the efficiency of the method.

Many methods are available in the literature; we have chosen to present eight of them which seem to us the most widely used in the calculation of reliability. These simulation methods can be classified according to the information used to choose sampling: without previous information (this section) or with the FORM/SORM results (the following section). The simplest to implement, for limit-states of general form, is the crude Monte Carlo method. However, it represents an enormous cost for real problems: to estimate a probability of the order of 10^{-n} , it is necessary to perform about 10^{n+2} to 10^{n+3} samples, as Equation (8.6) will show; that is to say, a great many calculations of the mechanical model, which can be very complex.

8.4.2 Crude Monte Carlo simulations

The Monte Carlo method, in its classic form, is simple to apply in principle. It avoids preparation and, from this point of view, it leads to an economy of thought. However, it involves many calculations, without providing the certainty of being able to reach a conclusion.

Principle of the method [AT84]

The sampling is carried out in the whole space, following a multinormal distribution (Figure 8.4). The integral to be evaluated is:

$$P_f = \int_{\mathcal{D}_f} \phi_n(u_k) du_1 du_2 \cdots du_n \quad (8.2)$$

where P_f is the probability of failure, $\phi_n(u_k)$ is a the n -dimensional multinormal density function and \mathcal{D}_f is the failure domain defined by $H(u_k) \leq 0$ (or $G(x_k) \leq 0$). By introducing the failure counter $\mathbf{I}_{\mathcal{D}_f}$ defined by:

$$\mathbf{I}_{\mathcal{D}_f} = \begin{cases} 1 & \text{if } H(u_k) \leq 0 \\ 0 & \text{if } H(u_k) > 0 \end{cases}$$

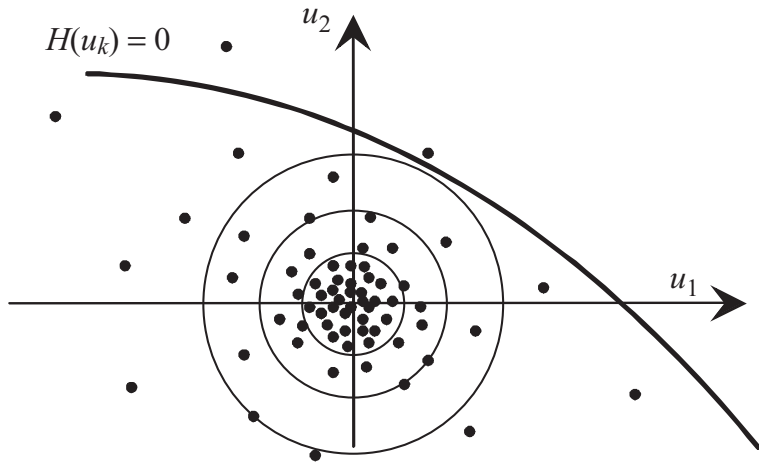


Figure 8.4 Monte Carlo simulations.

integral (8.2) can be written in the form:

$$P_f = \int_{R^n} \mathbf{I}_{\mathcal{D}_f} \phi_n(u_k) du_1 du_2 \cdots du_n = E[\mathbf{I}_{\mathcal{D}_f}]$$

where $E[\cdot]$ is the mathematical expectation.

Statistical estimates

For N random samples, the empirical average of $\mathbf{I}_{\mathcal{D}_f}$ is a non-biased estimation of P_f :

$$P_f = E[\mathbf{I}_{\mathcal{D}_f}] \approx \tilde{P}_f = \frac{1}{N} \sum_{r=1}^N \mathbf{I}_{\mathcal{D}_f}^{(r)} \quad (8.3)$$

whose variance is obtained by the following calculation:

$$\text{var}[\tilde{P}_f] = \text{var} \left[\frac{1}{N} \sum_{r=1}^N \mathbf{I}_{\mathcal{D}_f}^{(r)} \right] = \frac{1}{N^2} \text{var} \left[\sum_{r=1}^N \mathbf{I}_{\mathcal{D}_f}^{(r)} \right] = \frac{1}{N^2} \sum_{r=1}^N \text{var} \left[\mathbf{I}_{\mathcal{D}_f}^{(r)} \right]$$

because the random variables $\mathbf{I}_{\mathcal{D}_f}^{(r)}$ come from independent outcomes of the limit-state variables:

$$\text{var} \left[\tilde{P}_f \right] = \frac{1}{N^2} N \text{var} \left[\mathbf{I}_{\mathcal{D}_f}^{(r)} \right] = \frac{1}{N} \left(E \left[\mathbf{I}_{\mathcal{D}_f}^{(r)} \right]^2 \right) - E \left[\mathbf{I}_{\mathcal{D}_f}^{(r)} \right]^2 \quad (8.4)$$

because the variables are identically distributed.

However, we can show that this estimate is biased and that the non-biased estimate is obtained multiplying by $1/(N-1)$. An approximation of the variance estimate is then obtained by introducing (8.3):

$$\widetilde{\text{var}}[\tilde{P}_f] \approx \frac{1}{N-1} \left(\frac{1}{N} \sum_{r=1}^N \mathbf{I}_{\mathcal{D}_f}^{(r)} - \left(\frac{1}{N} \sum_{r=1}^N \mathbf{I}_{\mathcal{D}_f}^{(r)} \right)^2 \right) \quad (8.5)$$

Estimate distribution

By noting that $E[\mathbf{I}_{\mathcal{D}_f}] = P_f$ and $E[\mathbf{I}_{\mathcal{D}_f}^2] = E[\mathbf{I}_{\mathcal{D}_f}]$ because $\mathbf{I}_{\mathcal{D}_f}^2 = \mathbf{I}_{\mathcal{D}_f}$, Equation (8.4) becomes:

$$\text{var}[\tilde{P}_f] = \frac{1}{N} P_f (1 - P_f) \approx \frac{1}{N} \tilde{P}_f (1 - \tilde{P}_f)$$

which can be found again in another way. A numerical experiment consists of sampling the variable $\mathbf{I}_{\mathcal{D}_f}$. Let us note $p = \text{Prob}(\mathbf{I}_{\mathcal{D}_f} = 1) = P_f, q = \text{Prob}(\mathbf{I}_{\mathcal{D}_f} = 0) = (1 - P_f)$ and $K = \sum_{r=1}^N \mathbf{I}_{\mathcal{D}_f}^{(r)}$. The random variable K has a binomial distribution:

$$\text{Prob}(k) = \frac{N!}{k!(N-k)!} p^k q^{N-k}$$

whose average is $E[K] = Np$ and variance $[K] = Npq = Np(1-p)$, whence:

$$\text{var}[\tilde{P}_f] = \frac{1}{N^2} \text{var}[K] = \frac{1}{N} P_f (1 - P_f)$$

which is the expression sought. The distribution to be associated with the probability estimate is therefore binomial, whose limit, when $N \rightarrow \infty$, is a Gaussian distribution.

The coefficient of variation of the estimate is then written as:

$$\text{cov} = \sqrt{\frac{1-P_f}{NP_f}} \approx \sqrt{\frac{1}{NP_f}} \Big|_{P_f \rightarrow 0} \quad (8.6)$$

For an objective $\text{cov} = 0.1$ and a probability $P_f = 10^{-n}$, we obtain $N = 10^{n+2}$.

Confidence interval

This is obtained in the context of an estimation of the average with unknown variance, for a symmetric bilateral confidence interval at threshold α :

$$\tilde{P}_f - t_{1-\frac{\alpha}{2}}(\nu) \sqrt{\text{var}[\tilde{P}_f]} \leq P_f \leq \tilde{P}_f + t_{1-\frac{\alpha}{2}}(\nu) \sqrt{\text{var}[\tilde{P}_f]}$$

where $t_{1-\alpha/2}(\nu)$ is Student's variable of parameter $\nu = N - 1$. For a large N , it is replaced by the quartile of the normal distribution (difference of 0.12% for $N = 1,000$).

For an interval with 95% $t_{0.975} \approx u_{0.975} = 1.96$, whence:

$$\tilde{P}_f \left(1 - 1.96 \sqrt{\frac{1 - \tilde{P}_f}{N P_f}} \right) \leq P_f \leq \tilde{P}_f \left(1 + 1.96 \sqrt{\frac{1 - \tilde{P}_f}{N P_f}} \right)$$

which leads to Shooman's equation [Sho68] by admitting $1.96 \approx 2$:

$$\% S = 200 \sqrt{\frac{1 - \tilde{P}_f}{N \tilde{P}_f}} \quad (8.7)$$

\tilde{P}_f is the estimate of P_f and N is the number of simulations. This percentage corresponds to a probability of 95% that the exact value of P_f belonged to the interval \tilde{P}_f ($1 \pm \% S$); this is the 95% confidence interval.

Reliability index estimate

The reliability index associated with the estimate \tilde{P}_f is given by the usual equation:

$$\tilde{\beta} = -\Phi^{-1}(\tilde{P}_f)$$

This is a random variable whose moments can be known based on P_f following a Gaussian distribution $\mathcal{N}(\tilde{P}_f, \text{var}[\tilde{P}_f])$. In fact, remembering that if:

$$y = y(x) \quad E[Y(X)] = \int_{-\infty}^{+\infty} y(x) f_X(x) dx$$

then:

$$\begin{aligned} E[\tilde{\beta}] &= \int_0^1 -\Phi^{-1}(t) \frac{1}{\sqrt{\text{var}[\tilde{P}_f]}} \phi \left(\frac{t - \tilde{P}_f}{\sqrt{\text{var}[\tilde{P}_f]}} \right) dt \\ \text{var}[\tilde{\beta}] &= \int_0^1 \left(-\Phi^{-1}(t) - E[\tilde{\beta}] \right)^2 \frac{1}{\sqrt{\text{var}[\tilde{P}_f]}} \phi \left(\frac{t - \tilde{P}_f}{\sqrt{\text{var}[\tilde{P}_f]}} \right) dt \end{aligned}$$

Conclusion

Generally, to evaluate a probability of order 10^{-n} correctly, it is necessary to carry out between 10^{n+2} and 10^{n+3} simulations. It is evident that this

method is impossible to use for large systems with a weak probability of failure and with a high calculation cost for each outcome. A solution for this will be to look to maximize the number of failing outcomes through appropriate conditioning, knowing the weight of successful outcomes that the conditioning avoids calculating. An illustration is given in Section 8.6.1.

Variance reduction

A judicious choice of the correlation between variables enables us to improve the performance of Monte Carlo methods [AT84]. If two random variables Y and Z are correlated, the expectation of their half-sum $X = (Y + Z)/2$ is given by $E[X] = (E[Y] + E[Z])/2$ and their variance by:

$$\text{var}[X] = \frac{1}{4}(\text{var}[Y] + \text{var}[Z] + 2\text{cov}[Y, Z])$$

which can lead to better efficiency when the covariance is chosen as negative.

The implementation of this technique consists of sampling the estimates of P_f with negative correlation. To generate two estimates $\tilde{P}_f^{(1)}$ and $\tilde{P}_f^{(2)}$ correlated negatively, [HM56, HH64] have proposed to draw a sample $u_i, i = 1, 2, \dots, N$ to calculate $\tilde{P}_f^{(1)}$ and then to use variables $1 - u_i, i = 1, 2, \dots, N$ to evaluate $\tilde{P}_f^{(2)}$. The efficiency of this technique depends on the problem dealt with.

8.4.3 Directional simulations (DS) [Dea80, DBOH88, DMG90, Bje88]

Directional simulations are more economical than Monte Carlo simulations, while not requiring additional information. In standardized space, the multinormal probability density presents a rotational symmetry. It can be advantageous to carry out the sampling in a radial manner, particularly when the limit-state comes close to a hypersphere.

The procedure proposed by Ditlevsen and Bjerager is as follows (Figure 8.5):

- We generate radial directions $\delta_k^{(r)}$ uniformly distributed on the unit hypersphere centered at the origin, r being the sample number. The standardized Gaussian vector is defined by $U_k = R \Delta_k$, where R is the length of the vector.
- For every random direction, we determine the intersection with the limit-state by a linear search method. Second degree polynomial approximations can be used: see Section 5.6.
- If there is only one intersection for which the radius is written $\rho^{(r)}$, it becomes $R = \rho^{(r)}$ and $H(\rho^{(r)} \delta_k^{(r)}) = 0$ and the probability of failure can

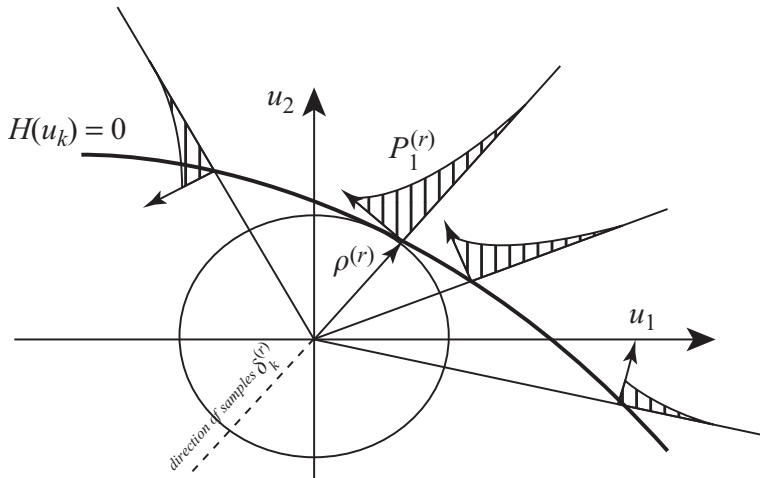


Figure 8.5 Directional sampling on a unit sphere.

be written in the form:

$$\begin{aligned} P_f &= \int_{\delta_k} \text{Prob}[H(R\Delta_k) \leq 0 \mid \Delta_k = \delta_k] f_{\Delta_k}(\delta_k) d\delta_1 \cdots d\delta_n \\ &= \int_{\delta_k} P_1 f_{\Delta_k}(\delta_k) d\delta_1 \cdots d\delta_n \end{aligned}$$

where $f_{\Delta_k}(\delta_k)$ is a density function of Δ_k (constant density on the unit sphere). For a given direction $\Delta_k = \delta_k^{(r)}$, the failure domain is defined as $R \geq \rho^{(r)}$. Probability P_1 is therefore:

$$\begin{aligned} P_1^{(r)} &= \text{Prob} [H(R \Delta_k) \leq 0 \mid \Delta_k = \delta_k^{(r)}] \\ &= \text{Prob} [R \geq \rho^{(r)}] = 1 - \chi_n^2 \left((\rho^{(r)})^2 \right) \end{aligned}$$

and the estimate of P_f is:

$$\tilde{P}_f = \frac{1}{N} \sum_{r=1}^N P_1^{(r)} = \frac{1}{N} \sum_{r=1}^N \left(1 - \chi_n^2 \left((\rho^{(r)})^2 \right) \right)$$

- If there are several intersections, the radius must be split into segments belonging to the failure domain.

This method enables the most probable failure point to be determined. An illustration is given Section 8.6.2.

8.5 Sampling methods using P^*

Methods based on knowledge of the design point P^* are definitely more effective and give a good control of the FORM or SORM approximation, but they do not allow us to detect the presence of possible local minima – or even the global minimum if the search algorithm does not converge toward the global optimum – located far from the considered point. This can be dangerous because the estimation has no meaning if the point used for the sampling is not the global minimum.

8.5.1 Importance sampling (IS) [Mel90]

As the weight of the failure probability is generally located in the vicinity of the design point P^* , it is more efficient to concentrate the sampling around this point (Figure 8.6). The center of the sampling is calculated using one of the methods cited in Chapter 5. The integral to be evaluated is given in the form:

$$P_f = \int_{R^n} \mathbf{I}_{\mathcal{D}_f} \frac{\phi_n(u_k)}{\psi(u_k)} \psi(u_k) du_1 du_2 \cdots du_n$$

where $\psi(u_k)$ is a new density function of the sampling, which must be chosen judiciously. We must suppose that function ψ does not cancel out on domain \mathcal{D}_f , thus avoiding the problems resulting from a possible singularity. A first

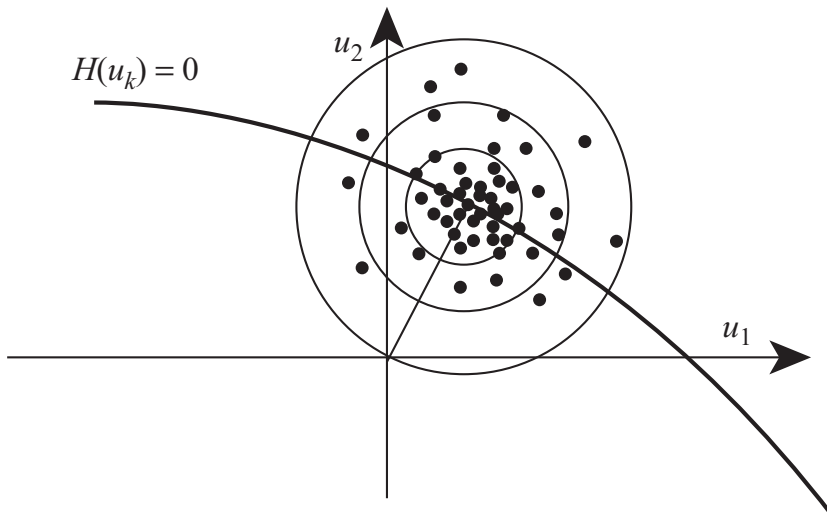


Figure 8.6 Samples concentrated around the most probable failure point.

solution is to choose for this function a reduced normal density centered at the design point u_k^* :

$$\psi(u_k) = \frac{1}{(2\pi)^{n/2}} \exp\left(-\frac{(u_i - u_k^*)^2}{2}\right)$$

To simulate the random variables according to this density, it is sufficient to generate reduced normal variables centered at $u_k^{(r)}$ and to carry out the change of variables $\tilde{u}_k^{(r)} = u_k^{(r)} s + u_k^*$ (r being the number of the sample). Failure probability is estimated as:

$$\tilde{P}_f = \frac{1}{N} \sum_{r=1}^N \mathbf{I}_{\mathcal{D}_f}^{(r)} \frac{\phi_n(\tilde{u}_k^{(r)})}{\psi(\tilde{u}_k^{(r)})} = \frac{1}{N} \sum_{r=1}^N \left(\mathbf{I}_{\mathcal{D}_f}^{(r)} \exp\left(-\sum_i u_i^* u_i^{(r)} - \frac{\beta^2}{2}\right) \right)$$

β being the Hasofer-Lind index, given by $\sqrt{\sum_i u_i^{*2}}$. A non-Gaussian distribution can be chosen as long as the support of ψ contains that of ϕ_n ($-\infty, +\infty$), so that the estimate is without bias.

Demonstration

$$\begin{aligned} \frac{\phi_n(\tilde{u}_k)}{\psi(\tilde{u}_k)} &= \frac{(2\pi)^{-n/2} \exp\left(-\frac{1}{2}(u_i + u_i^*)^2\right)}{(2\pi)^{-n/2} \exp\left(-\frac{1}{2}(\tilde{u}_i - u_i^*)^2\right)} = \frac{\exp\left(-\frac{1}{2}(u_i + u_i^*)^2\right)}{\exp\left(-\frac{1}{2}u_i^2\right)} (\Sigma_i)! \\ &= \exp\left(-u_i u_i^* - \frac{1}{2}u_i^{*2}\right) = \exp\left(-u_i u_i^* - \frac{\beta^2}{2}\right) \end{aligned}$$

where $(\Sigma_i)!$ represents the index summation i . A variance estimate of P_f is given by the usual definition:

$$\widetilde{\text{var}}(\tilde{P}_f) \approx \frac{1}{N-1} \left(\frac{1}{N} \sum_{r=1}^N \left(\mathbf{I}_{\mathcal{D}_f}^{(r)} \left(\frac{\phi_n(\tilde{u}_k^{(r)})}{\psi(\tilde{u}_k^{(r)})} \right)^2 \right) - \tilde{P}_f^2 \right)$$

Importance sampling gives satisfactory results if point P^* has been well identified and if there are no secondary minima at neighboring distances. It is possible to spread out or tighten the conditioning by introducing a standard deviation different from that of function $\psi(u_k)$. An illustration is given in Section 8.6.3.

8.5.2 Conditional sampling (CS) [BF87]

The objective of this approach is to eliminate a maximum number of samples which have no chance of belonging to the failure domain. As the design point is

the nearest point to the origin belonging to the failure domain, we can exclude domain S_n^β defined by the hypersphere centered at the origin and having a radius equal to the reliability index β (Figure 8.7).

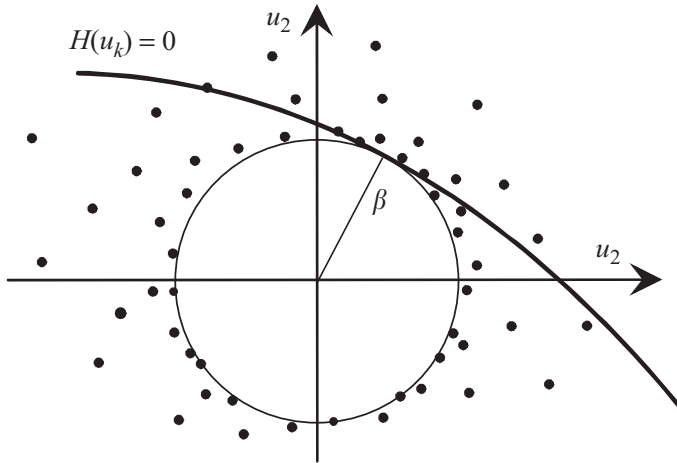


Figure 8.7 Samples outside the sphere of radius β .

The probability of failure is then:

$$P_f = \text{Prob}[u_k \in \mathcal{D}_f \mid u_k \notin S_n^\beta] \text{ Prob}[u_k \notin S_n^\beta] = P_1 P_2$$

Probability P_2 , corresponding to the probability of not having samples inside the hypersphere, is given by:

$$P_2 = \text{Prob}[u_k \notin S_n^\beta] = \text{Prob}[\|u\| > \beta] = 1 - \chi_n^2(\beta^2)$$

where χ_n^2 is the χ^2 distribution with n degrees of freedom. The first term P_1 , which is generally the greatest, is obtained by conditional sampling by generating a random direction Δ_i (outcome δ_i) uniformly distributed on the hypersphere in \mathbb{R}^n and a random radius R (outcome ρ) distributed according to the conditional Rayleigh distribution by $R > \beta$ (let us remember that the combination of a uniform direction and a Rayleigh radius gives a normal standardized distribution). The variables used in the simulations are given by $u_k^{(r)} = \rho^{(r)} \delta_k^{(r)}$. This probability is therefore estimated by:

$$\tilde{P}_1 = \frac{1}{N} \sum_{r=1}^N \mathbf{I}_{\mathcal{D}_f}^{(r)}$$

and, finally:

$$\tilde{P}_f = (1 - \chi_n^2(\beta^2)) \frac{1}{N} \sum_{r=1}^N \mathbf{I}_{\mathcal{D}_f}^{(r)}$$

The interest of such a procedure is to produce simulations with a high probability and to scan all the space outside the sphere of radius β . An illustration is given in Section 8.6.3.

8.5.3 Latin hypercube (LH)

In this method, the sampling is carried out in a uniform manner in a hypercube whose center is the design point (Figure 8.8); in general, it is sufficient to take a hypercube p varying from $-k$ to $+k$, $k = 3$ or more centered on u_k^* . The sides of the hypercube are parallel to the reference axes. The uniform density function on the hypercube is $f_{U_k}(u_k) = 1/V(p)$, where $V(p)$ is the volume of the hypercube. The probability of failure is written as:

$$P_f = \int_p \mathbf{I}_{\mathcal{D}_f} \frac{\phi_n(u_k)}{V(p)} V(p) d(vol)$$

The estimate of this integral is given by the mathematical expectation of the variable $\mathbf{I}_{\mathcal{D}_f} \phi_n(u_k) V(p)$ for a random vector u_k uniformly distributed in $V(p)$:

$$\tilde{P}_f = \frac{V(p)}{N} \sum_{r=1}^N \mathbf{I}_{\mathcal{D}_f}^{(r)} \phi_n \left(u_k^{(r)} \right)$$

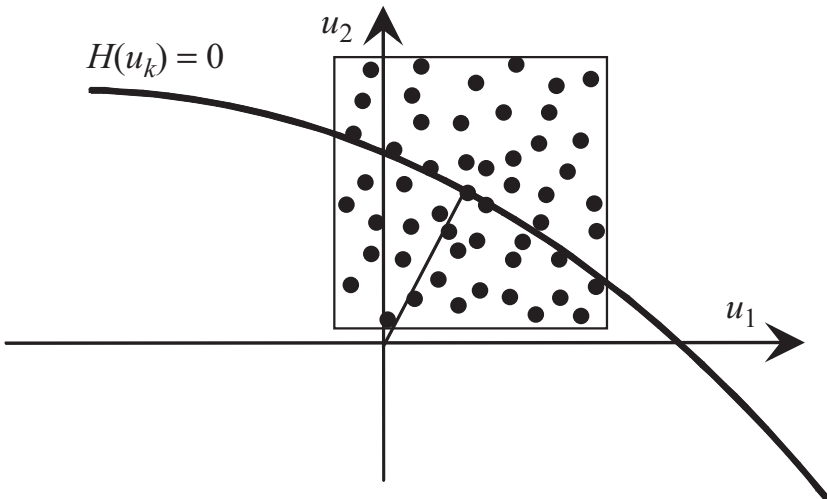


Figure 8.8 Uniform samples in a cube.

The Latin hypercube method is reputed to be inefficient for weak probabilities. An illustration is given in Section 8.6.3.

8.5.4 Adaptive sampling (AS) [Buc88]

To estimate the probability of failure, it would be sufficient to make a single sampling if we knew the probability function conditioned by belonging to the failure domain $f_{U_k}(u_k \mid u_k \in \mathcal{D}_f)$. However, this function is not known in advance. The adaptive sampling method (Figure 8.9) uses the information acquired during the previous simulations carried out to estimate the conditional distribution from statistics on the points obtained in the failure domain. The new distribution is therefore used to carry out the subsequent sampling.

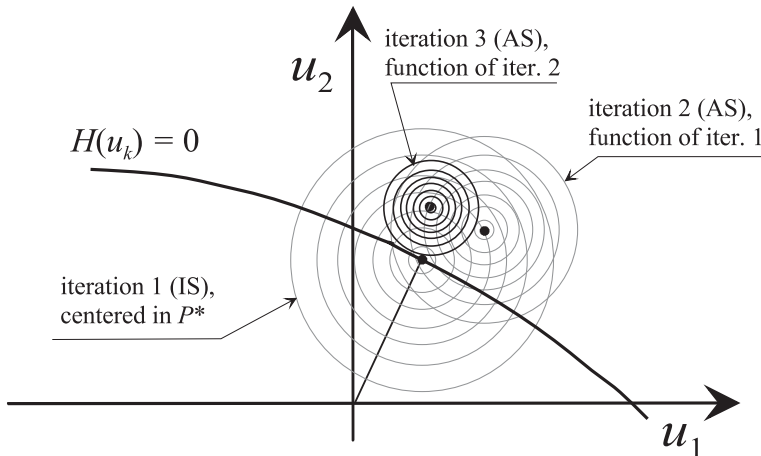


Figure 8.9 Iterations of adaptive sampling.

The first set of samples is performed using the importance sampling (IS) method. The average and the standard deviation obtained from the conditional function are calculated from the points found in the failure domain. A second set of samples is carried out according to this distribution.

New parameters are calculated, and so on. This is a good principle whose efficiency and economy have not been demonstrated through numerical examples.

8.5.5 Conditional importance sampling method

We combine importance sampling and conditional sampling to aim for maximum efficiency of the calculation by localizing the calculation without

taking into account the points situated at a distance from the origin of less than β . [SM93] gives a comparative approach to the different methods.

8.5.6 Stratified sampling method [Rub81]

This method is based on separating the integration space into a certain number of discrete domains for which the probabilities can be calculated in an independent manner. Variance reduction is obtained by increasing the number of samples in the ‘important’ domains.

8.6 Illustration of the methods

In order to show the implementation of these methods, we again take the resistance – stress example in which the two variables are uniform.

The correlation coefficient is taken as equal to 0.5. The limit-state is simply:

$$G(R, S) = R - S$$

The results available are those of the FORM analysis – $\beta_{\text{FORM}} = 1.546 - P_{f,\text{FORM}} = 0.061$ – and of the SORM analysis (Equation (7.20)) – $\beta_{\text{SORM}} = 1.787 - P_{f,\text{SORM}} = 0.037$. The exact probability is $P_f = 0.032$. The conditioning methods are implemented from the point P^* obtained by FORM analysis: $u_1 = -0.852$ and $u_2 = 1.291$.

8.6.1 Crude Monte Carlo (MC)

Figure 8.10 shows the convergence obtained for the estimate of failure probability and the coefficient of variation of the latter. As foreseen, the convergence is slow, by the square root of the number of simulations. The two black lines frame the estimate of P_f with ± 2 standard deviations. The coefficient of variation is weak because the target probability is high: Equation (8.6) gives 3,125 simulations, for $\text{cov} = 0.1$. Another simulation would lead to a different appearance of the convergence scheme.

8.6.2 Directional simulations (DS)

Figure 8.11 shows the convergence obtained for the estimate of failure probability and of the coefficient of variation of the latter. In comparison with the direct Monte Carlo method, the number of simulations is divided by 10 and we ascertain that a coefficient of variation of 0.1 is reached for about 600 simulations instead of 3,125. The failure point is obtained by looking for the minimum radius. The cost depends on the difficulty of the search on the intersection of a direction with the limit-state.

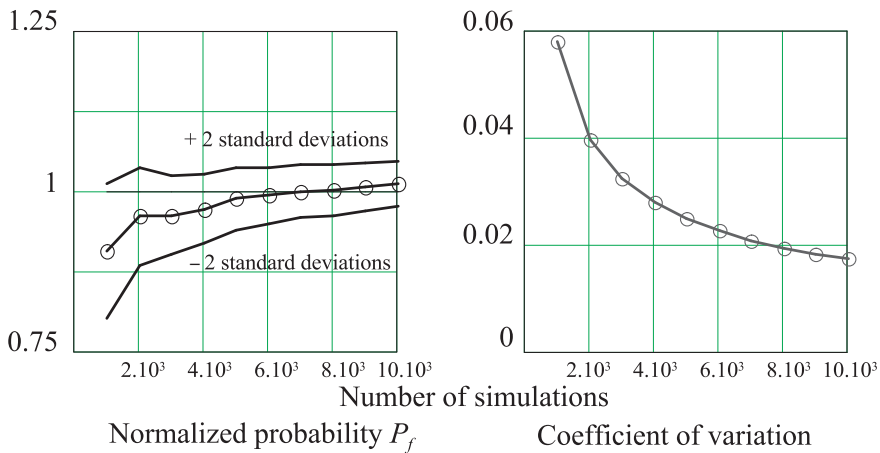


Figure 8.10 Convergence of Monte Carlo simulations (10^4) for the example. Probability is normalized to the expected value.

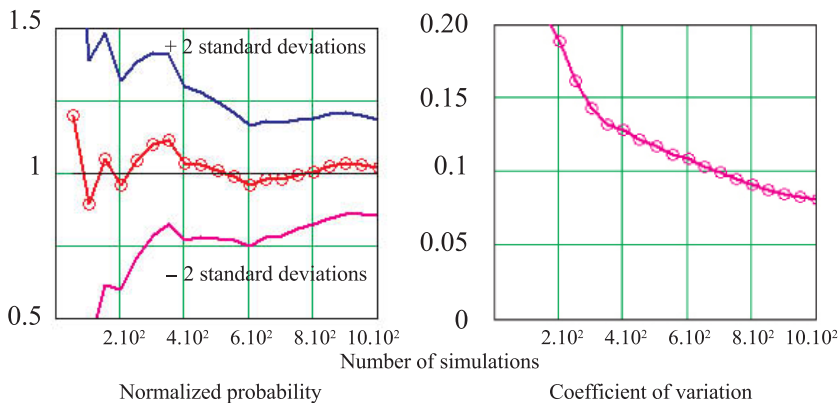


Figure 8.11 Convergence of directional simulations (10^3) for the example. Probability is normalized to the expected value.

8.6.3 Conditional sampling with the knowledge of P^* (IS, CS, LH)

Figure 8.12 illustrates the results obtained for 1,000 simulations according to three of the methods set forth. For each, the number of simulations for a coefficient of variation of 0.1 is given:

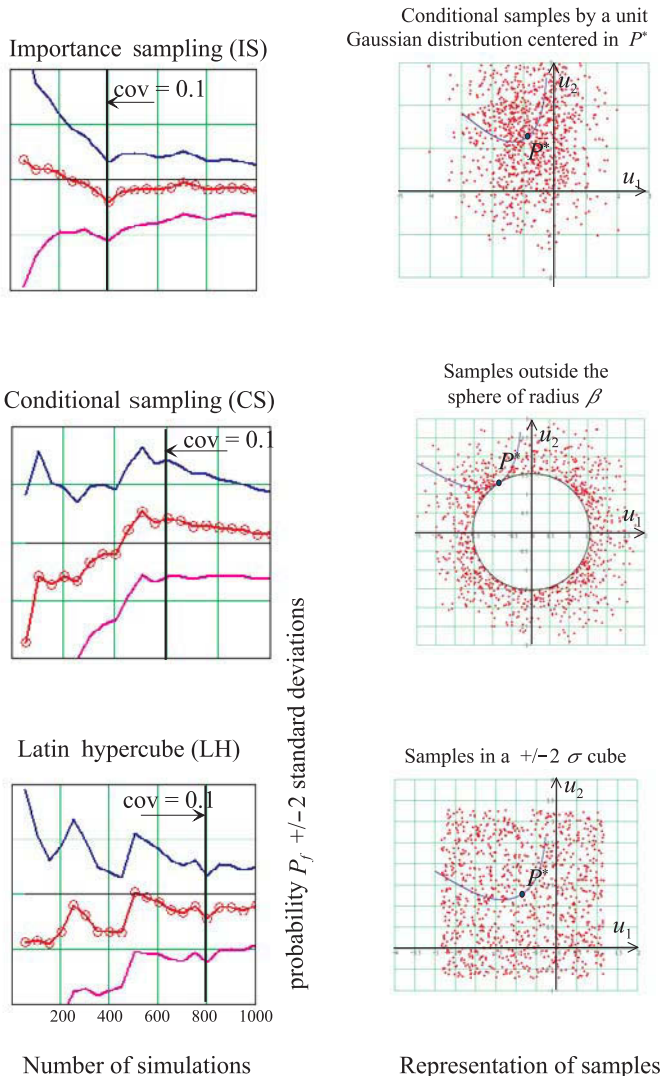


Figure 8.12 Illustration of conditional sampling for the example.

- importance sampling is carried out around point P^* , precisely calculated, and there are no secondary minima. This conditioning is then very efficient,
- conditional samples outside the sphere of radius β are less efficient but this method allows us to be certain of the existence – or not – of secondary minima. It is necessary to use it if the presence of such minima cannot be discounted,

- sampling according to a Latin hypercube does not bring a significant advantage and convergence is slow.

8.6.4 Outcome of the illustration

Table 8.1 summarizes the number of simulations N according to each method for an objective $\text{cov} = 0.1$. The additional necessary calculations are indicated in the comment column. The conclusions to be drawn can be applied only to the case of a unique and dominant, well-identified point P^* . The number of simulations remains high but the analysis of results has focused on the convergence of P_f , which is much more severe than an analysis of the reliability index β . Thus, importance sampling leads to a value of $\beta = -\Phi^{-1}(P_f)$, correct within 10% for about 40 simulations in most of the trials.

Method	$N \text{cv} = 0.1$	Comment
MC	3,125	—
DS	600	Intersection of a direction with the limit-state
IS	400	Search for point P^*
CS	600	Search for point P^*
LH	800	Search for point P^*

Table 8.1 Comparison of the number of simulations according to various methods.

8.7 Conclusion

Simulation methods have the advantage of being able to handle very complex cases, for example, irregular or non-differential limit-states or the combined limit-states of series or parallel systems. The efficiency of a method is increased by integrating the information available on the problem if the latter is pertinent.

In real structures, the probabilities of failure are generally very weak (10^{-2} to 10^{-8}) and the choice of the method must therefore be adapted to the number of samples necessary to stabilize the estimation of this probability. However, despite the large number of evaluations of the mechanical model, simulations do not offer much information on the reliability behavior of the system. Only directional simulations allow us to obtain indications concerning the most probable failure point and importance factors (sensitivities, partial coefficients, etc.).

Methods based on knowledge of the design point are generally efficient but can give a wrong estimation of failure probability if the point of calculation is a local minimum or if there are several minima. We must therefore be certain that we have indeed only one significant minimum for the problem.

A general calculation procedure can thus be proposed:

1. carry out a FORM reliability analysis,
2. complete possibly by a SORM analysis,
3. carry out conditional sampling around the point P^* found and observe the convergence of the P_f estimate and its coefficient of variation:
 - if the estimate converges rapidly, then the solution obtained is satisfactory and point P^* is indeed an absolute minimum and no secondary minimum is found at a greater, but comparable distance,
 - if the estimate does not converge rapidly, this conveys the existence of ‘probability attractors’ other than point P^* . Two possibilities exist: look for the secondary points P and use an approximate system or else pass on to a simulation method not using the FORM information: the cost of calculation will be high!

Because each sample is a complete calculation of the mechanical model, direct simulations are coupled with numerical models (finite elements for example) only for simple cases with a moderate probability of failure. They are used essentially to provide reference results, with a view to validating other methods of calculation, such as the search for the reliability index.

Besides their intrinsic interest, sampling methods, in one of their adapted formulations, constitute at present the best means of validating a result obtained by an approximation method.

Chapter 9

Reliability of Systems

The reliability of a mechanical system does not depend, in general, on only one event. In the previous chapters, the notion of the failure scenario, describing an event, was introduced. A failure scenario is associated with a limit-state function separating the safety domain from the failure domain. A *component* is defined by *a failure scenario* and *a limit-state*. Such a definition does not prejudge the physical nature of a component. It can completely correspond to a physical component, but that is not necessary.

In this chapter, several components, in the sense referred to above, are considered. Each component contributes to reliability or to failure and the *combination* of success or failure events leads to the success or to the failure of a *resulting system*. It is then the failure of the system which is studied. This approach enables us to represent complex failure scenarios obtained by a combination of elementary scenarios. In fact, the failure of a structure or of a mechanical system generally results from several combined reasons.

The study of failure requires an accurate analysis of operation and dysfunction conditions. This constitutes an essential step before any calculation of reliability. We can even say that all reliability calculations are useless if the analysis of the failure is not performed with care. In fact, any identification of a risk leads naturally to taking measures to compensate for it, and this, too, is independent of any calculation. Some methods have been proposed to this end and we will not describe them in this work. They are based in general on *Failure Modes and Effects Analysis* (FMEA) and result in the construction of cause trees or consequence trees; see for example [Vil88].

The objective of this chapter is limited to an examination of simple combinations of events. Later it proposes some methods to evaluate the probability of failure associated with any type of combination.

9.1 Combination of failure modes

The following combinations are examined:

- series combination,

- parallel combination,
- series combination of parallel combinations,
- parallel combination of series combinations,
- conditional parallel combinations.

9.1.1 Series combination

Let a set of failure events be E_i with probabilities $P(E_i)$. The system formed by the events E_i is a *series system* if the occurrence of one single event brings about a failure of the system. The probability of failure of the system, P_{f_sys} , is then the probability of the union of failure events:

$$\text{series system: } P_{f_sys} = \text{Prob}(\cup E_i) \quad (9.1)$$

For example, for two events:

$$\text{Prob}(E_1 \cup E_2) = P(E_1) + P(E_2) - P(E_1 \cap E_2)$$

This formula can be extended for any number of events. This is then the Poincaré formula:

$$\begin{aligned} & \text{Prob}\left(\bigcup_{i=1}^n E_i\right) \\ &= \sum_{i=1}^n P(E_i) - \sum_{j=2}^n \sum_{i=1}^{j-1} P(E_i \cap E_j) + \dots + (-1)^n P(E_1 \cap E_2 \cap \dots \cap E_n) \end{aligned}$$

The classic example is that of a chain whose failure is related to any of its links. The series representation is given in Figure 9.1.

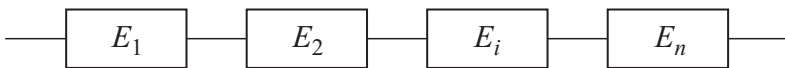


Figure 9.1 Representation of a series system.

9.1.2 Parallel combination

Let a set of failure events be E_i , with probabilities $P(E_i)$. The system formed by the events E_i is a *parallel system* if the failure of all the events is necessary for the failure of the system. The probability of failure of the system, P_{f_sys} , is then the probability of the intersection of the failure events:

$$\text{parallel system: } P_{f_sys} = \text{Prob}(\cap E_i) \quad (9.2)$$

For example, for two events:

$$\text{Prob}(E_1 \cap E_2) = P(E_1) P(E_2 | E_1) = P(E_2) P(E_1 | E_2)$$

where $P(E_2|E_1)$ signifies ‘probability of E_2 when E_1 is realized’.

The parallel combination expresses in principle a redundancy, but this is true only if the events of the intersection are independent. Two types of redundancies are possible:

- *active redundancy*, in which all the components contribute at every instant to the operation of the system (a car with four wheels capable of continuing to drive on three wheels in degraded mode),
- *passive redundancy*, in which some components (on *standby*) participate in the operation only in case of necessity in the case of certain failures (a car with its spare wheel).

The parallel representation is given in Figure 9.2.

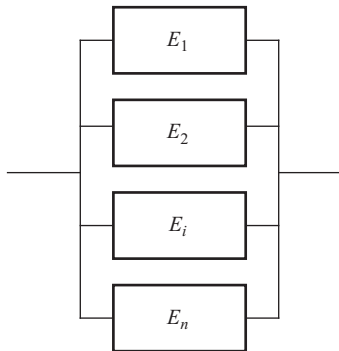


Figure 9.2 Representation of a parallel system.

9.1.3 Series combination of parallel systems

The series system is composed of events E_j themselves composed of parallel events E_i . By combining equations (9.1) and (9.2), it becomes:

$$P_{f_sys} = \text{Prob} \left(\bigcup_j \left(\bigcap_i E_i \right)_j \right)$$

The representation of a failure scenario by a set of parallel events in series is not always possible. Such a representation is called a ‘cut set’. The cut set is

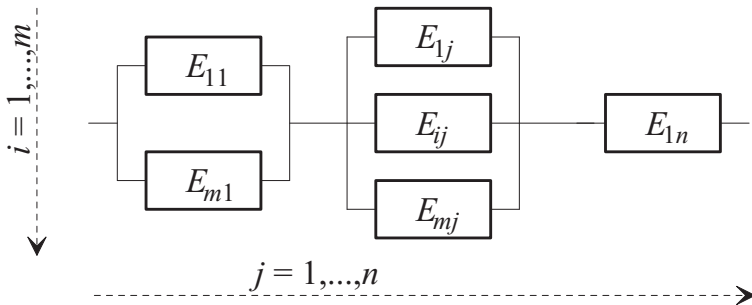


Figure 9.3 Representation of a series system of parallel systems.

minimal if it does not contain another cut set as its own subset, and is then called a *minimal cut set*. The diagram in Figure 9.3 represents a minimal cut set of a series system of parallel systems.

9.1.4 Parallel combination of series systems

The parallel system is composed of events E_j themselves composed of series events E_i . By combining equations (9.1) and (9.2), it becomes:

$$P_{f_sys} = \text{Prob} \left(\bigcap_j \left(\bigcup_i E_i \right)_j \right)$$

The representation of a failure scenario by a set of series events in parallel is not always possible. It is composed of parallel ties of series systems, and is called a (*minimal*) *tie set*.

9.1.5 Conditional parallel combination

This is a special presentation of series combinations of parallel systems, illustrated in Figure 9.4. We consider a set of failure events E_i (rupture of the bar i). The first step consists of looking at the probabilities $P(E_i)$. The next step looks at the conditional probabilities $P(E_j | E_i)$. This outline is repeated as many times as necessary and the probability of failure is obtained by taking the union of probabilities of each intersection, $P(E_i) \cap P(E_j | E_i) \cap P(E_k | E_i E_j) \cap \dots$, for all possible intersections.

An example illustrates this approach. The system is composed of two bars in parallel from the mechanical point of view, and the failure system is a series system of two parallel systems (Figure 9.4).

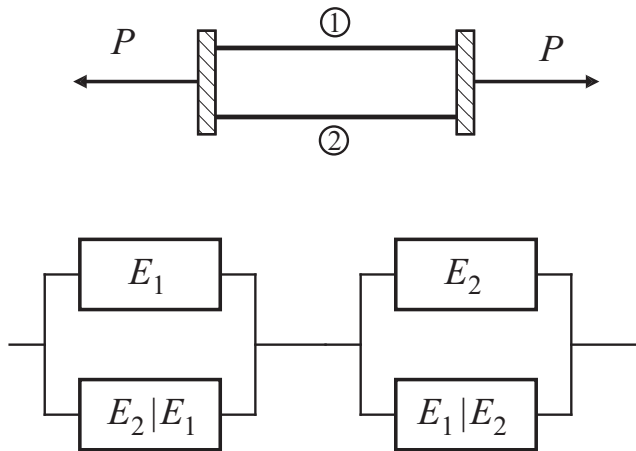


Figure 9.4 Mechanical system of two bars and system of associated failure.

9.1.6 Implementation and application

We are not concerned here with studying the general methods of construction of the system representation. The bases presented here constitute elements of a model aimed at reliability calculation, of which three stages can be recalled:

1. carry out an accurate analysis of all the causes of failure, by identification of components and of their interactions,
2. organize the information under an explicit presentation, for example, of the type *minimal cut set*,
3. finally, evaluate the probabilities of the components and of the system.

The first stage is particularly delicate and requires a wide knowledge of the real operation of the mechanical system studied; it is most difficult because *it does not serve any purpose to have accurate calculations if an essential cause of failure has been missed*. From this point of view, it is necessary to remember that the reliability analysis starts with a very fine analysis of the mechanical system whose consequences on reliability are always positive even if no calculation is carried out later.

This chapter is mainly devoted to the third stage; implementation in situations in which the first two are dealt with in a satisfactory manner.

It is necessary to note that modeling failure in the form of a system depends on the way in which the mechanical model is constructed, and the same mechanical limit-state can, in fact, be reached in different ways. Example 2 (infinitesimal elastoplasticity) supports this assertion. However, a first example is presented to illustrate the concepts introduced.

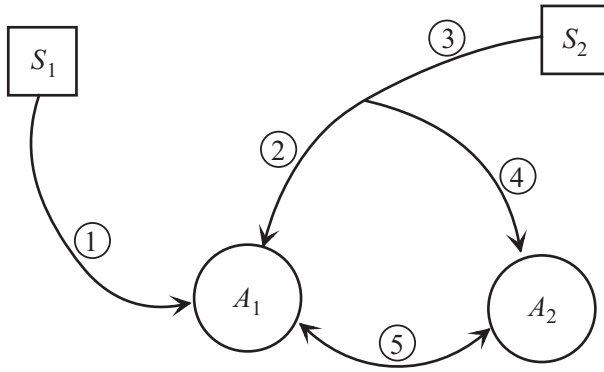


Figure 9.5 Example: water supply.

Example 1: supplying water

This example is given by Rackwitz [Rac89]. Two reservoirs S_1 and S_2 supply water to two towns A_1 and A_2 . The arcs i indicate the possible circulation of water (Figure 9.5). The failure of the system is non-supply to A_1 or A_2 . Let us mark as E_i the failure of arc i and as A_i the failure of the supply to town A_i . By examining directly the causes of failure for each town, it is possible to write the combinations of events which bring about the undesirable event. Thus, for non-supply to town A_1 :

$$\text{Prob}(A_1) = \text{Prob}\{E_1 \cap (E_2 \cup E_3) \cap (E_3 \cup E_4 \cup E_5)\} \quad (9.3)$$

and for A_2 :

$$\text{Prob}(A_2) = \text{Prob}\{(E_1 \cup E_5) \cap (E_3 \cup E_4) \cap (E_2 \cup E_3 \cup E_5)\} \quad (9.4)$$

The possible representations of the cuts are given in Figure 9.6. Diagram (1) illustrates directly the two formulae written as (9.3) and (9.4). Every parallel event of the series system is a cut leading to failure.

The classic equations:

$$E_i \cap (E_j \cup E_k) = (E_i \cap E_j) \cup (E_i \cap E_k)$$

$$E_i \cup (E_j \cap E_k) = (E_i \cup E_j) \cap (E_i \cup E_k)$$

allow us to extract any possible cuts. Equation (9.3) becomes:

$$\begin{aligned} \text{Prob}(A_1) &= \{(E_1 \cap E_2 \cap E_3) \cup (E_1 \cap E_2 \cap E_4) \\ &\quad \cup (E_1 \cap E_2 \cap E_5) \cup (E_1 \cap E_3 \cap E_4) \cup (E_1 \cap E_3 \cap E_5)\} \end{aligned}$$

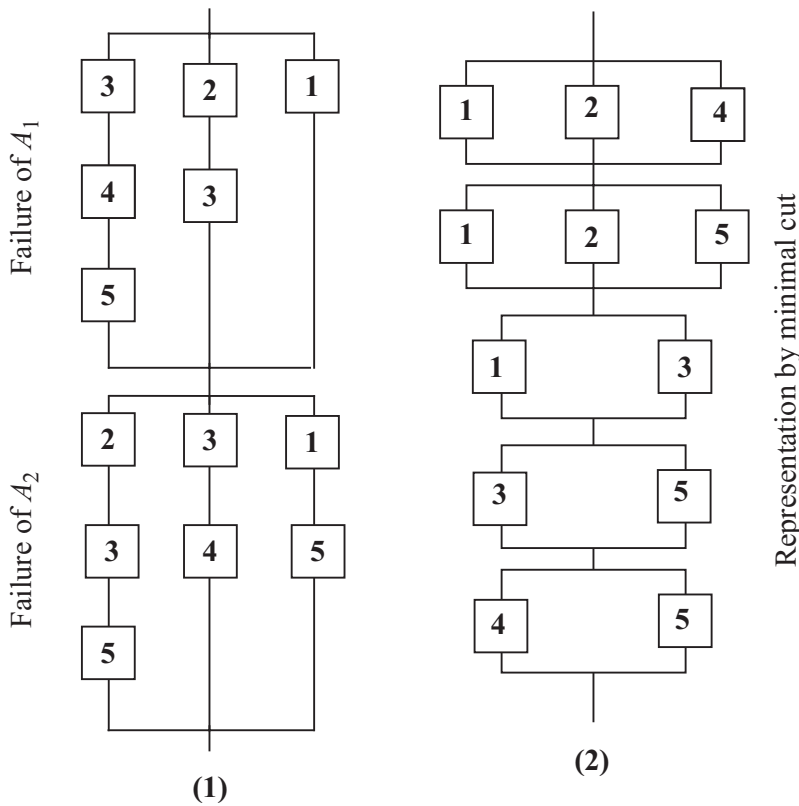


Figure 9.6 Representation of the failure by cuts.

and likewise for (9.4). By developing and simplifying it, considering that if $E_i \subseteq E_j$, then $E_i \cup E_j = E_j$ and $E_i \cap E_j = E_i$, after elimination of the redundant terms, we obtain:

$$\begin{aligned} \text{Prob}(A_1 \cup A_2) &= \{(E_1 \cap E_3) \cup (E_3 \cap E_5) \cup (E_4 \cap E_5) \\ &\quad \cup (E_1 \cap E_2 \cap E_4) \cup (E_1 \cap E_2 \cap E_5)\} \end{aligned}$$

The illustration of this equation is diagram (2) of Figure 9.6. It constitutes a representation by a *minimal cut set* which is the smallest combination of events bringing about the undesirable event.

A representation by parallel ties of series systems is also given in Figure 9.7; this representation constitutes a minimal tie set. Each tie corresponds to a possible supply for the two towns.

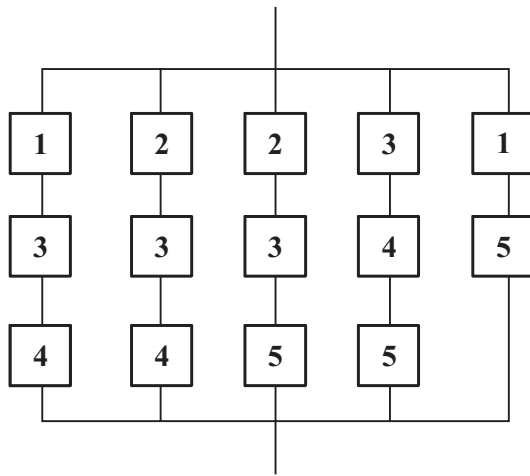


Figure 9.7 Representation of ‘minimal tie set’.

Example 2: infinitesimal elastoplasticity

To reach the load limit of an elastoplastic structure without stress hardening, three methods are possible:

1. the incremental method,
2. limit analysis using the kinematics theorem,
3. limit analysis using the static theorem.

These three analyses lead evidently to the same load limit, but their expressions in terms of the system are different. They are illustrated in the example of the frame in Figure 9.8. Cross-sections 2 and 3 are the sections of the extreme bending moments in which the plastic resisting moments M_{P_1} and M_{P_2} are supposedly independent.

Incremental method. The following events are identified:

1. E_2 : section 2 reaches the yield stress; \bar{E}_2 : section 2 does not,
2. E_3 : section 3 reaches the yield stress; \bar{E}_3 : section 3 does not.

Failure is then:

$$\text{elastoplastic failure: } \text{Prob}(((E_2 \mid \bar{E}_3) \cap E_3) \cup ((E_3 \mid \bar{E}_2) \cap E_2))$$

Kinematics method. A single event is possible, E_c , since there is only one mechanism whose equation is $H - M_{P_2}/h - M_{P_3}/h'$. It becomes:

$$\text{elastoplastic failure: } \text{Prob}(E_c)$$

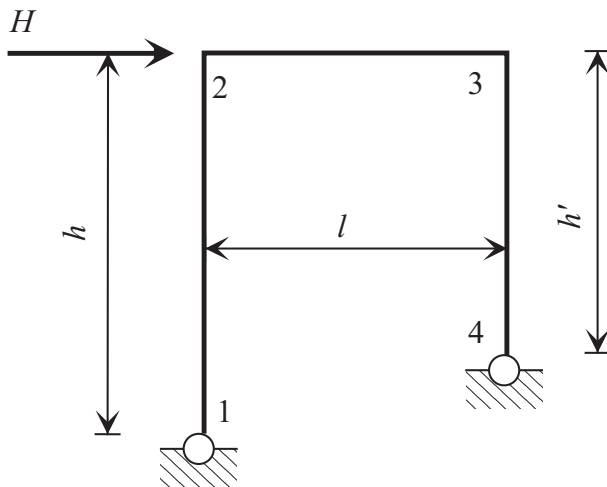


Figure 9.8 Example 2: simple frame.

Static method. The statically and plastically admissible system is of the form:

$$\left| H + \frac{X}{h'} \right| h \leq M_{P_2} \quad |X| \leq M_{P_3}$$

where X is the bending moment in cross-section 3. The static theorem leads us to look for the solution which maximizes H . Taking the absolute value into account, four events E_{si} are possible, each leading to failure:

$$\text{Elastoplastic failure: } \text{Prob}(E_{s1} \cup E_{s2} \cup E_{s3} \cup E_{s4})$$

Without entering into the details of the calculations, this example shows that the choice of the mechanical model leads to a more or less complex system representation.

9.2 Bounds of the failure probability of a system

9.2.1 Hypothesis

We will consider here a system presenting k potential failure modes. The event E_i is associated with each mode, and the complementary event is \bar{E}_i . The study is concerned with a series failure system or a parallel safety system. The probability of failure of the series system is $P(E) = P(\cup_i E_i)$; it is analyzed in the FORM context.

9.2.2 A classic approximation

The first obvious point is to note that the probability of a system is found between 0 and 1. This is not unnecessary because some approximate values do not respect this restriction. A classic approximation is obtained by first considering two events:

$$\begin{aligned}\text{Prob}(E_1 \cup E_2) &= \text{Prob}(E_1) + \text{Prob}(E_2) - \text{Prob}(E_1 \cap E_2) \\ &\leq \text{Prob}(E_1) + \text{Prob}(E_2)\end{aligned}$$

The probability of the union of two events is lower than or equal to the sum of the probabilities of the elementary events, which leads to an acceptable generalization to n events if the probabilities of intersections from the third order can be neglected:

$$P(\bigcup_i E_i) \approx \min \left(\sum_i \text{Prob}(E_i); 1 \right)$$

The limits of this formula are discussed in Section 9.2.5.

9.2.3 Correlation of events E_i and E_j

Let us consider events E_i and E_j whose associated hyperplanes in approximation FORM are respectively Z_i and Z_j . The standardized forms of the hyperplanes are:

$$\begin{aligned}Z_i &= \beta_i + \langle \alpha_i \rangle \{u\} \\ Z_j &= \beta_j + \langle \alpha_j \rangle \{u\}\end{aligned}$$

The averages of Z_i and Z_j are:

$$\text{E}[Z_i] = \beta_i \quad \text{E}[Z_j] = \beta_j$$

because variables $\{u\}$ are of zero averages. For variances and covariances, they become:

$$\begin{aligned}\text{var}[Z_i] &= \text{E}[Z_i^2] - \beta_i^2 = \beta_i^2 + \langle \alpha_i \rangle \text{cov}[\{u\}\{u\}^t] \{\alpha_i\} - \beta_i^2 = \langle \alpha_i \rangle \{\alpha_i\} = 1 \\ \text{var}[Z_j] &= \langle \alpha_j \rangle \{\alpha_j\} = 1\end{aligned}$$

$$\text{cov}[Z_i, Z_j] = \text{E}[Z_i Z_j] - \beta_i \beta_j = \langle \alpha_i \rangle \text{cov}[\{u\}\{u\}^t] \{\alpha_j\} = \langle \alpha_i \rangle \{\alpha_j\}$$

because $\text{cov}[\{u\}\{u\}^t]$ is the unit matrix. Correlation is then given by:

$$\text{cor}(Z_i, Z_j) = \langle \alpha_i \rangle \{\alpha_j\} = \rho_{ij}$$

The geometric interpretation is immediate; correlation is equal to the cosine of the angle formed by the vectors normal to the two hyperplanes. Different representations are given in Figure 9.9. Correlation is zero when the hyperplanes are orthogonal. By misuse of language, we consider then that if $\text{cor}(Z_i, Z_j) \geq 0$, then $P(E_j | E_i) \geq P(E_j)$, and the events are called ‘positively correlated’.

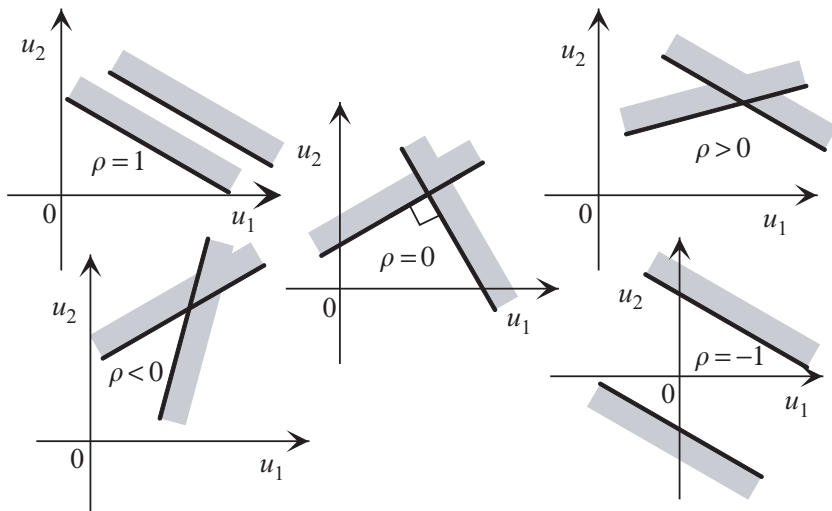


Figure 9.9 Representation of the correlation of Z_i and Z_j .

9.2.4 Uni-modal bounds

The bounds are called ‘uni-modal’ if they use only the probabilities of simple events, of type $P(E_i)$, and the sign of their dependence.

Case of positive dependence

Let the two events be E_i and E_j correlated positively. It becomes [AT84]:

$$\begin{aligned} P(E_j|E_i) &\geq P(E_j) \quad \text{and} \quad P(\bar{E}_j|\bar{E}_i) \geq P(\bar{E}_j) \\ P(\bar{E}_i \cap \bar{E}_j) &\geq P(\bar{E}_i) P(\bar{E}_j) \end{aligned}$$

For k events, all correlated positively:

$$P(\bar{E}) = P(\bar{E}_1 \cap \bar{E}_2 \cdots \cap \bar{E}_k) = P\left(\bigcap_{i=1}^k \bar{E}_i\right) \geq \prod_{i=1}^k P(\bar{E}_i) \quad (9.5)$$

and in the case of independent events:

$$P\left(\bigcap_{i=1}^k \bar{E}_i\right) = \prod_{i=1}^k P(\bar{E}_i)$$

Furthermore, event \bar{E} is contained in \bar{E}_i for every i , and hence:

$$P(\bar{E}) \leq \min_i P(\bar{E}_i) \quad (9.6)$$

Equations (9.5) and (9.6) frame the probability of the parallel system, whence:

$$\text{Correlation} > 0 \quad \min_i P(\bar{E}_i) \geq P(\bar{E}) \geq \prod_{i=1}^k P(\bar{E}_i)$$

To obtain the failure of the series system, it is sufficient to return to events E_i :

$$\text{Correlation} > 0 \quad \max_i P(E_i) \leq P(E) = P(\cup E_i) \leq 1 - \prod_{i=1}^k (1 - P(E_i)) \quad (9.7)$$

When probabilities $P(E_i)$ are weak, the second member is simplified by neglecting the products; it becomes:

$$\text{Correlation} > 0 \quad \max_i P(E_i) \leq P(E) \lesssim \min \left(\sum_{i=1}^k P(E_i); 1 \right)$$

Case of negative dependence

For k events correlated negatively:

$$\begin{aligned} P(E_j|E_i) &\leq P(E_j) \quad \text{and} \quad P(\bar{E}_j|\bar{E}_i) \leq P(\bar{E}_j) \\ P(\bar{E}_i \cap \bar{E}_j) &\leq P(\bar{E}_i) P(\bar{E}_j) \\ P\left(\bigcap_{i=1}^k \bar{E}_i\right) &\leq \prod_{i=1}^k P(\bar{E}_i) \end{aligned}$$

The lower bound is then trivially 0:

$$\begin{aligned} \text{correlation} < 0 \quad \prod_{i=1}^k P(\bar{E}_i) &\geq P(\bar{E}) \geq 0 \\ \text{correlation} < 0 \quad 1 - \prod_{i=1}^k (1 - P(E_i)) &\leq P(E) = P(\cup E_i) \leq 1 \end{aligned} \quad (9.8)$$

These equations can give a preliminary idea of the failure probability bounds of a system. For this, it is necessary that all the correlations be of the same sign. Quite obviously, the restriction obtained is often very large.

9.2.5 Bi-modal bounds

The bi-modal bounds are obtained from probabilities of events taken one by one and from probabilities of events taken two by two.

The result obtained by Ditlevsen [Dit79] is as follows:

$$P(E_1) + \sum_{i=2}^k \max \left(P(E_i) - \sum_{j=1}^{i-1} P(E_i \cap E_j); 0 \right) \leq P(E) \quad (9.9)$$

$$P(E) \leq \sum_{i=1}^k P(E_i) - \sum_{i=2}^k \max_{j < i} P(E_i \cap E_j) \quad (9.10)$$

In this expression, $P(E_1) = \max_i P(E_i)$. Its application is based on an estimation of probabilities $P(E_i \cap E_j)$, which is possible in the FORM approximation.

As a special case, let us consider that of two events. The application of the equation of the higher bound or that of the lower bound gives the same result: the exact expression of the probability of the union of two events:

$$P(E_1 \cup E_2) = P(E_1) + P(E_2) - P(E_1 \cap E_2)$$

9.3 First-order approximation bounds

9.3.1 Hypothesis

Continuing further, the failure of a system component is represented by a first-order approximation. This amounts to replacing the real limit-state by its linear approximation at the most probable failure point in standardized centered variable space. Event E_i is therefore represented by its reliability index β_i and the hyperplane $Z_i = a_{0i} + \langle a_i \rangle \{u\} = 0$. It is, however, possible to use SORM results or the best approximation obtained from $P(E_i)$ by substituting for β_i the value $\beta_i = -\Phi^{-1}(P(E_i))$.

9.3.2 Probability bounds of the intersection $P(E_i \cap E_j)$

Case of positive correlation

Figure 9.10 represents the two hyperplanes Z_i and Z_j . $P(E_i \cap E_j)$ is represented by the dihedron limited by the two hyperplanes, on the side of the failure events. To evaluate this quantity, two new planes are introduced:

- Z_A is perpendicular to Z_i , the associated event is $A = E_{\perp i}$,
- Z_B is perpendicular to Z_j , the associated event is $B = E_{\perp j}$.

The distances of planes Z_i , Z_j , Z_A and Z_B from the origin are respectively β_i , β_j , a and b and the associated probabilities $P(E_i) = \Phi(-\beta_i)$, $P(E_j) = \Phi(-\beta_j)$.

From Figure 9.10, it becomes:

$$P(A) \leq P(E_i \cap E_j)$$

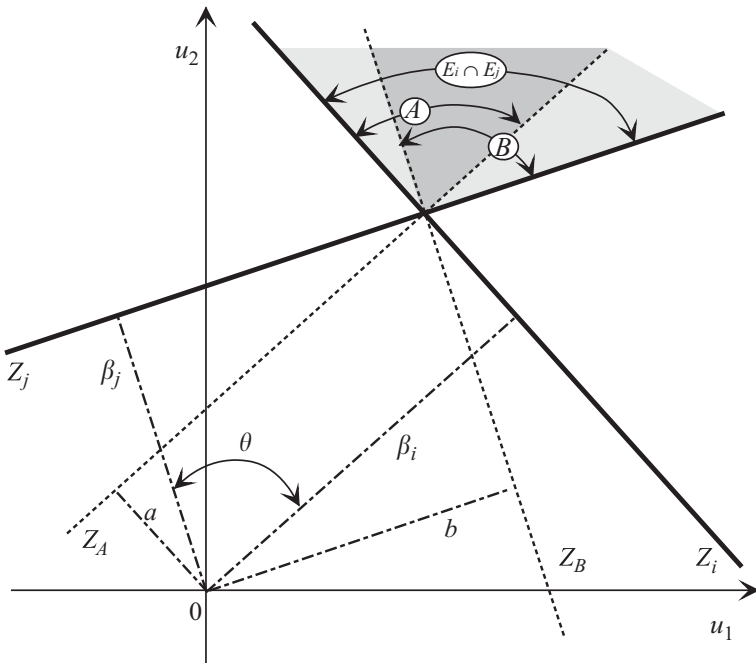


Figure 9.10 Positive correlation.

$$\begin{aligned} P(B) &\leq P(E_i \cap E_j) \\ P(A) + P(B) &\geq P(E_i \cap E_j) \end{aligned}$$

hence:

$$\max(P(A); P(B)) \leq P(E_i \cap E_j) \leq P(A) + P(B)$$

A simple calculation in the triangles gives the equations:

$$a = \frac{\beta_j - \rho_{ij}\beta_i}{\sqrt{1 - \rho_{ij}^2}} \quad b = \frac{\beta_i - \rho_{ij}\beta_j}{\sqrt{1 - \rho_{ij}^2}} \quad \text{with } \rho_{ij} = \cos(\theta) = \langle \alpha_i \rangle \{ \alpha_j \}$$

From the observation that $P(A)$ is the probability of the intersection of half-spaces limited by the orthogonal hyperplanes Z_i and Z_A , it results that $P(A) = \Phi(-\beta_i)\Phi(-a)$; likewise $P(B) = \Phi(-\beta_j)\Phi(-b)$ and finally:

$$P(A) = \Phi(-\beta_i)\Phi\left(-\frac{\beta_j - \rho_{ij}\beta_i}{\sqrt{1 - \rho_{ij}^2}}\right) \quad P(B) = \Phi(-\beta_j)\Phi\left(-\frac{\beta_i - \rho_{ij}\beta_j}{\sqrt{1 - \rho_{ij}^2}}\right)$$

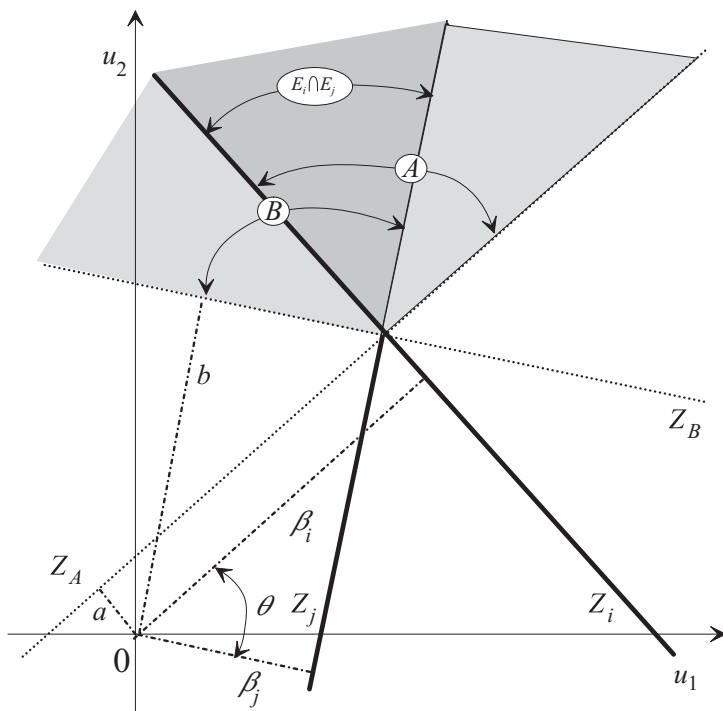


Figure 9.11 Negative correlation.

Case of negative correlation

Figure 9.11 illustrates a negative correlation. By reasoning, as in the case of positive correlation, it becomes:

$$\begin{aligned} P(A) &\geq P(E_i \cap E_j) \\ P(B) &\geq P(E_i \cap E_j) \end{aligned}$$

The lower bound is trivially 0 and:

$$0 \leq P(E_i \cap E_j) \leq \min(P(A); P(B))$$

9.3.3 Equivalent hyperplane

When two events represented by hyperplanes are combined, an evaluation of the probability of their union or of their intersection can be obtained:

$$\begin{aligned} \text{intersection } P(E_i \cap E_j) \\ \text{union } P(E_i \cup E_j) = P(E_i) + P(E_j) - P(E_i \cap E_j) \end{aligned}$$

From the probability evaluation, an equivalent index is deduced as:

$$\beta^E = -\Phi^{-1}(P(E)) = -\Phi^{-1}(P_{f_sys})$$

by retaining the most unfavorable evaluation.

Hohenbichler (cited by [TCM86]) gives a method of determining the direction cosines of a hyperplane equivalent to distance β^E . For this, this author studies the weight of each random variable by slightly increasing variable u_l .

The equation of an equivalent hyperplane is given by:

$$\beta^E = -\langle \alpha^E \rangle \{u\}$$

The hyperplane is disturbed by a slight increase of one of the components of $\{u\}$, for instance u_l :

$$\beta^E(\varepsilon) = -\langle \alpha^E \rangle (\{u\} + \Delta\{u(\varepsilon)\}) = \beta^E - \langle \alpha^E \rangle \{\Delta u(\varepsilon)\}$$

This perturbation is carried out on each of the limit-states, and an equivalent perturbed index $\beta^E(\varepsilon)$ for u_l obtained. The direction cosines are approximated by:

$$\bar{\alpha}_l^E = \frac{d\beta^E(\varepsilon)}{d\varepsilon} \underset{\varepsilon \text{ small}}{\sim} \left. \frac{\beta^E(\varepsilon) - \beta^E}{\varepsilon} \right|_{\varepsilon \text{ small}}$$

This operation is applied to each component, which leads to a vector $\{\bar{\alpha}^E\}$ of non-standardized components. It is sufficient to standardize it to obtain $\{\alpha^E\}$ and to choose the sign in such a manner that $\{\alpha^E\}^t(\{\alpha_i\} + \{\alpha_j\}) > 0$.

A hyperplane is associated with each pair of limit-states, and the procedure can later be repeated; however, approximations by bounds tend to lead to larger restrictions.

Example

We consider the two limit-states in parallel:

$$Z_1: 0.800 u_1 - 0.600 u_2 + 3.0 = 0$$

$$Z_2: 0.100 u_1 - 0.995 u_2 + 3.5 = 0$$

Probability is obtained from the calculation of the bounds:

$$\rho = 0.677 \quad a = 1.996 \quad b = 0.857 \quad P(A) = 0.307 \times 10^{-4} \quad P(B) = 0.453 \times 10^{-4}$$

$$0.453 \times 10^{-4} \leq P_{f_sys} \leq 0.760 \times 10^{-4}$$

The value retained is the higher bound and:

$$\beta^E = -\Phi^{-1}(0.760 \times 10^{-4}) = 3.79$$

The exact value is $\beta^E = 3.83$, see Equation (9.12).

For the calculation of the hyperplane, an increment on u_1 is first introduced:

$$\beta_1(\varepsilon = 0.1) = 3.0 - \langle 0.800 - 0.600 \rangle \begin{Bmatrix} 0.1 \\ 0 \end{Bmatrix} = 2.92$$

$$\beta_2(\varepsilon = 0, 1) = 3.5 - \langle 0.100 - 0.995 \rangle \begin{Bmatrix} 0.1 \\ 0 \end{Bmatrix} = 3.49$$

which gives:

$$\rho = 0.677 \quad a = 2.06 \quad b = 0.76 \quad P(A) = 0.345 \times 10^{-4} \quad P(B) = 0.540 \times 10^{-4}$$

and hence $\beta^E(\varepsilon) = 3.75$ and $\bar{\alpha}_1^E = -0.38$.

By introducing an increment on the second variable u_2 :

$$\beta_1(\varepsilon = 0.1) = 3.0 - \langle 0.800 - 0.600 \rangle \begin{Bmatrix} 0 \\ 0.1 \end{Bmatrix} = 3.06$$

$$\beta_2(\varepsilon = 0.1) = 3.5 - \langle 0.100 - 0.995 \rangle \begin{Bmatrix} 0 \\ 0.1 \end{Bmatrix} = 3.60$$

which gives:

$$\rho = 0.677 \quad a = 2.08 \quad b = 0.85 \quad P(A) = 0.208 \times 10^{-4} \quad P(B) = 0.315 \times 10^{-4}$$

and hence $\beta^E(\varepsilon) = 3.88$ and $\bar{\alpha}_2^E = 0.90$. Finally, after standardizing, it becomes:

$$\alpha^E = \langle 0.39 \quad -0.92 \rangle$$

9.4 First-order system probability

A solution for parallel systems or series systems can be obtained from the multinormal density ϕ_n , with the hypothesis of a first order approximation on each component, where:

$$\phi_n(\{\hat{u}\}) = \frac{1}{(2\pi)^{n/2} \sqrt{\det[\rho]}} e^{-(1/2)\{\hat{u}\}^t [\rho]^{-1} \{\hat{u}\}}$$

is the Gauss multinormal density, for the n variables $\{\hat{u}\}$ standardized and centered but correlated with the matrix of correlation $[\rho]$ and:

$$\Phi_n(\{-\beta\}) = \int_{-\infty}^{-\beta_1} \int_{-\infty}^{-\beta_2} \cdots \int_{-\infty}^{-\beta_n} \phi_n(\{\hat{u}\}) d\beta_1 d\beta_2 \cdots d\beta_n$$

9.4.1 Parallel system

The probability of failure of a component $i, 1 \leq i \leq k$, is given from the hyperplane equation:

$$P(E_i) = \text{Prob}(\langle \alpha_i \rangle \{U\} + \beta_i \leq 0) = \Phi(-\beta_i)$$

and for the parallel system:

$$P(E) = P(\cap E_i) = \text{Prob}\left(\bigcap_{i=1}^k (\langle \alpha_i \rangle \{U\} + \beta_i \leq 0)\right)$$

Let us note that $\{\beta\}$ is the vector formed by the k reliability indexes of the components and $[\rho]$ is the matrix of the limit-state correlation coefficients. The variables $\langle \alpha_i \rangle \{U\} = V_i$ are standardized, reduced, centered but correlated variables, and:

$$P(E) = \text{Prob}(V_1 \leq -\beta_1, V_2 \leq -\beta_2, \dots, V_k \leq -\beta_k)$$

with:

$$P(E) = \int_{-\infty}^{-\beta_1} \int_{-\infty}^{-\beta_2} \cdots \int_{-\infty}^{-\beta_k} f_{\{V\}}(v_1, v_2, \dots, v_n) dv_1 dv_2 \cdots dv_k$$

where the random variables V_i are $\mathcal{N}(0, 1)$, and hence:

$$\text{Parallel system: } P(\cap E_i) = \Phi_k(-\{\beta\}; [\rho]) \quad (9.11)$$

9.4.2 Series system

In the same manner, it becomes:

$$P(E) = P(\cup E_i) = \text{Prob}\left(\bigcup_{i=1}^k (\langle \alpha_i \rangle \{U\} + \beta_i \leq 0)\right)$$

$$\text{Series system: } P(\cup E_i) = 1 - \Phi_k(\{\beta\}; [\rho])$$

9.4.3 Multinormal distribution function

Evaluation of Φ_2

In two dimensions, the Gaussian density is given by:

$$\phi_2(u_1, u_2; \rho) = \frac{1}{2\pi\sqrt{1-\rho^2}} \exp\left(-\frac{1}{2(1-\rho^2)}(u_1^2 + u_2^2 - 2\rho u_1 u_2)\right)$$

and the distribution function by:

$$\Phi_2(x_1, x_2; \rho) = \int_{-\infty}^{x_1} \int_{-\infty}^{x_2} \phi_2(u_1, u_2, \rho) du_1 du_2$$

To integrate this equation, we note [MKL86] that:

$$\frac{\partial^2 \Phi_2(x_1, x_2; \rho)}{\partial x_1 \partial x_2} = \frac{\partial \Phi_2(x_1, x_2; \rho)}{\partial \rho}$$

and it then becomes:

$$\begin{aligned}\Phi_2(x_1, x_2; \rho) &= \Phi_2(x_1, x_2; 0) + \int_0^\rho \left. \frac{\partial \Phi_2(x_1, x_2; \lambda)}{\partial \lambda} \right|_{\lambda=t} dt \quad \rho > 0 \\ \Phi_2(x_1, x_2; \rho) &= \Phi(x_1) \Phi(x_2) + \int_0^\rho \phi_2(x_1, x_2; t) dt \quad \rho > 0\end{aligned}\tag{9.12}$$

and likewise:

$$\Phi_2(x_1, x_2; \rho) = \Phi(x_1) \Phi(x_2) - \int_\rho^0 \phi_2(x_1, x_2; t) dt \quad \rho < 0$$

This equation contains no more than a simple integral. It can be evaluated by numerical integration.

Another solution uses a Hermite polynomial expansion:

$$\begin{aligned}H_0(x) &= 1 \\ H_1(x) &= x \\ H_2(x) &= x^2 - 1 \\ H_k(x) &= x H_{k-1}(x) - (k-1) H_{k-2}(x) \\ \Phi_2(x_1, x_2; \rho) &= \Phi(x_1) \Phi(x_2) \\ &\quad + \frac{1}{2\pi} e^{(-(x_1^2/2+x_2^2/2))} \sum_{i=1}^{\infty} \frac{\rho^i}{i!} H_{i-1}(x_1) H_{i-1}(x_2)\end{aligned}$$

by retaining about 20–30 terms.

Some useful equations:

$$\begin{aligned}\Phi_2(x_1, x_2; \rho = 0) &= \Phi(x_1) \Phi(x_2) \\ \Phi_2(x_1, x_2; \rho = -1) &= \begin{cases} 0 & \text{if } x_1 + x_2 \leq 0 \\ 1 - \Phi(-x_1) - \Phi(-x_2) & \text{if } x_1 + x_2 \geq 0 \end{cases} \\ \Phi_2(x_1, x_2; \rho = +1) &= 1 - \Phi(\max(-x_1, -x_2, 0))\end{aligned}$$

Evaluation of Φ_k

Hohenbichler approximation: Hohenbichler gives a recurrence formulation [Rac89], [HR85], [TCM86]:

$$\begin{aligned} \Phi_k & \left(\left\{ \begin{array}{c} x_1 \\ x_2 \\ \vdots \\ x_k \end{array} \right\}; \left[\begin{array}{cccc} \rho_{11} & \rho_{12} & \cdots & \rho_{1k} \\ \rho_{21} & \rho_{22} & \cdots & \rho_{2k} \\ \vdots & \vdots & \ddots & \dots \\ \rho_{k1} & \rho_{k2} & \cdots & \rho_{kk} \end{array} \right] \right) \\ & \approx \Phi(x_1) \Phi_{k-1} \left(\left\{ \begin{array}{c} x_2^E \\ \vdots \\ x_k^E \end{array} \right\}; \left[\begin{array}{ccc} \rho_{22}^E & \cdots & \rho_{2k}^E \\ \vdots & \ddots & \dots \\ \rho_{k2}^E & \cdots & \rho_{kk}^E \end{array} \right] \right) \end{aligned}$$

where the terms x_i^E and ρ_{ij}^E are obtained by a linearization procedure.

The expression $\Phi_k(\{x\}; [\rho])$ is the probability:

$$\begin{aligned} \Phi_k(\{x\}; [\rho]) & = \text{Prob}(Z_1 \leq x_1, Z_2 \leq x_2, Z_3 \leq x_3, \dots, Z_k \leq x_k) \\ & = \text{Prob}\left(\bigcap_{i=1}^k Z_i \leq x_i\right) \end{aligned}$$

where the random variables Z_i are standardized but correlated. The probability of the intersection is split:

$$\text{Prob}\left(\bigcap_{i=1}^k Z_i \leq x_i\right) = \text{Prob}\left(\bigcap_{i=2}^k (Z_i \leq x_i) \mid Z_1 \leq x_1\right) \text{Prob}(Z_1 \leq x_1)$$

To decorrelate the random variables, it is sufficient to use the Cholesky decomposition:

$$[\rho] = [L] [L]^t \rightarrow Z_i = \sum_{j=1}^k l_{ij} U_j$$

where the random variables U_j constitute a vector of k independent random variables, not to be confused with the vector of n random variables of standardized space. It becomes:

$$\Phi_k(\{x\}; [\rho]) = \text{Prob}\left(\bigcap_{i=2}^k \left(\sum_{j=1}^i l_{ij} U_j \leq x_i \right) \mid U_1 \leq x_1\right) \text{Prob}(U_1 \leq x_1) \quad (9.13)$$

by noting that $Z_1 = U_1$ because $l_{11} = 1$ and $l_{1j} = 0$, for any $j \neq 1$. The summation on j is limited to i because $l_{ij} = 0$ if $j > i$. The condition $U_1 \leq x_1$

affects only the first variable. A distribution function of a variable V_1 , including such a condition, is:

$$\begin{aligned} F_{V_1}(v_1 | U_1 \leq x_1) &= \text{Prob}(U_1 \leq v_1 | U_1 \leq x_1) \\ &= \frac{\text{Prob}((U_1 \leq v_1) \cap (U_1 \leq x_1))}{\text{Prob}(U_1 \leq x_1)} = \frac{\Phi(v_1)}{\Phi(x_1)} \end{aligned}$$

It is necessary to take into account the maximum at 1 of the function and note finally:

$$F_{V_1}(v_1 | U_1 \leq x_1) = \min\left(\frac{\Phi(v_1)}{\Phi(x_1)}, 1\right)$$

Let:

$$F_{V_1}(v_1 | U_1 \leq x_1) = \Phi(u_1) = \min\left(\frac{\Phi(v_1)}{\Phi(x_1)}, 1\right)$$

which introduces a new standardized auxiliary variable. V_1 is then replaced by:

$$V_1 = \Phi^{-1}(\Phi(U_1) \Phi(x_1))$$

Expression (9.13) becomes, by substituting V_1 for $U_1 | U_1 \leq x_1$:

$$\begin{aligned} \Phi_k(\{x\}; [\rho]) &= \text{Prob}\left(\bigcap_{i=2}^k \left(l_{i1}V_1 + \sum_{j=2}^i l_{ij}U_j\right) \leq x_i\right) \text{Prob}(U_1 \leq x_1) \\ \Phi_k(\{x\}; [\rho]) &= \text{Prob}\left(\bigcap_{i=2}^k \left(l_{i1}\Phi^{-1}(\Phi(U_1) \Phi(x_1)) + \sum_{j=2}^i l_{ij}U_j\right) \leq x_i\right) \Phi(x_1) \end{aligned}$$

Each expression:

$$l_{i1}\Phi^{-1}(\Phi(U_1) \Phi(x_1)) + \sum_{j=2}^i l_{ij}U_j \leq x_i$$

is a limit-state i (non-linear with respect to U_1) of the variables U_j for which it is possible to find the distance x_i^E and the direction cosines $\{\alpha_i^E\}$ at the nearest point, which amounts to linearizing the limit-state in the form:

$$l_{i1}\Phi^{-1}(\Phi(U_1) \Phi(x_1)) + \sum_{j=2}^i l_{ij}U_j \leq x_i \approx -\{\alpha_i^E\}\{U\} \leq x_i^E$$

and the correlation matrix is given by the coefficients $\rho_{ij}^E = \{\alpha_i^E\}^t \{\alpha_j^E\}$.

It remains for us to choose the point of linearization. The problem:

to find $\{u^*\}$ which minimizes $d = \sqrt{\{u\}^t \{u\}}$

under the constraints $H_i(\{u\}) \leq 0$ with $i = 1, 2, \dots, n$

defines the domain of admissible solutions by the intersection of the failure domains: that is, $(H_1 \leq 0) \cap (H_2 \leq 0) \cap \dots \cap (H_k \leq 0)$. Generally, not all the limit-states are active at the minimum (i.e. $H_i(\{u^*\}) = 0$; with $1 \leq i \leq k$). In this case, we assume that the weight of inactive limit-states is neglected. Better precision is obtained by linearizing the active limit-states at point $\{u^*\}$ and by linearizing each of the inactive limit-states at the nearest point to $\{u^*\}$ belonging to the corresponding failure domain. This approach is illustrated in Section 9.6.3.

Simulation methods: once the problem is posed in standardized variable space, there is no further obstacle to the use of direct simulation methods, which can be implemented with a large number of outcomes. A now somewhat old procedure was proposed by [FMTE81] and a more recent approach is presented in [ADKOS98]. A technique of conditioning by importance sampling has been explored by [MK03].

9.5 Second-order system probability

Just as in the study of components, a second-order SORM approximation is proposed. Let us consider the intersection of k limit-states $H_i(\{u\})$ defined in multinormal space with n random variables. We are interested in the probability of the intersection of these limit-states: $\text{Prob}(\bigcap_{i=1}^k H_i(\{u\}) \leq 0)$. Let us suppose that there is a unique design point $\{u^*\}$ on the limit of domain $\mathcal{D}_f \in \mathbb{R}^n$ (the origin of the reference does not belong to \mathcal{D}_f) and that the following hypotheses are true:

1. For $\{u^*\}$ unique $\in \mathcal{D}_f$ and $\beta = \|u^*\| > 0$, we define the domain $\mathcal{D}_f^* \subset \mathcal{D}_f$ by the vicinity of $\{u^*\}$ in the failure domain and, by supposing that $H_i(\{u\})$ are twice derivable in $\{u^*\}$, it becomes:

$$H_r(\{u^*\}) = 0 \quad \text{for } r = 1, 2, \dots, p \text{ and } 1 \leq p \leq k$$

$$H_s(\{u^*\}) < 0 \quad \text{for } s = p + 1, \dots, k$$

$$\mathcal{D}_f \cap \mathcal{D}_f^* = \left(\bigcap_{i=1}^k H_i(\{u\}) \right) \bigcap \mathcal{D}_f^*$$

where $H_r(\{u\})$ are the limit-states passing through $\{u^*\}$ (i.e. active limit-states) and $H_s(\{u\})$ are the inactive limit-states; p is the number of active limit-states. Figure 9.12 shows the example of three limit-states of which two are active (H_1 and H_3) and one is inactive.

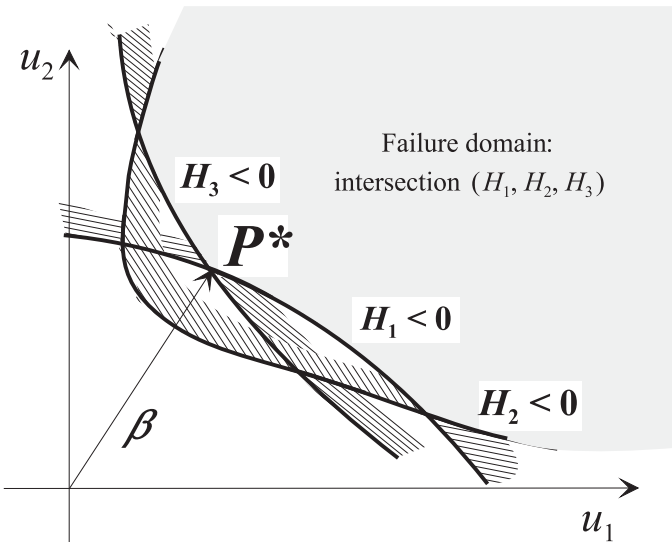


Figure 9.12 Intersection of limit-states and design point P^* ; H_1 and H_3 are active and H_2 is inactive.

2. The gradient vectors of the active limit-states are linearly independent. It results that $k \leq n$ and $\{\nabla H_r\} \neq \{0\}$ for $r = 1, 2, \dots, p$ and $1 \leq p \leq k$.
3. For $p+1 \leq i \leq n$, we can carry out an acceptable orthogonalization of the system so that $\partial H_r / \partial u_i = 0$ for $r = 1, 2, \dots, p$ with $1 \leq p \leq k$ (if $p = n$, this condition disappears). The resulting system takes the form:

$$\frac{\partial H_r}{\partial u_i} = \begin{bmatrix} \partial H_1 / \partial u_1 & \cdots & \partial H_1 / \partial u_p & 0 & \cdots & 0 \\ \vdots & \ddots & \vdots & \vdots & \ddots & \vdots \\ \partial H_p / \partial u_1 & \cdots & \partial H_p / \partial u_p & 0 & \cdots & 0 \end{bmatrix}$$

4. According to the extreme Lagrange conditions, the minimum point is a linear combination of the gradients of the active limit-states:

$$\{u^*\} = \sum_{r=1}^p \lambda_r \{\nabla H_r\} \quad \text{with } \lambda_r < 0 \text{ (if the origin } O \notin \mathcal{D}_f \text{) and } 1 \leq p \leq k$$

The works of Breitung (see Section 7.4.1) and of Hohenbichler *et al.* [HGKR84, Hoh84, HR83] lead to the following theorem.

Theorem 4. *For an affine transformation of the failure domain, $b\mathcal{D}_f \equiv \{b\{u\} : \{u\} \in \mathcal{D}_f\}$ (b being the affinity factor) and with $d = \det([I] - [D]) > 0$*

$(d_{ij} = \sum_{r=1}^p \lambda_r \partial^2 H_r / \partial u_i \partial u_j \text{ with } i, j = 1, 2, \dots, n)$, we have:

$$\lim_{b \rightarrow \infty} \frac{\text{Prob}[b \mathcal{D}_f]}{\Phi_p(-b\{\beta\}; [\rho])} = \frac{1}{\sqrt{d}} \quad (9.14)$$

with:

$$\beta_i = -\frac{\{\nabla H_i\}^t}{\|\nabla H_i\|} \{u^*\} \quad \text{and} \quad \rho_{ij} = \frac{\{\nabla H_i\}^t \{\nabla H_j\}}{\|\nabla H_i\| \|\nabla H_j\|} \quad \text{for } 1 \leq i, j \leq p$$

Let us write $\hat{\mathcal{D}}_f$, the failure domain given by the linearization of the limit-states; $\hat{\mathcal{D}}_f \equiv \bigcap_{r=1}^p (\{\nabla H_r\}^t (\{u\} - \{u^*\}) \leq 0)$; we have, therefore:

$$\text{Prob}\left[b \hat{\mathcal{D}}_f\right] = \Phi_p(-b\{\beta\}; [\rho])$$

By defining domain D_1 by the affine transformation $\mathcal{D}_1 = (1/b)\mathcal{D}_f$, as the asymptotic limit $(1/\sqrt{d})$ is not a function of the affinity factor b , Hohenbichler deduces:

$$\text{Prob}[\mathcal{D}_f] \approx \text{Prob}\left[\hat{\mathcal{D}}_f\right] \frac{1}{\sqrt{d}} = \Phi_p(-\{\beta\}; [\rho]) \frac{1}{\sqrt{d}} \quad (9.15)$$

When $\beta_i \rightarrow \infty$, the asymptotic approximation [Rub64] $\Phi(-\beta_i) \sim \phi(\beta_i)/\beta_i$ permits us to rewrite the previous expression:

$$\text{Prob}[\mathcal{D}_f] \approx \phi_p(-\{\beta\}; [\rho]) \frac{1}{\sqrt{d}} \prod_{j=1}^p \frac{1}{([\rho]^{-1}\{\beta\})_j}$$

where $(\cdot)_j$ indicates the j th component of the vector $[\rho]^{-1}\{\beta\}$.

Special case: a single limit-state is considered ($k = p = 1$). It becomes:

$$d_{ij} = \lambda_1 \frac{\partial^2 H_1}{\partial u_i \partial u_j}$$

$$d = \det([I] - \lambda_1 [\nabla^2 H_1]) = \det \begin{bmatrix} \ddots & & \\ & \delta_{ii} - \lambda_1 \kappa_{ii} & \\ & & \ddots \end{bmatrix} = \prod_{i=1}^n (1 - \lambda_1 \kappa_{ii})$$

if $[\nabla^2 H]$ is expressed as the main values κ_{ii} . To retrieve the Breitung formula (7.20) established for a parabolic form, it is sufficient to note that:

- $\kappa_{nn} = 0$ because of the parabolic form for which the coefficient of u_n^2 is zero,

- $\{u^*\} = \lambda_1 \{\nabla H_1\} = -\beta_1 \{\alpha_1\} = -\beta_1 (\{\nabla H_1\}/\|\nabla H_1\|)$, hence $\lambda_1 = -\beta_1$ by choosing H_1 standardized ($\|\nabla H_1\| = 1$). It then becomes:

$$P_f \approx \Phi(-\beta) \left(\prod_{i=1}^{n-1} \frac{1}{\sqrt{1 + \beta \kappa_{ii}}} \right)$$

This approach is illustrated in Section 9.6.4.

9.6 System of two bars in parallel

This example illustrates the concepts presented in this chapter. It concerns two bars placed in parallel from the point of view of the mechanical system. The data and results are summarized in Figure 9.13.

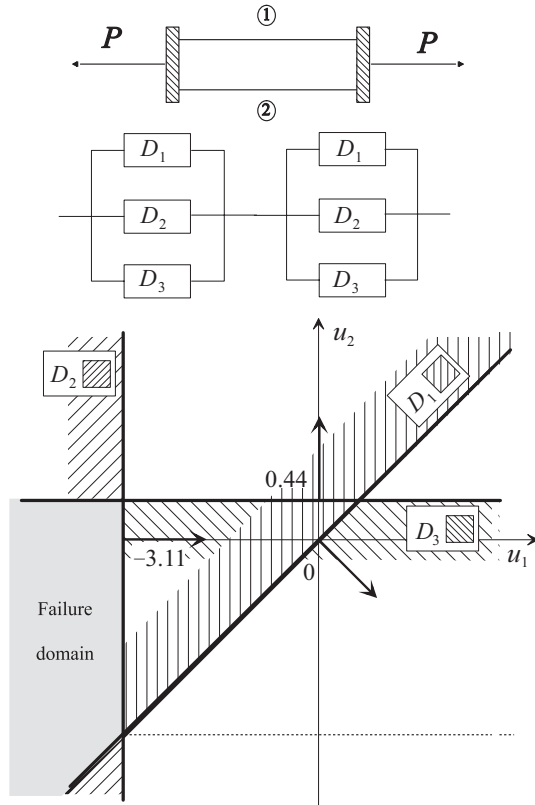


Figure 9.13 System of two parallel bars (the shaded domain is the failure domain).

9.6.1 Statement of the problem and data

The system is submitted to a traction P . The two bars ($i = 1, 2$) have a cross-section A_i and a resistance equal to R_i . These are non-correlated Gaussian random variables of the same mean and of the same standard deviation. This choice is retained only for the convenience of calculation. The system operates in the following manner:

- In the normal operating state, each bar transmits half of the traction:

$$r_1 > p/2 \quad \text{and} \quad r_2 > p/2$$

- The first failure is the rupture of *one or the other of the bars* by reaching the resistance; this is a fragile rupture in traction, and the residual resistance is zero. The degraded functioning of the system is then given by:

$$r_1 = 0 \quad \text{and} \quad r_2 > p \quad (\text{rupture of 1})$$

or otherwise:

$$r_2 = 0 \quad \text{and} \quad r_1 > p \quad (\text{rupture of 2})$$

The small letters designate outcomes of the random variables.

- Failure of the system is obtained when there is successive rupture of both bars.

The numerical data are given in Table 9.1. The reduced variables are associated with physical variables in the following order: R_1 and U_1 , R_2 and U_2 , P and U_3 .

Variable		Mean	Standard deviation
Resistance bar 1	R_1	75	11.25
Resistance bar 2	R_2	75	11.25
Traction	P	80	20

Table 9.1 Random variables.

First part: failure of a bar

1. We assume the first failure is the rupture of bar 1. Calculate the index β , the failure probability and the direction cosines of the tangent hyperplane at the most probable failure point.
2. For the first failure to be the rupture of bar 1, it is necessary that $r_2 > r_1$. What is the probability of the event $r_2 > r_1$? Give a frame of the probability of the event: $\{\text{rupture of the bar 1}\} \cap \{r_2 > r_1\}$.

3. The first failure is the rupture of one or other of the bars. Show that it is a matter of a series system from the reliability point of view; calculate the probability bounds of the first failure.

Second part: failure of the system

We call the rupture of the two bars *failure of the system*. To simplify, variable P is taken to be deterministic and equal to its mean:

1. The first failure mode is the rupture of bar 1 and then that of bar 2. Represent in the plane u_1, u_2 , the three limit-states (hyperplanes) corresponding to this mode. For each of these limit-states, give the values of β , P_f and the direction cosines. Represent the domain corresponding to the failure events. Deduce the probability.
2. The failure of the system occurs according to mode 1 or 2: rupture of 1 then 2 or rupture of 2 then 1. Give a representation of a chain of elementary events in series and in parallel. Write the expression of failure probability as a function of the indexes β , of the correlation coefficients and of the multinormal distribution function.

9.6.2 Solution

Rupture of bar 1

It is characterized by:

$$r_1 - p/2 = 0$$

Suppose, by carrying out a change of variables:

$$11.25u_1 - 10u_3 + 75 - 40 = 0$$

Then:

$$0.7474u_1 + 0u_2 - 0.6644u_3 + 2.3253 = 0$$

Hence:

$$\beta = 2.3253 \quad \langle \alpha \rangle = \langle 0.7474 \mid 0 \mid -0.6644 \rangle \quad P_f = 0.010028 \quad (9.16)$$

Rupture of 1 and $r_2 > r_1$

The probability of the event $r_2 > r_1$ is 0.5 because the two variables have the same Gaussian distribution, with the same parameters. The corresponding limit-state is:

$$r_1 - r_2 = 0$$

and, by carrying out the change of variables:

$$\begin{aligned} u_1 - u_2 &= 0 \\ 0.7071 u_1 - 0.7071 u_2 &= 0 \end{aligned}$$

Hence:

$$\beta = 0 \quad \langle \alpha \rangle = \langle 0.7071 | -0.7071 | 0 \rangle \quad P_f = 0.5 \quad (9.17)$$

There is rupture of 1 in the first place, with $r_2 > r_1$. It is necessary that the two events $\{E_2: r_1 \leq p/2\}$ and $\{E_1: r_2 > r_1\}$ be verified. It is a question of a parallel combination whose bi-modal bounds are calculated from (9.16) and (9.17). The events are correlated, $\rho = 0.5284$ and:

$$0.00929 \leq P(E_1 \cap E_2) \leq 0.01080$$

First failure

The first failure is the rupture of *either* of the bars. This is a series system whose two events are exclusive by the condition of the event E_1 and:

$$\begin{aligned} \text{Prob(first failure)} &= \text{Prob(rupture 1)} \cup \text{Prob(rupture 2)} \\ \text{Prob(first failure)} &= \text{Prob(rupture 1)} + \text{Prob(rupture 2)} \\ 0.0186 &\leq \text{Prob(first failure)} \leq 0.0216 \end{aligned}$$

By way of verification, 100,000 Monte Carlo simulations gives the following result:

$$P_f = 0.0191 \quad \text{with an interval of } 4.5\%$$

Rupture of 1 then 2

Three events in parallel are necessary:

1. E_2 : resistance r_1 is lower than $p/2$,
2. E_1 : resistance r_1 is lower than r_2 ,
3. E_3 : resistance r_2 is lower than p .

$$E_2 : r_1 \leq p/2 \quad E_1 : r_1 \leq r_2 \quad E_3 : r_2 \leq p$$

which correspond to the three straight lines of the plane:

$$\begin{aligned} D_2 : u_1 + 3.111 &= 0 \quad \beta = 3.111 \quad P_f = 0.000932 \\ D_1 : u_1 - u_2 &= 0 \quad \beta = 0 \quad P_f = 0.5 \\ D_3 : u_2 - 0.444 &= 0 \quad \beta = -0.444 \quad P_f = 0.67164 \end{aligned}$$

In Figure 9.13, the hatched domains D_1 , D_2 and D_3 represent the safety domains for each event. There is a failure in the non-hatched domain where all the events are failures. Its probability must be calculated. From geometric considerations, this is obtained from:

$$P_f = P(E_2)P(E_3) - \frac{1}{2}P(E_2)P(E_2) = 0.000625 \quad (9.18)$$

In this expression, the correction given by the second term is negligible.

Failure of the system

Failure is the rupture of 1 and then 2 or of 2 and then 1, which are exclusive events. Figure 9.13 can be completed by symmetry and the two failure domains do not intersect. The probability of failure (failure of two bars) is therefore equal to 2×0.000625 , or 0.00125.

Simulations of 100,000 events give 0.00124 ($\pm 18\%$); this first result is unexpired-for! A second trial gives 0.00128.

The representation of the combination of events is given in Figure 9.13, noting \bar{D}_1 , \bar{D}_2 , \bar{D}_3 , the failure events by rupture of 2 and then 1.

9.6.3 First-order solution

The probability of failure of the system is also given by:

$$P_{f_sys} = 2\Phi_3 \left(\begin{Bmatrix} -\beta_1 = 0 \\ -\beta_2 = -3.111 \\ -\beta_3 = 0.444 \end{Bmatrix}; \begin{bmatrix} 1 & 0.707 & -0.707 \\ 0.707 & 1 & 0 \\ -0.707 & 0 & 1 \end{bmatrix} \right)$$

The Cholesky decomposition gives:

$$[L] = \begin{bmatrix} 1 & 0 & 0 \\ 0.707 & 0.707 & 0 \\ -0.707 & 0.707 & 0 \end{bmatrix}.$$

We try to calculate:

$$\begin{aligned} & \text{Prob}[D_1 \leq -\beta_1, D_2 \leq -\beta_2, D_3 \leq -\beta_3] \\ &= \text{Prob} \left[\bigcap_{i=1}^3 (D_i \leq -\beta_i) \right] = \text{Prob} \left[\bigcap_{i=1}^3 \left(\sum_{j=1}^i l_{ij} U_j \leq -\beta_i \right) \right] \\ &= \text{Prob} \left[\bigcap_{i=2}^3 \left(\sum_{j=1}^i l_{ij} U_j \leq -\beta_i \right) | (U_1 \leq -\beta_1) \right] \text{Prob} [U_1 \leq -\beta_1] \\ &= \text{Prob} \left[\begin{array}{l} (l_{21}U_1 + l_{22}U_2 \leq -\beta_2) \cap \\ (l_{31}U_1 + l_{32}U_2 + l_{33}U_3 \leq -\beta_3) \end{array} | (U_1 \leq -\beta_1) \right] \text{Prob} [U_1 \leq -\beta_1] \end{aligned} \quad (9.19)$$

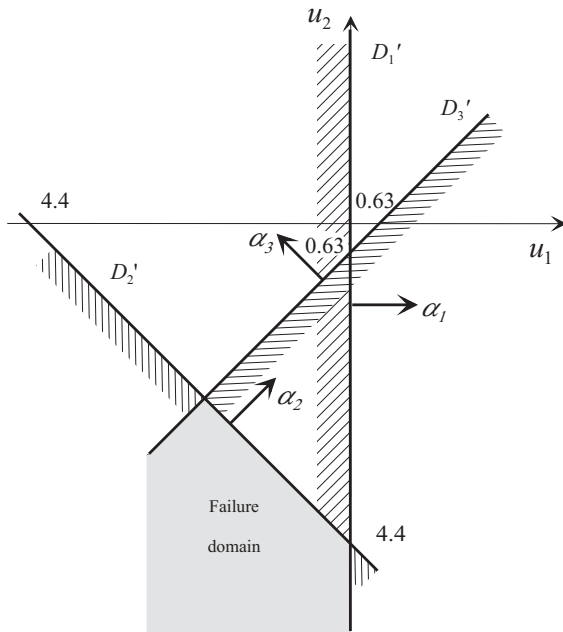


Figure 9.14 Representation of three limit-states defined by Equation (9.19).

Figure 9.14 gives the representation of straight lines contained in expression (9.19).

As:

$$\text{Prob} [(U_1 \leq v_1) | (U_1 \leq -\beta_1)] = \frac{\Phi(v_1)}{\Phi(-\beta_1)}$$

$$V_1 = \Phi^{-1} (\Phi(-\beta_1) \Phi(U_1))$$

and:

$$\Phi_3(\dots) = \Phi(-\beta_1) \text{Prob} [(D_2'' \leq 0) \cap (D_3'' \leq 0)]$$

$$D_2'' = l_{21} \Phi^{-1} (\Phi(-\beta_1) \Phi(U_1)) + l_{22} U_2 + \beta_2 \quad (9.20)$$

$$D_3'' = l_{31} \Phi^{-1} (\Phi(-\beta_1) \Phi(U_1)) + l_{32} U_2 + \beta_3 \quad (9.21)$$

The limit-states D_2'' and D_3'' lead to the following solutions:

1. D_2'' active and D_3'' inactive: $\beta_{2'} = 2.915$ and $\langle U \rangle = \langle -1.954; -2.164 \rangle$, linearization point P_2^* in Figure 9.15,
2. D_2'' violated (because $P_3^* \notin \mathcal{D}_f$) and D_3'' active: $\beta_{3'} = 0.040$ and $\langle U \rangle = \langle 0.021; -0.034 \rangle$ linearization point P_3^* in Figure 9.15,

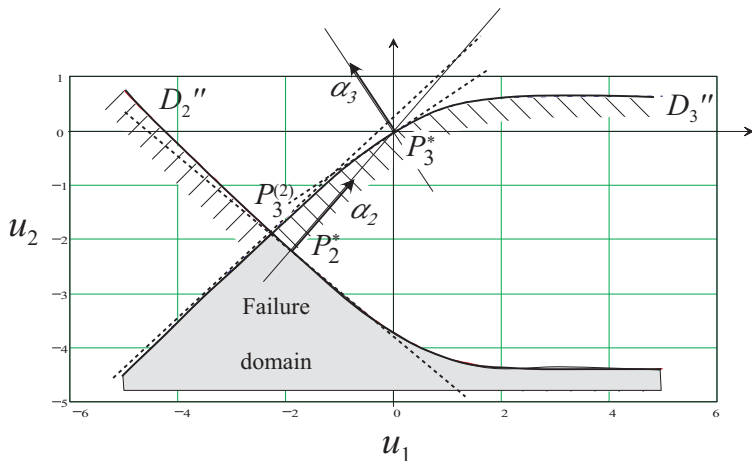


Figure 9.15 Representation of limit-states D_2'' and D_3'' and choice of linearization points.

3. D_2'' active and D_3'' active: $\beta_{23} = 2.917$ and $\langle U \rangle = \langle -1.973; -2.148 \rangle$, linearization point $P_3^{(2)}$ in Figure 9.15.

The limit-states are linearized at their design points (respectively P_2^* and P_3^*):

$$\begin{aligned} D_2'' &\approx 0.670 u_1 + 0.742 u_2 + 2.915 \quad \text{at point } P_2^* \\ D_3'' &\approx -0.528 u_1 + 0.849 u_2 + 0.040 \quad \text{at point } P_3^* \end{aligned}$$

As the design point P_2^* is not on $D_3'' = 0$, the limit-state D_3'' is not taken into account and the approximation of P_{f_sys} is given by:

$$P_{f_sys} = 2 \Phi(-\beta_1) \Phi(-\beta_{2'}) = 0.00178$$

This result is poor, because the inactive limit-state is completely ignored, but as it is close to P_2^* , its weight is not negligible, contrary to the basic hypothesis in the theory proposed by Hohenbichler *et al.* [HR83].

To improve accuracy, the inactive limit-state D_3'' can be linearized at the nearest point to the global minimum P_2^* belonging to the failure domain ($D_3'' = 0$) $\cap (D_2'' \leq 0)$. This is the intersection of two curves, point $P_3^{(2)}$ in Figure 9.15. It then becomes:

$$D_3'' \approx -0.677 u_1 + 0.736 u_2 - 0.139 \quad \text{with } \beta_{3''} = -0.139 \quad \text{at point } P_3^{(2)}$$

The coefficient of correlation of D_2'' and D_3'' linearized is $\rho = 0.0934$ and:

$$P_{f\text{-sys}} = 2\Phi(-\beta_1)\Phi_2\left(\begin{Bmatrix} -\beta_{2'} \\ -\beta_{3''} \end{Bmatrix}; \begin{bmatrix} 1 & \rho \\ \rho & 1 \end{bmatrix}\right) = 0.00119$$

Figure 9.15 shows that the curvatures are weak at the design point. However, a last improvement is obtained taking this into account through the second-order correction.

9.6.4 Second-order solution

In P_2^* , the curvature of D_2'' is given by $\kappa_2 = -0.0238$ and that of D_3'' in $P_3^{(2)}$ by $\kappa_3 = 0.0184$. These curvatures are those of osculating parabolas.

Linearization point P_2^ only:* given that only D_2'' is active at the design point, we have:

$$\begin{aligned} k = 2 \quad p = 1 \quad \Rightarrow \quad \lambda_1 &= -2.915 \\ \Rightarrow \quad d &= 1 - [(-2.915) \times (-0.0238)] = 0.9305 \quad \Rightarrow \quad \sqrt{d} = 0.9646 \end{aligned}$$

$$P_f = \Phi_p(-\{\beta\}; [\rho]) \frac{1}{\sqrt{d}} = \frac{0.00178}{0.9646} = 0.00184$$

Linearization points P_2^ and $P_3^{(2)}$:* the two limit-states are active. D_3'' presents a negative reliability index. It becomes:

$$\begin{aligned} k = 2 \quad p = 2 \quad \Rightarrow \quad \lambda_1 &= -2.915 \\ \lambda_2 &= 0.139 \\ \Rightarrow \quad d &= 1 - [(-2.915) \times (-0.0238) + (0.139) \times (0.0184)] \\ P_f = \Phi_p(-\{\beta\}; [\rho]) \frac{1}{\sqrt{d}} &= \frac{0.00119}{0.9633} = 0.00124 \end{aligned}$$

This result is very close to the theoretical solution (1.25×10^{-3}). It is obtained by the linearization of D_2'' in P_2^* and that of D_3'' in $P_3^{(2)}$. Another approximate solution would be obtained by linearizing the two limit-states in $P_3^{(2)}$. It is proved to be less accurate ($P_f = 1.20 \times 10^{-3}$). It is noted that the curvatures of two limit-states are of opposite signs in $P_3^{(2)}$.

9.6.5 Conclusion of the illustration

This example has illustrated the implementation of the methods proposed in this chapter. It is particularly severe because it introduces into the retained formulation a high-probability failure which requires a special discussion. The final result obtained by the FORM and SORM approximation methods is satisfactory.

9.7 Conclusion

System reliability, through the approach presented in this chapter, deals with simple compositions with a few components capable of being complex. As for operating safety methods, such as RAMS, these are more suitable for a complex composition of simple components and it is to such methods that we must resort in the case of large systems.

This chapter first recalled the necessity of a thorough analysis of the failure modes and emphasized that different models of representation lead to identical results after more or less simple calculations. Hence it is important to be vigilant in the choice of calculations.

The results on the bounds present a undeniable interest since they allow a rapid approximation which is sometimes sufficient, as well as a consistency check for the values derived from more complex methods.

The FORM approximation approach is now robust, the only difficulty being the calculation of the multinormal distribution function Φ_n for which the best solutions are now found in simulation, which represents a negligible cost when the calculation is performed in standardized space. Linearization methods have shown the difficulty of going beyond the FORM approximation.

This page intentionally left blank

Chapter 10

‘Safety’ Coefficients

The title of this chapter uses a vocabulary devoted to a concept that does not exist. A *safety* coefficient only denotes a number, which, associated with data selection, a failure scenario and a rule, generally results in a satisfactory design. It is validated by positive experience feedback. The coefficient does not measure safety. It is politically correct, as it draws on a positive and reassuring vocabulary. In reality, it is all our ignorance and all our uncertainties that are masked. The plural already introduces a part of the point of view developed in this chapter, which shows how safety can be evaluated and associated with the knowledge of coefficients, particularly *partial* coefficients.

10.1 Bases of design

10.1.1 General information

From the time when man became aware that there could be a defect in a design, in other words, ever since the time a tree placed across a stream snapped when a prehistoric man heavier than the tribe’s average weight walked on it, empirical and theoretical knowhow has advanced through trial and error (e.g. in the construction of cathedrals). The quest for safety coefficients is almost as old as the world, and Randall [Ran76] traces it back to the Egyptian Imhotep, about 2700 B.C.

Today, increasingly audacious technical challenges are made reasonable by the simultaneous recourse to algorithmic knowledge (resulting from reasoning) and heuristic knowledge (resulting from experience).

If algorithmic knowledge is progressing, it nonetheless remains and will always remain unsatisfactory. Everyday experience and feedback are the most essential elements of our collective knowhow. To preserve the memory of experience, to achieve the widest possible dissemination of algorithmic knowledge and to lay down prescriptions that must be respected by the various parties involved in a design, a construction or an industrial product, the knowhow is codified in open-ended documents: regulations and standards.

- A *regulation* is a set of prescriptions stipulated by an authority. It applies to all. For example, the French regulations on civil constructions are promulgated by the government.
- A *standard* is also a set of prescriptions that are established between the parties concerned. They codify a practice common to partners of the same profession. For example, we can cite the French standards published by the French Association for Standardization (AFNOR).

This basic distinction is tending to fade with a debate that has become international and European. The International Organization for Standardization (ISO) publishes normative texts. Among these, we must note the reference [ISO86] on the reliability of constructions for its historical interest and for its Appendix B stating the first principles. These texts are regularly updated. The European Union, through the European Committee for Standardization (CEN), has launched a vast project for the drafting of *Eurocodes* (CEN/TC 250) which, eventually, will harmonize the practices of the various countries [Cal96]. There are also a very large number of texts specific to products, for example, the French code for the construction of pressure vessels (CODAP).

These texts will guide the designer in the process, that is, in the choice of the values of design variables that help meet a functional objective while respecting constraints regarding the reliability level associated with this design. For this, he must make two decisions:

1. Choice of one (or more) failure scenario(s), each being represented by a set of design equations that can be very simple (e.g. $R - S > 0$) or very complex if they result from numerical solutions of partial differential equations, for example.
2. Choice of design values, that is the values to be taken into account in the application of the equations and to forecast values in production. It is this point that will be discussed in this chapter.

Design is therefore the association of a mechanical model, a data set and a decision on the values to give to the parameters in order to meet all the constraints.

10.1.2 Values associated with a variable

As indicated above, and according to the model whose formulation is represented by Equations (10.1), (10.2), (10.24), the design rules use particular values of variables that are either *representative values*, or *design values* or partial coefficients. A typology of these special values is given below. It systematizes, in the form of a table (Figure 10.1), which is used in the Eurocodes¹ [AFN96].

¹ Eurocodes seek to build a set of European standards for civil construction. Documents for national application are under preparation in the various countries.

Names of particular values associated with a variable			Examples of characteristic values
x_{rep}	x_k	Nominal values x_n	- dimension $x_k = d_n$ - yield limit $x_k = f_{yn}$
		Statistical content values	- mathematical expectation: $x_k = E[X]$ - p -fractile: $x_k = x_p$ with $\text{Prob}(X < x_p) = p$
		Combination values (actions only): $x_{comb} = \Psi x_k$	
			Design values: $x_d = \gamma x_{rep}$ (actions) or $x_d = x_{rep} / \gamma$ (resistances)

Figure 10.1 Representative values and design values of a variable. To comply with the notation used in this book, particular outcomes of random variables are written in lower case.

Representative values

These are either characteristic values x_k or combination values x_{comb} .

Characteristic values: these are the main representative values of the variables. Characteristic values are subdivided into *nominal values* x_n and *values with statistical content*. They are familiar to the designer and are introduced into the rules in conjunction with γ coefficients, called *partial coefficients* and Ψ -values (for combinations).

Nominal values: a nominal value is a value assigned to a quantity by the project or imposed on the designer by the code or the regulation. This is the case with dimensions, appearing on a plan or a catalog, or the yield limit values to be taken into account for the material. For example, steel of grade E 24: $f_{yn} = 235$ MPa; it is possible to impose tolerances on it.

Values with statistical content: values with statistical content are the main characteristic values. They are evaluated based on a more or less rich knowledge of random variable distributions: it is sometimes possible to have a complete stochastic description – known or assumed – of these variables, that is, of the joint distribution $f_{\{X\}}(\{x\})$. More often, we only know the marginal distribution of each variable and the correlations, or, otherwise, only the estimates of various statistical moments. Variables with statistical content can also, depending on the case, be:

- characteristics of central tendency or their estimates. For example:
 - a. the mathematical expectation of the variable $x_k = E[X]$,
 - b. an outcome of the estimate of the mathematical expectation of the variable. If $x_i, i = 1, \dots, n$ is a sample of n independent outcomes of X , then the estimate is $x_k = (\sum_{i=1}^n x_i/n)$,
- Shifted values (to the top or to the bottom) of the variable:
 - c. a p -fractile: $x_k = x_p$ where $\text{Prob}(X \leq x_p) = p$ with $p = 0.95$ for variables of load effect type and $p = 0.05$ for those of resistance type,
 - d. a shifted value of the average, greater or less by a number of k standard deviations: $x_k = m_X \pm k\sigma_X$ with $k = 2$ or 3 ,
 - e. a shifted value from the outcome of the estimate of the average: $x_k = \tilde{m}_X \pm k\hat{\sigma}_X$ where $\hat{\sigma}_X$ is an outcome of the estimate of the standard deviation.

Combination values: combination values are those which occur in the combinations of actions used in the design rules of codes and regulations. They are equal, for secondary action variables associated with a main action, to the product of the characteristic values and the Ψ coefficients that take into account the probability of the simultaneous occurrence of the secondary actions and the main action.

The choice of characteristic values: let us cite a few examples:

- the characteristic values of *permanent actions* are generally deduced from the nominal means of the volume masses and geometric dimensions stated on the plan,
- the characteristic values of *variable actions* are generally p -fractiles corresponding to extreme value distributions, for example, the height of the hundred-year wave in the North Sea,
- the characteristic values of *geometric dimensions* are the nominal values cited on the plan,
- the characteristic values of *material characteristics* are the nominal values of the supplier, corresponding in general to a given fractile.

From the viewpoint of reliability analysis, the choice of a characteristic value implies a certain partial coefficient, and this choice has no consequence on the target reliability sought. The engineer's usual working value is therefore often chosen as the characteristic value.

Design values

Design values x_d (d for design) are representative values weighted by partial coefficients noted γ which confer on the design a given reliability level. While

representative values – whether they are characteristic values x_k or combination values Ψx_k – are values comprehensible by the designer insofar as they are means or moderately high (or low) values; the design values result from a procedure requiring expert algorithmic knowledge used to target very weak probabilities of failure, to the order of 10^{-4} to 10^{-7} . They are therefore very high (or very low) values to which the designer is not necessarily accustomed, all the more so as he is often unfamiliar with the procedure for formulating the γ coefficients.

To give an illustration, let us consider a random variable X following a normal distribution with a mean of 100 and a coefficient of variation of 0.25:

- the 95% fractile gives $x_k = 141.12$,
- the design value $x_d = \gamma_X x_k$, which gives for $\gamma = 1.5$ – which is usual in the case of a variable action – $x_d = 211.68$,
- the probability $\text{Prob}(X \geq x_k)$ is 0.05 whereas $\text{Prob}(X \geq x_d) = 3.961 \times 10^{-6}$; the probability of exceeding the characteristic value and that of exceeding the design value are not of the same order of magnitude (the ratio here is of the order of 10^4).

The design rules can then be expressed either as a function of the representative values and the associated partial coefficients, or directly as a function of the design values. The very definition of design values introduces an equation between representative values and design values; partial coefficients summarize this equation in a certain manner:

$$\gamma = \frac{x_d}{x_{rep}} \quad (\text{load effect or stress}) \quad \text{or} \quad \gamma = \frac{x_{rep}}{x_d} \quad (\text{resistance})$$

In certain procedures used to obtain partial coefficients, the physical space coordinates of the failure point P^* are used to calculate the coefficients γ to be applied in the usual design rules. The coordinates of P^* then play the role of design values; P^* is then called the design point, and:

$$x_d = x^*$$

The choice of P^* as the design point satisfies two requirements: placing ourselves in the situation that the reliability analyst considers the most hazardous and controlling the distance to the median operating point by measuring the reliability index.

10.1.3 Design rule

The basic principle is to build a rule based on characteristic values and partial coefficients. This rule, in principle, can also be interpreted by referring not to characteristic values but only to design values. Such an approach has the

advantage of proposing to the designer rules whose elements are familiar to him. They target a reliability level that the designer can use without having to carry out a reliability analysis.

In the simplest case, resistance-stress, this rule is written as:

$$s_d - r_d < 0 \implies \gamma_S s_k < \frac{r_k}{\gamma_R} \quad (10.1)$$

where γ_X is the partial coefficient associated with the variable X ; it is determined by a procedure named calibration (Section 10.4.2) for whole application domain.

We seek coefficients in general greater than 1 (which is not systematic), and that is why we must divide the resistance variables and multiply the stress variables, when they can be identified as such.

Equation (10.1) can be simplified by writing:

$$r_k - \gamma_R \gamma_S s_k > 0 \implies r_k - \gamma s_k > 0$$

where γ is the usual ‘safety coefficient’. However, writing it in this manner does not help us know what the respective roles of resistance and stress in reliability are.

More generally, in the face of a failure scenario represented by a limit-state function $G(\{x\}) = 0$, a design rule is an equation between the characteristic values and the partial coefficients, in the form:

$$G(\{x_k\}, \{\gamma_X\}) > 0 \quad (10.2)$$

Code format: the characteristic values x_k , the partial coefficients γ_X and the Ψ -values are the main constitutive elements of a design *format*, named in this case, the *partial coefficient format*. The format defines the verification philosophy used. In such a format, the designer is obliged to verify that the value of a performance function G – in general a limit-state function – is positive or zero when each basic variable is taken as equal to its design value.

10.1.4 Levels in the design approach

Depending on the quality of the information available, the design method can be ordered according to various levels [MKL86]. Though the spirit is the same, the classification differs according to the authors. We have chosen the following:

- *Level 0* corresponds to a purely deterministic analysis. The loads (or stresses) and resistances are determined values based on expertise, and a global safety coefficient is chosen. Experience feedback alone justifies the design and the qualitative evaluation of the reliability.

- *Level 1* is called semi-probabilistic. The loads (or stresses) and resistances are introduced by representative values derived from a more or less rich statistical content. Partial coefficients are also introduced into the design rules. This level is the most widely used.
- *Level 2* corresponds to a partial application of probabilistic methods. It requires the definition of a reference period, and FOSM² (*first order second moment*) or FORM/SORM (*first/second order reliability methods*) approximations are allowed. Level 2 is also the basis for the partial coefficient calibration procedure defined in level 1.
- *Level 3* is the fully probabilistic method. It requires knowledge of the joint probability densities of all the variables, which is inaccessible in practice in most situations.

10.1.5 Illustration

Figure 10.2 illustrates the concepts introduced. Two variables, the resistance R and the stress S , are known by their probability marginal densities $f_R(r)$ and $f_S(s)$. Particular outcomes are: the means m_R and m_S , the characteristic values r_k and s_k and the design values $r_d = r^*$ and $s_d = s^*$.

These coordinates define three points: the mean point P_{mean} , the characteristic point P_k and the design point P^* . The limit-state $r - s = 0$ separates the safety domain from the failure domain. Around the point P_{mean} , the joint probability isodensity curves indicate the volume which measures the probability of failure in D_f . A simple equation is given between characteristic values and design values, taking into account the role of the stress or resistance:

$$r^* = \frac{r_k}{\gamma_R} \implies r_k - r^* = r_k \left(1 - \frac{1}{\gamma_R}\right)$$

$$s^* = \gamma_S s_k \implies s^* - s_k = s_k (\gamma_S - 1)$$

This figure illustrates the fact that partial coefficients must distance the characteristic point from the most probable failure point, if possible orthogonally to the boundary of the limit-state in standardized space.

The photo shows the great column of Suchères in central France, the work (1984) of Anne and Patrick Poirier, built on highway A72, at the boundary between the Auvergne and Rhône-Alpes regions. It is certainly one of the rare examples of a structure built intentionally at an apparent failure point, ... and maintained in this state.

² FOSM supposes the knowledge of the first two statistical moments (mean and standard deviation). FORM/SORM introduces furthermore an at least partial knowledge of the probability distributions (marginal densities).

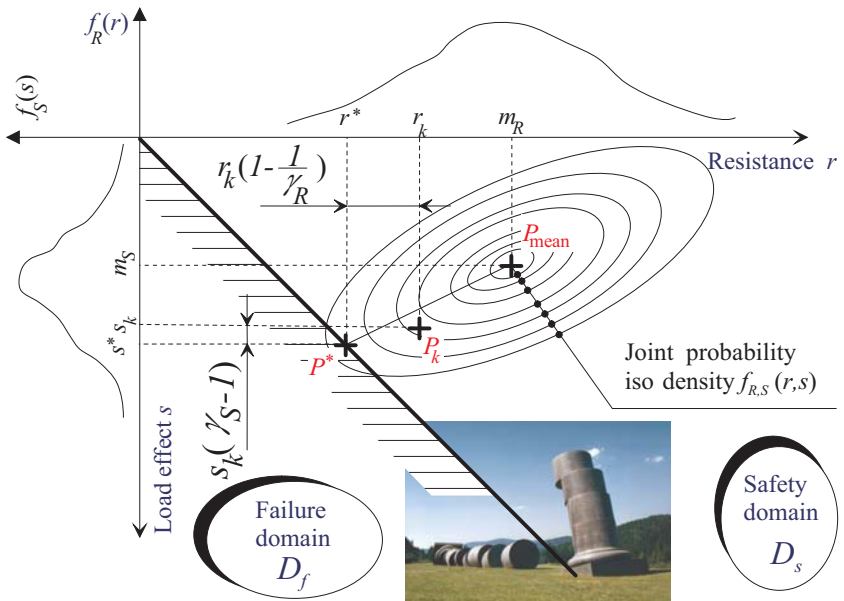


Figure 10.2 Design values and partial coefficients.

10.2 Safety coefficients – elementary case

The elementary scheme $R-S$, normally used in the description of reliability methods, is analyzed here from the design perspective. The design variable is the mean m_R of the resistance. The basic case is the one where R and S are normal; it is then studied in the case where R and S are lognormal.

10.2.1 Probabilistic design

Independent normal variables

Under the assumptions stated, the reliability index in the elementary case is:

$$\beta = \frac{m_R - m_S}{\sqrt{\sigma_R^2 + \sigma_S^2}} \quad (10.3)$$

The choice of a target reliability index $\bar{\beta}$ results in the value to be given to m_R . We only need to solve Equation (10.3) for $\beta = \bar{\beta}$. We obtain:

$$m_R = m_S C(\bar{\beta}, c_R, c_S) \quad \text{with } C(\bar{\beta}, c_R, c_S) = \frac{1 + \bar{\beta} \sqrt{c_R^2 + c_S^2 - \bar{\beta}^2 c_R^2 c_S^2}}{1 - \bar{\beta}^2 c_R^2} \quad (10.4)$$

Equation (10.4) shows that the coefficient $C(\bar{\beta}, c_R, c_S)$, equal by construction to the ratio of the means m_R/m_S , depends only on the target index $\bar{\beta}$ and the coefficient of variation (c.o.v.) c_R and c_S . A probabilistic design can:

- either leave the designer the task of calculating $C(\bar{\beta}, c_R, c_S)$ for a particular case,
- or establish an umbrella design rule covering all situations (the rule’s validity domain).

Table 10.1, calculated for a target index $\bar{\beta} = 3.8$, yields the values of C for various combinations of the coefficient of variation set. An umbrella design rule can be established, for example, depending on knowledge of the dispersion of a fabrication, $c_R = 0.10$ and an assumption of the variability of the load: $0.20 \leq c_S \leq 0.30$ (values in bold). We only need to take $\bar{C} = 2.48$.

	$c_R = 0.05$	$c_R = 0.10$	$c_R = 0.15$	$c_R = 0.20$
$c_S = 0.10$	1.472	1.774	2.444	4.259
$c_S = 0.15$	1.651	1.928	2.574	4.369
$c_S = 0.20$	1.836	2.103	2.734	4.513
$c_S = 0.25$	2.025	2.288	2.913	4.686
$c_S = 0.30$	2.215	2.479	3.105	4.880
$c_S = 0.35$	2.406	2.674	3.307	5.092
$c_S = 0.40$	2.598	2.871	3.515	5.318

Table 10.1 Elementary case for normal variables: values of $C(\bar{\beta}, c_R, c_S)$ for various situations.

Such a rule yields non-homogeneous values of the resulting reliability index β_{res} for the scope of application of the rule. In fact, by introducing \bar{C} and the coefficients of variation into (10.3), we obtain:

$$\beta_{\text{res}} = \frac{\bar{C} - 1}{\sqrt{c_R^2 \bar{C}^2 + c_S^2}}$$

which yields indices 4.65, 4.20 and 3.80 for the three values chosen. Furthermore, if $\bar{C} = 2.48$ is imposed systematically, this does not motivate the designer to control the variability of the stress better, even if possible.

Independent lognormal variables

In this case, the reliability index is given by (see Section 4.2.2):

$$\beta = \frac{\lambda_R - \lambda_S}{\sqrt{\xi_R^2 + \xi_S^2}} \quad (10.5)$$

and we obtain:

$$m_R = m_S C_{\ln}(\bar{\beta}, c_R, c_S)$$

$$C_{\ln}(\bar{\beta}, c_R, c_S) = \sqrt{\frac{1 + c_R^2}{1 + c_S^2}} \exp\left(\bar{\beta} \sqrt{\ln((1 + c_R^2)(1 + c_S^2))}\right) \quad (10.6)$$

By performing a limited expansion for the small variation ($c_X^2 \ll 1$), this expression can be simplified into a commonly used equation:

$$C_{\ln}(\bar{\beta}, c_R, c_S) \approx \exp(\bar{\beta} \sqrt{c_R^2 + c_S^2}) \quad (10.7)$$

Table 10.2, calculated for a target index $\bar{\beta} = 3.8$, gives the values of C_{\ln} for various combinations of the set of the coefficients of variation. An umbrella design rule can be established, for example, depending on knowledge of the dispersion of a fabrication $c_R = 0.10$ and an assumption of the variability of the stress: $0.20 \leq c_S \leq 0.30$ (values in bold). We only have to take $\bar{C} = 3.13$.

	$c_R = 0.05$	$c_R = 0.10$	$c_R = 0.15$	$c_R = 0.20$
$c_S = 0.10$	1.522	1.709	1.990	2.357
$c_S = 0.15$	1.800	1.965	2.229	2.587
$c_S = 0.20$	2.134	2.289	2.544	2.899
$c_S = 0.25$	2.524	2.676	2.929	3.287
$c_S = 0.30$	2.973	3.127	3.385	3.752
$c_S = 0.35$	3.487	3.645	3.912	4.292
$c_S = 0.40$	4.068	4.233	4.512	4.911

Table 10.2 Elementary case of lognormal variables: values of $C_{\ln}(\bar{\beta}, c_R, c_S)$ for various situations.

Such a rule yields non-homogeneous values of the resulting reliability index β_{res} for the scope of application of the rule. In fact, according to (10.5) and taking into account the equations of the lognormal distribution:

$$\lambda_R = \ln\left(\frac{m_R}{\sqrt{1 + c_R^2}}\right) = \ln m_R - \frac{1}{2} \ln(1 + c_R^2) \quad \text{and} \quad \xi_R = \sqrt{\ln(1 + c_R^2)} \quad (10.8)$$

we obtain:

$$\beta_{\text{res}} = \frac{\ln \bar{C}_{\ln} - \frac{1}{2} \ln((1 + c_R^2)/(1 + c_S^2))}{\sqrt{\ln((1 + c_R^2)(1 + c_S^2))}}$$

which results in indices 5.21, 4.39 and 3.80 for the values chosen.

Comparing Tables 10.1 and 10.2, it is possible to find a rule whose validity domain encompasses normal and lognormal distributions.

Conclusion

Such expressions were given by Rjanitzyne [Rja59] 50 years ago. They draw our attention to the essential role of the coefficients of variation. They show that a target reliability index and a mean coefficient $C = m_R/m_S$ are equivalent.

Illustration: designing for fatigue

For problems of fatigue, the ‘ S - N curve’ approach considers that the failure of a welded joint subject to a constant amplitude variation S follows the distribution $N = KS^{-m}$ where N is the number of cycles and m and K two adjustment parameters.

In a ln-ln diagram, this distribution is written as:

$$\ln N = \ln K - m \ln S$$

If the amplitude S is a lognormal random variable, then the number of cycles to fracture N is itself a lognormal random variable.

Let \bar{N} equal the number of stress cycles, also assumed to be lognormal. The probability of failure is:

$$P_f = \text{Prob}(N \leq \bar{N}) = \text{Prob}(\ln N \leq \ln \bar{N}) = \text{Prob}(\underbrace{\ln K - m \ln S}_{\text{resistance}} \leq \underbrace{\ln \bar{N}}_{\text{stress}})$$

The application of Equation (10.7) (small coefficients of variation) gives:

- Resistance coefficient of variation:

$$R = KS^{-m} : c_R \approx \xi_R = \sigma_{(\ln K - m \ln S)} = m \xi_S \approx m c_S$$

$m c_S$ is the product of the slope of the S - N curve and the coefficient of variation of the constant amplitude variation, S which is, in the present case, the resistance coefficient of variation, c_R , noted in Equation (10.7).

- Stress coefficient of variation, $c_{\bar{N}}$, and:

$$C_{\ln}(\beta, c_S, c_N) \approx \exp \left(\beta \sqrt{m^2 c_S^2 + c_{\bar{N}}^2} \right)$$

10.2.2 Global characteristic coefficient

To justify the reliability of a design, but without measuring it, the regulation uses two steps:

- the first is to extract from a random variable X a characteristic value x_k which, to be unfavorable, presents sufficiently little risk of being exceeded, if it is a stress, or of being reached if it is a resistance; it is often a p -fractile,
- the second is to assign this value of a partial (safety) coefficient γ_X , generally taken to be greater than 1.

The advantage of this decomposition results in:

- separately taking into account that what can be reached statistically directly or using a moderated extrapolation, and that which must be added outright,
- the fact that representative values are a necessary reference for controls, that they have a legal role and that they can be used in calculations where the variables are not ‘fundamental’.

The thorny problem of the calculation of a probability of failure, for which we must furthermore decide an admissible value \bar{P}_f , is replaced by the simple verification of the rule (see Equation (10.1)):

$$P_f = \text{Prob}(R - S \leq 0) < \bar{P}_f \implies \gamma_S s_k < \frac{r_k}{\gamma_R} \quad (10.9)$$

The choice of the characteristic values r_k and s_k and the calibration of partial coefficients γ_R and γ_S guarantee a reliability confirmed by experience. Reliability is provided in this example by four choices, two for two characteristic values and two for two partial coefficients.

By noting $\gamma = \gamma_S \gamma_R$, the global characteristic coefficient, Equation (10.9) becomes:

$$\gamma s_k < r_k \quad \text{or} \quad s_k < \frac{r_k}{\gamma} \quad (10.10)$$

If the means are chosen as characteristic values, the γ coefficient is a mean coefficient; if fractile values are chosen, γ is a fractile coefficient. The breakdown of γ according to each variable – formulation by partial coefficients – is presented in Section 10.2.3.

Means and mean coefficient

The characteristic values are means and Equation (10.10) becomes:

$$m_R > \gamma m_S$$

Coefficient γ is a mean coefficient whose expression is given by Equation (10.4) or (10.6):

$$\begin{aligned} \gamma_{\text{mean}} &= \frac{m_R}{m_S} = C(\bar{\beta}, c_R, c_S) && \text{normal variables} \\ &= C_{\ln}(\bar{\beta}, c_R, c_S) && \text{lognormal variables} \end{aligned}$$

The identity of γ_{mean} with coefficients $C(\bar{\beta}, c_R, c_S)$ or $C_{\ln}(\bar{\beta}, c_R, c_S)$, defined in Section 10.2.1 and tabulated in Tables 10.1 and 10.2 for various values of the coefficients of variation c_R and c_S , gives rise to the same comments as those given in the case of probabilistic design: an umbrella rule can be established by associating a single value of γ_{mean} with a more or less large set of situations.

Fractile values and global ‘fractile’ coefficient

The choice of a fractile is common practice in statistics. The fractile characteristic values are x_p values associated with the p -fractile of the random variable distribution:

$$\begin{aligned} r_k = r_p & \quad \text{with } \text{Prob}(R \leq r_p) = p_R \\ s_k = s_p & \quad \text{with } \text{Prob}(S \leq s_p) = p_S \end{aligned}$$

It must be noted that this presentation retains the same definition of the fractile irrespective of the type of variable. As a result, p_R must be close to 0, whereas p_S must be close to 1. We often choose $p_R = 5\%$ and $p_S = 95\%$.

The definition of the fractile value u_p is based on Gaussian distribution $\mathcal{N}(0, 1)$ by equation:

$$\begin{aligned} \Phi(u_{p_R}) &= \text{Prob}(R \leq r_p) = F_R(r_p) = p_R \\ \Phi(u_{p_S}) &= \text{Prob}(S \leq s_p) = F_S(s_p) = p_S \end{aligned}$$

If the distribution is known, choosing a p -fractile is equivalent to shifting the mean of $\pm k$ ($k > 0$) standard deviations:

$$\begin{aligned} r_k = r_p & \quad \text{with } \text{Prob}(R \leq r_p) = p_R \quad \text{or} \quad r_p = m_R - k_R \sigma_R \\ s_k = s_p & \quad \text{with } \text{Prob}(S \leq s_p) = p_S \quad \text{or} \quad s_p = m_S + k_S \sigma_S \end{aligned}$$

Case of Gaussian variables: for variable R , we obtain:

$$\begin{aligned} \text{Prob}(R \leq r_p) &= \text{Prob}\left(\frac{R - m_R}{\sigma_R} \leq \frac{r_p - m_R}{\sigma_R}\right) = \Phi(u_{p_R}) = p_R \\ \text{with } u_{p_R} &= \frac{r_p - m_R}{\sigma_R}, \quad \text{that is, } r_p = m_R + u_{p_R} \sigma_R. \end{aligned}$$

and likewise for S :

$$\begin{aligned} \text{Prob}(S \leq s_p) &= \text{Prob}\left(\frac{S - m_S}{\sigma_S} \leq \frac{s_p - m_S}{\sigma_S}\right) = \Phi(u_{p_S}) = p_S \\ \text{with } u_{p_S} &= \frac{s_p - m_S}{\sigma_S}, \quad \text{that is, } s_p = m_S + u_{p_S} \sigma_S. \end{aligned}$$

hence:

$$k_R = -u_{p_R} \quad k_S = u_{p_S}$$

Equation (10.10) becomes:

$$r_p > \gamma s_p \quad \text{that is:} \quad m_R(1 + u_{p_R} c_R) > \gamma m_S(1 + u_{p_S} c_S) \quad (10.11)$$

By choosing m_R as the design variable, Equation (10.11) results in the rule:

$$m_R > \frac{\gamma s_p}{1 + u_{p_R} c_R} \quad \text{with } \Phi(u_{p_R}) = \text{Prob}(R \leq r_p) = p_R \quad (10.12)$$

The coefficient γ to be chosen for a target index $\bar{\beta}$ is obtained by the following equation, introducing the expression $C(\bar{\beta}, c_R, c_S)$ defined in (10.4):

$$\begin{aligned} \gamma_{\text{fractile}} &= \frac{r_p}{s_p} = \frac{1 + u_{p_R} c_R}{1 + u_{p_S} c_S} C(\bar{\beta}, c_R, c_S) \\ &= \frac{1 + u_{p_R} c_R}{1 + u_{p_S} c_S} \frac{1 + \bar{\beta} \sqrt{c_R^2 + c_S^2 - \bar{\beta}^2 c_R^2 c_S^2}}{1 - \bar{\beta}^2 c_R^2} \end{aligned} \quad (10.13)$$

The equation with the mean coefficient is then:

$$\gamma_{\text{fractile}} = \frac{1 + u_{p_R} c_R}{1 + u_{p_S} c_S} \gamma_{\text{mean}}$$

Case of lognormal variables: the characteristic values are x_p values associated with the p -fractile of the random variable distribution:

$$\begin{aligned} r_k &= r_p \quad \text{with} \quad \text{Prob}(R \leq r_p) = p_R \\ s_k &= s_p \quad \text{with} \quad \text{Prob}(S \leq s_p) = p_S \end{aligned}$$

We obtain, for variable R :

$$\begin{aligned} \text{Prob}(R \leq r_p) &= \text{Prob}\left(\frac{\ln R - \lambda_R}{\xi_R} \leq \frac{\ln r_p - \lambda_R}{\xi_R}\right) \\ &= \text{Prob}\left(U \leq u_{p_R} = \frac{\ln r_p - \lambda_R}{\xi_R}\right) = \Phi(u_{p_R}) = p_R \end{aligned}$$

and likewise:

$$\text{Prob}(S \leq s_p) = \text{Prob}\left(U \leq \frac{\ln s_p - \lambda_S}{\xi_S}\right) = \Phi(u_{p_S}) = p_S$$

hence:

$$\begin{aligned} r_k &= r_p = \exp(\xi_R u_{p_R} + \lambda_R) \\ \text{similarly} \quad s_k &= s_p = \exp(\xi_S u_{p_S} + \lambda_S) \end{aligned}$$

Equation (10.10) is still written as $r_p > \gamma s_p$; that is, using (10.8):

$$r_p = \exp \left(\xi_R u_{p_R} + \ln m_R - \frac{\xi_R^2}{2} \right)$$

$$> \gamma s_p \quad ; \text{ that is: } m_R > \frac{\gamma s_p}{\exp(\xi_R u_{p_R} - (\xi_R^2/2))} \quad (10.14)$$

The value to be assigned to coefficient γ for a reliability index $\bar{\beta}$ is (with (10.6)):

$$\begin{aligned} \gamma_{\text{fractile}} &= \frac{r_p}{s_p} = \frac{\exp(\xi_R u_{p_R} - (\xi_R^2/2))}{\exp(\xi_S u_{p_S} - (\xi_S^2/2))} \frac{m_R}{m_S} \\ &= \frac{\exp(\xi_R u_{p_R} - (\xi_R^2/2))}{\exp(\xi_S u_{p_S} - (\xi_S^2/2))} C_{\ln}(\bar{\beta}, c_R, c_S) \\ &= \frac{\exp(\xi_R u_{p_R} - (\xi_R^2/2))}{\exp(\xi_S u_{p_S} - (\xi_S^2/2))} \sqrt{\frac{1+c_R^2}{1+c_S^2}} \exp\left(\bar{\beta} \sqrt{\ln((1+c_R^2)(1+c_S^2))}\right) \end{aligned}$$

$$\gamma_{\text{fractile}} =$$

$$\exp\left(u_{p_R} \sqrt{\ln(1+c_R^2)} - u_{p_S} \sqrt{\ln(1+c_S^2)} + \bar{\beta} \sqrt{\ln((1+c_R^2)(1+c_S^2))}\right)$$

The equation with the mean coefficient is then:

$$\gamma_{\text{fractile}} = \sqrt{\frac{1+c_S^2}{1+c_R^2}} \exp\left(u_{p_R} \sqrt{\ln(1+c_R^2)} - u_{p_S} \sqrt{\ln(1+c_S^2)}\right) \gamma_{\text{mean}}$$

Conclusion

Table 10.3, like the tables presented in Section 10.2.1 for normal variables, shows a lower amplitude of the γ coefficients according to the values of the coefficients of variation. This is due to the fact that a large proportion of the uncertainties is taken into account in the choice of the fractile. As a result, such an approach helps obtain a single rule in a large validity domain. The same conclusion is observed for lognormal distribution (Table 10.4).

Example: rod under tension

This example is presented in Section 3.6. It is now possible to explain the choice of the value of section A . To determine it, we must first of all decide characteristic variables and then partial safety coefficients.

The choice made is $k = 2$, which corresponds to a $p = 2.275\%$ fractile.

$$f_{yk} = m_{f_y} - 2\sigma_{f_y} = 240 \text{ MPa} \quad P_k = m_P + 2\sigma_P = 100 \text{ MN}$$

	$c_R = 0.05$	$c_R = 0.10$	$c_R = 0.15$	$c_R = 0.20$
$c_S = 0.10$	1.160	1.273	1.581	2.454
$c_S = 0.15$	1.215	1.292	1.555	2.352
$c_S = 0.20$	1.268	1.322	1.549	2.279
$c_S = 0.25$	1.317	1.354	1.555	2.228
$c_S = 0.30$	1.361	1.387	1.566	2.193
$c_S = 0.35$	1.402	1.418	1.581	2.169
$c_S = 0.40$	1.438	1.447	1.597	2.152

Table 10.3 Values of γ_{fractile} for various situations by assuming normal variables (5% and 95% fractiles).

	$c_R = 0.05$	$c_R = 0.10$	$c_R = 0.15$	$c_R = 0.20$
$c_S = 0.10$	1.194	1.231	1.313	1.423
$c_S = 0.15$	1.310	1.313	1.365	1.449
$c_S = 0.20$	1.445	1.423	1.449	1.511
$c_S = 0.25$	1.596	1.553	1.558	1.600
$c_S = 0.30$	1.762	1.701	1.687	1.711
$c_S = 0.35$	1.943	1.865	1.833	1.841
$c_S = 0.40$	2.139	2.043	1.995	1.987

Table 10.4 Values of γ_{fractile} for various situations by assuming lognormal variables (5% and 95% fractiles).

By accepting a characteristic safety coefficient γ_{fractile} of 1, we obtain:

$$A = \frac{P_k}{f_{yk}} = 0.42 \text{ m}^2$$

Interpretation of $k = 2$: choosing $k = 2$ is to accept the risk of having an insufficient resistance, or an excessive load. Let us call R the random resistance variable and r_k its characteristic value. The risk of having an insufficient resistance is:

$$P_R(r_k) = \text{Prob}(R \leq r_k)$$

which can be calculated with the assumption of Gaussian distribution:

$$P_R(r_k) = \frac{1}{\sigma_R \sqrt{2\pi}} \int_{-\infty}^{r_k} \exp\left(-\frac{(r - m_R)^2}{2 \sigma_R^2}\right) dr$$

After a change of variable:

$$u = \frac{r - m_R}{\sigma_R}$$

we obtain:

$$P_R(r_k) = \frac{1}{\sqrt{2\pi}} \int_{-\infty}^{-k} \exp\left(-\frac{u^2}{2}\right) du$$

which gives, for $k = 2$, $P_R(r_k) = 0.02275$.

The choice $k = 2$ is more severe than the choice regarding the 5% fractile, which corresponds to $k = 1.645$.

10.2.3 Designing using partial coefficients

Instead of applying a global coefficient to the rule, we choose to apply a coefficient to each characteristic value (Equation (10.9)):

$$s_d = \gamma_S s_k < \frac{r_k}{\gamma_R} = r_d \quad (10.15)$$

The product $s_d = \gamma_S s_k$ is a particular outcome of S : it is the design value. This also applies to r_d . The verification of (10.15) is tantamount to designing by comparing these two values. The choice of the design values helps calculate the partial coefficients. It is arbitrary, and the probabilistic approach provides a criterion: the design values are taken as equal to the coordinates of the most probable failure point, hence its name ‘design point’:

$$s_d = s^* \quad r_d = r^*$$

This choice gives coefficients γ_R and γ_S values that can be interpreted with respect to the basic data characterizing the problem, studied from a reliability point of view.

Case of independent normal variables

The equation with γ_{fractile} is immediate:

$$\gamma_R \gamma_S = \gamma_{\text{fractile}} = \frac{1 + u_{p_R} c_R}{1 + u_{p_S} c_S} C(\bar{\beta}, c_R, c_S) \quad (10.16)$$

Remembering that (see Section 3.7.4):

$$\begin{aligned} r^* &= m_R - \bar{\beta} \alpha_R \sigma_R = m_R(1 - \bar{\beta} \alpha_R c_R) \\ s^* &= m_S - \bar{\beta} \alpha_S \sigma_S = m_S(1 - \bar{\beta} \alpha_S c_S) \end{aligned}$$

the partial coefficients are written ($s_k = s_p$ and $r_k = r_p$) as:

$$\gamma_S = \frac{s^*}{s_p} = \frac{1 - \bar{\beta} \alpha_S c_S}{1 + u_{p_S} c_S} = \frac{1 + \left(\bar{\beta} c_S^2 / \sqrt{(c_R C)^2 + c_S^2} \right)}{1 + u_{p_S} c_S} \quad (10.17)$$

$$\gamma_R = \frac{r_p}{r^*} = \frac{1 + u_{p_R} c_R}{1 - \bar{\beta} \alpha_R c_R} = \frac{1 + u_{p_R} c_R}{1 - \left(\bar{\beta} c_R^2 / \sqrt{c_R^2 + (c_S/C)^2} \right)} \quad (10.18)$$

Each of the coefficients γ_R and γ_S is thus a function of the target reliability index, of the coefficients of variation and the choice made for the characteristic value. It must be noted that the coefficient of one variable depends on the variability of the other. The partial coefficients are therefore not intrinsic to a variable but to a variable within a rule. They depend on the coefficients of variation of the variables and the influence coefficients (the direction cosines α) which themselves depend on the expression of the limit-state function G .

Numerical example: target reliability is taken as equal to $\bar{\beta} = 3.8$. Variables R and S are normal, $C_R = C_S = 0.10$ and $p_R = 0.05$ and $p_S = 0.95$.

We obtain:

$$p_R = 0.05 \implies \text{Prob}(R \leq r_p) = p_R = \Phi(u_{p_R}) = 0.05 \implies u_{p_R} = -1.645$$

$$p_S = 0.95 \implies \text{Prob}(S \leq s_p) = p_S = \Phi(u_{p_S}) = 0.95 \implies u_{p_S} = +1.645$$

and by choosing $m_S = 100$:

$$s_p = m_S (1 + u_{p_S} c_S) = 116.45$$

$$r_p = m_R (1 + u_{p_R} c_R) = 0.836 m_R$$

$$C(\bar{\beta}, c_R, c_S) = \frac{1 + \bar{\beta} \sqrt{c_R^2 + c_S^2 - \bar{\beta}^2 c_R^2 c_S^2}}{1 - \bar{\beta}^2 c_R^2} = 1.774 \implies m_R = 177.4$$

$$\gamma_{\text{fractile}} = \frac{1 + u_{p_R} c_R}{1 + u_{p_S} c_S} C(\bar{\beta}, c_R, c_S) = 1.273$$

A solution such as $\gamma_R \gamma_S = \gamma_{\text{fractile}} = 1.273$ is acceptable. To choose the solution that corresponds to the design point, we only need to calculate the direction cosines:

$$\alpha_R = \frac{\sigma_R}{\sqrt{\sigma_R^2 + \sigma_S^2}} = 0.871$$

$$\alpha_S = -\frac{\sigma_R}{\sqrt{\sigma_R^2 + \sigma_S^2}} = -0.491$$

$$\gamma_S = \frac{s^*}{s_p} = \frac{1 - \bar{\beta} \alpha_S c_S}{1 + u_{p_S} c_S} = 1.019$$

$$\gamma_R = \frac{r_p}{r^*} = \frac{1 + u_{p_R} c_R}{1 - \bar{\beta} \alpha_R c_R} = 1.249$$

which results in $r_d = s_d = r^* = s^* = 118.66$ and $\gamma_S \gamma_R = \gamma_{\text{fractile}}$.

Correlation study – normal variables

R and S are always assumed to be normal and their dependence is entirely defined by the correlation coefficient $\rho \in [-1, 1]$. Remembering that in this case:

$$\beta = \frac{m_R - m_S}{\sqrt{\sigma_R^2 + \sigma_S^2 - 2\rho\sigma_R\sigma_S}}$$

Equation (10.4) becomes:

$$C(\bar{\beta}, c_R, c_S, \rho) = \frac{1 - \rho c_R c_S \bar{\beta}^2 + \bar{\beta} \sqrt{c_R^2 + c_S^2 - 2\rho c_R c_S - (1 - \rho^2) \bar{\beta}^2 c_R^2 c_S^2}}{1 - \bar{\beta}^2 c_R^2}$$

The fractile coefficient of Equation (10.13) is written in the same manner:

$$\gamma_{\text{fractile}} = \frac{r_p}{s_p} = \frac{1 + u_{p_R} c_R}{1 + u_{p_S} c_S} C(\bar{\beta}, c_R, c_S, \rho)$$

We come up against a difficulty when we pass on to partial coefficients. The Rosenblatt transformation is not unique because of the order of the variables and the choices of the signs of the square roots occurring in the Cholesky decomposition.

The first choice is taken here (see Section 4.3.6):

$$[\rho] = \begin{bmatrix} 1 & \rho \\ \rho & 1 \end{bmatrix} = [L][L]^t \quad \text{with} \quad \begin{pmatrix} \frac{r - m_R}{\sigma_R} \\ \frac{s - m_S}{\sigma_S} \end{pmatrix} = \begin{bmatrix} 1 & 0 \\ \rho & \sqrt{1 - \rho^2} \end{bmatrix} \begin{pmatrix} u_R \\ u_S \end{pmatrix}$$

With this transformation, the limit-state R - S is written as:

$$(\sigma_R - \sigma_s \rho) u_R - \sigma_s \sqrt{1 - \rho^2} u_s + m_R - m_S = 0$$

Index β , defined as the distance from the origin to the limit-state straight line, is then:

$$\beta = \frac{m_R - m_S}{\sqrt{\sigma_R^2 + \sigma_S^2 - 2\rho\sigma_R\sigma_S}}$$

and the direction cosines are:

$$\alpha_R = \frac{\sigma_R - \rho\sigma_S}{\sqrt{\sigma_R^2 + \sigma_S^2 - 2\rho\sigma_R\sigma_S}} = \frac{c_R C - \rho c_S}{\sqrt{(c_R C)^2 + c_S^2 - 2\rho C c_R c_S}}$$

$$\alpha_S = -\frac{\sigma_S \sqrt{1 - \rho^2}}{\sqrt{\sigma_R^2 + \sigma_S^2 - 2\rho\sigma_R\sigma_S}} = -\frac{c_S \sqrt{1 - \rho^2}}{\sqrt{(c_R C)^2 + c_S^2 - 2\rho C c_R c_S}}$$

with $C = m_R/m_S$.

The equation between the standardized and physical coordinates is written as:

$$r^* = \sigma_R u_R^* + m_R = m_R(1 - \beta c_R \alpha_R)$$

$$s^* = \sigma_S \left(\left(\sqrt{1 - \rho^2} \right) u_S^* + \rho u_R^* \right) + m_S$$

$$= m_S \left(1 - \beta c_S \left(\sqrt{1 - \rho^2} \alpha_S + \rho \alpha_R \right) \right)$$

and by introducing the direction cosines:

$$r^* = m_R \left(1 - \beta c_R \frac{c_R C - \rho c_S}{\sqrt{(c_R C)^2 + c_S^2 - 2\rho C c_R c_S}} \right)$$

$$s^* = m_S \left(1 - \beta c_S \left(\frac{\rho c_R C - c_S}{\sqrt{(c_R C)^2 + c_S^2 - 2\rho C c_R c_S}} \right) \right)$$

The partial coefficients are obtained for a target index: $\beta = \bar{\beta}$:

$$\gamma_R = \frac{r_p}{r^*} = \frac{1 + u_{p_R} c_R}{1 - \bar{\beta} c_R \left((c_R C - \rho c_S)/\sqrt{(c_R C)^2 + c_S^2 - 2\rho C c_R c_S} \right)} \quad (10.19)$$

$$\gamma_{S|R} = \frac{s^*}{s_p} = \frac{1 - \bar{\beta} c_S \left((\rho c_R C - c_S)/\sqrt{(c_R C)^2 + c_S^2 - 2\rho C c_R c_S} \right)}{1 + u_{p_S} c_S} \quad (10.20)$$

The same calculation can be performed by choosing the inverse order (S then R) for the variables:

$$[\rho] = \begin{bmatrix} 1 & \rho \\ \rho & 1 \end{bmatrix} = [L][L]^t \quad \text{with} \quad \begin{pmatrix} (s - m_S)/\sigma_S \\ (r - m_R)/\sigma_R \end{pmatrix} = [L] \begin{pmatrix} u_S \\ u_R \end{pmatrix}$$

This results in the same set of partial coefficients γ_S and $\gamma_{R|S}$. More precisely:

- the limit-state straight lines in standardized space are different,
- the design points do not have the same coordinates in standardized space.

But:

- the design point in physical space is invariant,

and therefore:

- the partial coefficients of the resistance and the stress are invariant.

10.3 General definition of partial coefficients

This section discusses the general case where:

- there is any number of random variables,
- the distributions of these variables are *a priori* unrestricted.

The cases of independent and then dependent variables are discussed in that order.

10.3.1 Case of independent variables

A design must be performed for all the potential critical situations. Replacing a complete probabilistic analysis with the application of a design rule supposes the definition of a particular design point and, as was mentioned in Section 10.2.3, it is the most probable failure point P^* that is chosen. This point is characterized by its coordinates u^* in standardized space.

The semi-probabilistic format usually selected is written by separating the resistance and stress variables of Equation (10.2):

$$G(\{x_k\}, \{\gamma_X\}) > 0 \implies G(s_{i_d}, r_{i_d}) = G(\gamma_{S_i}, s_{i_k}, \gamma_{R_i}, r_{i_k}) > 0 \quad (10.21)$$

where:

- s_{i_d} and r_{i_d} denote the design values of the random variables,
- s_{i_k} and r_{i_k} denote the characteristic values of the random variables,
- γ_{S_i} and γ_{R_i} denote the partial coefficients associated with each of these variables.

The equation between a characteristic value x_k and a design value $x_d = x^*$ is then:

$$x_k = \gamma_{X^{(R)}} x^* \quad \text{that is, } \gamma_{X^{(R)}} = \frac{x_k}{x^*} \text{ if } X = X^{(R)} \text{ is a resistance variable } R_i,$$

$$x_k = \frac{1}{\gamma_{X^{(S)}}} x^* \quad \text{that is, } \gamma_{X^{(S)}} = \frac{x^*}{x_k} \text{ if } X = X^{(S)} \text{ is a stress variable } S_i.$$

These equations are chosen to obtain partial coefficients greater than 1. However, if a very high (stress) or very low (resistance) characteristic value is

chosen, the associated coefficient can be less than 1. Furthermore, the concept of resistance or stress variables is not intrinsic and depends on the limit-state considered. This is the case, for example, for the compound bending of a fragile material in which the axial force N is either resistance or stress, in the reliability meaning of the terms, depending on whether the limit-state considered is fragile rupture under tension or rupture by compression (see Section 10.5.2).

If a target value, denoted $\bar{\beta}$, is given to the reliability index, it is then possible to link this value to the coefficients:

$$\begin{aligned}\gamma_{X^{(R)}} &= \frac{x_k}{x^*} = \frac{x_k}{F_{X^{(R)}}^{-1}(\Phi(-\bar{\beta}\alpha_{X^{(R)}}))} \\ \gamma_{X^{(S)}} &= \frac{x^*}{x_k} = \frac{F_{X^{(S)}}^{-1}(\Phi(-\bar{\beta}\alpha_{X^{(S)}}))}{x_k}\end{aligned}\quad (10.22)$$

The choice of characteristic values and associated partial coefficients shows that the same reliability level can be obtained with different partial coefficients. The partial coefficients of Equation (10.22) depend on:

- the target reliability index chosen,
- the choice made for the characteristic value,
- the influence of each variable in the evaluation of the probability of failure, associated with the design rule and measured using direction cosines.

A rule is generally established for a maximum variability. If a lower dispersion than the one contained in the rule is ensured, then the rule is penalizing.

If the characteristic values are fractile values, then:

$$x_k = x_p \quad \text{with } \text{Prob}(X \leq x_p) = p_X \quad \text{and} \quad X = X^{(R)} \quad \text{or} \quad X^{(S)}$$

If $F_X(X)$ is the distribution function of the random variable, we obtain:

$$p_X = F_X(x_p) = \Phi(u_{p_X}) \implies u_{p_X} = \Phi^{-1}(F_X(x_p))$$

and:

$$\begin{aligned}\gamma_{X^{(R)}} &= \frac{x_p}{x^*} = \frac{F_{X^{(R)}}^{-1}(\Phi(u_{p_{X^{(R)}}}))}{F_{X^{(R)}}^{-1}(\Phi(-\bar{\beta}\alpha_{X^{(R)}}))} \\ \gamma_{X^{(S)}} &= \frac{x^*}{x_p} = \frac{F_{X^{(S)}}^{-1}(\Phi(-\bar{\beta}\alpha_{X^{(S)}}))}{F_{X^{(S)}}^{-1}(\Phi(u_{p_{X^{(S)}}}))}\end{aligned}\quad (10.23)$$

Equation (10.23) elucidates Equation (10.22) when the characteristic values x_k are taken as equal to p -fractiles. It generalizes Equations (10.17) and (10.18).

10.3.2 Case of dependent variables

Equations (10.22) and (10.23) are correct when the variables are independent. In the case of dependent variables, the coefficients must be defined by sets of dependent variables. Let X_1 and X_2 be two dependent resistance variables. There are then as many partial coefficients as there are Rosenblatt transformations, in other words $n!$ for n variables. It is then necessary to choose the order of variables and to define conditional partial coefficients:

$$\begin{aligned}\Phi(-\bar{\beta}\alpha_{X_1}) &= F_{X_1}(x_1^*) \\ \Phi(-\bar{\beta}\alpha_{X_2}) &= F_{X_2}(x_2^*|x_1^*)\end{aligned}$$

and:

$$\gamma_{X_1} = \frac{x_{1k}}{x_1^*} = \frac{x_{1k}}{F_{X_1}^{-1}(\Phi(-\bar{\beta}\alpha_{X_1}))} \quad \gamma_{X_2|X_1} = \frac{x_{2k}}{x_2^*} = \frac{x_{2k}}{F_{X_2}^{-1}(\Phi(-\bar{\beta}\alpha_{X_2})|x_1^*)}$$

or otherwise

$$\gamma_{X_1|X_2} = \frac{x_{1k}}{x_1^*} = \frac{x_{1k}}{F_{X_1}^{-1}(\Phi(-\bar{\beta}\alpha_{X_1}|x_2^*))} \quad \gamma_{X_2} = \frac{x_{2k}}{x_2^*} = \frac{x_{2k}}{F_{X_2}^{-1}(\Phi(-\bar{\beta}\alpha_{X_2}))}$$

Notes: the example of two Gaussian variables discussed in Section 10.2.3 shows that, in this case, the partial coefficients are identical, irrespective of the order of variables in the Rosenblatt transformation.

10.3.3 Comments

The equations obtained in (10.17)–(10.20) and (10.22) show the implicit relation between the partial coefficients γ , the coefficients of variation c_X and the reliability index β . A set of coefficients defines an index and a probability of failure that it is possible to approximate using the methods presented in the previous chapters. Conversely, several sets of coefficients and characteristic values can correspond to one probability of failure, which shows that reliability can be ensured in an equivalent manner by making different weighting choices. Whilst the choice of a tolerable probability of failure is tricky, the partial coefficient method helps build a rule by taking decisions at each step: on characteristic values, then on each partial coefficient introduced. In fact, the first step must also take into account the role of the characteristic values in serviceability limit-state equations.

The use of a reliability index as the basis for a format to replace current formats that use partial coefficients has been studied for nearly twenty years, as it would do away with the inconvenience of an apparent mutual independence between the partial coefficients. In fact, the practical difficulties

in the development of codes on this basis lead us to consider this eventuality as still remote. We have, on the other hand, already used the reliability index as a means of controlling the values of partial coefficients and, more importantly, adapting them in certain special cases. Lastly, in entirely new cases, for which we do not have any practice, a reliability index chosen by analogy can provide a safety margin with a good chance of being of a correct order of magnitude and that can serve as the basis for evaluation. This can be the case for assessing the reliability of a damaged structure or of a structure whose operating conditions we want to change, and for deciding any repairs necessary (case of offshore platforms).

The reliability index is also used to show the sensitivity of a design to certain deterministic parameters and to parameters of random variable distributions (mean, standard deviation).

The use of probabilistic methods in design must overcome cultural inertia and also demonstrate its efficacy. The field of civil engineering is no doubt the most advanced and the reader will find in [GJLM98] an in-depth discussion on this subject.

10.4 Calibration of partial coefficients

A design rule in the form of (10.2) introduces characteristic values and partial coefficients. We have seen that it is possible to associate partial coefficients with the design point (Equation (10.22)).

However, finding these partial coefficients is tantamount to the complete resolution of the reliability problem. The objective is to avoid such a calculation for each case by offering the designer a single rule within a certain validity domain. We must therefore search for the best set of partial coefficients for a given set of situations: this is the calibration procedure. A first simple approach was given in Section 10.2.1 based on Tables 10.1–10.4 and their comments. Comparison of mean coefficients and fractile coefficients has shown the advantage of this latter formulation which, by integrating a part of the variability in the characteristic value, yields less dispersed coefficients, which opens the way to unique global fractile coefficients applicable to wide ranges of situations. This section proposes a calibration method in the general case of partial coefficients applied to characteristic values taken as equal to p -fractiles.

10.4.1 Calibration principle

So-called safety coefficients currently exist in all design rules. They result from successive adjustments made possible by the accumulation of the experience of builders.

The principle developed here consists of logically searching for a set of coefficients based on the statistical knowledge of variables or even models. But as this knowledge is imperfect, a purely algorithmic procedure is insufficient, and calibration is often performed for a target reliability index equal to the implicit reliability index of the existing code. As a result, linking probabilistic calibration methods to the result of expertise guarantees the reliability level, but also provides knowledge of its structure – what is the reliability sensitivity to each data variation? – and opens a possibility for the evolution of the rules. Calibration is therefore only an evolution, not a revolution.

A priori, it would be possible to define codes based on a probabilistic format, that is, codes whose design rules consist of verifying that the probability of failure is less than a predefined admissible value [GB90]:

$$P_f = \int_{G(X_i) \leq 0} f_{X_i}(x_i) dx_1 dx_2 \cdots dx_n \leq P_{f_{admissible}}$$

Such an approach would require at least one codification of the marginal distributions of the variables contained in the joint probability density $f_{\{X\}}(\{x\})$ and their correlation matrix. Marginal densities and the correlation matrix form the minimum necessary for a reliability calculation when the joint distribution cannot be identified. This codification work has not until now been carried out successfully. We can nevertheless mention that the *Joint Committee on Structural Safety* (JCSS) is working on such a codification, and the first part of the *Probabilistic Model Code* is presented in [Vro01].

The format usually used is therefore a semi-probabilistic format, characterized by the choice of design rules based on partial coefficients and characteristic values:

$$G(\{\gamma_{S_i} s_{i_k}\}, \{r_{i_k}/\gamma_{R_i}\}) > 0 \quad (10.24)$$

Quantities s_{i_k} and r_{j_k} are respectively the characteristic values of the stress and resistance variables. This presentation seeks to obtain partial coefficients greater than 1, regardless of variable type.

For a given situation j , it is easy to associate a characteristic value with each variable and then to determine the corresponding partial coefficient by a reliability analysis. Calibration searches for the set of coefficients to be applied to a set of situations. As a result, the designer knows the implicit reliability level associated with a rule without having to perform a complex reliability calculation, provided he verifies the conditions of application of the rule.

To bring together into a single rule a set of situations $j = 1, \dots, L$ corresponding to a class of structures, we search for the single set of partial coefficients covering all the situations as well as possible. The calibration

procedure results from solving the following problem:

$$\min_{\gamma_{X_i}} W(\gamma_{X_i}) = \sum_{j=1}^L \omega_j M(\beta_j(\gamma_{X_i}), \bar{\beta})$$

subject to $G_j(x_{i_k}, \gamma_{X_i}) > 0, \quad j = 1, \dots, L$

in which we try to minimize function $W(\gamma_{X_i})$ for all the situations j with respective weights ω_j and for a target index $\bar{\beta}$. $\beta_j(\gamma_{X_i})$ is the reliability index corresponding to the optimal solution of the design problem, $G_j(x_{i_k}, \gamma_{X_i}) > 0$ relative to situation j . $M(\beta_j(\gamma_{X_i}), \bar{\beta})$ is a penalty function for which a possible choice is $(\beta_j(\gamma_{X_i}) - \bar{\beta})^2$.

10.4.2 A calibration method

Several authors have presented calibration methods [Kro94, SKF94]. [DM96] summarizes the procedure in six important steps:

1. Choose the class of structures to be calibrated by defining:
 - the mechanical element,
 - the failure mode(s),
 - the design variables,
 - their domains of variation (*mean, standard deviation, distribution*).
2. Select a certain number of design situations and evaluate their weights ω_j .
3. Define a target reliability index $\bar{\beta}$.
4. Design each situation j by adjusting a design variable in such a manner that $\beta_j = \bar{\beta}$ and deduce the sensitivities $\vec{\alpha}_j$.
5. Choose a penalty function M and calculate $\vec{\delta}$ by minimization of:

$$\Delta = \sum_{\text{domains}} \sum_{\text{materials}} \sum_{\text{scenarios}} \sum_{\text{parameters}} \omega_j M(\tilde{\beta}_j, \bar{\beta}) \quad (10.25)$$

The application of Equation (10.25) is detailed in the next section.

6. Calculate the partial coefficients by:

$$\gamma_X = \frac{x^c}{x_k} \quad \text{or} \quad \gamma_X = \frac{x_k}{x^c}$$

depending on whether the variable X is a load effect or a resistance, where $x^c = F_X^{-1}(\Phi(-\bar{\beta}\delta))$ (δ : component of $\vec{\delta}$ associated with variable X) is the design value and x_k is the characteristic value.

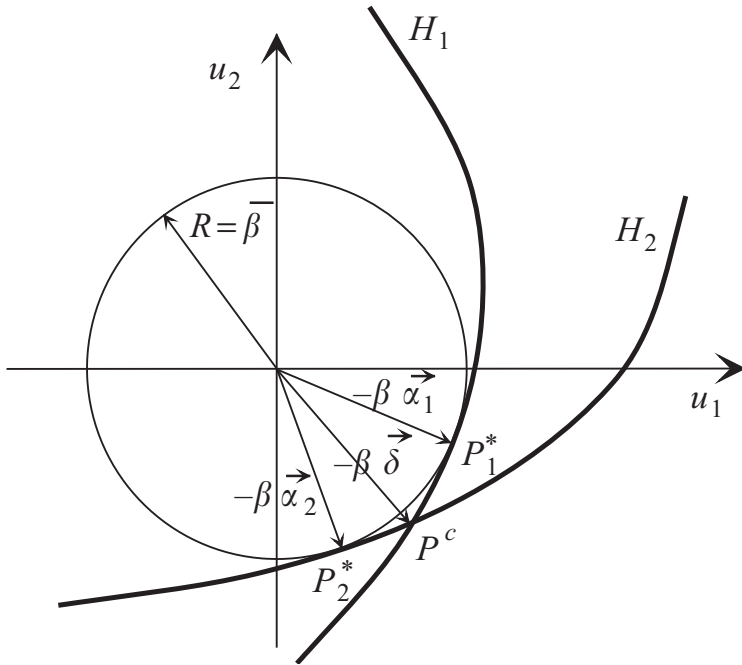


Figure 10.3 Combination of two limit-states: calculation of the joint calibration point.

Application of the optimization equation

Case of two situations: Figure 10.3 illustrates two situations represented by their limit-states H_1 and H_2 . For each one, the reliability index is $\bar{\beta}$. Apart from point P_i^* , any point belonging to the limit-state gives a combination of partial coefficients at least satisfying the requirement. The joint point P^c therefore gives a satisfactory solution for both situations, and the partial coefficients are calculated from the vector $\vec{\delta}$ used in substitution for vectors $\vec{\alpha}_1$ and $\vec{\alpha}_2$. Beyond the two situations, there is no joint point, apart from very special exceptions.

Case of more than two situations: vector $\vec{\delta}$ is then determined in such a manner as to minimize the function (10.25). Let us first consider (Figure 10.4) situation j with limit-state $H_j(u)$ and design point P_j^* such that $\overrightarrow{OP_j^*} = -\bar{\beta}\vec{\alpha}_j$. We replace $H_j(u) = 0$ with the limit-state $\tilde{H}_j(u) = 0$ such that the design point P^c belongs to this limit-state. P^c , with $\overrightarrow{OP^c} = -\bar{\beta}\vec{\delta}$, is not the design point of $\tilde{H}_j(u) = 0$. Let us note that later by \tilde{P}_j^* and by $\tilde{\beta}_j$ the distance OP_j^* . [DM96] then gives an approximate equation:

$$\tilde{\beta}_j \simeq \bar{\beta} \vec{\alpha}_j \vec{\delta}$$

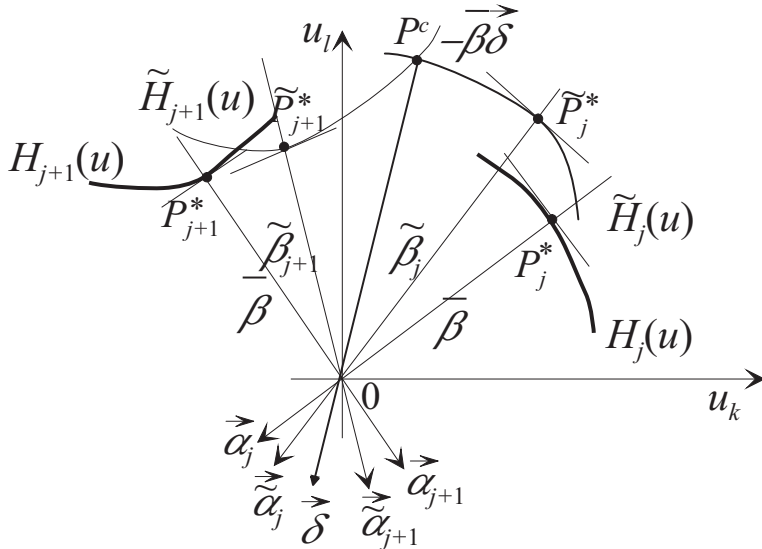


Figure 10.4 Illustration of the calibration procedure for any number of limit-states.

which supposes the following assumptions:

- the gradients of $H_j(u)$ and $\tilde{H}_j(u)$ remain almost parallel and $\overrightarrow{OP_j^*} \approx \lambda \overrightarrow{OP_j^*}$,
- the curvatures remain moderate and P^c projects itself approximately into \tilde{P}_j^* .

Due to this approximation and the penalty function, the result of optimization (10.25) does not exactly satisfy the target index, which must be verified.

10.4.3 Application example

Presentation of the problem

The application considered concerns the elastoplastic design already discussed in Section 7.7.3. It is applied here with different data.

The plastic resistance of a cross-section of a beam under bending is given by the equation:

$$M_{\text{plastic}} = z f_y$$

where M_{plastic} is the plastic moment, z is the plastic bending modulus and f_y is the yield limit. The stress is the bending moment M , and the elastoplastic failure is then given by:

$$G(\{x\}) = f_y z - M = x_1 x_2 - x_3$$

where $f_y = X_1$, $z = X_2$, $M = X_3$ are random variables. The design rule sought is then:

$$\frac{f_{y_p}}{\gamma_{f_y}} \frac{z_p}{\gamma_z} = \gamma_M M_p \implies z_p = \gamma_M \gamma_{f_y} \gamma_z \frac{M_p}{f_{y_p}} \quad (10.26)$$

The mean m_z of the variable z is chosen as the pilot variable, that is, the adjustment variable to obtain the target reliability $\bar{\beta} = 3.8$. The characteristic values x_p are 5% p -fractiles (resistance) or 95% p -fractiles (stress). The model selected for the random variables is given in Table 10.5.

	f_y (MPa)	z (m ³)	M (MNm)
m_X	200–400	m_z (pilot)	10–100
c_X	5–10%	5%	10–20%
law	lognormal or Gauss	Gauss	Gumbel
u_p	−1.645	−1.645	1.645

Table 10.5 Calibration variables.

Method

The general method (Section 10.4.2) is applied:

1. Choose the class of structures to be calibrated by defining:
 - the mechanical element: *the resistance of a section under elastoplastic bending*,
 - the failure mode(s): *the plastic moment is reached*,
 - the design variables: *the yield limit, the load effect and the plastic modulus of the cross-section*,
 - their domains of variation: *means and the coefficients of variation of the yield limit and the loading moment, distribution types (two in number) for f_y* .
2. Select a certain number of design situations and evaluate their weights ω_j : *these are the 2^5 possible combinations derived from the data in Table 10.5; all the situations are assumed to have identical weights*.
3. Define a target reliability index $\bar{\beta}$: *it is taken as equal to 3.8*.
4. Design each situation j by adjusting a design variable in such a manner that $\beta_j = \bar{\beta}$ and deduce the sensitivities α_j : *the design variable chosen is the mean of z* .

5. Choose a penalty function M and calculate $\vec{\delta}$ by minimization of:

$$\Delta = \sum_{\text{situations}} \left(\tilde{\beta}_j(\gamma_{X_i}) - \bar{\beta} \right)^2 \quad \text{with } \tilde{\beta}_j(\gamma_{X_i}) = \bar{\beta} \vec{\alpha}_j \cdot \vec{\delta} \quad (10.27)$$

for the validity domain of the rule.

6. Deduce the partial coefficients from the knowledge of point P^c .

Calibration

z is the pilot variable. The limit-state is rewritten in the form:

$$G(\{x\}) = f_y z - M = x_1 (\lambda x_2) - x_3 \quad \text{with } z = \lambda x_2$$

where λ is a scalar parameter and X_2 is a Gaussian variable with unit mean. As a result, λ is equal to the mean m_z of the variable z , that is, equal to the pilot parameter of the study.

We thus obtain $\lambda = m_z$ and $\sigma_{X_2} = c_z$. A parametric analysis is performed to determine λ such that $\beta = \bar{\beta} = 3.8$. This analysis shows first and foremost that partial coefficients are insensitive to the means with identical coefficients of variation and distributions. The lines in Table 10.6 show that:

$$\lambda = k \frac{m_M}{m_{f_y}} \quad \text{with } k = 2.63$$

which it must be possible to demonstrate.

m_{f_y}	σ_{f_y}	m_M	σ_M	λ	α_{f_y}	α_z	α_M
200	20	10	2	0.1315	0.348	0.180	-0.920
200	20	100	20	1.315	0.348	0.180	-0.920
400	40	100	20	0.657	0.347	0.180	-0.920
LogN.		Gumbel		Target index $\beta = 3.8$			
				β_{sorm}	γ_{f_y}	γ_z	γ_M
200	20	10	2	3.801	0.968	0.951	1.612
200	20	100	20	3.801	0.968	0.951	1.612
400	40	100	20	3.798	0.967	0.951	1.611

Table 10.6 Calibration calculations: influence of means.

The situations with variable means are thus identical. Therefore, we will consider only the situations in Table 10.7 whose results are given in Table 10.8.

cas	m_{f_y}	σ_{f_y}	law	f_{yp}	m_M	σ_M	law	M_p
1	200	10	Log-N	183.99	100	10	Gumbel	118.66
2	200	10	Gauss	183.55	100	10	Gumbel	118.66
3	200	20	Log-N	168.89	100	10	Gumbel	118.66
4	200	20	Gauss	167.10	100	10	Gumbel	118.66
5	200	10	Log-N	183.99	100	20	Gumbel	137.32
6	200	10	Gauss	183.55	100	20	Gumbel	137.32
7	200	20	Log-N	168.89	100	20	Gumbel	137.32
8	200	20	Gauss	167.10	100	20	Gumbel	137.32
$z: \text{Gauss } z_p = 0.918m_z$						Target index $\beta = 3.8$		

Table 10.7 Calibration calculations: choice of situations (5% fractiles for resistance variables and 95% fractiles for stress variables).

cas	λ	α_{f_y}	α_z	α_M	γ_{f_y}	γ_z	γ_M	β_{sorm}
1	0.897	0.254	0.268	-0.929	0.967	0.967	1.362	3.801
2	0.898	0.267	0.267	-0.926	0.967	0.967	1.369	3.800
3	0.966	0.473	0.249	-0.845	1.015	0.963	1.285	3.798
4	0.993	0.577	0.235	-0.783	1.070	0.961	1.233	3.801
5	1.245	0.183	0.190	-0.965	0.953	0.952	1.684	3.799
6	1.246	0.190	0.190	-0.963	0.952	0.952	1.682	3.799
7	1.315	0.348	0.180	-0.920	0.968	0.951	1.612	3.801
8	1.332	0.402	0.176	-0.899	0.986	0.950	1.577	3.801
		$\langle \alpha_j \rangle, j = 1, \dots, 8$						

Table 10.8 Calibration calculations: results obtained.

The following equations are used for the calculation of fractile values:

$$\text{Gaussian variable } x_p = m_X (1 + c_X u_p)$$

$$\text{Lognormal variable } x_p = m_X \exp(\lambda_X + \xi_X u_p)$$

$$x_p = m_X \frac{\exp(u_p \sqrt{\ln(1 + c_X^2)})}{\sqrt{1 + c_X^2}}$$

$$\text{Gumbel variable } x_p = m_X \left(1 - \frac{\sqrt{6}}{\pi} c_X (f + \ln(-\ln(\Phi(u_p)))) \right)$$

$$\text{with } f = 0.577215\dots$$

Equation (10.27) is written as:

$$\Delta = \sum_{\text{situations}} (\bar{\beta} \langle \alpha_j \rangle \{ \delta \} - \bar{\beta})^2 = \sum_j \bar{\beta}^2 \langle \delta \rangle \{ \alpha_j \} \langle \alpha_j \rangle \{ \delta \} - 2\bar{\beta}^2 \langle \delta \rangle \{ \alpha_j \} + \bar{\beta}^2$$

and by expressing the extreme of Δ :

$$\frac{\partial \Delta}{\partial \{ \delta \}} = 0 \implies \sum_j \{ \alpha_j \} \langle \alpha_j \rangle \{ \delta \} - \sum_j \{ \alpha_j \} = 0$$

which gives a linear system whose solution is vector $\{ \delta \}$. We obtain:

$$\{ \delta \} = \begin{bmatrix} 0.379 \\ 0.246 \\ -0.906 \end{bmatrix} \implies \{ u^c \} = -\bar{\beta} \{ \delta \} = \begin{bmatrix} -1.439 \\ -0.934 \\ 3.441 \end{bmatrix}$$

Calculation of partial coefficients

The partial coefficients depend on the quality of the information, and therefore on the variability. Furthermore, the choice of two possible distributions for f_y obliges us to select the most unfavorable case.

Coefficient of f_y

- *Gaussian case*: the characteristic value is $f_{yp} = m_{f_y} (1 + c_{f_y} u_p)$. The design value is given by $f_y^c = m_{f_y} (1 + c_{f_y} u_1^c)$; hence:

$$\gamma_{f_y} = \frac{1 + c_{f_y} u_p}{1 + c_{f_y} u_1^c} = \begin{cases} 0.989 & \text{for } c_{f_y} = 5\% \\ 0.976 & \text{for } c_{f_y} = 10\% \end{cases}$$

- *Lognormal case*: the characteristic value is $f_{yp} = m_{f_y} \exp(\lambda_{f_y} + \xi_{f_y} u_p) = m_{f_y} \exp(u_p \sqrt{\ln(1 + c_{f_y}^2)}) / (\sqrt{1 + c_{f_y}^2})$. The design value is given by:

$$f_y^c = m_{f_y} \exp(\lambda_{f_y} + \xi_{f_y} u_1^c) = m_{f_y} \frac{\exp(u_1^c \sqrt{\ln(1 + c_{f_y}^2)})}{\sqrt{1 + c_{f_y}^2}}$$

from which:

$$\begin{aligned} \gamma_{f_y} &= \exp(\xi_{f_y} (u_p - u_1^c)) = \exp\left(\sqrt{\ln(1 + c_{f_y}^2)}(u_p - u_1^c)\right) \\ &= \begin{cases} 0.990 & \text{for } c_{f_y} = 5\% \\ 0.980 & \text{for } c_{f_y} = 10\% \end{cases} \end{aligned}$$

Coefficient of z: the case is Gaussian, and we obtain $\gamma_z = 0.963$ for $c_z = 5\%$.

Coefficient of M: the characteristic value is given by

$$M_p = m_M \left(1 - (\sqrt{6}/\pi) c_M (f + \ln(-\ln(\Phi(u_p)))) \right)$$

and the design value by

$$M^c = m_M \left(1 - (\sqrt{6}/\pi) c_M (f + \ln(-\ln(\Phi(u_3^c)))) \right)$$

hence:

$$\gamma_M = \frac{1 - (\sqrt{6}/\pi) c_M (f + \ln(-\ln(\Phi(u_3^c))))}{1 - (\sqrt{6}/\pi) c_M (f + \ln(-\ln(\Phi(u_p))))} = \begin{cases} 1.340 & \text{for } c_M = 10\% \\ 1.588 & \text{for } c_M = 20\% \end{cases}$$

Design rule

The above results show that fractile values are sufficient for resistances, and coefficients γ_{f_y} and γ_z are taken as equal to 1. The rule thus helps determine the mean of the plastic modulus, according to (10.26):

$$z_p = m_z (1 + u_p c_z) = \gamma_M \gamma_{f_y} \gamma_z \frac{M_p}{f_{y_p}}$$

$$\text{that is } 0.918 m_z = \gamma_M \frac{M_p}{f_{y_p}} \implies m_z = \begin{cases} 1.46 \frac{M_p}{f_{y_p}} & \text{for } c_M = 10\% \\ 1.73 \frac{M_p}{f_{y_p}} & \text{for } c_M = 20\% \end{cases}$$

Verification

We must now verify that the target index is obtained by the application of the rule. Table 10.9 shows the results for the calibration values. Table 10.10 shows a few situations sorted randomly. Over-estimations yield a resultant index greater than the expected index, with a high level of homogeneity.

10.5 Application examples

Two examples are given as application exercises.

10.5.1 Linear fracture mechanics

Statement of the problem

This exercise is drawn freely from [BA96]. The simple model of the linear fracture mechanics yields the following limit-state equation:

$$J_{Ic} - F^2 \sigma^2 \frac{\pi a}{E} (1 - \nu^2) = 0$$

	m_{f_y}	σ_{f_y}	law	f_{yp}	m_M	σ_M	law	M_p	m_z	β
1	200	10	Log-N	183.99	100	10	G	118.66	0.942	4.05
2	200	10	Gauss	183.55	100	10	G	118.66	0.944	4.05
3	200	20	Log-N	168.89	100	10	G	118.66	1.026	4.09
4	200	20	Gauss	167.10	100	10	G	118.66	1.037	4.00
5	200	10	Log-N	183.99	100	20	G	137.32	1.291	3.93
6	200	10	Gauss	183.55	100	20	G	137.32	1.294	3.92
7	200	20	Log-N	168.89	100	20	G	137.32	1.407	4.04
8	200	20	Gauss	167.10	100	20	G	137.32	1.422	4.02
$z : \text{Gauss} z_p = 0.918 m_z$								Target index $\beta = 3.8$		

Table 10.9 Calibration calculations: verification.

	m_{f_y}	σ_{f_y}	law	f_{yp}	m_M	σ_M	law	M_p	m_z	β
1	400	30	Log-N	352.6	1,000	200	G	1373	6.736	4.00
2	100	10	Log-N	84.45	10,000	2,000	G	13732	281.3	4.04
3	400	40	Gauss	334.2	10	1	G	11.87	0.052	4.01
$z: \text{Gauss } z_p = 0.918 m_z$								Target index $\beta = 3.8$		

Table 10.10 Calibration calculations: situations sorted randomly.

where:

- J_{Ic} is the critical stress intensity factor of the material,
- F is a form factor,
- σ is the applied stress,
- a is the amplitude of the defect capable of initiating a crack,
- E and ν are respectively the elasticity modulus and the Poisson coefficient.

The three variables J_{Ic} , a , and σ are random, represented by lognormal distributions. For a variable X , we use the notations m_X for the mean, σ_X for the standard deviation, λ_X for $m_{\ln X}$ and ξ_X for $\sigma_{\ln X}$. The centered, reduced normal variable associated with X is U_X .

The coefficients of variation are assumed to be very small to allow the largest approximate equations in the expressions of the mean and the standard deviation of variables $\ln J_{Ic}$, $\ln a$ and $\ln \sigma$:

$$\lambda_X \approx \ln m_X \quad \xi_X \approx \frac{\sigma_X}{m_X} = c_X$$

1. Give the application conditions of the above approximations.

2. Establish the limit-state equation in centered and reduced Gaussian space.

Deduce from this the reliability index β and the direction cosines $\alpha_i, i = 1, 2, 3$. The results will be expressed as a function of the quantity $K = m_{J_{Ic}} E / m_a m_\sigma^2 - F^2 \pi (1 - \nu^2)$ and the coefficients of variation c_X of the random variables.

3. Calculate the standardized coordinates of the most probable failure point P^* .
4. Calculate the physical coordinates of P^* .
5. P^* is chosen as the design point. Calculate the partial coefficients $\gamma_{J_{Ic}}, \gamma_a$ and γ_σ for the characteristic values equal to the mean of each variable. (Take into account the stress or resistance effect of each variable to obtain partial coefficients greater than 1.)
6. Give a simple equation between K and the partial coefficients.

Approximations of the lognormal distribution

The exact equations are:

$$\begin{aligned}\lambda_X &= \ln \left(\frac{m_X}{\sqrt{1 + c_X^2}} \right) \approx \ln m_X - \frac{c_X^2}{2} \approx \ln m_X \\ \xi_X &= \sqrt{\ln(1 + c_X^2)} \approx \frac{\sigma_X}{m_X} = c_X\end{aligned}$$

Approximations are possible if $c_X^2 \ll 1$ and $c_X^2 \ll \ln m_X$. Note that these approximations result in confusing the median with the mean.

Limit-state equation and reliability index

By using logarithms:

$$\ln J_{Ic} - 2 \ln \sigma - \ln a - \ln(F^2 \frac{\pi}{E} (1 - \nu^2)) = 0$$

The transformation $u = T(x)$ – physical space \rightarrow standardized space – for each physical variable modeled by a random variable is:

$$u_X = \frac{\ln x - \ln m_X}{c_X}$$

Hence:

$$u_{J_{Ic}} c_{J_{Ic}} + \ln m_{J_{Ic}} - 2u_\sigma c_\sigma - 2 \ln m_\sigma - u_a c_a - \ln m_a - \ln \left(F^2 \frac{\pi(1 - \nu^2)}{E} \right) = 0$$

$$u_{J_{Ic}} c_{J_{Ic}} - 2u_\sigma c_\sigma - u_a c_a + \ln m_{J_{Ic}} - 2 \ln m_\sigma - \ln m_a - \ln \left(F^2 \frac{\pi(1 - \nu^2)}{E} \right) = 0$$

This is the equation of a straight line and:

$$\begin{aligned}\beta &= \frac{\ln m_{J_{Ic}} - 2 \ln m_\sigma - \ln m_a - \ln(F^2(\pi/E)(1-\nu^2))}{\sqrt{c_{J_{Ic}}^2 + 4c_\sigma^2 + c_a^2}} \\ &= \frac{\ln(m_{J_{Ic}} E / (m_\sigma^2 m_a F^2 \pi(1-\nu^2)))}{\sqrt{c_{J_{Ic}}^2 + 4c_\sigma^2 + c_a^2}} \\ \beta &= \frac{\ln K}{\sqrt{c_{J_{Ic}}^2 + 4c_\sigma^2 + c_a^2}}\end{aligned}$$

The direction cosines are then:

$$\begin{aligned}\alpha_{J_{Ic}} &= \frac{c_{J_{Ic}}}{\sqrt{c_{J_{Ic}}^2 + 4c_\sigma^2 + c_a^2}} \\ \alpha_\sigma &= -\frac{2 c_\sigma}{\sqrt{c_{J_{Ic}}^2 + 4c_\sigma^2 + c_a^2}} \\ \alpha_a &= -\frac{c_a}{\sqrt{c_{J_{Ic}}^2 + 4c_\sigma^2 + c_a^2}}\end{aligned}$$

The choice of signs is made in such a manner that a resistance variable gives a positive direction cosine and a stress variable a negative direction cosine.

Coordinates of the design point P^*

Standardized coordinates:

$$\begin{aligned}u_i^* &= -\beta \alpha_i \\ u_{J_{Ic}}^* &= -\frac{c_{J_{Ic}} \ln K}{c_{J_{Ic}}^2 + 4c_\sigma^2 + c_a^2} \\ u_\sigma^* &= \frac{2 c_\sigma \ln K}{c_{J_{Ic}}^2 + 4c_\sigma^2 + c_a^2} \\ u_a^* &= \frac{c_a \ln K}{c_{J_{Ic}}^2 + 4c_\sigma^2 + c_a^2}\end{aligned}$$

Physical coordinates – the transformation is:

$$u_X = \frac{\ln x - \ln m_X}{c_X} \quad x = m_X \exp(u_X c_X)$$

$$\begin{aligned}
 x^* &= m_X \exp(-\beta \alpha_X c_X) = m_X \exp\left(-\frac{\ln K}{\sqrt{c_{J_{Ic}}^2 + 4c_\sigma^2 + c_a^2}} \alpha_X c_X\right) \\
 &= m_X K^{-\frac{\alpha_X c_X}{\sqrt{c_{J_{Ic}}^2 + 4c_\sigma^2 + c_a^2}}} \\
 J_{Ic}^* &= m_{J_{Ic}} K^{\left(-c_{J_{Ic}}^2 / (c_{J_{Ic}}^2 + 4c_\sigma^2 + c_a^2)\right)} \\
 \sigma^* &= m_\sigma K^{\left(2c_\sigma^2 / (c_{J_{Ic}}^2 + 4c_\sigma^2 + c_a^2)\right)} \\
 a^* &= m_a K^{\left(c_a^2 / (c_{J_{Ic}}^2 + 4c_\sigma^2 + c_a^2)\right)}
 \end{aligned}$$

Partial coefficients

These are calculated for the means of the variables but also correspond to the median values in view of the approximations. To calibrate the design rule, that is, to determine the partial coefficients that are applied to it, we must express this rule (equality) at the optimum (the design point of coordinates x^*). This gives:

$$J_{Ic}^* - F^2 \sigma^{*2} \frac{\pi a^*}{E} (1 - \nu^2) = 0$$

or, in characteristic variables (means):

$$\frac{m_{J_{Ic}}}{\gamma_{J_{Ic}}} - F^2 \gamma_\sigma^2 m_\sigma^2 \frac{\pi \gamma_a m_a}{E} (1 - \nu^2) = 0 \quad (10.28)$$

J_{Ic} is a resistance ($\alpha_{J_{Ic}} > 0$):

$$\gamma_{J_{Ic}} = \frac{m_{J_{Ic}}}{J_{Ic}^*} = \frac{1}{K^{\left(-c_{J_{Ic}}^2 / (c_{J_{Ic}}^2 + 4c_\sigma^2 + c_a^2)\right)}}$$

and the other variables are stresses:

$$\begin{aligned}
 \gamma_\sigma &= \frac{\sigma^*}{m_\sigma} = K^{\left(2c_\sigma^2 / (c_{J_{Ic}}^2 + 4c_\sigma^2 + c_a^2)\right)} \\
 \gamma_a &= \frac{a^*}{m_a} = K^{\left(c_a^2 / (c_{J_{Ic}}^2 + 4c_\sigma^2 + c_a^2)\right)}
 \end{aligned}$$

Equation between the partial coefficients

The equation between the partial coefficients is obtained from Equation (10.28):

$$K = \gamma_{J_{Ic}} \gamma_\sigma^2 \gamma_a$$

where K appears as the mean coefficient between the resistance and the stress. It can be obtained directly from the product of the partial coefficients.

10.5.2 Compound bending of a fragile material

Statement of the problem

Let us consider a column clamped in its base (or a brick chimney³). It is subjected to a vertical action P – the dead load – and to a horizontal action density q . Its height is ℓ . The strength of materials efforts on the clamped cross-section are therefore:

$$\text{normal force } N = P \quad \text{bending moment } M = \frac{q\ell^2}{2} \quad \text{shear force } T = q\ell$$

The normal force is considered positive during compression. We are not interested in the design *vis-à-vis* the shear force. Normal stress on the cross-section is given algebraically by:

$$\sigma = -\frac{N}{S} + \frac{M}{I}y$$

where S and I are respectively the area and the inertia of the cross-section. y is the distance of the line considered from axis Gz passing through the center of gravity. The cross-section is considered symmetric with height h and the stress values at the points at $\pm h/2$ are given by:

$$\sigma_1 = -\frac{N}{S} + \frac{Mh}{2I} \quad \sigma_2 = -\frac{N}{S} - \frac{Mh}{2I}$$

These stresses are negative (if $N > 0$ and M is of limited amplitude) and we examine the design for their absolute values. Under these conditions, the rule to be taken into account, for a fragile material incapable of withstanding the tensile stress, is then:

$$f_y > \frac{N}{S} + \frac{Mh}{2I} > 0 \quad \text{and} \quad f_y > \frac{N}{S} - \frac{Mh}{2I} > 0$$

where $f_y > 0$ is the yield limit of the material. By considering that $m_N > 0$ and $m_M > 0$, two of the limit-states become very improbable and, finally, the design rule is reduced to:

$$f_y > \frac{N}{S} + \frac{Mh}{2I} \quad \text{and} \quad \frac{N}{S} - \frac{Mh}{2I} > 0$$

³ The inspiration for this example comes from an oral tradition. This attributes to A. Caquot, more than 50 years ago at ENPC, the illustration, through the example of a brick chimney, of the affirmation that systematically over-estimating actions tending toward safety is a misconception.

	Mean	Standard deviation	Distribution	c.o.v.
N	1 MN	0.05 MN	lognormal	0.05
M	0.025 MN m	0.0025 MN m	lognormal	0.10

Table 10.11 Probabilistic description of random variables.

Designing

For the design, we consider only two independent random variables, M and N , and we choose a cross-section characterized by radius $R(S = \pi R^2; I = \pi R^4/4$ and $h = 2R$). The two limit-states are:

- (1) $\pi R^3 f_y > N R + 4M$ (resistance condition)
- (2) $N R - 4M > 0$ (fragility condition)

The random data are given in Table 10.11. The resistance f_y is considered as a certain variable equal to 70 MPa.

Engineer Smith, from a school we will not name for reasons of discretion, decides to design the column by calculating the radius for characteristic actions corresponding to an exceedance probability of 1%:

1. Calculate the characteristic value N_k .
2. Calculate the characteristic value M_k .
3. Deduce from this the exact radius R for the second condition and verify that it also satisfies the first.
4. Calculate the reliability index and the probability of failure corresponding to the second condition.

We use the approximations allowed for lognormal distribution when the coefficients of variation are small. To summarize, if X is lognormal:

$$F_X(x) = \Phi\left(\frac{\ln x - \lambda}{\xi}\right) \quad \lambda = \ln(m_X) - \frac{\xi^2}{2} \quad \xi \approx \frac{\sigma_X}{m_X}$$

Calculation of characteristic values: a characteristic value is obtained by solving the equation:

$$\Phi\left(\frac{\ln x_k - \lambda}{\xi}\right) = 0.99 = \Phi(2.33)$$

Hence:

$$N_k = 1.122 \text{ MN} \quad M_k = 0.03139 \text{ MN m}$$

Calculation of the radius R for condition (2): designing using characteristic values therefore results in (upper rounding value):

$$R = \frac{4M_k}{N_k} = 0.112 \text{ m}$$

and the first condition (resistance):

$$\pi R^3 f_y = 0.3090 > N_k R + 4M_k = 0.2512$$

is also verified.

Reliability index and probability of failure of the limit-state (2): this limit-state can be written in the form:

$$\beta_2 = \frac{\ln R + \ln N - \ln M - \ln 4}{\sqrt{\xi_N^2 + \xi_M^2}} = 1.05 \quad P_{f_2} = 0.148$$

For $R = 0.12 \text{ m}$ (approximate value), $\beta_2 = 1.66$ and $P_{f_2} = 0.048$, which shows a very high sensitivity to R .

Designing for a reliability target

An IFMA engineer proposes to design for a reliability target, contending with engineer Smith that systematically over-estimating the actions is an error. The target index is $\beta = 3$, for each of the two limit-states taken independently.

To demonstrate his proposition, the IFMA engineer proposes to take the means as characteristic values and to calculate the partial coefficients to be applied to each limit-state.

Case of limit-state (2): it is written, for standardized variables $N \rightarrow u_N, M \rightarrow u_M$ as:

$$\begin{aligned} \ln R - \ln 4 + \ln N - \ln M &= 0 \\ \ln R - \ln 4 + \xi_N u_N + \lambda_N - \xi_M u_M - \lambda_M &= 0 \end{aligned}$$

hence:

$$\begin{aligned} \beta_2 &= \frac{\ln R - \ln 4 + \lambda_N - \lambda_M}{\sqrt{\xi_N^2 + \xi_M^2}} = 3 \\ \alpha_N &= \frac{\xi_N}{\sqrt{\xi_N^2 + \xi_M^2}} = 0.447 \quad \alpha_M = -\frac{\xi_M}{\sqrt{\xi_N^2 + \xi_M^2}} = -0.894 \end{aligned}$$

The target value of β gives R :

$$R = \exp \left(\beta_2 \sqrt{\xi_N^2 + \xi_M^2} - (\lambda_N - \lambda_M - \ln 4) \right) = 0.139 \text{ m}$$

The most probable failure point is:

$$u_N^* = -\beta_2 \alpha_N = -1.34 \quad N^* = \exp(u_N^* \xi_N + \lambda_N) = 0.934$$

$$u_M^* = -\beta_2 \alpha_M = 2.68 \quad M^* = \exp(u_M^* \xi_M + \lambda_M) = 0.0325$$

The partial coefficients to be applied are:

$$\gamma_N = \frac{N^*}{N_k (= m_N)} = 0.934 \quad \gamma_M = \frac{M^*}{M_k (= m_M)} = 1.301$$

This result shows that we must underestimate the normal force to be on the side of safety.

Case of limit-state (1): in the absence of an analytical solution, we must calculate R by iterations. We obtain:

$$\beta_1 = 3 \quad \alpha_N = -0.384 \quad \alpha_M = -0.923 \quad R = 0.103 \text{ m}$$

The most probable failure point is:

$$u_N^* = -\beta_1 \alpha_N = 1.15 \quad N^* = \exp(u_N^* \xi_N + \lambda_N) = 1.057$$

$$u_M^* = -\beta_1 \alpha_M = 2.77 \quad M^* = \exp(u_M^* \xi_M + \lambda_M) = 0.03281$$

The partial coefficients to be applied are:

$$\gamma_N = \frac{N^*}{N_k (= m_N)} = 1.058 \quad \gamma_M = \frac{M^*}{M_k (= m_M)} = 1.312$$

Example conclusion: the partial coefficient on M is practically the same in both cases. On the other hand, we must note that the mean of N must be underestimated for limit-state (2) but over-estimated for limit-state (1). The method used by engineer Smith is therefore dangerous!

10.6 Conclusion

Using simple examples, this chapter shows how we can give meaning today to the traditional concept of the ‘safety’ coefficient. ‘Safety coefficient’ does not have any intrinsic meaning, and we must at least associate it with the concept of a characteristic value to give it any sense. The contribution made by reliability theory is to help dissociate the content of a global coefficient according to each variable in a rule. Improvements can result from it, for example by rewarding a better production quality with a decrease in the partial coefficient associated with the variable in question.

The relation between reliability analysis and the evaluation of coefficients in a rule has been shown. If the reliability analysis has been performed as such,

there is no benefit in deducing the coefficients from it. Such a method becomes relevant when a prior study helps provide calibrated coefficients for a validity domain. Thus, a designer can use a calibrated rule without having to carry out a reliability study for each case. On the other hand, reliability analysis has shown that empirical rules often have defects in homogeneity, and that applying the reliability analysis makes it possible to improve the rules. Whereas the knowhow of builders is capitalized in these rules, the content of these rules evolves by adding an algorithmic component to the heuristic component.

For example, an analysis [GPL03] of rule BS5500 [Col] relative to the design of thin shells shows the heterogeneity of the reliability index contained in the rule according to the different situations and proposes partial coefficients to enhance their homogeneity. Without reliability analysis, any design optimization based on the satisfaction of a rule could only result in searching for situations in which the rule is the least penalizing.

The calibration method has been proposed as a principle. The choice of the control variable as well as its influence has not been discussed. An extensive discussion of this issue is presented in [GMS+04]. It offers several possible controls.

Chapter 11

Mechanical-Reliability Coupling

11.1 Introduction

The previous chapters presented the bases of reliability analysis. The few examples discussed were based on a performance function $G(X_i)$ defined explicitly. This function reflects mechanical behavior that must often be modeled by approximated numerical solutions, from which only outcomes of $G(X_i)$ are calculable. The application of reliability-based methods in real technical situations therefore requires us to be capable of ensuring the dialog between the mechanical model and the reliability model. This is the objective of mechanical-reliability coupling.

The most efficient numerical modeling of mechanical behavior is currently the finite element method (FEM). Every calculation of $G(X_i)$ is a complete finite element calculation that can have a wide scope, particularly in the case of non-linearity. The number of calculations necessary will therefore be a pertinent indicator of the efficiency of a coupled method: it must be the lowest possible.

Any coupled calculation is equivalent to repeating mechanical calculations. The difficulty lies in the choice of the *pilot* capable of selecting judicious outcomes x_i so as to obtain the most relevant information. The general schema is given in Figure 11.1. Two symmetric branches respectively deal with action (load effect) and state variables and resistance variables. Mechanical transformations, which can be very simple and reduced to identity or which can result from a very complex numerical calculation, respectively yield load and resistance models. These can be interleaved when the resistance depends on the load or on its history. Controlled by one of these methods, the reliability-based method defines the outcomes of the random data to be taken into account in the mechanical models.

After presenting a few coupling conditions, this chapter describes the three control methods introduced initially in [FML97]:

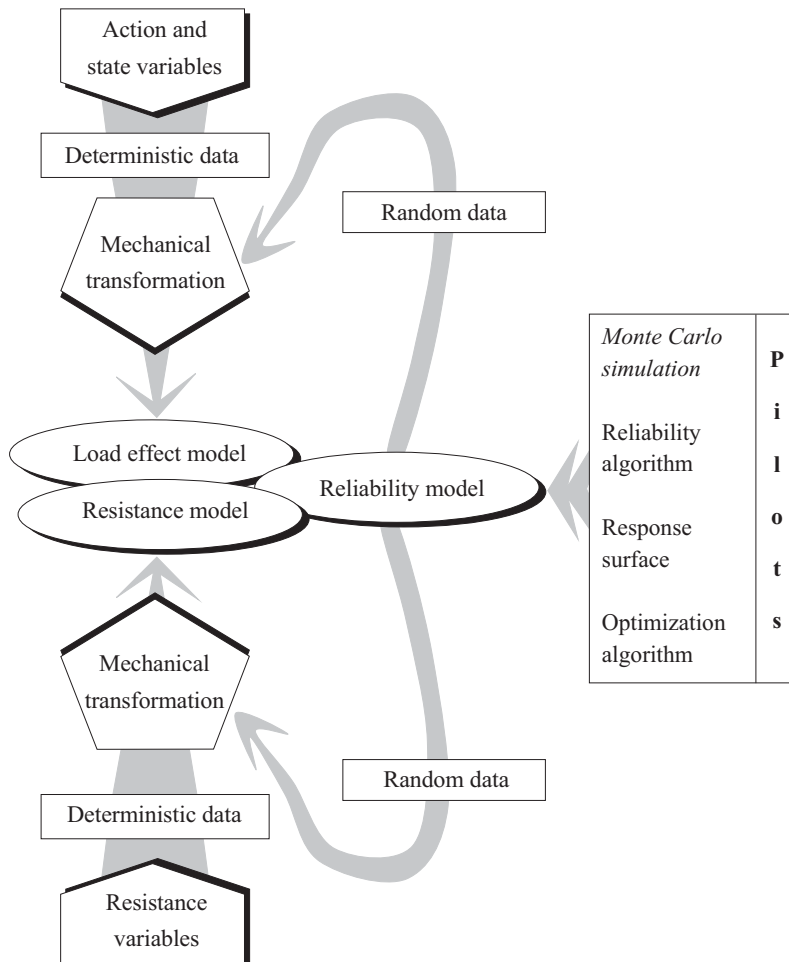


Figure 11.1 Principle of mechanical-reliability coupling. The various control methods.

- *direct coupling*, in which the reliability code calls the finite element code every time the calculation of $G(X_i)$ is necessary,
- *coupling by response surface*, in which a numerical design of experiments is used to construct an approximated explicit response of the performance function $G(X_i)$,
- *coupling by optimization*, in which the optimization problem resulting in the calculation of index β is solved using the optimization procedures available in the finite element code.

Direct coupling includes Monte Carlo simulation methods (Chapter 8). In their classical form, they are unrealistic in their application to the evaluation of weak probabilities. However, they are used in a conditioned form as a tool for validating FORM/SORM results.

In view of the current importance of FEM modeling, this presentation focuses on this mechanical model. However, it goes without saying that it applies to any mechanical model or any other model that can be solved numerically. The chapter is completed by simple examples, with an analytical solution or a numerical solution, which help illustrate and apply the results of the previous chapters.

11.2 General information on the coupling with a FEM code

11.2.1 Control of the FEM code

In a mechanical-reliability calculation, the finite element code must be controlled by the reliability module. The FEM code only executes the instructions of the reliability-based module. In each calculation loop, dialog must be established between the two modules: mechanical and reliability. This interaction is necessary, as it allows the reliability module to analyze the results of the FEM calculation and to make the appropriate decisions. Among these decisions, the reliability-based pilot must:

- define x_i coordinates of a new calculation point and evaluate a new outcome $G(x_i)$,
- validate the new step size depending on the consistency of the mechanical results,
- detect convergence in case of stabilization of the results during the iterations,
- stop the calculation in case of divergence and take appropriate actions,
- automatically change the algorithm used in order to speed up convergence depending on the nature of the problem posed.

11.2.2 Random variables

In a mechanical-reliability analysis, it is interesting to deduce, from the nature of random events and their interactions, their effects on the response of the system. Design variables for which we have more or less complete information are random. These basic variables X_i include the load variables S and resistance variables R used in the definition of the performance function $G(X_i)$ which can be separated into load and resistance parts – this is the case in Figure 11.1 –

(except if the load degrades the resistance):

$$G(X_i) = R(X_i) - S(X_i)$$

If we directly know the R and S distributions, the problem of reliability calculation becomes a simple mathematical operation. However, the functions of mechanical and physical transformations are often too complex to calculate the resistance and load variable distributions from the knowledge of the distributions of the basic variables X_i . Nevertheless, new approaches in stochastic finite elements (Chapter 12) are beginning to offer a solution to characterize the response distributions of any model.

In general, the FEM calculation data contain basic random variables X_i while the results help define the load variable $S(X_i)$. As for the resistance variable $R(X_i)$, it is often independent of the finite element calculation; it is therefore declared explicitly as a function of the basic variables X_i .

There can however be situations with a mixture of resistance and load variables intervening in finite element calculations. In this case, it is not possible to differentiate these two types of variables in the coupling between the probabilistic code and the mechanical code.

11.2.3 Mechanical-reliability variables

In a mechanical-reliability analysis, the processing of variables differs according to their nature and their relations. The variables of the model can be classified as in the following tree (Figure 11.2):

- *Elementary deterministic or random variables:* these are the lowest-level variables; they are declared by a simple assignment of a numerical value. Let us take the example of the axial stiffness of a bar $K_N = E S/L$ with $S = b h$ (rectangular cross-section area = base \times height); the variables E (elasticity modulus), L (length), b and h belong to this category. In the probabilistic model, these variables can be taken as random, by associating a distribution defined by its type with the associated parameters.
- *Random variables dependent on deterministic variables:* the variables are declared by a function involving other variables which remain deterministic in the entire tree up to the level of elementary variables. For example, the variables S and K_N can belong to this category, provided that b, h, L and E remain deterministic. In this probabilistic model, these variables are handled exactly as in the previous case; that is, we can assign them a distribution function without having to worry about the origin of their randomness. This is tantamount to considering the result S of the mechanical transformation $b, h \rightarrow S$ directly as an elementary random variable, without having to worry about the origin of the random event

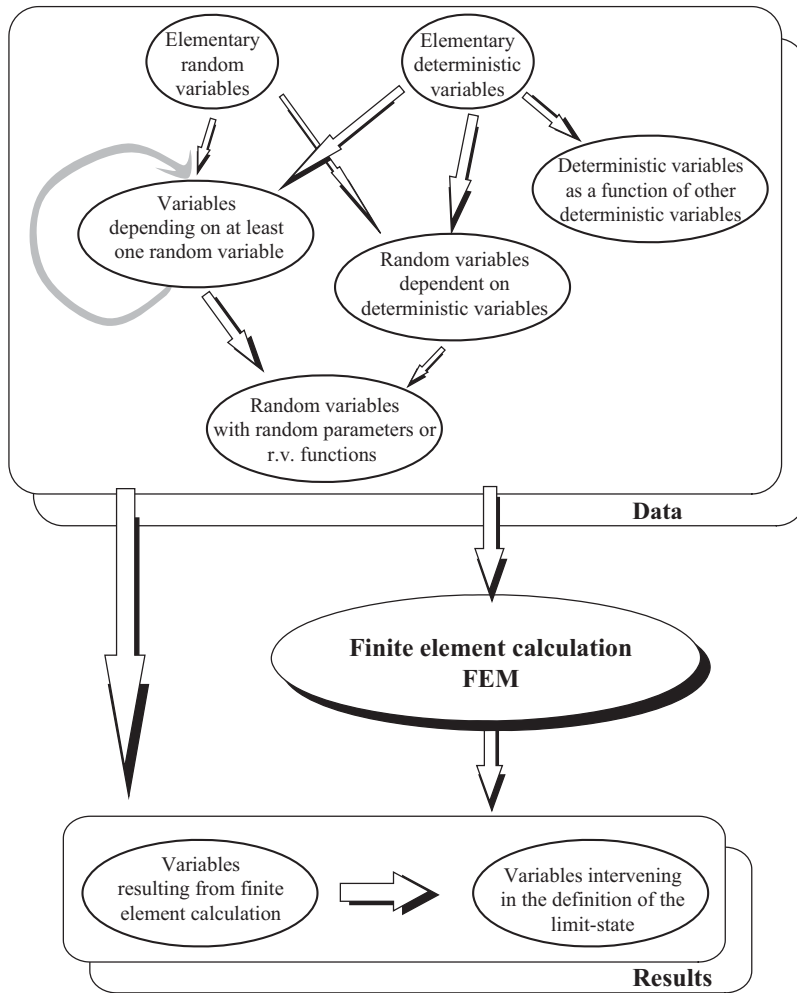


Figure 11.2 Tree of variables in the mechanical-reliability model.

through h and b , provided these latter do not themselves intervene as elementary random variables elsewhere.

- **Variables that are a function of at least one random variable:** these variables depend on random variables in the argument tree. For example, if the height h is random, variables S and K_N are also random. From the probabilistic point of view, their distribution is defined according to the combinations of random variables; we can therefore neither modify their distribution nor assign new probabilistic distributions; in brief, they are untouchable.

- *Variables that are a result of the finite element calculation:* some variables are the result of the analysis carried out by the FEM code, the stresses at a given point, a displacement, etc. In this case, it is very difficult to know, from a single FEM calculation, whether this type of variable is a function only of deterministic data or of some random data. In the former situation the result variable is deterministic, and in the latter situation it is a complex function of random variables; the result variable is therefore random. To verify whether a result variable is a function of random data, we can perform a sensitivity analysis by varying the data, one by one, and seeing whether the result changes or not; of course, this variability study will cost a few additional calculations, which are not indispensable, and it does not present any advantage for mechanical-reliability calculation.

In general, the result variables that are of interest to us are those that intervene in the expression of the performance function (and which generally deals with a load effect). These variables are therefore a function of random variables, hence the mechanical-reliability coupling. If this is not the case, the mechanical and reliability models are decoupled and we will therefore be able to do without the FEM calculation in the reliability analysis; a single FEM calculation is enough for reliability analysis. In general, the probabilistic model considers all the variables resulting from the FEM calculation as variables that are a function of random variables; they are therefore untouchable, as in the previous case.

- *Variables whose distribution parameters depend on other random variables:* this is the case for ‘compound’ variables. For these variables, the distribution parameters are defined by explicit functions of other variables in the model. From the probabilistic point of view, these variables are random with random parameters. We must therefore keep in mind the entire composition tree and the functions of random variables up to the level of elementary variables; this is indispensable for the calculation of gradients and for taking into account the interactions and dependences of the variables.

It must be noted that variables can change their category depending on the nature of the analysis and in particular depending on the failure scenario envisaged. Let us take the example of reaching the yield limit; the criterion is:

$$G = f_y - \sigma(X_i)$$

where f_y is the yield limit and σ is a reference stress which is a function of the basic random variables. If we are interested in the elastic analysis, the yield limit does not intervene in the FEM calculation. However, in an elastoplastic post-elastic analysis with strain hardening, it can have a direct role as it enters into the material behavior model used in the FEM software.

11.2.4 Dialog between FEM and reliability procedures

We have just seen that dialog is indispensable in a coupling software package; the reliability-based module controls the calculation operations and the FEM code, which is considered as a black box. This dialog must be established using interfacing procedures between the two modules, mechanical and reliability.

It is therefore imperative for the reliability module to recognize and modify the values of the random variables of the FEM code data, and to recognize the load effects (output variables) in the FEM results. Furthermore, it must be alerted in case of problems in the execution of the mechanical calculation.

The choice that seems preferable is that of adapting the procedures of reading, analyzing and interpreting to the FEM code format; that is, it is the reliability-based module that makes the effort to converse with the FEM procedures, which remain intact. This solution is probably less direct, but it has the advantage of not intervening at the FEM code level, thus helping to preserve its qualities without any disturbance. This is also the only solution when the coupling is performed with a code for which we do not have any source programs.

Among the FEM codes available in engineering, we can distinguish two families according to whether the code has – or does not have – a parametrized language. The presence of such a language largely facilitates the task, as the variables are declared explicitly. Moreover, some codes are currently equipped with a general purpose optimization module, which can be used for the mechanical-reliability calculation (the calculation of the design point is in fact a particular optimization problem). Depending on the possibilities of each code, we must therefore adapt the interfacing procedure on a case-by-case basis.

11.2.5 Implementation of the procedures

The coupling between mechanical and reliability models requires an exchange of information. The protocol to be implemented depends on the capacities of the coupled software packages and the possibilities for dialog. The reliability module controls the mechanical module, which is generally the largest consumer of calculation resources, and a good performance indicator is the number of calls to the mechanical model. Figure 11.3 shows the main links possible.

By using a commercial mechanical module, four interface possibilities may be envisaged:

1. *Graphic user interface*: all the information is entered and read through graphic windows. The coupling is hardly flexible at all, and may even be impossible.
2. *Formatted files interface*: the information is entered and retrieved in numerical data exchange files, while retaining all the significant figures.

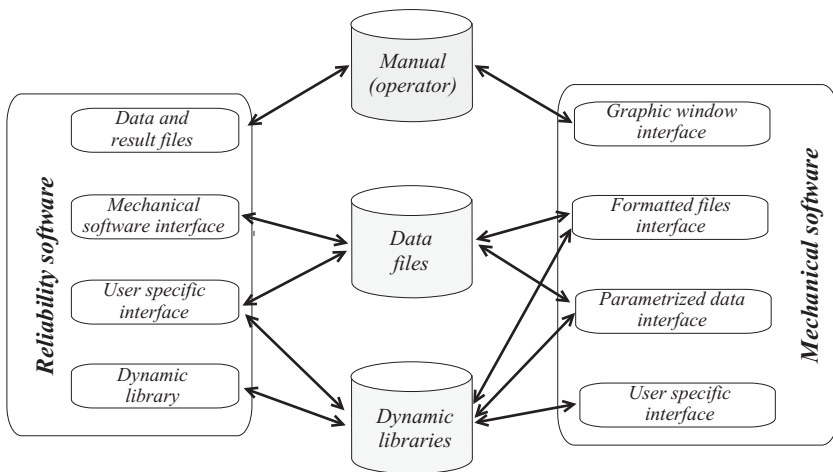


Figure 11.3 A few possible links between a mechanical calculation module and a reliability calculation module.

It is then possible to write, for each problem, a procedure for creating such files as long as the variables likely to vary do not modify the very definition of the geometric model (case of variables modifying the mesh of a FEM model).

3. *Parametrized data interface*: coupling is largely facilitated if the mechanical module has an integrated parametrized language. The random variables are then parameters of the mechanical model.
4. *User-specific interface*: such an interface exists in certain calculation codes. The user creates his own procedures for the exchange of results and the control of calculations; the reliability module is then completely integrated into the mechanical module and any risk of loss of accuracy by truncation is eliminated.

The reliability module offers the following interfaces.

1. *Writing data and results in an interpreted file*: the module is closed and automatic exchange is not possible.
2. *Interface compatible with the mechanical module*: such a possibility requires that the reliability module recognize the mechanical module. It provides a real coupling but must be developed on a case-by-case basis.
3. *User-specific procedure*: this consists of a procedure developed by the user to construct the limit-state function, or even its gradients, and to read the necessary data. The reliability module must be capable of managing such

an external procedure, which is compiled with the mechanical module to obtain an executable procedure.

4. *Dynamic library interface*: new calculator technologies allow the exchange of information via a dynamic library link (DLL), which is independent of the reliability module. This interface is an optimal form of dialog, as all the conditions are met: accuracy, efficiency, flexibility and portability.

11.2.6 Numerical evaluation of gradients

Most of the mechanical-reliability calculation procedures require calculation of the gradients in order to define the descent direction that minimizes the objective function (distance between the origin and the limit-state). During the mechanical-reliability coupling, this gradient can be obtained by numerical finite differences (direct method) or by derivation of an approximated explicit function of the limit-state (response surface method). In the context of finite elements, Section 12.4 also gives indications of the direct calculation of gradients.

Finite differences

Derivation with respect to a variable: in reliability algorithms, the calculation is essentially performed in standardized space. The Jacobian of the probabilistic transformation expresses the transformation from physical space to standardized space. Moreover, the calculation of gradients is necessary for the evaluation of the distribution parameter sensitivities. We therefore search for quantities of the form:

$$\frac{\partial G(x_k)}{\partial x_i}$$

In general, the function $G(x_k)$ is non-linear and no explicit form is known. It is, however, considered derivable. The analytical calculation of gradients is impossible in this case without admitting simplifying assumptions likely to lead to significant errors.

Gradients must therefore be calculated by finite differences. A Taylor expansion leads to three possible formulae, recalled here for function $G(x)$ and step size h :

$$G(x + h) = G(x) + \frac{\partial G(x)}{\partial x} h + \frac{1}{2} \frac{\partial^2 G(x)}{\partial x^2} h^2 + O^3 \quad (11.1)$$

- The direct application of this formula, retaining only the first two terms and assuming $h > 0$, gives the *forward finite difference* with an error of

order O^2 :

$$\frac{\partial G(x)}{\partial x} \approx \frac{G(x+h) - G(x)}{h}$$

- A negative step size ($h > 0$) gives the *backward finite difference*:

$$\frac{\partial G(x)}{\partial x} \approx \frac{G(x) - G(x-h)}{h}$$

- Lastly, by applying Equation (11.1) twice, respectively with $+h$ and $-h$ and by applying the difference, we obtain:

$$G(x+h) \approx G(x) + \frac{\partial G(x)}{\partial x} h + \frac{1}{2} \frac{\partial^2 G(x)}{\partial x^2} h^2 \quad (11.2)$$

$$G(x-h) \approx G(x) - \frac{\partial G(x)}{\partial x} h + \frac{1}{2} \frac{\partial^2 G(x)}{\partial x^2} h^2 \quad (11.3)$$

$$\frac{\partial G(x)}{\partial x} \approx \frac{G(x+h) - G(x-h)}{2h} \quad (11.4)$$

which constitutes the *centered finite difference*, of a better accuracy of order O^3 .

- If, as is generally the case, $G(x)$ is known, then the second derivatives are obtained for the same calculation effort as the first-order centered finite difference. By adding (11.2) and (11.3):

$$\frac{\partial^2 G(x)}{\partial x^2} \approx \frac{G(x+h) + G(x-h) - 2G(x)}{h^2} \quad (11.5)$$

with a remainder of order O^4 as the terms in h^3 cancel each other out.

Finite difference equations are particularly useful and efficient, provided we choose the step size well and we do not forget that the approximation tends toward $\frac{0}{0}$, which is mathematically satisfactory but can be numerically disastrous.

Derivation with respect to two variables: the previous equations apply variable by variable. We must still calculate the crossed second derivative (mixed), for respective step sizes $h > 0$ and $k > 0$, using:

$$\begin{aligned} & \frac{\partial^2 G(x, y)}{\partial x \partial y} \\ & \approx \frac{G(x+h, y+k) - G(x+h, y-k) - G(x-h, y+k) + G(x-h, y-k)}{4hk} \end{aligned} \quad (11.6)$$

Figure 11.4 shows a second-order finite difference mesh. For the one-dimensional derivatives (Equation (11.5)), we must use three points along each

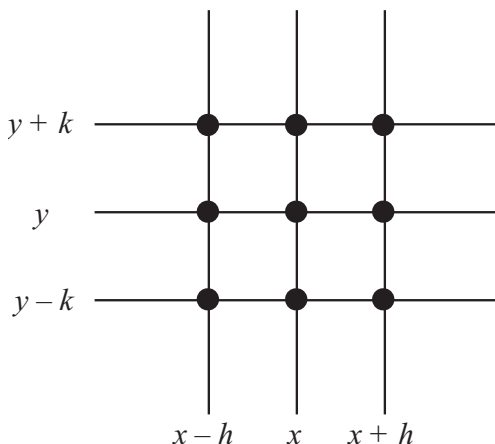


Figure 11.4 Two-dimensional finite difference mesh.

axis, whereas for the mixed derivative, two points are sufficient along each axis. As a result, Equation (11.6) can be applied to each domain defined by four points, and therefore to the center of each domain appearing in the figure. The step size is then $h/2$ and $k/2$.

If n is the number of variables, the number of calculations necessary to know the gradients is $n + 1$. The error is of second order for Equation (11.4) of the forward or backward difference. A better approximation is obtained in centered difference (error of third order), but at the cost of $1 + 2n$ calculations, which also provide the second derivatives, useful for the calculation of curvatures and the SORM approximation.

Comments

- Given that failure implies the decrease of resistance variables and the increase of load variables, we can choose the incrementation of the variables in the direction that brings us closer to failure. However, as the increments are relatively small, the direction of the increments can only have a very small influence on the convergence of the algorithm.
- In the case of variation of geometric data, the finite difference calculation implies a remeshing of the structure. Without error control, discretization errors in the two meshes can disturb the calculation of the gradients. Here again, we can suppose that this error will have a minimum effect, in view of the small variable increments, but we must validate this conclusion, particularly when we approach the minimum (when the derivatives approach zero).

Conclusion

The calculation of gradients is a key phase in mechanical-reliability procedures. The cost can be considerably decreased if the FEM code has an integrated gradient operator. A single analysis is then enough to obtain, in addition to the usual results, all the gradients of the various results with respect to the input variables. Current developments of new optimization procedures in FEM codes offer new tools for mechanical-reliability coupling.

11.3 Direct method

11.3.1 Description of the method

In the direct method, the *pilot* is the reliability algorithm selected for the calculation of the reliability index (Chapter 5). Every time an outcome of the performance function $G(X_i)$ must be calculated, the *pilot* chooses the outcome x_i and calls the FEM code. The calculation of gradients is performed by finite differences. The calculation of curvatures around P^* requires additional calls. Figure 11.5 summarizes the sequence of steps and underlines the calls made to the FEM code.

The number of calls depends on the performance of the algorithm selected and on the accuracy required for the iteration stop tests. Additional calls are made for the calculation of curvatures (SORM approximation) and for the conditional simulations necessary for the validation of the results.

11.3.2 Overview

As an overview, we can mention the following:

1 Advantages:

- conservation of the accuracy of the mechanical calculation of $G(X_i)$,
- efficiency of specialized reliability algorithms,
- automatic procedure (no intervention by the designer),
- robustness,
- compatibility with any calculation code accepting data on file,
- etc.

2 Disadvantages:

- complex automation if the mechanical module is not parametrized,
- automatic procedure (risk of useless, even physically unrealistic, calculations),
- possible lack of convergence of FORM toward the real design point,
- numerical calculation of gradients,
- difficult calculation of curvatures to obtain SORM results,

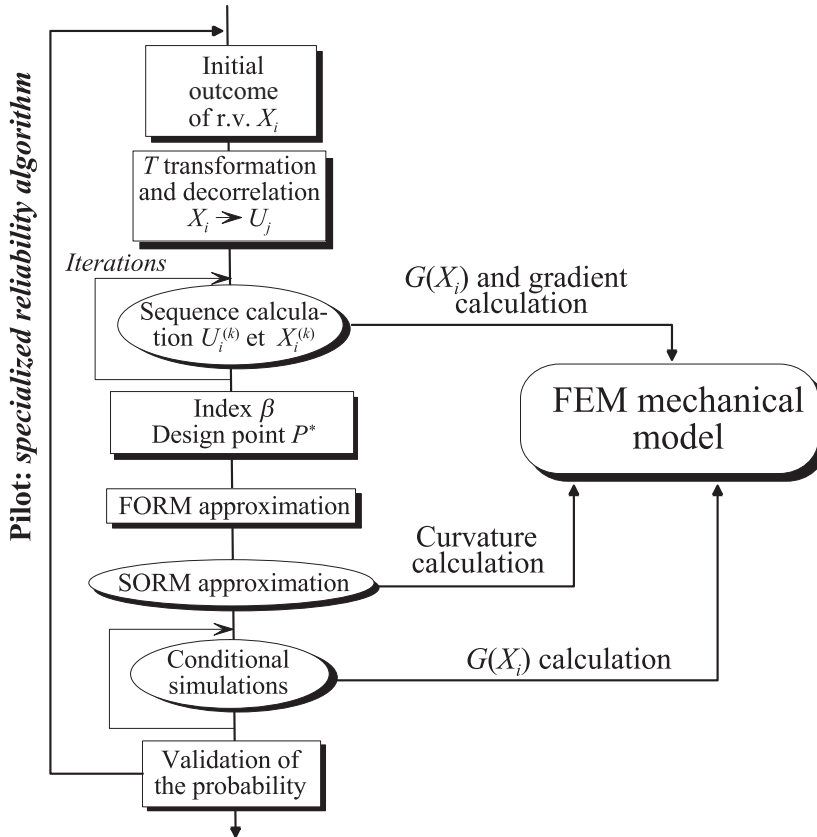


Figure 11.5 Coupling by direct method.

- large number of calls, depending on the quality of the control algorithm and given the necessity of evaluating the gradients by finite differences,
- etc.

11.4 Response surface method

11.4.1 Introduction: polynomial response surface

The use of response surfaces in reliability problems is not recent and has always benefited from new contributions. Research has established the concepts [Far89, ETML91, RE93, Lem98], constructed solutions in the physical space [BB90] and

proposed methods of evolution [EFS94, Dev96, KN97]. The reliability model is in general FORM/SORM, but the response surface can also be coupled with simulations [LM94].

The solutions offered can be distinguished by the choice of working space (physical or standardized) and by the method of evolution toward the most probable failure point, this method requiring the construction of design of experiment (DOE). The general schema is given in Figure 11.6. The essential interest lies in the numerical decoupling between the mechanical model and

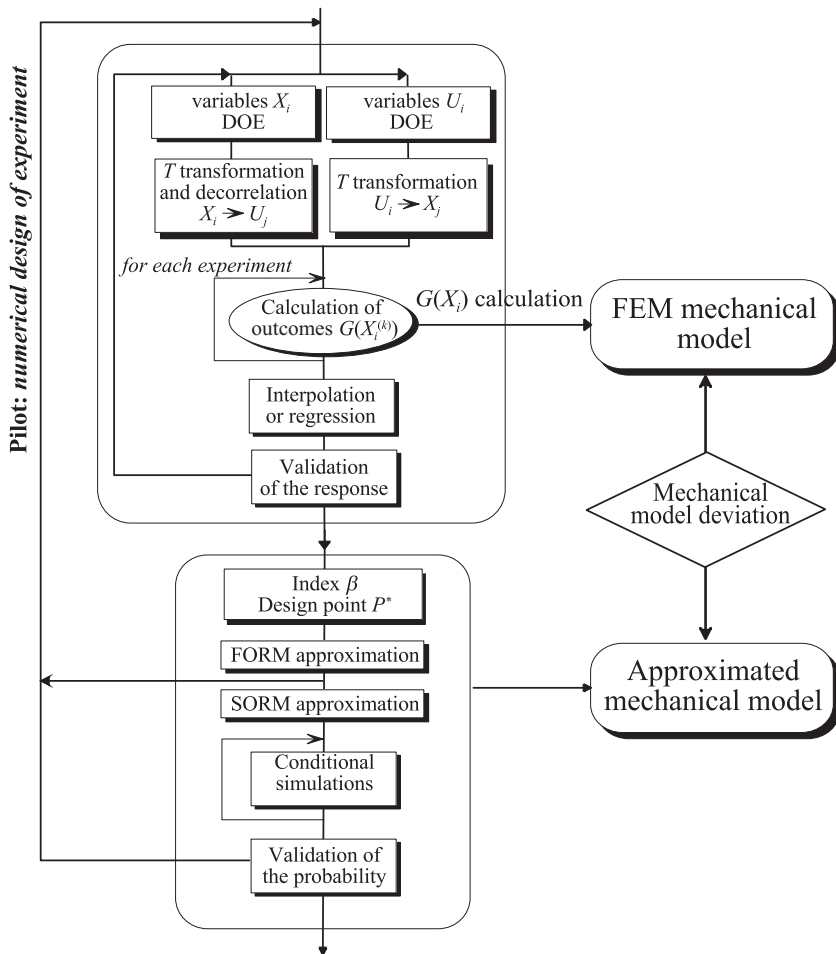


Figure 11.6 Principle of the response surface method.

the reliability model. The main drawback results from the fact that the reliability-based calculations are performed with an approximated mechanical model.

11.4.2 Description of the method

Reliability calculation requires, whatever the method used, an ever-increasing number of evaluations of outcomes of the performance function $G(X_i)$. This number is a good indicator of the efficiency of the method; as each outcome can result from a complex model associated with a complex numerical solution, it is indispensable in limiting the total number of outcomes. For this, one of the possible methods is to construct a simple analytical representation in the neighborhood of the design point. The name ‘response surface’ (RS) is given to such a representation. Its interest lies in an explicit form in which the reliability calculation is largely simplified and at practically zero cost; its difficulty is in justifying the approximation selected in a given domain.

For this, two problems must be addressed:

1. choice of a base for the development of the RS and identification of the unknown coefficients,
2. construction of the RS around the most probable failure point.

Bases for the development of the RS

Three cases must be considered, according to the information available:

1. The mechanical model results in an explicit form of the RS dependent on l parameters. It is then enough to identify the l parameters from l calculations, ensuring that the equation system is well-conditioned. We come across such a situation when the independent influence coefficients of the random variables can be calculated (see example in Section 6.4).
2. A theoretical study gives indications of the form of the RS. This is the case, for instance, of a limited expansion of the response around a point (Taylor expansion, asymptotic development). This is also the case when simplified theories exist beside more accurate models (beam theory instead of FEM calculation in elasticity).
3. In the absence of information, the RS must be constructed blindly. An *a priori* base is chosen and the coefficients are identified by interpolation or by regression.

In our case, an expansion on a polynomial basis seems the most efficient currently, but other attempts [PCH00] are being made on the basis of neural networks, which we will discuss in Section 11.4.5. The polynomial basis is selected by most of the authors. The degree $d = 2$ (quadratic response

surface, QRS) then corresponds to a good compromise, as it includes a possible calculation of curvatures, and it avoids oscillations, which are always possible with a high degree. For n random variables, the number of coefficients for the complete development is $l = (n + d)!/n!/d!$, that is, $l = (n + 2)(n + 1)/2$ for $d = 2$. For an approximation of $H(u)$, the general form is then:

$$\tilde{H}(\{u\}) = [\cdots \quad (u_i^p u_j^q)_k \quad \cdots] \begin{bmatrix} \vdots \\ a_k \\ \vdots \end{bmatrix} \quad (11.7)$$

with $p + q = \begin{cases} 0 & i, j = 1, \dots, n \ k = 1, \dots, l \\ 1 & \\ 2 & \end{cases}$

However, the designer also has information that enables him to eliminate certain interactions; that is, to consider certain a_k coefficients as zero or known, which reduces the dimension of the problem to $l^r \leq l$. The coefficients are determined by regression from n_e experiments.

Construction of the RS: ‘oriented’ design of experiment

The basis for the development of the RS having been chosen, we must construct it around the most probable failure point P^* , whose position is unknown. The solution proposed is to search for a series of points $P^{*(s)}$ associated with a series of RS(s) whose definition domain finally contains $P^{*(s)}$.

A numerical design of experiment (NDOE) defines the outcomes to be calculated; at least l^r for an interpolation, but a greater number is necessary to guarantee the quality of the approximation.

The theory of design of experiment (see, e.g. [BTG94]) proposes classical designs and tabulated designs:

1. Centered design of experiment:

- star design of experiment of type $1, u, v, u^2, v^2, \dots$, without interaction between the factors,
- factorial design of experiment 2^n of type $1, u, v, uv, \dots$,
- star + factorial design of experiment of type $1, u, v, u^2, uv, v^2 \dots$,

2. Tabulated design of experiment: the use of predefined tables, of the Taguchi type, requires information on the interactions between factors or variables.

Such designs have been tested on reference examples and have produced satisfactory results, showing their capability of converging toward the exact solution after a sufficient number of steps [ML96]. However, this first approach

does not take into account what the mechanical designer knows about the functioning of the structure under study. In fact, for most random variables, the resistance or load nature is known and the direction of shift from the median toward the failure point is therefore known *a priori*. Such designs, which include all the expert knowledge of the designer, are called ‘oriented’ and they must be preferred during the starting phase, whereas centered designs must be constructed around the failure point when its position is confirmed.

The choice of a first design of an experiment helps to construct a first response surface and thereby obtain a first point $P^{*(1)}$. The analysis of the results helps introduce new experiments around this first point to repeat the process by translation, change of scale [MLET92] or projection [KN97] of the NDOE. Figure 11.7 illustrates the construction. The first design (on the left), with one standard deviation, is oriented by the resistance or load character. It leads to point $P^{*(1)}$. Centered on this point, a second design (on the right) is constructed, with 0.75 standard deviation, which gives point $P^{*(2)}$.

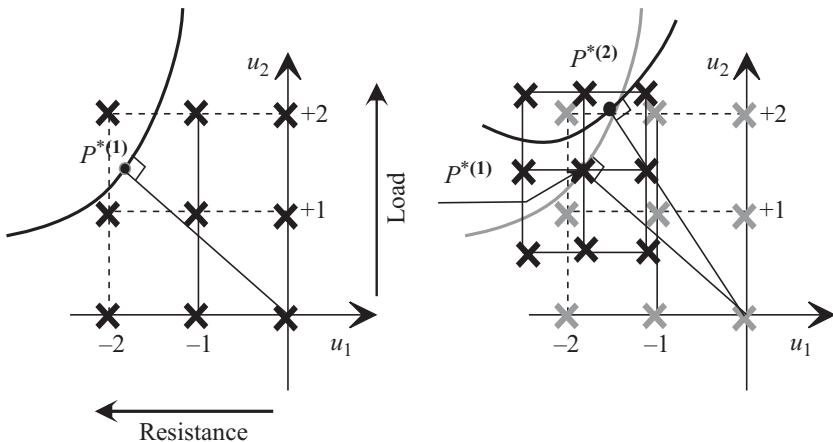


Figure 11.7 Two successive designs of experiment.

Choice of the working space

In view of the solution scheme of reliability problems, two possibilities are offered for the construction of an RS: in physical space or in standardized space. *Physical space:* placing ourselves in physical space offers the advantage of directly working with physically realizable solutions, which is close to the habits of the designer. However, the choice of physical points can lead to points very removed from the origin in standardized space or, on the contrary, to almost overlapping points, depending on the importance of standard deviation.

Furthermore, the designer knows the mean operating domain well, but can have great difficulties in identifying points around the failure. Lastly, the quality of the reliability-based solution depends on writing the limit-state in standardized variables obtained in this case by application of transformation T on the approximated form $\tilde{G}(X_i)$. Physical space is more favorable for a study of sensitivity around the mean than for a reliability study.

Standardized space: working directly in standardized space guarantees a choice of variables around a point, distant from a well-controlled number of standard deviations, which favors good numerical conditioning. The validity domain of the RS is then well known. However, it is possible for the physical origin point not to be physically admissible. We then search for aberrant physical solutions, hence the importance of examining the realistic – or unrealistic – nature of the physical origins of the calculation points.

A study *a priori* of the admissible domains of physical variables helps to obtain, by application of the isoprobabilistic transformation T , the standardized domain in which to place the calculation points of the RS.

In addition, the rules of correlation, composition and truncation of variables can lead to non-unique transformations T . An outcome $u_i^{(r)}$ always enables a physical origin outcome $x_i^{(r)}$ to be found, but the converse is not true.

Lastly, since the variables are standardized, adimensional indicators can be constructed, which makes their interpretation easier.

Conclusion: a response surface must be constructed in the acceptable physical neighborhood and include points which are sufficiently distributed in standardized space. A constant shuttling between physical points and standardized points is indispensable.

Shuttling between physical and standardized variables is independent of the mechanical model and can largely be done at practically zero cost.

However, the points around P^* whose position depends on the limit-state are interesting. To determine a domain for P^* , it is possible to use *a priori* information like the resistance or load quality of a variable or a simplified model of the mechanical behavior, by using a simplified theory or by a reduced FEM mesh.

A methodology

The response of a mechanical model around P^* is estimated by a process involving successive steps toward convergent mechanical and reliability contents:

- *Successive steps:* a few RS are constructed by ensuring an evolution of the NDOE center which converges toward a minimum. This minimum must belong to the construction domain; it is in general easy to show that it is an absolute minimum on the RS, but not necessary for the origin problem.

- *Mechanical convergence*: the mechanical model is refined during the successive steps. In fact, it is useless to use the most refined solutions in the first outcomes, but the management of successive models can be complex.
- *Reliability convergence*: apart from the reliability index and the FORM probability obtained at each step, the additional indicators are calculated as we change the steps (SORM, conditioned simulations).

Two approaches are possible:

- construct a large NDOE and then make it draw closer around the first point obtained, which is then generally inside the first design,
- construct an NDOE in a reduced domain and then move it around the first point obtained.

The choice of the NDOEs is the most difficult problem to solve. We cannot opt for an algorithmic response alone, and it is up to the engineer to introduce his expert knowledge. To ensure validation, we must enter the maximum quantity of information at each step and pay attention to the quality of this information, for example if it results from an approximated or refined mechanical calculation. The creation of a database enables experiments to be accumulated and reused in successive designs. Depending on the progress of the reliability calculation, it is possible to eliminate variables by fixing them to their medians if they appear to be of little significance from the stochastic point of view.

The reliability problem is then solved in the RS. It must be borne in mind that the RS is valid only in a restricted domain around the point P^* obtained and that it must not be used outside its domain of definition.

11.4.3 Calculation of the coefficients of a QRS

Matrix of experiment

The limit-state $H(u_i)$ is approximated by the second degree polynomial $\tilde{H}(u_i)$ (Equation (11.7)). Each experiment defines a line of the matrix of experiment $[Z]$. For experiment (r) :

$$\langle z^{(r)} \rangle = \left\langle 1, \dots, u_i^{(r)}, \dots, u_i^{(r)} u_j^{(r)}, \dots \right\rangle \text{ with } [Z] = \begin{bmatrix} \vdots \\ \langle z^{(r)} \rangle \\ \vdots \end{bmatrix} \text{ dimension } n_e \times l$$

and hence:

$$H(u_i^{(r)}) = \langle z^{(r)} \rangle \{a\} \implies \{H(u_i^{(r)})\} = [Z]\{a\}$$

Solution

An estimate $\{\hat{a}\}$ of l coefficients $\{a\}$ is deduced by a least squares approximation:

$$\text{minimize} \sum_{r=1}^{n_e} \left(\tilde{H}(u_i^{(r)}) - H(u_i^{(r)}) \right)^2$$

Let:

$$\text{minimize } \langle \hat{a} \rangle [Z]^t [Z] \{\hat{a}\} - 2 \langle \hat{a} \rangle [Z]^t \{H(u_i^{(r)})\} + \left\langle H(u_i^{(r)}) \right\rangle \{H(u_i^{(r)})\}$$

hence:

$$\frac{\partial}{\partial \{\hat{a}\}} = \{0\} \implies [Z]^t [Z] \{\hat{a}\} = [Z]^t \{H(u_i^{(r)})\}$$

and:

$$\{\hat{a}\} = ([Z]^t [Z])^{-1} [Z]^t \{H(u_i^{(r)})\} \quad (11.8)$$

Measures associated with the matrix of experiment $[Z]$

The DOE theory suggests three measures:

1. *D-optimal design criterion*: the value of the determinant of $[[Z]^t [Z]]$ must be the greatest possible,
2. *A-optimal design criterion*: the trace of the matrix $[[Z]^t [Z]]^{-1}$ must be the smallest possible,
3. *G-optimal design criterion*: the value of the largest element of the diagonal of $[[Z]^t [Z]]^{-1}$ must be the smallest possible.

It must be noted that these indicators can be constructed in the absence of any mechanical calculation and are therefore economic to evaluate. They can help answer the following question: if I have n numerical experiments, how can I choose the $(n+1)$ th experiment to improve the indicators?

11.4.4 Validation

For each set s of outcomes r constituting a design of experiment and resulting in the construction of a response surface, a set of tests gives indications on the quality of the approximations obtained. They complete the measures associated with the matrix of experiment and can be classified according to the information necessary for their evaluation.

Physically admissible outcomes

The choice of a outcome $u_i^{(r)}$ implies a physical outcome $x_i^{(r)} = T_i^{-1}(u_j^{(r)})$ which must be physically admissible and correspond to a situation compatible with the hypotheses of the mechanical model. If this is not the case, it is an aberrant point to be excluded from the numerical design of experiment.

Quality of the regression [Sap90]

This is measured after calculation of the outcomes $H(u_i^{(r)})$. The indicator is the measure of the correlation R^2 between the calculated responses and the approximate responses evaluated by the RS:

$$R^2 = 1 - \frac{\sum_{r=1}^{n_e} \left(H(u_i^{(r)}) - \tilde{H}(u_i^{(r)}) \right)^2}{\sum_{r=1}^{n_e} \left(E[H(u_i^{(r)})] - H(u_i^{(r)}) \right)^2} \longrightarrow 1$$

where $E[\cdot]$ is the expectation. This indicator is equal to 1 in the case of an interpolation; it must be used only to control a regression where a value greater than 0.9 must be obtained, but practice shows that this indicator is not very selective.

Value of the limit-state function in P^*

After a reliability calculation, point P^* is obtained. Two indicators are proposed:

- The first measures that P^* belongs to the design of experiment:

$$I_{ppc} = 1 - \left(\frac{1}{\sum_t N_t} \sum_{t=1}^j \frac{N_t}{t!} \right)^{-1} \longrightarrow 0$$

where j is the limit chosen for the expansion and N_t is the number of points of the design of experiment located at less than t standard deviations from P^* according to a given norm; that is:

$$N_t = \text{card} \left(P^{(r)} \left| \max_{i=1,m} \left(u_i^{(r)} - \tilde{u}_i^* \right) < t \right. \right)$$

or:

$$N_t = \text{card} \left(P^{(r)} \left| \sqrt{\sum_{i=1}^m \left(u_i^{(r)} - \tilde{u}_i^* \right)^2} < t \right. \right) \text{ with } m = \dim(u_i)$$

Each point intervenes only once. This indicator tends toward 0 when the response surface surrounds point P^* with less than one standard deviation. It gives a large weight to the close points, but does not help to verify the good distribution around P^* . This results from an ‘inertia’ measure, which is tantamount to adding the squares of the distances and therefore to finding the indicator R^2 .

- The second verifies that point P^* belongs to the limit-state function. It requires an additional mechanical calculation:

$$I_a = \frac{H(\tilde{u}_i^*)}{H(\mathbb{E}[u_i])} = \frac{H(\tilde{u}_i^*)}{H(\{0\})} \longrightarrow 0$$

However, it does not prove that this is a minimum in the limit-state function.

Reliability sensitivity of the RS

Reliability software packages easily evaluate the sensitivity, or better, the elasticity of index β with respect to the parameters of the RS. This additional information illustrates the robustness (or otherwise) of the surface. A low elasticity shows that the approximations carried out have only a small influence on the reliability results.

Validation by repetition of the design of experiment [BBF92]

The evaluation of the indicators proposed by Böhm and Brückner-Foit supposes the repetition of the design of experiment. The outcome of a single design helps calculate an approximation $\tilde{H}(u_i)$ of the performance function. The adjustment error is measured by the quantity:

$$\varepsilon_a(u_i) = H(u_i) - \tilde{H}(u_i)$$

which is a systematic and deterministic error. It is supposed that outcomes $H(u_i^{(r)})$ have a Gaussian experimental error ε_e , with zero mean and variance σ_e^2 . It exists in the case of physical experiments in which it is not possible to repeat the same conditions exactly. It is zero in the numerical case with the same software and the same modeling where the repetition of an experiment always gives the same result with a very adequate number of significant figures. We get:

$$\{H(u_i^{(r)})\} = [Z]\{a\} + \{\varepsilon_a(u_i^{(r)})\} + \{\varepsilon_e^{(r)}\} \approx \{\hat{H}(u_i^{(r)})\} = [Z]\{\hat{a}\}$$

and the estimates $\{\hat{a}\}$ of the parameters of $\hat{H}(u_i)$ are obtained from n_e experiments according to Equation (11.8). The authors build criteria for the

acceptance of the response surface by evaluating the adjustment error and the experimental error through a repetition of the design of experiment. If the discussion and the examples of the paper show the quality of the indicators, we must underline the high cost of the calculation necessary owing to the repetitions.

Validation by resampling [GBL02]

The principle of the method proposed lies in the multiple utilization of the same set of outcomes of the design of experiment, without this procedure requiring additional mechanical calculations.

Construction of an application \mathbf{P} : let $j = 1, \dots, p$, be the p experiments and $\{u^{(j)}\}$ the n coordinates of outcome j in standardized space. Let us denote by $\{\tilde{u}^*\}$ the coordinates of the approximated point \tilde{P}^* obtained by application of the reliability analysis on the response surface. Let us define the following application \mathbf{P} :

$$\begin{aligned} \{u^{(1)}\}, \{u^{(2)}\}, \dots, \{u^{(j)}\}, \dots, \{u^{(p)}\} &\xrightarrow{\mathbf{P}} \{\tilde{u}^*\} \\ \mathbf{P}: \mathbb{R}^{p \times n} &\longrightarrow \mathbb{R}^n \end{aligned}$$

The entire process of calculating the $\{\tilde{u}^*\}$ is considered as an application including:

- the calculations of outcomes $H(\{u^{(j)}\})$ of each experiment,
- the least squares regression yielding the coefficients of the QRS,
- the calculation of coordinates $\{\tilde{u}^*\}$ by application of a classical reliability algorithm.

The approximation of the response results in a deviation between the calculated values and the approximated values:

$$\varepsilon^{(j)} = H(\{u^{(j)}\}) - \tilde{H}(\{u^{(j)}\})$$

This deviation arises from the least squares approximation and is a centered Gaussian random variable; $\tilde{H}(\{u^{(j)}\})$ is therefore also a Gaussian random variable, as is each coordinate of \tilde{P}^* . An exhaustive knowledge of the population $\{u^{(j)}\}$, or of $H(\{u^{(j)}\})$, would lead to the knowledge of $\{u^*\}$, the solution of the following optimization problem:

$$\{u^*\} = \min_{j=1, \dots, \infty} \sqrt{\{u^{(j)}\}^t \{u^{(j)}\}} \text{ subject to } H(\{u^{(j)}\}) \leq 0$$

with:

$$\{u^{(1)}\}, \{u^{(2)}\}, \dots, \{u^{(j)}\}, \dots, \{u^{(p)}\} \Big|_{p \rightarrow \infty} \implies \{u^*\}$$

Application \mathbf{P} can be seen as an operator calculating a characteristic value of the population $\{u\}$ through a reduced sample of this population. This value $\{\tilde{u}^*\}$ is a random variable dependent on the calculation sample whose best estimate must be found.

Point estimate: the estimate obtained from a single set of experiments is often considered as the final estimate, but it is not robust. To obtain such an estimate from a single sample, we can use the Jack-knife technique [Sap90] which consists of extracting p sub-samples by withdrawing each time a different outcome from the initial sample. Each sub-sample j results in an estimation $\{\tilde{u}^{*(j)}\}$.

A point estimate $m_{\{\tilde{u}^*\}}$ of the mean is obtained by taking the arithmetic mean $\{\bar{u}^*\}$ of $\{\tilde{u}^{*(j)}\}$. Likewise, a point estimate of the standard deviation is possible:

$$m_{\{\tilde{u}^*\}} = \{\bar{u}^*\} = \frac{1}{p} \sum_{j=1}^p \{\tilde{u}^{*(j)}\} \quad s_{\{\tilde{u}^*\}} = \sqrt{\frac{1}{p-1} \sum_{j=1}^p (\{\tilde{u}^{*(j)}\} - \{\bar{u}^*\})^2}$$

Interval estimate: the variance of $\{\tilde{u}^*\}$ is unknown and the random variable $\{\bar{u}^*\} - m_{\{\tilde{u}^*\}}/s/\sqrt{p}$ is a Student variable of degree $\nu = p - 1$. The confidence interval at the threshold $1 - \alpha$ is then:

$$\{\bar{u}^*\} - t_{\alpha/2, p-1} \frac{s_{\{\tilde{u}^*\}}}{\sqrt{p}} \leq m_{\{\tilde{u}^*\}} \leq \{\bar{u}^*\} + t_{\alpha/2, p-1} \frac{s_{\{\tilde{u}^*\}}}{\sqrt{p}}$$

where $t_{\alpha/2, \nu}$ is the Student distribution of degree ν .

Definition of new experiments: the confidence interval indicates which domain is likely to contain point P^* . A new design of experiment is constructed, centered in $\{\bar{u}^*\}$:

$$\{u^{(j)}\} = \{\bar{u}^*\} \pm K \cdot t_{\alpha/2, p-1} \frac{s_{\{\tilde{u}^*\}}}{\sqrt{p}} \quad K \geq 1$$

and the procedure is repeated until a satisfactory estimation is obtained. It must be noted that this procedure ensures convergence in distance (index β) but also in each component of vector $\{u^*\}$.

11.4.5 Construction of a neural network

An alternative to the construction of a polynomial response surface is the construction of a neural network.

Principle [Hay94, FLSHC99]

A neural network consists of artificial neurons. Each neuron j receives an input datum \mathbf{i}_j and transmits an output value \mathbf{o}_j via an activation function ϕ_j : $\mathbf{o}_j =$

$\phi_j(\mathbf{i}_j)$. The neurons are organized in a network of which one of the simplest topologies is made up of several layers (Figure 11.8). The inputs of each neuron of a particular layer are the outputs of the previous layer.

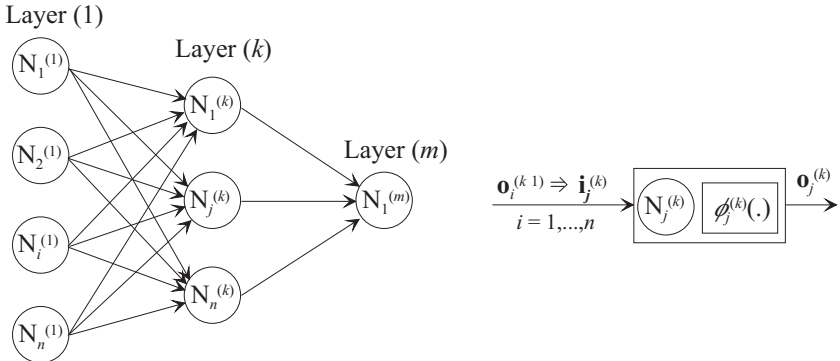


Figure 11.8 Representation of a neuron and architecture of a network.

For the reliability problem, the first layer contains as many neurons as there are design variables and the last layer contains a number equal to that of the performance functions, only one in the case of the reliability component. Intermediate (hidden) layers are defined between the first and the last layers.

Five steps are required to construct the neural network:

1. Choose the architecture of the neural network; that is, the number of hidden layers and the number of neurons on each layer.
2. Choose the input data of each neuron:
the input data $\mathbf{i}_j^{(k)}$ of neuron j in the layer (k) is a weighted linear combination of i outputs $\mathbf{o}_i^{(k-1)} = \mathbf{i}_{ij}^{(k)}$ of the previous layer:

$$\mathbf{i}_j^{(k)} = \sum_i w_{ij}^{(k)} \cdot \mathbf{i}_{ij}^{(k)} + b_j^{(k)}$$

where $w_{ij}^{(k)}$ are the weights of the i inputs of neuron $N_j^{(k)}$ and $b_j^{(k)}$ is a threshold termed bias.

3. Choose the activation function:

$$\phi_j^{(k)} = \begin{cases} F\left(\sum_i w_{ij}^{(k)} \mathbf{i}_{ij}^{(k)} + b_j^{(k)}\right) & \text{if } k > 1 \\ F\left(\mathbf{o}_j^{(0)}\right) & \text{if } k = 1 \end{cases}$$

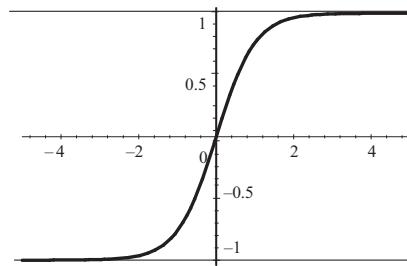


Figure 11.9 Hyperbolic tangent function.

One of the most judicious choices is to select the exponential sigmoid or hyperbolic tangent function (Figure 11.9):

$$F(t) = \alpha \tanh(\gamma \cdot t) \quad \alpha, \gamma \in \mathbb{R}$$

4. Determine the values of the weights and the bias that minimize the cost function: this is the learning procedure.
5. Validate the learning procedure.

The first three steps constitute the degrees of freedom defining the best architecture. Step 4 requires us to choose a cost function that minimizes the error between the experimental and approximated values; this step requires us to choose a judicious set of learning experiments. Lastly, Step 5 validates the network using a new set of numerical experiments.

Typical learning and validation curves are given in Figure 11.10.

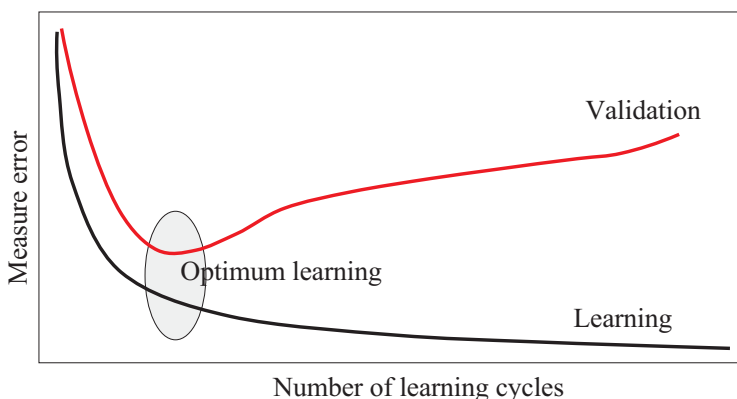


Figure 11.10 Typical learning and validation curves of a neural network.

11.4.6 Summary

Figure 11.11 summarizes all the control tests and their inter-relations.

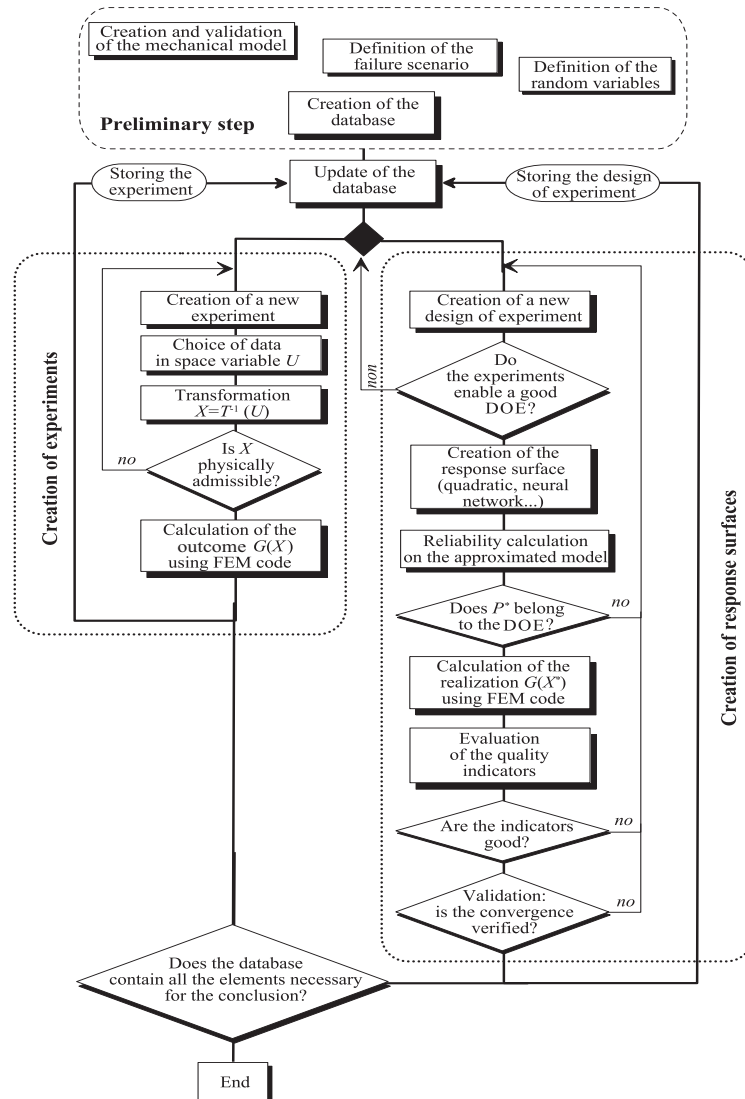


Figure 11.11 Application of the response surface method.

Database

The construction of a database enables us to collect the information derived from the numerical calculation and the reliability-based calculation. The database is made up of three sets:

1. data relative to a numerical experiment r : $u_i^{(r)}; x_i^{(r)}; \langle z^{(r)} \rangle; H(u_i^{(r)})$,
2. data relative to a numerical design of experiment s : $[Z^{(s)}]; \tilde{H}(u_i); a_k^{(s)}$; list of experiments; indicators,
3. data resulting from the reliability calculation: $\beta; u_i^{*(s)}; \alpha_i^{(s)}$; sensitivities of $a_k^{(s)}$.

Overview

As an overview, we can mention the following:

1 Advantages:

- reliability-based calculations on a simple but approximated model,
- decoupling of the mechanical and reliability calculations,
- numerical design of experiment including the expertise of the designer,
- number of calls to the FEM code can be limited,
- creation of a database of physically admissible outcomes,
- possibility of reusing certain experiments calculated previously to build new designs,
- etc.

2 Disadvantages:

- difficulty of automation,
- approximated mechanical model,
- minimum number of calls for a regression,
- location of the response surface,
- absence of a convergence rule as a function of the number of experiments,
- requires a qualified user for a validation of the steps using expertise,
- etc.

11.5 Two applications as examples

Two applications are proposed to illustrate both the response surface methodology and the interpretation of the results of the reliability calculation.

11.5.1 Sphere under pressure

The example given here [Pen97] is a reference case intended to illustrate the construction of a response surface.

Mechanical model

This example concerns the reliability of a sphere under pressure. The material is considered as homogeneous, without spatial variability. Several failure scenarios can be envisaged and we will consider only reaching the equivalent von Mises stress σ_{eq} . The interest of this example is that it has an analytical solution giving target results to be obtained:

$$\sigma_{eq}(r = r_0) = \sqrt{\sigma_r^2 + \sigma_\theta^2 - 2\sigma_r \sigma_\theta} = |\sigma_r - \sigma_\theta| = \frac{3 p_0}{2} \frac{r_1^3}{r_1^3 - r_0^3}$$

an equation whose variables are defined in Figure 11.12.

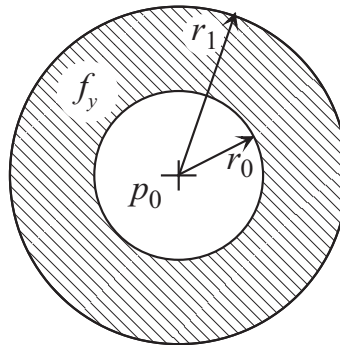


Figure 11.12 Sphere under pressure.

Elastoplastic failure

The limit-state function considered expresses elastoplastic failure; that is, the von Mises stress reaching the yield stress f_y at a point of the sphere:

$$f_y - \sigma_{eq} = f_y - \frac{3 p_0}{2} \frac{r_1^3}{r_1^3 - r_0^3} \quad (11.9)$$

The four variables are considered as random. They are represented by lognormal distributions. The data are collected in Table 11.1.

Variable X	m_X	σ_X	Distribution
Pressure p_0	130 MPa	8 MPa	log-N
Int. radius r_0	50 mm	2.5 mm	log-N
Ext. radius r_1	100 mm	5 mm	log-N
Yield stress f_y	300 MPa	20 MPa	log-N

Table 11.1 Sphere under pressure – data.

β	$\Phi(-\beta)$	$u_{p_0}^*$	$u_{r_0}^*$	$u_{r_1}^*$	$u_{f_y}^*$
3.055	1.127×10^{-3}	1.884	0.899	-0.899	-2.041

Table 11.2 Sphere under pressure – results of reliability analysis (FORM).

The FORM results obtained by PHIMECA-SOFT [Phi04] are given in Table 11.2.

The SORM corrections (Breitung) and directional simulations confirm the values obtained, respectively $\beta = 3.003$ and $\beta = 3.004$.

Solution by polynomial response surface

In view of the form of Equation (11.9), it is possible to separate the resistance component from the load component and an RS is constructed only for the second member. There are three random variables, and a first calculation is performed by interpolation with 10 experiments. Table 11.3 summarizes the results. The errors (absolute) are calculated with respect to the FORM results in Table 11.2. The results are hardly satisfactory, particularly for variable r_1 , and the indicators reflect this fact, excluding R^2 , without significance in case of interpolation. Two experiments are added to improve the I_{ppc} indicator (Table 11.4). An even greater distance between the points does not change I_{ppc} but I_a shows that the new point belongs to the limit-state. A last regression

	β	$u_{p_0}^*$	$u_{r_0}^*$	$u_{r_1}^*$	$u_{f_y}^*$
Results	3.196	1.851	0.715	1.880	-1.661
Error	0.141	-0.033	-0.184	2.779	0.380
$I_a = 31.59\%$			$I_{ppc} = -12.33$		
			$R^2 = \text{insignificant}$		

Table 11.3 Sphere under pressure – interpolation from 10 experiments.

	β	$u_{p_0}^*$	$u_{r_0}^*$	$u_{r_1}^*$	$u_{f_y}^*$
Results	3.113	1.923	0.826	-0.661	-2.208
Error	0.058	0.039	-0.073	0.238	-0.167
$I_a = 1.56\%$		$I_{ppc} = -12.33$		$R^2 = 99.9\%$	

Table 11.4 Sphere under pressure – regression from 12 experiments.

	β	$u_{p_0}^*$	$u_{r_0}^*$	$u_{r_1}^*$	$u_{f_y}^*$
Results	3.053	1.884	0.895	-0.897	-2.040
Error	-0.002	0.000	-0.004	0.002	0.001
$I_a = 0.07\%$		$I_{ppc} = 0$		$R^2 = 100\%$	

Table 11.5 Sphere under pressure – regression from 12 re-centered experiments.

is carried out by bringing the points closer, in order to improve I_{ppc} (all the points are chosen with less than one standard deviation). Table 11.5 shows the results obtained.

Solution by neural networks [LM00]

This is applied using SNNS software [Ins99] developed at the University of Stuttgart. It has the advantage of having multiple parameters to construct the neural network as well as possible and to generate a procedure in C programming language, which can be directly included in a design point calculation algorithm. A few tests result in a network with only one hidden layer of three neurons. Two successive designs of experiment are necessary to obtain a very high accuracy (0.5% on the coordinates of P^*), the first large ($\pm 3\sigma$) and the second refined ($\pm 0.5\sigma$) around the first design point found.

11.5.2 Two correlated uniform distributions

This application illustrates the response surface method and shows how to obtain the best possible approximation of the probability of failure by applying the methods described in Chapter 7.

Search for the design point

We take the example of two correlated uniform distributions for which a first solution is given in Chapter 5. It is processed using the response surface method.

It helps, in the application presented here, to construct an approximated representation of the limit-state surface and to deduce the curvature for the application of SORM methods. Correlation is $\rho = 0.5$ and the index and probability sought are respectively $\beta = 1.546$ and $P_f = 0.032$.

To construct a first response surface, a meshing is performed in standardized space. Table 11.6 gives the points calculated.

Experiment	r	s	u_R	u_S	H
0	4	2	-0.253	0.153	2
1	2.793	1.209	-1.000	0.000	0.098
2	4.500	0.784	0.000	-1.000	0.030
3	6.207	2.791	1.000	0.000	0.087
4	4.500	3.216	0.000	1.000	0.058
5	6.207	3.661	1.000	1.000	0.039
$I_{ppc} = -1.12$					

Table 11.6 Two uniform distributions – first design of experiment.

A regression yields a first approximated surface of the limit-state, and the sequential quadratic programming (SQP) algorithm is applied to deduce a first design point $P^{(1)}$ whose coordinates are:

$$\begin{aligned} u_R &= -0.8343 & r &= 3.0102 \\ u_S &= 1.1913 & s &= 2.8861 \end{aligned}$$

and index $\beta^{(1)} = 1.4544$.

A new starting point is chosen by slightly amplifying the coordinates of $P^{(1)}$. The second design of experiment is constructed with fewer dispersed points than the first; the points are placed on a mesh of side 0.5 (Table 11.7).

The solution obtained is given by:

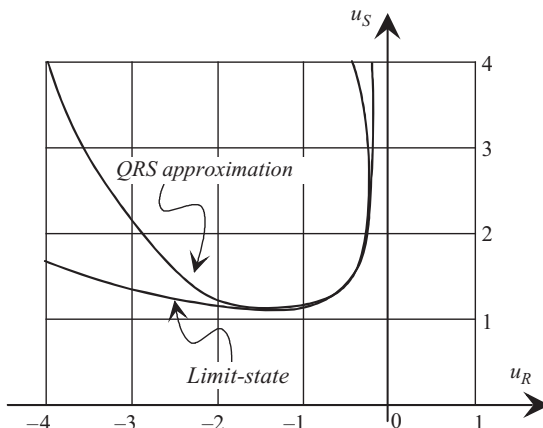
$$\begin{aligned} u_R^* &= -0.8546 & r^* &= 2.9819 \\ u_S^* &= 1.2888 & s^* &= 2.9819 \end{aligned}$$

and the reliability index is $\beta = 1.5469$.

In the neighborhood of the design point, the limit-state surface (Figure 11.13) is approximated by:

$$\begin{aligned} H(u_R, u_S) &\approx 2.504 + [1.32665 \quad -1.45636] \begin{bmatrix} u_R \\ u_S \end{bmatrix} \\ &\quad + \frac{1}{2} [u_R \quad u_S] \begin{bmatrix} 1.35088 & 0.41876 \\ 0.41876 & 0.57188 \end{bmatrix} \begin{bmatrix} u_R \\ u_S \end{bmatrix} \end{aligned}$$

Experiment	r	s	u_R	u_S	H
0	2.955	2.924	-0.875	1.249	0.031
1	2.423	2.558	-1.375	1.249	-0.134
2	2.955	2.298	-0.875	0.749	0.657
3	3.770	3.236	-0.375	1.249	0.534
4	2.955	3.407	-0.875	1.749	-0.452
5	3.770	3.614	-0.375	1.749	0.015
$I_{ppc} = 0$					

Table 11.7 Two uniform distributions – second design of experiment.**Figure 11.13** Two uniform distributions – limit-state and approximated quadratic response surface.

FORM calculation of the probability of failure

The FORM first-order approximation is obtained from the tangent at the design point. The probability of failure is given by:

$$P_f \approx \Phi(-1.5469) = 0.0609 \quad \text{error equal to } 103\%$$

SORM calculation of the probability of failure

Calculation of the curvature: the second-order approximation is based on the calculation of the curvature at the design point. The Hessian of the quadratic form is given by:

$$[H] = \begin{bmatrix} 1.35088 & 0.41876 \\ 0.41876 & 0.57188 \end{bmatrix}$$

The Gram-Schmidt method is used to define the orthonormal reference frame with the last column oriented along vector $\{\alpha\}$; the rotation matrix is:

$$[R] = \begin{bmatrix} 0.8343 & 0.5514 \\ -0.5514 & 0.8343 \end{bmatrix}$$

Moving to the new base gives:

$$[A] = \frac{1}{2 \left\| \frac{\partial H}{\partial u} \right\|} [R]^t [H] [R] = \begin{bmatrix} 0.5806 & -0.0752 \\ -0.0752 & 0.1640 \end{bmatrix}$$

The main curvature in the new reference frame is then:

$$\kappa_1 = 1.1612$$

The corresponding curvature radius is $R = 0.86118$.

Centered hypersphere method: the probability estimation can be given by the domain outside a circle centered at the origin and with radius β , by:

$$P_f \leq 1 - \chi_{n=2}^2 (\beta^2) = 0.302$$

but this equation is of no interest as the limit-state is convex, which implies more strongly:

$$P_f \leq \Phi(-\beta) = 0.0609$$

A quick inspection of the geometry of the problem allows this estimation to be improved. By tracing tangents to the limit-state starting from the origin of the reference frame, we find that the failure domain is contained in an envelope defined by an angle equal to 63° (Figure 11.14). Therefore, we only need to consider the domain outside the circle with radius β limited by the two tangents passing through O . By taking advantage of the property of axial symmetry of the probability density, a good estimation of the probability of failure is given by:

$$P_f \leq \frac{63}{360} [1 - \chi_{n=2}^2 (\beta^2)] = 0.053$$

Now, let us examine the case of a circle tangential to the design point (hypersphere method). The radius of the circle is equal to the radius of curvature in $\{u^*\}$; therefore $R = 0.86118$. The center of the circle is therefore displaced by a distance $\delta = \beta + R$ along the direction of vector $\{\alpha\}$; the components of this decentering are therefore:

$$\delta = 1.5469 + 0.86118 = 2.4081$$

$$\delta_x = \delta \alpha_1 = (2.4081)(-0.5514) = -1.3278$$

$$\delta_y = \delta \alpha_2 = (2.4081)(+0.8343) = +2.0091$$

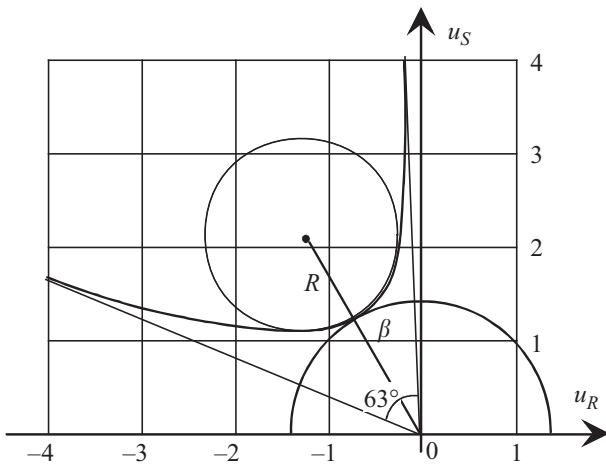


Figure 11.14 Two uniform distributions – hypersphere method.

The probability of failure is therefore estimated by the distribution of χ^2 decentered in δ :

$$P_f \approx \chi_{n,\delta}^2(R^2)$$

In our case:

$$P_f \geq \frac{1}{2\pi} \int_0^{2\pi} \int_0^{0.86118} r e^{-(1/2)[(r \cos \theta - 1.3278)^2 + (r \sin \theta + 2.0091)^2]} dr d\theta = 0.0273$$

The error obtained is equal to -15% . These approximations help define the bounds of the probability of failure:

$$0.027 \leq P_f \leq 0.053$$

Breitung formula: the probability approximation is given by:

$$P_f \approx \Phi(-\beta) \frac{1}{\sqrt{1 + \beta \kappa_1}} = 0.0364$$

The result is markedly improved, and the error on P_f is equal to 13% .

Tvedt method: the first term of the probability is that of Breitung (Equation (7.20)):

$$A_1 = 0.03644$$

The second term is (Equation (7.23)):

$$A_2 = [\beta \Phi(-\beta) - \phi(\beta)] \left[\prod_{j=1}^{n-1} \frac{1}{\sqrt{1 + \beta \kappa_j}} - \prod_{j=1}^{n-1} \frac{1}{\sqrt{1 + (\beta + 1) \kappa_j}} \right] \\ = -0.002508$$

The third term gives (Equation (7.24)):

$$A_3 = (\beta + 1) [\beta \Phi(-\beta) - \phi(\beta)] \\ \times \left[\prod_{j=1}^{n-1} \frac{1}{\sqrt{1 + \beta \kappa_j}} - \operatorname{Re} \left\{ \prod_{j=1}^{n-1} \frac{1}{\sqrt{1 + (\beta + i) \kappa_j}} \right\} \right] \\ = (\beta + 1) [\beta \Phi(-\beta) - \phi(\beta)] (0.034411) = -0.002306$$

Thus, the probability of failure is estimated at (Equation (7.22)):

$$P_f = A_1 + A_2 + A_3 = 0.0316$$

The result is slightly improved compared to the Breitung formula; the error is brought down to -1% .

11.5.3 Conclusion

The response surface method results in a reliability problem whose solution is greatly simplified. Its application can provide interesting information at a limited cost if the number of random variables is limited. In fact, a complete identification requires at least $(n + 1)(n + 2)/2$ numerical experiments, which is insufficient to validate the result obtained.

The approach developed here seeks to organize the method after making a few methodological choices:

- construction of the numerical design of experiment in standardized variables,
- proposal of indicators to be evaluated in order to assess the quality of the solution.

More than simply placing our hopes in an automatic method, which will always be complex, we must trust the expertise of the designer to choose the successive numeric experiments judiciously. This simply means using the information available in the database as efficiently as possible.

The application of the method proposed helps to address any reliability problem whose mechanical model is based on a finite element calculation. No adaptation of the FEM code is necessary.

If another method is used, it implies, in every case, the calculation of particular outcomes of the limit-state function. These outcomes can be stored in the database and used to construct a response surface, thus providing additional information on the quality of the result obtained.

11.6 Optimization method

11.6.1 Description of the method

The reliability calculation can be boiled down to an optimization problem that must be solved in standardized space. The most probable failure point is the closest point to the origin belonging to the limit-state surface; this problem is written as:

$$\min \left(\sqrt{\sum_i u_i^2} \right) \quad \text{subject to the constraint } H(u_i) \leq 0$$

where $H(u_i)$ is the limit-state function in standardized space u_i . The constraint selected is defined by $H(u_i) \leq 0$, which is more general than $H(u_i) = 0$; it is therefore simpler to handle it by an optimization module but this supposes that the origin point does not belong to the failure domain.

If the FEM code has an optimization module it is possible to solve this problem, provided it is formulated correctly in a classical optimization scheme. We can then leave the optimization module of the finite element code to search for the failure point and the reliability index [FM94].

Let us first analyze the optimization scheme of the FEM codes. In an optimization problem, there are three types of variables:

- Design variables $V_i (i = 1, \dots, n)$: these are control variables that are modified by the program to reach the optimal solution.
- State variables $g_j(V_i) (j = 1, \dots, m)$: these are variables that define the admissible state of the system; these variables represent the constraints to be imposed to obtain a realizable solution. They are defined by conditions of equality or inequality.
- Objective function $F(V_i)$: this is the variable to be minimized; it represents the cost function.

The optimization problem is therefore:

$$\begin{aligned} &\text{minimize} && F(V_i) \\ &\text{subject to} && V_{i_{\min}} \leq V_i \leq V_{i_{\max}} \quad (i = 1, \dots, n) \\ &&& \text{and} \quad g_{j_{\min}} \leq g_j(V_i) \leq g_{j_{\max}} \quad (i = 1, \dots, m) \end{aligned}$$

where $V_{i_{\min}}, V_{i_{\max}}, g_{j_{\min}}, g_{j_{\max}}$ are, respectively, the lower and upper bounds of the design variables and the state variables. In the reliability problem, the design variables V_i are standardized variables u_i that can vary from $-\infty$ to $+\infty$; the only constraint imposed is $H(u_i) \leq 0$ and the function to be minimized is the length of any vector in standardized space $d(u_i) = \sqrt{\sum_i u_i^2}$.

However, in a FEM optimization module the design variables are those used for the construction of the mechanical model. These are *physical variables*. Similarly, the limit-state function is known only in physical space $G(x_i)$; the optimization problem is then written as:

$$\begin{aligned} & \text{minimize} && d(u_i) \\ & \text{subject to} && G(x_i) \leq 0 \end{aligned}$$

It is obvious that this kind of problem cannot be solved correctly by the FEM optimization module for two reasons: the first is that the problem is defined as a function of two types of variables u_i and x_i , respectively belonging to standardized and physical spaces (the optimization module recognizes only one type of variable V_i); and the second is that variables u_i and x_i are not independent; they are linked by the isoprobabilistic transformation T .

To solve these difficulties, we can redefine the optimization problem as follows:

- the design variables V_i are represented by the physical variables x_i of the system,
- the state variables represent:
 - the fact that the limit-state function belongs to physical space, which can be calculated easily by the FEM code,
 - the links between physical and standardized spaces, translating the transformation functions T_i ,
- the objective function is always the length of the vector in standardized space.

Thus, the introduction of additional constraints which represent equations T_i helps solve the problem, as there is now only one type of variable x_i ; the objective function is indirectly defined as a function of x_i through these new constraints.

The new optimization problem has the following form:

$$\begin{aligned} & \text{minimize} && d(u_i) \\ & \text{subject to} && G(x_i) \leq 0 \\ & \text{and} && u_i - T_i(x_j) = 0 \end{aligned}$$

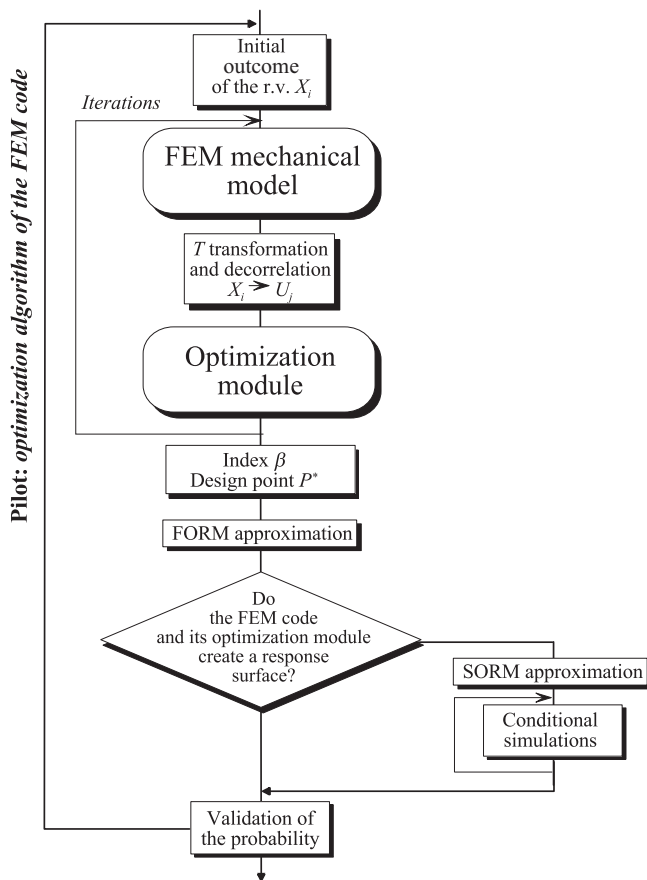


Figure 11.15 Control by optimization module.

The schema of the analysis consists of redefining the reliability problem in the form of an optimization (Figure 11.15). The optimization procedure is initiated in a classical manner. The results are the reliability index, the design point and, as the case may be, a response surface. Then an approximation of the first or second order is performed for the reliability calculation.

The convergence of such a system depends on the power of the algorithm implemented in the FEM code. Our experience [LMFM97] with ANSYS^R software [ANS94] shows that a general optimization module is not necessarily the best choice when addressing reliability problems. However, with new developments in the field of optimization, the algorithms will become increasingly robust and efficient, to the great advantage of mechanical-reliability coupling.

11.6.2 Overview

As an overview, we can mention the following:

1 Advantages:

- direct use of an existing code (mechanical model + optimization),
- etc.

2 Disadvantages:

- necessity to have an efficient optimization module,
- difficult to write the mechanical-reliability problem in the formalism of the optimization module,
- difficult to go beyond the FORM approximation,
- the number of calls can be high (depending on the quality of the general purpose optimization module),
- etc.

11.6.3 Application

The example of the sphere under pressure, described in Section 11.5.1, was also worked out by directly using the optimization module of the ANSYS code [ANS94] on the one hand and the CASTEM2000 code [CEA97] on the other. The procedures showed their efficiency and the expected results were obtained.

11.7 Example: isostatic truss

This academic example, which is very simple from the mechanical point of view, shows the application of the methods proposed in the previous chapters and illustrates the results obtained. It is limited to the study of the first reliability component and must be completed by a system approach.

11.7.1 Data

Geometric data

Let us consider the truss illustrated in Figure 11.16 in which the connections are simple ball pivots. All the bars have full circular cross-sections with diameter d . E and f_y are, respectively, the elasticity modulus and the yield limit of the material. The truss is subject to two load systems P and Q .

Stochastic data

The stochastic model of the variables is given in Table 11.8. We allow the hypothesis that the diameters of all the bars are perfectly correlated. The same

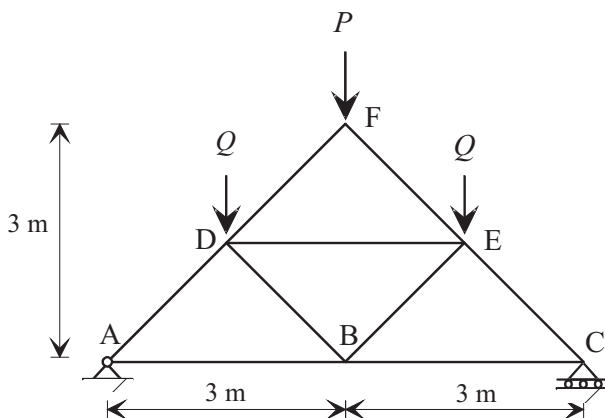


Figure 11.16 Isostatic truss.

Variable	Distribution	Mean	Standard deviation	Correlation
P	Normal	3 MN	0.6 MN	$\text{cor}[P, Q] = \rho$
Q	Normal	2 MN	0.4 MN	$\text{cor}[Q, P] = \rho$
f_y	Lognormal/Gauss	200 MPa	30 MPa	—
d	Lognormal/Gauss	0.22 m	0.01 m	—

Table 11.8 Isostatic truss – variable data.

is true for yield limits. All the bars are therefore identical. Furthermore, the risk of buckling is negligible.

Failure scenario

Failure is the reaching of the yield limit under traction or under compression in any bar; the truss being isostatic, it cannot withstand an increase in the load. To be rigorous, we must consider the series system made up of events:

$$\{\text{failure of the bar } i \text{ under traction OR under compression}\}$$

One of the events {traction or compression} necessarily has a very weak probability, and it can be ignored. The system is not analyzed and the example remains limited to the failure of the most loaded bar in the deterministic sense. The questions posed are as follows:

1. The failure scenario to be considered is plastic damage of the most loaded bar of the truss. If P and Q are not correlated, study the reliability of the truss and deduce the importance factors. On which parameters must we act to enhance the reliability of the structure?
2. What is the effect of the hypothesis of f_y and d being distributed according to Gaussian distribution, instead of lognormal distributions?
3. For the previous case (f_y and d normal variables), calculate the reliability of the system as a function of the correlation of P and Q .

11.7.2 Mechanical analysis

The mechanical analysis of the truss can be performed analytically. For loads P and Q , the absolute values of the normal forces are summarized in Table 11.9. The most loaded bars are AD and CE.

Bar	Normal force $ N_i $	
AB, BC	$Q + P/2$	Traction
AD, EC	$\sqrt{2}(Q + P/2)$	Compression
DF, EF	$P/\sqrt{2}$	Compression
DB, BE	0	—
DE	Q	Compression

Table 11.9 Isostatic truss – normal forces; P and Q are assumed to be positive.

11.7.3 Reliability analysis

For any bar, the failure limit-state is given by:

$$G = R_i - |N_i| \leq 0$$

where R_i and N_i are, respectively, the resistance of bar i and the normal force in the same bar. Resistance is defined by the plastic normal force:

$$R_i = f_{y_i} \frac{\pi d_i^2}{4}$$

where the outcomes of f_y and d are identical in the entire structure.

For bars AD and EC, the limit-state function is:

$$G = R - |N_{\max}| = f_y \frac{\pi d^2}{4} - \sqrt{2} \left(Q + \frac{P}{2} \right)$$

ignoring the possible negative outcomes of the normal force.

Products of reliability analysis

The reliability analysis is performed using PHIMECA-SOFT, with direct coupling and the Rackwitz-Fiessler algorithm.

For outcomes of X_i equal to the means, the limit-state function is $H_0 \equiv G_0 = 2.653$. The gradient in physical space is calculated by finite differences:

$$\left\{ \frac{\partial G}{\partial x_i} \right\} = \begin{bmatrix} -0.707 \\ -1.414 \\ 0.0380 \\ 69.12 \end{bmatrix} \quad \text{for } \{x\} = \begin{bmatrix} P \\ Q \\ f_y \\ d \end{bmatrix}$$

To move to standardized space, we must calculate the Jacobian matrix of the isoprobabilistic transformation:

$$[J] = \left[\frac{\partial T_i}{\partial x_j} \right]_{\text{mean}} = \begin{bmatrix} 1.667 & 0 & 0 & 0 \\ 0 & 2.500 & 0 & 0 \\ 0 & 0 & 0.034 & 0 \\ 0 & 0 & 0 & 100.052 \end{bmatrix}$$

The gradient in standardized space is therefore:

$$\left\{ \frac{\partial H}{\partial u_i} \right\} = [J]^{-1} \left\{ \frac{\partial G}{\partial x_i} \right\} = \begin{bmatrix} -0.424 \\ -0.566 \\ 1.134 \\ 0.691 \end{bmatrix}$$

On the first iteration, the reliability index is obtained as:

$$\beta^{(1)} = \frac{H_0 - \{\partial H / \partial u_i\}^t \{u\}}{\|\partial H / \partial u_i\|} = 1.697$$

Convergence is achieved at the end of the third iteration (Table 11.10); this is illustrated in Figure 11.17.

Iteration	β	G/G_0
0	0	1
1	1.697 ...	0.099
2	1.8971	0.00012
3	1.8974	-3.8×10^{-7}

Table 11.10 Isostatic truss – convergence of the reliability analysis.

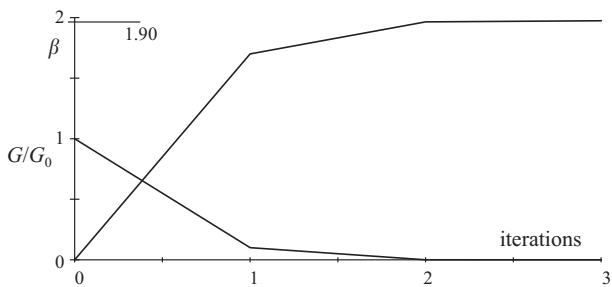


Figure 11.17 Isostatic truss – convergence of the reliability index and the limit-state.

In the first order, the probability of failure is estimated as:

$$P_f = \Phi(-\beta) = 0.0289$$

The second-order approximation is given according to two methods as:

$$\text{Breitung formula} \quad P_f = 0.0277$$

$$\text{Tvedt formula} \quad P_f = 0.0274$$

The results, at the design point, are summarized in Table 11.11, giving:

	x^* u^*	α	α_m	α_σ	e_m	e_σ	γ
P MN	3.394 0.657	-0.346	-0.577	-0.380	-0.913	-0.120	1.131
	2.350 0.876		-0.462	-1.155	-1.012	-1.217	-0.213
f_y MPa	162.36 -1.323	0.697	0.031	-0.039	3.315	-0.619	1/1.232
	0.212 -0.806		0.425	44.60	-37.74	5.172	-0.199
							1/1.037

Table 11.11 Isostatic truss – results of reliability analysis.

- the coordinates of the design point,
- the direction cosines α ,
- the sensitivities and elasticities of the reliability index with respect to means α_m and e_m ,
- the sensitivities and elasticities of the reliability index with respect to standard deviations α_σ and e_σ ,
- the partial coefficients with respect to the mean.

In standardized space, the quadratic response surface is:

$$H = 2.534 + \begin{bmatrix} -0.424 \\ -0.566 \\ 1.086 \\ 0.662 \end{bmatrix}^t \begin{bmatrix} u_P \\ u_Q \\ u_{f_y} \\ u_d \end{bmatrix} + \frac{1}{2} \begin{bmatrix} u_P \\ u_Q \\ u_{f_y} \\ u_d \end{bmatrix}^t \begin{bmatrix} 0 & 0 & 0 & 0 \\ 0 & 0 & 0 & 0 \\ 0 & 0 & 0.127 & 0.0785 \\ 0 & 0 & 0.0785 & 0.0472 \end{bmatrix} \begin{bmatrix} u_P \\ u_Q \\ u_{f_y} \\ u_d \end{bmatrix}$$

Figures 11.18–11.20, respectively, give the direction cosines, the elasticities of the means and standard deviations, and the partial coefficients. These are given the sign + for load variables and the sign - for resistance variables.

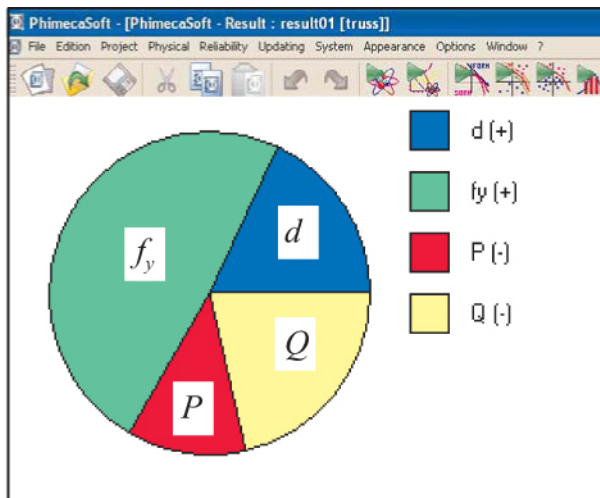


Figure 11.18 Isostatic truss – direction cosines.

Optimizing the design

To improve reliability, we must correctly analyze the importance factors of the various parameters. The histogram of the elasticities of means shows that the mean of the diameter of the bars plays the largest role in the reliability

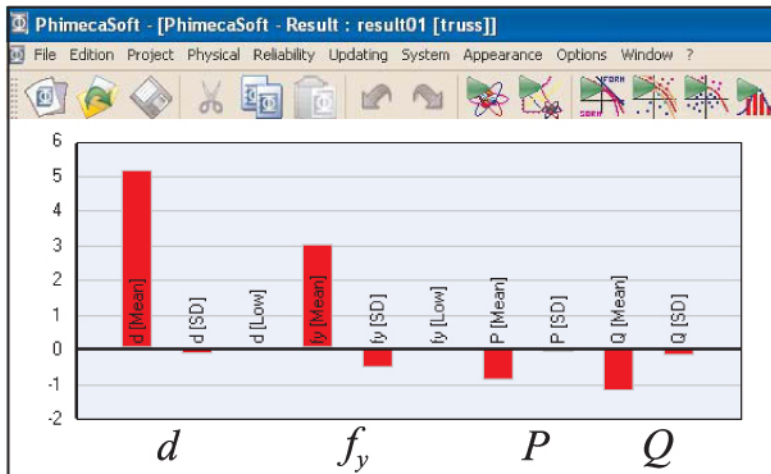


Figure 11.19 Isostatic truss – elasticities of the means and standard deviations.

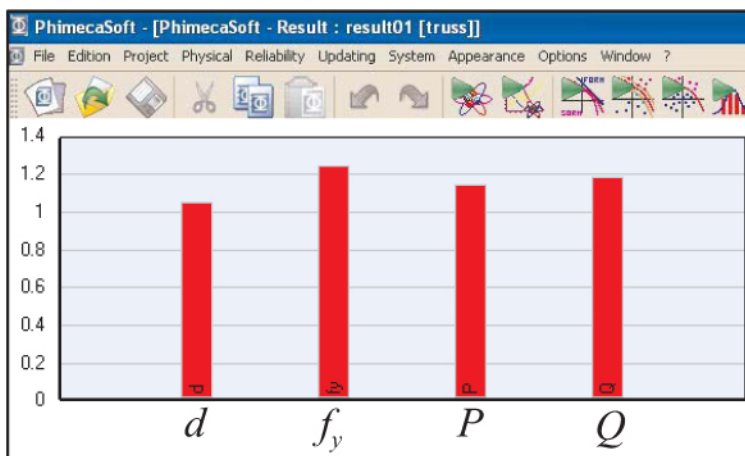


Figure 11.20 Isostatic truss – partial coefficients.

of the system; a solution is therefore to use bars with a larger mean (or nominal) diameter. However, the factor presenting maximum elasticity is not necessarily the one for which the cost of modification is the lowest. Case 1 in Table 11.12 shows the effect of an increase in the diameter with a constant standard deviation and not with a constant coefficient of variation.

Initial configuration: $\bar{\beta} = 1.897$						
For $m_d = 22$ cm and $\sigma_{f_y} = 30$ MPa						
Case 1		Case 2		Case 3		
m_d	β	σ_{f_y}	β	m_d	σ_{f_y}	β
25	3.18	25	2.07	25	25	3.49
27	3.98	20	2.26	27	20	4.86
29	4.75	15	2.45	29	15	6.52

Table 11.12 Isostatic truss – calculation of the reliability level by modification of one or two parameters.

The histogram of standard deviations shows that the dispersion of the yield limit has an important role. It is therefore recommended to set up rigorous quality controls on the material in order to decrease the variance of the yield limit. Case 2 in Table 11.12 shows this effect. Lastly, case 3 gives the reliability calculation performed with various values for the mean of d and the standard deviation of f_y , the other parameters remaining unchanged.

Such an intuitive approach to mechanical-reliability optimization paves the way for more systematic methods [KML02a].

Approximation by normal variables

The reliability analysis is carried out for f_y and d distributed according to normal distribution by retaining the same means and standard deviations. The reliability index found is $\beta = 1.837$ instead of 1.897; the gap is 3.2%, with a lower value approximation.

Study of the effect of load correlation

By retaining the assumption of normal distributions for f_y and d and for the initial data, the reliability index is calculated for a correlation ρ of actions P and Q . The evolution is given in Figure 11.21.

11.8 Conclusion

No coupling method appears *a priori* the best. We can get a result economically with good methodology just as well as with good control of the iterative procedures during the optimization phase (setting parameters and stop tests).

Furthermore, depending on the mechanical problem addressed, the number of random variables and the tools available, one or other of the various methods will prove to be the most efficient. Comparing them will help validate the most appropriate from among all the methods. In this sense, methodological redundancy is a necessity.

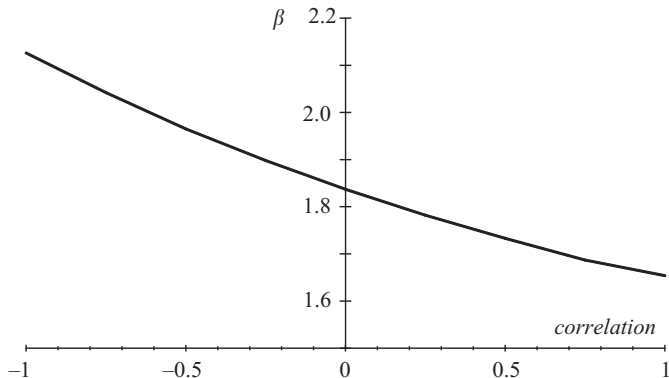


Figure 11.21 Isostatic truss – evolution of reliability as a function of load correlation.

In practice, the choices are imposed by the availability of tools and skills.

The response surface method is suitable for coupling any mechanical model with a reliability model without having to ensure direct dialog between the software packages. In this context, it is not at all necessary to have tools on the same computer platform or even on computer platforms that can converse with each other. This method sometimes enables the re-use of already performed calculations or uses the expertise of mechanical engineers in the definition of the response surface or the numerical design of experiment to be retained. It further imposes a constant dialog between the mechanical engineer and reliability engineer in the case where a single person does not possess these two skills.

As for direct coupling, it allows an automation of the procedure. The advantage is then to be able to use the resources of modern computers without having to resort to considerable human resources.

If we want to develop suitable procedures and interfaces, it is advantageous to focus our effort on the calculation of gradients and to build a database. In all cases, it is important to store all the mechanical calculations performed, as these consume a large amount of the calculation time. In fact, even in the case of direct coupling, the results can be validated *a posteriori* by performing a calculation by the response surface method reusing the calculations already performed and stored.

Beyond the FORM/SORM methods, conditional simulations also open possibilities for coupling explored by Waarts [Waa00].

Regardless of the method used, storing any calculation can only enhance the value of the results. In fact, value remains an essential difficulty, which will be overcome more by an increased experience in the application of coupled methods than by automated algorithms.

This chapter focused on introducing the methods and illustrating them using a simple and demonstrative example. Mechanical-reliability coupling is now capable of contributing additional accuracy in industrial problems, such as those we will present in Chapter 13.

This page intentionally left blank

Chapter 12

Stochastic Finite Elements

12.1 Introduction

Devoting one chapter to stochastic finite elements while whole books can be written on them [GS91, KH92] and limiting ourselves to certain aspects only, will allow us to give the definitions and introduce a subject that is still far from having stabilized, as testified by two articles [Col97, MBBGS97] and by the report by Sudret and Der Kiureghian [SDK00] giving the state of the art. These contain a very complete presentation and several hundreds of references that the reader can consult for an in-depth study of the subject, without forgetting to consult more recent papers. Our objective is therefore simply to give an idea about a concept that is still novel, to classify the various approaches and to indicate a few tools for their development.

12.1.1 Definition and purpose

We must first of all give a definition that can be more or less comprehensive. We term as a *stochastic finite element method* a numerical modeling approach based on a finite element method in which certain design variables (intervening in the stiffness matrix K) or actions (intervening in the actions vector F and, as the case may be, in the prescribed displacements vector) are random fields, expressed by the equation:

$$K(\omega)q(\omega) = F(\omega) \quad \omega \in \Omega \tag{12.1}$$

assuming the linearity of the mechanical model. In this wide meaning, the mechanical-reliability methods described in Chapter 11 could have been qualified as stochastic finite element methods. However, the coupling approach was elucidated there with the purpose of showing how a mechanical model, by finite elements or any other way, could be applied in a reliability analysis. From the point of view of stochastic finite elements, we will focus more on searching for the stochastic properties of the response of the mechanical model; that

is, perform a sensitivity analysis rather than a reliability analysis. Of course, these two methods are inter-related, as knowing the stochastic properties of the mechanical model offers a great interest for reliability analysis [FM94, FML97, SDK02].

In a more restricted usage, the stochastic finite element method is limited to the case where the random variables belong to the stiffness matrix. This is the important case of the spatial variability of the material's characteristics (Young's modulus E and Poisson's coefficient ν), particularly studied by soil mechanics engineers.

The objective of a stochastic finite element method is therefore primarily to study the variability of the random response given by the finite element model whose inputs are random. As well as the term 'stochastic finite element method' (SFEM), we can also find the 'random finite element method' (RFEM) or the 'probabilistic finite element method' (PFEM).

12.1.2 Random variables and random fields

In the displacement model of finite elements, the variability of the data appears as input in the action vector and in the stiffness matrix, and as output in the displacement vector.

If the operation of a mechanical system is represented by a finite set of parameters, the vector of random variables is included in the vector of parameters. However, FEM is a method of discretization of a continuous medium, and variability exists both in the continuous medium and in the discretized medium. Thus, the question arises as to the representation of a random field and its discretization, which is different from mechanical discretization. Stochastic discretization then consists of the construction of a vector V_i of correlated random variables. This point was introduced in Chapter 2 (Section 2.3.3).

Let us consider a function $V(x, t, \omega)$ of the space x , time t and random event ω . It is possible to perform a discretization of this function in space with fixed t . A vector $\{V\}$, whose components are correlated (with matrix $[\rho]$), is then substituted for the random field:

$$V(x, t, \omega) \longrightarrow \{V(\omega)\} = \begin{Bmatrix} v_1(\omega) \\ v_2(\omega) \\ \vdots \\ v_n(\omega) \end{Bmatrix} \quad [\rho] = \begin{bmatrix} 1 & \rho_{12} & \cdots & \rho_{1n} \\ \rho_{21} & 1 & \cdots & \rho_{2n} \\ \vdots & \vdots & \ddots & \vdots \\ \rho_{n1} & \rho_{n2} & \cdots & 1 \end{bmatrix} \quad (12.2)$$

Here, stochastic discretization forms an important part of the stochastic finite element method. It concerns all the fields: material, dimensions, loadings. It can be performed both on a geometric discretization basis (as in deterministic FEM) by choosing physical nodal values $v_i(\omega)$ in nodes (Section 12.2) and

by an expansion on a well-chosen function basis (Section 12.3). The random variables are then either nodal components of the physical discretization, or the amplitudes of the discretization modes.

The previous chapters covered the questions of mechanical reliability in the presence of random variables. The ambition of stochastic finite elements also involves the presence of a random field whose discretization must be performed in the most efficient manner in order to limit the size of the random vector of the design variables.

12.1.3 Chapter plan

The first question to ask concerns the representation of the random event. Sections 12.2 and 12.3 examine the two modes of discretization possible: spatial or spectral:

- If the random event is finally represented by a vector of centered random variables denoted by $\alpha(\omega)$, the stiffness equation is written as:

$$K(\alpha(\omega)) q(\omega) = F(\alpha(\omega)) \quad \omega \in \Omega$$

Section 12.4 introduces the calculation of the derivatives whose use is highlighted in the perturbation method in Section 12.5. However, this method is limited to the calculation of the first moments, and Section 12.6 shows how to go toward a more complete representation of the stochastic response.

- If the random event is represented by a centered random field, denoted by $\alpha(x, \omega)$, we must go back to the foundations of the finite element method to express a stochastic stiffness matrix, with classical notations:

$$K_e(\omega) = \int_{V_e} B^t(x, \omega) H(x, \omega) B(x, \omega) \mathrm{d}V$$

Section 12.7 describes two continuous field methods: the weighted integral method and the spectral method.

- Lastly, Section 12.8 illustrates the concepts introduced using a very simple example, and Section 12.9 gives the conclusion.

The final objective of the stochastic finite element method is to calculate the complete response of the mechanical model, i.e. to know the joint probability density of the vector $q(\omega)$. Then the response given both to the reliability analysis and to the sensitivity analysis would be perfect. We will see that this is not the case and that the information about the response remains limited: means, variances-covariances, limited expansions, etc.

12.2 Spatial discretization of a random field

12.2.1 Random field [Cau88, CL67]

We will now summarize a few essential results necessary for our study. Let us consider a random field $V(x, t, \omega)$ with fixed t . It is therefore a field $V(x, \omega)$, function of a space variable x , $x = (x_1, x_2, x_3)$; the indexes of the components are omitted and the indexation position is used to denote the various points. The same logic is valid for a time-dependent field; $\omega \in \Omega$ expresses the random event, $V(x, \omega = \omega_0)$ is a trajectory and $V(x = x_0, \omega)$ is a random variable.

Definitions

A random (or stochastic) process, representing a random field, can be defined by a family of random variables $V(\omega)$ indexed in space by the coordinate $x \in \mathcal{D}$. In the case of second-order processes, a simple description is obtained from the first two moments, when they exist and are finite:

$$\begin{aligned} \text{mean } m_V(x) &= E[V(x, \omega)] \\ \text{variance/covariance } \Sigma_V(x_1, x_2) &= \text{cov}[V(x_1, \omega), V(x_2, \omega)] \end{aligned}$$

Covariance expresses the spatial dependence of the process between two points x_1 and x_2 . It is then called the autocovariance function. An autocorrelation function is defined by:

$$\begin{aligned} R_V(x_1, x_2) &= E[V(x_1, \omega)V(x_2, \omega)] \\ &= \Sigma_V(x_1, x_2) + E[V(x_1, \omega)]E[V(x_2, \omega)] \end{aligned} \tag{12.3}$$

This function is symmetric and positive defined.

Second-order stationary process

The processes can be separated into two classes: stationary processes and non-stationary processes. The properties of a stationary process do not depend on the indexation position (in space or time), whereas those of a non-stationary process depend on it.

Formally, a second-order process is stationary if its properties are invariant by translation. Strict (or strong) stationarity affects all the properties, and it is unusable in practice. Second-order (or weak) stationarity is limited to the second-order properties. A process is second-order stationary if:

- its autocorrelation function $R_V(x_1, x_2)$ is a function only of $x_2 - x_1$,
- its expectation $E[V(x, \omega)]$ is independent of x , equal to m_V .

The autocorrelation function then depends only on $\ell = x_2 - x_1$, and it is denoted by:

$$\Gamma_V(\ell) = R_V(x_1, x_1 + \ell) \quad \forall x_1$$

and, according to (12.3):

$$\Gamma_V(\ell) = \text{cov} [V(x_1, \omega), V(x_1 + \ell, \omega)] + m_V^2$$

Function $\Gamma_V(\ell)$ is symmetric with respect to the origin. Value $\Gamma_V(0) = E[V(x, \omega)^2]$ is the mean power and $|\Gamma_V(\ell)| \leq \Gamma_V(0), \forall \ell$.

Harmonic analysis of a second-order stationary process

The autocorrelation function is positive, continuous in 0; it is the Fourier transform of a bounded positive measure. The spectral measure μ_V represents the distribution of the mean power according to the frequency spectrum; it is equal to:

$$\mu_V(u) = \int_{-\infty}^{\infty} \Gamma_V(\ell) e^{-i\ell u} d\ell$$

The spectral density $g_V(u)$ is given by $d\mu_V(u) = g_V(u)du$, if it exists.

Table 12.1 gives a few examples. The exponential and triangular functions are particularly useful for taking into account the *neighborhood correlation* effect, often in direct relation to the physics of the phenomena. The cosine function shows the evident spectral content. Finally, the last line characterizes white noise; that is, a process whose frequencies are uniformly distributed (as in white light). If B is a standardized white noise, then:

$$R_B(x_1, x_2) = \Gamma_B(x_2 - x_1) = \begin{cases} 1 & \text{if } x_1 = x_2 \\ 0 & \text{if } x_1 \neq x_2 \end{cases}$$

Two points, however close they might be, are decorrelated.

$\Gamma_V(\ell)$	$g_V(u)$ or $\mu_V(u)$
$\exp\left(-\frac{a^2}{2}\ell^2\right)$	$g_V(u) = \frac{i}{2\pi} \exp\left(-\frac{iu^2}{2a^2}\right)$
$\exp(- \ell)$	$g_V(u) = \frac{i}{\pi} \frac{1}{(1+u^2)} \text{ (Cauchy density)}$
$\begin{cases} 1 - \ell /a & \text{if } \ell \leq a \\ 0 & \text{if } \ell \geq a \end{cases}$	$g_V(u) = \frac{a}{\pi} \left(\frac{\sin(ua/2)}{ua/2} \right)^2$
$(a^2/2) \cos \frac{2\pi\ell}{L}$	$\mu_V(u) = (a^2/2)\delta_{1/L}$ (δ is the Dirac function)
$\frac{N_0}{2}\delta_\ell$	$\mu_V(u) = N_0/2$ (white noise)

Table 12.1 Examples of autocorrelation functions.

Scale of fluctuation

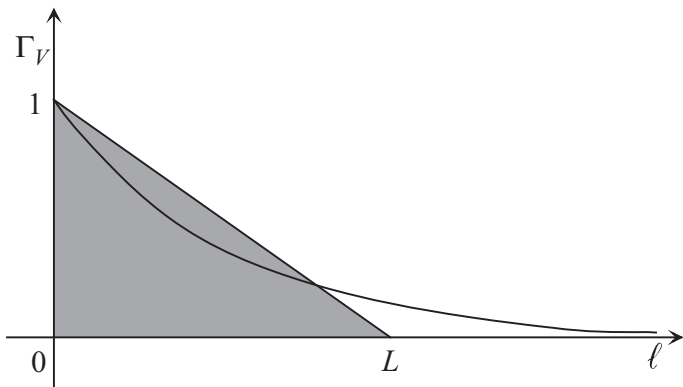


Figure 12.1 Illustration of the scale of fluctuation.

Vanmarcke [Van83] introduces a characteristic θ of the field that he calls *scale of fluctuation*, which expresses a certain form of the spatial correlation.

Let us consider the autocorrelation function $\Gamma_V(\ell)$. The integral:

$$\theta = \int_{-\infty}^{+\infty} \Gamma_V(\ell) d\ell$$

represents the area of the surface under the curve, and the length L (Figure 12.1) is such that the area of the gray-shaded triangle is:

$$\frac{1}{2}L = \frac{\theta}{2} = \int_0^{+\infty} \Gamma_V(\ell) d\ell$$

Example – for $\Gamma_V(\ell) = \exp(-\ell/a)$, we obtain:

$$\theta = 2 \int_0^{\infty} \exp\left(-\frac{\ell}{a}\right) d\ell = 2a$$

and for $\Gamma_V(\ell) = \exp(-\ell^2/a^2)$:

$$\theta = 2 \int_0^{\infty} \exp\left(-\frac{\ell^2}{a^2}\right) d\ell = a \sqrt{\pi}$$

The scale of fluctuation can also be expressed as a function of the spectral density: $\theta = \pi g(0)$. For line 3 of Table 12.1, we obtain $\theta = \pi g(0) = a$.

Process with two variables – an area of correlation is given by:

$$\alpha = \int_{-\infty}^{+\infty} \int_{-\infty}^{+\infty} \Gamma_V(\ell_1, \ell_2) d\ell_1 d\ell_2 = \pi^2 g(0, 0)$$

A characteristic length L then expresses the fluctuation of the random field. [MKL86] gives an example:

$$\pi L^2 = \int_{-\infty}^{\infty} \int_{-\infty}^{\infty} \frac{\text{cov}[V(x_1, x_2, \omega), V(x_1 + \ell_1, x_2 + \ell_2, \omega)]}{\text{cov}[V(x_1, x_2, \omega), V(x_1, x_2, \omega)]} d\ell_1 d\ell_2$$

The choice of an autocovariance function is a tricky question of identification and we must often be content with classical forms. For a second-order plane stationary spatial field, with zero mean and for two coordinate points (x_1, x_2) and $(x_1 + \ell_1, x_2 + \ell_2)$, [MKL86] proposes:

$$\text{cov}[V(x_1, x_2, \omega), V(x_1 + \ell_1, x_2 + \ell_2, \omega)] = \Gamma_V(\ell_1, \ell_2)$$

$$\Gamma_V(\ell_1, \ell_2) = \begin{cases} \sigma_V^2 \delta_{\ell_1} \delta_{\ell_2} & L = \frac{1}{\sqrt{\pi}} \text{ white noise} \\ \sigma_V^2 \exp\left(-\frac{\sqrt{\ell_1^2 + \ell_2^2}}{\ell}\right) & L = \ell\sqrt{2} \text{ isotropic field} \\ \sigma_V^2 \exp\left(-\frac{(\ell_1^2 + \ell_2^2)}{\ell^2}\right) & L = \ell \text{ isotropic field} \\ \sigma_V^2 \exp(-|\ell_1|/\ell) \exp(-|\ell_2|/\ell) & L = \frac{2}{\sqrt{\pi}}\ell \text{ anisotropic field} \end{cases}$$

where $\sigma_V^2 = \text{cov}[V(x, \omega), V(x, \omega)] = \text{constant}$.

To illustrate, we easily verify, for line 3, that:

$$\pi L^2 = \int_{-\infty}^{\infty} \int_{-\infty}^{\infty} \frac{\sigma_V^2 \exp(-(\ell_1^2 + \ell_2^2)/\ell^2)}{\sigma_V^2 \exp(0)} d\ell_1 d\ell_2 = \pi \ell^2$$

Phenomenological description of the random field

A second-order stationary random field has good mathematical properties, but physics has the freedom to conform to them or not. Physical observations can result in a direct description, incomplete but sufficient, of a process. Such an example was proposed by Electricité de France [RPLB98] to represent the field of external temperature $T(x, \omega)$ along a wall of width b of a power station boiler. It is constructed as below:

- *Mean:* $m_T(x) = A \exp(-(x - a)^2/\ell^2)$ where A, a and ℓ are constants adjusted on experimental measurements.

- *Standard deviation:* $\sigma_T(x) = B \exp(-(x-a)^2/k^2)$ where B and k are also constants.
- *Autocorrelation:* $\rho_{ij} = \pm \exp(-(x_j-x_i)^2/(\lambda^2 b^2))$ where λ is an adjustment parameter to study the influence of the autocorrelation.
- *Random event ω :* Gaussian variables.

Figure 12.2 gives the mean profile and an outcome defined by three points T_i , $i = 1, 2, 3$.

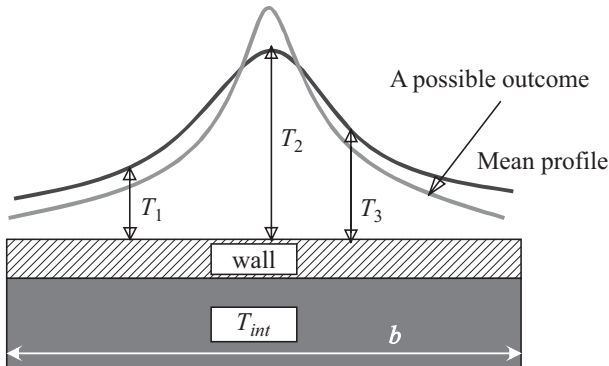


Figure 12.2 Distribution of temperatures along a wall.

12.2.2 Stochastic mesh

In a stochastic finite element method, a first discretization draws from the deterministic method. The latter is guided by the strain gradient; the mesh is denser when the strain is likely to vary rapidly. In the stochastic method, discretization depends on two factors:

- The first is the correlation length expressing the rate of variability of the random field. The distance between two stochastic discretization points must be relatively short, of the order of half the correlation length.
- The second is the dimension of the discretized vector $\{V(\omega)\}$. A large dimension is theoretically favorable but will require considerable calculation resources, whereas the determinant of the correlation matrix tends to 0 and this matrix becomes singular.

It is therefore natural to think that the two discretizations, deterministic and stochastic, are different. Furthermore, it is difficult to increase the fineness of the stochastic mesh, and other hierarchical approaches are proposed for the expansion of the stochastic field.

12.2.3 A few discretization methods

Let $V(x, \omega) \in \mathcal{D}$ be a multidimensional random field defined in domain \mathcal{D} . We consider that the field is completely described by its mean $m(x)$, by its variance $\sigma^2(x)$ and by its autocorrelation function $R(x, x')$. Let $\{V(\omega)\}$ be the vector of the random variables that describe the random field. All current methods link $V(x, \omega)$ to $\{V(\omega)\}$ using a linear transformation. For a Gaussian random field, $\{V(\omega)\}$ is also Gaussian, and as a result, completely defined by its mean $\{m_V\}$ and its covariance matrix $[C_V]$.

Discretization at the center of gravity

The value of the field at the geometric center of gravity G of element \mathcal{D}_e is chosen as a constant value over element e :

$$V(x \in \mathcal{D}_e, \omega) \implies \tilde{V}(x \in \mathcal{D}_e, \omega) = V(x = x_G, \omega)$$

Such a representation introduces discontinuities between the elements and tends to over-estimate the variability within the element. Its advantage resides in its ease of application for the calculation of the covariance matrix (positively defined) and in its independence as regards the distribution of the random event. However, it can require elements of reduced size.

Discretization based on nodal values

The principle of interpolation used in the deterministic formulation of finite elements is used here, for an element e having n_e nodes i :

$$\begin{aligned} V(x \in \mathcal{D}_e, \omega) &\implies V_i(x = x_i, \omega) \\ \tilde{V}(x \in \mathcal{D}_e, \omega) &= \sum_{i=1}^{n_e} N_i(x) V_i(x = x_i, \omega) \end{aligned}$$

where $N_i(x)$ is the vector of the finite element interpolation functions, assumed to be non-random, which implies a geometric mesh independent of the random event. The discretized random field then shows properties of inter-element continuity. The interpolation functions and the nodal points of the deterministic displacement field and the random field can be identical or not.

The following equations give the mean and the covariance:

$$\begin{aligned} \mathbb{E}[\tilde{V}(x \in \mathcal{D}_e, \omega)] &= \sum_{i=1}^{n_e} N_i(x) \mathbb{E}[V_i(x = x_i, \omega)] \\ \text{cov}[\tilde{V}_i(.), \tilde{V}_j(.)] &= \sum_{i=1}^{n_e} \sum_{j=1}^{n_e} N_i(x) N_j(x) \text{cov} [V_i(x = x_i, \omega), V_j(x = x_j, \omega)] \end{aligned}$$

Discretization at the integration points

The random field can also be discretized at the numerical integration points of the finite element (classically at the Gauss or Hammer points). Its advantage is obvious when discretization at the center of gravity becomes inefficient owing to too short a correlation length.

Discretization by spatial mean

The field within the element is taken as constant and equal to the spatial mean over the element:

$$V(x \in \mathcal{D}_e, \omega) \implies \tilde{V}(x \in \mathcal{D}_e, \omega) = \frac{1}{\text{vol}(\mathcal{D}_e)} \int_{\mathcal{D}_e} V(x, \omega) d(\text{vol})$$

This method shows inter-element discontinuities and tends to underestimate variability within the element. The calculation of the covariance matrix has been performed for certain elements [Van83], but it seems difficult to generalize it.

Discretization by optimal linear estimation

The random field is represented by a linear form:

$$V(x \in \mathcal{D}_e, \omega) \implies \tilde{V}(x \in \mathcal{D}_e, \omega) = a(x) + \sum_{i=1}^{n_e} b_i(x) V_i(x = x_i, \omega)$$

in which coefficients $a(x)$ and $b_i(x)$ are chosen in such a manner as to minimize the variance of the approximation error. The calculation points x_i form a mesh that can be different from a deterministic mesh.

This method seems like a particular application of the kriging techniques [Mat65] and is limited to Gaussian fields. It is considered more efficient than the previous methods.

12.2.4 Conclusion

The development of various stochastic discretization methods shows that the situation is not stabilized and that a good method has not yet been established. The selection criteria which must be taken into account are:

- do we have the calculation capacity to control a large number of random variables?
- is the variability of the random field high or low?
- is the random field Gaussian or not?

In this form of discretization, a random field is approximated by a random vector and a correlation matrix (Equation (12.2)). The correlation matrix can be brought to an eigenbasis (it is positive defined), which can thereafter be truncated.

In the absence of efficient physical discretization, an alternative is provided by series expansion methods, presented in the next section.

12.3 Series expansion of a random field

The discretization methods presented in the previous section involve linear forms and the calculation of the covariance matrix is therefore possible for Gaussian fields. In the absence of this assumption, non-linear expansions do not introduce additional complexity. Three expansions are discussed below.

12.3.1 Cholesky decomposition

A random field $V(x, \omega)$ can be decomposed on the basis of n functions of random, standardized, centered and independent variables $\zeta_i(\omega)$ and m deterministic functions $\phi_j(x)$, linearly independent and preferably orthogonal, verifying the kinematic conditions. By limiting ourselves to the second order:

$$V(x, \omega) \approx \tilde{V}(x, \omega) = \sum_{j=1}^m h_{0j} \phi_j(x) + \sum_{i=1}^n \sum_{j=1}^m h_{ij} \zeta_i(\omega) \phi_j(x)$$

Lawrence [Law87, Law89] uses Legendre polynomials for functions $\phi_j(x)$. In a given interval $[a, b]$, coefficients h_{ij} are evaluated by adjustment on the first and second moments of $\tilde{V}(x, \omega)$ over those of $V(x, \omega)$:

$$h_{0j} = \int_a^b m_V(x) \phi_j(x) dx$$

$$\nu_{ij} = \sum_{k=1}^{\min(i,j)} h_{ki} h_{kj} = \int_a^b \int_a^b \text{cov} [V(x_1, \omega), V(x_2, \omega)] \phi_i(x_1) \phi_j(x_2) dx_1 dx_2$$

where $\nu_{ij} = \nu_{ji}$ because covariance is symmetric. The Cholesky decomposition then gives coefficients h_{ij} :

$$h_{ii} = \sqrt{\nu_{ii} - \sum_{k=1}^{i-1} h_{ki}^2} \quad h_{ij} = \frac{\nu_{ij} - \sum_{k=1}^i h_{ki} h_{kj}}{h_{ii}} \quad j \geq i$$

Such a method helps limit the expansion of the random field by choosing only n random variables $\zeta_i(\omega)$ and m functions $\phi_j(x)$, depending on the accuracy desired.

12.3.2 Karhunen-Loève expansion [GS91]

A random field $V(x, \omega)$ is separated into a deterministic part, the mean $m_V(x)$ and a decomposed random part on the basis of n eigenvalues λ_i and eigenfunctions $\phi_i(x)$ of the covariance function:

$$V(x, \omega) \approx \tilde{V}(x, \omega) = m_V(x) + \sum_{i=1}^n \sqrt{\lambda_i} \zeta_i(\omega) \phi_i(x) \quad (12.4)$$

where $\zeta_i(\omega)$ is a set of standardized centered random variables ($E[\zeta_i(\omega)] = 0$, $E[\zeta_i(\omega) \zeta_j(\omega)] = \delta_{ij}$) to be chosen depending on the distribution associated with the random field, for example, Gaussian. The eigenvalues and eigenfunctions are solutions to the homogeneous Fredholm integral equation of the second kind:

$$\int_{\mathcal{D}} \Sigma_V(x_1, x_2) \phi_i(x_2) dx_2 = \lambda_i \phi_i(x_1) \quad (12.5)$$

An illustration is given in the one-dimensional case for the autocovariance function $\Sigma_V(x_1, x_2) = \exp(-c|x_2 - x_1|)$ defined in the interval $[-a, a]$:

$$\lambda_i = \frac{2c}{\omega_i^2 + c^2}$$

$$\phi_i(x) = \begin{cases} \frac{\cos(\omega_i x)}{\sqrt{a + \sin(2\omega_i a)/(2\omega_i)}} & \text{for } i \text{ odd} \\ \frac{\sin(\omega_i x)}{\sqrt{a - \sin(2\omega_i a)/(2\omega_i)}} & \text{for } i \text{ even} \end{cases}$$

where ω_i are solutions of:

$$c - \omega_i \tan(\omega_i a) = 0 \quad \text{for } i \text{ odd}$$

$$\omega_i + c \tan(\omega_i a) = 0 \quad \text{for } i \text{ even}$$

The main difficulty of this decomposition is the solution of Equation (12.5), particularly if the random field is two- or three-dimensional and numerical solutions are proposed.

12.3.3 Polynomial chaos

The same authors [GS91] have proposed a particular choice for functions $\zeta_i(\omega)$ found in (12.4), under the name ‘polynomial chaos’.

Let us consider a set of Gaussian independent random variables. $\xi_i(\omega), i = 1, \infty$. The polynomial chaos $\Gamma_p(\xi_1(\omega), \xi_2(\omega), \dots, \xi_\infty(\omega))$ of order p is then the set of polynomials formed by a combination of the $\xi_i(\omega)$ with a power not exceeding p .

Ghanem *et al.* show that any elements $\mu(\omega)$ in space Ω of the random variables can be expressed thus:

$$\begin{aligned}\mu(\omega) = & a_0 \Gamma_0 + \sum_{i_1=1}^{\infty} a_{i_1} \Gamma_1(\xi_{i_1}(\omega)) + \sum_{i_1=1}^{\infty} \sum_{i_2=1}^{i_1} a_{i_1 i_2} \Gamma_2(\xi_{i_1}(\omega), \xi_{i_2}(\omega)) \\ & + \sum_{i_1=1}^{\infty} \sum_{i_2=1}^{i_1} \sum_{i_3=1}^{i_2} a_{i_1 i_2 i_3} \Gamma_3(\xi_{i_1}(\omega), \xi_{i_2}(\omega), \xi_{i_3}(\omega)) + \dots\end{aligned}$$

which we can write, after truncation to m variables, in a condensed form:

$$\mu(\omega) = \sum_{j=0}^{J(m,p)-1} \tilde{a}_j \Psi_j[\xi_1(\omega), \dots, \xi_m(\omega)] \quad (12.6)$$

where \tilde{a}_j are identical to $a_{i_1}, a_{i_1 i_2} \dots$ and $\Psi_j[\xi_r(\omega)]$ to $\Gamma_k(\xi_r(\omega))$ for $k = 1, \dots, p$. Polynomials $\Psi_j[\xi_r(\omega)]$ are orthogonal and, at dimension $m = 1$, we find Hermite polynomials whose variance is equal to $p!$.

The total number of terms in the expansion $J = J(m, p)$ is given by:

$$J(m, p) = \sum_{k=0}^p \binom{m+k-1}{k} = \frac{(m+p)!}{m! p!} \quad (12.7)$$

where p is the chaos order and m its dimension.

As an illustration, $\mu(\omega)$ is developed for $m = 2$ and $p = 3$, $J(m, p) = 10$:

$$\begin{aligned}\mu(\omega) = & a_0 \Gamma_0 + a_1 \Gamma_1(\xi_1) + a_2 \Gamma_1(\xi_2) \\ & + a_{11} \Gamma_2(\xi_1, \xi_1) + a_{12} \Gamma_2(\xi_1, \xi_2) + a_{22} \Gamma_2(\xi_2, \xi_2) \\ & + a_{111} \Gamma_3(\xi_1, \xi_1, \xi_1) + a_{211} \Gamma_3(\xi_2, \xi_1, \xi_1) \\ & + a_{221} \Gamma_3(\xi_2, \xi_2, \xi_1) + a_{222} \Gamma_3(\xi_2, \xi_2, \xi_2) \\ = & \langle \tilde{a} \rangle \{ \Psi \}\end{aligned}$$

with:

$$\begin{aligned}\langle \tilde{a} \rangle &= \langle a_0, a_1, a_2, a_{11}, \dots, a_{222} \rangle \\ \{ \Psi \}^t &= \{ \Gamma_0, \Gamma_1(\xi_1), \Gamma_1(\xi_2), \dots, \Gamma_3(\xi_2, \xi_2, \xi_2) \}^t\end{aligned}$$

The polynomial chaos $\Gamma_p(\xi_i)$ is built by successively imposing orthogonality conditions to the polynomials of order 0 to $p - 1$. Tables 12.2 and 12.3, drawn from [GS91], give the 1- and 2-dimensional polynomials as well as their variances for the first four degrees. Irrespective of the polynomial, we impose $\Gamma_0 = 1$ and $E[\Gamma_p(\xi_i)] = 0$ (the polynomials have zero mean, except for degree 0). The polynomials of Table 12.2 are, not surprisingly, the Hermite polynomials whose orthogonality conditions we know (see Section 4.8).

j	Chaos of order p	j th polynomial Ψ_j	variance $\langle \Psi_j^2 \rangle$
0	0	1	
1	1	ξ_1	1
2	2	$\xi_1^2 - 1$	2
3	3	$\xi_1^3 - 3\xi_1$	6
4	4	$\xi_1^4 - 6\xi_1^2 + 3$	24

Table 12.2 One-dimensional polynomial chaos and variance ($m = 1$).

j	Chaos of order p	j th polynomial Ψ_j	variance $\langle \Psi_j^2 \rangle$
0	0	1	
1	1	ξ_1	1
2	1	ξ_2	1
3	2	$\xi_1^2 - 1$	2
4	2	$\xi_1 \xi_2$	1
5	2	$\xi_2^2 - 1$	2
6	3	$\xi_1^3 - 3\xi_1$	6
7	3	$\xi_1^2 \xi_2 - \xi_2$	2
8	3	$\xi_1 \xi_2^2 - \xi_1$	2
9	3	$\xi_2^3 - 3\xi_2$	6
10	4	$\xi_1^4 - 6\xi_1^2 + 3$	24
11	4	$\xi_1^3 \xi_2 - 3\xi_1 \xi_2$	6
12	4	$\xi_1^2 \xi_2^2 - \xi_1^2 - \xi_2^2 + 1$	4
13	4	$\xi_1 \xi_2^3 - 3\xi_1 \xi_2$	6
14	4	$\xi_2^4 - 6\xi_2^2 + 3$	24

Table 12.3 Two-dimensional polynomial chaos and variances ($m = 2$).

12.3.4 Conclusion

The methods introduced in Sections 12.2 and 12.3 sought to represent a random field. These solutions are not yet definitive and other propositions are being explored by researchers [SDK00, Waa00, Van03].

As for the classic methods of deterministic mechanics, we have direct discretization methods and expansion methods with truncation. In both cases, questions arise as to convergence, the size of the mesh or the number of terms in the expansions. This highlights a dimension of the stochastic problem characterized by the number of random variables chosen and the size of the autocorrelation matrix.

12.4 Finite element method and gradient calculation

Whether the random variables are nodal variables or amplitudes of a series expansion, it is interesting to calculate, directly if possible, the derivatives of particular functions with respect to these variables. Such calculations are necessary for a sensitivity analysis, but also for an efficient application of the reliability algorithms described in Chapter 5.

12.4.1 Assumptions and notations

Certain variables of external random events (actions represented by the vector F) and internal random events (variables relative to the material and to the geometry of the stiffness matrix K) are random. They are represented in a vector X including the nodal variables of the stochastic discretization or the coefficients of an expansion. The first and second moments of vector X are assumed to be known. In the displacement model of the FEM, the direct output variable is the displacement q and the resulting variables are the strain ε and the stress σ .

12.4.2 FEM linear equations

Reminder [BD90]

In order to facilitate the presentation and to fix the notations, we will give a brief summary of the finite element method for linear static problems.

Let N be an appropriate form function; the displacement u of an element e is given by:

$$u = N q_e$$

where q_e is the vector of the nodal displacements of an element. By derivation of this equation, we can obtain the strain:

$$\varepsilon = B q_e \quad (12.8)$$

where B is a matrix of the geometric conditions of the element. The stress σ is given by:

$$\sigma = H \varepsilon$$

where H is the elasticity matrix. The elementary stiffness matrix K_e is obtained by applying the virtual work principle on the volume of the element:

$$K_e = \int_{V_e} B^t H B \, dV \quad (12.9)$$

The global stiffness matrix K is obtained by assembling the elements in a domain. Then the application of boundary conditions yields:

$$K q = F \quad (12.10)$$

where q is the vector of unknown displacements and F is the vector of equivalent external nodal forces.

12.4.3 Gradient calculation with constant mesh

Let us assume $\alpha = x - m_X$ to obtain a centered random variable (for uniformity with the rest of the chapter). The differentiation of (12.10) directly gives for a variable:

$$K \frac{\partial q}{\partial \alpha} = \frac{\partial F}{\partial \alpha} - \frac{\partial K}{\partial \alpha} q$$

The influence of variables α on the displacements, strains and stresses is obtained from the Jacobian of the mechanical transformations:

$$\begin{aligned} q &= K^{-1} F \quad J_{q,\alpha} = \frac{\partial q}{\partial \alpha} = K^{-1} \left(\frac{\partial F}{\partial \alpha} - \frac{\partial K}{\partial \alpha} q \right) = K^{-1} (J_{F,\alpha} - J_{K,\alpha} q), \\ \varepsilon &= B q \quad J_{\varepsilon,\alpha} = B \frac{\partial q}{\partial \alpha} = B J_{q,\alpha} \quad (\text{if } B \text{ does not depend on the random variables}), \\ \sigma &= H \varepsilon \quad J_{\sigma,\alpha} = H B J_{q,\alpha} + J_{H,\alpha} B q. \end{aligned}$$

It is noted that the mesh and the form functions must not be a function of the random variables. The direct introduction of these equations into a FEM code, under linear assumptions, is an efficient but complex procedure to apply, except if the random variable vector is limited to certain types of random events. In addition, the expected results allow only one linearization around a point, which is interesting for a sensitivity analysis around a known point (the mean, in general) but is inadequate for a reliability analysis. However, the reliability algorithms (Chapter 5) use gradients and their application is made easier.

The generalization to random variables α_k gives:

$$\frac{\partial q}{\partial \alpha_j} = K^{-1} \left(\frac{\partial F}{\partial \alpha_j} - \frac{\partial K}{\partial \alpha_j} q \right) \quad (12.11)$$

and, if the second order is desired:

$$\frac{\partial^2 q}{\partial \alpha_j \partial \alpha_l} = K^{-1} \left(\frac{\partial^2 F}{\partial \alpha_j \partial \alpha_l} - \frac{\partial K}{\partial \alpha_j} \frac{\partial q}{\partial \alpha_l} - \frac{\partial K}{\partial \alpha_l} \frac{\partial q}{\partial \alpha_j} - \frac{\partial^2 K}{\partial \alpha_j \partial \alpha_l} q \right) \quad (12.12)$$

In Equations (12.11) and (12.12), the main calculation effort lies in the calculation of the derivatives of the stiffness matrix, except in particular cases.

Case of material variability

In this case, only the stress-strain equation is involved. By introducing the random variable into Equation (12.9), we obtain:

$$\frac{\partial K}{\partial \alpha_j} = \int_V B^t \frac{\partial H(\alpha_k)}{\partial \alpha_j} B dV$$

12.4.4 Calculation of derivatives with a variable mesh

A particularly interesting approach in the finite element method involves isoparametric elements. Its interest lies in performing integration equation (12.9) on a parent element independent of all geometric uncertainty (Figure 12.3). Equation (12.9) becomes:

$$K = \int_{\gamma V} {}^0 B^t H {}^0 B dV = \int_{\gamma V} {}^\gamma B^t H {}^\gamma B \det {}_0^\gamma J dV \quad (12.13)$$

where γV is the volume of the parent element and ${}^\gamma J$ is the Jacobian of the transformation between the physical configuration ${}^0 V$ and the parent configuration γV .

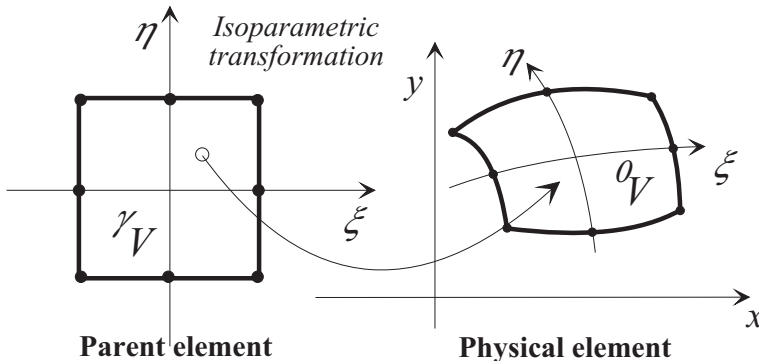


Figure 12.3 Isoparametric transformation.

First-order sensitivity

As the integration of (12.13) is on the parent element γV , which is independent of the disturbance of the mesh, there is no convection term and the computation of the derivative is reduced to the differentiation of B , of $|{}^\gamma J| = \det {}_0^\gamma J$ for the geometric variables and of H for the material variables.

Geometric variables: let us consider matrix B , Equation (12.8), in plane elasticity:

$$\boldsymbol{\varepsilon} = \begin{bmatrix} \frac{\partial u_1}{\partial x} \\ \frac{\partial u_2}{\partial y} \\ \frac{\partial u_1}{\partial y} + \frac{\partial u_2}{\partial x} \end{bmatrix} \implies {}^0B = \begin{bmatrix} {}^0N_{1,x} & 0 & {}^0N_{n,x} & 0 \\ 0 & {}^0N_{1,y} & \dots & 0 & {}^0N_{n,y} \\ {}^0N_{1,y} & {}^0N_{1,x} & {}^0N_{n,y} & {}^0N_{n,x} \end{bmatrix}$$

where n is the number of nodes in the element. The derivative $\partial B / \partial \alpha_j$ is calculated as a function of $\partial N_{i,x} / \partial \alpha_j$ and $\partial N_{i,y} / \partial \alpha_j$ by:

$$\begin{bmatrix} \frac{\partial {}^0N_{i,x}}{\partial \alpha_j} \\ \frac{\partial {}^0N_{i,y}}{\partial \alpha_j} \end{bmatrix} = \frac{\partial {}^0J^{-1}}{\partial \alpha_j} \begin{bmatrix} {}^\gamma N_{i,\xi} \\ {}^\gamma N_{i,\eta} \end{bmatrix}$$

However, as ${}^0J^{-1}$ and 0J are orthogonal (i.e. ${}^0J^{-1} \cdot {}^0J = I$), the derivative of ${}^0J^{-1}$ is given as a function of $\partial {}^0J / \partial \alpha_j$ by:

$$\frac{\partial {}^0J^{-1}}{\partial \alpha_j} = -{}^0J^{-1} \frac{\partial {}^0J}{\partial \alpha_j} {}^0J^{-1}$$

Lund [Lun94] proposes evaluating the Jacobian by finite differences, but we can see that an analytical differentiation is possible by writing J in the form:

$${}^0J = \begin{bmatrix} {}^\gamma N_{1,\xi} & {}^\gamma N_{2,\xi} & \dots & {}^\gamma N_{n,\xi} \\ {}^\gamma N_{1,\eta} & {}^\gamma N_{2,\eta} & \dots & {}^\gamma N_{n,\eta} \end{bmatrix} \begin{bmatrix} x_1 & y_1 \\ x_2 & y_2 \\ \dots & \dots \\ x_n & y_n \end{bmatrix}$$

and the differentiation of the Jacobian is given directly by:

$$\frac{\partial J}{\partial \alpha_j} = \begin{bmatrix} {}^\gamma N_{1,\xi} & {}^\gamma N_{2,\xi} & \dots & {}^\gamma N_{n,\xi} \\ {}^\gamma N_{1,\eta} & {}^\gamma N_{2,\eta} & \dots & {}^\gamma N_{n,\eta} \end{bmatrix} \begin{bmatrix} \frac{\partial x_1}{\partial \alpha_j} & \frac{\partial y_1}{\partial \alpha_j} \\ \frac{\partial x_2}{\partial \alpha_j} & \frac{\partial y_2}{\partial \alpha_j} \\ \dots & \dots \\ \frac{\partial x_n}{\partial \alpha_j} & \frac{\partial y_n}{\partial \alpha_j} \end{bmatrix}$$

which can be evaluated analytically, that is, without finite differences. For example, if $\alpha_j = x_i$ or $\alpha_j = y_j$, the derivatives are simply:

$$\frac{\partial {}^0J}{\partial x_i} = \begin{bmatrix} {}^\gamma N_{i,\xi} & 0 \\ {}^\gamma N_{i,\eta} & 0 \end{bmatrix} \quad \text{or} \quad \frac{\partial {}^0J}{\partial y_j} = \begin{bmatrix} 0 & {}^\gamma N_{j,\xi} \\ 0 & {}^\gamma N_{j,\eta} \end{bmatrix}$$

However, as the derivative of the Jacobian determinant is also required, it can be evaluated by a finite difference:

$$\frac{\partial |\gamma_0 J|}{\partial \alpha_j} \approx \frac{|\gamma_0 J(\alpha_j + \Delta \alpha_j)| - |\gamma_0 J(\alpha_j)|}{\Delta \alpha_j}$$

or by direct differentiation of the determinant's expression, for example, for a plane problem:

$$\frac{\partial |\gamma_0 J|}{\partial \alpha_j} = \frac{\partial \gamma_0 J_{11}}{\partial \alpha_j} \gamma_0 J_{22} + \gamma_0 J_{11} \frac{\partial \gamma_0 J_{22}}{\partial \alpha_j} - \frac{\partial \gamma_0 J_{12}}{\partial \alpha_j} \gamma_0 J_{21} - \gamma_0 J_{12} \frac{\partial \gamma_0 J_{21}}{\partial \alpha_j}$$

where $\gamma_0 J_{mn}$ is term (m, n) of the Jacobian $\gamma_0 J$. Finally, the derivative of the stiffness matrix is given by:

$$\frac{\partial K}{\partial \alpha_j} = \int_{\gamma V} \left(\frac{\partial \gamma B^t}{\partial \alpha_j} H \gamma B |\gamma_0 J| + \gamma B^t H \frac{\partial \gamma B}{\partial \alpha_j} |\gamma_0 J| + \gamma B^t H \gamma B \frac{\partial |\gamma_0 J|}{\partial \alpha_j} \right) dV \quad (12.14)$$

To facilitate the implementation of the equations, (12.14) can be put in the form [Lun94]:

$$\frac{\partial K}{\partial \alpha_j} = 2 \left[\int (\gamma B^t H \gamma \hat{B} |\gamma_0 J|) dV \right]_s \quad (12.15)$$

where:

$$\gamma \hat{B} = \frac{\partial \gamma B}{\partial \alpha_j} + \frac{\gamma B}{2 |J|} \frac{\partial |J|}{\partial \alpha_j}$$

and $[\cdot]_s = \frac{1}{2} ([\cdot] + [\cdot]^t)$.

Material variables: in the case of variables relative to the material, such as Young's modulus or Poisson's coefficient, the stiffness derivative is given by:

$$\frac{\partial K}{\partial \alpha_j} = \int_{\gamma V} \gamma B^t \frac{\partial H(\alpha_k)}{\partial \alpha_j} \gamma B |\gamma_0 J| dV$$

In the case of non-linear behavior, Kleiber [Kle97] gives various techniques to apply in incremental analysis.

Second-order sensitivity

The developments presented in the previous section can be extended to the second order [ML98].

12.5 Perturbation method

This method is based on the calculation of the derivatives of the stiffness matrix. These can be obtained from the equations of the FEM (previous section) or by finite differences. The objective is to obtain the mean and the covariance of the results of finite element analysis (displacements, stresses, etc.).

12.5.1 Taylor expansion

The perturbation method assumes that the effect of the random event forms a small variation around a reference value, in general, the mean. For this, the random design variables X_k are replaced by centered variables $\alpha_k = X_k - m_{X_k}$. A Taylor expansion is then carried out. Equation (12.10) is written by making the random variables explicit:

$$K(\alpha_k) q(\alpha_k) = F(\alpha_k) \quad (12.16)$$

where the indexes are written only for the n random variables α_k whereas the indexes of the components of K with dimension $m \times m$, $q(m)$ and $F(m)$ are systematically omitted.

We note, for any variable V :

$$\frac{\partial V}{\partial \alpha_i} \Big|_{\alpha=0} = V_i^I \quad \text{and} \quad \frac{\partial^2 V}{\partial \alpha_i \partial \alpha_j} \Big|_{\alpha=0} = V_{ij}^{II}$$

K , q and F are expanded to the second order around the reference value:

$$\begin{aligned} K &= K^0 + \sum_{i=1}^n K_i^I \alpha_i + \frac{1}{2} \sum_{i=1}^n \sum_{j=1}^n K_{ij}^{II} \alpha_i \alpha_j + \dots \\ q &= q^0 + \sum_{i=1}^n q_i^I \alpha_i + \frac{1}{2} \sum_{i=1}^n \sum_{j=1}^n q_{ij}^{II} \alpha_i \alpha_j + \dots \\ F &= F^0 + \sum_{i=1}^n F_i^I \alpha_i + \frac{1}{2} \sum_{i=1}^n \sum_{j=1}^n F_{ij}^{II} \alpha_i \alpha_j + \dots \end{aligned} \quad (12.17)$$

The application of Equation (12.16) gives, by term-by-term identification, the following systems:

$$\begin{aligned} q^0 &= (K^0)^{-1} F^0 \\ q_i^I &= (K^0)^{-1} (F_i^I - K_i^I q^0) \\ q_{ij}^{II} &= (K^0)^{-1} (F_{ij}^{II} - (K_i^I q_j^I + K_j^I q_i^I + K_{ij}^{II} q^0)) \end{aligned}$$

A single inversion of the stiffness matrix is enough to compute the $(2 + 3n + n^2)/2$ linear systems above, in view of the symmetry $q_{ij}^{II} = q_{ji}^{II}$.

Strains are calculated in each element:

$$\varepsilon = \varepsilon^0 + \sum_{k=1}^n \varepsilon_k^I \alpha_k + \frac{1}{2} \sum_{k=1}^n \sum_{l=1}^n \varepsilon_{kl}^{II} \alpha_k \alpha_l + \dots$$

with $\varepsilon^0 = Bq^0 \quad \varepsilon_k^I = Bq_k^I \quad \varepsilon_{kl}^{II} = Bq_{kl}^{II}$ (B does not depend on α_k)

and stresses are similarly calculated, taking into account that a random event is possible in the Hooke matrix H :

$$H = H^0 + \sum_{i=1}^n H_i^I \alpha_i + \frac{1}{2} \sum_{i=1}^n \sum_{j=1}^n H_{ij}^{II} \alpha_i \alpha_j + \dots$$

$$\sigma = \sigma^0 + \sum_{i=1}^n \sigma_i^I \alpha_i + \frac{1}{2} \sum_{i=1}^n \sum_{j=1}^n \sigma_{ij}^{II} \alpha_i \alpha_j + \dots$$

$$\sigma^0 = H^0 \varepsilon^0 \quad \sigma_i^I = H^0 \varepsilon_i^I + H_i^I \varepsilon^0 \quad \sigma_{ij}^{II} = H^0 \varepsilon_{ij}^{II} + H_i^I \varepsilon_j^I + H_j^I \varepsilon_i^I + H_{ij}^{II} \varepsilon^0$$

12.5.2 Mean and covariance

Limiting ourselves initially to a first-order expansion, we can obtain the mean and the covariance of any variable, q for example, by taking into account on the one hand the linear form and on the other the nullity of the means m_{α_i} :

$$q = q^0 + \sum_{i=1}^n q_i^I \alpha_i$$

$$\mathbb{E}^I[q] = \mathbb{E}[q^0]$$

$$\text{cov}^I[q, q] = \mathbb{E}[(q - \mathbb{E}^I[q])(q - \mathbb{E}^I[q])^t] = \sum_{i=1}^n \sum_{j=1}^n q_i^I (q_j^I)^t \mathbb{E}[\alpha_i \alpha_j]$$

where $\mathbb{E}[\alpha_i \alpha_j]$ is the covariance matrix of random vector α_k with zero mean.

In the second order, the form is no longer linear and [SY88] assumes that variables α_k are Gaussian to obtain the following results:

$$\mathbb{E}^{II}[q] = q^0 + \frac{1}{2} \sum_{i=1}^n \sum_{j=1}^n q_{ij}^{II} \mathbb{E}[\alpha_i \alpha_j] \tag{12.18}$$

$$\text{cov}^{II}[q, q] = \text{cov}^I[q, q] + \frac{1}{4} \sum_{i=1}^n \sum_{j=1}^n \sum_{m=1}^n \sum_{n=1}^n q_{ij}^{II} (q_{mn}^{II})^t$$

$$\times (\mathbb{E}[\alpha_i \alpha_n] \mathbb{E}[\alpha_j \alpha_m] + \mathbb{E}[\alpha_i \alpha_m] \mathbb{E}[\alpha_j \alpha_n]) \tag{12.19}$$

Knowledge of the first two moments does not enable a reliability analysis. At best, the Chebychev inequality can be used to obtain an over-estimation, which is generally very high:

$$\text{Prob} \left[|X - \mathbb{E}[X]| > k \sqrt{\text{var}[X]} \right] \leq \frac{1}{k^2}$$

which gives 0.25 with $k = 2$, compared to 0.046 if the distribution is Gaussian!

12.5.3 Example: deflection of a beam

The previous equations are used here in a particularly simple case, with one degree of freedom, for which an exact solution can be found.

Let us consider a problem of beam theory in which the deflection f is given by an expression as a function of the Young's modulus E and a concentrated load P , both of which are assumed to be random, and with a deterministic coefficient k including the geometric characteristics (length, inertia). We therefore note:

$$f = k \frac{P}{E}$$

Deflection f is a random variable. The respective means and standard deviations of E and P are denoted by m_E and σ_E and by m_P and σ_P . We introduce the centered random variables:

$$\alpha_1 = E - m_E \quad \alpha_2 = P - m_P$$

and we consider that the α_k are small perturbations or disturbances ($\alpha_k \approx d\alpha_k$) with zero mean and with a covariance matrix $\mathbb{E}[\alpha_i \alpha_j]$, $i, j = 1, 2$.

Characterization of the deflection: let us suppose two variables X and Y ; the distribution function of $Z = k X/Y$ is given by [Rad91] (including k):

$$F_Z(z) = \int_0^{+\infty} \left\{ \int_{-\infty}^{yz/k} f_{X,Y}(x,y) dx \right\} dy + \int_{-\infty}^0 \left\{ \int_{yz/k}^{+\infty} f_{X,Y}(x,y) dx \right\} dy$$

and the density:

$$f_Z(z) = \int_{-\infty}^{+\infty} \frac{|y|}{k} f_{X,Y} \left(\frac{y z}{k}, y \right) dy$$

Case of Gaussian variables: the variables are assumed to be independent (no correlation between the loading and the Young's modulus) and the constant k is positive. Let us first consider centered standardized variables. We obtain:

$$f_{X,Y}(x,y) = \frac{1}{2\pi} \exp \left(-\frac{x^2 + y^2}{2} \right)$$

and with $x = y z/k$:

$$\begin{aligned} f_Z(z) &= \frac{1}{2k\pi} \int_{-\infty}^{+\infty} |y| \exp\left(-\frac{(yz/k)^2 + y^2}{2}\right) dy \\ &= \frac{1}{2k\pi} \int_0^{+\infty} \exp\left(-\frac{y^2}{2} \left(1 + \frac{z^2}{k^2}\right)\right) d(y^2) \\ f_Z(z) &= \frac{1}{k\pi} \left(1 + \frac{z^2}{k^2}\right)^{-1} \end{aligned}$$

For any Gaussian variable:

$$\begin{aligned} f_{X,Y}(x, y) &= \frac{1}{2\pi\sigma_X\sigma_Y} \exp\left(-\frac{1}{2} \left(\left(\frac{x - m_X}{\sigma_X}\right)^2 + \left(\frac{y - m_Y}{\sigma_Y}\right)^2\right)\right) \\ f_Z(z) &= \frac{1}{2k\pi\sigma_X\sigma_Y} \int_{-\infty}^{+\infty} |y| \exp\left(-\frac{1}{2} \left(\left(\frac{yz/k - m_X}{\sigma_X}\right)^2 + \left(\frac{y - m_Y}{\sigma_Y}\right)^2\right)\right) dy \\ f_Z(z) &= \frac{1}{2k\pi\sigma_X\sigma_Y} \int_{-\infty}^{+\infty} |y| \exp\left(-\frac{1}{2} \left(y^2 \underbrace{\left(\frac{z^2}{k^2\sigma_X^2} + \frac{1}{\sigma_Y^2}\right)}_A\right.\right. \\ &\quad \left.\left.+ y \underbrace{\left(-\frac{2m_X z}{k\sigma_X^2} - \frac{2m_Y}{\sigma_Y^2}\right)}_B + \underbrace{\left(\frac{m_X^2}{\sigma_X^2} + \frac{m_Y^2}{\sigma_Y^2}\right)}_C\right)\right) dy \\ f_Z(z) &= \frac{1}{2k\pi\sigma_X\sigma_Y} \int_{-\infty}^{+\infty} |y| \exp\left(-\frac{1}{2} (Ay^2 + By + C)\right) dy \end{aligned}$$

but:

$$Ay^2 + By + C = \left(\sqrt{A}y + \frac{B}{2\sqrt{A}}\right)^2 - \frac{B^2}{4A} + C$$

and:

$$f_Z(z) = \underbrace{\frac{\exp\left(-\frac{1}{2} \left(-\frac{B^2}{4A} + C\right)\right)}{2k\pi\sigma_X\sigma_Y}}_K \int_{-\infty}^{+\infty} |y| \exp\left(-\frac{1}{2} \left(\sqrt{A}y + \frac{B}{2\sqrt{A}}\right)^2\right) dy$$

By carrying out the change of variable:

$$u = \sqrt{A}y + \frac{B}{2\sqrt{A}} \quad y = \frac{u}{\sqrt{A}} - \frac{B}{2A} \quad dy = \frac{du}{\sqrt{A}}$$

$$f_Z(z) = K \int_{-\infty}^{+\infty} \left| \frac{u}{\sqrt{A}} - \frac{B}{2A} \right| \exp\left(-\frac{1}{2}u^2\right) \frac{du}{\sqrt{A}}$$

$$f_Z(z) = K \left(\int_{-\infty}^{\frac{B}{2\sqrt{A}}} \left(\frac{B}{2A\sqrt{A}} - \frac{u}{A} \right) e^{-\frac{1}{2}u^2} du \right.$$

$$\left. + \int_{\frac{B}{2\sqrt{A}}}^{\infty} \left(\frac{u}{A} - \frac{B}{2A\sqrt{A}} \right) e^{-\frac{1}{2}u^2} du \right)$$

which gives the following integrals¹:

$$\frac{B}{2A\sqrt{A}} \int_{-\infty}^{\frac{B}{2\sqrt{A}}} \exp\left(-\frac{1}{2}u^2\right) du = \frac{B\sqrt{2\pi}}{4A\sqrt{A}} \left(\operatorname{erf}\left(\frac{\sqrt{2}B}{4\sqrt{A}}\right) + 1 \right)$$

$$\frac{1}{A} \int_{-\infty}^{\frac{B}{2\sqrt{A}}} -u \exp\left(-\frac{1}{2}u^2\right) du = \frac{1}{A} \exp\left(-\frac{B^2}{8A}\right)$$

$$-\frac{B}{2A\sqrt{A}} \int_{\frac{B}{2\sqrt{A}}}^{\infty} \exp\left(-\frac{1}{2}u^2\right) du = -\frac{B\sqrt{2\pi}}{4A\sqrt{A}} \left(1 - \operatorname{erf}\left(\frac{\sqrt{2}B}{4\sqrt{A}}\right) \right)$$

$$-\frac{1}{A} \int_{\frac{B}{2\sqrt{A}}}^{\infty} -u \exp\left(-\frac{1}{2}u^2\right) du = \frac{1}{A} \exp\left(-\frac{B^2}{8A}\right)$$

and finally:

$$f_Z(z) = \frac{\exp\left(-\frac{1}{2}\left(-\frac{B^2}{4A} + C\right)\right)}{2k\pi\sigma_X\sigma_Y} \left(\frac{\sqrt{2\pi}B}{2A\sqrt{A}} \operatorname{erf}\left(\frac{\sqrt{2}B}{4\sqrt{A}}\right) + \frac{2}{A} \exp\left(-\frac{B^2}{8A}\right) \right)$$

Case of lognormal variables: this case does not require the use of general formulae. In fact, it is enough to note that:

$$f = k \frac{P}{E} \iff \ln f = \ln k + \ln P - \ln E$$

which leads to the algebraic addition of three Gaussian variables. Let us assume $W = \ln f$, W is a Gaussian variable with parameters:

$$m_W = \ln k + \lambda_P - \lambda_E \quad \sigma_W = \sqrt{\xi_P^2 + \xi_E^2}$$

¹ The function $\operatorname{erf}(x)$ is defined by $\operatorname{erf}(x) = (2/\sqrt{\pi}) \int_0^x e^{-u^2/2} du$. It is calculated by most software applications under the name erf (*error function*).

and:

$$f_f(f) = \frac{1}{f \sqrt{2\pi} \sqrt{\xi_P^2 + \xi_E^2}} \exp \left(-\frac{1}{2} \frac{(\ln f - \ln k - \lambda_P + \lambda_E)^2}{\xi_P^2 + \xi_E^2} \right)$$

f is therefore a lognormal variable with mean:

$$m_f = \exp \left(m_W + \frac{\sigma_W^2}{2} \right) = k \frac{m_P}{m_E} \left(1 + \frac{\sigma_E^2}{m_E^2} \right)$$

and standard deviation:

$$\begin{aligned} \sigma_f &= \exp(m_W + \sigma_W^2) \sqrt{1 - \exp(-\sigma_W^2)} \\ &= k \frac{m_P}{m_E} \sqrt{1 + c_P^2} (1 + c_E^2)^{3/2} \sqrt{1 - \frac{1}{1 + c_P^2} \frac{1}{1 + c_E^2}} \\ &= k \frac{m_P}{m_E} (1 + c_E^2) \sqrt{c_P^2 + c_E^2 + c_P^2 c_E^2} \end{aligned}$$

where c_X is the coefficient of variation of variable X .

Approximation by Taylor expansion: the expansion is written as:

$$f = f_0 + \frac{\partial f}{\partial \alpha_1} d\alpha_1 + \frac{\partial f}{\partial \alpha_2} d\alpha_2 + \frac{1}{2} \left(\frac{\partial^2 f}{\partial \alpha_1^2} d\alpha_1^2 + 2 \frac{\partial^2 f}{\partial \alpha_1 \partial \alpha_2} d\alpha_1 d\alpha_2 + \frac{\partial^2 f}{\partial \alpha_2^2} d\alpha_2^2 \right)$$

that is, with $\alpha_1 = E - m_E$ and $\alpha_2 = P - m_P$:

$$\begin{aligned} f &= k \left(\frac{m_P}{m_E} - \frac{m_P}{m_E^2} \alpha_1 + \frac{1}{m_E} \alpha_2 + \frac{1}{2} \left(\frac{2 m_P}{m_E^3} \alpha_1^2 - \frac{2}{m_E^2} \alpha_1 \alpha_2 \right) \right) \\ f &= k \left(\frac{m_P}{m_E} + \begin{bmatrix} -\frac{m_P}{m_E^2} & \frac{1}{m_E} \end{bmatrix} \begin{bmatrix} \alpha_1 \\ \alpha_2 \end{bmatrix} \right. \\ &\quad \left. + \frac{1}{2} [\alpha_1 \ \alpha_2] \begin{bmatrix} 2 m_P/m_E^3 & -1/m_E^2 \\ -1/m_E^2 & 0 \end{bmatrix} \begin{bmatrix} \alpha_1 \\ \alpha_2 \end{bmatrix} \right) \end{aligned}$$

First-order approximations.

$$E^I[f] = m_f = k m_P / m_E$$

$$E[f^2] = k^2 \left(m_P^2 / m_E^2 + \begin{bmatrix} -m_P & 1 \\ -m_E^2 & m_E \end{bmatrix} \begin{bmatrix} E[\alpha_1^2] & E[\alpha_1 \alpha_2] \\ E[\alpha_2 \alpha_1] & E[\alpha_2^2] \end{bmatrix} \begin{bmatrix} -m_P / m_E^2 \\ 1 / m_E \end{bmatrix} \right)$$

and as $\sigma_f^2 = E[f^2] - E[f]^2$, we obtain:

$$\sigma_f^{2I} = k^2 \begin{bmatrix} -\frac{m_P}{m_E^2} & \frac{1}{m_E} \\ \frac{1}{m_E} & \frac{1}{m_E} \end{bmatrix} \begin{bmatrix} E[\alpha_1^2] & E[\alpha_1\alpha_2] \\ E[\alpha_2\alpha_1] & E[\alpha_2^2] \end{bmatrix} \begin{bmatrix} -m_P/m_E^2 \\ 1/m_E \end{bmatrix}$$

Second-order approximations.

$$\begin{aligned} E^{II}[f] &= m_f = k \left(\frac{m_P}{m_E} + \frac{1}{2} \left(\frac{2m_P}{m_E^3} E[\alpha_1^2] - \frac{2}{m_E^2} E[\alpha_1\alpha_2] + 0 E[\alpha_2^2] \right) \right) \\ \sigma_f^{2II} &= \sigma_f^{2I} + k^2 \left(\frac{2m_P^2}{m_E^6} E[\alpha_1^2]^2 - \frac{4m_P}{m_E^5} E[\alpha_1\alpha_2] E[\alpha_1^2] \right. \\ &\quad \left. + \frac{1}{m_E^4} (E[\alpha_1\alpha_2]^2 + E[\alpha_1^2] E[\alpha_2^2]) \right) \end{aligned}$$

Comparison: the density of the deflection being known, it is possible to compare the exact results for the first two moments with those obtained by the Taylor expansions. This comparison is made here with arbitrary data (Table 12.4) and shows, in this case, negligible differences (Table 12.5). We must however note that the mean and standard deviation of the Gaussian case are obtained by numerical integrations of the density expression on a truncated support. In fact, the quotient of two Gaussian distributions is a Cauchy distribution that does not have any moments.

Variable	Distribution	m_X	σ_X	c_X
P	Gauss or LogN	100,000	15,000	15%
E	Gauss or LogN	210×10^9	21×10^9	10%
k	Deter.	0.105×10^6		

Table 12.4 Variable data (units: N, m).

Method	Truncated Gauss	Exact LogN	Taylor ^I	Taylor ^{II}
m_f	0.050516	0.050500	0.050000	0.050500
σ_f	0.009270	0.009135	0.009014	0.009073

Table 12.5 Comparison of the approximations.

12.5.4 Neumann expansion

The calculation of the mean and covariance using Equations (12.18) and (12.19) can be replaced by a Monte Carlo simulation in order to eliminate the Gaussian nature. The Neumann expansion [SY88] gives an economic means of generating a large sample of outcomes.

Cholesky decomposition

The FEM equation (12.10) with a linear assumption is formally solved by calculating the inverse matrix K^{-1} , which is often very complex. The Cholesky decomposition offers an interesting alternative. Let us assume (which is possible, since K is positive defined):

$$L L^t = K$$

where L is a lower triangular matrix. The solution is decomposed into two triangular systems:

$$L X = F \quad L^t q = X$$

Neumann expansion

The stiffness matrix is decomposed into one part K^0 , independent of random events (calculated with the means) and another part $\Delta K(\alpha)$, a function of the random events (Equation (12.17)). The latter part can be built from a discretized random field or otherwise on another basis. The Neumann expansion gives the inverse matrix:

$$K(\alpha)^{-1} = (K^0 + \Delta K(\alpha))^{-1} = (I - P(\alpha) + P(\alpha)^2 - P(\alpha)^3 + \dots) K^{0^{-1}}$$

with $P(\alpha) = K^{0^{-1}} \Delta K(\alpha)$.

$$K(\alpha)^{-1} = \sum_{i=0}^{\infty} (-1)^i \left(K^{0^{-1}} \Delta K(\alpha) \right)^i K^{0^{-1}} = \sum_{i=0}^{\infty} (-1)^i P(\alpha)^i K^{0^{-1}} \quad (12.20)$$

Hence:

$$\begin{aligned} q &= K(\alpha)^{-1} F(\alpha) \\ q &= (I - P(\alpha) + P(\alpha)^2 - P(\alpha)^3 + \dots) K^{0^{-1}} F \\ q &= q^0 - P(\alpha) q^0 + P(\alpha)^2 q^0 - P(\alpha)^3 q^0 + \dots \\ q &= q^0 - q^1 + q^2 - q^3 + \dots \end{aligned}$$

and the successive terms q^i are obtained from the equation:

$$K^0 q^i = \Delta K(\alpha) q^{i-1}$$

inverted by the Cholesky decomposition.

The series is truncated according to the following criterion:

$$\frac{\|q^i\|}{\left\| \sum_{k=0}^i (-1)^k q^k \right\|} < \varepsilon \quad (\text{sufficiently small}), \quad \text{with } \|q\| = \sqrt{q^t q}$$

The Neumann series converges if the absolute values of all the eigenvalues of the product $K^{0^{-1}} \Delta K$ are less than 1.

Monte Carlo simulation

Associated with the Cholesky decomposition of the stiffness matrix K , the Neumann expansion is an economic means of building large samples from which we can thereafter extract a statistic.

Statistical moments

First order [SD88]:

$$\begin{aligned} q &\approx (I - P)q^0 \\ E[q] &\approx q^0 \\ \text{cov}[q, q] &\approx E[P q^0 q^{0^t} P^t] \end{aligned}$$

12.6 Polynomial chaos expansion

Section 4.8 introduced a first application of the Hermite polynomials. The works of Ghanem and Spanos, which are presented in Section 12.7.2, show the entire advantage of Hermite multidimensional polynomials in relation to the spectral decomposition of the random field. More recently, it has been proposed to use the polynomial chaos directly on the discretized expression (12.1). This application presupposes first of all an expansion of the random variables entering into the stiffness matrix or the vector of external actions and building after the assembly of the random variables.

12.6.1 Random variable expansion

Let us consider a random variable X with finite variance. It can be decomposed on the basis of the Hermite polynomials [Mal97] of the random variable ξ ,

$\mathcal{N}(0, 1)$:

$$X(\xi) = \sum_{i=0}^{\infty} a_i H_i(\xi) \quad (12.21)$$

If $F_X(x)$ is the distribution function of this variable, the isoprobabilistic transformation is written as:

$$F_X(x) = \Phi(\xi) \implies x = F_X^{-1}(\Phi(\xi))$$

Two methods are used to calculate the coefficients.

Projection method [PPS02]

By multiplying the two terms of (12.21) and then by taking the expectation, we obtain, in view of the orthogonality:

$$\mathbb{E}[X H_i(\xi)] = a_i \mathbb{E}[H_i(\xi)^2] = a_i i! \implies a_i = \frac{1}{i!} \mathbb{E}[X(\xi) H_i(\xi)]$$

and by introducing the isoprobabilistic transformation:

$$a_i = \frac{1}{i!} \int_{\mathbb{R}} F_X^{-1}(\Phi(t)) H_i(t) \phi(t) dt$$

For Gaussian or lognormal variables, integration is possible:

$$\begin{aligned} X \equiv \mathcal{N}(m, \sigma^2) &\implies a_0 = m \quad a_1 = \sigma \quad a_i = 0 \quad \text{for } i \geq 2 \\ X \equiv \mathcal{LN}(\lambda, \zeta^2) &\implies a_i = \frac{\zeta^i}{i!} \exp\left(\lambda + \frac{1}{2}\zeta^2\right) \quad \text{for } i \geq 0 \end{aligned}$$

If this is not the case, we must perform a numerical integration [SBL03].

Collocation method [Isu99]

Instead of searching for the successive terms of the expansion, we choose to limit (12.21) to order p :

$$\tilde{X}(\xi) = \sum_{i=0}^p a_i H_i(\xi)$$

Coefficients a_i are then determined as being the best approximation in the least squares sense for a given set of experiments $\{\xi^{(1)}, \dots, \xi^{(n)}\} \implies \{x^{(1)}, \dots, x^{(n)}\}$. The deviation to be minimized is:

$$\Delta X = \sum_{j=1}^n (x^{(j)} - \tilde{x}^{(j)})^2 = \sum_{j=1}^n \left(x^{(j)} - \sum_{i=0}^p a_i H_i(\xi) \right)^2$$

that is:

$$\sum_{l=0}^p \left(\sum_{j=1}^n H_k(\xi^{(j)}) H_l(\xi^{(j)}) \right) a_l = \sum_{j=1}^n H_k(\xi^{(j)}) \quad k, l = 0, \dots, p$$

The choice of collocation points can either be made using random strategy such as Monte Carlo or from a deterministic strategy, for example, by a uniform distribution in space.

The projection method aims to find the exact coefficients a_i , whereas the collocation method seeks the best compromise at a given level of truncation. Apart from analytical cases, both methods require numerical approximations, either because of numerical integration or because of the choice of collocation points, and a verification of convergence is necessary.

12.6.2 Application to the finite element method

Assemblage of random variables

The principle [SBL04] consists of assembling the random variables, each represented by an expansion on the basis of one-dimensional Hermite polynomials, on the basis of a polynomial chaos. A simple allocation procedure is sufficient, and the projection of a random variable vector² is written finally in the simplified form:

$$X(\omega) = \sum_{i=0}^{\infty} \tilde{a}_i \Psi_i(\omega)$$

and after truncation of order p :

$$X(\omega) = \sum_{i=0}^{J-1} \tilde{a}_i \Psi_i(\omega) \quad \text{with } J = \sum_{k=0}^p \binom{m+k-1}{k}$$

Let us consider, for example, variables X_1 and X_2 developed to the second order, $J = 6$. From Tables 12.2 and 12.3:

$$X_1 \approx a_{01} \Psi_0 + a_{11} \Psi_1 + a_{21} \Psi_2 = a_{01} 1 + a_{11} \xi_1 + a_{21} (\xi_1^2 - 1)$$

$$X_2 \approx a_{02} \Psi_0 + a_{12} \Psi_1 + a_{22} \Psi_2 = a_{02} 1 + a_{12} \xi_2 + a_{22} (\xi_2^2 - 1)$$

$$\begin{bmatrix} X_1 \\ X_2 \end{bmatrix} \approx \begin{bmatrix} a_{01} & a_{11} & 0 & a_{21} & 0 & 0 \\ a_{02} & 0 & a_{12} & 0 & 0 & a_{22} \end{bmatrix} \begin{bmatrix} 1 \\ \xi_1 \\ \xi_2 \\ \xi_1^2 - 1 \\ \xi_1 \xi_2 \\ \xi_2^2 - 1 \end{bmatrix}$$

² The indexes of the vectors and the matrices are omitted: $X \equiv X_j$ or $\{X\}$ and $K \equiv K_{ij}$ or $[K]$.

$$X_j = \sum_{i=0}^{\infty} a_{ij} H_i(\xi_j) \implies X_j = \sum_{i=0}^{\infty} \tilde{a}_{ij} \Psi_i[\xi_r(\omega)] \quad r = 1, \dots, m$$

Projection of the stiffness matrix and the external action vector

Similarly, the stiffness matrix and the action vector are decomposed in the same polynomial chaos:

$$K(\omega) = \sum_{j=0}^{\infty} K_j \Psi_j(\omega) \quad F(\omega) = \sum_{j=0}^{\infty} F_j \Psi_j(\omega)$$

where K_j is the matrix:

$$K_j = \frac{\mathbb{E}[K(\omega) \Psi_j(\omega)]}{\mathbb{E}[\Psi_j(\omega)^2]} = \bigcup_{\text{elements}} \frac{\int_{V_e} B^t \mathbb{E}[H(\omega) \Psi_j(\omega)] B \, dV}{\mathbb{E}[\Psi_j(\omega)^2]}$$

in which the random event is contained only in the Hooke matrix H . To go further, we must characterize the stochastic models of H and F , see [SBL04].

Solution

The displacement response is also expanded on the same basis:

$$q(\omega) = \sum_{j=0}^{\infty} q_j \Psi_j(\omega) \quad (12.22)$$

in which parameters q_j , equal in number to the product of the dimension of the stiffness matrix $ndof$ and the number of terms J of the truncation, are the unknowns of the problem. Equation (12.1) is written as:

$$\left(\sum_{i=0}^{\infty} K_i \Psi_i(\omega) \right) \left(\sum_{j=0}^{\infty} q_j \Psi_j(\omega) \right) = \sum_{j=0}^{\infty} F_j \Psi_j(\omega)$$

After truncation of order J , there is a residue:

$$\varepsilon_J = \left(\sum_{i=0}^{J-1} K_i \Psi_i(\omega) \right) \left(\sum_{j=0}^{J-1} q_j \Psi_j(\omega) \right) - \sum_{j=0}^{J-1} F_j \Psi_j(\omega)$$

whose minimization is obtained by imposing that it be orthogonal to the subspace engendered by vectors $\Psi_j(\omega)$, $j = 0, \dots, J-1$ [GS91]:

$$\mathbb{E}[\varepsilon_J \Psi_k(\omega)] = 0$$

We obtain the following linear system, with $M = J - 1$:

$$\begin{bmatrix} [\mathcal{K}_{00}] & [\mathcal{K}_{0k}] & [\mathcal{K}_{0M}] \\ [\mathcal{K}_{j0}] & [\mathcal{K}_{jk}] & [\mathcal{K}_{jM}] \\ [\mathcal{K}_{M0}] & [\mathcal{K}_{Mk}] & [\mathcal{K}_{MM}] \end{bmatrix}_{(J)\cdot(ndof) \times (J)\cdot(ndof)} \begin{Bmatrix} \{q_0\} \\ \vdots \\ \{q_k\} \\ \vdots \\ \{q_M\} \end{Bmatrix}_{(J)\cdot(ndof)} = \begin{Bmatrix} \{\mathcal{F}_0\} \\ \vdots \\ \{\mathcal{F}_k\} \\ \vdots \\ \{\mathcal{F}_M\} \end{Bmatrix}_{(J)\cdot(ndof)} \quad (12.23)$$

whose elements are given by:

$$\begin{aligned} \{\mathcal{F}_k\} &= F_k \text{ E}[\Psi_j(\omega) \Psi_k(\omega)] \\ [\mathcal{K}_{jk}] &= \sum_{i=0}^{J-1} K_i \text{ E}[\Psi_i(\omega) \Psi_j(\omega) \Psi_k(\omega)] \end{aligned}$$

The expectations of the products are obtained without numerical integration based on formulae [SDK00, SDK02].

Post-processing

After solving, the mean and standard deviation of the mechanical response are obtained immediately, thanks to the properties of the polynomial chaos:

$$\begin{aligned} \text{E}[q] &= q_0 \\ \text{cov}[q, q] &= \sum_{i=1}^{J-1} \text{E}[\Psi_i(\omega) \Psi_i(\omega)] q q^t \end{aligned}$$

The expansion of the response also enables us to build its density with an accuracy that depends on the order of the truncation, and to use this density in a reliability analysis [SBL04].

Illustration

The example discussed in Section 12.5.3 is taken up again, without detailing all the calculations. The variables are lognormal. The expansion of two random variables is given from analytical equations:

$$a_{iE} = \frac{\xi_E^i \exp(\lambda_E + (\xi_E^2/2))}{i!} \quad a_{iP} = \frac{\xi_P^i \exp(\lambda_P + (\xi_P^2/2))}{i!}$$

For a chaos of order $p = 4$, $m = 2$, we obtain $J = 15$:

$$\begin{bmatrix} E \\ P \end{bmatrix} = \begin{bmatrix} a_{0E} & a_{1E} & 0 & \dots & a_{4E} & 0 & 0 & 0 & 0 \\ a_{0P} & 0 & a_{1P} & \dots & 0 & 0 & 0 & 0 & a_{4P} \end{bmatrix} \Psi_i[\xi_r(\omega)]_{r=1}^{r=2}$$

Equation (12.1) is written simply:

$$\frac{E(\omega)}{k} f(\omega) = P(\omega)$$

The second member of system (12.23), with dimension $J \times 1 = 15$, is given by:

$$\{\mathcal{F}_k\} = \tilde{a}_{kP} E[\Psi_k \Psi_k]$$

where $\{\mathcal{F}_k\}$ is a one-dimensional vector. The matrix of the equation system is given by the elements of dimension 1×1 :

$$[\mathcal{K}_{jk}] = \sum_{i=0}^{J-1} \frac{\tilde{a}_{iE}}{k} E[\Psi_i(\omega) \Psi_j(\omega) \Psi_k(\omega)]$$

The solution gives the expansion of the deflection:

$$q = \langle 0.0505 - 5.037 \times 10^{-3} 7.533 \times 10^{-3} 2.512 \times 10^{-4} - 7.514 \times 10^{-4} \dots \rangle \quad (12.24)$$

from which the calculation of the mean gives 0.050500 and the calculation of the standard deviation gives 0.0091355. These are the exact figures at the given accuracy. With the choice of an admissible deflection threshold, chosen at $f_{\text{adm}} = 0.1$, a reliability calculation is performed.

Table 12.6 gives the results obtained for the first four orders p . If the results are very satisfactory for an estimation of the first moments, we must note the much slower convergence in the reliability index, for a level of β of the order of that which is often sought. If the method seems attractive, we must keep in mind the extent of the calculations. The number of unknowns is equal to the number of degrees of freedom multiplied by dimension J of the chaos (Equation (12.7)).

	$p = 1, J = 3$	$p = 2, J = 6$	$p = 3, J = 10$	$p = 4, J = 15$
$E[\hat{f}_p]$	0.050500	0.050500	0.050500	0.050500
$\sigma_{\hat{f}_p}$	0.0090003	0.0091323	0.0091355	0.0091355
β_p	5.500	4.077	3.919	3.910
Exact	$E[f] = 0.050500$		$\sigma_f = 0.0091355$	$\beta = 3.897$

Table 12.6 Means and standard deviations obtained for various powers of the chaos.

12.6.3 Perspectives

New methods are being developed to avoid having to solve the large system (12.23) and to take into account non-linear mechanical models. Another important challenge is to use the current finite codes as such; the method is then called *non-intrusive* [FJRHP00, GG02]. This is based on the direct use of Equation (12.22). By multiplying term-by-term and taking into account the orthogonality of the chaos, we obtain:

$$\mathbb{E}[\Psi_k(\omega) q(\omega)] = \mathbb{E} \left[\sum_{j=0}^{\infty} q_j \Psi_j(\omega) \Psi_k(\omega) \right] \implies q_j = \frac{\mathbb{E}[\Psi_j(\omega) q(\omega)]}{\mathbb{E}[\Psi_j(\omega)^2]} \quad j=0, \dots, J-1$$

an expression in which the denominator results from a simple calculation [SDK00] and the numerator is written by integrating with respect to variables $\mathcal{N}(0, 1)$:

$$\mathbb{E}[\Psi_j(\omega) q(\omega)] = \int_{\mathbb{R}^m} q(\xi) \Psi_j(\xi) \phi_m(\xi) d\xi_1 \dots d\xi_m$$

This integration can be done by simulation or quadrature. It is enough to know how to calculate $q(\xi)$ at the points considered by numerical solution under any assumption whatsoever. For a linear problem:

$$q_j = \frac{\int_{\mathbb{R}^m} K(\xi)^{-1} F(\xi) \Psi_j(\xi) \phi_m(\xi) d\xi_1 \dots d\xi_m}{\mathbb{E}[\Psi_j(\xi)^2]}$$

Illustration – let us return to the example of the deflection of a beam:

$$q_j = \frac{\int_{\mathbb{R}^2} (k P(\omega)/E(\omega)) \Psi_j(\xi_1, \xi_2) \phi_2(\xi_1, \xi_2) d\xi_1 d\xi_2}{\mathbb{E}[\Psi_j(\xi_1, \xi_2)^2]}$$

by introducing the isoprobabilistic transformation of the lognormal distribution:

$$q_j = \frac{\int_{\mathbb{R}^2} k(\exp(\zeta_P \xi_2 + \lambda_P)/\exp(\zeta_E \xi_1 + \lambda_E)) \Psi_j(\xi_1, \xi_2) \phi_2(\xi_1, \xi_2) d\xi_1 d\xi_2}{\mathbb{E}[\Psi_j(\xi_1, \xi_2)^2]}$$

and the numerical integration arrives at results (12.24). If integration seems attractive for such a simple example, we must not forget that each requires a mechanical calculation at each integration point, to be repeated for the J coefficients.

12.6.4 Conclusion

Expansion on polynomial chaos offers the possibility of searching for the statistical moments of a high-order response. The theory reminds us that the knowledge of all the moments is equivalent to the knowledge of the density. The inevitable truncations allow only an approximation, for which the error is all the more sensitive as it is used for the purpose of reliability for high indexes. A certain apparent simplicity of the formulation must not cause us to forget the considerable amount of numerical calculation that it engenders.

12.7 Continuous random field methods

The methods proposed in the previous sections apply directly to discretized FEM modeling. Those that are described below intervene as early as the formulation of the problem, upstream of the discretization.

12.7.1 Weighted integral method

Stochastic stiffness matrix

The method of weighted integrals was introduced by Takada [Tak90b,Tak90a] and Deodatis [Deo91, DS91]. There is no longer direct discretization of the random field, whose influence is integrated on each element of the deterministic discretization. The random field $V(x, \omega)$ is first decomposed into a deterministic mean part $m_V(x)$ and a random fluctuation in the form:

$$V(x, \omega) = m_V(x)(1 + \alpha(x, \omega))$$

where $\alpha(x, \omega)$ is a field with zero mean and autocovariance $\Sigma_\alpha(x_1, x_2)$. The elementary stiffness matrix (12.9) is then decomposed into a deterministic part and a random part. As an illustration, let us consider the Young's modulus as a random field. We obtain:

$$H = m_E(x)(1 + \alpha(x, \omega)) H_{E=1}$$

where $H_{E=1}$ is the elasticity matrix for $E = 1$:

$$\begin{aligned} K_e &= \int_{V_e} B^t H B dV \\ &= \int_{V_e} m_E(x) B^t H_{E=1} B dV + \int_{V_e} m_E(x) \alpha(x, \omega) B^t H_{E=1} B dV \\ K_e &= K_e^0 + \Delta K_e(\omega) \quad (\text{deterministic part at mean + random part}) \end{aligned}$$

$\Delta K_e(\omega)$ is the elementary stochastic stiffness matrix.

Decomposition of $K_e(\omega)$

The quantity under the integral sign is a function of space variable x by the random field and also by matrix B . Matrix B is decomposed into a sum of p terms as a function of the powers of x , that is:

$$B^t H_{E=1} B = \sum_{i=0}^p \Delta K_{e_i} x^i \quad (x^i = x_1^r x_2^s x_3^t \text{ in 3 dimensions})$$

and we obtain:

$$\Delta K_e(\omega) = \sum_{i=0}^p \left(\int_{V_e} x^i m_E(x) \alpha(x, \omega) dV \right) \Delta K_{e_i}$$

where the integral on the volume is the weighted integral $X_e(\omega)_i$ relative to power i and matrix ΔK_{e_i} . Finally:

$$K_e(\omega) = K_e^0 + \sum_{i=0}^p X_e(\omega)_i \Delta K_{e_i}$$

which forms the elementary stochastic stiffness matrix. For nel elements, the assembly gives:

$$K(\omega) = \sum_{e=1}^{nel} \left(K_e^0 + \sum_{i=0}^p X_e(\omega)_i \Delta K_{e_i} \right) \quad (12.25)$$

The number of weighted integrals is equal, for each element, to $n + 1$ ((degree of the product $B^t B$) + 1), for each coordinate x . For a lineic bar element under tension-compression, the number of degrees of freedom is 1 and the power of $B^t B$ is $p = 0$. There is consequently only one weighted integral. For a beam element, the normal force part ($B = \text{constant}$) gives one integral (i.e. the bar) and the bending part (B of degree 1) gives two integrals.

Statistical moments

These can be obtained by expanding the displacement vector q to the first order, around the means, with respect to the weighted integrals:

$$q \approx q^0 + \sum_{e=1}^{nel} \sum_{i=0}^p \frac{\partial q}{\partial X_e(\omega)_i} (X_e(\omega)_i - E[X_e(\omega)_i])$$

The partial derivative of q is deduced from $K q = F$; if F does not depend on the random event:

$$K \frac{\partial q}{\partial X_e(\omega)_i} + \frac{\partial K}{\partial X_e(\omega)_i} q = 0$$

$$\frac{\partial q}{\partial X_e(\omega)_i} = -K^{0-1} \frac{\partial K}{\partial X_e(\omega)_i} q^0$$

and:

$$q \approx q_0 - \sum_{e=1}^{nel} \sum_{i=0}^p K^{0-1} \frac{\partial K}{\partial X_e(\omega)_i} q^0 (X_e(\omega)_i - E[X_e(\omega)_i])$$

With the first order:

$$E[q] \approx q^0$$

$$\text{cov}[q, q] \approx \sum_{e_1=1}^{nel} \sum_{e_2=1}^{nel} \sum_{i=0}^p \sum_{j=0}^p K^{0-1} \frac{\partial K}{\partial X_{e_1}(\omega)_i} q^0 q^{0t} \frac{\partial K^t}{\partial X_{e_2}(\omega)_j} K^{0-1t}$$

$$E[(X_{e_1}(\omega)_i - E[X_{e_1}(\omega)_i])(X_{e_2}(\omega)_j - E[X_{e_2}(\omega)_j])]$$

and using (12.25):

$$\text{cov}[q, q] \approx \sum_{e_1=1}^{nel} \sum_{e_2=1}^{nel} \sum_{i=0}^p \sum_{j=0}^p K^{0-1} \Delta K_{e_1 i} q^0 q^{0t} \Delta K_{e_2 j}^t K^{0-1t}$$

$$E[(X_{e_1}(\omega)_i - E[X_{e_1}(\omega)_i])(X_{e_2}(\omega)_j - E[X_{e_2}(\omega)_j])]$$

From the Neumann expansion (see Section 12.5.4), means and covariance can be obtained by simulation.

Conclusion

If this method appears attractive, since it does away with stochastic discretization, stochastic discretization in fact underlies deterministic discretization. The calculation of only first-order statistical moments is also a limitation. Lastly, it would be tricky to extend it to the combination of several random fields.

12.7.2 Spectral method

The weighted integral method projects the random field to the deterministic FEM discretization basis. Other expansion bases are possible, particularly those discussed in Section 12.3.

Structural behavior model

Formally, a displacement model (variable $q(x, \omega)$) of structural behavior is written:

$$\begin{aligned}(L(x) + \Pi(\alpha(x, \omega))) q &= f(x, \omega) \text{ in } V \\ \Sigma(x, \omega) q &= 0 \text{ on } S\end{aligned}$$

where L is an operator function of position x (deterministic part of the stiffness), Π is an operator applied to the random field $\alpha(x, \omega)$ (random part of the stiffness, internal random event, with zero mean) and $f(x, \omega)$ and $\Sigma(x, \omega)$ are random fields respectively expressing the loading conditions on the volume V and the displacement conditions on the lateral surface S (external random event).

For the sake of simplification, this formulation is not used with all its possible generality and we will introduce the following two assumptions:

- the boundary conditions are deterministic,
- the internal random event depends on only one field.

This gives the simplified formulation:

$$\begin{aligned}(L(x) + \alpha(x, \omega) R(x)) q &= f(x, \omega) \text{ in } V \\ \Sigma(x) q &= 0 \text{ on } S\end{aligned}$$

where $R(x)$ is an operator of the unique variable x . By choosing a basis of m kinematically admissible test functions $g_i(x)$ to decompose q and by integrating for any $\delta g_j(x)$ function, we obtain the variational form:

$$\begin{aligned}\sum_i^m \int_V \delta g_j(x) (L(x) + \alpha(x, \omega) R(x)) g_i(x) q_i \, dV &= \int_V \delta g_j(x) f(x, \omega) \, dV \\ \sum_i^m \left(\int_V \delta g_j(x) L(x) g_i(x) \, dV + \int_V \delta g_j(x) \alpha(x, \omega) R(x) g_i(x) \, dV \right) q_i &\\ = \int_V \delta g_j(x) f(x, \omega) \, dV &\quad (12.26)\end{aligned}$$

in which the part independent of ω yields the usual deterministic stiffness matrix:

$$\int_V \delta g_j(x) L(x) g_i(x) \, dV = K_{ij}^0$$

Application of the Karhunen-Loève expansion

The integrals of expression (12.26) give the various terms of a stochastic stiffness matrix. The random field in the second integral is decomposed according to

(12.4), the mean being zero:

$$\sum_{k=1}^n \zeta_k(\omega) \int_V \delta g_j(x) \sqrt{\lambda_k} \phi_k(x) R(x) g_i(x) dV = \sum_{k=1}^n \zeta_k(\omega) \Delta K_{ijk} \quad (12.27)$$

$$\int_V \delta g_j(x) f(x, \omega) dV = F_j(\omega)$$

and, after assembly:

$$\left(K^0 + \sum_{k=1}^n \zeta_k(\omega) \Delta K_k \right) q(\omega) = F(\omega) \quad (12.28)$$

whose matrix representation is:

$$\left([K^0] + \sum_{k=1}^n \zeta_k(\omega) [\Delta K_k] \right) \{q(\omega)\} = \{F(\omega)\}$$

The notations used previously have been retained; however, matrices K^0 , ΔK and vector F now depend on the choice of the functions used. By application of the Neumann expansion (12.20):

$$q(\omega) = \sum_{i=0}^{\infty} (-1)^i \left(\sum_{k=1}^n \zeta_k(\omega) K^{0^{-1}} \Delta K_k \right)^i K^{0^{-1}} F(\omega)$$

Ghanem and Spanos [GS91] then give the first two statistical moments of q ; however, it is more interesting to introduce the polynomial chaos because of its orthogonality properties.

Polynomial chaos

The random part of the displacement (with zero mean) is given by the Karhunen-Loëve expansion (12.4):

$$q(x, \omega) = \sum_{j=1}^n \sqrt{\lambda_j} \zeta_j(\omega) \phi_j(x)$$

in which the random functions $\zeta_j(\omega)$ form a set of standardized centered random variables. Ghanem and Spanos [GS91] propose to use the polynomial chaos (12.6):

$$\begin{aligned} \zeta_j(\omega) &= \sum_{i=0}^{J-1} \tilde{a}_i \Psi_i[\xi_r(\omega)]|_j = \sum_{i=0}^{J-1} \tilde{a}_{ij} \Psi_i(\omega) \\ &= \sum_{i=0}^{J-1} \tilde{a}_{ij} \Psi_i(\omega) \end{aligned}$$

where J is the total number of terms in the expansion, a function of the chaos order and its dimension. We obtain:

$$q(x, \omega) = \sum_{j=1}^n \sum_{i=0}^{J-1} \sqrt{\lambda_j} \tilde{a}_{ij} \Psi_i(\omega) \phi_j(x)$$

Let us assume:

$$\begin{aligned} \sqrt{\lambda_j} \phi_j(x) &= c_j(x) \\ \sum_{j=1}^n \tilde{a}_{ij} c_j(x) &= d_i(x) \\ q(x, \omega) &= \sum_{i=0}^{J-1} d_i(x) \Psi_i(\omega) \end{aligned}$$

and let us discretize the displacement ($x = x_l$) to obtain component l of the displacement vector q :

$$q_l(\omega) = \sum_{i=0}^{J-1} d_{li} \Psi_i(\omega) \quad l = 1, \dots, ndof \text{ (degree of freedom number)}$$

and finally, for the nodal displacement vector:

$$q(\omega) = \sum_{i=0}^{J-1} d_i \Psi_i(\omega) \iff \{q(\omega)\} = \sum_{i=0}^{J-1} \Psi_i(\omega) \{d_i\} \quad (12.29)$$

where d_i is now a vector with the same dimension as q .

The unknowns of the problem are the J vectors d_i . They are obtained by a procedure identical to the one in Section 12.6.2. Let us multiply (12.28) by $K^{0^{-1}}$ and introduce the expression $q(\omega)$:

$$\sum_{i=0}^{J-1} \left(I + \sum_{k=1}^n \zeta_k(\omega) K^{0^{-1}} \Delta K_k \right) d_i \Psi_i(\omega) = K^{0^{-1}} F(\omega)$$

By multiplying this equation by $\Psi_j(\omega)$, $j = 0, \dots, J - 1$, a least squares approximation gives the solutions d_i after introducing the boundary conditions:

$$\left(\sum_{k=0}^n \sum_{i=0}^{J-1} E[\zeta_k(\omega) \Psi_i(\omega) \Psi_j(\omega)] K^{0^{-1}} \Delta K_k \right) d_i = E[\Psi_j(\omega) K^{0^{-1}} F(\omega)] \quad (12.30)$$

where, for $k = 0$, $\zeta_0 = 1$ and $K^{0^{-1}} \Delta K_0 = I$. The random nodal field is given by (12.29):

$$q(\omega) = \sum_{i=0}^{J-1} d_i \Psi_i(\omega) \iff \{q(\omega)\} = \sum_{i=0}^{J-1} \Psi_i(\omega) \{d_i\}$$

This expression is particularly useful for the calculation of the first two statistical moments. In fact $E[\Psi_i(\omega)] = 0$ – except for zero order, where $E[\Psi_0(\omega)] = 1$ – and $E[\Psi_i(\omega) \Psi_j(\omega)] = \delta_{ij} E[\Psi_i(\omega) \Psi_i(\omega)]$. We obtain:

$$\begin{aligned} E[q(\omega)] &= d_0 \\ \text{cov}[q, q] &= \sum_{i=1}^{J-1} E[\Psi_i(\omega) \Psi_i(\omega)] d_i d_i^t \end{aligned}$$

Calculation of the terms of Equation (12.30)

The equation obtained constitutes a matrix equation system. By identifying the matrix or vector character of each term, (12.30) is written as:

$$[[\mathcal{K}_{j0}] \quad \cdots \quad [\mathcal{K}_{ji}] \quad \cdots \quad [\mathcal{K}_{j(J-1)}]] \begin{Bmatrix} \{d_0\} \\ \vdots \\ \{d_i\} \\ \vdots \\ \{d_{J-1}\} \end{Bmatrix} = \begin{Bmatrix} \{\mathcal{F}_0\} \\ \vdots \\ \{\mathcal{F}_j\} \\ \vdots \\ \{\mathcal{F}_{J-1}\} \end{Bmatrix}$$

where, by denoting by $ndof$ the dimension of the stiffness matrix:

$$\begin{aligned} [\mathcal{K}_{ji}] &= \sum_{k=0}^n E[\zeta_k(\omega) \Psi_i(\omega) \Psi_j(\omega)] [K^0]^{-1} [\Delta K]_k \quad \text{dimension } ndof \times ndof \\ \{\mathcal{F}_j\} &= E[\Psi_j(\omega) [K^0]^{-1} F(\omega)] \quad \text{dimension } ndof \end{aligned}$$

The linear system to be solved is then, with $M = J - 1$:

$$\begin{bmatrix} [\mathcal{K}_{00}] & [\mathcal{K}_{0i}] & [\mathcal{K}_{0M}] \\ [\mathcal{K}_{j0}] & [\mathcal{K}_{ji}] & [\mathcal{K}_{jM}] \\ [\mathcal{K}_{M0}] & [\mathcal{K}_{Mi}] & [\mathcal{K}_{MM}] \end{bmatrix}_{(J) \cdot (ndof) \times (J) \cdot (ndof)} \begin{Bmatrix} \{d_0\} \\ \vdots \\ \{d_i\} \\ \vdots \\ \{d_M\} \end{Bmatrix}_{(J) \cdot (ndof)} = \begin{Bmatrix} \{\mathcal{F}_0\} \\ \vdots \\ \{\mathcal{F}_j\} \\ \vdots \\ \{\mathcal{F}_M\} \end{Bmatrix}_{(J) \cdot (ndof)}$$

The dimension of the equation system is therefore equal to the number of degrees of freedom of the discretized structure $ndof$ multiplied by the number of polynomials J . The calculation of matrices $[\mathcal{K}_{ji}]$ includes the calculation of matrices $[\Delta K]_k$ derived from (12.27):

$$[\Delta K]_k = \int_V \{\delta g(x)\} \sqrt{\lambda_k} \phi_k(x) R(x) \{g(x)\}^t dV$$

and the expectation $E[\zeta_k(\omega)\Psi_i(\omega)\Psi_j(\omega)] = c_{kij}$. Functions $\zeta_k(\omega)$ are chosen as being Gaussian, $\zeta_k(\omega) = \xi_k(\omega)$; [GS91] gives the calculation method and some results including those indicated in Table 12.7.

k	i	j	c_{kij}	k	i	j	c_{kij}	k	i	j	c_{kij}
1	0	1	1	1	0	1	1	2	0	2	1
	1	2	2		1	3	2		1	4	1
	2	3	6		2	4	1		2	5	2
	3	4	24		3	6	6		3	7	2
					4	7	2		4	8	2

Table 12.7 Non-zero coefficients c_{kij} for one- and two-dimensional polynomials.

12.7.3 Conclusion

Regardless of whether the calculation is by a perturbation method or by a series expansion, it results in the construction of a stiffness matrix in the form of a term independent of random events, in general the stiffness with mean K^0 and with a stochastic stiffness matrix $\Delta K(\alpha)$ combining all the matrices which are a function of the random event; this stochastic stiffness matrix is necessarily truncated.

The expansion of $\Delta K(\alpha)$ to the first order, or even the second order, gives directly usable expressions for the estimation of the mean and the covariance of the responses of the finite element model. It is also possible to use the Monte Carlo simulation, which then applies to expressions that no longer call for the mechanical model. The advantage of polynomial chaos lies in its orthogonality properties.

The construction of efficient stochastic finite elements is still under research and it is certain that the tool of tomorrow will not draw solely from the ideas presented here.

12.8 An illustration

We will take up here the example of the rod under tension already discussed in Chapter 3. The numerical data are however different. A few methods proposed in this chapter are applied. This example, as well as other applications, is described by Scheffer [Sch97].

12.8.1 Statement of the problem

A rod (Figure 12.4) of length L is fixed at one of its ends and subjected to an axial force P on the other end. This rod, with cross-section A , is made up of material with Young's modulus E .

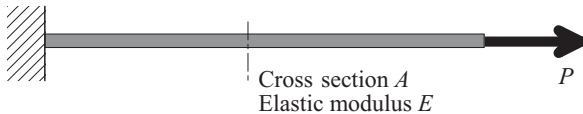


Figure 12.4 Rod under tension.

The numerical data used are presented in Table 12.8. The problem here is a simple formulation, as only one bar element is necessary for the finite element model. The stiffness matrix of the system is reduced to $K^0 = E^0 A^0 / L^0$; the deterministic displacement at the end is then $q^0 = P^0 L^0 / E^0 A^0$, corresponding to the numerical value $q^0 = 0.121$ mm.

Parameter	Mean	Standard deviation	c.o.v. %
Young's modulus	$E^0=210,000$ MPa	15,000 MPa	7.1
Cross-section	$A^0=314$ mm ²	20 mm ²	6.4
Length	$L^0=1,000$ mm	200 mm	20.0
Applied force	$P^0=8,000$ N	400 N	5.0

Table 12.8 Numerical values used for the example of the rod under tension.

12.8.2 Case 1: 4 random variables

The variables E , A , L and P are random variables. The solution is obtained by the perturbation method, Neumann expansion and Monte Carlo simulation.

Perturbation method

This example, already studied by various authors including [KH92], offers the advantage of having simple formulations for the mean and standard deviation of response q when we use the perturbation method. We have several options for choosing the random parameters. In the most general case, the mean and the variance of q are expressed by (12.18) and (12.19):

$$\begin{aligned} E^{II}[q] &= q^0 + \frac{P^0 L^0}{E^{0^3} A^0} \text{cov}[E, E] + \frac{P^0 L^0}{E^{0^2} A^{0^2}} \text{cov}[E, A] - \frac{P^0}{E^{0^2} A^0} \text{cov}[E, L] \\ &\quad - \frac{L^0}{E^{0^2} A^0} \text{cov}[E, P] + \frac{P^0 L^0}{E^0 A^{0^3}} \text{cov}[A, A] - \frac{P^0}{E^0 A^{0^2}} \text{cov}[A, L] \\ &\quad - \frac{L^0}{E^0 A^{0^2}} \text{cov}[A, P] + \frac{1}{E^0 A^0} \text{cov}[L, P] \end{aligned}$$

$$\begin{aligned}
\text{var}^I[q] = & \frac{P^0 L^0}{E^0 A^0} \text{cov}[E, E] \\
& + 2 \frac{P^0 L^0}{E^0 A^0} \text{cov}[E, A] - 2 \frac{P^0 L^0}{E^0 A^0} \text{cov}[E, L] - 2 \frac{P^0 L^0}{E^0 A^0} \text{cov}[E, P] \\
& + \frac{P^0 L^0}{E^0 A^0} \text{cov}[A, A] - 2 \frac{P^0 L^0}{E^0 A^0} \text{cov}[A, L] - 2 \frac{P^0 L^0}{E^0 A^0} \text{cov}[A, P] \\
& + \frac{P^0 L^0}{E^0 A^0} \text{cov}[L, L] + 2 \frac{P^0 L^0}{E^0 A^0} \text{cov}[L, P] \\
& + \frac{L^0}{E^0 A^0} \text{cov}[P, P] + \text{second-order term}
\end{aligned}$$

The numerical application described in Table 12.9 gives the values obtained by the second-order perturbation method. The covariance matrix is chosen arbitrarily (it takes into account only a correlation coefficient of -0.4 between the cross-section and the length of the bar). The second line of results in the table shows that the effect of variable P is zero, given the standard deviation chosen here.

Variables	Covariance matrix				$E[q]$	$\text{cov}[q, q]$
E, A, L, P	$15,000^2$	0	0	0	0.123	0.030^2
	0	20^2	$-1,600$	0		
	0	$-1,600$	200^2	0		
	0	0	0	400^2		
E, A, L	$15,000^2$	0	0	0.123	0.030^2	
	0	20^2	$-1,600$			
	0	$-1,600$	200^2			

Table 12.9 Results obtained by the perturbation method (displacement in millimeters).

Neumann expansion

Based on the numerical values in Table 12.9 for the case of three variables (Gaussian) we observe, in Figure 12.5, convergence in mean and standard deviation for 2,000 simulations. The final values are $E[q] = 0.123$ and $\text{cov}[q, q] = 0.031^2$.

Monte Carlo simulation

The results obtained by a direct simulation are identical to those obtained by Neumann expansion, but they require greater calculation resources.

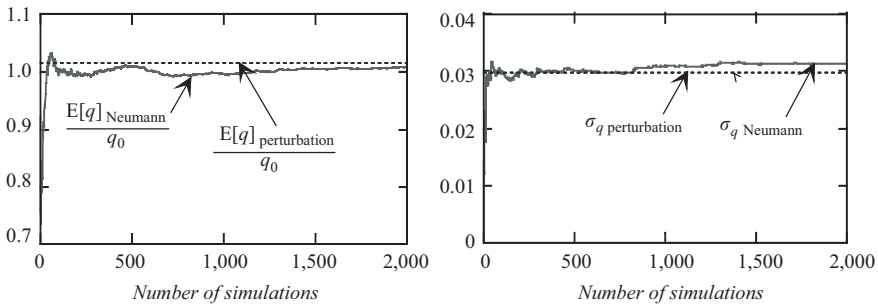


Figure 12.5 Mean and standard deviation calculated by simulation.

12.8.3 Case 2: stiffness EA is a random field

Statement of the problem

Let us now assume that the stiffness EA of the bar is a stochastic field $EA(x, \omega)$, characterized by its mean m_{EA} and its autocorrelation function of exponential form:

$$R(x_1, x_2) = \sigma_{EA}^2 e^{-c|x_1 - x_2|} \quad \text{for } x_1, x_2 \in [0; L] \quad c = \frac{1}{L_c} \quad (12.31)$$

The eigenvalues and eigenfunctions of the autocorrelation function are given by the solutions of (12.5), in the interval $[0, L_c]$:

$$\lambda_i = \frac{2c}{\omega_i^2 + c^2} \sigma_{EA}^2$$

$$\phi_i(x) = \frac{1}{\sqrt{L_c + \frac{1 - \cos 2\omega_i L_c}{2\omega_i}}} [\cos(\omega_i x) + \sin(\omega_i x)] \quad \text{for } x \in [0, L_c]$$

where the ω_i are solutions of $2\omega_i c + (c^2 - \omega_i^2) \tan(\omega_i L_c) = 0$ for $x \in [0, L_c]$.

Based on the numerical data in Table 12.10, the first four modes and eigenvalues obtained are represented in Figure 12.6. The objective is to calculate the statistical displacement parameters q .

Solution

The following methods are applied:

1. *Perturbation method:* the field is discretized using a single random variable, with mean m_{EA} and standard deviation σ_{EA} : spatial variability is therefore not taken into account.

Parameter	Mean	Standard deviation
Stiffness	6.594×10^7 N	6.594×10^6 N
Length	1,000 mm	—
Applied force	8,000 N	—
	Correlation length $L_c = L$	

Table 12.10 Numerical values used when the stiffness of the bar is a random field.

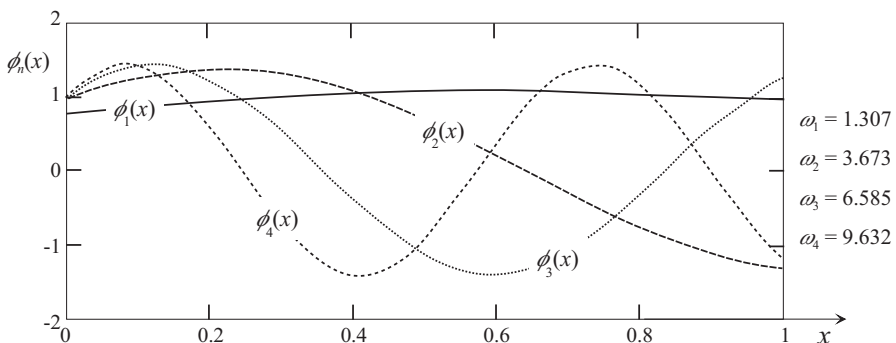


Figure 12.6 Eigenfunctions of the stiffness autocorrelation function EA.

2. *Direct Monte Carlo simulation*: here again, there is only one random variable, Gaussian, with mean m_{EA} and standard deviation σ_{EA} .
3. *Weighted integral method*.
4. *Karhunen-Loève method coupled with a Neumann expansion*: the mean of response q is calculated using three terms in the Neumann expansion, against only two for the standard deviation. The Karhunen-Loève expansion of the random field contains six terms.
5. *Polynomial chaos method*: the expansion basis of polynomial chaos is two-dimensional and we use the terms up to the second order. The Karhunen-Loève expansion of the random field contains six terms.

The results obtained are summarized in Table 12.11 and are represented in Figures 12.7 and 12.8, where we can observe the deviations between the methods with discretized parameters and the spectral methods, both in the mean of displacement q and in its standard deviation.

	Method	$m_q(10^{-4}\text{m})$	$\sigma_q(10^{-4}\text{m})$	c.o.v. (%)
1	Direct simulation	1.2254	0.12548	10.3
2	Perturbation	1.2254	0.12132	9.9
3	Weighted integrals	1.2133	0.12128	10.0
4	Karhunen-Loëve + Neumann	1.2530	0.21667	17.3
5	Polynomial chaos	1.2536	0.24251	19.3

Table 12.11 Results obtained by various methods for a random stiffness of the bar.

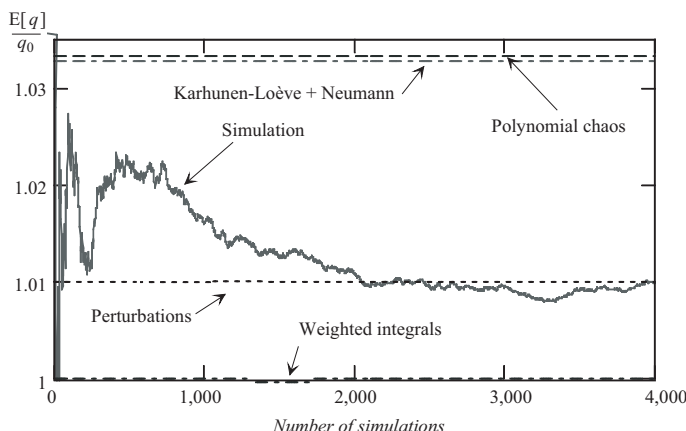


Figure 12.7 Mean of displacement q for a random field $EA(x, w)$, with respect to the deterministic displacement.

12.9 Conclusion

As the mechanical-reliability coupling introduces many possibilities, what can the advantage of stochastic finite elements be? It lies of course in the limitations of the coupling, which proves efficient as long as the number of random variables is limited and is therefore difficult to apply for the representation of random fields.

The *perturbation method* is limited and provides a response around a known position, in general the mean. It could be used sequentially, like response surfaces, of which it is a particular case. Must we prefer a numerical design of experiment to a Taylor expansion? It certainly remains the preferred means for sensitivity analysis around the mean or another known point.

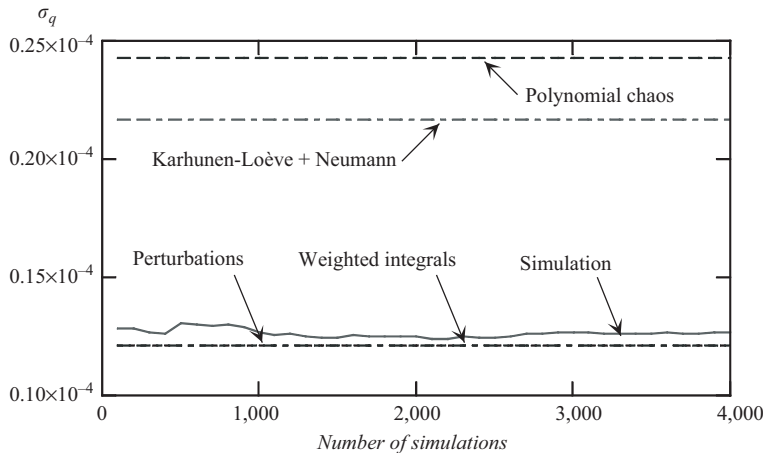


Figure 12.8 Standard deviation of displacement q for a random field $EA(x, w)$.

The *stochastic discretization methods* are efficient if they can be adapted according to the spatial variability of the random events, independent of the spatial variability of the strain that governs FEM discretization. From this point of view, the spectral methods have potential for the future, as they can show that the first modes capture the spatial variability of the random events. The approach is identical for the space-time problems solved by modal decomposition. These methods introduce a promising path recently open to non-linear problems.

12.9.1 Combination of the coupling and stochastic finite elements

Each of these approaches has advantages and drawbacks. The combination of the two is interesting if dissociation conditions enable us to identify the performance function as the combination of several functions capable of being studied separately.

If the load effect $S(X_{k+1}, \dots, X_n)$ results from a linear FEM calculation, the first two moments of S can be obtained by stochastic finite element methods, at the cost of a degradation of the information, since the distribution of S is not known, but with the considerable gain of a reduction of the size of the stochastic problem and a better representation of a random field in space. However, the information obtained then involves S^* , from which we must know how to come back to X_i^* .

12.9.2 Conclusion

The origins of finite element methods saw the progressive conquest of discretization and the widest possible behavioral assumptions. Thirty years later, methods coupling finite elements and reliability have opened up a new field of research and development, of which we have presented the main avenues.

This page intentionally left blank

Chapter 13

A Few Applications

It is not possible to conclude this book without giving the reader some ideas about the fields of application in which the proposed methods are used. The examples described are very limited, and they have been given with the sole aim of showing what the necessary assumptions and expected results are. The studies or articles available are cited as references.

The author wishes to thank all those, researchers in his team and industrial partners, who are the inspiration for these applications and who have supported their development.

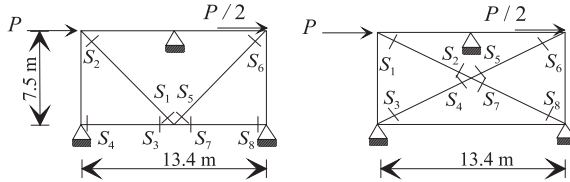
13.1 Design of a wind bracing

The problem, first posed by Elf-Aquitaine (today TOTAL), is that of the choice between a principle of wind bracing in **K**- or in **X**-form in the design of offshore structures (Figure 13.1). The criterion is reliability. Mechanical analysis first shows a difference in behavior: **X** is more ductile than **K** and a first failure is therefore *a priori* less hazardous. The failure is characterized by an incremental elastoplastic mechanical model. The first level is the failure of a cross-section. The second level is the failure of a second cross-section, following the failure of the first. The results give successive reliability indexes. **X** shows a better performance on the first failure ($\min \beta = 4.1$), whereas **K** is more efficient on the second ($\min \beta = 4.6$)! This result perhaps explains why both these solutions coexist.

The reliability calculation here illustrates the application of a model linearized by parts and a *branch and bound* approach. At level 1, failure occurs when the limit-state function is reached in any cross-section: the mechanical model is then constructed with the initial properties of the cross-sections. At level 2, failure occurs when the limit-state function is reached in a second cross-section, knowing that the first is in plasticity. As a result, the mechanical model is modified. The number of branches increases very rapidly, but a large number of them quickly lose their significance because of the high values of the indexes

Objective: compare reliability of two technical solutions:

K frame and **X** frame.



Data: the random variables are the force P , the plastic moments M_p and the plastic axial strength N_p .

Mechanical model: incremental elastoplastic – the failure of a cross-section is given by the equation:

$$G = 1 - f\left(\frac{N}{N_p} + \frac{M}{M_p}\right) \leq 0$$

Failure of the structure: level 1 – failure of any cross-section, level 2 – failure of any cross-section, knowing the failure of a previous cross-section.

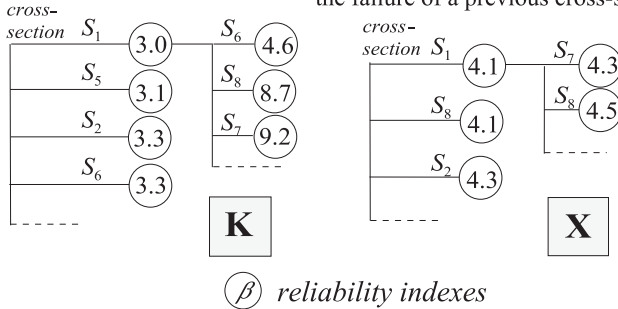


Figure 13.1 Comparison of *K* and *X* wind bracings.

found. At a given level, the probability of failure results from the union of the failure events of each cross-section. This application is developed in [ML95, Lem97].

13.2 Modeling of a mandrel

The axis of a sheet winding mandrel is a massive structure modeled here by finite elements with a linear elastic model (Figure 13.2). Its interest lies in one of the first applications of the reliability-based calculation with a finite element model. The result shown in the RYFES window (Reliability with Your

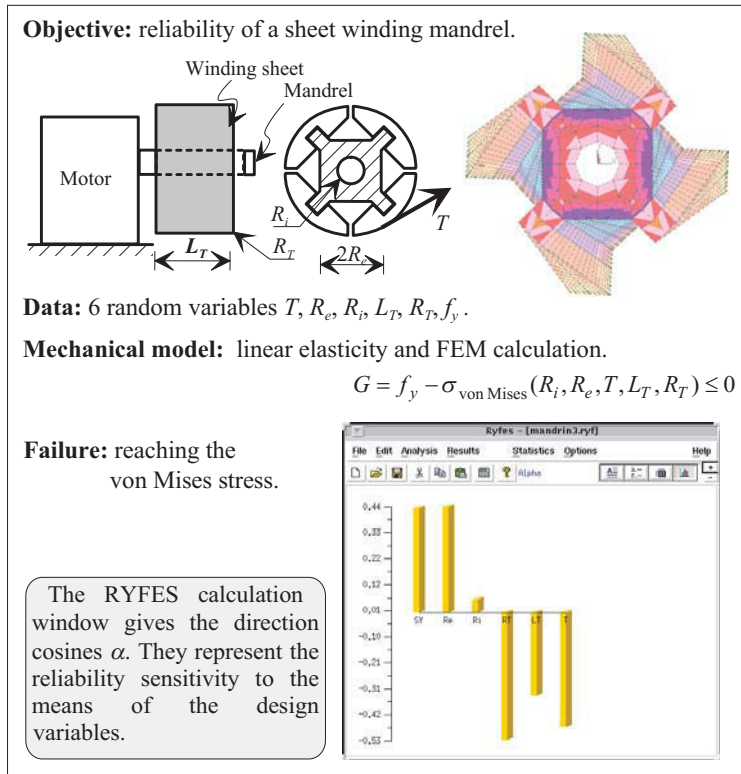


Figure 13.2 Modeling of a mandrel.

Finite Element Software, a code developed at LARAMA¹⁾ illustrates the products of the reliability analysis, in this case: the elasticities of the six design variable means. Given the insufficient lifespan of this mandrel, the elasticities of the means, to which we must add those of the standard deviations, provide indications for defining a new design as a function of the weight of the variables and the cost of progress on each. This application is presented in [LMFM97].

13.3 Failure of a cracked plate

This application is a theoretical example intended to show the influence of the variability of the Young's modulus random field (Figure 13.3). Failure, according to the classic fracture mechanics model, does not involve the Young's

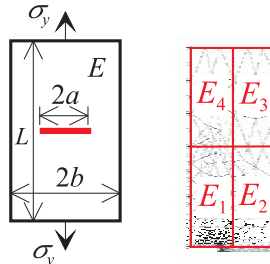
¹ At the time, the Laboratory of Research and Applications for Advanced Mechanics, French Institute for Advanced Mechanics and Blaise Pascal University, Clermont-Ferrand.

Objective: study of the influence of the Young's modulus variability on the failure of a cracked plate.

Data: rectangular plate element including the crack.

Mechanical model: linear fracture mechanics.

$$G = K_{lc} - K_I(a, b, \sigma_y, E_i)$$

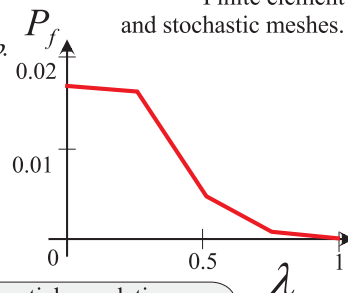


Failure: reaching toughness K_{lc} for a random field $E(x, \omega)$ with correlation ρ .

$$\rho_{ij} = \exp\left(-\frac{\text{distance } ij}{\lambda L}\right)$$

where L is a reference length.

Finite element and stochastic meshes.



The parameter λ expresses the spatial correlation of the Young's modulus.

$\lambda \rightarrow 0$ indicates spatial independence of the modulus,
 $\lambda \rightarrow \infty$ indicates perfect correlation of the modulus.

Figure 13.3 Failure of a cracked plate.

modulus since it is assumed to be identical at all points. Taking into account its spatial variability, characterized here by a correlation ρ_{ij} , it shows a probability of failure that tends naturally to zero when the correlation becomes perfect. This application is developed in [FML97].

13.4 Cooling of a cracked plate

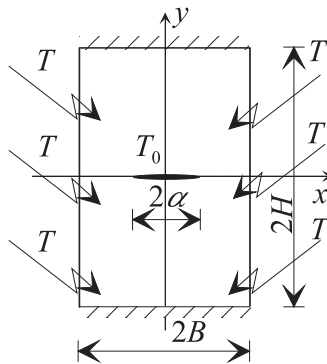
This application is taken from a problem posed by Electricité de France (EDF) (Figure 13.4). The complexity of the problem arises from a very thorough analysis of variability conditions undertaken by EDF. The stochastic model yields compound variables. The mean and standard deviation of K_{Ic} are functions of the temperature. The result illustrates a convergence toward the limit-state as a function of the number of calls for the construction of the performance function $G(X)$. This application is presented in [MLMM97, MLMM98].

Objective: study of the risk of propagation during the cooling of a cracked plate.

Data: evolution of the external thermal field T , internal temperature T_0 , crack aperture 2α .

Mechanical model: linear fracture mechanics.

Failure: $K_{lc} - K = 0$.
random variables are
 α, T, K_{lc} , the latter a function of T .



The graph shows the convergence to the solution $G(X) = 0$ as a function of the number of calls to the performance function: each call is a FEM calculation; this is the main computing cost.

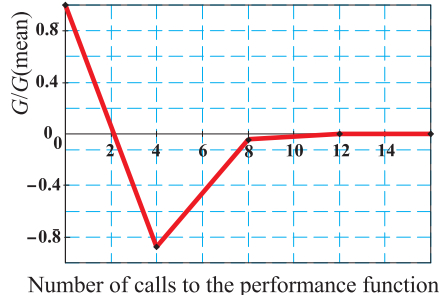


Figure 13.4 Cooling of a cracked plate.

13.5 Boiler casing subjected to a thermal field

This application is also the result of one of EDF's preoccupations (Figure 13.5). The temperature distribution on a boiler casing depends on the circulation of water taking the heat from the combustion chamber. The question is whether it is advisable or not to control the system by avoiding thermal gradients. The stochastic model was discussed in Section 12.2.1. The mechanical model results from a homogenization of the casing in the form of an orthotropic plate, whose characteristics are different in membrane and in bending. The calculation is performed using finite elements and the result shows the importance of correlating the temperature. This application is presented in [RPLB98].

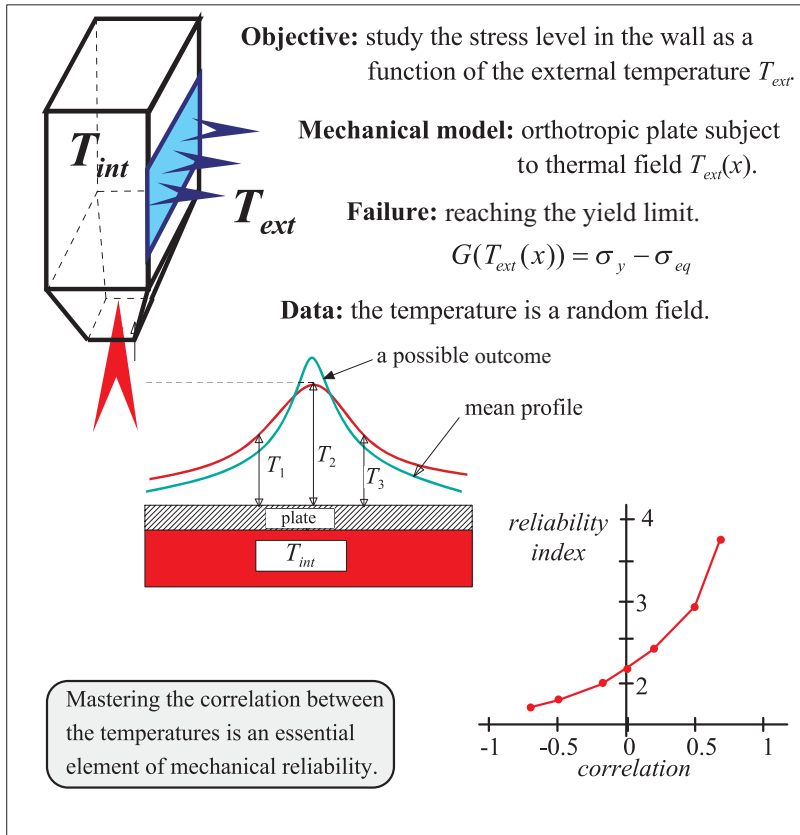


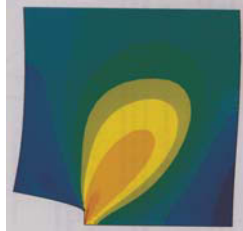
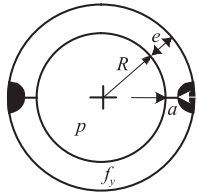
Figure 13.5 Boiler casing subjected to a thermal field.

13.6 Pressurized tank

This application results from a request by the Atomic Energy Commission (CEA, Bruyères le Châtel). It was implemented by C. Fournier as part of the preparation of his thesis (Figure 13.6). Depending on the manufacturing quality, that is, on the knowledge of the variability of the physical outcomes (material, geometry), what are the partial coefficients that must be applied for a given reliability target? The mechanical model is a fracture mechanics model solved using finite elements (integral J). The results show the very high influence of the coefficient on the material toughness, whereas the accuracy of the geometric dimensions means that they have no real influence on reliability. This application is presented in [Fou97].

Objective: reliability study of a pressurized tank,
determination of the partial coefficients.

Data: geometric characteristics R and e , pressure p , crack a ,
toughness J_{lc} and yield limit f_y



Mechanical model: calculation of the integral J .
Failure by rupture: – on the weld,
– elsewhere in the tank structure.

Results: partial coefficients.

Variables	PDF	c.o.v.	Partial coeff.
J_{lc}	Normal	13.75%	3.01
a	Uniform	11.55%	1.16
p	Parameter		1.03
f_y	Normal	7.4%	1.01
e	Normal	0.2%	1
R	Normal	0.18%	1

Taking into account the knowledge of the data variability in production, partial coefficients are deduced for each variable.

Figure 13.6 Pressurized tank.

13.7 Stability of a cylindrical shell

This application concerns the stability of a cylindrical shell under external pressure (Figure 13.7). After verifying the correct functioning of the elastic models with respect to available analytical formulations, failure with respect to the elastoplastic buckling modes is sought. The resistance is the pressure limit for a random defect and the load is the external pressure applied to the shell. The INCA FEM-code offers an efficient and economical solution to the mechanical calculation. The results obtained involve the reliability index associated with the most significant buckling modes. We must then calculate

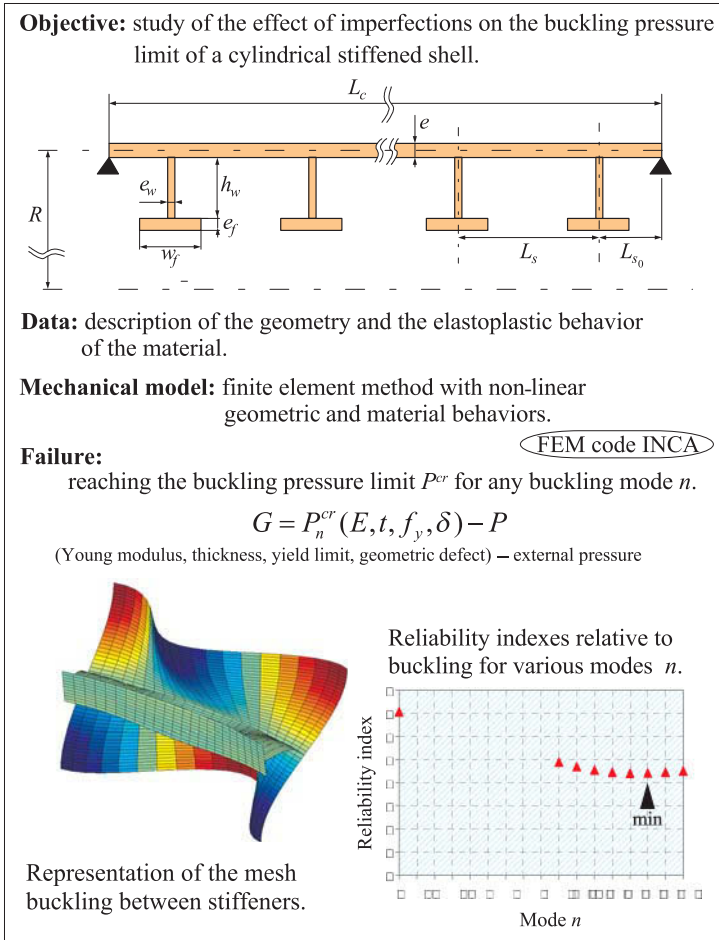


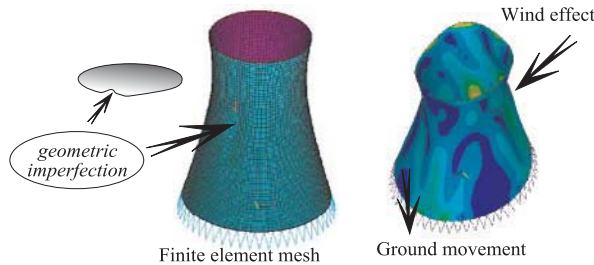
Figure 13.7 Elastoplastic stability of a cylindrical stiffened shell under external pressure.

the index associated with the serial combination of the modes. This application is described in [BGLC00, LM00].

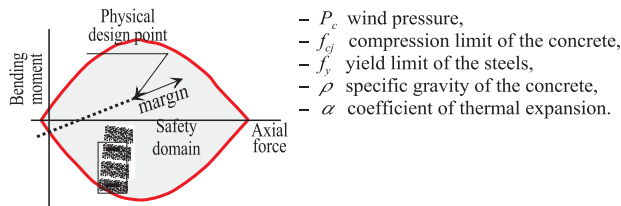
13.8 Reliability sensitivity for a cooling tower

The gradual deterioration of cooling towers over time under the effect of operating and environmental conditions (ground movement, wind, thermal gradient) results in certain amplifications of geometric defects (Figure 13.8).

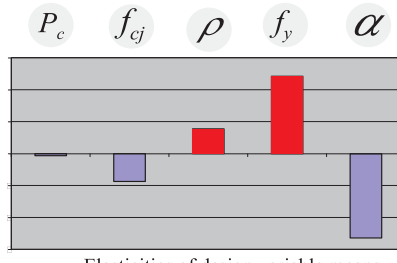
Objective: study the sensitivity of the margin between the design point and the limit-state in a cooling tower with respect to geometric imperfections.



Data: geometric and material, the random variables are:



Mechanical model: search for the design point in an interaction diagram between bending moment and axial force.



Reliability analysis: obtaining the elasticity of the means of the random variables; the most important parameters to monitor are f_y and α .

Figure 13.8 Sensitivity of the margin between the design point and the limit-state for a cooling tower.

In order to plan the required maintenance operations as judiciously as possible, EDF wanted to know the distance between the physical design point (current operating point) and the acceptable limit of the interaction domain between the bending moment and the axial force.

The result presented here shows the relative importance of the variables. The yield point of the steels and the coefficient of thermal expansion are the most important variables to observe. This result is an initial step for a problem whose mechanical model must be improved by taking creep into account. This application is described in [LM00].

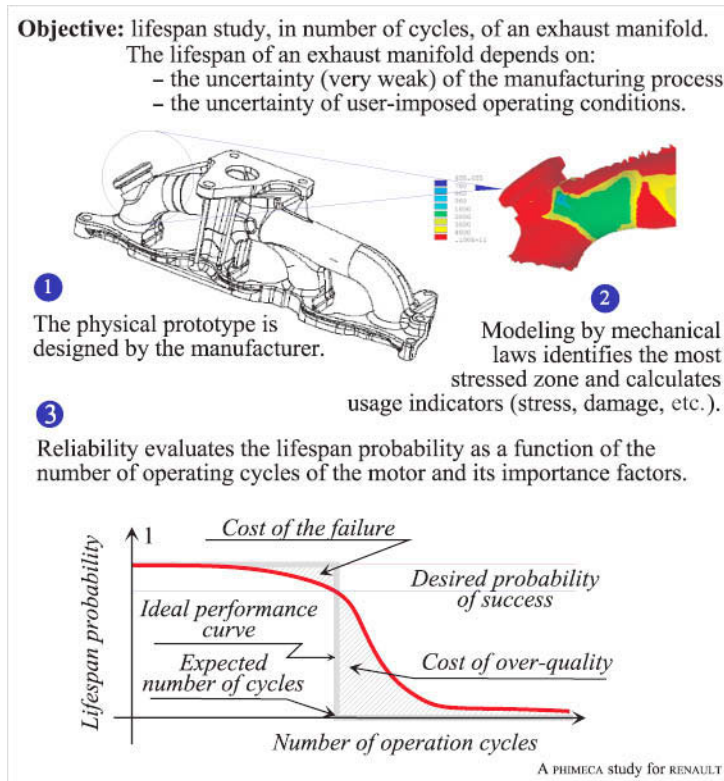


Figure 13.9 Lifespan of an exhaust manifold.

13.9 Lifespan of an exhaust manifold

The lifespan of an exhaust manifold (Figure 13.9) depends on the manufacturing process and user-imposed operating conditions. The study undertaken by PHIMECA for RENAULT has enabled the importance factors of the different variables to be evaluated, at the cost of the stochastic modeling of the manufacturing process and a complex finite element model with more

than 100,000 degrees of freedom, including geometric variation, elastoplasticity and damage. Extending the study, the figure illustrates a form of optimization to be sought. The ideal would be to provide a guaranteed number of cycles to the user: it is represented by a step function. The non-provided cycles result in a guarantee cost for the manufacturer, whereas the cycles available beyond the guarantee are considered as over-quality. This application is described in [PMMR03].

This page intentionally left blank

Chapter 14

Conclusion

This brief chapter, by way of conclusion, summarizes all the results described in this book. It then gives some indications as to the potential fields of application of reliability methods, and it concludes with perspectives for the future, since the field of mechanical reliability is constantly progressing.

14.1 Reliability methods in mechanics

The 19th century saw the first approaches to design by the evaluation of a resistance value and that of a load effect value, and the introduction of a ‘safety’ coefficient between these two values. It was the century of characteristic values with a more or less defined content. The 20th century introduced variability through the coefficient of variation. It was the century of means and standard deviations. Better still, it introduced the modeling of random variables. Each level of approach has its own methods of calculation and justification. This book helps us study mechanical design, taking into account the following assumptions.

1. There is a performance function dependent on random variables and whose probability of negative outcomes we must calculate; there is a combination of performance functions (system reliability).
2. The random variables are identified using a stochastic model. In principle, we must know the joint probability density of a random variable vector, which is often inaccessible. In practice, only knowledge of the marginal distributions of each variable and their correlations is at our disposal.

In accordance with these two assumptions, time-independent mechanical-reliability methods enable us calculate a probability of failure, a probability conditioned on the quality of the information available: the quality of the mechanical representation of the performance function and the quality of the stochastic model. They also enable us to calculate the importance factors (sensitivities and elasticities) which are relevant in optimizing the design of a

mechanical part. Ignoring them would be tantamount to rejecting an additional precision that is available to us.

Of course, these two assumptions limit the field of application and we will discuss this further in Section 14.3 in the perspectives for progress.

Three summary sheets, presented in the following pages, summarize the objective and the method. The first (Figure 14.1) recalls the methodology:

The goal: FORM /SORM approximation methods are efficient for the calculation of weak probabilities, less than $10^{-2} \sim 10^{-3}$. They can be used alone or in combination with conditional Monte Carlo methods.

Methodology:

- 1 – Selection of design variables and modeling of *random variables* X_p ,
- 2 – Construction of the performance function $G(X_i)$ of random variables X_p
such that $G(X_i) > 0$ defines success
and $G(X_i) \leq 0$ defines failure.
- 3 – Definition of the *probability of failure*: $P_f = \text{Prob}(G(X_i) \leq 0)$
- 4 – Evaluation using FORM/SORM methods:
 - of the *reliability index* β ,
 - of the *probability of failure* P_f ,
 - of the *reliability sensitivity factors*.

Variables X_i : they are modeled with random variables by choosing their probability density function:

$$X_i \rightarrow f_{X_1, X_2, \dots, X_n}(x_1, x_2, \dots, x_n)$$

or, at least:

the marginal distribution of each variable,

$$X_i \rightarrow f_{X_i}(x_i)$$

and the correlation between each couple.

$$X_i, X_j \rightarrow \rho_{ij}(X_i, X_j)$$

Performance function: $G(X_i)$ expresses the mechanical link between variables,
such that a positive value indicates success:

Elementary case: $X_1 = R$, R is a *resistance* or a resource,
 $X_2 = S$, S is an *internal strength* (stress) or a need,
and then $G(R,S) = R - S$.

General case: $G(X_i)$ is any function resulting from a physical, mechanical,
economic, etc ... model.

If $G(X_i)$ is *explicit* and *derivable*, FORM/SORM algorithms
can be easily applied,

If $G(X_i)$ is *implicit*, various approaches enable us to implement
FORM /SORM methods, like *numerical design of
experiment*.

Obtained results: the *reliability index* β , which forms an intermediate calculation
but also a reliability measure; the *probability of failure* P_f and
the *importance factors* (sensitivity or elasticity) of type: $\frac{\partial f}{\partial X_i}, \dots, \frac{\partial \beta}{\partial X_i}$

Figure 14.1 FORM/SORM methods – assumptions and expected results.

- choosing a stochastic model of design variables; in general, marginal densities and correlations,
- choosing the mechanical model and the performance function $G(X_i)$ and its numerical implementation, validated in the entire variation domain of the design variables.

Depending on the nature of the performance function, simple explicit or more complex models, often based on finite element discretization, will result in either an easy or a much more complicated solution. The results expected are the probability of failure and the importance factors.

The second sheet (Figure 14.2) illustrates the calculation of the reliability index through the following two operations:

- application of the isoprobabilistic transformation to move from physical space to the space of standardized, centered and independent Gaussian variables,
- solution of the optimization problem to locate the most probable failure point (or design point).

The third sheet (Figure 14.3) summarizes the first-order approximation and the higher-order approximations:

- asymptotic Breitung approximation,
- ‘exact’ SORM calculations by integration along a quadric,
- exact RGMR integration.

Lastly, it underlines the fact that the results must be meticulously validated by conditional simulations, and that the duality between approximation methods and simulation methods must always be borne in mind in order to achieve optimum efficiency.

Among the results of the analysis, importance factors link the probability of failure to the partial coefficients of the design rules. It comes to the same thing either to choose partial coefficients or to choose target reliability as an index associated with a stochastic model. The door is then open for the calibration of design rules.

14.2 Application of the methods

14.2.1 Design and maintenance

Let us recall once again the observation made by Hasofer: reliability methods ‘offer an additional precision’ to the designer who can use them both in the initial design phase of a structure or mechanical part, and to optimize inspection, maintenance and repair operations. It is this latter aspect that seems the most likely to stimulate motivation, given the economic stakes. In fact,

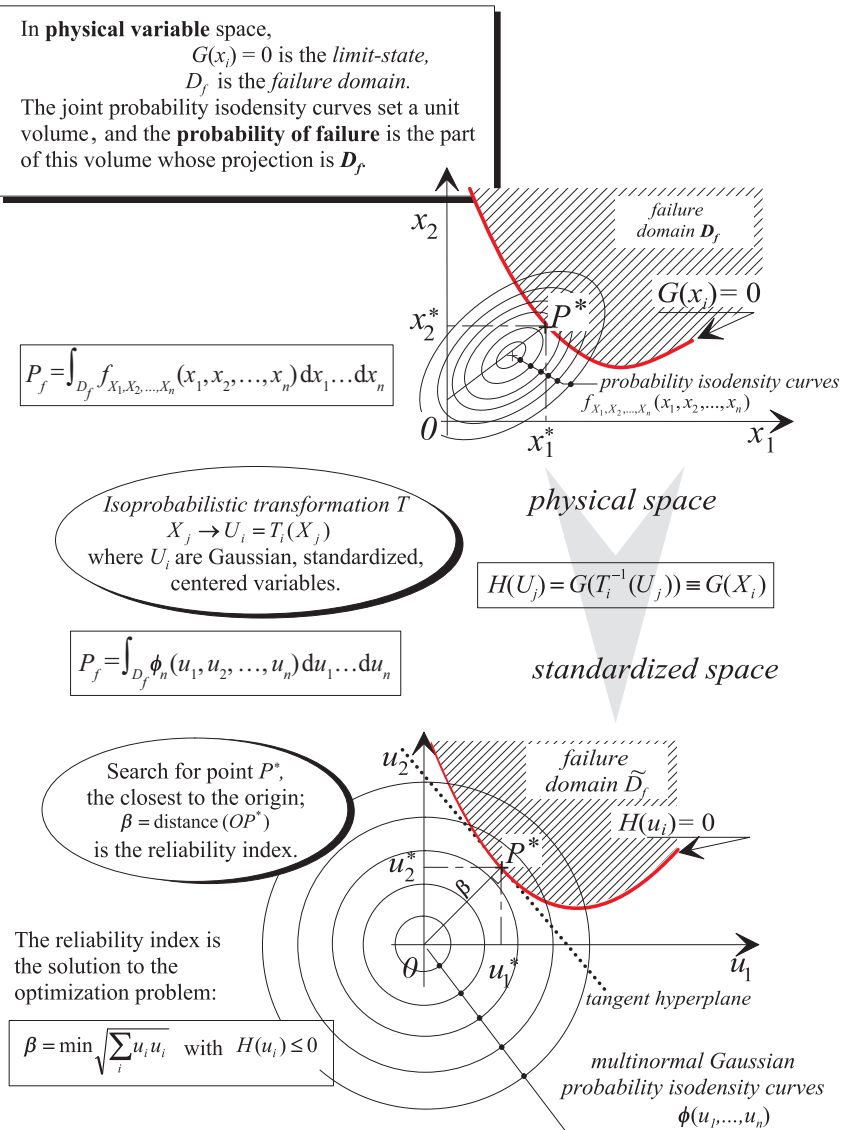
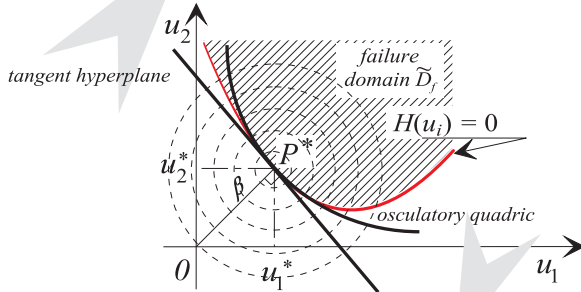


Figure 14.2 FORM/SORM methods – calculation of the reliability index.

deterministic design methods are very often capable of providing satisfactory designs in the case of prototypes (unique constructions) at a time when it is not possible to imagine all the defects and all the deviations between physical reality

FORM approximation: $H(U_i) = 0$ is replaced by a hyperplane:

Φ : Gaussian distribution, zero mean, unit standard deviation $P_f \approx \Phi(-\beta)$



SORM approximations:

asymptotic correction due to the curvatures κ_j of $H(U)$ at P^* :

(Breitung formula)

$$P_f \approx \Phi(-\beta) f(\kappa_j)$$

Exact' SORM calculations:

integration along the quadric Q osculatory to $H(U)$ at P^* :

$$P_f \approx \int_Q \phi_n(u_1, u_2, \dots, u_n) du_1 \dots du_n$$

(Rice and Tvedt formulae)

Exact integration with RGMR:

$$P_f = \int_{B_1} f(\bar{OM}) |J| du_1 \dots du_n$$

(integration on the unit sphere)

Correction of the approximation and validation:

with a small number of simulations by **Monte Carlo**
methods **conditioned** by the knowledge of P^* .

Simulations are now

centered at P^* , instead of the origin:
The conditional probability sought is of order 1/2 instead of 10^{-n} .

Figure 14.3 FORM/SORM methods – approximation and validation of the probability of failure.

and the model. On the other hand, when a structure is in service, the question is to know whether it is still capable of performing its mission, in view of the actual deviations, this time not imagined but observed. The variation of the reliability index and the evolution of importance factors are then precious indications. In the case of mass production, the initial reliability analysis contributes to the definition of tolerances.

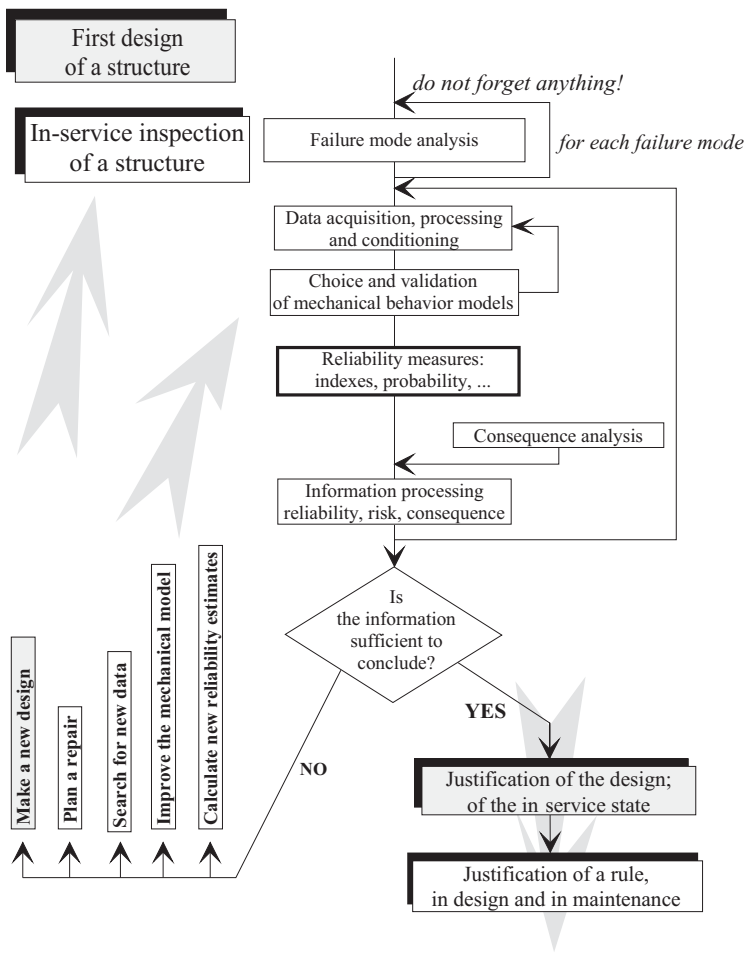


Figure 14.4 Sequence of actions for a reliable design.

Figure 14.4 illustrates the entire procedure. Reliability methods appear as an element in a set of actions to be undertaken for a reliable and optimal design, during both initial analysis and follow-up.

14.2.2 Software tools

It is clear that such an approach will require considerable software resources to analyze the failure modes and their criticality, to acquire and process data, and, in the light of this book, to apply reliability methods. As mechanical modeling is essential, it is necessary to have tools capable of conversing with the tools to

which the designer is accustomed. It is for this purpose that the RYFES tool was developed at the initiative of A. Mohamed: *Reliability with Your Finite Element Software*. Depending on the needs and resources available, a first solution is to develop a tool to couple the mechanical model and the reliability model. If the needs are limited, it can be advantageous to write the reliability procedures directly; if they are considerable, we can use commercially-distributed software, among which we can mention the following:

- STRUREL (STRUCTURAL RELIABILITY) is the fruit of research by Professor Rackwitz at the Technical University of Munich. It comprises modules for component reliability and system reliability as well as time-invariant and time-variant approaches. Contact: <http://www.strurel.de/>.
- PROBAN (PROBABILISTIC ANALYSIS) was developed by Det Norske Veritas, evolving from the first versions oriented toward the offshore oil industry to a general code available today. Contact: <http://www.dnv.at/services/software/products/safeti/safetiqra/proban.asp>.
- PHIMECA software is the general purpose software whose development is based on the research carried out by the author of this book. Its specificity lies in its openness and the possibilities of dialog with any mechanical or physical behavior model. Contact:<http://www.phimeca.com/>.
- OPENTURNS is an Open source initiative to Treat Uncertainties, Risks 'N Statistics in a structured industrial approach. Since the beginning of 2005, a partnership of three companies – Electricité de France (EDF), European Aeronautic Defense and Space (EADS) and an engineering consultancy company (PHIMECA) – has been working on building together a tool designed to perform reliability analyses. Contact: <http://trac.openturns.org/>.

The reader can also refer to Structural Safety (28), 2006. This reference presents an overview of general purpose software in structural reliability.

14.3 Perspectives

We hope that this book has convinced the reader of the advantages of probabilistic methods. Furthermore, we hope it has enabled the reader to discover the bases of these methods so that he/she can himself/herself apply them and validate the results obtained with a clear knowledge of the assumptions. These assumptions will certainly leave him/her dissatisfied. To discover the probabilistic approach is also to discover its limits.

To go further, the reader can consult the international literature on the subject as well as review books; see, for example, [DM96].

In a scientific and industrial context, the author would point out the following four avenues for progress.

14.3.1 Stochastic finite elements

As during the early years of the development of finite element codes for the number of degrees of freedom, the question today concerns solution capacity, considering the number of random variables. We have indicated that the efficiency of FORM/SORM methods can decrease with an increase in the number of variables, which then call for other approaches or a greater use of conditional simulations. Moreover, the volume of calculation increases very rapidly.

Gordon Moore's law, which predicts that the power of computers will double every two years – up to what limit? – will come to our aid.

From a scientific point of view, it is the stochastic finite element method that should result in the creation of codes. The challenge today is to find the correct spectral decomposition capable of capturing the maximum variability with a minimum number of modes. The creation of software tools will promote their application in increasingly complex real cases. As for deterministic finite element methods, it will be more by an accumulation of experiences than by algorithmic justifications – indispensable but insufficient – that we can gradually develop a skill.

14.3.2 The time factor

The time factor has been discussed very little in this book. Two approaches are associated with it.

First, stochastic dynamics deals with the response of a dynamic system excited by a random signal and having, as the case may be, parameters of stiffness, mass and damping that are also random. This is a field in its own right described in depth in the works of Krée and Soize [KS83] in France and in Chapter V of [Soi01].

In addition, all the time-dependent phenomena urge us to replace modeling with a random variable by modeling with a stochastic process. A time-invariant approach results in the probability calculation:

$$P_{f,i}(t) = \text{Prob} (G(t, \mathbf{x}(t), \omega) \leq 0) \quad \text{at fixed } t$$

whereas a time-variant approach poses the question of the calculation of cumulative probability:

$$P_{f,c}(t) = \text{Prob} (\exists \tau \in [t_0, t] \text{ such that } G(\tau, \mathbf{x}(\tau), \omega) \leq 0)$$

where t_0 is the date of commissioning of the mechanical system.

The response to this question can be addressed using several methods based on the concept of outcrossing rate according to the Rice formula [Ric44a],

Ric44b]. This involves estimating the number of trajectories of the process entering the failure domain in the interval $[t_0, t]$:

- The Monte Carlo method can be applied under broad assumptions, but at the cost of very great demand on computing resources.
- For differentiable or jump processes [BFR91, SFR91], there are explicit equations for the outcrossing rate.
- Hagen and Tvedt [HT91b, HT91a] have suggested considering outcrossing as a system formed by the intersection of a positive outcome on date t and a negative outcome on date $t + dt$. Such an approach has been developed further in [ARSL04].

Under certain assumptions, often verified in the degradation of materials, point-in-time probability is equal to cumulative probability. This is the case if all the trajectories are decreasing.

14.3.3 Data acquisition and processing

The reliability methods described in this book are based on an exhaustive knowledge of the stochastic modeling of the variables. Of course, the information available is always poor and we only have estimates for the parameters of the random variable distributions. They introduce an additional uncertainty that can be offset at the cost of an increase in the number of random variables. It is then possible to construct a reliability index as a function of the size of the samples available. This information indicates whether it is advisable or not to increase the statistical richness of the sample, at the price of additional tests. [PHLM00, Pen00] describe this approach.

The quality of the data model is essential. It will never be satisfactory, particularly because of the importance of distribution tails. However, it always provides better information than the choice of a deterministic characteristic value. The absence of standards for the modeling of variables is currently an obstacle to the dissemination of probabilistic methods. We can imagine that one day a code for the representation of variables will be adopted, as there is today a code for the partial coefficient approach.

14.3.4 Mechanical-reliability optimization

The design of mechanical structures and systems progressed by leaps and bounds in the second half of the 20th century. This is primarily thanks to the considerable increase in computing power. Thus, the following milestones were crossed:

- linear calculation of structures during the 1970s,
- geometric and material non-linear calculation during the 1980s,

- coupling between the calculation of structures and optimization on the one hand and design of the geometry on the other hand during the 1990s,
- coupling between reliability methods and mechanical models, also in the 1990s.

Tomorrow's tools will see the development of optimization methods. Firstly, classic optimization in a deterministic context, but also reliability-based design optimization (RBDO), as the criterion of data variability must enter into the optimization scheme for the latter to guarantee a minimum level of reliability. In fact, neglecting it can lead to solutions that are perhaps theoretically optimal, but in reality hardly robust in the face of the deviations between the target values and the physical outcomes.

Such an approach has been developed by the author of this book and his team, in the laboratory [KML02b, KOML04]. As the search for the design point is itself an optimization problem, RBDO is tantamount to building two interleaved optimization loops.

By denoting:

1. the optimization variables $\{x\}$; these are the deterministic variables to be controlled in order to optimize the design; they represent the control parameters of the mechanical system (i.e. dimensions, materials, loads, etc.) and of the probabilistic model (i.e. means and standard deviations of the random variables),
2. the random variables $\{y\}$, which represent the uncertainties; each of these variables is identified by its distribution type and the associated parameters; these variables can be geometric dimensions, material characteristics or external loadings,
3. $f(\{x\})$, the objective function of the design variables to be optimized,
4. $G(\{x\}, \{y\})$, the performance function,
5. $g_k(\{x\}, \{y\}) \geq 0$, the set of k constraints of the optimization.

Then the two optimization procedures are:

1. The deterministic optimization of the system, by integrating the reliability constraint:

$$\min_{\{x\}} f(\{x\})$$

under the constraints: $g_k(\{x\}, \{y\}) \geq 0$ and $\beta(\{x\}, \{y\}) \geq \bar{\beta}$

where $\bar{\beta}$ is the target reliability index and $\beta(\{x\}, \{y\})$ is that of the structure.

2. The search for the design point by an optimization procedure:

$$\min_{\{y\}} d^2(\{x\}, \{y\}) \quad \text{under the constraint} \quad G(\{x\}, \{y\}) \geq 0$$

where $d(\{x\}, \{y\}) = \|T(\{x\}, \{y\})\|$ is the distance, in standardized space, between the origin and the design point.

14.4 Reliability analysis and sensitivity analysis

Reliability analysis consists of searching for a particular point of the distribution function of the performance function. By introducing a threshold and by varying the reliability level, it becomes possible to construct the density point by point. Sensitivity analysis consists of developing the performance function from its first statistical moments. By increasing the number of moments, their density can be approximated, and thus a reliability analysis can be performed. If there are in fact two ways to address the same problem, the expected results are indeed different.

The first analysis prefers an accurate study at a given point, located generally in a distribution tail, whereas the second favors the knowledge of the central tendencies. The choice therefore depends on the questions posed.

- *Static mechanical-reliability coupling is a tool already at the disposal of engineers for an optimal and reliable design. It will be complemented in the coming years with the arrival of tools integrating spatial variability, the time dimension and optimization.*
- *These tools will be used to refine prediction methods by the development of specific tools, according to the type of behavior of materials and structures: fracture mechanics, fatigue, instability, etc.*
- *They will one day join with failure analysis tools to integrate reliability more completely into operating safety.*

To be continued ...

This page intentionally left blank

Bibliography

- [ADKOS98] R. Ambartzumian, A. Der Kiureghian, V. Ohanian and H. Suskiasian. Multinormal probability by sequential conditioned importance sampling: Theory and application. *Probabilistic Engineering Mechanics*, 13(4): 299–308, 1998.
- [AFN96] AFNOR. Eurocode 1: Bases du Calcul et Actions sur les Structures et Document d'Application Nationale. Technical Report XP ENV 1991–1, AFNOR, April 1996.
- [And02] C. Andrieu. *Fiabilité mécanique des structures soumises à des phénomènes physiques dépendant du temps*. PhD thesis, Blaise Pascal University – LaRAMA IFMA/UBP, 13 December 2002.
- [ANS94] Inc. ANSYS. *ANSYS 5.1: Finite Element Software*. ANSYS Inc, Houston, USA, 1994.
- [AR90] T. Abdo and R. Rackwitz. A new beta-point algorithm for large time-invariant and time variant reliability problems. In *Reliability and Optimization of Structures*, 1–11. 3rd WG 7.5 IFIP conference, Berkeley, 1990.
- [ARSL04] C. Andrieu-Renaud, B. Sudret and M. Lemaire. The PHI2 method: A way to compute time-variant reliability. *Reliability Engineering and System Safety*, 84: 75–86, 2004.
- [AS72] M. Abramowitz and A. Stegun. *Handbook of Mathematical Functions*. Dover Publications, New York, 10th edition, 1972.
- [ASC83] Committee on Reliability of Offshore Structures ASCE. Application of reliability methods in design and analysis of offshore platforms. *Journal of Structural Engineering*, 109(10): 2265–2291, October 1983.
- [AT84] A.H.S. Ang and A.W. Tang. *Probability Concepts in Engineering Planning and Design, volume 2: Decision, Risk and Reliability*. John Wiley & Sons, New York, 1984.
- [BA96] B. Barthelet and E. Ardillon. Approche probabiliste simplifiée pour déterminer les coefficients de sécurité des critères d'acceptabilité des défauts. In *Troisième Conférence Nationale INSTRUC 3*, SFM Paris, 27 and 28 November 1996.

- [Bal99] H. Baldeweck. *Méthode des éléments finis stochastiques. Applications à la géotechnique et à la mécanique de la rupture.* PhD thesis, University of Evry – INSTN, 16 April 1999.
- [BB90] C.G. Bucher and U. Bourgund. A fast and efficient response surface approach for structural reliability problems. *Structural Safety*, (7): 57–66, 1990.
- [BBF92] F. Böhm and A. Brückner-Foit. On criteria for accepting a response surface model. *Probabilistic Engineering Mechanics*, 7: 183–190, 1992.
- [BC70] J.R. Benjamin and A. Cornell. *Probability, Statistics and Decision for Civil Engineers*. McGraw-Hill Book Co., 1970.
- [BD90] J.L. Batoz and G. Dhatt. *Modélisation des Structures par Éléments finis – Solides Elastiques*, volume 1. Hermès, Paris, 1990.
- [BF87] P. Bernard and M. Fogli. Une méthode de Monte Carlo performante pour le calcul de la probabilité de ruine. *Construction Métallique*, (4): 23–39, 1987.
- [BFR91] P. Bryla, M.H. Faber and R. Rackwitz. Second Order Methods in Time Variant Reliability Problems. *Proceedings of the OMAE'91*, II: 143–150, 1991.
- [BGLC00] J.M. Bourinet, N. Gayton, M. Lemaire and A. Combescure. Reliability analysis of stability of shells based on combined finite element and response surface methods. In M. Papadrakakis, A. Samartin and E. Onate, editors, *Computational Methods for Shell and Spatial Structures*, 20p. ISASR-NTUA, Athens, Greece, June 5–7, 2000.
- [Bje88] P. Bjerager. Probability integration by directional simulation. *Journal of Engineering Mechanics*, 114(8): 1285–1302, 1988.
- [BM58] G.E.P. Box and M.E. Muller. A note on the generation of random normal deviates. *Annals of Mathematical Statistics*, (29): 610–611, 1958.
- [BMB01] D. Breysse, A. Mébarki and D. Boissier, editors. *Fiabilité des Matériaux et des Structures*. JN'Fiab 3, CDGA, Bordeaux, 1–2 février 2001.
- [Bre84] K. Breitung. Asymptotic approximations for multinormal integrals. *Journal of the Engineering Mechanical Division, ASCE*, 110(3): 357–366, March 1984.
- [Bro70] C.G. Broyden. The convergence of a class of double-rank minimization algorithms – 2. the new algorithm. *Journal of the Institute of Mathematics and its Applications*, 6: 222–231, 1970.
- [BTG94] D. Benoist, Y. Tourbier and S. Germain. *Plans d'expériences : construction et analyse*. Lavoisier, 1994.
- [Buc88] C.G. Bucher. Adaptative Sampling: an Iterative Fast Monte Carlo Procedure. *Structural Safety*, 5: 119–126, 1988.

- [But56] J.W. Butler. Machine sampling from given probability distributions. In M.A. Meyer, editor, *Symposium on Monte Carlo Methods*. Wiley, New York, 1956.
- [Cal96] J.A. Calgaro. *Introduction aux Eurocodes – Sécurité des constructions et bases de la théorie de la fiabilité*. Presses de l'ENPC, Paris, 1996.
- [Cau88] Y. Caumel. *Probabilités: théorie et applications*. Eyrolles, Paris, 1988.
- [CEA97] CEA/LAMS – Saclay. *Castem 2000*, 1997.
- [CL67] H. Cramer and M.R. Leadbetter. *Stationary and Related Stochastic Processes*. Wiley, New York, 1967.
- [Col] Collectif. Unfired fusion welded pressure vessels. Technical Report BS 5500, British Standards Institution.
- [Col95] Collectif. *Aide-Mémoire Statistique*. CISIA-CERESTA, Saint-Mandé, 1995.
- [Col97] Collectif. IASSAR report on computational stochastic mechanics. 4 – stochastic finite elements. *Probabilistic Mechanics*, 12(4): 285–321, October 1997.
- [Dav59] W.C. Davidon. Variable metric method for optimization. Technical Report ANL-5990, Atomic Energy Commission Research and Development, November 1959.
- [DBOH88] O. Ditlevsen, P. Bjerager, R. Olesen and A.M. Hasofer. Directional simulation in Gaussian processes. *Probabilistic Engineering Mechanics*, 3(4): 207–217, 1988.
- [DC75] H. Dalgas Christiansen. Random number generators in several dimensions. Theory, tests and examples. Technical report, IMSOR, Techn. Univ. of Denmark, Lyngby, 1975.
- [Dea80] I. Deák. Three digits accurate multiple normal probabilities. *Numerical Mathematics*, 35: 369–380, 1980.
- [Dea90] I. Deák. *Random Number Generators and Simulation*. Akadémiai Kiado, Budapest, 1990.
- [Deo91] G. Deodatis. The Weighted Integral Method. I: Stochastic Stiffness Matrix. *Journal of Engineering Mechanics*, 117(8): 1851–1864, August 1991.
- [Dev96] N. Devictor. *Fiabilité et mécanique : méthodes FORM/SORM et couplages avec des codes d'éléments finis par des surfaces de réponse adaptatives*. PhD thesis, Blaise Pascal University – Clermont II, December 1996.
- [Dit79] O. Ditlevsen. Narrow reliability bounds for structural systems. *Journal of Structural Mechanics*, 7(4): 453–472, 1979.
- [DKD98] A. Der Kiureghian and T. Dakessian. Multiple design points in first and second-order reliability. *Structural Safety*, 20(1): 37–50, 1998.

- [DKL86] A. Der Kiureghian and P.L. Liu. Structural reliability under incomplete probability information. *Journal of Engineering Mechanics*, 112(1), 1986.
- [DM96] O. Ditlevsen and H.O. Madsen. *Structural Reliability Methods*. John Wiley & Sons, New York, 1996.
- [DMG90] O. Ditlevsen, R.E. Melchers and H. Gluver. General multi-dimensional probability integration by directional simulation. *Computers and Structures*, 36(2): 355–368, 1990.
- [Dol83] K. Dolinski. First-order second-moment approximation in reliability of structural systems: critical review and alternative approach. *Structural Safety*, 1: 211–231, 1983.
- [DS91] G. Deodatis and M. Shinozuka. The weighted integral method. II: Response variability and reliability. *Journal of Engineering Mechanics*, 117(8): 1865–1877, August 1991.
- [EFS94] I. Enevoldsen, M.H. Faber and J.D. Sorensen. Adaptative response surface techniques in reliability estimation. In Schuëller, Shinozuka and Yao, editors, *Structural Safety and Reliability*, A.A. Balkema Publications, Rotterdam, The Netherlands, 1257–1264, 1994.
- [Er98] G.K. Er. A method for multi-parameter PDF estimation of random variables. *Structural Safety*, (20): 25–36, 1998.
- [ESR98] Working Group ESReDA. *Industrial Application of Structural Reliability Theory*. Det Norske Veritas, 1998.
- [ETML91] K. El-Tawil, J.P. Muzeau and M. Lemaire. Reliability method to solve mechanical problems with implicit limit state. In R. Rackwitz and P. Thoft-Christensen, editors, *Reliability and Optimization of Structures, Proceedings of the 4th IFIP WG 7.5 Conference*, 181–190. Springer-Verlag, 1991.
- [Far89] L. Faravelli. Response surface approach for reliability analysis. *Journal of Engineering Mechanics*, 115(12), 1989.
- [FJRHP00] R.V. Field Jr., J. Red-Horse and T. Paez. A non-deterministic shock and vibration application using polynomial chaos expansion. In *8th ASCE Speciality Conference on Probabilistic Mechanics and Structural Reliability*, 2000.
- [Fle70] R. Fletcher. A new approach to variable metric algorithms. *Computer Journal*, 13: 317–322, 1970.
- [FLSHC99] C. Forgez, B. Lemaire-Semail, J.P. Hautier and S. Clénet. Réseaux de neurones appliqués à la modélisation de systèmes électrotechniques. *Revue Internationale de Génie Electrique*, 2(3): 305–333, 1999.
- [FM94] O. Florès Macias. *Modèles fiabilistes et mécaniques: Eléments finis Stochastiques. Méthodes de Couplage et Applications*. PhD thesis, Blaise Pascal University, Clermont-Ferrand, 1994.

- [FML97] O. Florès Macias and M. Lemaire. Eléments finis stochastiques et fiabilité – application en mécanique de la rupture. *Revue Française de Génie Civil*, (2), 1997.
- [FMTE81] G. Ferregut, E. Mendoza, F. Tellez and L. Esteva. Programme d'Analyse de Fiabilité par Simulation de Monte Carlo. Technical Report Projet 9172, Institute of Engineering, National University of Mexico, Mexico, 1981.
- [Fou97] C. Fournier. Dimensionnement probabiliste des structures (utilisation de la règle R6): Application au dimensionnement de réservoirs. *Revue Française de Mécanique*, 1(1): 35–42, 1997.
- [FP63] R. Fletcher and M.J.D. Powell. A rapidly convergent descent method for minimization. *Computer Journal*, 6: 163–168, 1963.
- [GB90] J. Goyet and A. Bureau. Sécurité probabiliste des structures – évaluation de coefficients partiels de sécurité pour l’élaboration des nouveaux règlements. *Construction Métallique*, (1): 3–31, 1990.
- [GBL02] N. Gayton, J.M. Bourinet and M. Lemaire. CQ2RS: A new statistical approach to the response surface method for reliability analysis. *Structural Safety*, 25: 99–121, 2002.
- [GG02] D. Ghiocel and R.G. Ghanem. Stochastic finite element analysis of seismic soil-structure interaction. *Journal of Engineering Mechanics*, 128: 66–77, 2002.
- [Gib71] J.D. Gibbons. *Non-parametric Statistical Inference*. McGraw-Hill, Tokyo, Kogakusha, 1971.
- [GJLM98] J. Goyet, B. Jacob, M. Lemaire and H. Mathieu. Fiabilité des constructions. *Revue Française de Génie Civil*, 2(5): 529–610, September 1998.
- [Gle89] J. Gleick. *La Théorie du Chaos*. Albin Michel, 1989.
- [GMS⁺04] N. Gayton, A. Mohamed, J.D. Sorensen, M. Pendola and M. Lemaire. Calibration methods for reliability-based design codes. *Structural Safety*, 26: 91–121, 2004.
- [Gol70] D. Goldfarb. A family of variable-metric methods derived by variational means. *Mathematics of Computation*, 24: 23–26, 1970.
- [Gor67] S. Gorenstein. Testing a random number generator. *Communications of the Association for Computing Machinery*, (10): 111–118, 1967.
- [GPL03] N. Gayton, M. Pendola and M. Lemaire. Reliable design of thin axisymmetric shells using partial factor calibration. In G. Gogu, D. Coutellier, P. Chedmail and P. Ray, editors, *Recent Advances in Integrated Design and Manufacturing in Mechanical Engineering*, 411–420. IDMME, Kluwer Academic Publishers, 2003.

- [Gre61] M. Greenberger. Notes on a new pseudo-random number generator. *Journal of the Association for Computing Machinery*, (8): 163–167, 1961.
- [GS91] R.G. Ghanem and P.D. Spanos. *Stochastic Finite Elements: A Spectral Approach*. Springer, Berlin, 1991.
- [Gum58] E.J. Gumbel. *Statistics of Extremes*. Columbia University Press, New York, 1958.
- [Hay94] S. Haykin. *Neural Networks*. Prentice Hall, 1994.
- [HGKR84] M. Hohenbichler, S. Goldwitzer, W. Kruse and R. Rackwitz. New light on first and second-order reliability methods. Technical report, Technical University of Munich, 1984.
- [HGKR87] M. Hohenbichler, S. Goldwitzer, W. Kruse and R. Rackwitz. New light on first- and second-order reliability methods. *Structural Safety*, 4: 267–284, 1987.
- [HH64] I.M. Hammersley and D.C. Handscomb. *Monte Carlo Methods*. Wiley, New York, 1964.
- [HK85] R.T. Haftka and M.P. Kamat. *Elements of Structural Optimization*. Martinus Nijhoff, 1985.
- [HL74] A.M. Hasofer and N.C. Lind. Exact and invariant second moment code format. *Journal of Engineering Mechanics*, 100: 111–121, 1974.
- [HM56] I.M. Hammersley and K.W. Morton. A New Monte Carlo Technique with Antithetic Variates. *Proceedings Cambridge Philosophy Society*, 52: 442–474, 1956.
- [Hoh84] M. Hohenbichler. Numerical Evaluation of the Error Term in Breitung’s Formula. Technical Report 69, Technical University of Munich, 1984.
- [HR83] M. Hohenbichler and R. Rackwitz. First order concepts in system reliability. *Structural Safety*, 1(3): 177–188, 1983.
- [HR85] M. Hohenbichler and R. Rackwitz. A bound and an approximation to the multivariate normal distribution function. *Mathematica Japonica*, 30(5), 1985.
- [HT91a] O. Hagen and L. Tvedt. Parallel system approach for vector out-crossing. In *Proceedings of the OMAE’91, Volume II*, 165–172, 1991.
- [HT91b] O. Hagen and L. Tvedt. Vector process out-crossing as parallel system sensitivity measure. *Journal of Engineering Mechanics, ASCE*, 121(10): 2201–2220, 1991.
- [Ins99] Institut für Parallele und Verteilte Höchstleistungsrechner – IPVR – Stuttgart University. *Stuttgart Neural Network Simulator (SNNS)*, www.informatik.uni.stuttgart.de/ipvr/bv/projekte/snns edition, 1999.

- [ISO86] International Organization for Standardization. *Principes généraux de la fiabilité des constructions.* Technical Report ISO 2394-1986(F), ISO, 1986.
- [Isu99] S.S. Isukapalli. *Uncertainty Analysis of Transport-Transformation Models.* PhD thesis, The State University of New Jersey, 1999.
- [JK70] N.L. Johnson and S. Kotz. *Distributions in Statistics – Continuous Univariate Distributions.* John Wiley, New York, 1970.
- [Kar39] W. Karush. *Minima of Functions of Several Variables with Inequalities as Side Conditions.* PhD thesis, University of Chicago, Dept. of Mathematics, 1939.
- [KH92] M. Kleiber and T.D. Hien. *The Stochastic Finite Element Method, basic Perturbation Technique and Computer Implementation.* John Wiley & Sons, New York, 1992.
- [Kle97] M. Kleiber. *Parameter Sensitivity in Non-Linear Mechanics – Theory and Finite Element Computations.* John Wiley & Sons, New York, 1997.
- [KML02a] G. Kharmanda, A. Mohamed and M. Lemaire. CAROD: Computer-aided reliable and optimal design as a concurrent system for real structures. *International Journal of CAD/CAM*, 2: 1–22, 2002.
- [KML02b] G. Kharmanda, A. Mohamed and M. Lemaire. Efficient reliability-based design optimization using hybrid space with application to finite element analysis. *Structural and Multidisciplinary Optimization*, 24(3): 233–245, September 2002.
- [KN94] H.U. Köylüoğlu and S.R. Nielsen. New approximations for SORM integrals. *Structural Safety*, 13: 235–246, 1994.
- [KN97] S.H. Kim and S.W. Na. Response surface method using vector projected sampling points. *Structural Safety*, 19(1): 3–19, 1997.
- [Knu81] D.E. Knuth. *The Art of Computer Programming*, volume 2. Addison Wesley, 1981.
- [KOML04] G. Kharmanda, N. Olhoff, A. Mohamed and M. Lemaire. Reliability-based topology optimization. *Structural and Multidisciplinary Optimization*, 26: 295–307, 2004.
- [Kro94] I.B. Kroon. *Decision Theory Applied to Structural Engineering Problems.* PhD thesis, Institutte for Bygningsteknik, Aalborg University, Denmark, June 1994.
- [KS83] P. Krée and C. Soize. *Mécanique Aléatoire.* Dunod, Paris, 1983.
- [Law87] M.A. Lawrence. Basis random variables in finite element analysis. *International Journal for Numerical Methods in Engineering*, 24: 1849–1863, 1987.

- [Law89] M.A. Lawrence. An introduction to reliability methods. In W.K. Liu and T. Belytschko, editors, *Computational Mechanics for Probabilistic and Reliability Analysis*, 9–46. Elmepress International, Lausanne, 1989.
- [LDK90] P.L. Liu and A. Der Kiureghian. Optimization algorithms for structural reliability. *Structural Safety*, 9(3): 161–177, 1990.
- [Lem97] M. Lemaire. Reliability and mechanical design. *Reliability Engineering & System Safety*, 55(2): 163–170, February 1997.
- [Lem98] M. Lemaire. Finite element and reliability: combined methods by response surface. In G.N. Frantziskonis, editor, *PROBAMAT-21st Century: Probabilities and Materials. Tests, Models and Applications for the 21st Century*, volume NATO ASI series 3. High Technology – vol. 46, 317–331, Kluwer Academic Publishers, September 10–12, 1998.
- [LFM95] M. Lemaire, J.L. Favre and A. Mébarki, editors. *Applications of Statistics and Probability*, volume I, II, III. International Conference on Applications of Statistics and Probability, ICASP7, Paris, 10–13 July 1995, Balkema, 1995.
- [LG03] X. Lin and C. Gengdong. Discussion on: Moment methods for structural reliability. *Structural Safety*, 1(25): 193–199, 2003.
- [LM94] Y.W. Liu and F. Moses. A sequential response surface method and its application in the reliability analysis of aircraft structural systems. *Structural Safety*, 16(1+2): 39–46, 1994.
- [LM00] M. Lemaire and A. Mohamed. Finite element and reliability: A happy marriage? In A. Nowak and Szerszen M., editors, 9th IFIP WG 7.5 Working Conference, The University of Michigan, *Reliability and Optimization of Structural Systems*, 3–14, September 2000.
- [LMFM97] M. Lemaire, A. Mohamed and O. Florès-Macias. The use of finite element codes for the reliability of structural systems. In D.M. Frangopol, R.B. Corotis and R. Rackwitz, editors, *Reliability and Optimization of Structural Systems'96, 7th IFIP WG 7.5 Working Conference, Boulder, 2–4 April*. Elsevier (Pergamon), 1997.
- [Lue86] D. Luenberger. *Introduction to Linear and Non Linear Programming*. Addison & Wesley, Reading, MA, 1986.
- [Lun94] E. Lund. *Finite Element Based Design Sensitivity Analysis and Optimization*. PhD thesis, Aalborg University, Denmark, 1994.
- [Mal97] P. Malliavin. *Stochastic Analysis*. Springer, Berlin 1997.
- [Mat65] G. Matheron. *Les variables régionalisées et leur estimation*. Masson, Paris, 1965.

- [MBB98] A. Mébarki, D. Boissier and D. Breysse, editors. *Fiabilité des matériaux et des structures*. 2ème conférence nationale JN-FIAB'98, Hermès, 1998.
- [MBBGS97] G.H. Matthies, C.E. Brenner, C.G. Bucher and C. Guedes Soares. Uncertainties in probabilistic numerical analysis of structures and solids – stochastic finite elements. *Structural Safety*, 19(3): 283–336, 1997.
- [MBL95] J-C. Mitteau, A. Béakou and M. Lemaire. Less approximations for SORM integrals. In M. Lemaire, J.L. Favre and A. Mébarki, editors, *Applications of Statistics and Probability*, volume 1, 1003–1010. A.A. Balkema, July 1995.
- [Méb90] A. Mébarki. *Sur l'approche probabiliste de la fiabilité des structures de génie civil: la méthode de l'hypercone et ses algorithmes*. PhD thesis, University of Toulouse, 1990.
- [Mel90] R.E. Melchers. Radial importance sampling for structural reliability. *Journal of Engineering Mechanics*, 116(1): 189–203, January 1990.
- [Mit95] J-C. Mitteau. Discussion on the paper: Less approximations for SORM integrals. In M. Lemaire, J.L. Favre and A. Mébarki, editors, *Applications of Statistics and Probability*, volume 3, 1529–1531. A.A. Balkema, July 1995.
- [Mit96] J.C. Mitteau. Error estimates for FORM and SORM computations of failure probability. In D. Frangopol and M. Mircea, editors, *Probabilistic Mechanics and Structural Reliability*, 562–565. Worcester, MA, USA, ASCE, 7–9 August 1996.
- [Mit99] J.C. Mitteau. Error evaluations for the computation of failure probability in static structural reliability problems. *Probabilistic Engineering Mechanics*, 14(1–2): 119–135, January/April 1999.
- [MK03] Y. Mori and T. Kato. Multinormal integrals by importance sampling for series system reliability. *Structural Safety*, 25: 363–378, 2003.
- [MKL86] H.O. Madsen, S. Krenk and N.C. Lind. *Methods of Structural Safety*. Prentice Hall, New York, 1986.
- [ML95] A. Mohamed and M. Lemaire. Linearized mechanical model to evaluate reliability of offshore structures. *Structural Safety*, 17: 167–193, 1995.
- [ML96] M. Meynet and M. Lemaire. Utilisation de plans d'expériences dans l'espace normé pour la construction de surface de réponse. Technical report, LaRAMA – Institut Français de Mécanique Avancée and Blaise Pascal University, Clermont-Fd, France, 1996.

- [ML98] A. Mohamed and M. Lemaire. The use of sensitivity operators in the reliability analysis of structures. In *Third International Conference on Computational Stochastics Mechanics*, Santorini, Greece, 14–17 June 1998.
- [MLET92] J.P. Muzeau, M. Lemaire and K. El-Tawil. Méthode fiabiliste des surfaces de réponse quadratiques (srq) et évaluation des règlements. *Construction Métallique*, (3): 41–52, September 1992.
- [MLMM97] A. Mohamed, M. Lemaire, J.C. Mitteau and E. Meister. Éléments Finis et Fiabilité; Méthodes de Couplage et Application à une Pièce Fissurée. *Revue Française de Mécanique*, (3): 171–177, 1997.
- [MLMM98] A. Mohamed, M. Lemaire, J.C. Mitteau and E. Meister. Finite element and reliability: A method for compound variables – application on a cracked heating system. *Nuclear Engineering and Design*, (185): 185–202, 1998.
- [MML94] A. Mébarki, J.P. Muzeau and M. Lemaire, editors. *Applications des Statistiques et des Probabilités en Analyse des Matériaux et des Ouvrages*. Journées Nationales CERRA-ICASP 7, Ecole Normale Supérieure de Cachan, 30–31 March, 1994.
- [MN98] M. Matsumoto and T. Nishimura. Mersenne twister: A 623-dimensionally equidistributed uniform pseudorandom number generator. *ACM Transaction on Modeling and Computer Simulation*, 8(1): 3–30, January 1998.
- [MS99] R.E. Melchers and M. Stewart, editors. *Applications of Statistics and Probability – Civil Engineering Reliability and Risk Analysis*. Proceedings of the ICASP 8 Conference, Sydney, Australia, Balkema, Rotterdam, 12–15 December 1999.
- [MSL96] A. Mohamed, F. Suau and M. Lemaire. A new tool for reliability based design with ANSYS FEA. In *ANSYS Conference & Exhibition, Houston, USA*, 3.13–3.23. ANSYS, Inc, 1996.
- [Nat62] A. Nataf. Détermination des distributions dont les marges sont données. *Comptes Rendus Académie des Sciences*, (225): 42–43, 1962.
- [Nie94] H. Niederreiter. New developments in uniform pseudorandom number and vector generation. In *Monte Carlo and Quasi-Monte Carlo Methods in Scientific Computing*, 87–120, 1994.
- [PCH00] M. Pendola, E. Chatelet and P. Hornet. Structural reliability using finite element analyses and artificial neural networks. In *Mathematical Methods in Reliability*, Bordeaux, 2000.
- [Pen97] M. Pendola. Couplage mécano-fiabiliste par surfaces de réponse - Application aux tuyauteries droites fissurées. Rapport de projet de fin d'études et de DEA, Blaise Pascal University and Institut Français de Mécanique Avancée, 1997.

- [Pen00] M. Pendola. *Fiabilité des structures en contexte d'incertitudes statistiques et d'écart de modélisation*. PhD thesis, Blaise Pascal University, 6 December 2000.
- [Phi04] Phimeca S.A., <http://www.phimeca.com>. *Phimeca-Soft*, 2004.
- [PHLM00] M. Pendola, P. Hornet, M. Lemaire and A. Mohamed. The influence of data sampling uncertainties in reliability analysis. In R.E. Melchers and M.G. Stewart, editors, *ICASP 8 – Applications of Statistics and Probability*, (2), 1095–1100, Rotterdam/Brookfield, 2000. ICASP'8, A.A. Balkema.
- [PMMR03] M. Pendola, G. Morin, A. Mohamed and P. Ragot. Reliability analysis of exhaust system. In *Simulation: An Essential Tool for Risk Management in Industrial Product Development*. SIA, Paris, 17–18 September 2003.
- [PPS02] B. Puig, F. Poirion and C. Soize. Non-Gaussian simulation using hermite polynomial expansion: Convergences. *Probabilistic Engineering Mechanics*, 17: 253–264, 2002.
- [PTVF92] W.H. Press, A.A. Teukolsky, W.T. Vetterling and B.P. Flannery. *Numerical Recipes in FORTRAN – The Art of Scientific Computing*. Cambridge University Press, 1992.
- [PW88] P.Y. Papalambros and D.J. Wilde. *Principles of Optimal Design*. Cambridge University Press, NY, USA, 1988.
- [Rac76] R. Rackwitz. Practical probabilistic approach to design. First order reliability concepts for design codes. Bulletin d'Information du CEB 112, Comité Européen du Béton, July 1976.
- [Rac89] R. Rackwitz. Methods of system reliability evaluation. Joint Research Centre, Ispra, Italy, Commission of the European Communities, November 1989.
- [Rad91] J.C. Radix. *Pratique moderne des Probabilités*. Lavoisier Tec & Doc, 1991.
- [Ran76] F.A. Randall. The safety factor of structures in history. *Professional Safety*, 12–18, January 1976.
- [RE93] M.R. Rajashekhar and B.R. Ellingwood. A new look at the response surface approach for reliability analysis. *Structural Safety*, 12(3): 205–220, 1993.
- [RF79] R. Rackwitz and B. Fiessler. Structural reliability under combined random load sequences. *Computers and Structures*, 9: 489–494, 1979.
- [Ric44a] S.O. Rice. Mathematical analysis of random noise, part I and II. *Bell System Technical Journal*, 32: 282–332, 1944.
- [Ric44b] S.O. Rice. Mathematical analysis of random noise, part III and IV. *Bell System Technical Journal*, 46–156, 1944.

- [Ric80] S.O. Rice. Distribution of quadratic forms in normal random variables – evaluation by numerical integrations. *SIAM Journal of Scientific Computing*, 1(4): 438–448, December 1980.
- [Rja59] A.R. Rjanitzyn. *Calcul à la Rupture et Plasticité des Constructions*. Eyrolles, Paris, 1959.
- [Ros52] M. Rosenblatt. Remarks on a multivariate transformation. *The Annals of Mathematical Statistics*, 23: 470–472, 1952.
- [RPLB98] O. Rollot, M. Pendola, M. Lemaire and I. Boutemy. Reliability indexes calculation of industrial boilers under stochastic thermal process. In *Proceedings of DETC'98*. ASME Design Engineering Technical Conferences, Atlanta, Georgia, USA, ASME, 13–16 September 1998.
- [Rub64] H. Ruben. An asymptotic expansion for the multivariate normal distribution and mill's ratio. *Journal of Research NBS*, 68B(1): 3–11, 1964.
- [Rub81] R.Y. Rubinstein. *Simulation and the Monte Carlo Methods*. John Wiley & Sons, New York, 1981.
- [Rud75] W. Rudin. *Analyse réelle et complexe*. Masson, Paris, 1975.
- [Rzh49] R.A. Rzhanitzyn. Design of structures with considerations of plastic properties of materials. *Stroivoenmorizdat*, 1949.
- [Sap90] G. Saporta. *Probabilités, Analyse des Données et Statistique*. éditions Technip, Paris, 1990.
- [SBL03] B. Sudret, M. Berveiller and M. Lemaire. Eléments finis stochastiques spectraux: nouvelles perspectives. In *Actes du 16ème Congrès Français de Mécanique*. CFM, Nice, 1–5 September 2003, AFM, 2003.
- [SBL04] B. Sudret, M. Berveiller and M. Lemaire. Eléments finis stochastiques en Elasticité linéaire. *CRAS – Mécanique*, 332: 531–537, 2004.
- [Sch86] K. Schittkowski. NLPQL: A Fortran subroutine solving constrained non linear programming problems. *Annals Operations Research*, 5: 485–500, 1986.
- [Sch97] F. Scheffer. Approche par Eléments Finis Stochastiques de la Fiabilité de Composants mécaniques. Rapport de projet de fin d'études et de DEA, Blaise Pascal University and Institut Français de Mécanique Avancée, 1997.
- [SD88] M. Shinozuka and G. Deodatis. Response variability of stochastic finite element systems. *Journal of Engineering Mechanics*, 114(3), March 1988.
- [SDK00] B. Sudret and A. Der Kiureghian. Stochastic finite element methods and reliability – a state-of-the-art report. Technical Report UCB/SEMM-2000/08, Dept. of Civil and Environmental Engineering, University of California, Berkeley, November 2000.

- [SDK02] B. Sudret and A. Der Kiureghian. Comparison of finite element reliability methods. *Probabilistic Engineering Mechanics*, 17: 337–348, 2002.
- [SFR91] G. Schall, M.H. Faber and R. Rackwitz. The ergodicity assumption for sea states in the reliability estimation of offshore structures. *Journal of Offshore Mechanics and Arctic Engineering*, 113: 241–246, August 1991.
- [Sha70] D.F. Shanno. Conditioning of quasi-newton methods for function minimization. *Mathematics of Computation*, 24: 647–656, 1970.
- [Sha78] D.F. Shanno. Conjugate gradient methods with inexact line searches. *Mathematics of Operations Research*, 3: 244–256, 1978.
- [Sho68] M.L. Shooman. *Probabilistic Reliability: An Engineering Approach*. McGraw-Hill Book Co, New York, 1968.
- [SKF94] J.D. Sorensen, I.B. Kroon and M.H. Faber. Optimal reliability-based code calibration. *Structural Safety*, 15(3), September 1994.
- [SM93] A. Sellier and A. Mébarki. Evaluation de la probabilité d'occurrence d'un événement rare par utilisation du tirage d'importance conditionné. *Annales des Ponts et Chaussées*, 3–23, July 1993.
- [Sof01] Math Soft. *Mathcad 2001 professionnel*, 2001.
- [Soi94] C. Soize. *The Fokker-Planck Equation for Stochastic Dynamical Systems and its Explicit Steady State Solutions*. World Scientific, Singapore, 1994.
- [Soi01] C. Soize. *Dynamique des Structures – éléments de base et concepts fondamentaux*. Ellipses, Paris, 2001.
- [SS97] Shinozuka and Shiraishi, editors. *7th International Conference on Structural Safety and Reliability*. International Association for Structural Safety and Reliability (IASSAR), 24–28 November 1997.
- [SS01] M. Shinozuka and G.I. Schuëller, editors. *8th International Conference on Structural Safety and Reliability*. International Association for Structural Safety and Reliability (IASSAR), 17–22 June 2001.
- [SY88] M. Shinozuka and F. Yamazaki. Stochastic finite element analysis: an introduction. In *Stochastic Structural Dynamics, Progress in Theory and Applications*, 241–291. Elsevier Applied Science, 1988.
- [Tak90a] T. Takada. Weighted integral method in multi-dimensional stochastic finite element analysis. *Probabilistic Engineering Mechanics*, 5(4): 158–166, 1990.
- [Tak90b] T. Takada. Weighted integral method in stochastic finite element analysis. *Probabilistic Engineering Mechanics*, 5(3): 146–156, 1990.
- [TCM86] P. Thoft-Christensen and Y. Murotsu. *Application of Structural Systems Reliability Theory*. Springer-Verlag, Berlin, 1986.

- [Tve83] L. Tvedt. Two second-order approximations to the failure probability. Technical Report RDIV/20-004-83, Det Norske Veritas, 1983.
- [Tve88] L. Tvedt. Second order reliability by an exact integral. Technical report, A.S. Veritas Research, Høvik, Norway, 1988.
- [Tve90] L. Tvedt. Distributions of quadratic forms in normal space – application to structural reliability. *Journal of Engineering Mechanics*, 116(6): 1183–1197, June 1990.
- [Van83] E.H. Vanmarcke. *Random Fields: Analysis and Synthesis*. MIT Press, Cambridge, MA, 1983.
- [Van03] B. Van den Nieuwenhof. *Stochastic Finite Elements for Elastodynamics: Random Field and Shape Uncertainty Modelling Using Direct and Modal Perturbation-Based Approaches*. PhD thesis, Université catholique de Louvain – Faculté des sciences appliquées – unité de Génie Civil et Environnemental, May 2003.
- [Ver94] V. Verderaime. Illustrated structural application of universal first-order reliability method. Technical Report 3501, NASA, August 1994.
- [Vil88] A. Villemeur. *Sûreté de fonctionnement des systèmes industriels*. Eyrolles, Paris, 1988.
- [VN51] J. Von Neumann. Various techniques used in connection with random digits. Technical Report 12, US Nat. Bur. Stand. Appl. Math. Serv., 1951.
- [Vro01] A. Vrouwenvelder. The JCSS probabilistic model code. In Safety, risk and reliability – trends in engineering. *Proceedings of the Malta Conference*, 21–23 March 2001.
- [Waa00] P.H. Waarts. *Structural Reliability Using Finite Element Methods*. PhD thesis, Delft University, 2000.
- [Wei51] W. Weibull. A statistical distribution function of wide applicability. *Journal of Applied Mechanics*, 18: 273–277, 1951.
- [Win87] S. Winterstein. Moment-based Hermite models of random vibration. Technical Report R-219, Technical University of Denmark – Department of Structural Engineering, 1987.
- [Win88] S.R. Winterstein. Nonlinear vibration models for extremes and fatigue. *Journal of Engineering Mechanics, ASCE*, 114: 1172–1190, 1988.
- [ZDK95] Y. Zhang and A. Der Kiureghian. Two improved algorithms for reliability analysis. In R. Rackwitz, A. Augusti and A. Borri, editors, *Proceedings of the 6th IFIP WG7.5 Reliability and Optimization of Structural Systems*, 1995.
- [ZO99a] Y.G. Zhao and T. Ono. New approximations for SORM: Part 1. *Journal of Engineering Mechanics*, 125(1): 79–85, January 1999.

- [ZO99b] Y.G. Zhao and T. Ono. New approximations for SORM: Part 2. *Journal of Engineering Mechanics*, 125(1): 86–93, January 1999.
- [ZO00] Y.G. Zhao and T. Ono. New point-estimates for probability moments. *Journal of Engineering Mechanics ASCE*, 4(126): 433–436, 2000.
- [ZO01] Y.G. Zhao and T. Ono. Moment methods for structural reliability. *Structural Safety*, 1(23): 47–75, 2001.

This page intentionally left blank

Annotations

A.1 Vectors and matrices

$\langle V \rangle$	Line vector
$\{V\}$ or v_k or \mathbf{u}	Column vector
v_k	Vector or component, depending on the context
$[M]$ or M_{ij}	Matrix
$[M]^t$	Transposition
$\ V \ $	Euclidean norm

A.2 Operators

$\sum_i a_i b_i = a_i b_i$	Einstein convention
$\delta_{ij} = 1 \quad \text{if } i = j \\ \delta_{ij} = 0 \quad \text{if } i \neq j$	Kronecker symbol
$\{v\}^t \{u\}$ or $\mathbf{u} \cdot \mathbf{v}$	Scalar product
$c_i = a_j \wedge b_k = \epsilon_{ijk} a_j b_k$	Vectorial product

with

- $\epsilon_{ijk} = 1$ if i, j, k form a direct permutation,
 $\epsilon_{ijk} = -1$ if i, j, k form an indirect permutation,
 $\epsilon_{ijk} = 0$ if i, j, k , do not form a permutation.

$\vec{\text{grad}} \ u = \partial u / \partial x_i = u_{,i} = \nabla u$	Gradient
$\nabla_u H = \partial H / \partial u_i$	Gradient with indication of the variable
$\text{div } \vec{v} = \text{div } v_i = \partial v_i / \partial x_i = v_{i,i}$	Divergence
$\vec{\text{rot}} \ \vec{v} = \epsilon_{ijk} v_{k,j}$	Rotational

A.3 Random values

A.3.1 Scalar values and random variable couples

r.v.	Random variable
X	Random variable, in principle, in upper case
x	Outcome of the random variable X , in principle, in lower case
x_k	Characteristic value of X
m_X	Mean of the random variable X
σ_X	Standard deviation of the random variable X
c_X	Coefficient of variation (c.o.v.) of random variable $X (c_X = \sigma_X/m_X)$
ρ	Coefficient of correlation of two random variables
$E[X]$	Expectation (mean) of X
$\text{var}[X]$	Variance of X
$F_X(x)$	Cumulative Distribution Function (CDF) of the random variable X
$f_X(x)$	Probability Density Function (PDF) of the random variable X
θ	Parameters of a probability function, for example, $f_X(x \theta)$
Θ	Random parameters of a probability function
$\text{cov}[X_i, X_j]$	Covariance of X_i, X_j
$\text{cor}[X_i, X_j]$	Correlation of X_i, X_j
$\rho_{X_i X_j} = \rho_{ij}$	Coefficient of correlation of X_i, X_j

A.3.2 Statistical values

(x_1, \dots, x_n)	n -dimensional sample of the random variable X
\bar{x}	Empirical mean $\frac{1}{n} \sum_{i=1, \dots, n} x_i$
m'_r	Statistical moment of order r ; $\frac{1}{n} \sum_{i=1, \dots, n} x_i^r$
m_r	Centered statistical moment of order r ; $\frac{1}{n} \sum_{i=1, \dots, n} (x_i^r - \bar{x})^r$
μ'_r	Moment of order r of the r.v. X , $E[X^r]$
μ_r	Centered moment of order r of the r.v. X , $E[(X - E[X])^r]$
α_3	Skewness $E[(X - E[X])^3]/\text{var}[X]^{3/2}$
α_4	Kurtosis $E[(X - E[X])^4]/\text{var}[X]^2$

A.3.3 Vectorial values

X_i or $\{X\}$	Vector of physical random variables
m_{X_i} or $\{m_X\}$	Vector of means of X_i or $\{X\}$
σ_{X_i} or $\{\sigma_X\}$	Vector of standard deviations of σ_i or $\{\sigma\}$
$[C_X]$	Covariance matrix of $\{X\}$
ρ_{ij} or $[\rho]$	Correlation matrix of $\{X\}$
$f_{X_i}(x_i)$ or $f_{\{X\}}(\{x\})$	Joint probability density function of X_i or $\{X\}$
U_i or $\{U\}$	Uncorrelated, centered, standardized random variables

P or Prob	Probability, e.g. $P(X > x)$ or $\text{Prob}(X > x)$
$\mathcal{N}(0, 1)$	Normal distribution with zero mean and unit variance
$\phi(x)$	Probability density of the normal distribution $\mathcal{N}(0, 1)$
$\Phi(x)$	Distribution function of the normal distribution $\mathcal{N}(0, 1)$
S	Random load effect or stress
R	Random resistance
Z	Margin $Z = R - S$

A	Random action
K	State variable (geometry or material)
U	Standardized variable $\mathcal{N}(0, 1)$
$G_k(X_j)$	Performance function of the random variables X_j
$G_k(X_j) = 0$	Limit-state function
$H_k(U_j) = 0$	Limit-state function in standardized variables
\mathcal{D}_s	Safety domain
\mathcal{D}_f	Failure domain

P_f	Probability of failure
P_f^*	Approximated value of P_f
\tilde{P}_f	Estimated value of P_f
\bar{P}_f	Required value of P_f

β_c	Rjanitzyne-Cornell index
β_{HL} or β	Hasofer-Lind index
$\bar{\beta}$	Target value of an index
P^*	The most probable failure point or design point
α_i	Direction cosines of the limit-state function in P^*
γ_X	Partial safety factor associated with the random variable X
$\bar{\gamma}$	Mean (safety) factor $\bar{\gamma} = m_R/m_S$

A.3.4 Mechanical values

f_y	Yield limit (another notation σ_e)
f_u	Resistance under tension
E	Elasticity (or Young's) modulus

Index

- Application
 - Boiler, 445
 - Cooling tower, 448
 - Cracked plate, 443
 - Cracked plate cooling, 444
 - Design and maintenance, 455
 - Exhaust manifold, 450
 - Mandrel, 442
 - Pressurized tank, 446
 - Stability, 447
 - Wind bracing, 441
- Cornell, 60
- Design point, 64, 84
 - Multiplicity, 218
- Optimization algorithms, 119
 - Abdo-Rackwitz algorithm, 137, 143
 - BFGS method, 137
 - Gradient method, 124, 132
 - HLRF algorithm, 128, 141, 383
 - iHLRF algorithm, 131
 - Lagrangian method, 127
 - Newton method, 135
 - Penalty method, 126
 - SQP algorithm, 136, 143
- Optimization problem, 116, 455
- Partial coefficients, 303
- Search, 115, 144, 371
- Several minima, 138
- Design variables, 21
 - Characteristic values, 301
 - Correlation, 45, 46, 93, 317, 387
 - Design values, 302
 - Independence, 48
 - Modeling, 23, 39, 344, 392, 453, 461
 - Nominal values, 301
 - Polynomial chaos expansion, 418
 - Safety coefficients, 300
 - Sensitivity, 150
- Distribution
 - Exponential, 85, 227
 - Extreme value, 27
 - Fractile, 311
 - Gamma, 108
 - Gauss, 25, 46, 52, 167, 172, 242, 282, 412
 - Gaussian couple, 87
 - Gumbel, 81
 - Joint probability density, 44
 - Kurtosis, 105
 - Lognormal, 80, 244, 333, 414
 - Skewness, 105
 - Uniform, 53, 101, 371
 - Weibull, 244
- Elementary case
 - Probability of failure, 48
 - Reliability modeling, 65
 - Rod under tension, 57
 - Safety coefficients, 306

- Finite element method, 341, 343, 391
- Gradient calculation, 405
- Isoparametric transformation, 407
- Polynomial chaos, 420
- SFEM linear system, 422, 431
- Stochastic FEM, 391, 428, 460
- Freudenthal, 11
- Gödel, 5
- Galileo, 3
- Hammurabi, 1
- Hasofer, 63
- Hermite polynomials, 102
- Leonardo da Vinci, 3
- Lind, 63
- Mechanical modeling
 - Example, 42
 - Failure scenario, 29, 41
 - Need, 29
 - Performance function, 29
 - Resource, 29
- Mechanical-reliability coupling, 33, 115, 341
 - Actors, 33
 - Application, 34
 - Sphere, 368
 - Truss, 380
 - Uniform distributions, 371
 - Design of experiment, 356
 - Direct coupling, 342
 - Direct method, 352
 - FEM implementation, 347
 - Gradient calculation, 349, 405
 - Neural networks, 364, 371
 - Optimization, 342, 377, 461
 - Quadratic response surface, 359, 370, 371
 - Resampling, 363
- Response surface, 342, 353
 - Polynomial, 353
- Stochastic FEM, 438
- Validation, 360
- Pascal, 3
- Poincaré, 4
- Probabilistic design
 - Characteristic coefficient, 309
 - Fatigue, 309
 - Fractile coefficient, 311, 315
 - Gauss, 306
 - Lognormal, 307
- Probability of failure, 68
 - Asymptotic SORM, 190
 - Breitung formula, 190, 219, 222, 225, 230, 288, 375, 384
- Calculation, 85, 167, 218
 - Reference example, 166, 168, 174, 185, 194, 202, 215, 218
- Characteristic function, 196
- Elementary case, 48
- FORM approximation, 168, 212, 373, 455
 - Counter-example, 172
- Hohenbichler formula, 194
- Integration, 53
- Plastic failure, 221
- RGMR method, 203, 220, 226, 230
- Rod under tension, 219
- Sensitivity, 156
- Simulation, 54
- SORM approximation, 196, 207, 373, 455
- SORM approximation, 175
- Tvedt formula, 194, 375, 384
- Random field
 - Autocorrelation, 394, 445
 - Cholesky decomposition, 401

- Correlation length, 396, 444
- Definition, 26, 392, 394
- Discretization, 399
 - OLE (kriging), 400
- KL expansion, 402, 428
- Perturbation, 410
- Phenomenological description, 397
- Polynomial chaos, 402, 429
- Second-order, 395
- Spectral method, 427
- Stationarity, 394
- Stochastic mesh, 398
- Weighted integral method, 425
- Regulations, 300
 - Code format, 304
 - Eurocodes, 300
 - Standard, 300
- Reliability index
 - Cholesky decomposition, 89, 401
 - Design point, 64, 84
 - Direction cosines, 64, 150
 - Hasofer-Lind, 63, 70, 77
 - Hermite transformation, 104, 111
 - Isoprobabilistic
 - transformation, 63, 79, 167, 455
 - Linear case, 101
 - Most probable failure point (*see:* Design point), 63
 - Nataf transformation, 92
 - Normal distribution, 89
 - Rjanitzne-Cornell, 61, 70
 - Rosenblatt transformation, 82, 100
 - Standardized space, 63
 - Transformation, 85, 112
 - Example, 98, 101, 109
- Reliability methods, 453
 - Branch and bound, 441
- Definition, 6
- Design levels, 304
- Direction cosines, 150, 385
- Distribution parameters, 152
- Elasticity, 156, 386, 450
- Failure domain, 381
- Illustration, 161
- Importance factors, 149, 385, 443
- Mechanical analysis, 148
- Mechanical-reliability coupling, 438
- Neumann expansion, 417
- Omission factors, 157
- Overview, 19
- Performance function, 155, 341, 444, 453
- Perturbation, 410, 437
- Polynomial chaos, 424
 - Beam deflection, 422
- Polynomial chaos expansion, 418, 438
- Reliability analysis, 31, 463
- Sensitivity analysis, 30, 392, 407, 463
- Software tools, 458
- Spectral method, 427
- Taylor expansion, 410
 - Beam deflection, 412
- Theoretical reliability, 22
- Reliability modeling
 - Component, 21
 - Elementary case, 44, 65
 - Failure domain, 43
 - Limit-state, 43, 75, 157
 - Curvature, 176, 188, 222
 - Gradient calculation, 349
 - Parabolic approximation, 183, 188
 - Quadratic approximation, 179, 186
 - Quadratic approximation, 181, 198

- Random spaces, 42, 357
- Safety domain, 43
- Reliability of systems
 - Bounds, 275, 276
 - Conditional parallel combination, 268
 - Correlation, 274
 - Design point, 139
 - Equivalent hyperplane, 279
 - First-order approximation, 281, 293
 - First-order bounds, 277
 - Illustration, 270, 272, 289
 - Optimization, 117
 - Parallel combination, 266
 - Poincaré formula, 266
 - Second-order approximation, 286, 296
 - Series combination, 266
 - Wind bracing, 441
- Risk, 2
 - Acceptability, 6
 - Construction, 9
 - Farmer graph, 2
 - Technological, 5
- Rjanitzyn, 11, 60
- Rod under tension
 - Elementary case, 57
 - Hasofer-Lind index, 66
 - KL expansion, 435, 436
 - Neumann expansion, 434
 - Perturbation, 433, 435
 - Probability of failure, 219
 - Safety coefficients, 313
 - Simulation, 436
- Safety coefficients
 - Application
 - Calibration, 326
 - Fracture mechanics, 331
 - Fragile material, 336
 - Calibration, 322
 - Characteristic values, 301
- Comments, 321
- Correlation, 317
- Design rule, 303
- Design values, 302
- Design variables, 300
- Elementary case, 306
- Illustration, 305
- Nominal values, 301
- Partial coefficients, 299, 315, 319, 386
 - Design point, 303
- Pressurized tank, 446
- Rod under tension, 313
- Simulation
 - Adaptive sampling, 259
 - Conditional sampling, 256, 261
 - Crude Monte Carlo, 249, 260
 - Directional simulations, 253, 260
 - Estimates, 250
 - Gauss, 242
 - Generators, 237
 - Importance sampling, 255
 - Latin hypercube, 258
 - Lognormal, 244
 - Monte Carlo, 54, 233, 247
 - Non-uniform numbers, 240
 - Random numbers, 234
 - Random vector, 244
 - Shooman formula, 55, 252
 - Variance reduction, 253
 - Weibull, 244
- Time factor, 460